NOTE TO USERS

PETROLOGIC AND EXPERIMENTAL CONSTRAINTS ON MAGMA MINGLING AND ASCENT: EXAMPLES FROM JAPAN AND ALASKA

A

THESIS

Presented to the Faculty

of the University of Alaska Fairbanks

in Partial Fulfillment of the Requirements

for the Degree of

DOCTOR OF PHILOSOPHY

By

Brandon Lanquist Browne B.S., M.S.

Fairbanks, Alaska

May 2005

PETROLOGIC AND EXPERIMENTAL CONSTRAINTS ON MAGMA MINGLING AND ASCENT: EXAMPLES FROM JAPAN AND ALASKA

By

Brandon Lanquist Browne

RECOMMENDED:

Advisory Committee Chair

Vice Chair, Department of Geology and Geophysics

APPROVED:

Dean, College of Natural Science and Mathematics

Dean of the Graduate School

April 11, 2005
Date

ABSTRACT

This study investigates how magma is physically, chemically, and mineralogically modified in two regions in the shallow crust: the magma chamber and the conduit through which magma ascends from the chamber to the surface during eruption. Chapter 1 includes findings from 2 studies on how contrasting magmas interact in the chamber during basaltic replenishment events, which is performed by documenting different characteristics of mafic-to-intermediate enclaves and coexisting silicic host lavas from Unzen volcano, Japan. Two types of magmatic enclaves, referred to as Equigranular and Porphyritic, are easily distinguished texturally. Equigranular enclaves are andesitic, non-porphyritic, and consist of tabular shaped, medium grained microphenocrysts in a matrix glass in equilibrium with host dacite magma. Equigranular enclaves are a product of a more prolonged mixing and gradual crystallization at a slower cooling rate within the interior of mafic intrusions. Porphyritic enclaves display a wide range in composition from basalt to andesite and are porphyritic, where large resorbed plagioclase phenocrysts exist in a matrix of acicular crystals and glass. Porphyritic enclaves are produced when intruding basaltic magma engulfs melt and phenocrysts of resident silicic magma at their mutual interface. In response to the sudden compositional and temperature change in the surrounding melt, engulfed plagioclases develop resorption zones at their edges that are composed of a micron-sized network of glass inclusions and calcic plagioclase that is identical in composition to plagioclase microphenocrysts inherent to the enclave-forming magma. Over time, engulfed plagioclases are recycled back to the host as enclaves disaggregate.

Chapter 2 describes results of a study that experimentally constrains the rate and manner in which reaction rims form on hornblende during decompression (magma ascent) using samples from Redoubt volcano, Alaska. Findings from this study show that the development of reaction rims depends on a balance between the rate of hornblende dissolution, which supplies the necessary components for reaction rims to the crystal-melt boundary, and the rate that dissolved components are transported away from the destabilized crystal to crystal faces of other pre-existing minerals. This reaction is strongly influenced by melt viscosity, which varies with changing water content, temperature, and pressure.

TABLE OF CONTENTS

LIST OF FIGURES

LIST OF TABLES

LIST OF APPENDICES

ACKNOWLEDGEMENTS

The following people have supported me in completing this thesis in countless ways. My advisor and friend, Dr. John Eichelberger, has taught me a great deal about science, cooperation, and the world, for which I am eternally grateful. John is an inspiring mentor who champions the physical, intellectual, and cultural challenges (and rewards) unique to studies of North Pacific volcanoes like no other. He is also one of the most selfless and generous people I have ever met whose endless pursuit of a life embodied by kindness, honesty, and peace will forever earn my admiration and respect.

After guiding me through a Masters degree in the precarious fields of western Mexico in 1999-2001, Dr. Jim Gardner moved 4,000 miles south during my second year as a Ph.D. student. Was it something I said? In spite of the distance between Alaska and Texas, Jim has remained committed and dedicated to my development as a physical scientist. I deeply appreciate his willingness to remain an active participant of my committee; and I thank him for his advice, patience, and all that he continues to teach me about volcanoes, academic politics, and baseball. Drs. Jessica Larsen, Paul Layer, and Chris Nye also acted on my committee and always supported my research with genuine interest and enthusiasm. I am indebted to them for their numerous pep talks, reference letters, and insightful input into this research.

My involvement with the Alaska Volcano Observatory has been nothing short of extraordinary. The cooperative arrangement that AVO has with the UAF Volcanology Research Group was central to my original decision to come to Fairbanks in 1999 for my Masters degree, and one of the main reasons I decided to stay in 2001 for my Ph.D. I am

forever grateful to all of my experiences with members within AVO, especially Tina Neal, Michelle Coombs, Game McGimsey, Janet (Carl, Henry, Rocky, & Max) Schaefer, John Paskievitch, John Power, Charlie Bacon, Tom Sisson, Jonathan Dehn, and Ken Dean. In addition, the Alaska Volcano Observatory provided me with invaluable funding for travel to fascinating and wonderfully unusual natural laboratories for volcanic research such as Japan, Kamchatka, and the Aleutian Islands, as well as important scientific conferences such as the 2004 IAVCEI Assembly in Pucón, Chile; the 2003 IUGG Assembly in Sapporo, Japan; and many American Geophysical Union conferences in San Francisco, California during Alaska's dark and cold winter, for which I am especially appreciative.

Tom Vogel, Lina Patino, Kozo Uto, Hideo Hoshizumi, Nguyen Hoang and Setsuya Nakada graciously and patiently contributed to my research at Unzen volcano, which is described in Chapter 1 of this thesis. I am grateful for all they have taught me and for the opportunity to have worked with them on this amazing project. In addition, I am proud to know many others who have helped me through this journey. They are Pavel Izbekov, Alain Burgisser, Ben Andrews, Sean Bemis, Ken Papp, Rob Nicholson (The Los Blue Ribbon Treehorn Guapos 5), Mary Keskinen, Ken Severin, Don Snyder, Robert Wiebe, Malcolm Rutherford, Steve McNutt, Jeffrey Freymueller, Charlie Mandeville, Jim Beget, Darren Chertkoff, Jim Webster, and John Pallister. Bill Witte and June Champlin of the UAF Geology and Geophysics Department are also acknowledged, for they are genuinely kind people who have assisted me a great deal.

Finally, I am sincerely appreciative of my parents, along with my many sisters and brother for their limitless ability to support and encourage my life decisions, even though many special family gatherings and events were often missed as a result. I also thank my second (in-lawed) set of parents, who continue to amaze me with their interest and enthusiasm for a science that they knew so little about just a few short years ago. They are an emerging pair of volcano experts, whose unavoidable inquiries about volcanoes, or rocks in general, motivate me to learn more, even if for no other reason than to have something new to share with them next time I see them. Carrie, my most miraculous and angelic wife, has remained a source of endless comfort, support, and patience throughout this thesis. Our six years in Alaska have presented unimaginable challenges and immeasurable rewards, all of which we faced together. She is my strength and my purpose- for there is absolutely positively no possible way that I could have survived these past 6 years without her.

PREFACE

This thesis is the result of three studies that investigate how magma is physically, chemically, and mineralogically modified in two regions in the shallow crust. One such region is a storage reservoir where magma ponds between eruptions, referred to as a magma chamber, and the other is the conduit through which magma ascends from the chamber to the surface during eruption. Magma may be modified externally by mixing with other magmas of different composition, or internally through crystallization and degassing. These modifications influence the composition, texture, and mineralogy of magma, as well as the style in which it erupts. Investigating processes that modify magma in the shallow crust are therefore critical to a comprehensive understanding of volcanic eruption processes.

Most silicic magma chambers in the crust appear to be sustained by episodic injection of basalt, and Chapter 1 combines two studies that investigate how basaltic replenishment occurs in the silicic magma chamber of Unzen Volcano, Japan. All sample collection, preparation, electron microprobe analyses, and data interpretation was performed by me under the guidance of Drs. John Eichelberger (University of Alaska Fairbanks Geophysical Institute); Thomas Vogel and Lina Patino (Michigan State University); and Kozo Uto and Hideo Hoshizumi (Japan Geological Survey). Dr. Lina Patino performed all whole-rock analysis of Unzen samples and laser ablation inductively coupled-mass spectrometry (LA ICP-MS) analysis of plagioclase. One study documents different textural, petrological, and geochemical characteristics of magmatic enclaves, which provide a record of how replenishing and resident magma interact physically.

Findings from this study indicate that two texturally distinct enclaves exist in Unzen lavas, and that both types of enclaves may be produced during the same replenishment event. One type records rapid cooling at an interface between host silicic magma and intruding basalt magma, and the other is the product of more prolonged mixing and crystallization within the mafic intrusion. The second study documents the textural and geochemical characteristics of plagioclase crystals from lavas and enclaves, which provide a temporal record of changes in temperature and melt composition. Findings from this study demonstrate that the style of magma mixing in the Unzen magma chamber involves the exchange of crystals between the two magmas, which cause the juxtaposition of plagioclase (and other) crystals with seemingly different histories.

Chapter 2 explores the process of magma as it ascends through a conduit from the chamber to the surface using samples erupted from Redoubt Volcano, Alaska during 1989 to 1990. Michelle Harbin and Ken Wolf collected the natural pumice and dome block samples used in this study. All sample preparation, experiments, electron microprobe analyses, and data interpretation was performed by me under the primary guidance of Dr. James Gardner (University of Texas at Austin), with additional input from Drs. Jessica Larsen and John Eichelberger. The rate of an important mineralogical breakdown reaction that occurs between destabilized amphibole and melts during ascent was measured experimentally. Results show that reaction rims develop through the dissolution of destabilized amphiboles, and that this reaction occurs preferentially at higher pressures, where melt viscosity is lower compared to near-surface conditions.

CHAPTER 1.

1.1 INTRODUCTION

The presence and textural characteristics of chilled mafic enclaves, also described as *under-cooled inclusions* (e.g. Bacon, 1986) in igneous rocks is well documented in andesitic to rhyolitic lava flows and domes (e.g. Eichelberger, 1978; 1980; Heiken and Eichelberger, 1980; Bacon and Metz, 1984; Clynne, 1999; Davidson et al., 2001; Singer et al., 1995), as well as in the plutonic record (e.g. Didier, 1973; Vernon, 1983, 1984; Wiebe, 1994; Wiebe and Collins, 1998; Wiebe et al., 2002). These enclaves are interpreted to form by the mingling of coexisting magmas with strongly contrasting physical properties in the liquid state (Eichelberger et al., 1976; Bacon, 1986; Sparks and Marshall, 1986; Koyaguchi and Blake, 1991; Stimac et al., 1990; Stimac and Pearce, 1992), as indicated by textural evidence such as a spherical or ellipsoidal shape with vesicular interiors, acicular groundmass minerals and/or cuspate margins. The types and morphologies of enclaves in host lavas preserve information on the style and dynamics of the mingling of magmas. Therefore, investigating the characteristics of enclaves promotes a more comprehensive understanding of the styles of mafic-silicic magma interactions, especially when considering if a discontinuity in magma composition can be stable in the magma body (e.g., Eichelberger et al., 2000).

Textural characteristics of phenocrysts are also often used to infer magmatic process (Vance, 1965; Tsuchiyama and Takahashi, 1983; Nelson and Montana, 1992;

Nakada et al., 1994; Dunbar et al., 1994; Singer et al., 1995; Feeley and Dungan, 1996; Izbekov et al., 2002). Chemical and textural zoning patterns preserved in plagioclase phenocrysts, for example, provide useful information that constrains the changing melt-crystal compositions, and therefore also bear on the general problem of how magmas of differing compositions and physical properties chemically interact in shallow reservoirs beneath arc volcanoes. Many studies have utilized the compositional and textural information recorded in plagioclase from volcanic rocks to infer various aspects of magma chamber dynamics (Anderson, 1983; Pearce et al., 1987; Stimac et al., 1990; Stimac and Pearce, 1992; Singer et al., 1995; Davidson and Tepley, 1997; Davidson et al., 1998; Nakamura and Shimakita, 1998; Clynne, 1989, 1999; Gamble et al., 1999; Tepley et al., 1999; Zellmer et al., 1999; Tepley et al., 2000; Davidson et al., 2001; Coombs et al., 2002; Izbekov et al., 2002). This is because: 1) Plagioclase is extremely common in rocks from volcanic arcs; 2) Plagioclase crystallizes over a wide range of temperatures and persists as a stable crystallizing phase throughout cooling and eruption; and 3) The compositional and textural zoning patterns develop during primary growth are preserved in plagioclase because the CaAl-NaSi diffusion exchange within the crystal structure is relatively slow (Grove et al., 1984).

This study documents the morphologic, geochemical, and petrologic characteristics of two texturally distinct types of enclaves sampled by flank drilling through virtually all magmas erupted from Mount Unzen for the past 500,000 years during the Unzen Scientific Drilling Project (USDP). This data is presented in concert with textural and high resolution major and trace element analysis of plagioclase crystals

from Unzen enclaves and host lavas. We also present petrologic and geochemical data from an andesite lava flow erupted from Mt. Unzen in 1663 because it is an unusually mafic lava composition not represented in the core stratigraphy. We begin with a brief overview of the geologic setting of Unzen volcano, and then review our sampling and analytical methods. We follow with descriptions of the enclave types and mineral phases. We then propose a model for the mingling of magmas in the Unzen chamber.

1.2 GEOLOGIC SETTING

Unzen volcano is situated in a volcano-tectonic depression known as the Unzen graben (Hoshizumi et al., 1999), located approximately 70 km behind the volcanic front of SW Japan (Fig. 1.1). The volcanic products of Unzen volcano are lava domes, thick lava flows, and pyroclastic deposits that range in composition from andesite to dacite (~57- 67 wt.% SiO_2), with abundant large hornblende and plagioclase phenocrysts, and minor orthopyroxene, clinopyroxene, quartz, biotite, olivine, magnetite, ilmenite, and apatite. Hoshizumi et al. (1999) and Uto et al. (2002) divided the eruptive history of the Unzen volcanic edifice into two main groups based on the age and composition of the erupted material, separated by a ~100,000 year repose period. Older Unzen is thought to be a complex of several different volcanic vents from which many lava domes, lava flows, and pyroclastic flows were erupted. K-Ar ages of Older Unzen deposits range from ~300 to 200 ka, although some deposits may be as old as 500 ka (NEDO, 1988). Younger Unzen yielded K-Ar, ^{14}C, and fission track ages of ~100 ka to present, and is a collection

Figure 1.1
Location map of Unzen volcano on Kyushu Island, Japan. The location of the Unzen Graben (after Hoshizumi et al., 1999), the Japanese volcanic front (shaded), and other nearby active volcanic centers (solid triangles), including Aso and Sakurajima, are also indicated.

of several volcanic edifices, including Nodake, Mayuyama, satellite Mayuyama, and the youngest, Fugendake. Eruptive deposits from younger Unzen are typically domes, lava flows, and block-and-ash pyroclastic deposits.

1.3 MATERIALS AND METHODS

Three groups of samples are used in this study. Group 1 consists of enclaves and coexisting dacite lavas and dacitic block-and-ash flow sequences intersected by the USDP-1 drill hole (752 meters depth, Hoshizumi et al., 2002) (Fig. 1.2). These samples were acquired at the USDP core storage facility, located at the Geological Survey of Japan (GSJ) in Tsukuba City. The core was described, photographed, and archived by the GSJ. Because the USDP core is an invaluable resource for future studies, only small pieces of enclave-bearing dacite lava were sampled by cutting the core into one-quarter, <5 cm longitudinal sections. Group 2 consists of enclaves and coexisting dacitic block-and-ash flow deposits from the 1991-1995 eruption. Samples of the lavas from groups 1 and 2 are referred to as "host" lavas in this study. Group 3 is from an andesite lava flow erupted from Unzen volcano in the year 1663.

The major-element compositions of mineral and glass phases from the host lavas, enclaves and 1663 lava were analyzed using the Cameca SX-50 Electron Microprobe, equipped with four wavelength-dispersive spectrometers and one energy-dispersive spectrometer system, located at the University of Alaska Fairbanks. The precision of measurements on the electron microprobe is a function of x-ray counting statistics, which

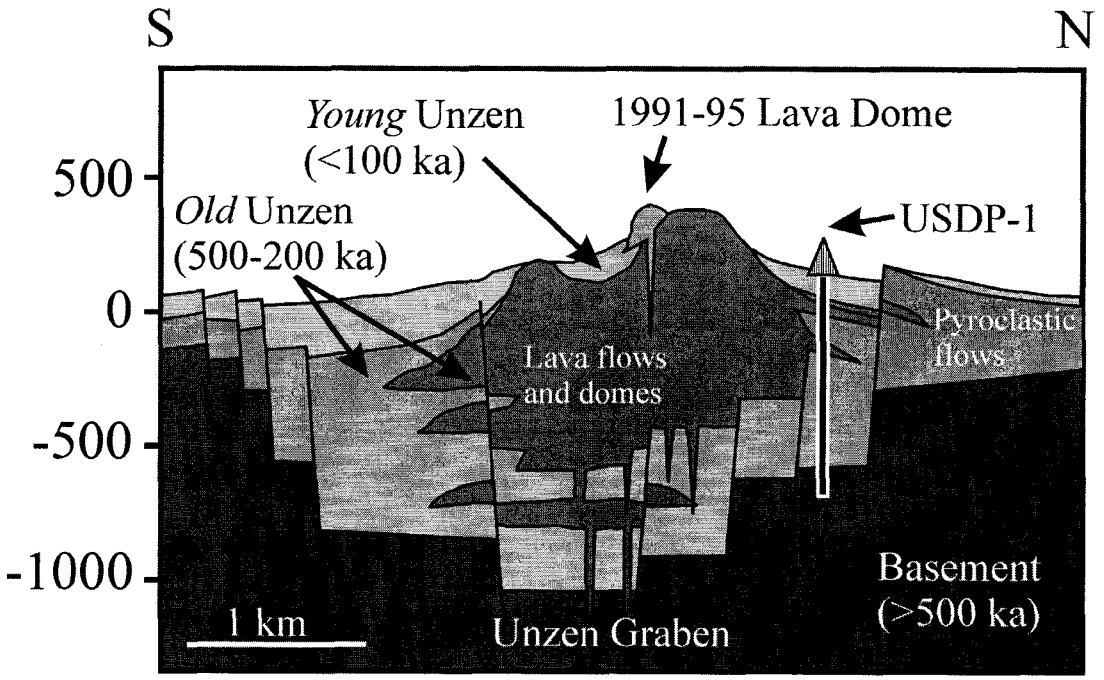

Figure 1.2
Schematic cross-section of Unzen volcano and USDP-1 frank drill path (modified after Hoshizumi et al., 2002)

depend on the total number of x-ray counts collected on both the standard used for calibration, and also on the counts collected on the sample. The minimum precision attainable on the instrument is ~0.5 wt.%, as determined by replicate measurements on Smithsonian standards. For all mineral phases, an accelerating voltage of 15 keV, a beam current of 10 nA, and a 2-3 μm focused electron beam was used. Beam conditions for all glass analysis used an accelerating voltage of 15 keV, a beam current of 10 nA, and a defocused electron beam (8-10 μm diameter) in order to minimize sodium migration. In addition, sodium was counted in two-second intervals for the first 10 seconds of each

analysis, and the counts were regressed to determine the initial sodium content as outlined in Devine et al. (1995).

For whole-rock analysis, samples were first pulverized into fine powder with a ceramic flat plate grinder. Next, for each sample, 3 grams of powdered sample were added to 9 grams of lithium tetraborate (used as a flux), and 0.50 grams of ammonium nitrate (used as an oxidizer). These materials were mixed, fused at 1000 °C while continuously stirred in a platinum crucible in an oxidizing flame for at least 30 minutes, and then poured into disk-shaped platinum molds. These glass disks were then analyzed by XRF and LA-ICP-MS at Michigan State University. X-ray florescence (XRF) data for major-elements were processed using fundamental parameter reduction method (Criss, 1980) using XRFWIN software (Omni Instruments), and USGS and GSJ standards. Analytical precisions of major elements are <0.2 wt.%, <3% for minor elements (www.glg.msu.edu/facilities/jb-1aXRF_ICP-MS-Stats.xls). XRF trace-element analyses were reduced by standard linear regression techniques. Precision for XRF trace elements is better than ± 4% (www.glg.msu.edu/facilities/jb-1aXRF_ICP-MS-Stats.xls). The standards span a wide range of silicate rock compositions, ensuring that unknown samples lie within the range of the standards. For the LA ICP-MS, analytical precisions of major elements are <0.5 wt.%, <5% for minor elements, and ±5%.

We utilize the Sr and Ba concentrations of Unzen plagioclase as a record of different crystallization conditions for two reasons. First, Sr and Ba are the most abundant trace elements found in plagioclase. Second, the partitioning behavior of Sr and Ba is well defined by analytical and experimental work (e.g., Blundy and Wood, 1991;

Bindeman and Bailey, 1999). Sr and Ba contents in multiple spots along microprobe traverses of representative plagioclase phenocrysts were analyzed by using a Micromass Plasma ICP-MS coupled with a Cetac LSX 200+ laser-ablation system at Michigan State University. The 266 nm Nd:YAG laser was focused to a 25 μm sampling spot size and propagated into the sample at a rate of 1 μm/ sec. The data acquisition time was 1 minute, starting before the ablation and continued after ablation had stopped. The first 0.3 minutes of data acquisition were used to measure the background. After ~0.3 minutes of data acquisition, ablation was initiated and continued for 10 seconds. As the ablated material reached the detector, the signal was observed as a well-developed peak. Results were quantified using the height of the peak above background for each element. Concentrations of Sr and Ba were calculated by using peak intensities of ^{88}Sr, ^{138}Ba, and ^{44}Ca calibrated against a NIST 612 glass standard and EMPA determinations of Ca in analyzed spots as outlined in Norman et al. (1996).

1.4 RESULTS

Morphology and Texture of Enclaves

Enclaves are distributed evenly through the host lavas, ranging in size from ~0.25 cm to 30 cm in diameter. Enclaves are not observed in the 1663 andesite lava flow. The most noticeable distinction between enclaves and their hosts is the high crystal content (70-90 vol.%), smaller grain size, and darker color of the enclaves compared to the host (Fig. 1.3). Two types of magmatic enclaves exist in all enclave-bearing samples and are

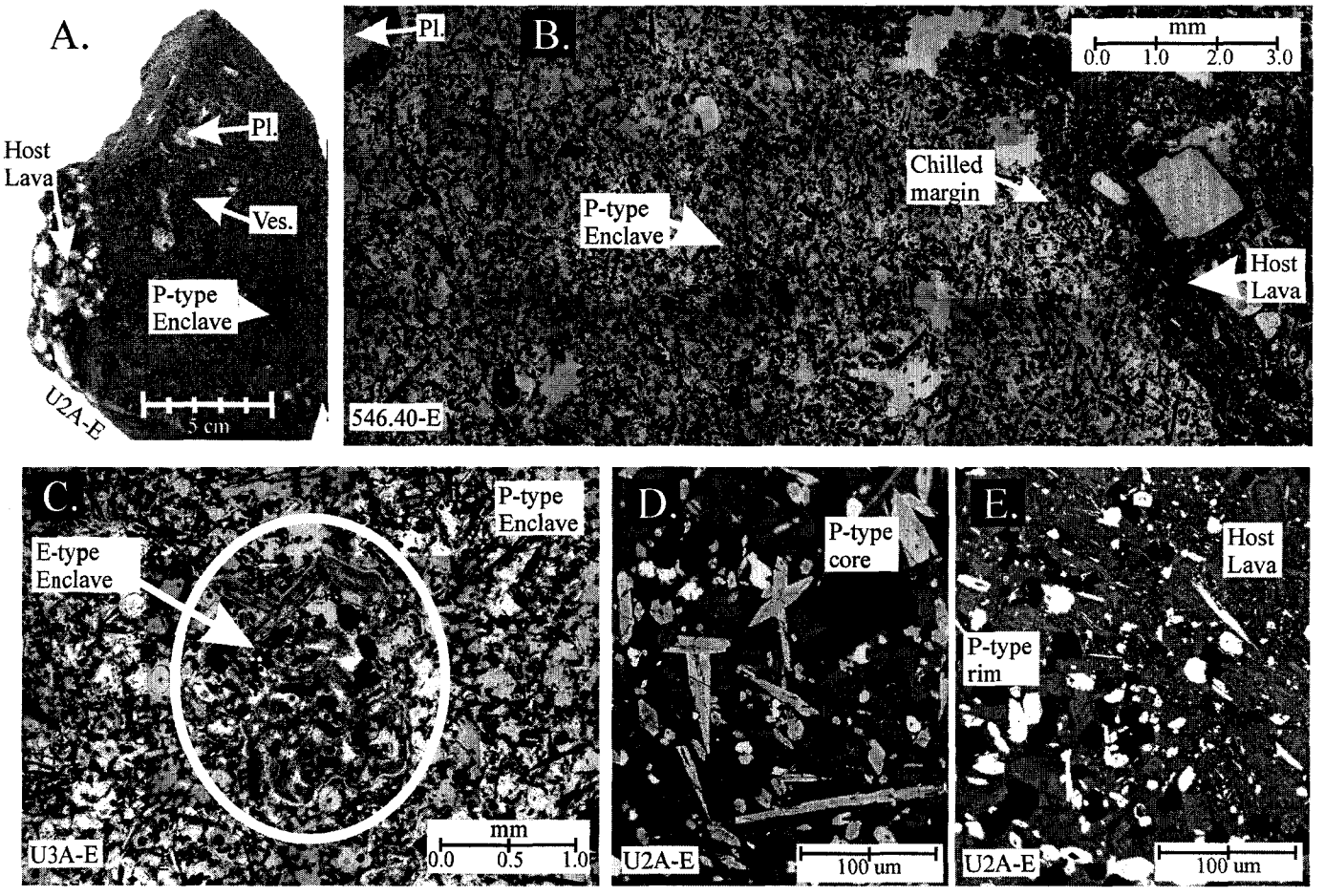

Figure 1.3
Photomicrographs and BSE images showing the texture of Porphyritic enclaves U2A-E, 546.40-E and U3A-E. P-type enclaves are finer-grained than host lava with plagioclase phenocrysts (A, B) and may contain Equigranular enclaves (C). P-type enclaves are texturally characterized as being glass rich with resorbed plagioclase phenocrysts in an acicular matrix. The cores of P-type enclaves are coarser grained and glass-poor (D) compared to enclave margins (E), indicative of chilling.

texturally distinguished, defined as Porphyritic (P-type in figures) and Equigranular (E-type in figures). Porphyritic enclaves are spherical in shape with well-developed crenulated, glassy margins, account for ~1 volume % (visual estimate), and range in size from 5 to 30 cm in diameter. Porphyritic enclaves contain abundant large plagioclase phenocrysts (Fig. 1.4) set in a groundmass of fine-grained, acicular microphenocrysts of mostly plagioclase and hornblende crystals and interstitial glass. Microphenocrysts decrease in size with approach to the contact with the host lava, indicative of a chilled margin. Porphyritic enclaves also contain hornblende phenocrysts with rounded, reacted margins surrounded by clean rims, minor amounts of clinopyroxene, and trace amounts of olivine (Table 1.1).

Porphyritic enclaves contain a bimodal population of vesicles (Fig. 1.5). Large, spherical vesicles (500- 1000 μm) occur most frequently in the center of enclaves, whereas smaller vesicles (50 to 100 μm) occur throughout the enclaves. Some of the larger vesicles appear to be partially coalesced smaller vesicles. A densely packed rim of plagioclase and hornblende microlites may surround large vesicles. Smaller vesicles are widespread, irregularly shaped, and exist in gaps between crystals.

Equigranular enclaves are smaller than Porphyritic enclaves with an average size of ~2 cm and a range of 0.1- 8 cm (Fig. 1.6), and may exist within Porphyritic enclaves but never the reverse. Equigranular enclaves are evenly distributed throughout lavas and are more abundant than Porphyritic enclaves, accounting for between 3 and 5 vol.% based on point counting. Equigranular enclaves become increasingly elliptical with increased size, with enclaves larger than 2 cm being characterized by length to width

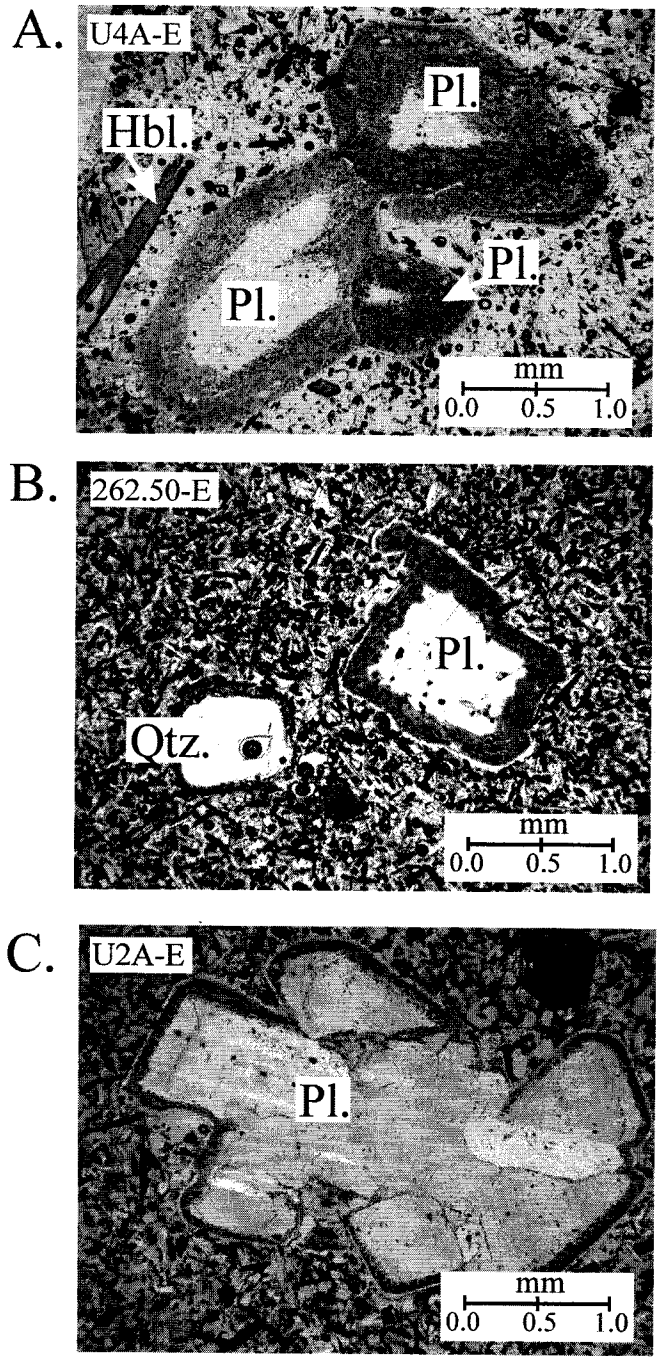

Figure 1.4
Photomicrographs of resorbed plagioclase phenocrysts in Porphyritic enclaves U4A-E, 262.50-E, and U2A-E

Table 1.1 Occurrence of phases in host lava, enclaves, and 1663 lava

	Host Dacite Lava	Porphyritic Enclave	Equigranular Enclave	1663 Lava
Glass	M	M	m	M
Plagioclase				
Oscillatory Zoned	M	m	A	M
Phenocryst	m	m	A	m
Sieved Core Phenocryst	m	M	A	m
Resorbed Rim Phenocrysts	A	M	M	M
Reversely Zoned Microphenocryst	A	M	M	A
Hornblende				
Phenocryst	m	m	A	A
Resorbed Phenocryst	m	m	A	A
Microphenocryst	A	M	m	A
Orthoyroxene	m	tr.	m	m
Clinopyroxene				
Phenocryst	tr.	m	A	m
Phenocryst with reaction rim	tr.	tr.	A	A
Olivine	tr.	tr.	A	tr.
Quartz				
Phenocryst	A	A	A	A
Resorbed phenocryst	tr.	tr.	A	tr.
Oxides	m	m	m	m
Vesicles				
Small (<150 μm)	m	m	m	tr.
Large (>250 μm)	tr.	m	A	A

Notes: M > 20%, 20% > m > 1%, tr. <1%; A = absent

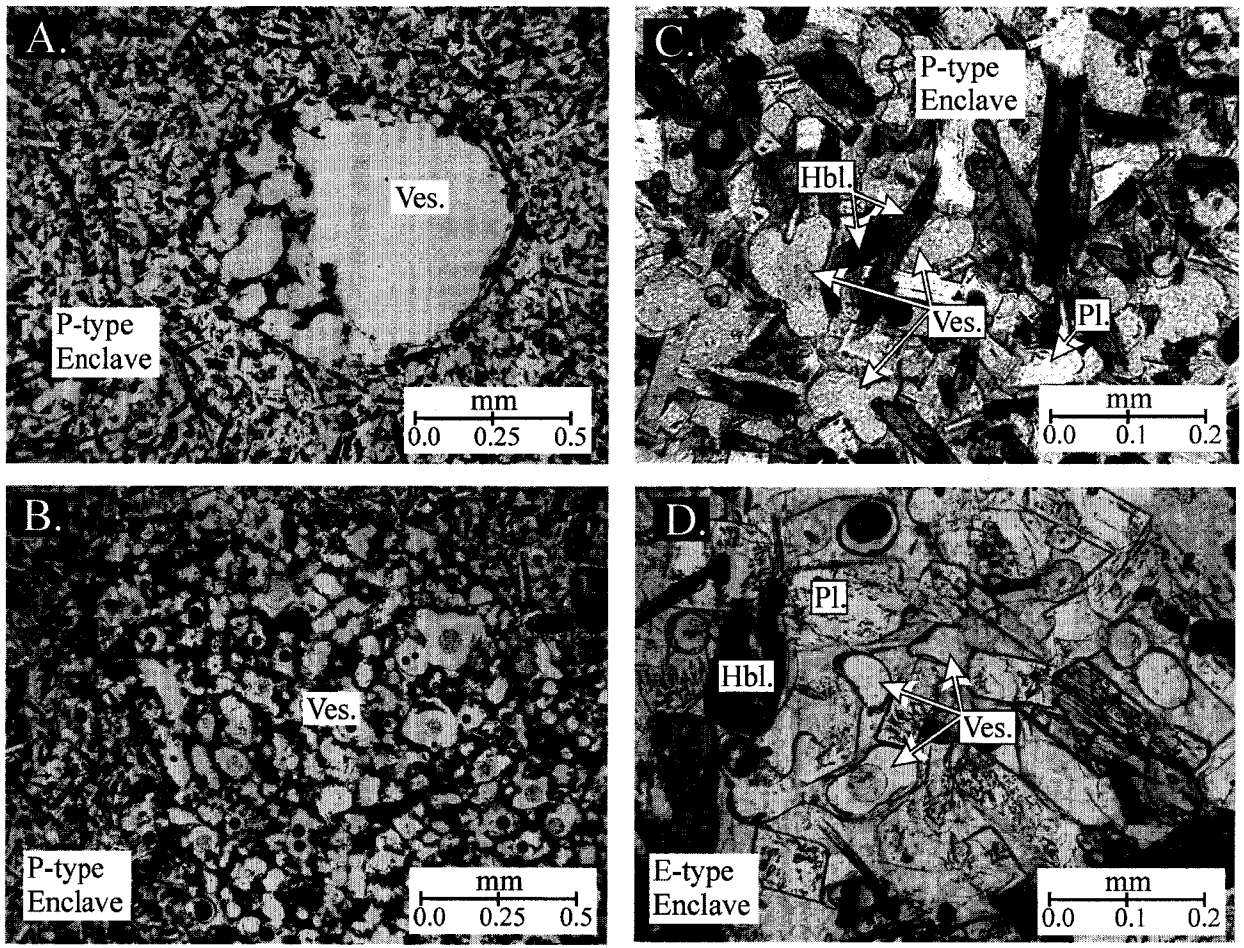

Figure 1.5
Photomicrographs of vesicles in Porphyritic and Equigranular enclaves. Porphyritic enclaves (A, B) contain large, spherical vesicles (500- 1000 mm) that occur most frequently in the center of enclaves and appear to be the result of smaller vesicles coalescing together. Both Porphyritic and Equigranular (C, D) enclave types contain abundant smaller vesicles ranging in diameter from 50 to 100 mm that occur throughout the enclaves.

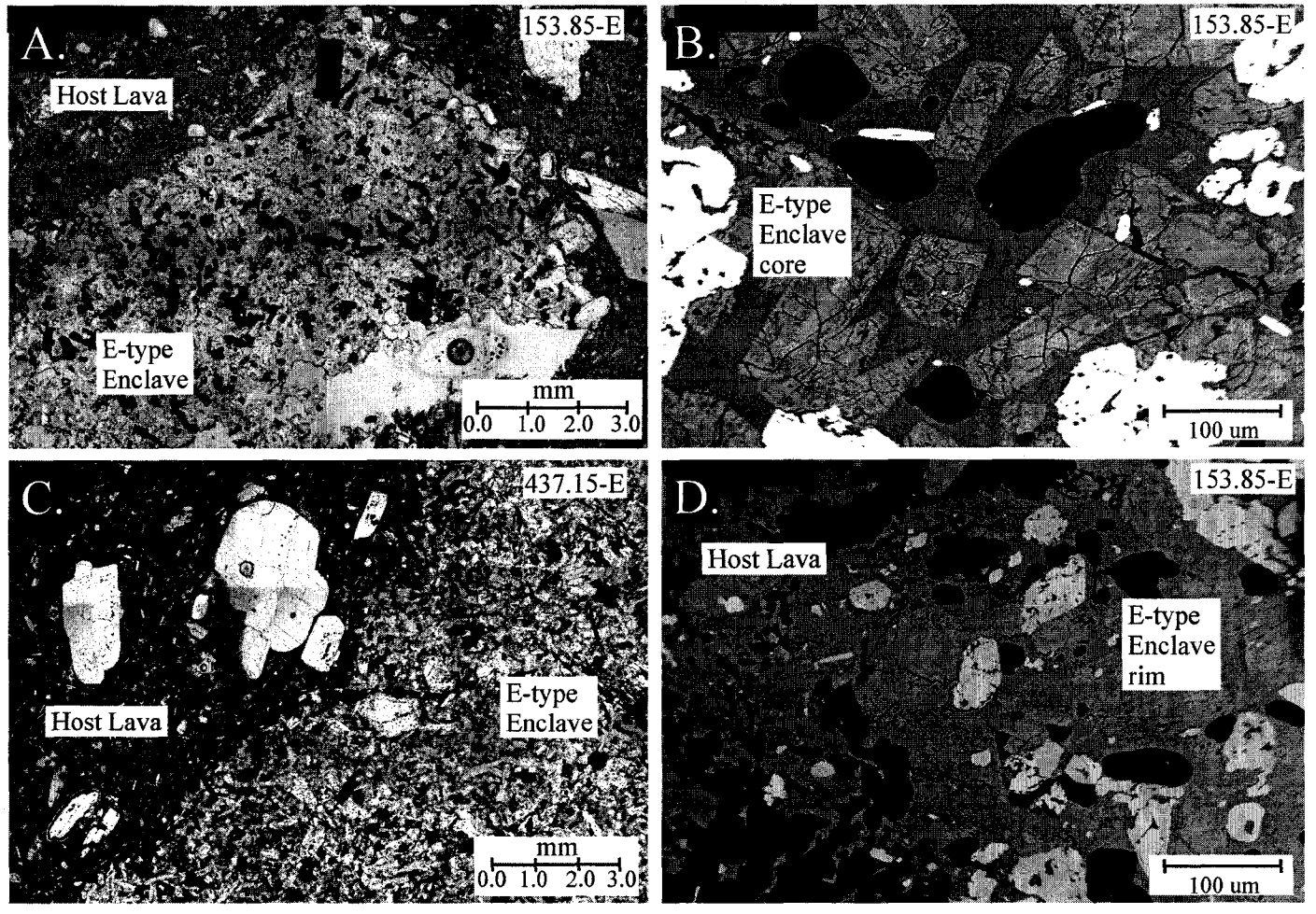

Figure 1.6
Photomicrographs and BSE images showing the texture of Equigranular enclave. E-type enclaves are glass poor, coarser grained than P-type enclaves (100-500 m), and non-porphyritic in a matrix glass of the same composition as the host. E-type microphenocrysts are tabular in the core (B) and rim (D), which are not crenulated or chilled like P-type enclaves, but rather are characterized by the protruding edges of microphenocrysts. Sample numbers are indicated.

aspect ratios from approximately 1.5 to 3. Equigranular enclaves are coarser grained (100-500 μm) than Porphyritic enclaves and are composed of tabular and equant microphenocrysts of ~60- 65 vol.% plagioclase, with less hornblende and orthopyroxene, trace amounts of clinopyroxene, and no olivine. Equigranular microphenocrysts do not decrease in size with approach to the margin, nor are margins crenulated or chilled like Porphyritic enclaves, but rather are defined by the protruding edges of microphenocrysts. Equigranular enclaves contain one population of 50- 100 μm sized subrounded vesicles, and <10 vol.% glass (Fig. 1.6). No change in vesicle size or abundance appears to exist towards the center of these enclaves.

A few enclaves exhibit textures that appear intermediate to the Porphyritic and Equigranular endmembers (Fig. 1.7). Intermediate enclaves contain a mineral assemblage of elongate shaped plagioclase, hornblende, orthopyroxene, and Fe-Ti oxides. Intermediate enclaves also display porphyritic texture by containing phenocrystic plagioclase and hornblende with embayed or dissolved reaction rims, as in Porphyritic enclaves. Like Equigranular enclaves, however, Intermediate enclaves are typically small in size (< 2 cm). Intermediate enclaves are rare compared to either enclave end member, occurring in only trace amounts in the host lava.

Whole Rock Geochemistry

Unzen host lava (i.e. the lavas containing enclaves) samples are calc-alkaline dacites and silicic andesites (Fig. 1.8, Table 1.2) (Gill, 1981; Miyashiro, 1974). Whole-rock host compositions range narrowly from 61.8 to 64.7 wt.% SiO_2, from 2.3 to 3.0 wt.% MgO,

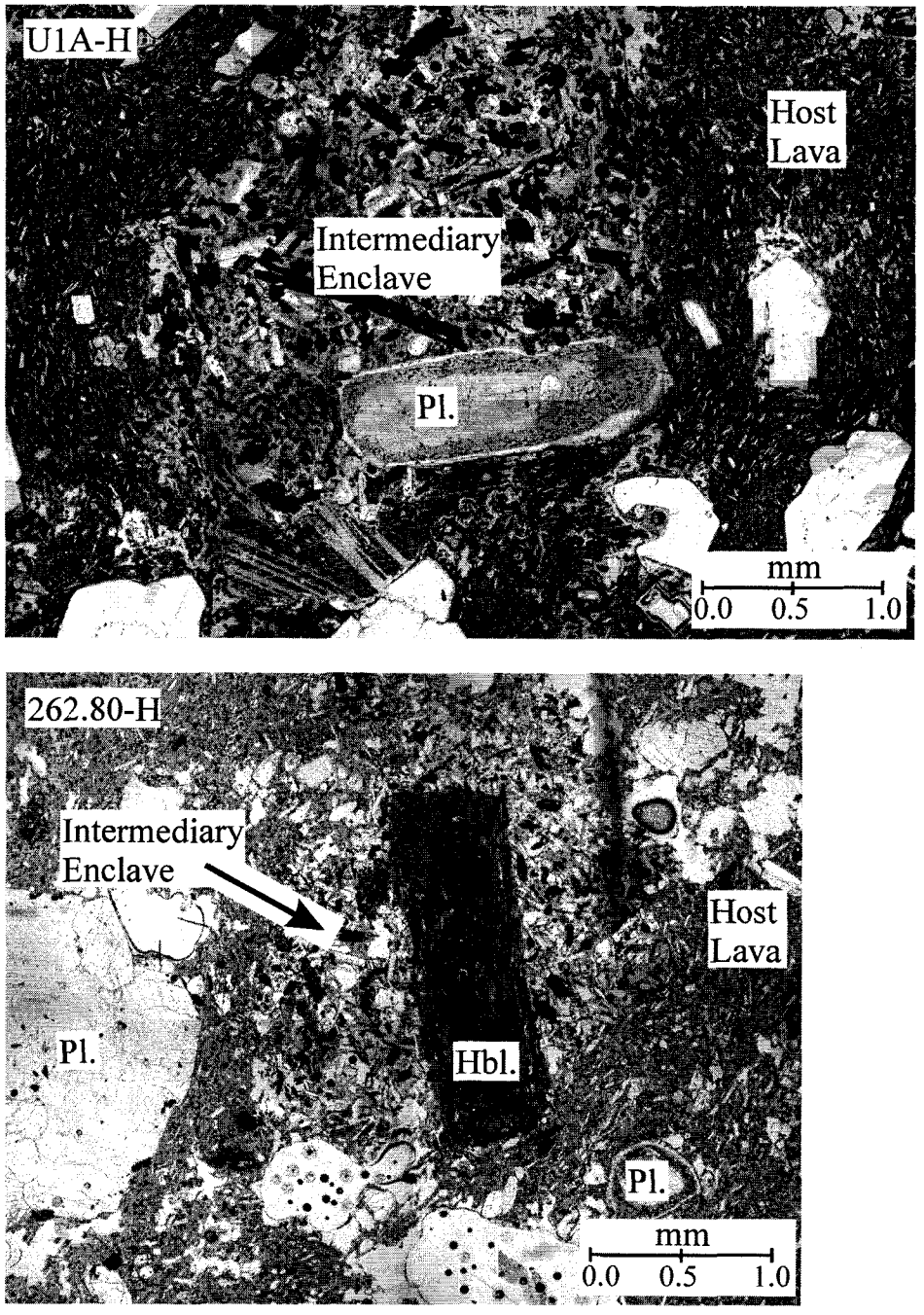

Figure 1.7
Photomicrographs showing the texture of enclaves with intermediate texture compared to P-type and E-type enclaves (samples U1A-H and 262.80-H). Intermediate enclaves are porphyritic, containing plagioclase and hornblende phenocrysts with embayed or dissolved reaction rims, as in P-type enclaves, but occur in only trace amounts in the host lava.

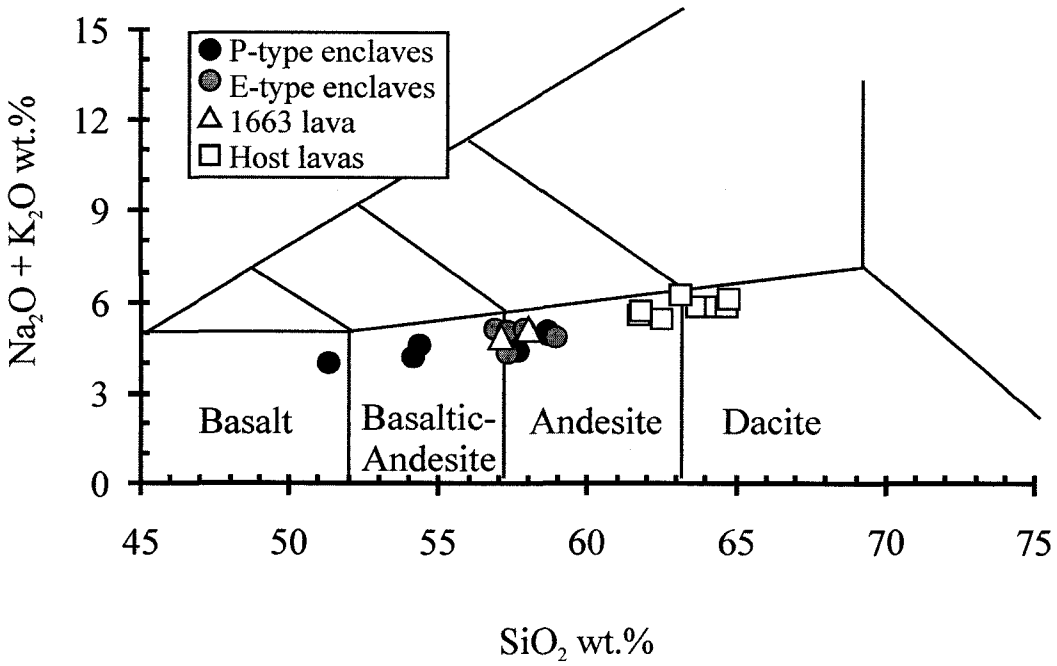

Figure 1.8
IUGS chemical classification scheme for Unzen samples. Samples include host lava (open squares), Porphyritic enclaves (solid circles), Equigranular enclaves (gray circles) and 1663 lava (open triangles). Note that E-type enclaves are narrowly distributed in composition with respect to silica and overlie the most silicic P-type enclave composition. E-type enclaves are also equivalent to the 1663 lava in bulk composition. Rock-type boundaries from Le Bas et al. (1986).

Table 1.2
Whole-rock compositions of host lava samples

Sample	U1A-H	103.80- H	153.85-H	198.90-H	262.80-H	390.00-H	437.15-H	546.45-H	602.80-H
Depth (m)	0.00	103.80	153.85	198.90	262.80	390.00	437.15	546.45	602.80
SiO_2 (wt.%)	63.95	61.75	63.69	64.30	61.78	64.69	62.50	63.12	64.72
TiO_2	0.67	0.73	0.69	0.70	0.78	0.71	0.78	0.70	0.79
Al_2O_3	16.15	17.04	15.68	15.96	16.49	15.65	16.30	15.84	15.58
Fe_2O_3 *	4.98	5.44	5.10	4.78	5.58	5.24	6.04	5.01	5.31
MnO	0.10	0.11	0.10	0.10	0.11	0.11	0.12	0.10	0.09
MgO	2.65	2.67	2.62	2.37	2.99	2.29	2.71	2.43	2.29
CaO	5.23	5.83	5.22	4.98	5.71	4.89	5.68	4.61	4.59
Na_2O	3.57	3.39	3.26	3.49	3.38	3.22	3.19	3.74	3.48
K_2O	2.24	2.16	2.57	2.38	2.31	2.59	2.26	2.49	2.61
P_2O_5	0.16	0.16	0.16	0.16	0.19	0.17	0.17	0.17	0.21
Total	99.70	99.28	99.09	99.22	99.32	99.56	99.75	97.91	99.67
Ni (ppm)	28.7	22.6	24.9	24.9	26.4	17.2	13.6	69.4	36.5
Cu	26.9	26.8	24.0	28.0	15.1	16.2	9.9	25.7	20.6
Zn	53.7	55.3	49.0	51.5	54.8	54.0	62.3	54.9	49.5
Rb	74.5	62.6	81.8	77.0	70.2	80.5	67.8	86.9	85.1
Zr	147.6	159.2	162.5	164.9	175.7	173.0	146.8	163.6	181.8
Sr	332.7	408.1	355.6	371.9	376.3	364.0	430.5	370.7	346.2
Y	14.85	17.42	15.18	16.16	19.72	16.52	18.98	15.67	17.65
Nb	19.09	18.00	25.42	26.56	24.80	22.22	16.66	25.86	32.25
Ba	458.91	474.38	515.05	529.71	485.32	534.94	449.53	571.19	530.53
La	22.03	22.70	22.95	23.55	26.10	23.67	22.01	24.56	26.37
Ce	44.30	41.05	45.69	47.79	46.79	46.27	38.91	49.02	50.99
Pr	4.62	4.70	4.90	5.27	5.68	5.36	4.86	5.33	5.99
Nd	16.01	17.08	17.20	18.69	20.98	18.68	18.79	18.47	21.15
Sm	3.09	3.45	3.28	3.67	4.13	3.56	3.84	3.47	4.10
Eu	1.02	1.10	1.00	1.07	1.18	1.07	1.14	1.07	1.10
Gd	2.60	2.80	2.72	2.87	3.39	2.93	3.22	2.80	3.27
Tb	0.41	0.46	0.41	0.45	0.55	0.46	0.52	0.43	0.52
Dy	2.29	2.71	2.36	2.52	3.12	2.66	2.96	2.49	2.95
Ho	0.46	0.55	0.46	0.49	0.62	0.53	0.58	0.49	0.58
Er	1.31	1.60	1.37	1.45	1.72	1.53	1.72	1.37	1.66
Yb	1.23	1.60	1.26	1.31	1.75	1.49	1.72	1.24	1.57
Lu	0.20	0.24	0.21	0.22	0.27	0.24	0.28	0.22	0.25
Hf	2.46	2.95	2.69	2.76	3.39	3.21	3.08	2.81	3.40
Ta	2.87	3.87	6.79	7.77	7.74	6.20	4.26	5.61	10.87
Pb	13.48	10.37	14.72	14.82	9.70	12.93	9.38	16.36	13.23
Th	7.18	7.27	7.19	7.11	7.45	8.17	7.35	8.12	8.68
U	2.66	1.84	2.67	2.62	1.83	2.44	1.81	2.97	2.60
Cr	45.20	47.20	57.80	45.80	45.40	32.70	35.40	63.20	21.00

All whole-rock analyses reflect normalization to 100 wt.% to factor out hydration of glassy groundmass.
Major oxides, and Ni-Sr by XRF, rest by LA ICP-MS. 1991- 1995 eruption sample group, U1A-H; Unzen Scientific Drilling Project USDP-1 Drill Core, 103.80-H, 153.85-H, 198.90-H, 262.80-H, 390.00-H, 437.15-H, 602.80-H
Fe_2O_3 * = all Fe calculated as Fe_2O_3

and from 2.2 to 2.6 wt.% K_2O (Fig. 1.9). Whole-rock host lava Fe, Ca, Mg, Al, Mn, Sr, and Y concentrations generally decrease with increasing silica, whereas concentrations of K, Rb, Ba, and Zr are positively correlated with whole-rock silica abundance (Fig. 1.10). Little variation is observed in Na, P, or Nd over the entire range of silica. Host lavas are medium-K in composition (Fig. 1.9).

Porphyritic enclaves range broadly from calc-alkaline basalt through basaltic andesite to andesite (Fig. 1.8, Table 1.3), with 51.3 to 58.7 wt.% SiO_2, 4.6 to 3.8 wt.% MgO, and 1.2 to 1.8 wt.% K_2O. Although whole-rock Fe, Ca, Mg, Mn, Al, Sr, and Y concentrations generally decrease with increasing silica and show broad correlation with host samples (Fig. 1.9 and 1.10), only a few elements (e.g. Ca and Y) form tight arrays collinear with host dacites, others show considerable scatter. Equigranular enclaves narrowly range in composition from basaltic-andesite to andesite with respect to Figure 1.8 (Fig. 1.9 and 1.10, Table 1.4). Their evident scatter likely results from their small size (~2 cm average diameter) and coarse-grained texture. Equigranular enclaves overlap in composition with the most silicic Porphyritic enclaves.

The sample of the 1663 enclave-absent lava flow is medium-K calc-alkaline and plots on the boundary between basaltic-andesite and andesite (Fig. 1.8 and 1.9). The 1663 lava contains 57.1 wt.% SiO_2, 4.5 wt.% MgO, and 1.7 wt.% K_2O, which is consistent with previous analyses performed by Nakada et al. (1999) (Table 1.5). The 1663 whole-rock compositions overlap the most silicic Porphyritic enclaves and Equigranular enclave in composition. 1663 lava has comparable concentrations of Sr, and Zr as host lavas, but lower Rb and Ba, and higher Y concentrations than the host lavas (Fig. 1.10, Table 1.5).

Concentrations of Rb and Y broadly plot on-trend between enclaves and host lava analyses on SiO_2 variation diagrams, whereas Sr does not.

Phenocryst and Glass Compositions

Lavas analyzed in this study are generally similar to those described previously by Hoshizumi et al. (1999) and Nakada and Motomura (1999). Host lava samples are crystal-rich, averaging between 30 and 40% crystals by volume, with large plagioclase and hornblende as the dominant phenocrystic phases. Other minerals such as clinopyroxene, orthopyroxene, quartz, magnetite, ilmenite, olivine (± opx rims), biotite, and apatite may also be present in varying amounts. In addition to individual phenocryst phases, glomeroporphyritic aggregates of calcic plagioclase, orthopyroxene, clinopyroxene, and Fe-Ti oxide crystals are observed throughout the lavas.

The 1663 lava contains between 20- 25 vol.% crystals of plagioclase (15-20 vol.%), clinopyroxene (3- 4 vol.%), and orthopyroxene (1- 2 vol.%). The remaining crystal phases are composed of magnetite, ilmenite, quartz and pseudomorphs of hornblende. Quartz and hornblende are considered to be unstable as indicated by reaction rims of clinopyroxene and plagioclase that always enclose quartz, and hornblendes are almost completely replaced with Fe-Ti oxides, plagioclase, and clinopyroxene.
Both types of enclaves are dominated by euhedral plagioclase and hornblende, with lesser amounts of orthopyroxene, magnetite, ilmenite, and glass. In addition, Porphyritic enclaves contain clinopyroxene, olivine, quartz (always reacted), and biotite (always reacted) exclusively, whereas Equigranular enclaves contain trace amounts of apatite.

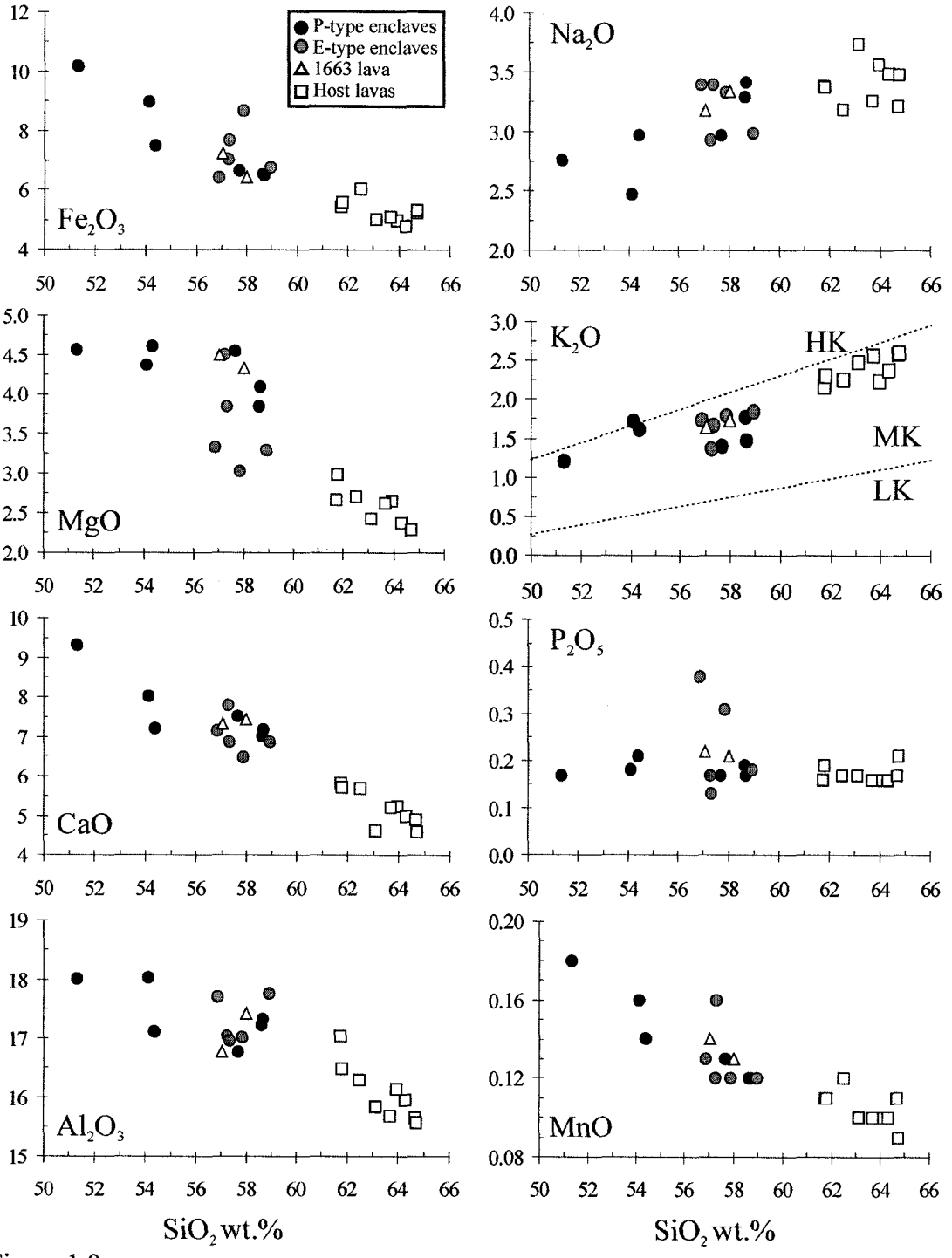

Figure 1.9
Major-oxide-SiO_2 variation diagrams for Unzen samples, including host lava, Porphyritic enclaves, Equigranular enclaves, and 1663 lava. High-K, Medium-K, and Low-K trends from Le Maitre et al. (1989).

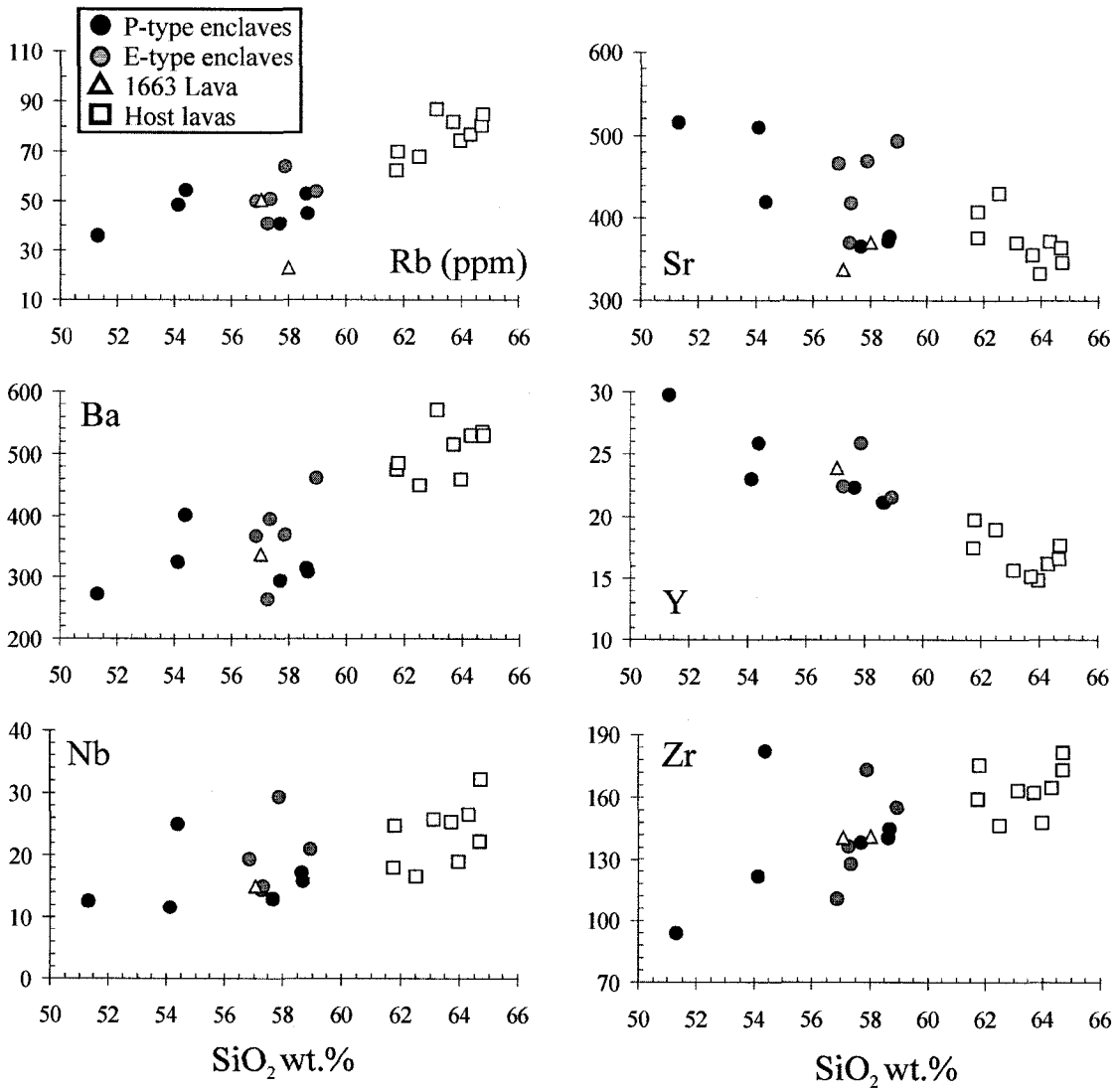

Figure 1.10
Trace-element-SiO_2 variation diagrams for Unzen samples, including host lava, Porphyritic enclaves, Equigranular enclaves, and 1663 lava.

Table 1.3
Whole-rock compositions of Porphyritic enclaves.

Sample	U2A-E	U3A-E	U4A-E	262.50-E	435.20-E	546.40-E
Depth (m)	0.00	0.00	0.00	262.50	435.20	546.40
SiO_2 (wt.%)	58.67	57.68	58.63	54.37	54.11	51.32
TiO_2	0.87	0.86	0.88	0.96	0.96	1.27
Al_2O_3	17.33	16.78	17.22	17.11	18.03	18.01
Fe_2O_3	6.51	6.65	6.55	7.48	8.97	10.17
MnO	0.12	0.13	0.12	0.14	0.16	0.18
MgO	4.10	4.56	3.85	4.61	4.37	4.57
CaO	7.18	7.53	7.02	7.22	8.03	9.33
Na_2O	3.42	2.97	3.29	2.97	2.47	2.76
K_2O	1.47	1.41	1.78	1.62	1.73	1.21
P_2O_5	0.17	0.17	0.19	0.21	0.18	0.17
Total	99.84	98.74	99.53	96.69	99.01	98.99
Ni (ppm)	40.2	47.3	40.0	171.8	16.2	15.7
Cu	42.6	51.7	54.7	40.6	3.8	20.5
Zn	61.5	56.2	60.0	61.5	77.0	69.1
Rb	44.9	41.2	53.0	54.5	48.3	36.0
Zr	144.6	137.9	140.5	182.1	122.0	94.1
Sr	378.4	366.2	372.5	420.3	510.6	515.9
Y	21.16	22.37	21.17	25.96	23.04	29.84
Nb	15.74	13.06	17.12	25.02	11.59	12.53
Ba	308.82	294.20	315.57	401.27	324.35	272.88
La	18.91	19.24	19.66	27.51	16.31	12.64
Ce	34.25	35.41	34.95	47.20	30.48	23.17
Pr	4.36	4.60	4.42	6.10	4.44	3.61
Nd	17.37	18.52	17.61	23.95	19.13	25.20
Sm	3.76	4.15	3.89	4.99	4.37	4.39
Eu	1.11	1.19	1.12	1.36	1.32	1.35
Gd	3.35	3.64	3.48	4.34	3.81	4.36
Tb	0.55	0.59	0.57	0.70	0.62	0.75
Dy	3.21	3.54	3.27	4.15	3.67	4.79
Ho	0.66	0.72	0.66	0.83	0.74	0.98
Er	1.92	2.07	1.91	2.35	2.10	2.80
Yb	1.94	2.05	1.95	2.28	2.10	2.67
Lu	0.29	0.32	0.30	0.35	0.33	0.41
Hf	2.95	3.01	2.90	3.84	2.73	2.38
Ta	4.40	2.37	5.77	7.93	4.28	5.81
Pb	6.57	6.87	7.22	7.03	8.43	3.49
Th	4.96	4.95	5.22	6.47	3.39	2.84
U	1.18	1.11	1.20	1.20	0.72	0.55
Cr	65.20	72.20	45.10	63.50	33.00	37.80

All enclave whole-rock analyses reflect normalization to 100 wt.% to factor out hydration of glassy groundmass. Major oxides, and Ni-Sr by XRF, rest by LA ICP-MS. 1991- 1995 eruption sample group, U2A-E, U3A-E, U4A-E; Unzen ScientificDrilling Project USDP-1 Drill Core, 262.50-E, 546.40-E, 435.20-E. Fe_2O_3 * = all Fe calculated as Fe_2O_3

Table 1.4
Whole-rock compositions of Equigranular enclaves

Sample	U5A-E	153.85-E	199.10-E	390.00-E	602.80-E
Depth (m)	0.0	153.9	199.1	390.0	602.8
SiO_2 (wt.%)	57.26	56.87	57.33	58.94	57.87
TiO_2	0.90	1.01	1.02	0.91	1.35
Al_2O_3	17.04	17.71	16.97	17.76	17.02
$Fe_2O_3^*$	7.02	6.44	7.66	6.77	8.65
MnO	0.12	0.13	0.16	0.12	0.12
MgO	4.52	3.33	3.85	3.29	3.03
CaO	7.79	7.16	6.88	6.86	6.48
Na_2O	2.93	3.40	3.40	2.99	3.33
K_2O	1.37	1.74	1.67	1.85	1.80
P_2O_5	0.17	0.38	0.13	0.18	0.31
Total	99.12	98.17	99.07	99.67	99.96
Ni (ppm)	46.7	34.1	29.6	19.2	32.2
Cu	33.4	127.4	91.9	17.4	19.9
Zn	58.6	63.4	75.9	60.3	73.4
Rb	41.2	50.1	50.9	54.2	63.9
Zr	136.3	110.8	127.6	154.8	173.2
Sr	370.7	467.0	418.3	492.9	470.1
Y	22.44	33.28	30.11	21.53	25.88
Nb	14.43	19.34	15.06	20.92	29.45
Ba	265.05	366.93	395.62	460.65	368.08
La	17.92	33.30	24.07	23.55	26.62
Ce	31.93	65.08	47.23	41.89	46.62
Pr	4.34	8.00	6.04	5.60	6.32
Nd	17.72	32.12	24.46	22.43	25.37
Sm	3.94	6.79	5.31	4.90	5.38
Eu	1.14	1.57	1.44	1.43	1.33
Gd	3.56	6.20	4.98	3.99	4.49
Tb	0.58	0.96	0.81	0.62	0.73
Dy	3.50	5.90	5.18	3.41	4.50
Ho	0.71	1.13	0.99	0.67	0.90
Er	2.11	3.52	3.10	1.92	2.50
Yb	2.13	3.32	3.11	1.88	2.42
Lu	0.32	0.50	0.49	0.29	0.36
Hf	2.99	3.28	4.10	3.34	3.71
Ta	4.69	1.52	1.27	10.60	9.87
Pb	5.90	8.94	8.04	7.41	7.23
Th	4.61	8.47	7.97	6.13	6.83
U	0.98	1.27	1.12	1.23	1.46
Cr	64.80	75.80	44.30	38.50	0.10

All enclave whole-rock analyses reflect normalization to 100 wt.% to factor out hydration of glassy groundmass. Major oxides, and Ni-Sr by XRF, rest by LA ICP-MS. 1991- 1995 eruption sample group, U5A-E; Unzen Scientific Drilling Project USDP-1 Drill Core sample group, 153.85-E, 199.10-E, 390.00-E, 602.80-E

$Fe_2O_3^*$ = all Fe calculated as Fe_2O_3

Table 1.5
Whole-rock compositions of 1663 lava

Sample	UZN-1663	Nakada et al. (1999)
Depth (m)	NA	NA
SiO_2 (wt.%)	57.05	58.01
TiO_2	1.01	0.94
Al_2O_3	16.77	17.42
$Fe_2O_3^*$	7.22	6.41
MnO	0.14	0.13
MgO	4.50	4.34
CaO	7.33	7.45
Na_2O	3.18	3.34
K_2O	1.65	1.74
P_2O_5	0.22	0.21
Total	99.07	99.99
Ni (ppm)	-	-
Cu	-	-
Zn	-	-
Rb	50.6	23.0
Zr	140.8	137.0
Sr	337.9	371.0
Y	23.92	-
Nb	14.77	-
Ba	336.55	-
La	18.55	-
Ce	36.73	-
Pr	4.43	-
Nd	17.57	-
Sm	3.65	-
Eu	1.15	-
Gd	3.82	-
Tb	0.64	-
Dy	3.45	-
Ho	0.81	-
Er	2.30	-
Yb	2.13	-
Lu	0.34	-
Hf	3.07	-
Ta	0.91	-
Pb	5.95	-
Th	5.95	-
U	0.91	-
Cr	57.88	-

All 1663 lava whole-rock analyses reflect normalization to 100 wt.% to factor out hydration of glassy groundmass. Major oxides, and Ni-Sr by XRF, rest by LA ICP-MS. 1663 Lava sample from Setsuya Nakada, UZN-1663. $Fe_2O_3^*$ = all Fe calculated as Fe_2O_3

Glass

Glass comprises 60- 70 vol.% of the host lava samples and the 1663 lava sample. Glass accounts for 15- 20 vol.% in Porphyritic enclaves (>20 vol.% at the enclave edge), and ~10 vol.% in Equigranular enclaves. Porphyritic enclave glasses overlap with 1663 lava glass with respect to Na_2O, K_2O, and CaO, but not Fe_2O_3, Al_2O_3, or TiO_2 (Fig. 1.11). Equigranular glass compositions have an identical range compared to host lava glasses (Fig. 1.11, Table 1.6). In addition, enclave glasses are clear whereas host lava matrix glasses are charged with microlites.

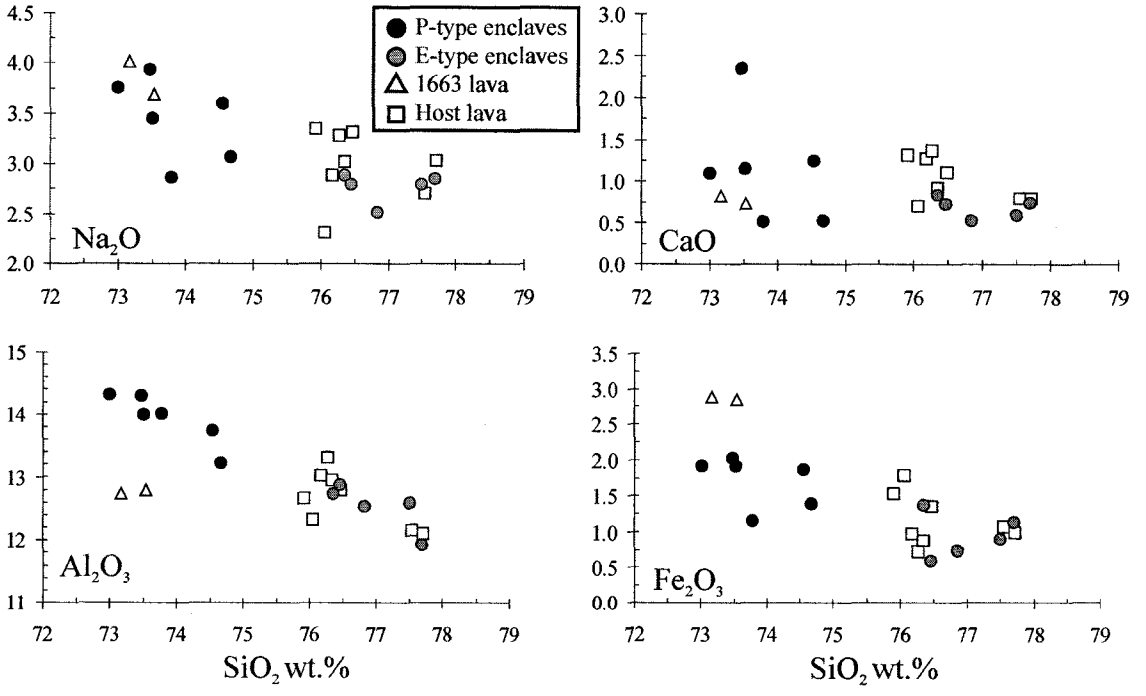

Figure 1.11
Major-oxide-SiO_2 variation diagrams in matrix glass for Unzen samples, including host lava (open squares), Porphyritic enclaves (solid circles), Equigranular enclaves (gray circles) and 1663 lava (open triangles).

Table 1.6
Electron microprobe (Oxides in wt.%) analyses of glass

Sample	*n*	SiO_2	Al_2O_3	TiO_2	Fe_2O_3	MgO	CaO	Na_2O	K_2O	Cl	Total
153.85-H (host lava)	*10*	73.67	12.29	0.16	1.33	0.17	0.81	2.79	5.17	0.10	96.49
Nonhydrous		76.35	12.74	0.17	1.38	0.18	0.84	2.89	5.36	0.10	100.00
199.10-H (host lava)	*10*	73.67	11.93	0.35	1.73	0.45	0.68	2.31	5.72	0.03	96.87
Nonhydrous		76.05	12.32	0.36	1.79	0.46	0.70	2.38	5.90	0.03	100.00
390.00-H (host lava)	*10*	74.66	11.47	0.21	1.09	0.12	0.72	2.74	4.98	0.10	96.09
Nonhydrous		77.70	11.94	0.22	1.13	0.12	0.75	2.85	5.18	0.10	100.00
435.20-H (host lava)	*10*	74.35	12.71	0.25	0.96	0.11	1.24	2.82	5.09	0.07	97.60
Nonhydrous		76.18	13.02	0.26	0.98	0.11	1.27	2.89	5.22	0.07	100.00
546.45-H (host lava)	*10*	74.71	12.68	0.16	0.86	0.18	0.90	2.96	5.37	0.04	97.86
Nonhydrous		76.34	12.96	0.16	0.88	0.18	0.92	3.02	5.49	0.04	100.00
602.80-H (host lava)	*10*	75.62	13.19	0.22	0.73	0.07	1.36	3.26	4.69	0.02	99.16
Nonhydrous		76.26	13.30	0.22	0.74	0.07	1.37	3.29	4.73	0.02	100.00
U5A-H (host lava)	*10*	76.52	12.81	0.38	1.36	0.16	1.12	3.32	4.36	0.05	100.08
Nonhydrous		76.46	12.80	0.38	1.36	0.16	1.12	3.32	4.36	0.05	100.00
262.5-E (P-type)	*10*	71.13	13.55	0.59	1.85	0.16	1.12	4.97	3.34	0.06	96.76
Nonhydrous		73.51	14.00	0.61	1.91	0.17	1.16	5.14	3.45	0.06	100.00
435.20-E (P-type)	*10*	71.38	13.56	0.31	1.11	0.07	0.49	6.91	2.78	0.05	96.74
Nonhydrous		73.79	14.02	0.32	1.15	0.07	0.51	7.14	2.87	0.05	100.00
546.25-E (P-type)	*10*	73.68	12.03	0.16	0.71	0.09	0.51	6.27	2.41	0.03	95.89
Nonhydrous		76.84	12.55	0.17	0.74	0.09	0.53	6.54	2.51	0.03	100.00
U1A-E (P-type)	*10*	72.62	14.24	0.35	1.91	0.13	1.09	5.31	3.74	0.09	99.48
Nonhydrous		73.00	14.31	0.35	1.92	0.13	1.10	5.34	3.76	0.09	100.00
U2A-E (P-type)	*10*	74.09	13.13	0.55	1.38	0.08	0.53	6.37	3.05	0.05	99.23
Nonhydrous		74.66	13.23	0.55	1.39	0.08	0.53	6.42	3.07	0.05	100.00
U4A-E (P-type)	*10*	73.55	13.56	0.32	1.84	0.24	1.23	4.31	3.55	0.07	98.67
Nonhydrous		74.54	13.74	0.32	1.86	0.24	1.25	4.37	3.60	0.07	100.00
153.85-E (E-type)	*10*	73.67	12.29	0.16	1.33	0.17	0.81	5.17	2.79	0.10	96.49
Nonhydrous		76.35	12.74	0.17	1.38	0.18	0.84	5.36	2.89	0.10	100.00
199.10-E (E-type)	*10*	73.00	12.10	0.10	0.70	0.20	0.60	2.20	4.90	0.10	93.90
Nonhydrous		77.74	12.89	0.11	0.75	0.21	0.64	2.34	5.22	0.11	100.00
390.00-E (E-type)	*10*	74.66	11.47	0.21	1.09	0.12	0.72	4.98	2.74	0.10	96.08
Nonhydrous		77.71	11.94	0.22	1.13	0.12	0.75	5.18	2.85	0.10	100.00
602.80-E (E-type)	*10*	76.36	12.87	0.23	0.60	0.14	0.74	6.12	2.80	0.01	99.88
Nonhydrous		76.45	12.89	0.23	0.60	0.14	0.74	6.13	2.80	0.01	100.00
UZN1663 (1663 Lava)	*20*	71.67	12.48	0.96	2.81	0.18	0.77	3.79	5.30	0.07	97.73
Nonhydrous		73.34	12.77	0.98	2.87	0.19	0.78	3.87	5.42	0.07	100.00

n gives number of analyses averaged

Plagioclase

Plagioclase is the most abundant phenocryst phase in Unzen host lavas, accounting for 15-25 vol.% total rock samples. The majority of host lava plagioclases fall into two populations based on texture and composition (Fig. 1.12A, B). The most common population of plagioclase is represented by large grains (0.25- 1 cm in length) that are oscillatory-zoned with core compositions of An_{45} to An_{60} and medial zones ranging from An_{50} to An_{70} (Fig. 1.13; Table 1.7). The second, less common plagioclase population consists of grains with a coarsely sieved interior that ranges in composition from An_{72} to An_{85} (Fig. 1.12C). The coarsely sieved texture results from the presence of abundant inclusions of pyroxene, hornblende and glass (melt), and contains an extensive network of interconnecting inclusions that appear to pervade the crystals interior. A densely packed dusty zone of micro-sieved texture (resorption zone) surrounds many of the interiors of oscillatory-zoned plagioclase phenocrysts, and occasionally surrounds coarsely sieved plagioclase (Fig. 1.12D). Resorption zones on host lava plagioclase range widely in thickness from 30 to 400 μm, and are more calcic in composition (An_{70}- An_{90}) compared to phenocryst interiors. The texture and composition of these resorption zones strongly resemble those replicated by Nakamura and Shimakita (1998) in heating experiments. A third population of plagioclase exists in host lavas, which are typically smaller than other populations (0.02 to 0.04 cm), and are characterized by cores with a resorption zone texture and a compositional range of An_{85}- An_{95} (Fig. 1.12F).

Clear, euhedral to subhedral rims enclose virtually all plagioclase grains found in the host lavas. In grains with resorption zones, rims exhibit strong normal zoning patterns

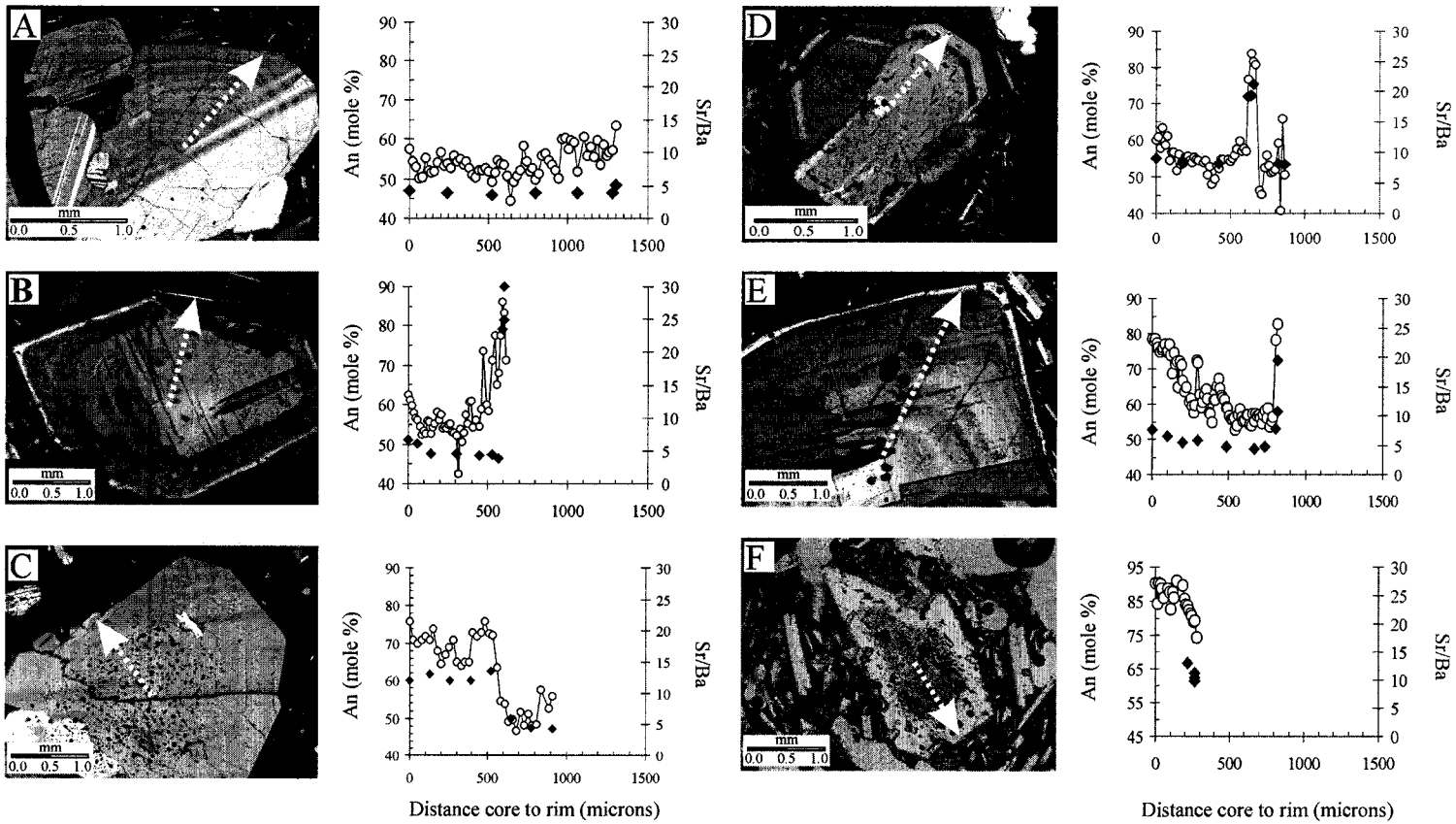

Figure 1.12
Photomicrographs of different Unzen plagioclase types from host lavas (A, B, C and D) and 1663 lava (E and F) with mole% An (open symbols) plotted with Sr/Ba ratios (filled symbols) along core to rim transects. A, Oscillatory zoned plagioclase; B, oscillatory zoned plagioclase with resorption zone; C, coarsely sieved plagioclase without resorption zone; D, coarsely sieved plagioclase with resorption zone; E, oscillatory zoned plagioclase with resorption zone; and F, resorption zone core plagioclase. Arrows indicate direction of sampling transects. Note the strong correlation between fluctuations in An content and Sr/Ba.

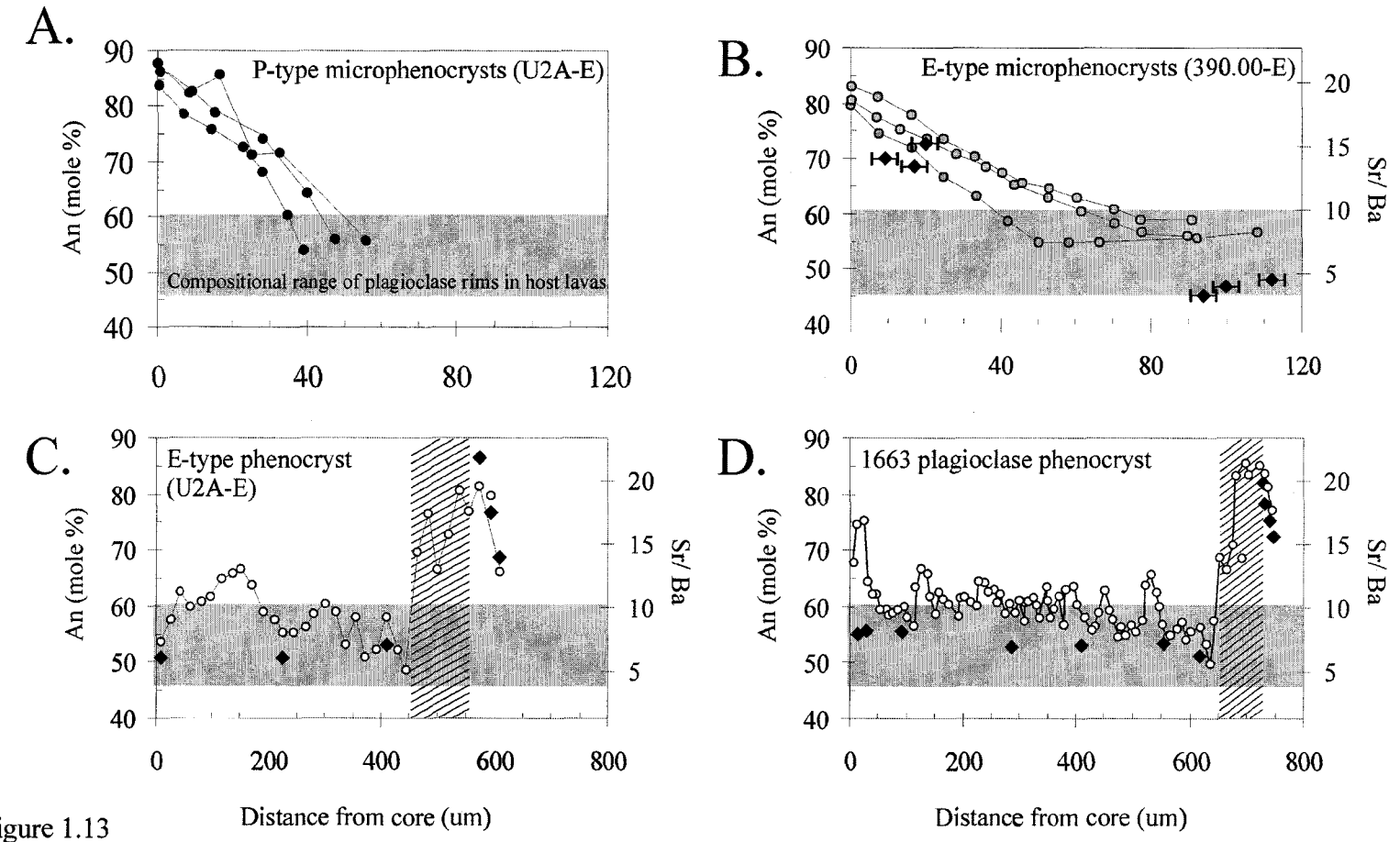

Figure 1.13
Selected samples of plagioclase from enclaves and 1663 lava. Plagioclase composition (mole% An in circles symbols) and Sr/Ba ratios (diamond symbols) are plotted along core to rim sampling transects. Shaded region on graphs represents the range of composition for the rims of coexisting plagioclase phenocrysts in host lava. Diagonally hatched region indicates resorption zone (see text). A, Microphenocryst plagioclase from Porphyritic enclaves (U2A-E); B microphenocryst plagioclase from Equigranular enclaves (390.00-E); C, plagioclase phenocryst from Porphyritic enclave (U2A-E); and D, plagioclase phenocryst from 1663 lava (1663A-01). Note that microphenocryst cores and resorbed phenocryst rims are characterized by high An content and Sr/Ba ratios compared to microphenocryst rims and phenocryst cores.

Table 1.7
Representative electron microprobe (Oxides in wt.%) analyses of plagioclase along rim-core traverses

Sample		SiO_2	Al_2O_3	FeO	CaO	Na_2O	K_2O	Total	An*	Sr/Ba
437.15-H (host lava)	rim	56.20	27.30	0.26	9.13	5.94	0.43	99.20	58.90	6.50
Plagioclase 1	middle	57.80	26.60	0.22	8.36	6.40	0.49	99.90	54.70	4.41
	core	57.70	26.40	0.22	8.25	6.42	0.51	99.60	54.30	4.14
602.80-H (host lava)	rim	58.90	25.20	0.88	7.74	5.28	0.48	98.50	57.30	8.02
Plagioclase 3	middle	55.10	28.20	0.48	10.13	4.72	0.26	98.90	66.10	8.15
	core	57.20	26.80	0.60	8.54	5.40	0.23	98.70	60.20	9.04
435.20-H (P-type)	rim	49.20	31.73	0.68	14.66	2.72	0.12	99.11	83.80	24.83
Plagioclase 5	middle	57.10	25.40	0.23	10.14	5.94	0.44	99.25	61.38	4.62
	core	56.90	27.10	0.21	8.85	6.18	0.42	99.66	57.28	6.67
262.50-E (P-type)	rim	52.90	29.00	0.41	11.54	4.55	0.27	98.70	70.10	5.21
Plagioclase 2	middle	55.40	26.70	0.28	9.10	5.85	0.38	97.70	59.30	5.90
	core	55.10	27.40	0.31	9.68	5.55	0.49	98.50	61.40	4.68
U2A-E (P-type)	rim	48.23	31.26	0.59	14.46	2.96	0.11	97.60	82.50	19.86
Plagioclase 1	middle	56.80	26.00	0.30	8.48	5.95	0.58	98.10	56.30	5.33
	core	54.80	27.60	0.22	9.91	5.65	0.31	98.50	62.40	5.10
262.50-E (P-type)	rim	48.19	32.61	0.53	15.96	2.19	0.12	99.60	87.30	NA
Microphenocryst 1	middle	50.28	31.11	0.58	13.61	3.24	0.17	98.90	79.90	NA
	core	56.80	26.90	0.28	9.09	5.89	0.33	99.30	59.40	NA
546.40-E (P-type)	rim	62.44	22.89	0.97	7.87	3.54	1.54	99.26	60.07	NA
Microphenocryst 1	middle	57.06	26.53	1.03	10.36	3.38	0.86	99.21	70.96	NA
	core	48.01	32.52	0.57	15.48	2.39	0.11	99.09	86.04	NA
390.00-E (E-type)	rim	57.59	25.86	0.35	8.64	6.45	0.30	99.19	56.15	4.79
Microphenocryst 3	middle	52.82	29.80	0.24	11.76	4.62	0.22	99.46	70.84	
	core	49.60	31.63	0.15	14.52	3.32	0.14	99.37	80.76	9.78
390.00-E (E-type)	rim	55.56	27.58	0.19	10.06	5.55	0.36	99.30	62.98	4.89
Microphenocryst 2	middle	51.98	31.35	0.24	12.03	4.39	0.16	100.15	72.53	
	core	48.64	31.37	0.37	15.15	3.03	0.14	98.71	82.69	11.88
UZN-1663 (1663 Lava)										
Plagioclase B04a	rim	51.26	29.02	0.75	14.57	3.24	0.30	99.13	80.48	19.49
	middle	54.64	29.46	0.15	11.50	5.05	0.26	101.05	68.41	5.78
	core	51.61	31.43	0.37	14.09	3.75	0.19	101.43	78.16	7.58
UZN-1663 (1663 Lava)										
Plagioclase A07	rim	48.30	33.58	0.48	16.82	2.19	0.07	101.44	88.17	20.05
	middle	57.16	27.63	0.22	9.46	6.01	0.36	100.85	59.74	4.51
	core	56.32	28.30	0.23	10.20	5.79	0.34	101.19	62.45	5.32

* Anorthite content (in weight %)

across a total thickness that ranges from 0.01 to 0.08 mm. Rim compositions immediately adjacent to the resorption zones range from An_{75} to An_{88} (referred to as resorption zone rims in figures). The outermost rim at the crystal edge in contact with matrix glass (referred to as outer rims in figures) ranges in composition from An_{50} to An_{70}. Plagioclase microphenocrysts make up 50-55 vol.% of Porphyritic enclaves and are euhedral, elongate grains (50-200 μm long, 20- 40 μm wide) compared to larger, tabular, and more equant microphenocryst plagioclase found in Equigranular enclaves (100- 500 μm long, 80- 300 μm wide) (Figs. 1.5). Plagioclase microphenocrysts comprise 60- 65 vol.% of Equigranular enclaves. Both Porphyritic and Equigranular enclave microphenocryst plagioclase have large normal compositional gradients from core to rim (Fig. 1.13A, B). Cores of Porphyritic enclave microphenocrysts range between An_{80} – An_{90}, whereas Equigranular plagioclase cores range from An_{75} –An_{85}; plagioclase from both types have rim compositions of An_{50}- An_{60}. Rim compositions of microphenocryst plagioclase overlap the range of host lava plagioclase rims. Finally, although the plagioclase core and rim compositions from Porphyritic and Equigranular enclaves are similar, the nature of the zoning from one type to another is distinct. Whereas elongate Porphyritic microphenocrysts are steeply normally zoned, tabular Equigranular microphenocrysts display a more gradual normal zonation towards the rim.

Phenocrystic plagioclase is an essential characteristic of porphyritic enclaves, accounting for between 3 and 5 vol.%. These plagioclase range in size from 0.2 to 8 mm in diameter, and commonly have oscillatory-zoned (An_{45} to An_{70}) cores. Calcic (An_{84} to An_{92}) resorption zones invariably enclose porphyritic enclave plagioclase phenocrysts

(Fig. 1.13C). Only rarely do phenocrystic plagioclase with coarsely sieved cores (An_{72} to An_{85}) exist in enclaves, and typically do not contain resorption zones. The thicknesses of phenocrystic resorption zones range from 30 to 500 μm when comparing grains from one enclave to another. However, the thicknesses of resorption zones on plagioclase within the same enclave are similar. This observation holds true even when oscillatory-zoned plagioclase phenocrysts occur in clusters of 2- 4 overlapping grains within a single enclave. In this case, resorption zones exist wherever in contact with enclave matrix glass. Finally, a thin, clear rim (<30 μm) encloses the resorption zone. Like plagioclase phenocrysts in 1663 lavas, these rims are strongly normally zoned, with resorption zone rim compositions ranging from An_{73} to An_{92} and outer rim compositions ranging from An_{49}- An_{67}.

Plagioclase is also the most common phase in the 1663 lava, accounting for 15-20 vol.%. Plagioclase in 1663 lava can be divided into the same three populations from host lavas based on texture and composition (Fig. 1.12E, Table 1.7). Similar to plagioclase phenocrysts in Porphyritic enclaves, all plagioclase in 1663 lava are surrounded by calcic (An_{75}- An_{85}), densely sieved resorption zone (Fig. 1.13D). A profuse network of fine-grained ~1 micron glass inclusions also characterizes these resorption zones, but 1663 plagioclase resorption zones have a narrower range of thickness (30- 90 μm) compared to that of other host lavas (30- 400 μm). Clear and euhedral rims enclose 1663 plagioclase where in contact with matrix glass. Rims are 0.01 to 0.03 mm thick, and exhibit strong normal zoning patterns from the rim immediately surrounding resorption zones (An_{72}- An_{91}) to the crystal edge (An_{70}- An_{85}). Many 1663 plagioclase grains appear broken as

evidenced by their cracked morphology and truncated oscillatory zoning patterns. It is unlikely, however, that these crystals were fractured during ascent or emplacement because they too are surrounded by dusty zones of high An content ranging from An_{75}-An_{85} and finally enclosed by thin, clear, An_{75}- An_{85} rims.

Specific points within plagioclase phenocrysts from Unzen host lavas, enclaves, and the 1663 lava were examined with laser ablation ICP-MS to determine Sr and Ba zoning patterns, and are clearly distinguished on the phenocryst surface (Fig. 1.12). Ba and Sr were measured along the same transects as those performed using EMPA. Resorption zones were not analyzed via laser ablation ICP-MS because of the interference between the 25-μm-wide spot size and the abundance of micron-sized glass inclusions. However, laser ablation ICP-MS analysis was performed on plagioclase rims. In order to avoid interference involving the 25-μm wide laser spot size and the matrix glass at the crystal edge, laser ablation ICP-MS analyses were performed in areas in between resorption zones and the crystal edge (RZ rims).

In most grains, fluctuations in anorthite content are mirrored by Sr/Ba ratio (Fig. 1.14). This is consistent with the findings of Blundy and Wood (1991), who determined that Sr and Ba partition coefficients in plagioclase systematically vary as a function of An content, which changes in response to temperature. The Sr/Ba ratios of interior regions of oscillatory-zoned plagioclase phenocrysts from host lavas, porphyritic enclaves, and 1663 lava range from 3 to 12 (Fig. 1.14). Conversely, the interior regions of coarsely sieved plagioclases from host lavas have higher Sr/Ba ratios, ranging from 4 to 22. Resorption zone rims on plagioclase phenocrysts from host lavas, porphyritic enclaves, and 1663

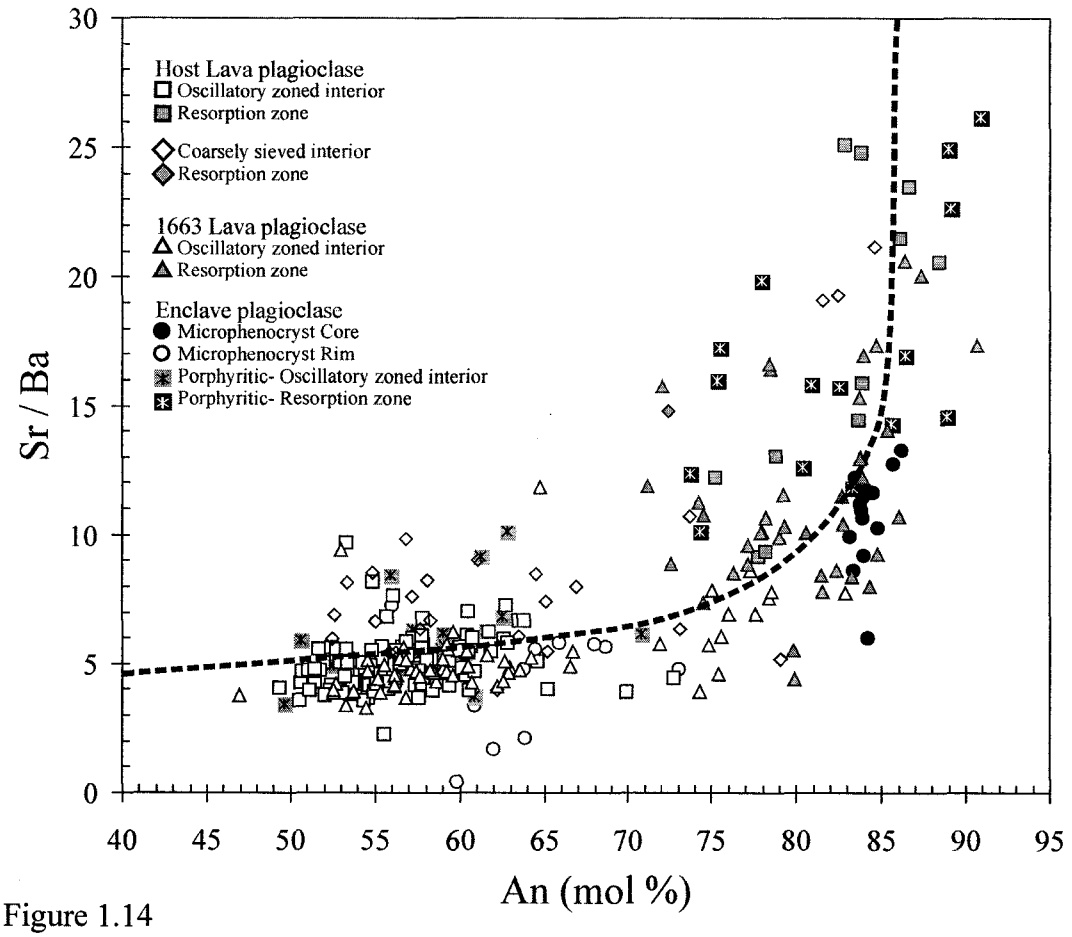

Figure 1.14
Trace element and anorthite compositions of Unzen plagioclase. Sr/Ba ratios of Unzen plagioclase plotted against An content (mole %) for host dacite lavas (HOI- host lava oscillatory interior, HORZ- host lava oscillatory resorption zone rims, HCI- host lava coarsely sieved interior, HCRZ- host lava coarsely sieved resorption zone rim), 1663 andesite lava (63OI- 1663 lava oscillatory interior, 63RZ- 1663 lava resorption zone rim), and the basalt enclaves (EMC- enclave microphenocryst core, EMR- enclave microphenocryst rim, EOI- enclave porphyritic oscillatory interior, EORZ- enclave porphyritic resorption zone rim). Note the strong correlation between Sr/Ba ratio and increasing An content, which occurs as a result of Ba becoming less compatible than Sr with increasing An content due to changes in the plagioclase crystal structure (Blundy and Wood, 1991). Also note that broad correlation between the samples analyzed in our study and what is predicted by Blundy and Wood's (1991) empirically derived relationship for changing partition coefficients of Sr and Ba as a function of An weight fraction.

lava also have high Sr/Ba ratios, ranging up to 31. Finally, equigranular enclave microphenocryst plagioclase cores have an elevated Sr/Ba concentration (4- 14) compared to the rims (1- 5).

Hornblende

Hornblende phenocrysts account for between 5 and 8 vol.% of host lavas, and occur as either dark brown, medium grained (1-5 mm), equant phenocrysts, or as tan colored, large (5-8 mm), equant phenocrysts with rounded or embayed rims. A thin rim of pyroxene, plagioclase, and Fe-Ti oxides may enclose phenocrystic hornblendes, while other grains appear to have no rims, even when separated from each other by less than a few millimeters. Hornblende phenocrysts commonly have inclusions of plagioclase, biotite, clinopyroxene, glass, and Fe-Ti oxides. Medium grained hornblendes typically do not have rounded or embayed rims, nor do they contain biotite or quartz inclusions. Hornblende microphenocrysts are the dominant mafic mineral phase in the enclaves, and account for 20-25 vol.% in Porphyritic enclaves, and 15-25 vol.% in Equigranular enclaves. Hornblendes found in Porphyritic enclaves are distinct from hornblendes of host lavas and Equigranular enclaves, in that they are smaller, highly elongate, compositionally zoned, and typically have hollow cores. Equigranular enclave hornblendes are larger, prismatic, and typically compositionally unzoned.

There is a large variation in hornblende composition found in enclaves and host lava. Cores of hornblendes in Porphyritic enclaves contain about twice the Al_2O_3, TiO_2, and Na_2O as the rim, and rim compositions of Porphyritic enclave hornblende approach

the composition of Equigranular enclave and host lava. Furthermore, hornblende cores from Porphyritic enclaves have elevated $Al^{(IV)}$ and (Na + K) compared to the host lava hornblende cores, although rim compositions may overlap (Fig. 1.15, Table 1.8). In contrast, Equigranular enclaves have hornblende core and rim $Al^{(IV)}$ and (Na + K) compositions similar to those in host lavas.

Hornblende in 1663 lava occurs as relics, having been almost completely replaced with Fe-Ti oxides, plagioclase, and clinopyroxene. Hornblende relics account for between 2 and 3 vol.% of the 1663 lava, and range in size from 5- 8 mm. Hornblende is also observed enclosing some olivine phenocrysts as reaction rims.

Pyroxenes

Pyroxenes account for <3 vol.% of host lavas and 2-5 vol.% in the enclaves. Orthopyroxene and clinopyroxene are commonly found in glomeroporphyritic aggregates with calcic plagioclase and Fe-Ti oxides that occur in host lavas and Porphyritic enclaves. These clinopyroxenes are invariably rimmed by orthopyroxene and plagioclase where in contact with host groundmass. When pyroxenes exist as single crystals in host lavas, clinopyroxenes are subhedral to anhedral, and many have resorbed rims, whereas orthopyroxenes are euhedral to subhedral. Orthopyroxene is found in both types of enclaves, and is typically euhedral in Porphyritic enclaves and subhedral in Equigranular enclaves. In contrast, clinopyroxene is found in all Porphyritic enclaves, but only a single grain was found in Equigranular enclaves. Orthopyroxenes of Porphyritic enclaves have a wide range in composition (Fig. 1.16, Table 1.9) compared to those in Equigranular

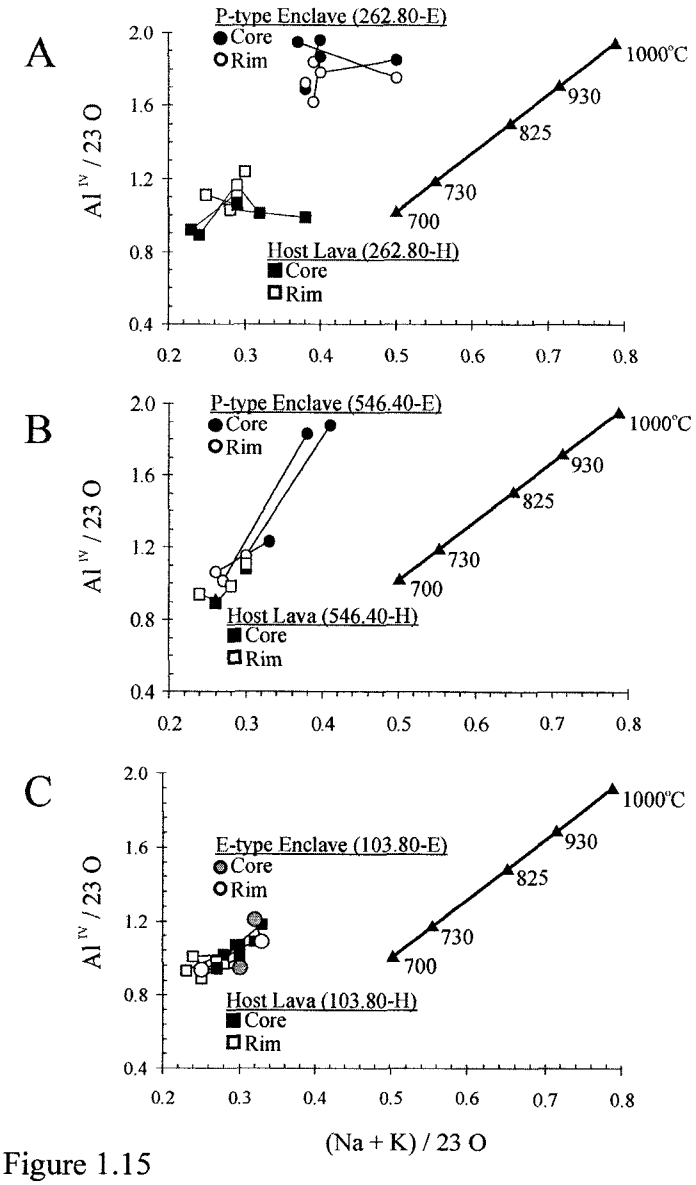

Figure 1.15
Composition of coexisting hornblende crystals in enclave and host lavas. A, P-type enclave and host (262.80-H, 262.80-E); B, P-type enclave and host (546.40-H, 546.40-E); and C, E-type enclave and host (103.80-H, 103.80-E). Lines connect intra-grain analyses at crystal core and rim. All structural formulas calculated on the basis of 23 oxygens (after Helz, 1979) and 15 cations (after Robinson et al., 1982). Heavy line is from Helz (1973), giving the composition of hornblende coexisting with melt in 1921 Kilauea basalt (QFM buffer and H2O saturated at 500 MPa at given temperatures). Note strong zoning in 546-40-E hornblende paralleling Helz's data. See text for further discussion on zoning patterns.

Table 1.8
Representative electron microprobe analyses (Oxides in wt.%) of hornblende rims and cores

Sample	103.80-H (host) HBL 2		103.80-E (E-type) Microphen. HBL 1		546.40-H (host) HBL 1		546.40-E (P-type) Microphen. HBL 3		262.80-H (host) HBL 2		262.80-E (P-type) Microphen. HBL 4	
	rim	core	rim	core	rim	core	rim	core	rim	core	rim	core
SiO_2	47.20	47.30	47.43	46.92	48.16	48.20	45.20	43.80	46.20	46.82	43.79	41.02
TiO_2	2.30	1.10	1.91	1.52	1.20	1.42	1.86	1.90	1.40	1.40	1.36	2.18
Al_2O_3	7.71	9.80	8.19	8.93	9.61	8.96	10.80	11.59	9.80	9.28	13.20	14.16
FeO $^{\$}$	13.15	10.89	11.14	11.01	10.44	11.11	10.85	10.20	11.82	11.20	9.68	10.73
Fe_2O_3 $^{\$}$	1.81	4.25	3.49	3.13	3.95	2.53	3.81	3.98	3.08	3.51	3.85	2.97
MgO	13.97	14.72	14.65	14.71	14.91	14.83	14.51	15.39	14.18	14.92	14.33	14.20
CaO	11.40	9.48	9.88	10.52	9.16	9.97	9.46	9.97	10.26	10.28	10.17	10.48
Na_2O	1.28	1.21	1.19	1.34	1.38	2.19	1.80	2.08	1.48	1.38	1.32	2.20
K_2O	0.71	0.40	0.58	0.52	0.43	0.51	0.58	0.50	0.71	0.60	0.59	0.42
MnO	0.43	0.41	0.32	0.41	0.46	0.60	0.41	0.20	0.50	0.70	0.46	0.40
F	0.00	0.10	0.20	0.10	0.10	0.00	0.30	0.40	0.20	0.00	0.56	0.30
Cl	0.09	0.20	0.20	0.20	0.10	0.07	0.10	0.10	0.10	0.00	0.08	0.10
Total	100.05	99.86	99.18	99.31	99.90	100.39	99.68	100.11	99.73	100.09	99.39	99.16
Cations per 23 Oxygens*												
Si	6.80	6.73	6.47	6.72	6.82	6.83	6.50	6.29	6.66	6.69	6.85	5.94
Al^{IV}	1.20	1.27	1.26	1.28	1.18	1.17	1.50	1.71	1.34	1.31	1.98	2.06
Ti	0.25	0.12	0.20	0.16	1.20	0.15	0.20	0.21	0.15	0.15	0.15	0.24
Al^{VI}	0.31	0.24	0.27	0.28	0.27	0.39	0.36	0.38	0.34	0.30	0.23	0.39
Fe^{2+}	1.58	1.30	1.32	1.44	1.24	1.32	1.30	1.22	1.42	1.34	1.43	1.30
Fe^{3+}	0.20	0.46	0.37	0.34	0.42	0.27	0.41	0.43	0.33	0.38	0.31	0.43
Mg	3.00	3.17	3.15	3.13	3.15	3.13	3.11	3.30	3.05	3.18	3.13	3.06
Mn	0.05	0.05	0.05	0.05	0.06	0.07	0.05	0.02	0.06	0.08	0.06	0.05
Ca	1.76	1.44	1.50	1.61	1.39	1.51	1.46	1.53	1.58	1.57	1.60	1.62
Na	0.18	0.17	0.16	0.19	0.19	0.30	0.25	0.29	0.21	0.19	0.19	0.31
K	0.13	0.07	0.11	0.10	0.08	0.09	0.11	0.09	0.13	0.11	0.11	0.08

*Structural formulas for all hornblendes calculated on the basis of 23 Oxygens (after Helz, 1979)

$^{\$}$Ferrous and ferric iron calculated on the basis of 15 cations (after Robinson et al., 1982)

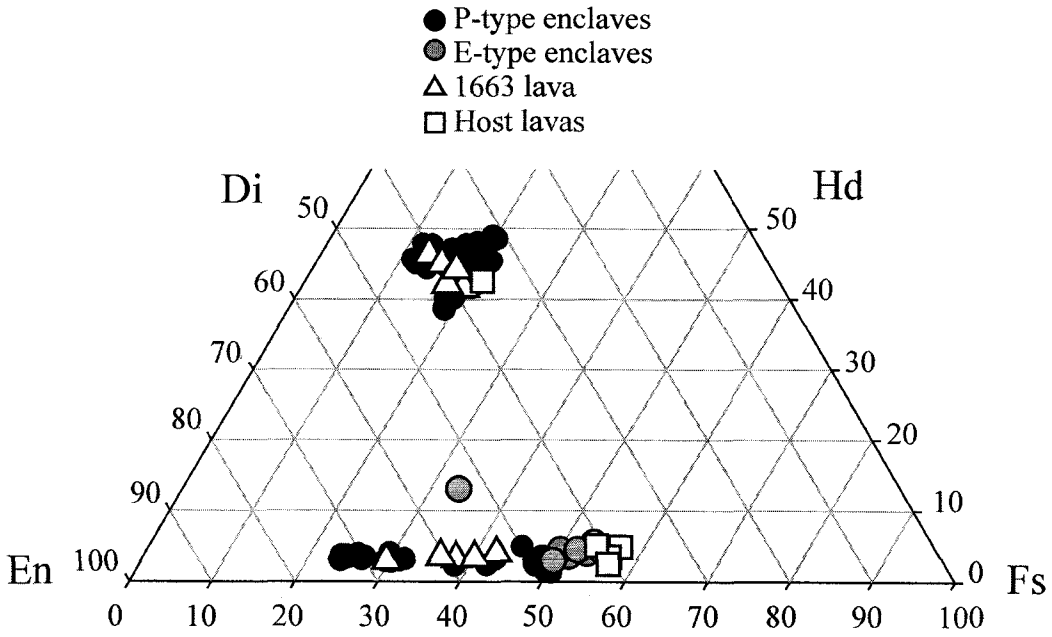

Figure 1.16
Pyroxene compositions in Unzen samples, including host lavas (open squares), Porphyritic enclaves (filled circles), Equigranular enclaves (gray circles), and 1663 lava (open triangles).

enclaves or host lavas. Compositions of clinopyroxenes in P-type enclave are clustered around $Wo_{45}En_{35}Fs_{10}$, and are unzoned. Pyroxenes account for 4- 7 vol.% of the 1663 lava, second in abundance to plagioclase, and commonly occur as phenocrysts rather than in glomeroporphyritic aggregates as in the host lava samples. Clinopyroxene phenocrysts are euhedral to subhedral, 20 to 200 μm in length, and have an average composition of $Wo_{42}En_{40}Fs_{18}$. Orthopyroxene phenocrysts are predominantly subhedral and range between 20 and 100 μm in size, and have an average composition of $Wo_5En_{58}Fs_{37}$.

Olivine

Olivine phenocrysts (Fo_{65}-Fo_{75}) range in size from 0.2- 0.5 mm, and may be found either as individual phenocrysts or in glomeroporphyritic aggregates in P-type enclaves (<1 vol.%). Olivine is not present in Equigranular enclaves. Although olivine does occur as individual phenocrysts in host lavas, it more commonly occurs in glomeroporphyritic aggregates with calcic plagioclase, clinopyroxene, and Fe-Ti oxides. Thin rims (<10μm) of orthopyroxene may surround olivine crystals in host lavas where in contact with surrounding matrix glass. Olivine crystals are usually unrimmed when observed in Porphyritic enclaves. Olivine is common in 1663 lava, accounting for ~2 vol.% and ranging in composition from Fo_{60} to Fo_{75} (Table 1.9) The 1663 lava olivine is slightly coarser grained compared to those found in host lavas or Porphyritic enclaves, ranging in size from 0.2 – 1.2 mm. Olivine phenocrysts found in the 1663 lava are typically subhedral or anhedral and enclosed by a reaction rim of either hornblende or orthopyroxene where in contact with matrix glass.

Table 1.9
Electron microprobe analyses (Oxides in wt.%) of pyroxenes and olivines

Sample	SiO_2	TiO_2	Al_2O_3	Cr_2O_3	FeO	MnO	MgO	CaO	NiO	Total
153.85-H (host lava)										
OPX 1	52.19	0.21	1.40	0.02	21.20	0.11	23.86	1.01	0.00	100.00
OPX 2	51.70	0.09	1.21	0.02	21.68	0.32	23.02	1.03	0.03	99.10
OPX 3	51.67	0.19	1.49	0.02	19.62	0.86	25.26	1.43	0.03	100.57
199.90-H (host lava)										
OPX 1	52.40	0.11	0.80	0.03	21.26	1.40	23.85	0.53	0.01	100.39
OPX 2	52.70	0.08	0.80	0.02	20.81	1.30	24.19	0.59	0.40	100.89
U2A-E (P-type)										
OPX 1	53.83	0.14	1.56	0.17	14.24	0.40	28.97	1.41	0.01	100.73
OPX 2	54.06	0.11	0.73	0.19	13.84	0.61	29.22	1.32	0.05	100.13
CPX 1	49.85	0.75	3.63	0.23	7.68	0.24	15.77	20.40	0.00	98.55
CPX 2	50.98	0.55	3.22	0.37	5.93	0.21	17.64	20.77	0.06	99.73
Olivine 1	36.10	0.00	0.10	0.00	20.90	0.50	42.50	0.10	0.00	100.20
Olivine 2	37.70	0.06	0.00	0.10	20.10	0.18	41.90	0.00	0.00	100.04
153.85-E (E-type)										
OPX-1	51.56	0.15	1.66	0.08	21.50	1.08	23.43	0.88	0.11	100.45
OPX-2	51.44	0.29	0.84	0.04	21.39	1.49	24.06	0.73	0.02	100.30
262.80-E (E-type)										
OPX 1	50.30	0.20	1.50	0.00	21.30	1.00	21.20	1.30	0.00	96.80
OPX 2	52.50	0.10	0.40	0.00	22.90	1.50	22.50	0.70	0.00	100.60
CPX 1	51.60	0.40	2.70	0.30	5.70	0.10	18.20	20.60	0.00	99.60
CPX 2	51.20	0.70	3.10	0.00	8.50	0.40	18.10	17.70	0.00	99.70
CPX 4	51.20	0.80	5.20	0.10	8.10	0.30	14.50	17.30	0.10	97.60
Olivine 1	38.48	0.04	0.08	0.01	17.25	0.24	43.62	0.10	0.11	99.93
Olivine 2	39.21	0.07	0.42	0.04	18.28	0.36	42.02	0.18	0.14	100.72
Olivine 3	38.16	0.03	0.10	0.02	17.18	0.28	44.71	0.08	0.11	100.67
199.90-E (E-type)										
OPX 1	52.60	0.10	0.70	0.00	21.10	1.40	23.80	0.60	0.00	100.30
OPX 2	52.40	0.10	0.90	0.00	21.40	1.40	23.90	0.50	0.00	100.60
602.80-E (E-type)										
OPX 1	51.85	0.14	0.83	0.05	21.67	1.37	23.58	0.69	0.02	100.20
OPX 2	52.13	0.20	1.05	0.00	19.81	0.72	24.72	0.91	0.04	99.58
OPX 3	52.01	0.15	0.85	0.04	20.75	1.14	23.70	0.73	0.04	99.41
UZN1663 (1663 Lava)										
OPX 1	53.40	0.45	1.72	0.00	17.33	0.48	23.74	2.36	0.01	99.48
OPX 2	53.90	0.35	2.42	0.00	14.37	0.42	25.61	2.26	0.04	99.37
CPX 1	51.73	0.38	1.94	0.00	5.93	0.23	17.59	19.28	0.00	97.08
CPX 2	52.25	0.55	3.05	0.10	7.50	0.22	18.29	17.57	0.00	99.54
CPX 3	53.24	0.46	1.45	0.00	9.51	0.43	17.40	17.35	0.04	99.87
CPX 4	51.10	0.70	3.38	0.00	8.74	0.37	16.62	17.89	0.00	98.80
CPX 5	50.30	1.29	5.26	0.00	7.88	0.28	16.96	17.39	0.00	99.35
Olivine 1	38.18	0.02	0.00	0.20	23.46	0.44	37.59	0.09	0.16	100.15
Olivine 2	38.18	0.01	0.03	0.10	24.05	0.30	36.81	0.12	0.15	99.75
Olivine 3	39.20	0.01	0.02	0.10	19.74	0.34	40.94	0.11	0.15	100.61
Olivine 4	39.31	0.03	0.03	0.00	18.79	0.36	41.96	0.06	0.14	100.67
Olivine 5	38.74	0.02	0.03	0.30	21.69	0.37	38.94	0.06	0.14	100.28

Fe-Ti Oxides

Magnetite and ilmenite are present in all host lavas, in the 1663 lava, and, in the majority of enclave samples. Together, magnetite and ilmenite account for between 1- 2 vol.% of host lavas and the 1663 lava, and slightly more in enclaves (1-3 vol.%). Magnetite occurs as small subhedral, or irregularly shaped phenocrysts in host lavas and the 1663 andesite, but is typically euhedral in enclaves. Many host lavas and Equigranular enclaves contain magnetite grains with ilmenite exsolution lamellae, probably resulting from slow cooling in the interior of lava flows and domes. Ilmenite occurs as small subhedral crystals in the host lavas and enclaves, but as anhedral or irregularly shaped crystals in the 1663 andesite. Ilmenite is less abundant than magnetite in all samples, occurring only in trace amounts (<1 vol.%).

Magnetite and ilmenite disequilibrium textures, such as irregular crystal faces in 1663 lava and exsolution textures in host lavas and enclaves, are widespread, thereby complicating efforts to make estimates of pre-eruptive temperatures. All such estimates presented in this study are limited to analyses of touching magnetite and ilmenite grains with euhedral crystal faces where the pair compositions are potentially in equilibrium, based on the model of Bacon and Hirschmann (1988). All geothermometry from this study employs the mineral recalculation scheme of Stormer (1983) and the algorithm of Andersen and Lindsley (1988), which has an associated error of ± 10°C.

Magnetite- ilmenite pairs from host lava samples are compositionally zoned (Table 1.10), yielding a temperature range of 725 to 810°C from pair cores from 820 to 830°C for pair rims. These estimates are similar to those obtained in an earlier study

(Venesky and Rutherford, 1999). Magnetite-ilmenite pairs from Porphyritic enclaves are either unzoned or are surrounded by a thin rim (<10 μm) of differing composition. Porphyritic enclave pairs yield temperatures ~150°C higher than pairs from host lavas, ranging between 955 and 1040°C (only 2 samples yield temperatures >1000°C). Where present, thin rims yield a temperature range of 825 to 895°C (n = 2). It seems likely, however, that most Porphyritic enclave magnetite-ilmenite pairs did not have enough time to fully re-equilibrate with the host before ascent and subsequent quenching, and thus these temperature estimates may not be a true indicator of the temperature of the enclaves upon mixing with the host. Magnetite-ilmenite pairs analyzed in Equigranular enclaves are not zoned, and yield temperatures between 805° and 840°C, which is ~20°C higher than pairs from host lavas.

Quartz

Quartz typically accounts for 1-2 volume % of dacite lavas, and always occurs as large, rounded and/or irregularly embayed phenocrysts with no reaction rim. Although rare, quartz occurs in Porphyritic enclaves and 1663 andesite, where a coarse-grained reaction rim of clinopyroxene, plagioclase, and glass invariably surrounds it.

Table 1.10
Representative electron microprobe analyses (Oxides in wt.%) of magnetite and ilmenite pairs

Sample		TiO_2	Al_2O_3	Cr_2O_3	FeO	MnO	MgO	NiO	V_2O_3	CaO	Total	Usp	Ilm	T°C	log fO_2
199.10-H (host lava)															
Magnetite	core	5.90	0.80	0.10	89.40	0.50	1.80	0.08	0.64	0.06	99.28	0.16			
Ilmenite	core	39.30	0.10	0.00	54.20	0.70	1.80	0.02	0.24	0.05	96.41		0.87	806°C +/- 20	-11.76
Magnetite	rim	9.50	1.15	0.00	86.49	0.58	1.15	0.04	0.38	0.04	99.34	0.26			
Ilmenite	rim	43.20	0.10	0.00	51.85	0.76	2.18	0.04	0.45	0.03	98.61		0.81	850°C +/- 20	-11.79
390.00-H (host lava)															
Magnetite	core	5.90	1.60	0.10	89.08	0.60	1.79	0.10	0.59	0.04	99.80	0.17			
Ilmenite	core	42.20	0.10	0.00	55.50	0.60	1.80	0.04	0.28	0.04	100.56		0.90	810°C +/- 15	-11.71
Magnetite	rim	9.30	0.80	0.00	86.70	0.60	1.78	0.04	0.44	0.04	99.70	0.26			
Ilmenite	rim	44.50	0.10	0.00	51.20	0.60	2.10	0.04	0.39	0.04	98.97		0.79	839°C +/- 20	-11.93
602.80-H (host lava)															
Magnetite	core	6.70	0.66	0.11	89.40	0.44	1.21	0.09	0.39	0.09	99.09	0.18			
Ilmenite	core	41.00	0.00	0.00	55.80	0.50	2.20	0.04	0.29	0.04	99.87		0.83	803°C +/- 25	-12.17
Magnetite	rim	7.60	0.78	0.00	88.70	0.44	1.22	0.04	0.29	0.09	99.16	0.21			
Ilmenite	rim	41.20	0.10	0.00	55.10	0.70	2.10	0.04	0.34	0.04	99.62		0.83	826°C +/- 15	-11.87
262.50-E (P-type)															
Magnetite	core	10.90	1.70	0.00	84.40	0.60	2.14	0.09	0.68	0.05	100.56	0.33			
Ilmenite	core	41.20	0.20	0.10	55.90	0.50	0.10	0.04	0.24	0.04	98.32		0.83	925°C +/- 20	-10.43
Magnetite	rim	9.40	0.80	0.20	86.40	0.40	1.90	0.04	0.59	0.04	99.77	0.21			
Ilmenite	rim	41.20	0.11	0.00	54.60	0.54	1.92	0.04	0.24	0.04	98.69		0.86	831°C +/- 20	-11.68
U2A-E (P-type)															
Magnetite	core	9.70	2.40	0.30	84.40	0.60	1.90	0.09	0.48	0.09	99.96	0.56			
Ilmenite	core	44.30	0.10	0.10	53.60	0.60	1.20	0.04	0.04	0.04	100.02		0.77	1040°C +/- 25	-9.84
Magnetite	rim	9.20	1.90	0.00	85.60	0.50	1.40	0.04	0.54	0.04	99.22	0.26			
Ilmenite	rim	42.10	0.10	0.00	55.60	0.70	1.80	0.04	0.04	0.04	100.42		0.89	895°C +/- 25	-10.90
199.10-E (E-type)															
Magnetite	core	7.70	1.74	0.10	88.50	0.40	1.20	0.08	0.38	0.04	100.14	0.21			
Ilmenite	core	40.20	0.20	0.00	57.40	0.60	2.20	0.04	0.21	0.04	100.89		0.96	840°C +/- 15	-11.13
Magnetite	rim	7.60	1.41	0.10	88.60	0.50	1.30	0.04	0.31	0.04	99.90	0.21			
Ilmenite	rim	43.20	0.10	0.00	52.85	0.76	2.18	0.04	0.14	0.04	99.31		0.82	837°C +/- 20	-11.96
390.00-E (E-type)															
Magnetite	core	6.30	1.84	0.10	89.80	0.50	1.20	0.04	0.46	0.04	100.28	0.17			
Ilmenite	core	41.60	0.10	0.10	55.60	0.60	1.50	0.04	0.28	0.04	99.86		0.89	815°C +/- 20	-11.65
Magnetite	rim	6.10	1.40	0.00	88.90	0.50	1.20	0.04	0.39	0.04	98.57	0.17			
Ilmenite	rim	41.20	0.10	0.00	55.50	0.60	1.80	0.04	0.18	0.04	99.46		0.90	810°C +/- 25	-11.73

Temperatures and oxygen fugacities after Anderson and Lindsley (1988) algorithm.
All oxides reported in wt.%, Usp = mol.% Ulvospinel, Ilm = mol.% Ilmenite

Biotite

Biotite is sometimes found in host lavas (<1 vol.%), and is invariably rimmed by pyroxenes, plagioclases, and Fe-Ti oxides (± amphibole). Rarely, angular pieces of biotite grains that were likely fractured during ascent are found with reaction rims on only a few sides where in contact with groundmass. In Porphyritic enclaves, biotite is a rare mineral phase that is always surrounded by a fine-grained reaction rim of pyroxene, plagioclase, and Fe-Ti oxides. Biotite is not found in Equigranular enclaves or in 1663 lava.

1.5 DISCUSSION

This section begins with an interpretation of the textural, petrological, and geochemical data presented above as strongly supporting a model for the origin of the Unzen magmas that involved mingling between basalt and dacite magma. Then, I propose a model to explain the formation of the texturally distinct enclaves where Porphyritic enclaves are the product of rapid cooling at the boundary between mafic magma intrusions and host dacite magma and Equigranular enclaves result from more prolonged development within the interior of the mafic magma intrusion. Plagioclase textural and geochemical data indicates that this mixing scenario involved extensive phenocryst exchange between the two interacting magmas. Finally, we argue that the mingling scenario presented here is widespread by briefly comparing examples from other volcanoes.

Mingling Constraints From Textural Data

The textures of Porphyritic and Equigranular enclaves are distinct, suggesting that they experienced different cooling rates during formation. Porphyritic enclave texture indicates quenching of a largely liquid magma within a cooler silicic host as indicated by their acicular texture, chilled and cuspate margins, and an outward decrease in grain size toward the enclave rim. This indicates an increase in cooling rate near the contact with the lower temperature host magma, and discredits the interpretation that they are the product of melting of a restite source or represent entrained cumulate material (Eichelberger, 1980). Basalt crystallization experiments have produced textures similar to those of Porphyritic enclaves, characterized by acicular and skeletal plagioclase, at undercooling conditions (ΔT) of between 140 to 185 °C (Lofgren, 1980, Coombs et al., 2002). This is consistent with an average difference in temperature from Porphyritic enclaves and host lava of 150°C as determined in this study. The outward increase in glass content, strong normal zoning in microphenocrysts, and widespread occurrence of vesicles also implies rapid quenching.

Like Porphyritic enclaves, Equigranular enclaves contain a pervasive population of small single vesicles that exist in the irregular spaces between microphenocrysts, implying a vesiculation event induced by crystallization. Unlike Porphyritic enclaves, however, Equigranular enclave texture is consistent with a more gradual and prolonged crystallization history as indicated by less steeply zoned and tabular to equant microphenocrysts that do not change in morphology with distance from the enclave rim. There is also the absence of chilled or crenulated margins, the enclave surface being

characterized by protruding edges of microphenocrysts. Basalt crystallization experiments have produced similar textures with tabular crystal morphologies where undercooling was <40°C (Lofgren, 1980, Coombs et al., 2002). This is consistent with inferred temperature difference between Equigranular enclaves and host lavas of 10 to 45°C. Finally, it is important to note that the characteristic Porphyritic enclave texture does not occur as a rind on Equigranular enclaves. This indicates that the differences between the two texturally distinct enclaves cannot be due merely to size (diffusion path-length) dependence resulting from direct contact with the host on the exterior of enclaves producing a Porphyritic texture with the Equigranular enclave texture developing in their interiors.

Mingling Constraints From Mineralogical Data

Plagioclase microphenocrysts, with calcic core compositions ranging from An_{75} to An_{90}, are the dominant phase in both types of Unzen enclaves. This suggests that microphenocryst plagioclase crystallized from the enclave-forming magma. The interiors of plagioclase phenocrysts from Porphyritic enclaves, however, are typically oscillatory zoned and have An compositions and Sr/Ba ratios identical to interiors of plagioclase grains in the host lavas, which are too sodic have been precipitated from the enclave-forming magma. Furthermore, sodic plagioclase phenocryst cores in Porphyritic enclaves are invariably surrounded by resorption zones that cut across oscillatory zoning profiles with major and trace element compositions equal to microphenocrysts. These zones strongly resemble experimentally developed resorption zones on plagioclase grains that

formed in response to sudden heating events (Tsuchiyama and Takahashi, 1983; Tsuchiyama, 1985; Nakamura and Shimakita, 1998). Therefore, Porphyritic enclave plagioclase phenocrysts are interpreted to have originated from the host magma and that the resorption zones record the mineralogical response to the abrupt change in surrounding melt composition and temperature from which the sodic oscillatory-zoned interior precipitated.

The presence of host-derived phenocrysts in Porphyritic enclaves requires that intruding mafic magma engulfed plagioclase phenocrysts from the host dacite magma during replenishment events. The thickness of resorption zones can be used to constrain the amount of time required for engulfment of host magma by intruding basaltic magma to occur. Resorption zones on sodic Porphyritic enclave plagioclase phenocrysts range in thickness from 30 to 500 μm. This range in thickness requires 0.3 to 8 days to develop given a surrounding temperature range of between 950 to 1050°C according to experiments (Tsuchiyama and Takahashi, 1983; Tsuchiyama, 1985; Nakamura and Shimakita, 1998). But does intruding basalt engulf host magma while in the form of enclaves? A simple conduction model predicts that a 30-cm diameter enclave at 1000 °C would approach thermal equilibration with the surrounding host magma (800 °C) in an hour (e.g. Jaeger, 1968). This suggests that host magma probably does not mix with intruding basalt while in the form of blobs or enclaves because rapid cooling leaves insufficient time for the resorption zones to form. Thus, most resorption zone development on host-derived plagioclases occurs when they are incorporated into the mafic intrusion, and continue to form as the mixed magma is dispersed.

Some host-derived plagioclase are clearly not engulfed by intruding basaltic magma during a replenishment event, as evidenced by abundant oscillatory-zoned plagioclase in host dacite lavas that are not enclosed by a resorption zone. The presence of both types of plagioclase phenocrysts is ubiquitous in Unzen dacitic lavas, which is consistent with replenishment events resulting in mingling of only a portion of the magma body that is eventually erupted.

The 1663 lava flow appears to be the rare exception to this rule. Whereas most mingling events result in the eruption of only a portion of the magma body, the 1663 lava appears to be the product of complete and thorough mixing between intruded basalt and host dacite. Such thorough mixing is only expected to result from a replenishment scenario where the mass fraction of intruded basalt accounted for $\geq 50\%$ of the mixture (Kouchi and Sunagwana, 1985; Bacon, 1986; Sparks and Marshall, 1986), which agrees with mixing calculations that require a 1:1 mixture of mafic and silicic end members to produce the 1663 composition. The similarity of the 1663 lava plagioclase population to that observed in the enclaves is consistent with the idea that the two differ only in post-mixing thermal history. Whereas the Porphyritic enclaves represent the hybrid magma from the mafic- silicic interface that was dispersed and quenched in the host dacite, the 1663 lava represents an eruption of hybrid magma directly from the mafic- silicic interface without the typical steps of dispersal and quenching in the silicic resident magma. This conclusion is supported by the fact that the 1663 andesitic lava flow does not contain enclaves.

Equigranular enclaves do not contain vestiges of incorporated crystalline phases from the host like the Porphyritic enclaves, nor do they contain olivine. In addition, Equigranular enclave interstitial melt appears to be in chemical equilibrium with the melt of the host, based on their identical composition. Why then, are they more equilibrated compared to the Porphyritic enclaves? One possibility is that Equigranular enclaves are derived from a third andesitic magma, different from the magma that formed Porphyritic enclaves. This hypothesis is rejected because of the strong compositional resemblance between the Equigranular enclaves and the obviously hybrid Porphyritic enclaves. In addition, eruptions at Unzen appear to be generated by mafic inputs to the system. For three magma batches to repeatedly participate in generating eruption products seems like a colossal coincidence. The hypothesis that Equigranular enclaves are cumulates is also rejected because cumulate products of magma would contain the same phases that the magma is precipitating. Crystal phases of Equigranular enclaves differ significantly in their composition and morphology from crystal phases in the dacite magma.

Equigranular enclaves therefore are thought to be basalt + dacite hybrids, as indicated by calcic plagioclase microphenocrysts An_{75}–An_{85}, elevated geothermometry temperatures compared to the host, and strong bulk chemical resemblance to the Porphyritic enclaves. Accepting this inference nonetheless requires an explanation for why they are more equilibrated than the Porphyritic enclaves. One possibility is that they are simply Porphyritic enclaves from previous replenishment events that have ripened with time. Porphyritic enclaves clearly disaggregate with time as indicated by the presence of formerly engulfed plagioclase crystals in the host and the presence of the

enclaves with intermediate textures to Porphyritic and Equigranular types. This hypothesis, however, is not the general mode of formation for Equigranular enclaves for several reasons. First, if Equigranular enclaves were the disaggregated remnants of Porphyritic enclaves, one would expect to find cores of engulfed host phenocrysts within Equigranular enclaves. Longer residence times within the cool dacitic magma would not result in the destruction of engulfed phenocrysts in aged Porphyritic enclaves, for the cores of those phenocrysts are already in equilibrium with the host. Second, the majority of Unzen enclaves can be easily distinguished as either Porphyritic or Equigranular based on texture. If Equigranular enclaves were the disaggregated remnants of Porphyritic enclaves one would to find a wide range of textures between them, but intermediary enclaves occur only in trace amounts in host lavas. Third, it is unlikely that the acicular and steeply normally zoned microphenocrystic plagioclase in Porphyritic enclaves would evolve into to tabular microphenocrysts with more gradual zoning over time.

Mingling Constraints From Geochemical Data

Many of the compositional arrays of Unzen lavas and Porphyritic enclaves are broadly linear (e.g. Fe, Ca, Y) over nearly 15 wt.% range in SiO_2, which supports a mixing relationship between basalt and dacite endmembers. Some elemental arrays, however, are quite scattered (e.g. Ba, Sr, P) or curvilinear (e.g. Al, Na). This suggests that processes such as crystallization, fractionation, and assimilation likely operate in the Unzen magma reservoir between mafic intrusions over time. Compositional scatter is also apparent among the Equigranular enclaves, which likely resulted from their small size (averaging

~2 cm in diameter) relative to grain size. In addition, some Porphyritic enclave elemental trends project to compositions that are depleted beyond host lava compositions (e.g. Sr, Ba, Rb), suggesting that enclaves may have experienced some separate form of crystal-liquid differentiation, such as gas-driven filter pressing (Anderson et al., 1984; Sisson and Bacon, 1999). Porphyritic enclaves do not contain segregation pipes of rhyolitic melt, however, which might be expected if filter pressing had occurred (e.g. Bacon, 1986).

Projection of the mixing lines yields information on the compositions of possible end members, though subject to the above uncertainties. The most silicic host dacite lava samples have a composition between 64 and 65 wt.% SiO_2. However, for the purposes of mixing calculations we estimate the silicic end member to have a SiO_2 content of ~66 wt.% because even the most silicic host dacite lava contains enclaves and reacted quartz and olivine crystals. Previous studies have used the 1663 lava as a mafic end member in mixing models (e.g. Nakada and Motomura, 1999; Chen et al., 1999), which contains ~57 wt.% SiO_2. Another candidate for the mafic end member is the most mafic Porphyritic enclave, which contains ~51 wt.% SiO_2. Both the 1663 lava and most mafic Porphyritic enclave contain abundant host-derived phenocrysts, which require some degree of mixing prior to quenching. In addition, a larger proportion of incorporated host-derived rhyolite liquid component undoubtedly accompanied the engulfment of host phenocrysts into the enclave-forming magma into the groundmass. Therefore, neither of these candidates can accurately represent a mafic mingling end member.

One proxy for the mafic end member is to analyze olivine crystals present in Porphyritic enclaves and Unzen lavas. Although olivines are usually unrimmed in

Porphyritic enclaves, they are clearly unstable in Unzen host lavas and the 1663 lava as evidenced by reaction rims of orthopyroxene or hornblende where crystal faces are in contact with the matrix glass. Olivines compositions from enclaves and lavas range from Fo_{65} to Fo_{75}, which is common for olivines in high-aluminum basaltic magmas of andesitic arcs.

After accounting for oxygen fugacity based on magnetite and ilmenite pairs to calculate correct proportions of Fe^{2+} and Fe^{3+} in olivine and glasses (Sack et al., 1980), the exchange equilibria of Mg and Fe^{2+} between olivine and melt (Roeder and Emslie) indicate that the Unzen residual olivines crystallized from a basaltic melt with a range of FeO/ MgO (mole%) ratios between 0.6 and 0.9. The calculated FeO/MgO (mole %) ratios for melts equivalent to the bulk composition of the Porphyritic enclaves and the 1663 andesite range from 0.75 to 1.1, which is consistent only with the most evolved Unzen olivine compositions (Fig. 1.17). The most primitive olivines could not be precipitated from the most primitive enclave, which is 51 wt.% SiO_2 and itself shows evidence of hybridization. Therefore, we estimate the mafic end member to have a SiO_2 content of ~50 wt.% for the purposes of mixing calculations based on the correlation of the most primitive predicted FeO/MgO (mole%) melt ratio (0.6) and mixing trend from the silicic end member. This is clearly not a "primitive" basaltic composition indicative of direct mantle derivation (Luhr and Carmichael, 1985; Bacon et al., 1997; Clynne and Borg, 1997), implying the possibility that the intruding basalt end member evolved substantially since extraction from the mantle and prior to intrusion into the Unzen magma reservoir.

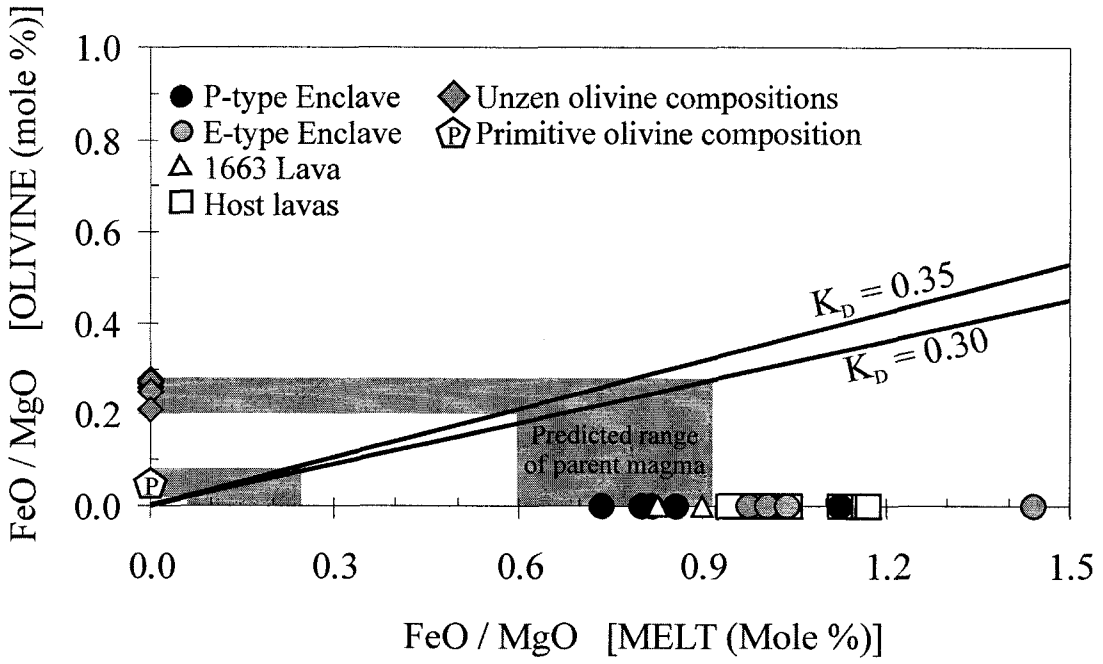

Figure 1.17
Olivine compositions from Unzen samples. The measured FeO to MgO ratio (mole %) for olivines from Porphyritic enclaves, host lavas, and the 1663 lava (shaded diamonds) corrected for oxygen fugacity (e.g. Sack et al., 1980) plotted against the measured FeO to MgO (mole%) for whole-rock compositions of the Porphyritic enclave (filled circles), Equigranular enclaves (gray circles), host lavas (open squares), and 1663 lava (open triangles). Given a range of distribution coefficients (K_D) for the exchange of Fe and Mg between olivine and coexisting melt of 0.30 and 0.35, (Roeder and Emslie, 1970; Ulmer, 1989), the olivine found in Unzen eruptive products are predicted to have crystallized from a basaltic melt with a range of FeO/ MgO (mole%) ratios between 0.6 and 0.9. Note that difference between olivine compositions from Unzen samples and those from more primitive magmas (data from Clynne and Borg, 1997).

Estimates of the proportion of end member magmas in Unzen lavas and enclave types suggest that both products of mingling are significantly hybridized (Fig. 1.18). Porphyritic enclaves contain a wide range of proportions of silicic end member from 5-55 wt.%. In contrast, Equigranular enclaves and 1663 andesite are made from nearly equal proportions of each end member, ranging from 45- 55 wt.% silicic end member component. Finally, host lavas contain between 10 to 25 wt.% of the mafic end member. These high mixing proportions are consistent with the disequilibrium mineral assemblage of Unzen lavas and enclaves where reaction rims and embayed and/or partially dissolved crystal faces like quartz and albitic-cored plagioclase exist in the Porphyritic enclaves and olivine and clinopyroxene exist in Unzen lavas.

Mingling Model

The occurrence of the two texturally distinct enclave types in all enclave-bearing lavas erupted from Unzen suggests that we might look for conditions that could give rise to both during a single intrusive event. The textural and petrologic differences between Equigranular and Porphyritic enclaves are interpreted to be the result of different, but not necessarily exclusive, modes of formation (Fig. 1.19). We propose that replenishment events at Unzen are characterized by the intrusion of high alumina olivine-bearing basaltic magma into the base of a silicic magma chamber (e.g. Wiebe, 1994; Snyder and Tait, 1995). Upon intrusion, the replenishing basalt engulfs, assimilates, and mixes with portions of adjacent magma and phenocrysts of the resident silicic magma. The intruded magma, now an andesite hybrid, experiences rapid crystallization and subsequent second

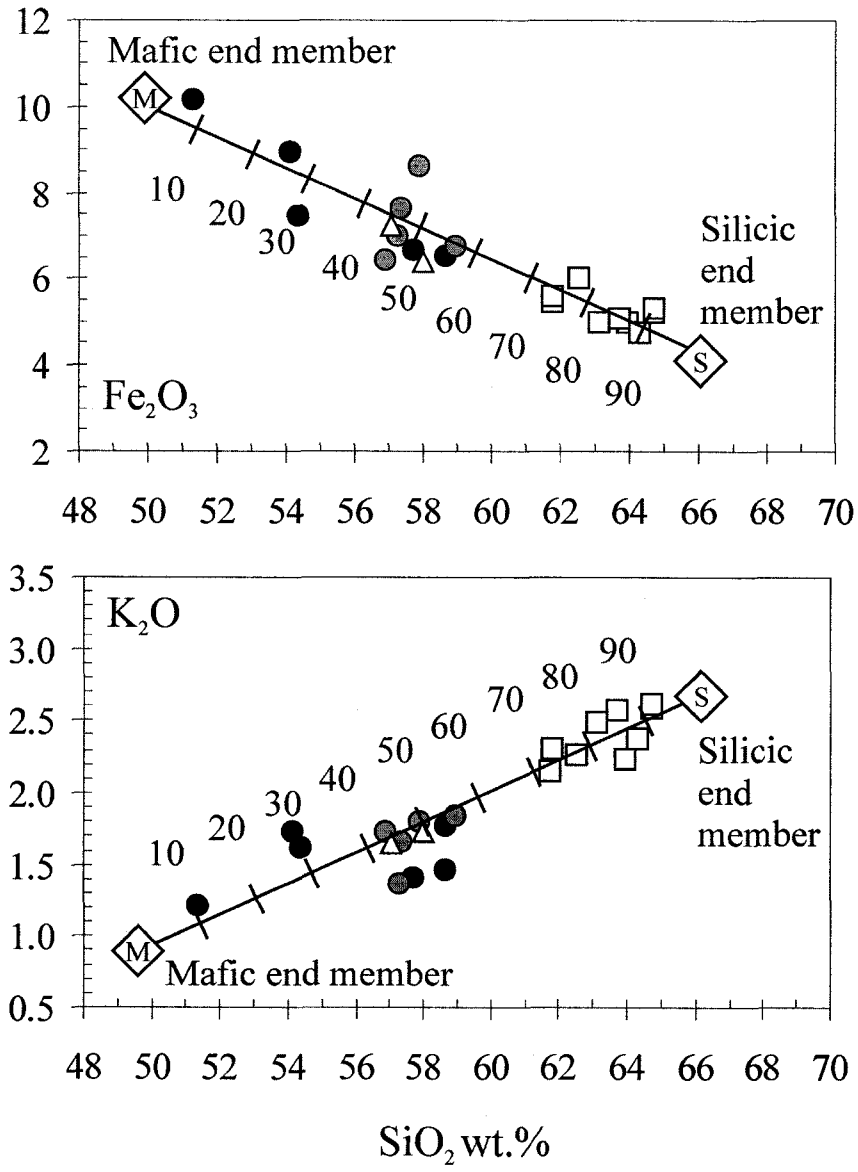

Figure 1.18
Mixing line showing proportions of a mafic (M) and silicic (S) end members in Unzen host lavas, P-type and E-type enclaves, and the 1663 lava flow plotted on K_2O and Fe_2O_3 versus SiO_2 variation diagrams. Tick marks on mixing line indicate weight percent of the silicic end member. See text for discussion of mixing end member compositions.

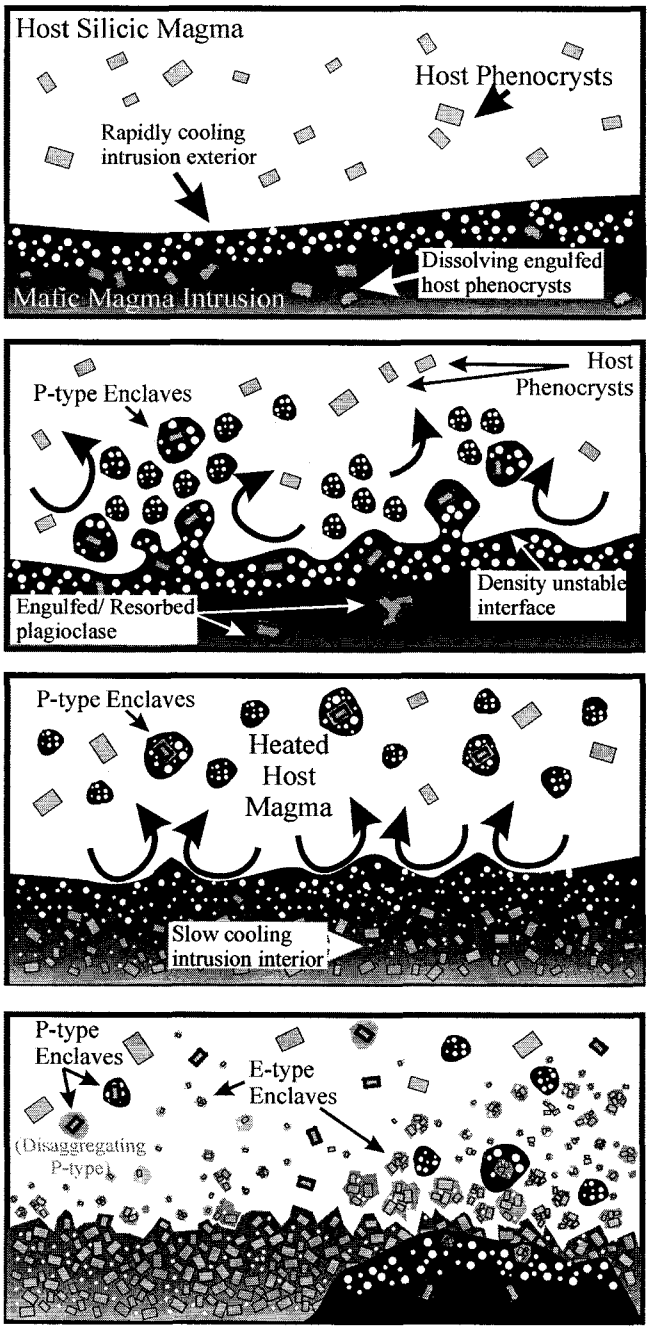

Figure 1.19
Schematic mingling model for the formation of Porphyritic and Equigranular enclaves in the Unzen magma chamber. See text for discussion.

boiling in response to heat loss to the overlying silicic host magma (Huppert et al., 1982b; Jaupart and Vergniolle, 1989). As a result, blobs of andesitic hybrid rise buoyantly into the overlying host magma- accelerating the cooling and crystallization process (Eichelberger, 1980; Huppert et al., 1982a). These become Porphyritic enclaves.

Meanwhile, the temperature contrast between the hybridizing intrusion and resident silicic host magma decreases. The portion of the intrusion in contact with the host magma cools through mixing with and conduction to the overlying cool silicic host. The silicic magma above the interface is warmed through conduction and by incorporation of disrupted mafic material. As the degree of undercooling diminishes, so does convection in the mafic intrusion interior, resulting in the slow crystallization of a framework of equigranular crystals in a vesicular matrix. This slower cooling permits thorough homogenization and hence the more limited range in composition. It also allows time for thorough digestion, rather than partial resorption, of engulfed phenocrysts from the silicic magma and dissolution of olivine inherited from the basalt.

Equigranular enclave clots are stripped off the cooling intrusion by convective stirring, or perhaps disrupted during subsequent replenishment events. Equigranular enclaves are subsequently dispersed throughout the host magma. Some may be engulfed by subsequent intrusion events as indicated by their occasional presence in Porphyritic enclaves. In examples of mafic intrusions in silicic plutons, the volume of the mafic intrusion interior typically exceeds the quenched exterior (e.g. Wiebe et al., 2002). This is consistent with Equigranular enclaves being 2 to 5 times more abundant compared to Porphyritic ones.

Variation of Mingling Model

We have discussed an intrusion of mafic magma in lava flow-like form (e.g. Wiebe, 1994; Snyder and Tait, 1995), but mafic magma may also replenish silicic reservoirs vigorously as a low viscosity, bubble-rich fluid due to CO_2-rich vapor exsolution prior to injection (e.g. Huppert et al., 1982a; Phillips and Woods, 2001). Instead of ponding at the base of the chamber, such a model predicts that a turbulent jet will be generated upon initial injection, then subsiding to produce a flow that cools relatively slowly on the floor of the chamber. In such a case, Porphyritic enclaves might represent quenched blobs in the turbulent "spray" from the basalt plume, and Equigranular enclaves might be produced by slow cooling of the flow on the magma chamber floor. This model is consistent with observations from Unzen, such as: (1) widespread distribution of mafic phenocrysts and enclaves in the host lavas; (2) the lack of intermediary enclave textures, for two distinct mingling mechanisms would likely produce two unique textures; (3) the large range in size for Porphyritic enclaves (5- 30 cm), which might be expected from a chaotic and turbulent plume; and (4), the large coalesced vesicles in Porphyritic enclaves, suggestive of two episodes of vesiculation, one prior to intrusion due to the exsolution of CO_2-rich vapor.

The crystallization of intruded mafic magma is not an instantaneous response to cooling, however. If it were, little or no mingling would occur at all. For example, experimental results cited previously indicate that 0.3 to 8 days are required for the growth of resorption zones of equivalent thickness on incorporated sodic plagioclase as

those observed in Unzen Porphyritic enclaves. This implies that a "spray model" origin for Unzen enclaves is unlikely due to the required time for resorption zone formation and microphenocryst growth. We concede, however, that if resorption and crystallization actually occur faster than experimentally observed thus far, for example because the resorption occurs at higher temperatures, the spray model could be viable.

Mingling Implications

The important aspect of the mixing style presented here is that 2 texturally distinct types of enclaves may be generated from single magma mixing events. Enclave-bearing lavas from some volcanoes, however, preferentially contain enclaves of one texture. For example, lavas erupted from Augustine volcano, Alaska; almost exclusively contain enclaves with porphyritic texture. Conversely, lavas erupted from Pinatubo volcano, Philippines; preferentially contain enclaves that are equigranular (Pallister et al., 1996). Nonetheless, both textural types are ubiquitous in the enclave-bearing lavas of Unzen, and are commonly found in enclave-bearing lavas elsewhere, such as Mount Lassen, California (Heiken and Eichelberger, 1980), Mount Dutton, Alaska (Miller et al., 1999), and Kizimen Volcano, Kamchatka. Wiebe (1994) and Wiebe et al. (2002) also observed both types of enclaves in plutonic rocks. This strongly suggests that both textural enclave types are likely products of interaction of the same magma, resulting from different styles of magma mingling during the same or successive mafic replenishment events. We have suggested one way in which this could occur during a single replenishment event.

1.6 CONCLUSIONS

(1) All erupted products from Mount Unzen record replenishment events of high-aluminum olivine basalt magma into the silicic magma reservoir as indicated by abundant and evenly distributed magmatic enclaves, disequilibrium phenocryst assemblages, and textures of both host and enclave-free lavas.

(2) Magmatic enclaves are divided into two texturally distinct groups, Porphyritic and Equigranular. The texture, petrology, and geochemistry of Porphyritic enclaves indicate that they formed by rapid cooling at the interface between intruded basalt and silicic magma, whereas Equigranular enclaves crystallized more slowly in the interior of the mafic intrusion.

(3) Even the most silicic host dacite lavas (~65 wt.% SiO_2) and mafic Porphyritic enclaves (~51 wt.% SiO_2) contain evidence of contamination, therefore silicic (~66 wt.% SiO_2) and mafic (~50 wt.% SiO_2) end members are assumed for mixing calculations. Significant incorporation of both end member magmas is necessary to explain the observed compositions, where Porphyritic enclaves contain 5- 55 wt.% silicic component, Equigranular enclaves and 1663 andesite contain nearly equal proportions of each end member, and host lavas contain between 10 to 25 wt.% mafic end member.

(4) Replenishment events at Unzen are characterized by the intrusion of high alumina olivine-bearing basaltic magma into the base of a silicic host magma chamber, engulfing and mixing with portions of surrounding host melt and phenocrysts. The intruded magma, now an andesitic hybrid, experiences rapid crystallization and subsequent second boiling in response to heat loss into overlying silicic host magma. As

a result, the hybrid buoyantly rises into the host magma, quenching in the cooler silicic host. The interior of the hybrid intrusion, however, cools more slowly, resulting in a crystallized framework of equigranular, tabular crystals in a poorly vesicular matrix. Equigranular enclaves and crystal clots are disrupted, stripped off, and subsequently dispersed in the host magma as a result of convective stirring or simply detaching along the preferentially weak zones of the microphenocryst framework. Equigranular enclaves may also be disrupted and subsequently engulfed by successive intrusion events.

(5) When a basaltic intrusion event occurs, many (but not all) host-derived phenocrysts are engulfed by the basaltic magma. Engulfed plagioclase phenocrysts react to the dramatically different surrounding melt composition and temperature with the development of a resorption zone, and crystallize a rim composition of identical An content and Sr/Ba ratio to plagioclase microphenocrysts crystallizing from the basalt. Over time, the engulfed plagioclase grains are recycled back into the host magma as Porphyritic enclaves disaggregate. This produces a diverse population of phenocrysts with distinctly different crystallization histories from distinctly different magmas.

(6) Both textural types of enclaves observed at Unzen are common in enclave-bearing lavas erupted from other volcanoes including Mount Lassen, Mount Dutton, and Kizimen volcano. Wiebe (1994) and Wiebe et al. (2002) also observed both types of enclaves in plutonic rocks, suggesting that both textural enclave types are products of the same magma, resulting from different styles of magma mingling during the same or successive mafic replenishment events.

CHAPTER 2.

2.1 INTRODUCTION

Many important characteristics of volcanic eruptions are controlled by the rate at which magma ascends to the surface. For example, the way magma ascends influences eruptive style (Sigurdsson et al., 1990; Martel et al., 1998), magma supply and withdrawal (Scandone and Malone, 1985; Carey and Sigurdsson, 1987), earthquake type and occurrence (Martin-del Pozzo and Cifuentes, 2003), magma mixing (Freundt and Tait, 1986; Koyaguchi and Blake, 1989), and mineralogical changes in the rising magma (Martel et al., 1998; Cashman and Blundy, 2000; Blundy and Sparks, 2002; Hammer and Rutherford, 2002). Therefore, understanding the manner in which magma ascends through the shallow crust to the surface during eruption is essential in resolving how volcanic eruptions occur and to aid in assessing risks for future eruptions.

The rate of magma ascent strongly controls important chemical and mineralogical reactions that occur when volatile-rich magmas rise to the surface as a result of substantial changes in confining pressure. One reaction that is a direct result of magma ascent is the exsolution of volatiles from the melt. Volatiles dissolved in the melt will tend to diffuse and exsolve into bubbles during ascent because of their lower solubility in melt at lower pressures (Shaw, 1974). Some minerals that crystallize in magmas in deep storage chambers contain volatiles in their structure. For example, amphiboles may contain up to 3 wt.% H_2O in their crystal structure (Deer et al., 1992). Because the

concentration of dissolved water species in melt decreases as magma rises to the surface, hydrous minerals like amphibole tend to become unstable and react with the surrounding melt (Rutherford and Devine, 1988). As a result, a reaction rim of anhydrous minerals, such as pyroxene, plagioclase, and Fe-Ti oxides may develop around the unstable amphibole (Fig. 2.1). Reaction rims can also occur if the thermal stability of amphibole is exceeded, for example, because of magma mixing. In this case, destabilized amphiboles react with the surrounding melt and crystallize reaction rims composed of minerals that are stable at higher temperatures.

The rates of amphibole breakdown in response to magma ascent and heating have generally not been determined because they are complex functions of many variables, including mineral and melt compositions, melt viscosity, temperature, and pressure. Rutherford and Hill (1993) performed decompression experiments using a hornblende-bearing dacite erupted at Mount St. Helens in 1980. These experiments were performed at a constant decompression rate from a pressure that correlates with a depth of approximately 8 km to near-surface conditions. Rutherford and Hill (1993) found that slower decompression rates resulted in hornblende phenocrysts having thicker reaction rims. Rutherford and Hill (1993) used their calibrated reaction rate to estimate magma ascent rates from Mount St. Helens by converting pressure changes to depth changes. More recent studies have used that calibration to estimate ascent during eruptions at Montserrat (Devine et al., 1997), Redoubt volcano (Wolf and Eichelberger, 1997), and Unzen volcano (Venezky and Rutherford, 1999).

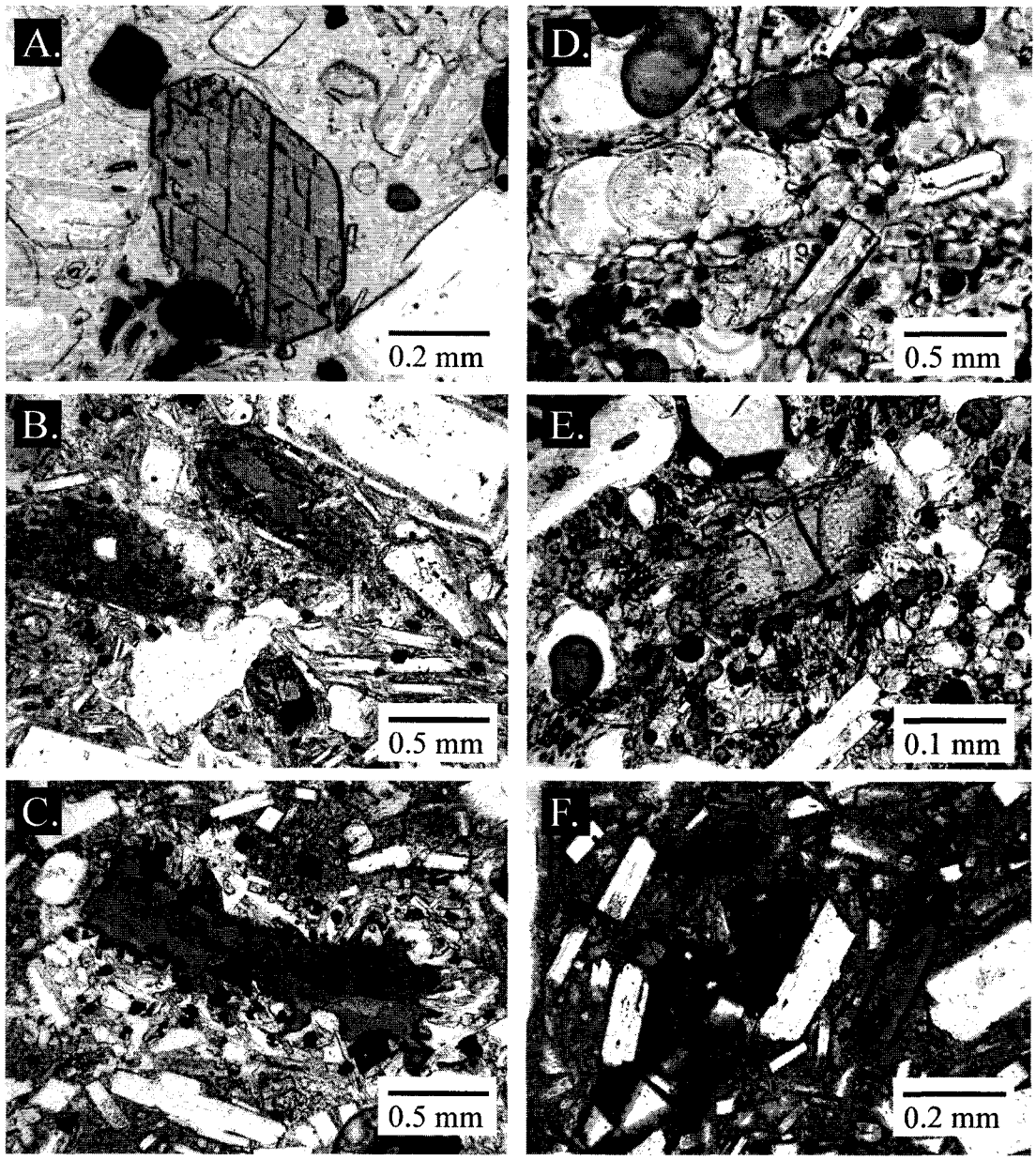

Figure 2.1
Photomicrographs of Redoubt amphibole erupted between 12/15/1989 and 6/20/1990. A, unrimmed hornblende typical of dacite pumice erupted on December 15 1989; B, Fine-grained reaction rims enclose hornblende amphiboles with subhedral crystal edges erupted on April 15 1990; C, Course-grained reaction rim of clinopyroxene and calcic plagioclase surround embayed and anhedral hornblende erupted on January 1, 1990; D, unrimmed pargasite typical of andesite pumice erupted on December 15 1989; E, Fine-grained reaction rim encloses subhedral pargasite crystal erupted on February 15 1990; F, hornblendes with "black rims" typical of the final dome (April- June, 1990).

Clearly, studies of amphibole reaction rims provide valuable data about the rates of mineralogical reactions that occur during magma mixing and ascent. Unfortunately, such information could not be fully utilized for many reasons. Firstly, decompression-induced amphibole breakdown was calibrated only for the 1980 Mount St. Helens dacite. Because this reaction is between the amphibole and surrounding melt, the rate is undoubtedly influenced by melt composition, and hence magma composition. Secondly, melt viscosity and melt water content, all of which change as pressure decreases during ascent and the melt crystallizes as driven by gas loss. At present, however, amphibole breakdown during decompression is calibrated only for constant ascent rates of a single bulk composition. Therefore, understanding reaction rate as a function of decompression path was needed to quantitatively evaluate magma ascent. Amphibole breakdown is also not calibrated for isobaric thermal breakdown, which prevents the ability to differentiate rims caused from magma mixing events and those that formed during ascent.

This study expands upon previous studies on magma ascent by experimentally examining the breakdown reactions of amphibole using the erupted magma from Redoubt volcano in 1989-1990. Two magmas were erupted during that time (Nye et al., 1994), providing an excellent opportunity to compare amphibole breakdown between magmas. One magma type is dacite that contains microphenocrysts (~35%) of plagioclase, orthopyroxene, magnetite, ilmenite, and hornblende that is similar to that in the 1980 Mount St. Helens magma. Although the bulk compositions of the Redoubt and Mount St. Helens dacites are the same, however, the Redoubt dacite melt composition is more silicic (~10% more SiO_2 wt.%) and cooler (~60°C) (Nye et al., 1994; Swanson et al.,

1994), allowing for an investigation of the influences of temperature and melt composition on amphibole breakdown. The other magma erupted from Redoubt is andesitic in composition and contains microphenocrysts (~30%) of plagioclase, clinopyroxene, orthopyroxene, magnetite, rare ilmenite, and pargasite (Nye et al., 1994). This magma enables the investigation whether pargasite reacts raster than hornblende.

2.2 GEOLOGIC SETTING

Redoubt Volcano, located 180 km southwest of Anchorage near the eastern margin of Lake Clark National Park and Wilderness, is a 3108-m-high stratovolcano that has produced at least 30 Holocene tephras in the Cook Inlet region (Fig. 2.2) (Riehle, 1985). The volcano is composed of intercalated lava flows and pyroclastic deposits and exists atop Mesozoic granitic rocks of the Alaska-Aleutian Range batholith (Reed and Lanphere, 1973; Till et al. 1994). Redoubt is capped by a 1.8-km-wide, ice-filled summit crater that is breached on the north side by the Drift Glacier, which flows northward and spreads into a piedmont lobe in the upper Drift River Valley.

Redoubt is one of six Quaternary volcanoes along the west margin of Cook Inlet. These volcanoes comprise the east end of the 2600-km-long Aleutian volcanic arc, formed as a result of subduction of the Pacific plate beneath the North American plate. Of the six volcanoes, Spurr, Augustine, and Redoubt have been historically active. Earlier historical explosive eruptions from Redoubt occurred in 1902 and 1966, with lesser phreatomagmatic activity in 1933, 1967, and 1968 (Beget and Nye, 1994). Vent-clearing

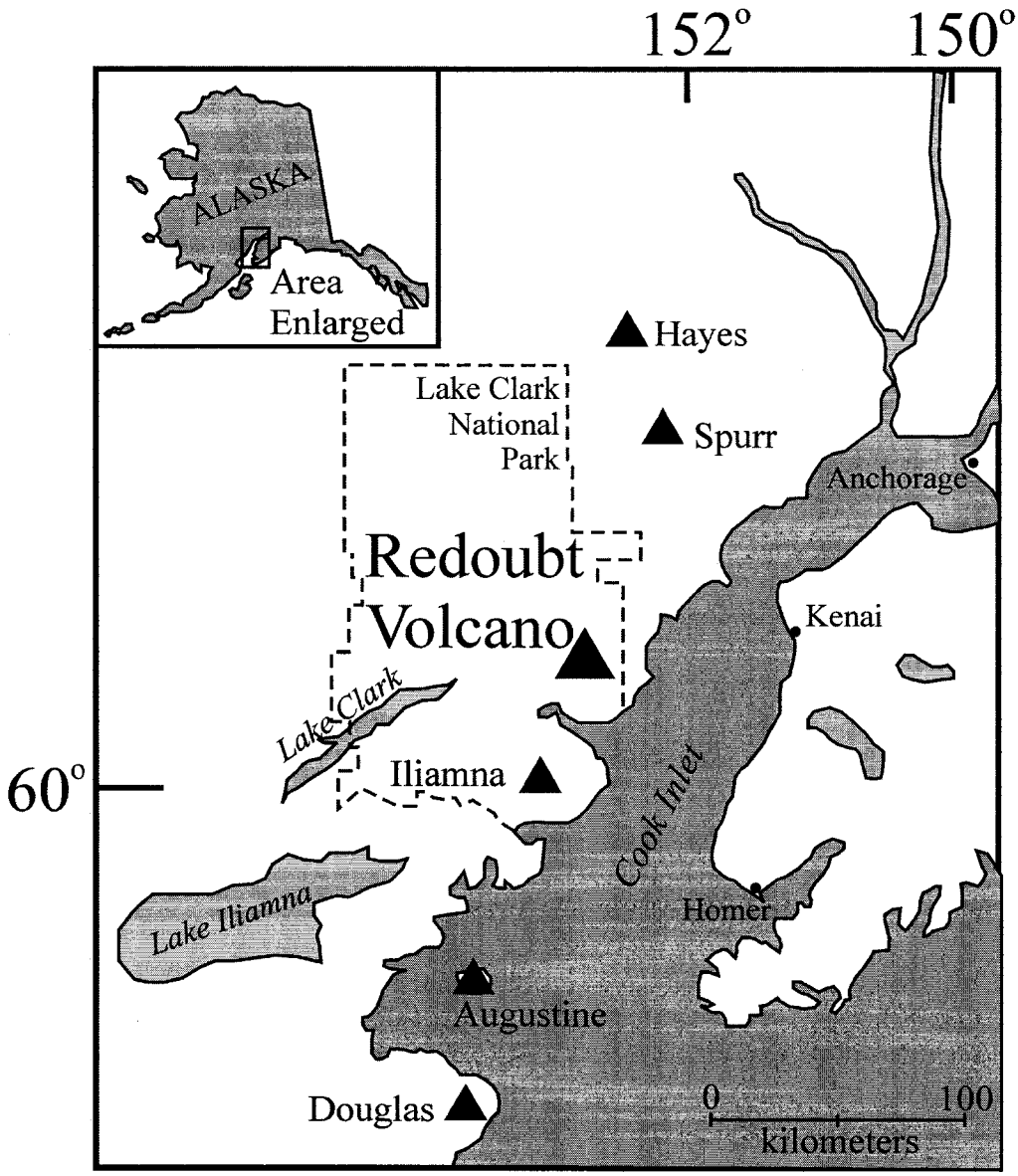

Figure 2.2
Location map of Cook Inlet volcanoes. Redoubt volcano exists within Lake Clark National Park (boundary shown), approximately 180 km SW of Anchorage.

explosions, repetitive dome emplacement and destruction events, and lahar formation typically characterize eruptions from Redoubt (Till et al., 1994).

Chronology of the 1989-90 Eruption

The 1989-90 eruption of Redoubt seriously impacted public transportation, commerce, commercial air traffic, and natural resource development efforts throughout Cook Inlet. The total economic loss from this eruption is estimated to be $160 million (Miller and Chouet, 1994), making the eruption of Redoubt the second most costly in U.S. history (1980 Mount St. Helens remains the most costly).

The 1989-90 Redoubt eruption lasted for 6 months, but activity was not continuous and the character of the eruption ranged from phreatic explosions to the formation of pyroclastic flows resulting from dome collapse. The eruption began with a phreatomagmatic, vent-clearing explosion at 9:47 am on December 14, 1989 after less than 24 hours of intense precursory seismicity (Brantley, 1990; Miller and Chouet, 1994). Over the next two days, several strong explosions resulted in ash plumes and clouds. The largest of which occurred on December 15, with the generation of an ash plume reaching >12 km above sea level and a pyroclastic flow that deposited juvenile pumice clasts down the Drift Glacier and Drift River valley.

The size and frequency of explosive events decreased after December 15, as the eruptive activity changed from being primarily explosive to repetitive building and destroying domes. The first and largest summit dome (20×10^6 m^3) was observed on December 26 (Miller, 1994). This was the first of 14 lava domes that were emplaced and

subsequently collapsed between December 21, 1989 and mid-April, 1990. Following an eruption on April 21, 1990, growth of the present dome began and continued through mid-June. The nature of earthquake activity changed after the December 15, 1989 eruption as volcano-tectonic events shifted from a depth of 0- 3 km to depths of 4- 10 km (Power et al., 1994).

Eruptions in December 1989 tapped two magmas, one a dacite (~63-64 wt.% SiO_2), the other an andesite (~58 wt.% SiO_2) (Nye et al., 1994; Swanson et al., 1994). The initial products from the December 15 eruption contain two unrimmed amphibole phenocryst types. The dacite contains hornblende, whereas the andesite contains pargasite (Swanson et al., 1994; Wolf and Eichelberger, 1997). Subsequent dome extrusions are composed primarily of magma that is a hybrid (~60 wt.% SiO_2) between the dacite and andesite end member compositions with both hornblende and pargasite surrounded by reaction rims of various widths (Swanson et al., 1994; Wolf and Eichelberger, 1997). Mineral and glass compositions in the hybrid magma, combined with seismic data suggest that a magma-mixing event immediately preceded the eruption in December 1989 (Nye et al., 1994; Swanson et al., 1994; Power et al., 1994).

2.3 METHODS

Experimental Techniques

A critical aspect of experimentally calibrating magma ascent rates is determining the depth that the magma last existed in the crust prior to ascent and eruption. Laboratory

determination of pre-eruptive magma storage conditions is based on analytical techniques and on experimental replication of the phase assemblage, natural compositions of melt and major minerals, and the appropriate mode of mineral phases (e.g. Rutherford et al., 1985; Gardner et al., 1995; Grove et al., 1997; Barclay et al., 1998; Hammer et al., 2002). Oxygen fugacity and temperature are first constrained by analyzing Fe-Ti oxide pairs in natural samples. A series of phase equilibria experiments then serve to establish the stability fields of the major phenocryst phases in pressure- temperature space. Finally, the compositions of coexisting experimental matrix glasses and phenocryst rims are compared with the rims of phenocrysts and matrix glass in natural samples to refine the equilibrium conditions because melts respond to the changes as functions of pressure and temperature of proportions and abundances of crystallizing phases.

The materials selected for pre-eruptive phase-equilibria experiments are large portions of lightly crushed dacite (92MHR6-1) and andesite (92MHR9-1) pumices erupted from Redoubt volcano on December 15, 1989 (Table 2.1). Samples were collected from a pyroclastic flow deposit 6 km to the north of Redoubt volcano in the Drift River Valley. No amphibole grains from dacite and andesite starting material contain reaction rims. All experiments were conducted in the UAF experimental petrology facility.

Table 2. 1.
Whole rock compositions 1989-90 Redoubt eruption samples (from Wolf and Eichelberger, 1997)

Sample #:	92MHR9-1	92MHR6-1	92MHR24-1	92MHR20-1	92MHR12-1	92MHR22-3	93KWRD11
Eruptive Event:	12/15/1989	12/15/1989	1/2/1990	1/2/1990	2/15/1990	4/15/1990	final dome
SiO_2	58.47	62.58	59.47	63.00	61.79	60.00	61.94
Al_2O_3	18.86	18.03	18.71	17.93	18.24	18.45	17.81
TiO_2	0.60	0.47	0.58	0.46	0.49	0.56	0.52
FeO *	6.20	4.69	5.74	4.57	4.92	5.72	5.42
MnO	0.15	0.13	0.14	0.13	0.13	0.14	0.14
CaO	7.44	6.03	7.10	5.90	3.27	6.88	3.06
MgO	2.67	1.95	2.48	1.86	2.03	2.47	2.16
K_2O	1.28	1.59	1.36	1.60	1.53	1.41	1.52
Na_2O	4.11	4.34	4.20	4.37	4.40	4.16	4.33
P_2O_5	0.22	0.19	0.22	0.19	0.20	0.21	0.12

* Total Fe is expressed as FeO

A series of phase equilibria experiments were performed at constant pressure and temperature to better constrain the field of amphibole stability. For dacite experiments, Ag or $Ag_{70}Pd_{30}$ tube charges with one end crimped and welded were filled with 0.1 to 0.5 grams of powdered dacite sample (92MHR6-1) and sufficient distilled water to ensure that all samples were water-saturated ($P_{H_2O} = P_{total}$) (Fig. 2.3A). The open end of the tubing was then crimped and the capsule weight was recorded. Then, the crimped end was welded and the capsule was heated for one hour on a 150°C hot plate to determine if any distilled water escaped during welding. Capsules were finally re-weighed, and discarded if water loss occurred. Experiments were performed in Rene cold-seal pressure vessels. Oxygen fugacity was buffered near the Ni-NiO (NNO) oxygen buffer curve by the reaction between the Ni-alloy vessel, a Ni filler rod, and water, which was also used as the pressurizing fluid (Geschwind and Rutherford, 1992). Temperature and pressure

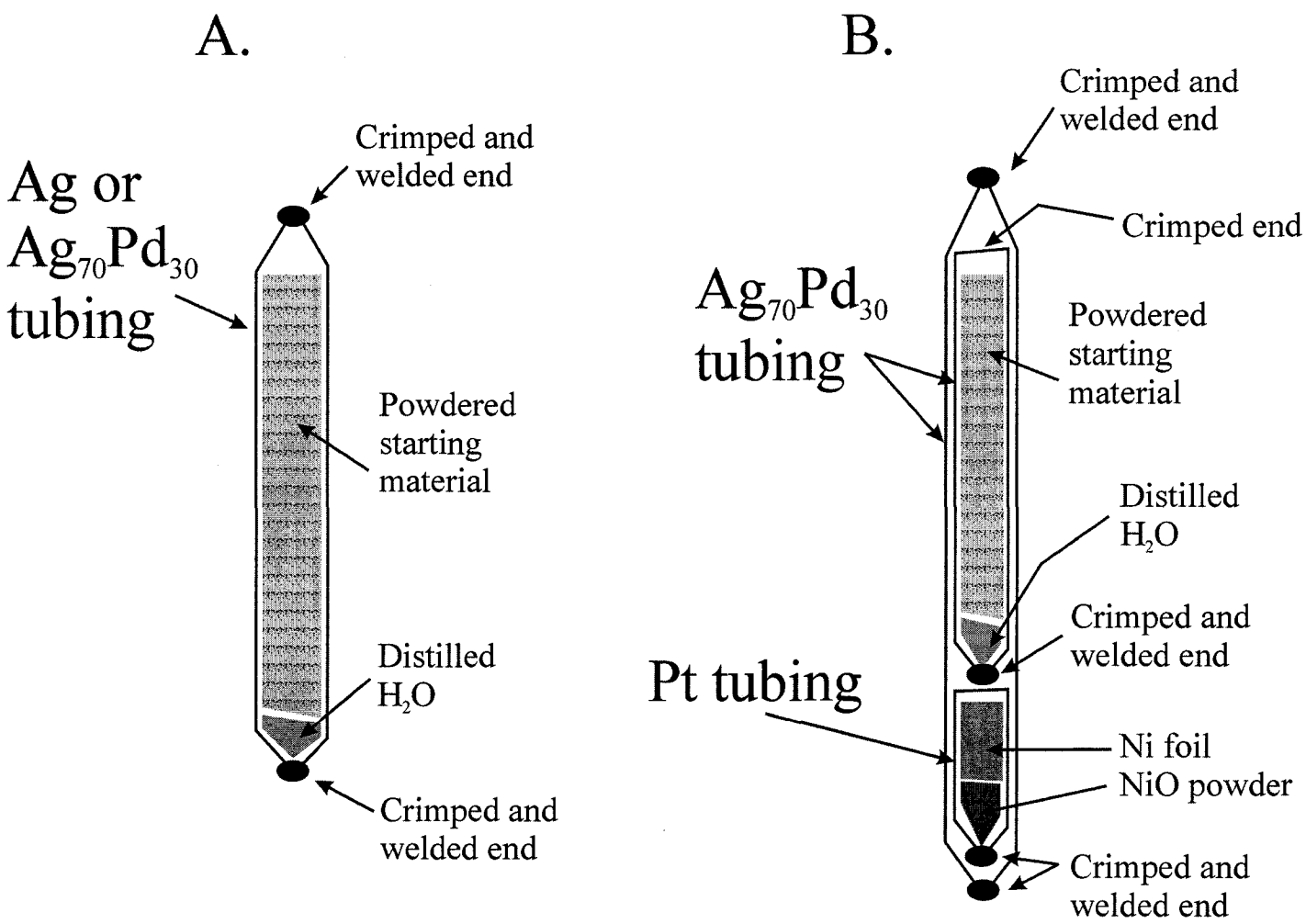

Figure 2.3
Schematic diagram of experimental sample configurations. See text for discussion.

settings are precise to ±3°C and ±0.5MPa, respectively. All phase equilibria experiments ran for between 3 and 5 days in order to grow crystals large enough to identify and analyze.

Phase equilibria experiments involving the andesite pumice were run in TZM (Tungsten-Zirconium-Molybdenum) pressure vessels, using a mixture of CH_4 gas with minor Ar as the pressurizing medium. Experimental charges consisted of powdered sample (92MHR9-1) in 2 or 3-mm-diameter $Ag_{70}Pd_{30}$ tubing and small amounts of Ni and NiO in 4-mm-diameter Pt tubing, which was used to monitor oxygen fugacity. Both capsules were then placed in 5-mm-diameter $Ag_{70}Pd_{30}$ tubing with sufficient distilled water to ensure that all experiments were water saturated ($P_{H_2O} = P_{total}$), weighed, and welded shut (Fig. 2.3B). Capsules were then placed on a 150°C hot plate for one hour and re-weighed to determine if any water loss resulted from welding. Capsules were discarded if water loss occurred. The oxygen fugacity of experiments were controlled by varying the composition of the Ar-CH_4 pressuring gas mixture. Examination of the remaining Ni in the capsules followed all experiments, where Ni loss was interpreted to indicate the experimental fO_2 was above the NNO buffer and below NNO +2 (Pownceby and O'Neill, 1994). Temperature and pressure settings are precise to ±5°C and ±5MPa, respectively. All phase equilibria experiments ran for at least 12 hours in order to grow crystals large enough to identify and analyze.

Isothermal decompression experiments were performed on dacite samples in two ways to investigate how hornblende reaction rims form. All decompression experiments were performed in Rene cold-seal pressure vessels where they were initially held at the

pre-eruptive pressure and temperature conditions, determined through phase-equilibria experiments, for 3 to 5 days before carrying out the pressure drop. Multi-step experiments were decompressed at regular time intervals using a controlled pressure intensifier to simulate magma ascent at a steady rate over 3 to 15 days down to 1 MPa, before being quenched. Single-step experiments were decompressed to lower pressures in one step using controlled pressure leaks from a valve and held for between 2 and 25 days before being quenched.

Isobaric heating experiments were performed on dacite samples to investigate the effect that an intrusion of higher temperature andesite magma into a dacite magma chamber prior to eruption would have on hornblende stability. All heating experiments were initially held at the pre-eruptive pressure and temperature conditions, determined through phase-equilibria experiments, for 5 days in Rene cold-seal pressure vessels. Samples were then heated isobarically to 950 °C in cold seal TZM pressure vessels, where they were held for 2 to 12 hours, and finally quenched.

Electron Microprobe Techniques

After experimental runs, samples were mounted in epoxy on thin sections and polished. Back-scattered electron (BSE) images and mineral and glass analyses were obtained from thin sections of natural and experimental samples using a Cameca SX-50 electron microprobe, located in the University of Alaska Fairbanks Advanced Instrumentation Laboratory. BSE images were conducted using a 2-μm-wide focused beam, an accelerating voltage of 15 KeV, and a beam current ranging from 25 to 50 nA.

Mineral analyses were done using a 2-μm-wide focused beam, an accelerating voltage of 15 KeV, and a beam current of 10 nA. Glass analyses were done with a 10-micron-wide defocused beam, an accelerating voltage of 15 KeV, and a beam current of 8 nA in order to minimize sodium migration. Sodium was counted in two-second intervals for the first 10 seconds of each analyses, and the counts were regressed to determine the initial sodium content. Test analyses of variably hydrated, standard reference glasses prior to and following analyses of unknowns were also performed (e.g. Devine et al., 1995). Mineral phases in the experiments were identified both optically and with energy dispersive spectroscopy on the electron microprobe. Phase stability was determined based on the presence of new, euhedral crystals that grew during the experiment.

Amphibole Rim Width Measurement Techniques

The widths of amphibole breakdown rims were measured in polished thin sections of both natural and experimental samples using a graduated micrometer mounted on the ocular of a stereomicroscope. The sections were examined in both transmitted and reflected light, as well as using BSE images. Rim width measurements were made using back-scattered electron images and reflected light analysis because they more clearly illustrate the true reaction rim. Repeated measurements of amphibole rims indicate that the uncertainty (1 σ) of this method is 10%.

2.4 RESULTS

Amphibole in Natural Redoubt Samples

Amphibole is the most abundant mafic mineral phase in all 1989-90 Redoubt samples, accounting for 4.5- 5 vol.% in pumice samples. The amphiboles are of two main types: hornblende that contains 7- 11 wt.% Al_2O_3 and pargasite that contains 12- 15 wt.% Al_2O_3 (Wolf and Eichelberger, 1997) (Fig. 2.4 and Table 2.2). Nearly all amphibole found in dacite and andesite pumice samples erupted on December 15, 1989 are euhedral and lack reaction rims (Fig 2.1A, Fig. 2.5). What reaction rims that do exist are thick (20-80 μm), coarse grained and composed of clinopyroxene and calcic plagioclase along embayed crystal edges of anhedral hornblende. Dacite dome samples erupted on December 26 1989 contain both rimmed and unrimmed hornblendes. Unrimmed hornblendes are subhedral (Fig. 2.6A), whereas anhedral grains have embayed crystal edges and are broadly enclosed by thick (20- 100 μm), coarse-grained rims composed of clinopyroxene, calcic plagioclase, and Fe-Ti oxides (Fig 2.6B). Most pargasite grains from December 15, 1989 dome samples are unrimmed (Fig. 2.6C), although some are surrounded by thin, fine-grained reaction rims (2- 8 μm) composed of plagioclase and orthopyroxene.

Most amphibole observed in dome samples erupted January 2 1990 are subhedral and unrimmed (Fig. 2.6D). Thick (10- 80 μm), coarse-grained reaction rims composed of calcic plagioclase, clinopyroxene, and Fe-Ti oxides exist around anhedral hornblendes (Fig. 2.6E). Most pargasite is unrimmed, although margins of some crystals appear partially dissolved, based on their diffuse texture (Fig. 2.6F). Amphiboles in subsequent

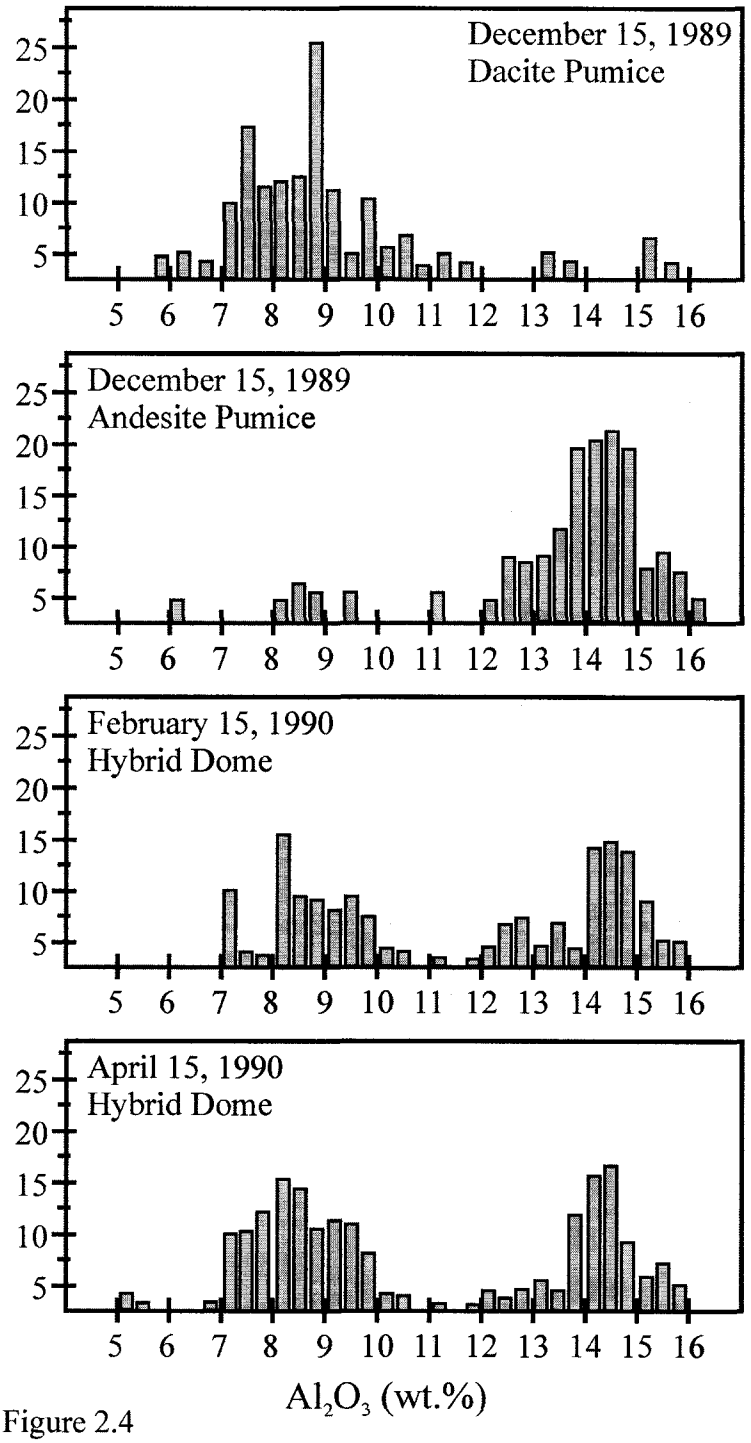

Figure 2.4
Amphibole Al_2O_3 (in wt. %) contents for eruptive products throughout the 1989-90 eruption (modified from Wolf and Eichelberger, 1997). Redoubt deposits contain two different amphiboles, hornblende (7- 11 wt.% Al_2O_3) and pargasite (12- 15 wt.% Al_2O_3).

Table 2.2
Electron microprobe analyses of amphiboles (Oxides in wt.%)

Sample	Amphibole	Event	microns	SiO_2	TiO_2
92MHR6-1	HBL	Dec 15 1989	0.00	45.57	1.81
			49.67	45.73	2.11
			66.79	45.38	2.40
			83.07	46.13	2.14
92MHR9-1	PG	Dec 15 1989	0.00	41.18	1.29
			25.00	41.07	1.32
			60.00	40.59	1.72
92MHR20-1	HBL	Jan 2 1990	0.00	45.33	1.62
			16.76	46.97	1.85
			32.57	44.71	1.97
			49.34	44.44	1.97
			66.10	45.29	1.46
			82.86	47.78	1.40
			98.67	48.34	1.38
92MHR20-1	PG	Jan 2 1990	0.00	40.34	1.44
			33.54	40.35	1.13
			60.84	40.56	1.25
			86.02	40.94	1.38
			127.99	40.54	1.32
			138.99	40.80	1.40
92MHR12-1	HBL	Feb 15 1989	15.30	48.29	1.77
			30.82	47.93	1.32
			77.92	48.12	1.61
			93.22	48.33	1.65
			109.50	48.33	1.47
			140.32	48.17	1.54

Al_2O_3	FeO	MnO	MgO	CaO	Na_2O	K_2O	F	Cl
8.49	12.56	0.40	14.54	10.79	1.87	0.72	0.46	0.42
8.45	12.99	0.49	14.66	11.06	1.77	0.47	0.00	0.09
8.50	12.21	0.70	14.68	11.10	1.79	0.43	0.00	0.10
9.34	11.64	0.33	14.90	11.35	2.13	0.36	0.39	0.09
15.68	11.09	0.39	12.16	12.60	2.89	0.38	0.00	0.05
15.54	11.86	0.33	12.15	12.69	2.85	0.34	0.26	0.00
15.35	11.61	0.41	11.69	12.83	2.72	0.28	0.20	0.05
8.94	13.21	0.65	14.33	11.09	1.75	0.35	0.00	0.05
7.49	11.76	0.40	15.12	10.85	1.42	0.33	0.00	0.07
9.41	13.48	0.60	13.96	11.14	1.79	0.38	0.00	0.09
9.23	12.87	0.48	14.00	10.93	1.79	0.39	0.26	0.07
9.31	12.57	0.55	13.96	11.19	1.79	0.38	0.00	0.09
7.31	11.89	0.64	15.80	11.00	1.38	0.23	0.20	0.07
6.72	11.65	0.42	15.97	10.96	1.48	0.29	0.39	0.07
15.07	11.39	0.42	13.83	12.19	2.85	0.33	0.00	0.06
15.29	11.94	0.38	13.41	12.62	2.91	0.31	0.19	0.01
15.23	11.82	0.40	13.86	12.74	2.09	0.26	0.51	0.02
15.19	12.07	0.31	12.65	12.66	1.77	0.37	0.13	0.02
15.06	11.49	0.26	12.72	11.80	2.98	0.29	0.00	0.05
15.22	11.65	0.36	12.70	11.21	2.82	0.30	0.19	0.06
6.70	11.69	0.43	15.46	11.34	1.59	0.26	0.20	0.11
6.61	10.69	0.39	15.88	11.29	1.47	0.29	0.00	0.08
6.58	11.70	0.35	15.87	11.14	1.38	0.32	0.00	0.06
6.55	11.59	0.52	15.88	10.83	1.53	0.22	0.00	0.12
6.55	11.10	0.35	15.60	11.21	1.42	0.31	0.00	0.11
6.44	11.95	0.41	15.60	10.99	1.29	0.27	0.07	0.11

Table 2.2 (cont.)
Electron microprobe analyses of amphiboles (Oxides in wt.%)

Sample	Amphibole*	Event	microns	SiO_2	TiO_2	Al_2O_3	FeO	MnO	MgO	CaO	Na_2O	K_2O	F	Cl
RDT-4	HBL		0.00	45.67	2.05	8.99	12.75	0.29	14.28	11.10	1.98	0.40	0.65	0.11
			16.49	45.26	2.78	8.77	12.91	0.36	14.00	11.29	1.90	0.44	0.20	0.10
RDT-4	HBL		0.00	45.81	1.95	8.78	12.38	0.28	14.26	10.80	1.86	0.44	0.46	0.13
			22.81	45.77	1.27	9.68	12.42	0.55	14.10	10.86	1.99	0.30	0.00	0.02
RDT-A-1	PG		0.00	41.74	1.75	14.06	11.97	0.23	12.37	12.07	2.55	0.44	0.00	0.07
			13.04	41.32	1.86	14.19	11.27	0.14	12.35	12.08	2.60	0.44	0.20	0.02
RDT-A-1	PG		0.00	41.39	2.39	13.37	11.34	0.26	14.39	11.61	2.56	0.44	0.52	0.06
			9.12	41.07	2.49	13.22	11.19	0.11	14.42	11.76	2.50	0.39	0.00	0.06
			18.24	42.00	1.94	13.46	11.58	0.19	14.72	11.86	2.56	0.43	0.00	0.00
RDT-A-2	PG		0.00	40.51	2.10	16.23	11.87	0.21	14.66	10.04	2.51	0.37	0.20	0.01
			9.44	40.72	2.21	16.42	11.30	0.15	14.38	10.95	2.42	0.41	0.00	0.03
			18.88	40.58	2.47	16.26	11.15	0.23	14.10	10.24	2.51	0.45	0.33	0.03

* HBL, Hornblende; PG, pargasite

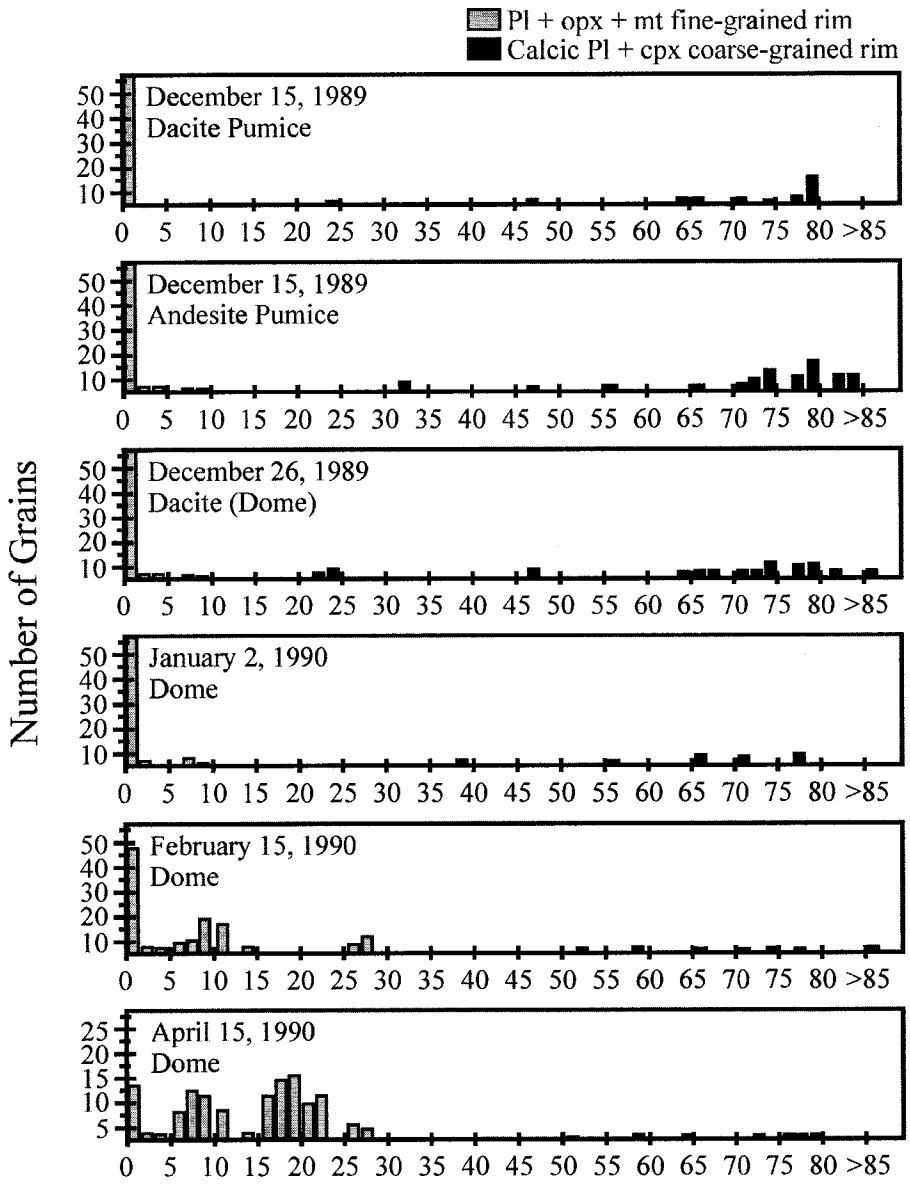

Figure 2.5
Abundance of amphibole reaction rim widths of varying thickness from natural samples emplaced during the 1989-90 eruptions. Shaded bars indicate fine-grained rims composed of plagioclase (Pl), orthopyroxene (opx), and titanomagnetite (mt) that enclose subhedral crystals, whereas solid bars indicate coarse-grained rims composed predominantly of calcic plagioclase and clinopyroxene (cpx) that surround anhedral and embayed crystals. Note that unrimmed amphiboles are present in every eruptive event and that fine-grained reaction rims become more abundant and thicker over time. Coarse grained reaction rims are common in samples erupted on December 15 1989, especially in andesite pumice samples, but only occur in trace amounts in deposits erupted afterwards.

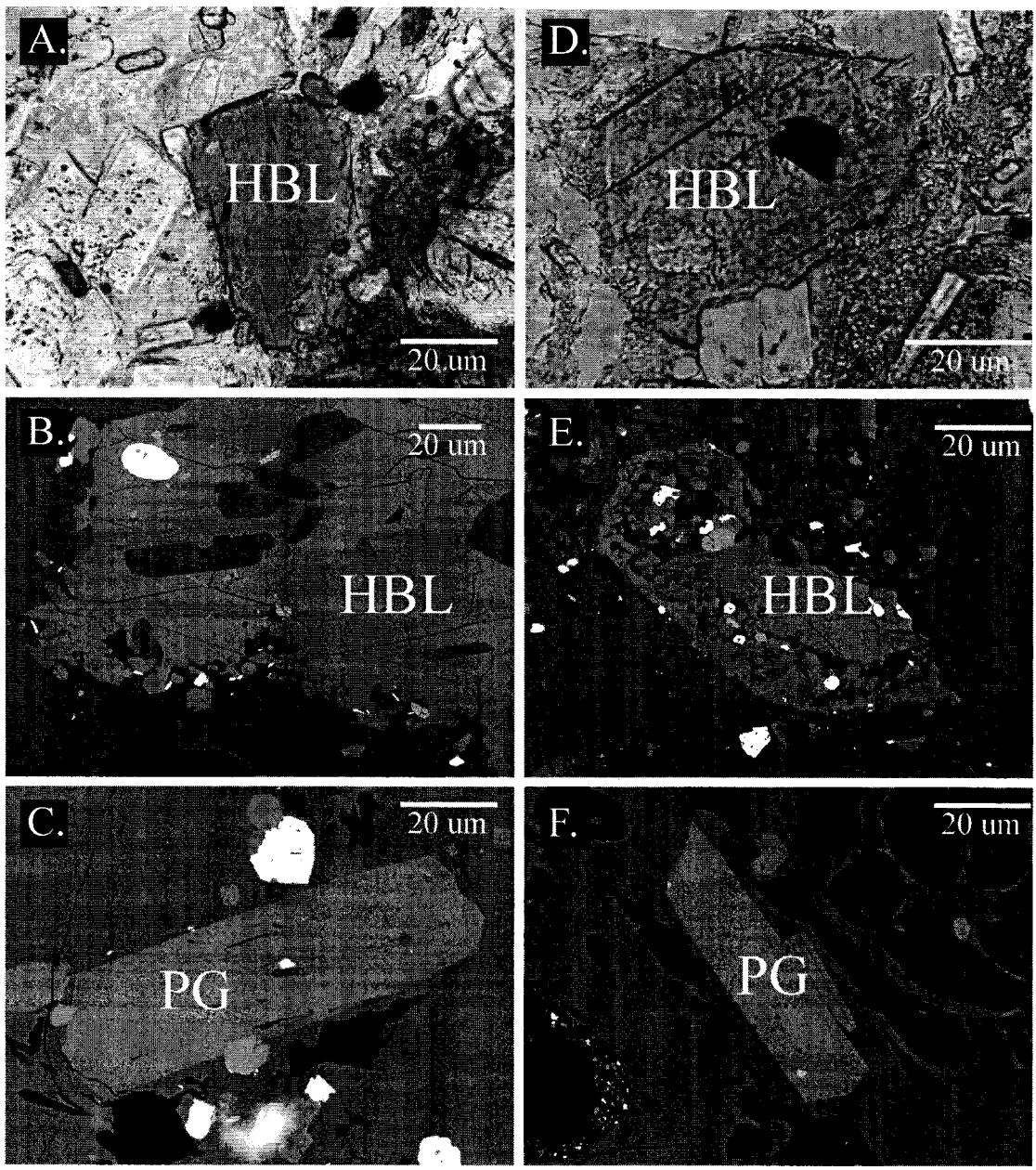

Figure 2.6
Photomicrographs and BSE images of amphiboles from natural samples erupted on December 15 1989 (A, B, C) and January 2 1990 (D, E, F) domes. A, photomicrograph of unrimmed hornblende with subhedral crystal edges; B, BSE image of embayed and anhedral hornblende with coarse-grained reaction rim composed of calcic plagioclase and clinopyroxene with minor titanomagnetite; C, BSE image of unrimmed pargasite with euhedral crystal edges; D, photomicrograph of unrimmed and subhedral hornblende; E, BSE image of coarse-grained reaction rim; F, BSE image of subhedral pargasite.

domes erupted February 15 and April 15, 1990, as well as the final dome that grew from April 21 to June 20, 1990 contain both rimmed and unrimmed hornblende and pargasite. There are two populations of rimmed hornblende (Fig. 2.7A). Thick (50- 120 μm), coarse-grained (15- 30 μm diameter crystals) clinopyroxene, calcic plagioclase, and Fe-Ti oxides (Fig. 2.7B and C) that surround anhedral, embayed hornblende crystal faces characterize one rim population. The other population is characterized by subhedral hornblende grains that are surrounded by rims <5- 28 μm thick, that consist of 2- 10-μm-diameter crystals of orthopyroxene and plagioclase with minor titanomagnetite (Fig. 2.7D). Many hornblende crystals from the final dome have rounded crystal faces bound by 'black rims' (Fig. 2.1F), similar to oxidation rims observed in blast samples from Mount St. Helens (Rutherford and Hill, 1993) and dome samples from Soufriere Hills (Devine et al., 1997). Some pargasite crystals are enclosed by 5- 35 μm thick rims composed of plagioclase and orthopyroxene (Fig. 2.7E), while others exist as unrimmed, subhedral grains (Fig. 2.7F).

Geothermometry

Titanomagnetite is abundant in the dacite sample 92MHR6-1, occurring as 0.02 to 0.5 mm, euhedral to subhedral phenocrysts or as inclusions in plagioclase, hornblende, and pyroxene. Although ilmenite is relatively rare, touching pairs of titanomagnetite and ilmenite are easily found. Titanomagnetite generally contains 6- 9 wt.% TiO_2 (16- 19 mole % ulvospinel) and are compositionally homogeneous (Table 2.3). Some dacite samples contain titanomagnetite grains with ilmenite exsolution lamellae, suggesting a

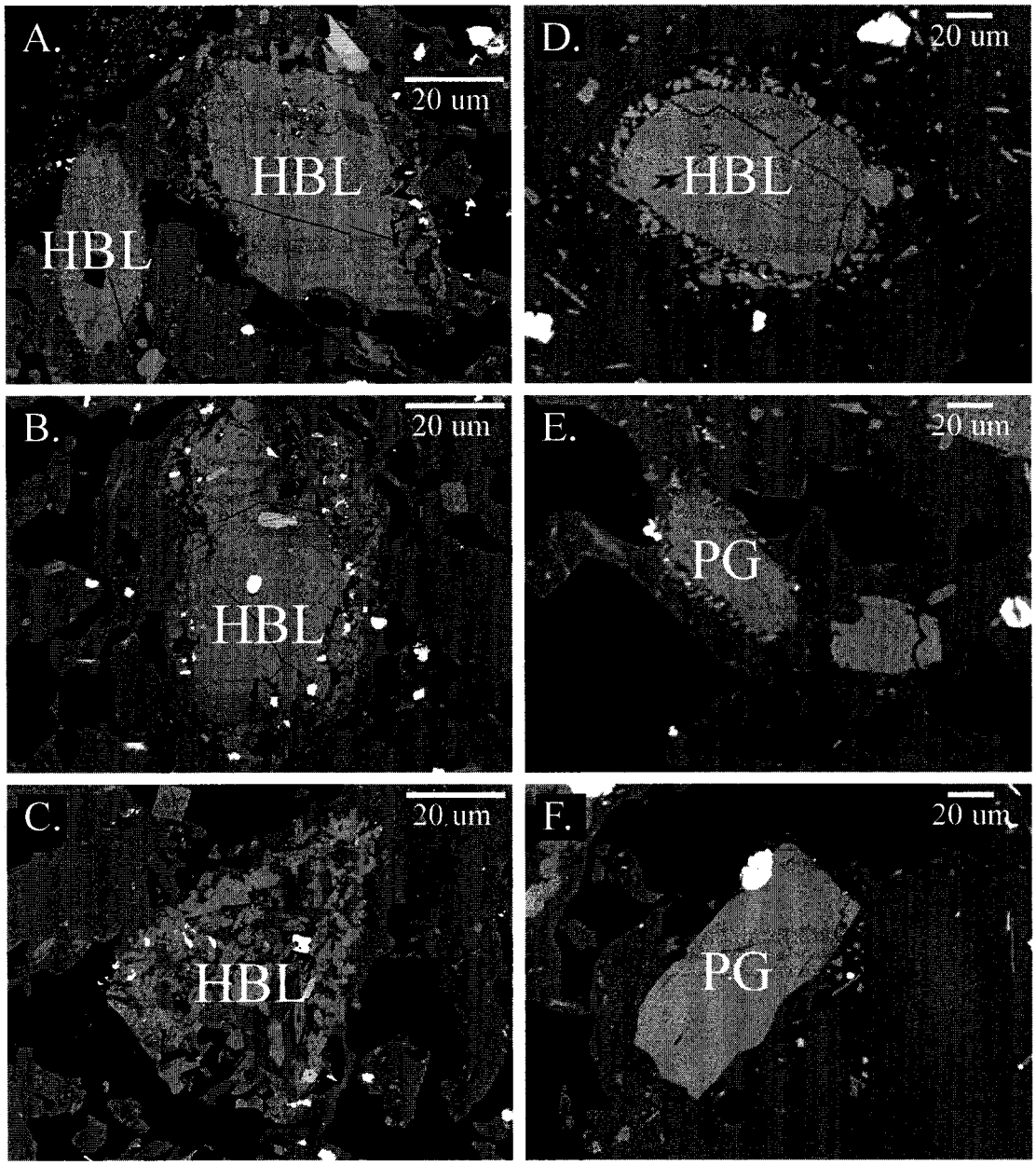

Figure 2.7
BSE images of amphiboles from natural samples erupted on February 15 1990 (A, B) and April 15 1990 (C, D, E, F) domes. A, BSE image of neighboring hornblende, one enclosed by a fine-grained reaction rim composed of plagioclase and orthopyroxene (left) and one surrounded by a coarse-grained reaction rim composed of calcic plagioclase, clinopyroxene, and titanomagnetite; B, BSE image of embayed and anhedral hornblende with coarse-grained reaction rim composed of calcic plagioclase and clinopyroxene with minor titanomagnetite; C, BSE image of thick coarse-grained rim; D and E, BSE images fine-grained reaction rims enclosing subhedral hornblende and pargasite, respectively; E, BSE image of unrimmed subhedral pargasite.

Table 2.3
Electron microprobe analyses of touching magnetite and ilmenite pairs (Oxides in wt.%)

Sample	SiO_2	TiO_2	Al_2O_3	MgO	FeO	MnO	Cr_2O_3	Total	Usp	Ilm	T°C	log fO_2
92MHR6-1 MT01 core	0.08	6.50	1.76	1.56	88.90	0.90	0.00	99.70				
92MHR6-1 MT01 rim	0.07	6.61	1.71	1.71	88.94	0.94	0.01	99.99	17.26			
92MHR6-1 ILM01 core	0.14	38.60	0.30	2.29	57.77	0.83	0.06	99.99				
92MHR6-1 ILM01 rim	0.15	38.58	0.28	2.21	57.75	0.81	0.08	99.86		70.16	843	-11.43
92MHR6-1 MT02 core	0.08	6.15	2.28	1.92	88.96	0.57	0.01	99.97				
92MHR6-1 MT02 rim	0.08	6.24	2.21	1.99	88.94	0.58	0.00	100.04	16.50			
92MHR6-1 ILM02 core	0.04	38.47	0.40	1.88	58.78	0.39	0.02	99.98				
92MHR6-1 ILM02 rim	0.10	38.41	0.38	1.89	57.82	0.42	0.00	99.02		70.14	839	-11.48
92MHR6-1 MT03 core	0.11	6.19	1.82	1.55	89.51	0.82	0.01	100.01				
92MHR6-1 MT03 rim	0.10	6.05	1.70	1.62	88.16	0.79	0.00	98.42	16.52			
92MHR6-1 ILM03 core	0.08	38.69	0.26	2.28	57.94	0.67	0.01	99.93				
92MHR6-1 ILM03 rim	0.07	38.91	0.20	2.42	57.19	0.72	0.00	99.51		69.94	850	-10.56
92MHR6-1 MT04 core	0.08	6.13	1.75	1.47	89.47	0.84	0.05	99.79				
92MHR6-1 MT04 rim	0.10	6.19	1.84	1.38	88.46	0.91	0.04	98.92	16.93			
92MHR6-1 ILM05 core	0.03	38.72	0.21	1.99	58.20	0.71	0.04	99.90				
92MHR6-1 ILM05 rim	0.07	39.91	0.28	1.48	58.26	0.72	0.00	100.72		70.69	840	-11.49
92MHR6-1 MT05 core	0.13	6.95	1.86	1.43	88.79	0.85	0.00	100.01				
92MHR6-1 MT05 rim	0.08	7.14	1.79	1.54	87.04	0.69	0.10	98.38	18.84			
92MHR6-1 ILM05 core	0.09	40.98	0.29	2.16	55.60	0.83	0.00	99.95				
92MHR6-1 ILM05 rim	0.08	41.82	0.27	2.10	55.04	0.76	0.00	100.07		74.02	842	-11.61
92MHR9-1 MT01 core	0.09	8.51	2.19	1.62	85.01	0.57	0.08	98.07				
92MHR9-1 MT01 rim	0.10	8.56	2.10	1.54	85.92	0.57	0.01	98.80	23.81			
92MHR9-1 ILM01 core	0.00	28.64	0.44	2.01	64.18	0.45	0.03	95.75				
92MHR9-1 ILM01 rim	0.04	28.61	0.52	2.17	63.94	0.52	0.01	95.81		52.73	959	-9.40
92MHR9-1 MT02 core	0.08	8.35	1.82	1.54	87.20	0.40	0.08	99.47				
92MHR9-1 MT02 rim	0.09	8.34	1.79	1.47	87.12	0.55	0.01	99.37	22.84			
92MHR9-1 ILM02 core	0.08	30.04	0.52	1.80	66.98	0.26	0.00	99.68				
92MHR9-1 ILM02 rim	0.07	30.18	0.49	1.77	67.18	0.23	0.03	99.95		54.01	942	-9.66
92MHR9-1 MT03 core	0.09	8.41	1.82	1.46	87.41	0.48	0.09	99.76				
92MHR9-1 MT03 rim	0.18	7.86	1.88	1.25	86.45	0.66	0.07	98.35	22.07			
92MHR9-1 ILM03 core	0.08	30.19	0.53	1.65	66.98	0.18	0.08	99.69				
92MHR9-1 ILM03 rim	0.06	29.43	0.45	1.16	68.49	0.33	0.06	99.98		53.28	940	-9.65

lack of equilibrium between the two phases. Titanomagnetite is also abundant in the andesite sample 92MHR9-1, where it typically occurs as 0.02 to 0.3 mm, euhedral to subhedral phenocrysts or less commonly as inclusions in plagioclase and pyroxene. Ilmenite is rare, making it difficult to find touching pairs with titanomagnetite. Titanomagnetite grains in sample 92MHR9-1 contains 7- 10 wt.% TiO_2 (22- 23 mole % ulvospinel).

All geothermometry estimates are limited to analyses of touching titanomagnetite and ilmenite grains with euhedral or subhedral crystal faces where the pair compositions are potentially in equilibrium, based on the model of Bacon and Hirschmann (1988). Geothermometry estimates from this study also employ the mineral recalculation procedure of Stormer (1983) and the algorithm of Andersen and Lindsley (1988). Titanomagnetite- ilmenite pairs from dacite sample 92MHR6-1 yield temperatures between 839°C and 850°C (average = 842°C) and oxygen fugacities ranging from $10^{-10.6}$ to $10^{-11.6}$ bars (Table 2.3). From the andesite, titanomagnetite- ilmenite pairs yield temperatures between 940°C and 959°C (average = 942°C) and oxygen fugacities ranging from $10^{-9.4}$ to $10^{-9.7}$ bars. Temperature estimates from both the dacite and andesite samples are equivalent to those obtained by Swanson et al. (1994).

Phase Equilibria Experiments

Phase equilibria experiments were performed in order to outline the stability field of amphibole, as well as other main mineral phases, in water-saturated Redoubt dacite and andesite compositions for a wide range of pressures and temperatures as illustrated in

Figure 2.8 (Table 2.4 and 2.5). Amphibole breakdown is expected to occur once it is outside these stability fields. All dacite phase equilibria experiments contain titanomagnetite and ilmenite. Plagioclase exists below 860°C, whereas pyroxene is stable below 880°C. Hornblende does not crystallize below 100 MPa at any temperature, and does not crystallize below 200 MPa at temperatures above 900°C. With decreasing pressure, at a given temperature, the crystallizing plagioclase becomes more calcic. Solidus conditions exist below 775°C and 30 MPa. Andesite phase equilibria experiments contain plagioclase below 1050°C at 50 MPa and 950°C at 200 MPa, pyroxene below 1050°C at 150 MPa. Pargasite is stable above 75 MPa at temperatures below 900°C, and above 200 MPa at temperatures below 1000°C.

The compositions of coexisting experimental phenocryst rims and matrix glasses and can be used to refine equilibrium conditions based on phase assemblage (Table 2.6 and 2.7). Compositions of experimental plagioclase rims and most oxides in matrix glass from dacite experiments run at 840°C and 150 MPa are most consistent with those observed in plagioclase rims and matrix glass from the natural dacite sample (Fig. 2.9 and 2.10). Compositions of experimental plagioclase rims and matrix glass from andesite experiments at 950°C and between 150 and 200 MPa are most consistent with those observed in plagioclase rims and matrix glass from the natural andesite sample (Fig. 2.9 and 2.10).

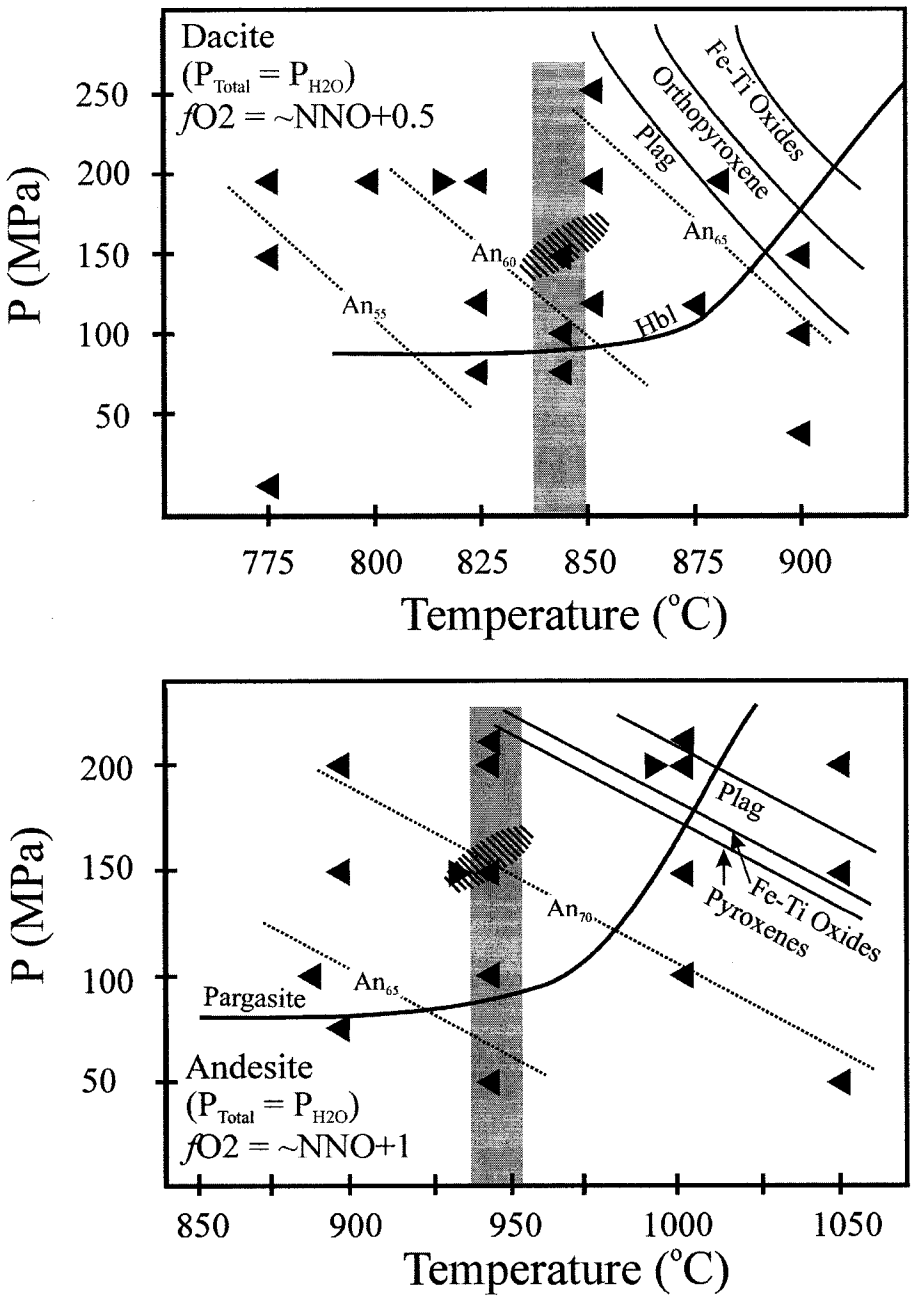

Figure 2.8
Phase equilibria diagrams for 12/15/1989 dacite (A) and andesite (B) experiments. Experiments ($P_{H2O = Ptotal}$) are given by triangles, where left and right-pointing triangles represent crystallization and melting experiments, respectively. Solid lines are "mineral in" curves for amphibole (hornblende or pargasite), plagioclase feldspar, pyroxene, and Fe-Ti oxides. Dotted lines are plagioclase compositions (in An mole %) for experimental plagioclase rims. The narrow, vertical darker shaded region brackets Fe-Ti oxide temperatures, and the experimental plagioclase rim compositions match the natural plagioclase rim compositions in the diagonally hatched region.

Table 2.4
Redoubt andesite and dacite phase equilibria experiments

Experiment	VSL*	SM**	P (MPa)	T (°C)	Duration (Days)	Products "
Dacite Experiments:						
G-235	1	D	50	900	4.0	Pl, Opx, Ox, gl
G-237	1	D	150	780	9.6	Pl, Hbl, Opx, Ox, gl
G-238	1	D	100	840	7.0	Pl, Hbl, Opx, Ox, gl
G-240	1	D	200	780	7.7	Pl, Hbl, Opx, Ox, gl
G-244A	1	D	200	850	5.0	Opx, Hbl, Ox, gl
G-247A	1	D	200	900	2.8	Pl, Opx, Ox, gl
G-257A	1	D	125	850	6.8	Pl, Hbl, Opx, Ox, gl
G-258A	1	D	125	825	5.8	Pl, Hbl, Opx, Ox, gl
G-296C	1	D	250	850	5.8	Pl, Hbl, Opx, Ox, gl
G-297C	1	D	200	800	8.8	Pl, Hbl, Opx, Ox, gl
G-301C	1	G-244A	200	825	10.8	Pl, Hbl, Opx, Ox, gl
G-301C	1	G-240	200	825	10.8	Pl, Hbl, Opx, Ox, gl
RDT-3	1	D	125	850	4.9	Pl, Hbl, Opx, Ox, gl
RDT-4	1	D	150	840	5.0	Pl, Hbl, Opx, Ox, gl
RDT-14	1	D	125	875	5.1	Pl, Opx, Ox, gl
RDT-15	1	D	100	900	5.1	Pl, Opx, Ox, gl
RDT-16	2	D	150	900	5.1	Pl, Opx, Ox, gl
RDT-17	1	D	30	775	5.1	Solidus
RDT-21	1	D	90	840	8.2	Pl, Opx, Ox, gl
RDT-51	1	D	80	840	2.1	Pl, Opx, Ox, gl
Andesite Experiments:						
RDT-A-1	2	A	150	940	0.6	Pl, Pg, Px, Ox, gl
RDT-A-2	2	A	210	940	0.6	Pl, Pg, Px, Ox, gl
RDT-A-3	2	A	100	940	1.9	Pl, Pg, Px, Ox, gl
RDT-A-4	2	A	200	1000	0.9	Pl, Pg, Px, Ox, gl
RDT-A-5	2	A	210	1000	1.0	gl
RDT-A-6	2	A	200	1050	0.5	gl
RDT-A-7	2	RDT-A-6	150	1000	1.0	Pl, Px, Ox, gl
RDT-A-8	2	RDT-A-6	50	1050	2.0	Pl, Px, Ox, gl
RDT-A-9	2	RDT-A-6	150	1050	0.9	Pl, gl
RDT-A-10	2	RDT-A-5	100	1000	1.9	Pl, Px, Ox, gl
RDT-A-11	1	A	100	880	2.8	Pl, Pg, Px, Ox, gl
RDT-A-12	1	RDT-A-5	75	900	2.8	Pl, Px, Ox, gl
RDT-30	1	A	150	900	3.2	Pl, Pg, Px, Ox, gl
RDT-31	2	A	200	900	3.2	Pl, Pg, Px, Ox, gl
RDT-32	2	A	50	940	3.2	Pl, Px, Ox, gl

* VSL, vessel; 1 is Rene cold seal; 2 is TZM

** SM, Starting Material; D, crushed 12/15/89 dacite pumice 92MHR6-1; A, crushed 12/15/89 andesite pumice 92MHR9-1; number, products of previous experiments used as SM

" Pl, plagioclase; Hbl, hornblende; Opx, orthopyroxene; Px, clino & ortho pyroxene; Ox, Fe-Ti Oxide; gl, glass

Table 2.5
Redoubt dacite decompression and heating experiments

Experiment	VSL*	D or H**	MS or SS[u]	Rate[v]	P_f (MPa)[w]	T_f (°C)[x]	Time (Days)[y]	Products[z] (Hbl rim in microns)
RDT-1	1	D	MS	30 MPa/day	30	840	3.5	E Hbl, no rim
RDT-2	1	D	MS	10 MPa/day	30	840	6.0	SR Hbl, no rim
RDT-5	1	D	MS	40 MPa/day	10	840	2.0	E Hbl, no rim
RDT-6	1	D	MS	30 MPa/day	80	840	1.5	E Hbl, no rim
RDT-7	1	D	MS	20 MPa/day	10	840	4.0	SA Hbl, rim = 6
RDT-8	1	D	MS	20 MPa/day	70	840	1.5	E Hbl, no rim
RDT-9	1	H	SS		150	900	1.9	E and SA Hbl, no rim
RDT-10	1	H	SS		150	880	4.5	E Hbl, no rim
RDT-11	1	H	SS		100	880	4.5	SR and A Hbl, rim = trace
RDT-12	1	D	MS	7 MPa/day	10	840	18.5	SR Hbl, rim = 16
RDT-13	1	D	MS	5 MPa/day	10	840	21.5	SR Hbl, rim = 20
RDT-14b	1	D	MS	20 MPa/day	50	840	1.6	SR Hbl, rim = 2
RDT-16b	1	D	MS	20 MPa/day	40	840	2.6	SR Hbl, rim = 2
RDT-17b	1	D	SS		100	840	0.0	E and SR Hbl, no rim
RDT-18	1	D	SS		110	840	0.0	SR Hbl, no rim
RDT-19	1	D	SS		85	840	8.1	SR Hbl, rim = trace
RDT-20	1	D	SS		85	840	4.3	SR Hbl, rim = 5
RDT-21	1	D	SS		90	840	8.2	SR Hbl, no rim
RDT-22	1	D	MS	5 MPa/day	40	840	10.1	SR Hbl, rim = 9
RDT-23	1	D	MS	5 MPa/day	85	840	3.3	SR Hbl, no rim
RDT-27	1	D	SS		20	840	6.8	SA Hbl, rim = 4
RDT-35	1	D	SS		60	840	7.5	SR Hbl, rim = 12
RDT-37	2	H	SS		150	940	0.1	A Hbl, rim = 10
RDT-38	2	H	SS		150	940	0.2	A Hbl, rim = 35
RDT-39	2	H	SS		150	940	0.4	A Hbl, rim = 78
RDT-40	2	H	SS		150	940	0.5	A Hbl, rim = 136
RDT-41	1	D	MS	5 MPa/day	20	840	15.5	SR Hbl, rim = 8
RDT-42	1	D	MS	5 MPa/day	40	840	11.5	SR Hbl, rim = 8
RDT-43	1	D	MS	5 MPa/day	60	840	7.5	SR Hbl, rim = 2
RDT-44	1	D	MS	5 MPa/day	80	840	3.5	SR Hbl, no rim
RDT-46	1	D	SS		110	840	0.5	E Hbl, no rim
RDT-47	1	D	SS		90	840	3.0	SR Hbl, no rim
RDT-48	1	D	SS		75	840	3.0	SR Hbl, rim = trace
RDT-49	1	D	SS		60	840	2.1	SR Hbl, rim = trace
RDT-50	1	D	SS		100	840	2.1	E Hbl, no rim
RDT-51	1	D	SS		80	840	2.1	SR Hbl, no rim
RDT-52	1	D	SS		50	840	1.9	SA Hbl, no rim
RDT-53	1	D	SS		40	840	1.9	SA Hbl, no rim
RDT-54	1	D	SS		45	840	2.8	SA Hbl, rim = trace
RDT-55	1	D	SS		20	840	2.0	SA Hbl, no rim
RDT-58	1	D	SS		65	840	2.8	SR Hbl, rim = 17
RDT-59	1	D	SS		70	840	2.8	SR Hbl, rim = 7
RDT-60	1	D	MS	5 MPa/day	80	840	4.5	SR Hbl, no rim
RDT-63	1	D	MS	5 MPa/day	40	840	14.1	SR Hbl, rim = 10
RDT-64	1	D	MS	10 MPa/day	5	840	7.2	SA Hbl, no rim
RDT-65	1	D	SS		20	840	3.8	SA Hbl, rim = 2
RDT-68	1	D	SS		20	840	6.0	SA Hbl, rim = 8
RDT-69	1	D	SS		10	840	6.0	SA Hbl, rim = 5
RDT-70	1	D	SS		30	840	9.9	SA Hbl, rim = 15
RDT-73	1	D	SS		20	840	17.0	SA Hbl, rim = 15
RDT-74	1	D	SS		30	840	17.0	SA Hbl, rim = 26
RDT-76	1	D	SS		5	840	26.0	SA Hbl, rim =5

* VSL, vessel; 1 is Rene cold seal; 2 is TZM

** D, Decompression experiment; H, Heating experiment

[u] MS, Multi-step experiment at constant rate; SS, Single-step

[v] Rate, Decompression Rate following >3 Day hold at 150 MPa and 840 oC

Table 2. 6
Electron microprobe analyses of natural dacite glass from phase equilibria experiments (in wt.%)

Sample	92MHR6-1	92MHR6-1C [w]	G-237	G-238	G-240	G-244A	G-247A
Remark [*]	12-15-89 Dacite Pumice	12-15-89 Dacite Pumice	780°C, 150 MPa	840°C, 100 MPa	780°C, 200 MPa	850°C, 200 MPa	880°C, 200 MPa
SiO_2	76.47 (0.46)	76.58	73.55 (0.06)	76.09 (0.06)	73.07 (0.08)	75.25 (0.34)	71.75 (0.07)
TiO_2	0.28 (0.07)	0.24	0.19 (0.05)	0.24 (0.05)	0.16 (0.09)	0.16 (0.12)	0.22 (0.03)
Al_2O_3	12.69 (0.11)	12.72	11.80 (0.04)	11.14 (0.04)	12.32 (0.04)	13.00 (0.14)	12.41 (0.09)
FeO	1.13 (0.06)	1.12	0.85 (0.04)	0.88 (0.29)	1.22 (0.10)	1.99 (0.25)	2.09 (0.06)
MgO	0.23 (0.04)	0.24	0.09 (0.08)	0.09 (0.04)	0.26 (0.03)	0.44 (0.05)	0.56 (0.05)
CaO	1.13 (0.03)	1.16	0.73 (0.03)	0.76 (0.03)	1.04 (0.03)	1.53 (0.22)	1.64 (0.04)
Na_2O	3.91(0.08)	3.93	4.45 (0.03)	3.16 (0.11)	4.01 (0.02)	3.72 (0.34)	3.50 (0.12)
K_2O	3.46 (0.05)	3.44	3.67 (0.09)	2.97 (0.37)	3.5 (0.05)	2.81 (0.09)	2.44 (0.09)
Total [**]	99.28 (0.49)	99.53	95.34 (0.17)	95.33 (0.48)	95.57 (0.24)	98.91 (0.68)	94.61 (0.15)
n [2]	10		10	10	8	10	10

Sample	G-258A	G-296C	G-297C	G-301C	RDT-4	RDT-14	RDT-15
Remark [*]	825°C, 125 MPa	850°C, 250 MPa	800°C, 200 MPa	825°C, 200 MPa	840°C, 150 MPa	875°C, 125 MPa	900°C, 100 MPa
SiO_2	75.36 (0.42)	70.19 (0.13)	72.89 (0.07)	73.09 (0.16)	73.02 (0.08)	73.94 (0.33)	74.02 (0.10)
TiO_2	0.27 (0.11)	0.13 (0.06)	0.16 (0.15)	0.17 (0.06)	0.26 (0.08)	0.29 (0.06)	0.32 (0.04)
Al_2O_3	12.10 (0.15)	12.78 (0.04)	12.29 (0.21)	12.47 (0.12)	12.09 (0.08)	12.03 (0.10)	11.64 (0.14)
FeO	0.99 (0.15)	2.20 (0.04)	1.33 (0.29)	1.61 (0.33)	1.21 (0.12)	1.58 (0.05)	1.97 (0.04)
MgO	0.16 (0.20)	0.54 (0.03)	0.36 (0.03)	0.37 (0.04)	0.25 (0.02)	0.33 (0.03)	0.34 (0.05)
CaO	0.97 (0.02)	1.74 (0.04)	1.28 (0.05)	1.45 (0.02)	1.11 (0.06)	1.23 (0.05)	1.32 (0.05)
Na_2O	4.13 (0.59)	3.22 (0.05)	3.67 (0.10)	3.64 (0.02)	3.73 (0.18)	3.87 (0.13)	4.29 (0.14)
K_2O	3.42 (0.28)	2.27 (0.05)	3.06 (0.04)	2.94 (0.06)	3.26 (0.11)	3.11 (0.07)	3.36 (0.05)
Total [**]	97.40 (0.61)	93.07 (0.19)	95.04 (0.43)	95.73 (0.53)	95.92 (0.17)	96.38 (0.27)	97.25 (0.34)
n [2]	4	7	6	6	6	6	6

[*] Date of eruptive event or phase equilibria experimental conditions

[**] prenormalized total

[1] standard deviation

[2] number of points per analysis

[w] data from Wolf and Eichelberger (1997)

Table 2. 6 (cont)
Electron microprobe analyses of natural andesite glass from phase equilibria experiments (in wt.%)

Sample	92MHR9-1	RDT-A-1	RDT-A-2	RDT-A-3	RDT-A-4	RDT-A-5	RDT-A-6
Remark *	12-15-89 Andesite Pumice	940°C, 150 MPa	940°C, 210 MPa	940°C, 100 MPa	1000°C, 200 MPa	1000°C, 200 MPa	1050°C, 200 MPa
SiO_2	68.33 (0.72)[1]	66.60 (1.28)	64.03 (0.40)	69.55 (0.83)	66.06 (0.83)	63.96 (0.22)	63.35 (0.20)
TiO_2	0.53 (0.31)	0.49 (0.19)	0.65 (0.16)	0.34 (0.15)	0.43 (0.24)	0.45 (0.12)	0.26 (0.23)
Al_2O_3	14.96 (0.22)	13.82 (0.33)	15.37 (0.25)	13.84 (0.41)	15.67 (0.66)	15.05 (0.46)	15.61 (0.26)
FeO	3.36 (0.18)	1.81 (0.37)	3.26 (0.40)	2.06 (0.21)	3.35 (1.07)	3.36 (0.41)	3.40 (0.79)
MgO	1.05 (0.02)	0.44 (0.40)	1.10 (0.40)	0.68 (0.72)	1.02 (0.96)	1.13 (0.47)	1.31 (0.44)
CaO	3.49 (0.52)	3.16 (0.22)	3.51 (0.26)	3.29 (0.26)	3.73 (0.29)	3.74 (0.54)	3.85 (0.67)
Na_2O	4.30 (0.54)	4.50 (0.12)	3.99 (0.24)	4.63 (0.35)	4.17 (0.28)	3.98 (0.28)	4.03 (0.10)
K_2O	2.53 (0.13)	2.50 (0.26)	2.08 (0.09)	2.58 (0.36)	1.96 (0.51)	1.87 (0.14)	1.90 (0.26)
Cl	0.19 (0.04)	0.07 (0.03)	0.13 (0.03)	0.14 (0.06)	0.15 (0.04)	0.13 (0.03)	0.19 (0.04)
Total **	98.55 (1.12)	93.38 (0.92)	94.11 (0.31)	97.11 (0.52)	95.55 (1.64)	93.67 (1.05)	93.90 (1.51)
n^2	17	5	5	5	5	5	3

Sample	RDT-A-7	RDT-A-8	RDT-A-9	RDT-A-10	RDT-A-11	RDT-30	RDT-31
Remark *	1000°C, 150 MPa	1050°C, 50 MPa	1050°C, 150 MPa	1000°C, 100 MPa	880°C, 100 MPa	900°C, 150 MPa	900°C, 200 MPa
SiO_2	67.12 (0.68)	68.55 (1.04)	65.06 (0.37)	67.24	70.10 (0.56)	70.89 (0.85)	66.11 (0.75)
TiO_2	0.35 (0.29)	0.18 (0.11)	0.09 (0.05)	0.20	0.39 (0.38)	0.52 (0.40)	0.63 (0.25)
Al_2O_3	14.84 (0.19)	14.51 (0.21)	15.01 (0.30)	14.36	13.61 (0.34)	14.71 (0.24)	15.02 (0.66)
FeO	2.65 (0.28)	2.46 (0.42)	2.78 (1.24)	2.39	1.70 (0.23)	1.93 (0.24)	2.75 (0.63)
MgO	0.76 (0.57)	0.52 (0.72)	1.21 (0.87)	0.54	0.35 (0.82)	0.47 (0.28)	1.06 (0.94)
CaO	3.46 (0.30)	3.44 (0.30)	3.56 (0.84)	3.35	3.14 (0.23)	3.36 (0.30)	3.31 (0.35)
Na_2O	4.27 (0.43)	4.62 (0.42)	4.14 (0.20)	4.47	4.80 (0.39)	4.79 (0.53)	4.32 (0.35)
K_2O	2.19 (0.35)	2.43 (0.27)	2.16 (0.23)	2.22	2.68 (1.36)	2.66 (0.32)	2.39 (0.52)
Cl	0.17 (0.04)	0.11 (0.00)	0.11 (0.04)	0.08	0.16 (0.05)	0.07 (1.04)	0.08 (0.04)
Total **	95.80 (0.68)	96.82 (0.84)	94.13 (0.87)	94.86	96.93 (0.54)	99.40 (1.21)	95.69 (0.60)
n^2		5	5	1	5	5	5

* Date of eruptive event or phase equilibria experimental conditions

** prenormalized total

[1] standard deviation

Table 2.7

Electron microprobe analyses of plagioclase rims from natural dacite and from dacite phase equilibria experiments (in wt.%)

Sample	92MHR6-1	G-237	G-238	G-240	G-244A	G-257A	G-258A
Remark *	12-15-89 Dacite Pumice	780°C, 150 MPa	840°C, 100 MPa	780°C, 200 MPa	850°C, 200 MPa	850°C, 125 MPa	825°C, 125 MPa
SiO_2	56.53 (0.26)[1]	58.46 (0.37)[1]	57.00 (2.28)	57.15 (0.44)	54.97 (1.12)	55.74 (0.08)	56.76 (0.05)
Al_2O_3	27.44 (0.12)	25.06 (0.37)	26.75 (1.19)	25.52 (0.23)	28.14 (0.74)	27.09 (0.66)	25.50 (0.13)
FeO	0.20 (0.04)	0.32 (0.06)	0.46 (0.11)	0.31 (0.12)	0.46 (0.08)	0.33 (0.09)	0.20 (0.05)
CaO	9.89 (0.35)	7.66 (0.04)	8.54 (0.75)	9.27 (0.31)	10.10 (0.39)	9.50 (0.10)	9.13 (0.14)
Na_2O	6.17 (0.22)	7.54 (0.05)	6.73 (0.76)	7.34 (0.44)	5.64 (0.32)	5.76 (0.10)	7.52 (0.14)
K_2O	0.14 (0.22)	0.48 (0.05)	0.32 (0.11)	0.25 (0.03)	0.26 (0.06)	0.30 (0.06)	0.25 (0.04)
Total **	100.36 (0.33)	99.51 (0.46)	99.79 (1.24)	99.84 (0.70)	99.58 (0.84)	98.73 (0.56)	99.35 (0.16)
Anorthite (mole %)	61.1	48.9	54.8	55.0	63.1	61.0	54.0
n^2	10	10	9	6	8	8	7
Sample	G-296C	G-297C	G-301C (244A)	G-301C (240)	RDT-4	RDT-14	RDT-15
Remark *	850°C, 250 MPa	800°C, 200 MPa	825°C, 200 MPa	825°C, 200 MPa	840°C, 150 MPa	875°C, 125 MPa	900°C, 100 MPa
SiO_2	51.69 (0.42)	57.63 (0.20)	55.95 (0.53)	56.02 (0.52)	56.66 (0.21)	55.46 (0.61)	55.81 (0.53)
Al_2O_3	29.85 (0.24)	25.36 (0.24)	27.03 (0.60)	27.25 (0.35)	27.44 (0.08)	27.55 (0.28)	27.79 (0.40)
FeO	0.50 (0.08)	0.20 (0.05)	0.34 (0.11)	0.27 (0.12)	0.19 (0.04)	0.39 (0.06)	0.32 (0.05)
CaO	12.85 (0.42)	9.13 (0.32)	9.76 (0.54)	9.46 (0.40)	9.87 (0.10)	9.97 (0.36)	9.48 (0.38)
Na_2O	4.64 (0.23)	6.81 (0.15)	6.22 (0.39)	6.24 (0.18)	6.10 (0.07)	5.74 (0.33)	5.72 (0.26)
K_2O	0.14 (0.03)	0.28 (0.03)	0.22 (0.03)	0.23 (0.03)	0.18 (0.04)	0.24 (0.04)	0.22 (0.03)
Total **	99.67 (0.27)	99.42 (0.62)	99.52 (0.65)	99.46 (0.70)	100.43 (0.33)	99.35 (0.37)	99.35 (0.64)
Anorthite (mole %)	72.9	56.3	60.2	59.4	61.1	62.5	61.5
n^2	7	8	9	6	8	8	8

* Date of eruptive event or phase equilibria experimental conditions

** prenormalized total

[1] standard deviation

[2] number of points per analysis

Table 2. 7 (cont.)
Electron microprobe analyses of natural and experimental plagioclase (in wt.%)

Sample	92MHR9-1	92MHR9-1	92MHR9-1	RDT-A-1	RDT-A-2	RDT-A-3	RDT-A-4
Remark *	12-15-89 Andesite Pumice	12-15-89 Andesite Pumice	12-15-89 Andesite Pumice	940°C, 150 Mpa	940°C, 210 Mpa	1000°C, 100 Mpa	1000°C, 200 Mpa
SiO_2	53.00	52.75	53.32	52.47 (0.25)	51.00 (0.98)	51.63 (0.61)	50.64 (1.10)
Al_2O_3	29.28	29.41	28.94	30.37 (0.93)	30.42 (0.42)	31.52 (0.50)	30.82 (1.47)
FeO	0.60	0.61	0.63	0.62 (0.09)	0.57 (0.09)	0.62 (0.11)	0.62 (0.09)
CaO	12.18	12.42	11.93	10.29 (0.05)	11.70 (0.49)	9.98 (0.16)	12.38 (1.10)
Na_2O	4.79	4.65	5.00	4.57 (0.24)	4.14 (0.27)	4.84 (0.44)	3.56 (0.32)
K_2O	0.15	0.16	0.17	0.08 (0.04)	0.18 (0.08)	0.15 (0.02)	0.18 (0.08)
Total **	100.00	100.00	100.00	98.28 (1.08)	98.05 (1.29)	98.74 (0.64)	98.20 (1.69)
An	71.2	72.1	69.8	68.9	72.9	66.6	76.8
n^2	5	5	5	3	5	6	9
Sample	RDT-A-7	RDT-A-8	RDT-A-9	RDT-A-10	RDT-A-11	RDT-30	RDT-31
Remark *	1000°C, 150 Mpa	1050°C, 50 MPa	1050°C, 150 MPa	1000°C, 100 MPa	880°C, 100 MPa	900°C, 150 MPa	900°C, 200 MPa
SiO_2	50.79 (0.81)	51.78 (0.76)	50.85 (1.12)	50.03 (1.14)	52.23 (1.06)	51.93 (0.54)	52.40 (0.77)
Al_2O_3	30.36 (0.83)	30.56 (0.39)	31.58 (1.20)	30.31 (0.53)	29.87 (1.50)	30.37 (0.92)	30.09 (0.60)
FeO	0.61 (0.15)	0.77 (0.17)	0.57 (0.30)	1.08 (1.06)	0.69 (0.06)	0.45 (0.15)	0.62 (0.15)
CaO	12.61 (0.60)	10.41 (0.62)	11.80 (0.66)	10.73 (0.45)	10.07 (0.50)	10.93 (0.44)	11.23 (1.06)
Na_2O	4.30 (0.60)	4.67 (0.39)	3.49 (0.37)	4.42 (0.40)	4.81 (0.17)	4.95 (0.71)	4.50 (0.44)
K_2O	0.13 (0.79)	0.28 (0.35)	0.32 (0.34)	0.24 (0.18)	0.16 (0.02)	0.16 (0.71)	0.20 (0.10)
Total **	98.79 (0.79)	98.46 (1.00)	98.61 (0.91)	97.80 (1.05)	97.83	98.79 (1.03)	99.03 (0.80)
An	74.0	67.8	75.6	69.8	66.9	68.1	70.5
n^2	10	9	9	9	6	8	9

* Date of eruptive event or phase equilibria experimental conditions

** prenormalized total

[1] standard deviation

[2] number of points per analysis

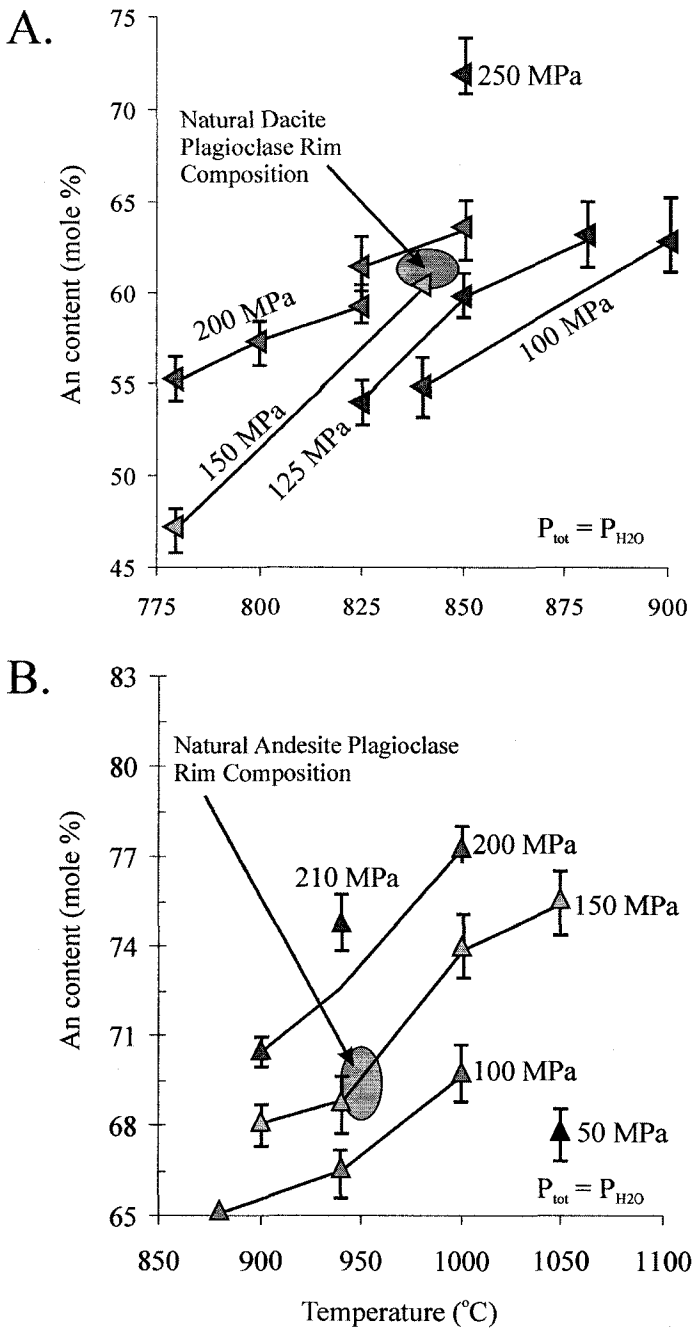

Figure 2.9
Plagioclase rim compositions for dacite and andesite experiments. Experimental plagioclase rim compositions for dacite (A) and andesite (B) compositions are plotted along pressure trends where the composition of natural samples is indicated by the shaded region. Plagioclase rim compositions from both andesite and dacite experiments run at 150 MPa most closely agree with natural compositions.

A.

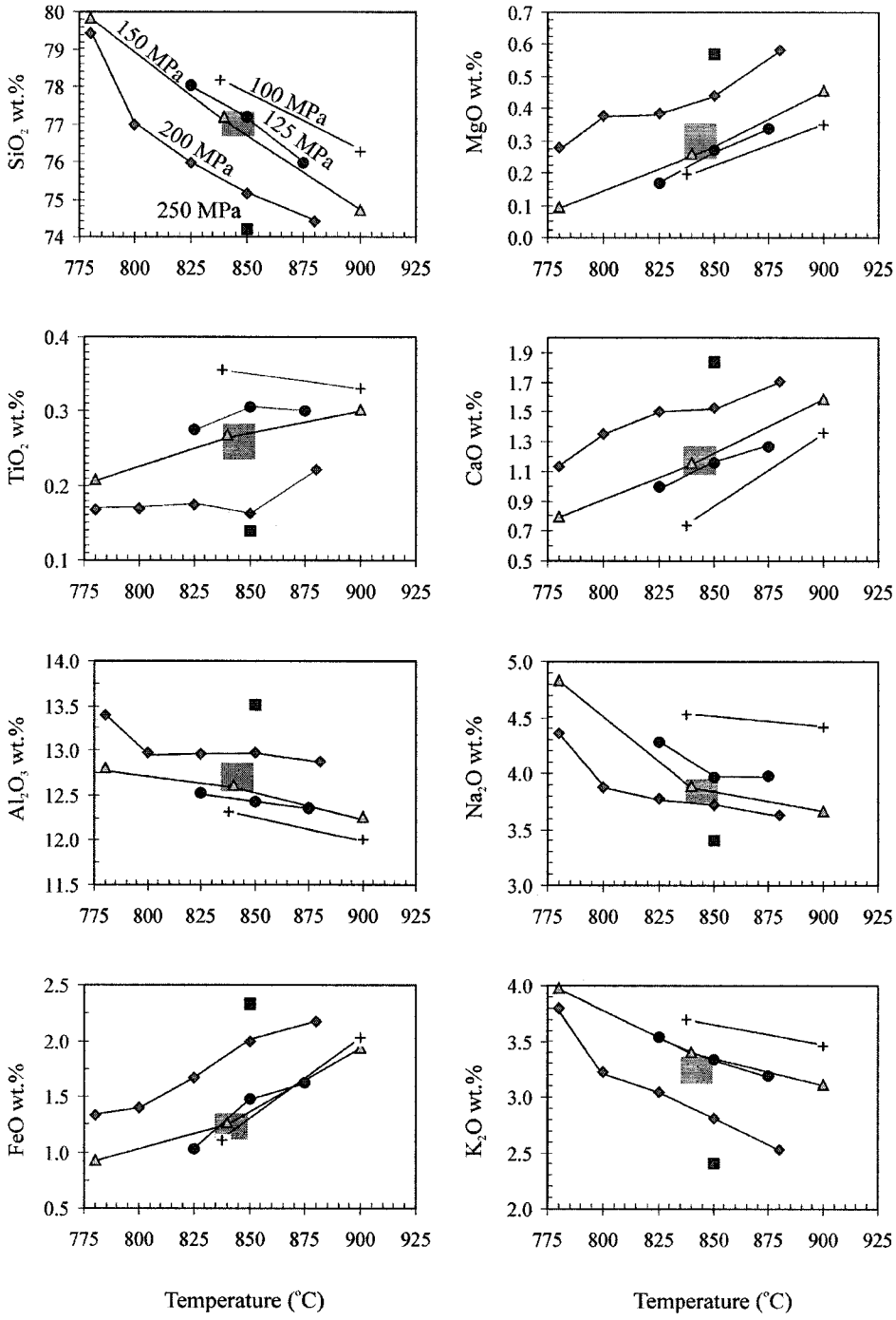

Figure 2.10
Matrix glass compositions for dacite and andesite experiments. Experimental matrix glass compositions for dacite (A) and andesite (B) are plotted along pressure trends where the composition of natural samples is indicated by the shaded region.

B.

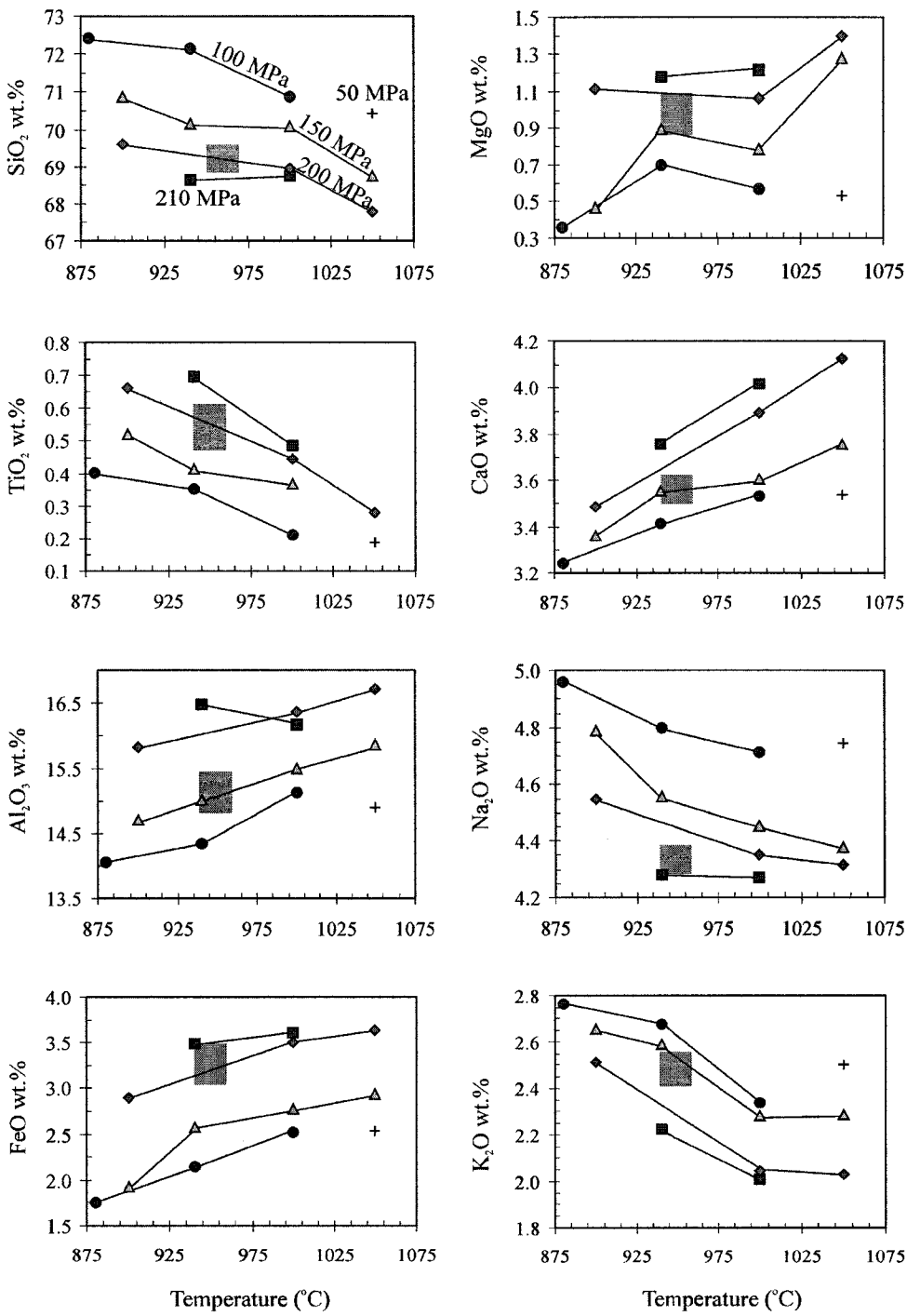

Figure 2.10 (cont.)

Decompression Experiments

Decompression experiments were initially held at 840°C and 150 MPa for 3 to 5 days, based on estimates of pre-eruptive storage conditions. Multi-step isothermal decompression experiments over 3- 21 days only produced breakdown rim growth on hornblendes that were decompressed below 20 MPa at rates slower than 20 MPa/ day, or approximately 5 days out of the hornblende stability field (Table 2.5). Breakdown rims induced by decompression at 20 MPa/ day have an average thickness of 5 μm, whereas rims from 10 MPa/day runs have an average thickness of 15 μm. Multi-step rims develop directly on boundary between coexisting melt and subhedral crystal edges, and are composed of fine-grained (~2 μm crystals) orthopyroxene and plagioclase, with trace amounts titanomagnetite (Figure 2.11).

Single-step isothermal decompression experiments produced a variety of breakdown rim thicknesses, textures, and mineralogy depending on the final pressure. Experiments rapidly decompressed to pressures between 80 and 90 MPa (20 to 10 MPa below hornblende stability) and held for 2 days contained fewer modal hornblende (2- 3 vol.%) compared to phase equilibria experiments and December 15, 1989 dacite pumice starting material. Also, hornblendes from these experiments have subrounded to rounded crystal edges, all of which are unrimmed (Table 2.5). Experiments held for 3 days also contained fewer modal hornblende characterized by subhedral crystal edges, but with fine-grained (<2 μm crystals) breakdown rims of orthopyroxene and plagioclase 1 to 8 μm thick. Experiments rapidly decompressed to 70- 60 MPa (30 to 40 MPa below the

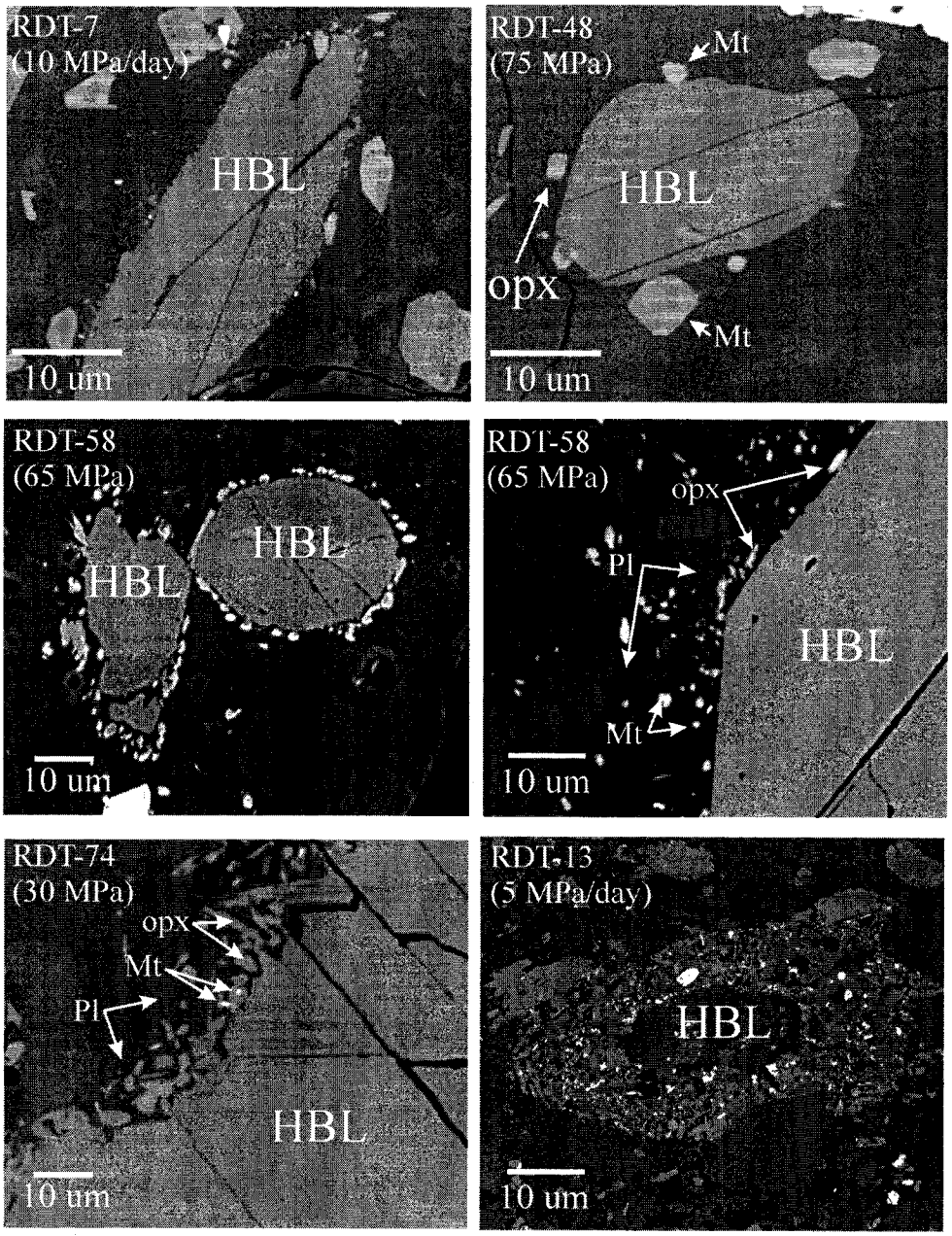

Figure 2.11
BSE images of decompression-induced reaction rims on Redoubt hornblende crystals. Experiment identification numbers are provided with the pressure that experiments were quenched at. All reaction rims are fine-grained and composed of plagioclase (Pl), orthopyroxene (opx), +/- titanomagnetite (Mt). Experiments quenched at higher pressures resulted in subrounded hornblendes with or without reaction rims with titanomagnetite compared to experiments quenched at lower pressures, which resulted in more angular hornblendes with reaction rims that lack titanomagnetite.

hornblende stability field) and held for 2 days contain unrimmed hornblende. Experiments held for 3- 4 days at this pressure, however contained hornblendes with medium grained (2- 5 μm crystals) breakdown rims of titanomagnetite, orthopyroxene, and plagioclase 5 to 18 μm thick. Reaction rim growth rate was notably higher at this pressure compared to others (Fig. 2.12). At this pressure reacting hornblende crystals are characterized by subrounded to subangular crystal edges. Finally, single-step decompression experiments performed at 20 to 50 MPa (80 to 50 MPa below the hornblende stability field) and held for 2 to 10 days produced no reaction rims. Runs lasting 12 to 25 days contained hornblende with breakdown rims 5 to 35 μm thick of fine grained (2- 10 μm crystals) orthopyroxene and plagioclase. Reacting hornblende crystals at this pressure develop reaction rims at the boundary between coexisting melt and the angular to subangular crystal edges.

Heating Experiments

Isobaric heating experiments on dacite samples produced hornblende breakdown rims distinctly different than those that formed in response to decompression. Experiments heated to 950°C and 150 MPa (50°C above hornblende stability) and held for 2 to12 hours produced thicker amphibole breakdown rims compared to decompression experiments (Fig. 2.13). Reaction rims are 2- 25 μm thick after 2 hours and 80- 140 μm thick after 12 hours, thus developing significantly more rapidly than decompression-induced rims. Thermally induced breakdown rims are coarser-grained than decompression rims, ranging from 5- 35 μm diameter crystals. Unlike decompression

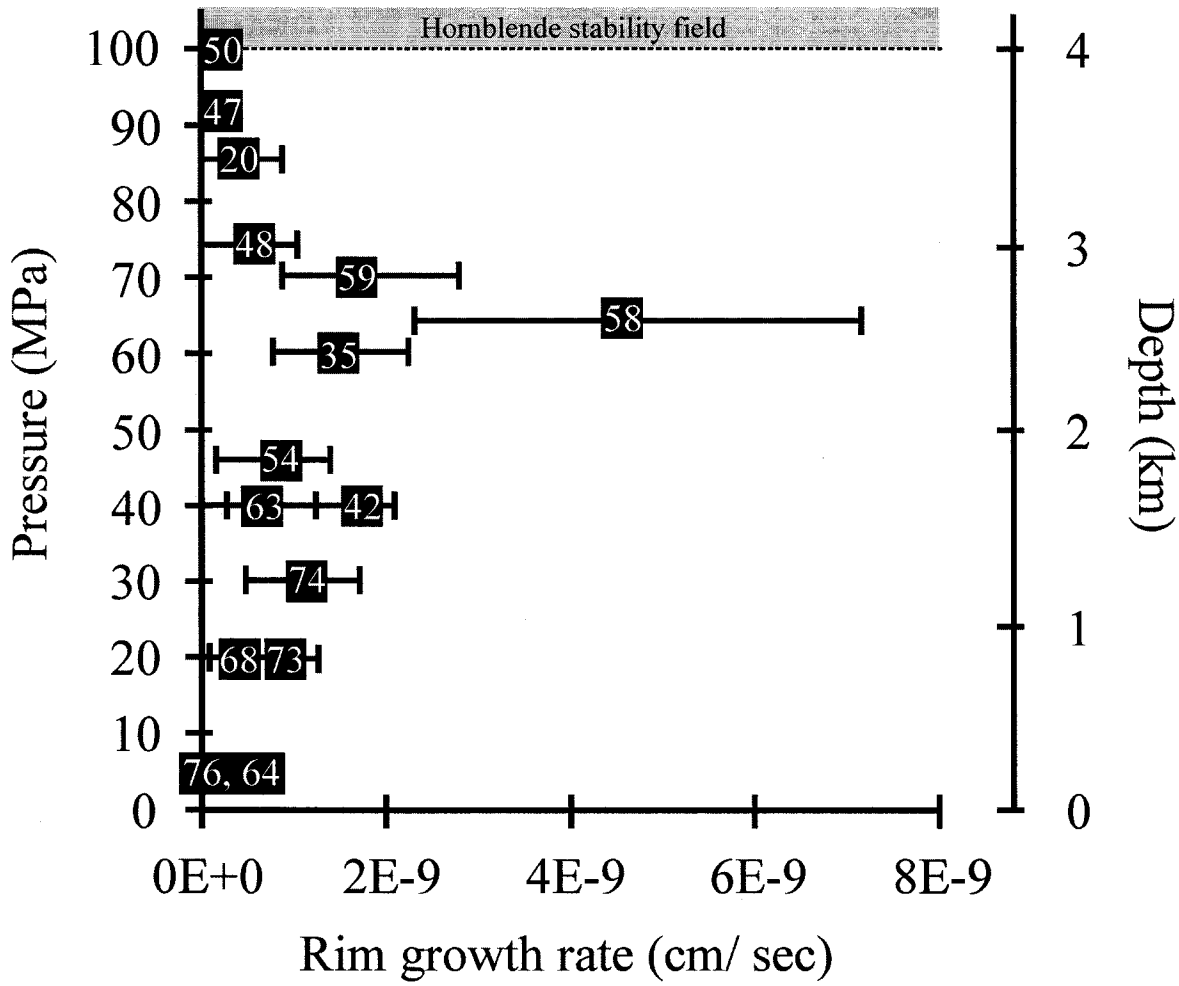

Figure 2.12
Reaction rim growth rate plotted against pressure and corresponding depths (in km) for single-step decompression experiments. Growth rate is extremely slow near the hornblende stability field and at pressures below 10 MPa. Growth occurs at the fastest rate at pressures between 60 and 70 MPa, or 40 to 30 MPa below the hornblende stability field. See text for discussion.

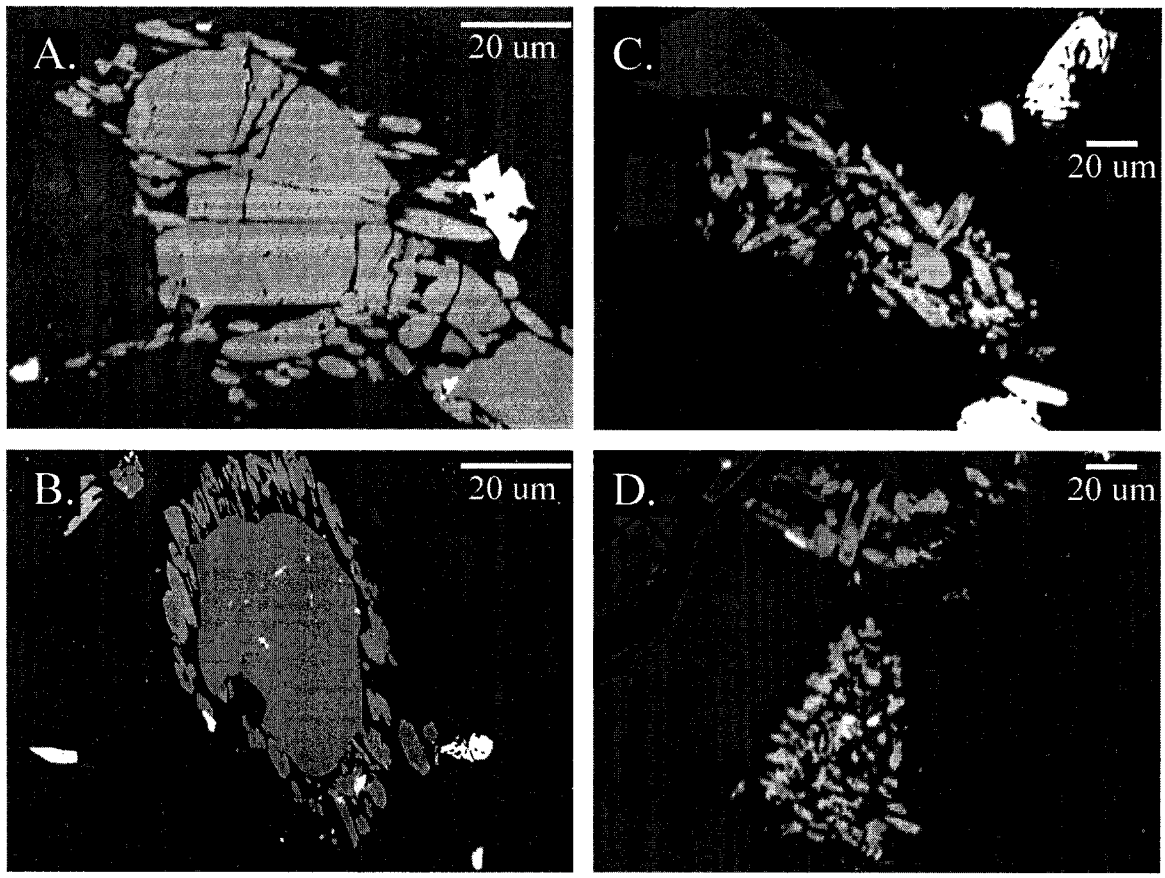

Figure 2.13
BSE images of heating-induced reaction rims on hornblende crystals. Experiments were heated to 940°C, (~40°C above the hornblende stability field) after 3-5 days at 840°C and 150 MPa and held for 2 (A), 4 (B), 6 (C), and 12 (D) hours before being quenched. All heating experiments produced reaction rims distinct from those that form in response to decompression. Heating rims are characterized as being coarse-grained, composed of calcic plagioclase, clinopyroxene, and titanomagnetite, and broadly surround embayed and anhedral crystal edges.

rims, heating rims are composed of clinopyroxene and calcic plagioclase, with minor amounts of pargasite and titanomagnetite. Finally, reaction rims on heated hornblendes exist as diffuse coronas that surround anhedral and pervasively embayed crystal edges.

2.5 DISCUSSION

In this section, the experimental results will first be used to constrain the pre-eruptive storage conditions of magmas erupted during the 1989-90 eruption of Redoubt volcano. Then, amphibole breakdown reactions that occur in response to decompression and heating will be discussed. Finally, experimental results will be applied to the 1989-90 Redoubt eruption.

Pre-Eruptive Storage Conditions

Agreement between the compositions of plagioclase rims and matrix glass from natural dacite pumice samples and experimental phase and glass compositions at water saturated conditions suggests that the dacite erupted on December 15, 1989 last equilibrated at 840°C and 150MPa (±25 MPa). Less consistency exists between plagioclase rim and matrix glass compositions from December 15, 1989 andesite pumices and experimental plagioclase rims and matrix glass compositions, resulting in an estimate of ~950°C and 175 MPa (±40 MPa) for the conditions of last equilibration for the andesite. These pressures correspond to depths of approximately 6 and 8 km for the dacite and andesite, respectively, assuming an average crustal density of 2600 kg/ m^3. This estimate is in good

agreement with a depth estimate of 6- 10 km from Power et al. (1994) and Lahr et al. (1994) based on hypocenter locations of volcano-tectonic earthquakes during the 1989-90 eruptions (Fig. 2.14).

Decompression Induced Amphibole Breakdown

The mineral assemblage present in amphibole (hornblende and pargasite) reaction rims that formed during decompression experiments is identical to that of the existing phenocryst assemblage. Reaction rims grow inward from the crystal edge with no breakdown in amphibole cores. These rims occur only when in contact with the surrounding melt, and not when amphibole is in contact with another crystal. This demonstrates that amphibole reacts with melt, most likely as a result of the reduction in the dissolved water content at lower pressure.

All multi-step experiments run at constant decompression rates of 5, 10, or 20 MPa/day produced samples with fewer modal hornblende compared to experiments run at pre-eruptive conditions (Table 2.8). In addition, these experiments contained unrimmed hornblende with subhedral crystal faces, unless decompressed below 20 MPa, in which case reaction rims developed. This clearly illustrates that the response of hornblende to decompression is strongly pressure dependent.

Single-step experiments clarify the relationship between pressure and reaction rim development in greater detail. Experiments run for <2 days at pressures less than 20 MPa below the stability limit of hornblende, did not produce visible reaction rims. Nonetheless, dissolution of hornblende clearly occurs at these conditions, as indicated by

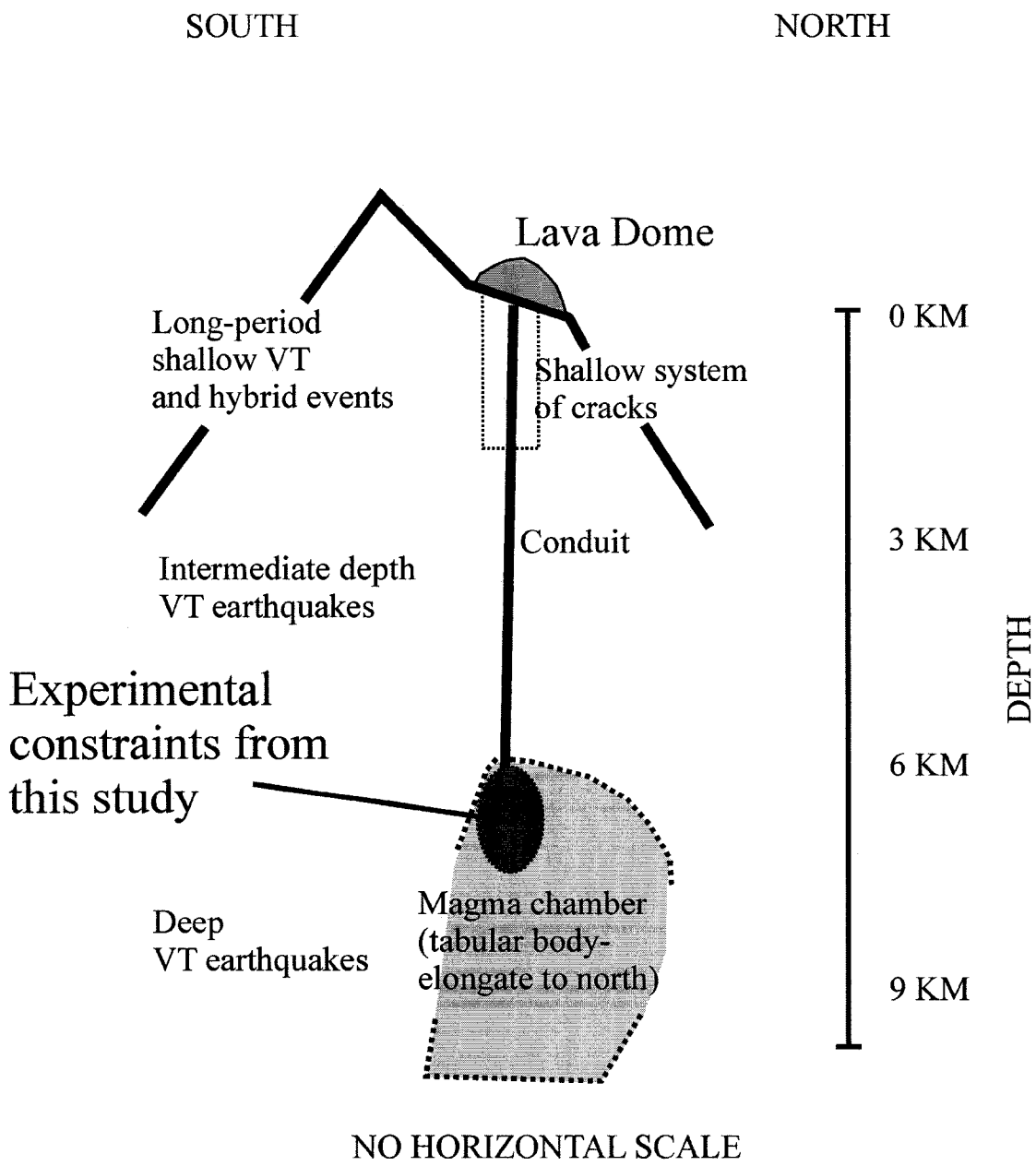

Figure 2.14
Schematic of pre-eruptive storage conditions for andesite and dacite magmas erupted December 15 1989 from Redoubt volcano (modified from Power et al., 1994). Experimental results suggest that the dacite and andesite magma last equilibrated at pressures of 150 MPa and 170 MPa, respectively, which correlate to a depth of 6- 7 km assuming an average crustal density of 2600 kg/ m^3. This estimate is consistent with previous studies (Power et al., 1994; Lahr et al., 1994) based on seismic evidence.

Table 2.8
Modal analyses of Redoubt natural and experimental samples

Sample	Type [x]	Event	P (MPa)	Phenocryst [y]					Counts	Modal Abundance [z]				
				Pl	Hbl	Px	Ox	gl		% Pl	% Hbl	% Px	% Ox	% gl
Natural Samples:														
92MHR6-1	P	Dec. 15, 1989		35	9	11	6	139	200	17.5	4.5	5.5	3.0	69.5
92MHR10-1	D	Dec. 15, 1989		70	6	10	4	110	200	35.0	3.0	5.0	2.0	55.0
92MHR20-1	D	Jan. 2, 1990		92	5	8	4	91	200	46.0	2.5	4.0	2.0	45.5
92MHR12-1	D	Feb. 15, 1990		80	13	9	5	93	200	40.0	6.5	4.5	2.5	46.5
92MHR12-2	D	Feb. 15, 1990		61	10	8	4	117	200	30.5	5.0	4.0	2.0	58.5
92MHR22-2	D	April 15 1990		76	10	9	4	101	200	38.0	5.0	4.5	2.0	50.5
92MHR22-3	D	April 15 1990		80	8	9	5	98	200	40.0	4.0	4.5	2.5	49.0
Experimental Samples:														
RDT-4	E		150	33	10	8	6	143	200	16.5	5.0	4.0	3.0	71.5
RDT-47	E		90	103	9	9	6	73	200	51.5	4.5	4.5	3.0	36.5
RDT-20	E		80	142	4	9	5	40	200	70.9	2.2	4.5	2.5	20.0
RDT-48	E		75	142	5	10	5	38	200	71.0	2.5	5.0	2.5	19.0
RDT-59	E		70	142	5	10	5	38	200	71.0	2.5	5.0	2.5	19.0
RDT-58	E		65	144	6	9	4	37	200	72.0	3.0	4.5	2.0	18.5
RDT-35	E		60	159	7	8	5	21	200	79.5	3.5	4.0	2.5	10.5
RDT-52	E		50	160	8	9	5	18	200	80.0	4.0	4.5	2.5	9.0
RDT-54	E		45	161	7	8	6	18	200	80.5	3.5	4.0	3.0	9.0
RDT-63	E		40	159	7	9	6	19	200	79.5	3.5	4.5	3.0	9.5
RDT-74	E		40	170	9	8	5	8	200	85.0	4.5	4.0	2.5	4.0
RDT-70	E		30	163	9	10	6	12	200	81.5	4.5	5.0	3.0	6.0
RDT-73	E		20	171	9	9	6	5	200	85.5	4.5	4.5	3.0	2.5
RDT-68	E		20	168	8	9	6	9	200	84.0	4.0	4.5	3.0	4.5
RDT-76	E		5	172	9	9	6	4	200	86.0	4.5	4.5	3.0	2.0
RDT-64	E		5	172	9	8	6	5	200	86.0	4.5	4.0	3.0	2.5

[x] Type: P, pumice; D, dome sample; E, experiment sample

[y] Phenocryst: Pl, plagioclase; Hbl, hornblende; Px, orthopyroxene; gl, glass

[z] Modal Abundance: Modal abundances based on 200 count points per sample

subrounded to rounded crystal edges. Dissolution is also indicated by the decrease in modal hornblende, which occurs simultaneously to increases in modal plagioclase, orthopyroxene, and titanomagnetite (Fig. 2.15, Table 2.8). Thus, the products of hornblende dissolution that are released to the surrounding melt appear to be transported away from the dissolving crystal margin before crystallization of reaction rims can occur. As a result, hornblende dissolution facilitates growth of pre-existing crystal phases away from the hornblende-melt boundary. This reaction is not observed at lower pressures, probably because melt viscosity is higher at lower pressures because of the lower water content of the interstitial melt (Shaw, 1974).

The growth rate of hornblende reaction rims is highest 30 to 40 MPa below the hornblende stability field. Like observations from experiments performed at higher pressures, hornblende dissolution also occurs at these pressures based on the presence of subhedral and rounded crystal edges and decreased modal abundance, but to a lesser extent (Fig. 2.15, Table 2.8). Unlike observations from experiments at higher pressures, however, reaction rims develop at particularly fast rates at these pressures. This suggests that the hornblende dissolution products that are released to the surrounding melt are not quickly transported away from the dissolving crystal margin, probably due to higher melt viscosity because of the lower water content of the melt (Fig. 2.15). As a result, reaction rim crystallization occurs because hornblende dissolution supplies necessary reaction rim components to the hornblende-melt boundary at a rate that exceeds the rate of material transport away from the crystal-melt boundary.

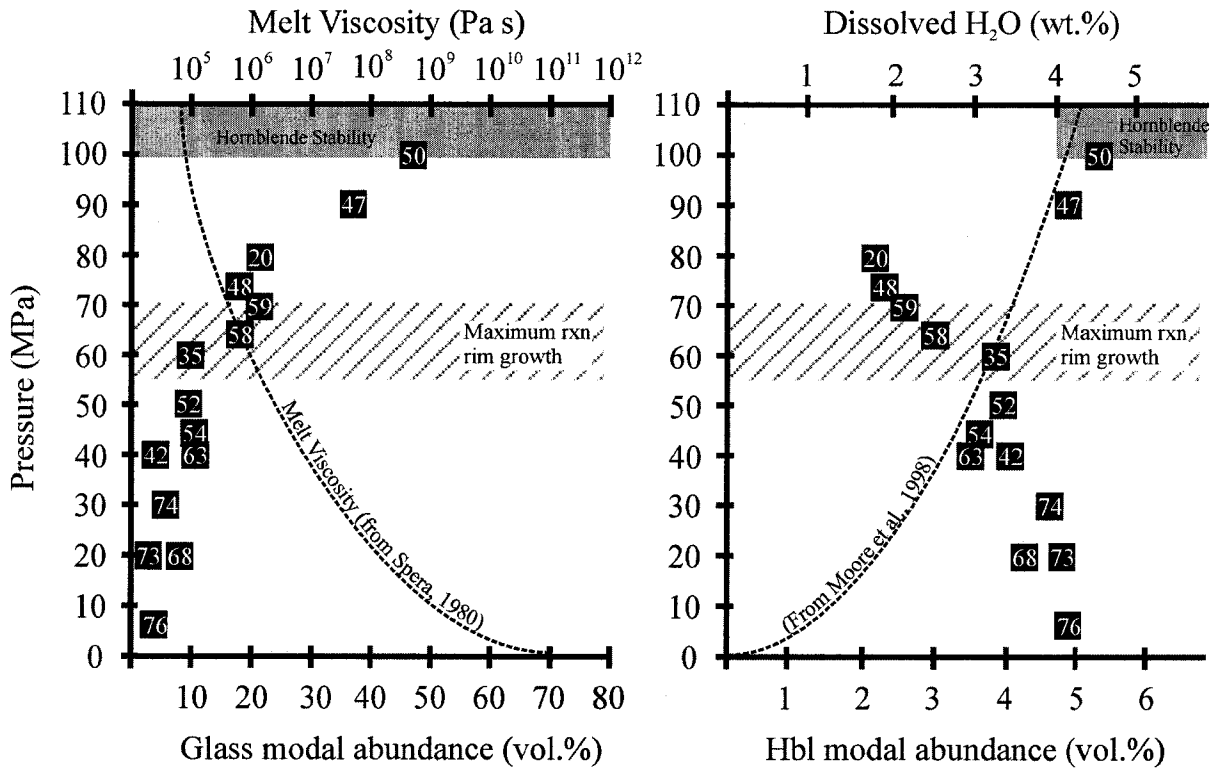

Figure 2.15
Modal abundance of matrix glass and hornblende phenocrysts from single-step decompression experiments with respect to pressure. Hatched pattern indicates region of maximum reaction rim growth. Phase equilibria experiments performed within the hornblende stability field (HSF) contain 5.5 vol.% hornblende phenocrysts (Table 2.8). Changes in hornblende abundance reflects dissolution, where experiments dropped to pressures <10 MPa and >70 MPa below HSF resulted in minor dissolution compared to experiments dropped to pressures 20- 40 MPa below HSF. The modal abundance of matrix glass also varies with pressure in decompression experiments, where experiments dropped to pressures <40 MPa below HSF contain 20-50 vol.% matrix glass, compared to <10 vol.% matrix glass in experiments dropped to >60 MPa below HDF. Melt viscosity increases by 4 orders of magnitude through this pressure range. See text for discussion.

The breakdown of hornblende at pressures 50- 90 MPa below the hornblende stability occurs at the slowest rate compared to experiments ran at higher pressures. Moreover, no visible hornblende reaction rims formed in experiments decompressed to >90 MPa below hornblende stability, even when held for 40 days. This may seem counterintuitive because these experiments occurred at conditions further away from the amphibole stability limit. The interstitial melt at 10- 50 MPa and 840°C contains less dissolved water (1- 3 wt.%) and more SiO_2, however, than melt at 80 MPa and 840°C, thereby causing it to be more viscous (e.g. Shaw, 1974). Thus, the slow rate of hornblende breakdown at 20 MPa is influenced by the high melt viscosity and microlite-rich nature of this near-solidus interstitial melt. In addition, rim morphologies at these low pressures are thin, fine-grained, and tightly enclose subangular hornblendes crystal edges. These observations are consistent with the relatively high hornblende modal abundance (Fig. 2.15, Table 2.8), suggesting that hornblende dissolution is limited at low pressure compared to the same reaction at higher pressures. The relatively slow reaction rim growth at low pressure may also reflect the limited supply of reaction products from the surrounding melt because the crystal rim has become effectively isolated.

Heating Induced Amphibole Breakdown

The reaction rim formed on heated hornblende consists of clinopyroxene, calcic plagioclase, and pargasite, all of which are stable at run temperature. Heating-induced reactions grow inward from the crystal edge and occur only where the hornblende is in

contact with the surrounding melt. Moreover, the anhedral and embayed morphology of destabilized hornblende edges suggests that the crystals are rapidly dissolving.

The breakdown of hornblende at 940°C occurs at rates 10 to 100 times faster than reaction rims grow when induced by decompression at 840 °C, and are characterized by thick, coarse-grained reaction rims around embayed, dissolving crystal edges. Instead, the rapid dissolution of hornblende margins drives the development of heating-induced reaction rims, which provides an abundance of necessary components for crystallization of coarse-grained rims of clinopyroxene, calcic plagioclase, and minor pargasite and titanomagnetite. Therefore, the rate of reaction rim growth in response to instability induced by decompression and heating appears to be largely controlled by the rate at which rim components are supplied from the hornblende to the coexisting melt through dissolution.

Experimental Results Compared to 1980 Mount St. Helens

The results from this study are generally consistent with the calibration of decompression-induced hornblende breakdown from magmas erupted during the 1980-86 eruption of Mount St. Helens. In both studies, progressively wider decompression-induced reaction rims are observed from a variety of decompression rates (magma ascent paths) where experiments are held outside the hornblende stability field for longer durations (Rutherford and Hill, 1993). Results from this study indicate that the rate of decompression reaction rim growth in 1989-90 Redoubt dacite occurs 30- 85% slower than Mount St. Helens 1980 dacite in experiments run at 900 °C and 15- 55% and 860 °C,

respectively (Fig. 2.16). It is unlikely that this discrepancy results from hornblende composition, for hornblende phenocrysts from both magmas are generally equivalent with respect to composition and size (Rutherford and Hill, 1993). Instead, results from this study indicate that reaction rim growth rate is strongly controlled by the rate at which rim components are supplied from the hornblende to the coexisting melt through dissolution of the crystal edges. Because this reaction was severely limited at low pressures, where interstitial melt was more viscous due to low water content and low temperature, it seems probable that the reaction rim growth rate in hornblendes from 1989-90 Redoubt dacite was slower compared to those from 1980-86 Mount St. Helens dacite for similar reasons (i.e. Redoubt magmas existed at a lower temperature with a more silicic melt than 1980 Mount St. Helens dacite).

Experimental Results Applied to the 1989-90 Redoubt Eruption

Two types of reaction rims occur together in nearly all magmas erupted from Redoubt during 1989-90 (e.g. Fig. 2.7). The profound differences in texture and mineralogy between the two types of reaction rims are interpreted to be the result of different modes of formation. Relatively thin, fine-grained rims that exist around subangular to subrounded crystal margins are interpreted to result from decompression, as suggested by their strong resemblance in texture and mineralogy to experimental rims that grew in response to decompression. The observations that fine-grained reaction rims exist on hornblendes that were erupted effusively, but not explosively, on December 26, 1989, are consistent with this inference because fine-grained reaction rims on hornblende

in dome samples originate as breakdown caused by H_2O loss from the coexisting melt during magma ascent in the conduit. Thicker (20- 120 μm), coarse-grained rims that exist around rounded and embayed crystal margins, however, are interpreted to form in response to heating. Intrusion of hotter andesitic magma into the Redoubt magma storage chamber is interpreted to have caused this thermal instability. This is consistent with other petrologic, geochemical, and seismic evidence suggesting that the ~940 °C andesite magma intruded the Redoubt dacitic storage region immediately prior to eruption (Swanson et al., 1994; Nye et al., 1994; Power et al., 1994). This conclusion is supported by the presence of coarse-grained reaction rims existing on hornblendes that were erupted explosively and effusively on December 15, 1989, because rims that form in response to heating grow while hornblendes were in the chamber. Therefore, naturally occurring reaction rims resembling those produced in decompression and heating experiments are hereafter referred to as 'decompression rims' or 'heating rims', respectively.

Given that amphiboles with decompression rims and heating rims are preserved in natural dacite samples, and that an ascent rate and heating duration can be estimated from experimental results (Fig. 2.16), a timescale for magma mixing prior to eruption and average magma ascent rates for magma erupted during eruption from Redoubt can be inferred. Estimates of ascent based on pargasite reaction rim thicknesses are based on experiments of Rutherford and Hill (1993).

The December 15, 1989, explosive eruption produced dacite pumice with hornblende crystals surrounded by 20-80-μm-thick heating reaction rims. This indicates a maximum reaction time of approximately 12 hours at 940°C, which is the predicted

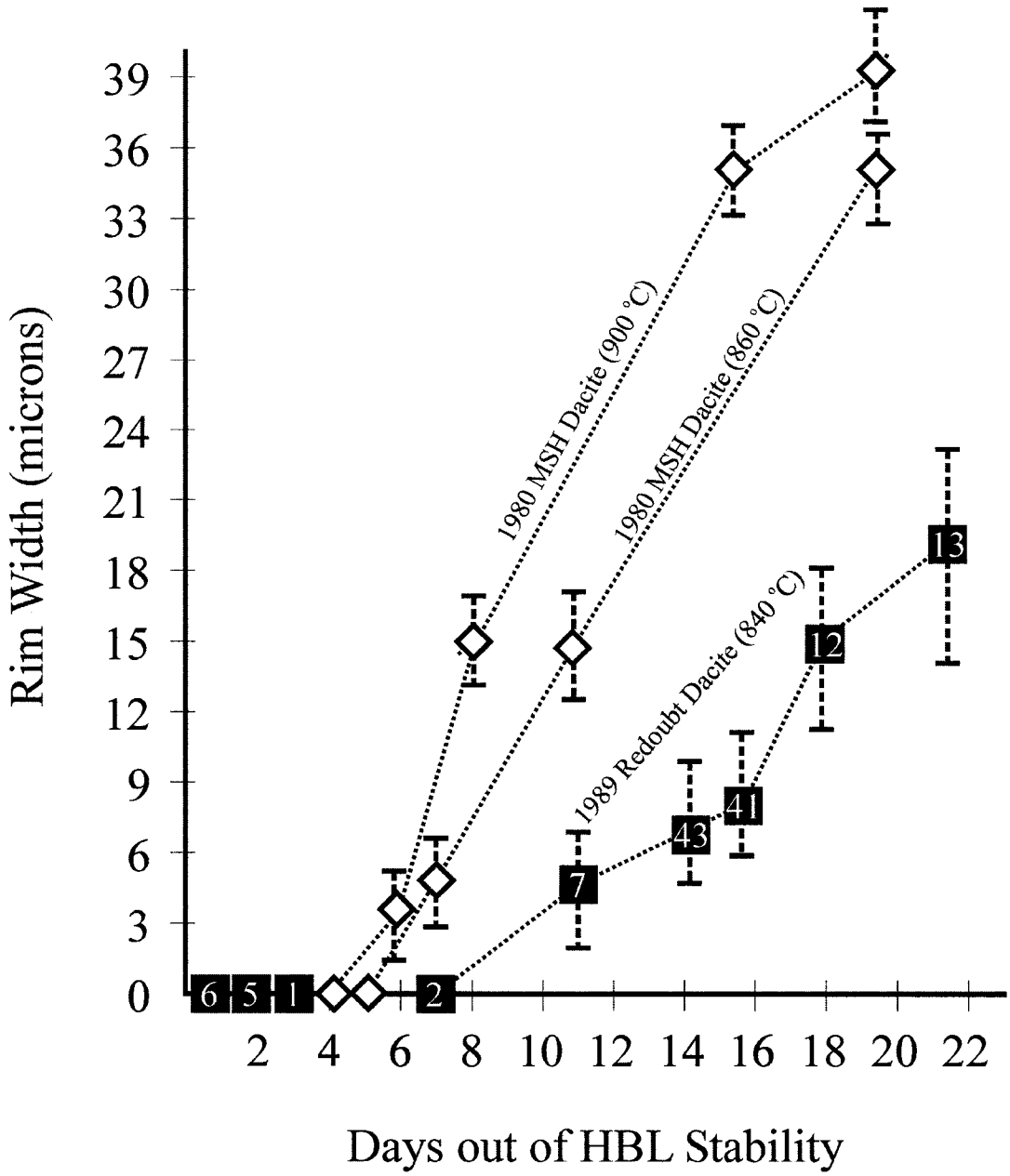

Figure 2.16
Hornblende reaction rim width versus time below the hornblende stability field (HSF) for multi-step experiments on December 15, 1989 Redoubt dacite. Additional curves are for constant rate decompression experiments at 900C and 860C on Mount St. Helens dacite performed by Rutherford and Hill (1993). The decompression-induced breakdown reaction of Redoubt hornblende is slower than the Mount St. Helens dacite, indicating that Redoubt hornblende phenocrysts must spend more time outside the HSF in order to develop reaction rims of equivalent thickness to those observed at Mount St. Helens.

tem

perature of the intruded andesite magma. This timescale is in good agreement with other petrologic evidence suggesting that mixing between the andesite and dacite magmas occurred immediately prior to eruption, such as the presence of sharp compositional contacts, without apparent diffusion, in banded pumice glasses as well as titanomagnetite-ilmenite pairs erupted on December 15 (Swanson et al., 1994).

Samples from the December 26, 1989, dome eruption also contain subhedral amphiboles with no decompression reaction rims, indicating rapid ascent from 6 km depth to the surface in <8 days, assuming the ascent rate was approximately constant. Assuming a constant ascent rate, however, is inconsistent with observations from Power et al. (1994) and Lahr et al. (1994) of an intense seismic swarm of long-period earthquakes at <3 km depth that preceded the eruption by 50 hours. This observation suggests that ascending magma may have stalled briefly (~2 days) at pressures <20 MPa below hornblende stability (~3 km) prior to erupting, which is in good agreement with the presence of abundant unrimmed and subrounded hornblende.

Rim widths of hornblende and pargasite from each dome-building eruptive event during the 1989-90 Redoubt activity vary greatly- even at thin section scale (Fig. 2.5). Approximately 60% of amphiboles observed in dome samples from eruptions on December 15 and January 2 are subhedral and lack decompression reaction rims, suggesting that the rising magma may have stalled briefly during an <8-day ascent. Decompression rims, ranging from 3- 12 μm in thickness, do exist on about one third of the hornblendes, indicating an ascent time of 10- 14 days. Pargasite reaction rims range up to 8 μm in thickness, suggesting ascent occurred over 7- 12 days (Rutherford and Hill,

1993). Approximately 40% of hornblende in domes emplaced in February and April, and ~30% of hornblende in the final dome emplaced between April and June 1990 contain unrimmed amphiboles, indicating an ascent in <8 days. The remaining hornblende crystals contain decompression rims from 5 to 28 μm thick, indicating an ascent time of 12 to 24 days. Pargasite decompression rims range from 5 to 35 μm, indicating an ascent time in 6 to 18 days. Therefore, the average resident time of Redoubt magmas (outside the hornblende stability field, 0 to 4 km depth) in the conduit steadily increased from <8 to 10 days in December 1989, to <8 to 14 days in January 1990, to <8 to 24 days in April and June 1990.

The observation that amphibole from each eruptive event exist with a wide variety in decompression rim thickness is strong evidence against a constant rate of magma ascent from a deep crystal storage chamber. The fact that the textures of amphibole-melt boundaries and reaction rim mineralogy also vary between grains in the same eruptive event supports this conclusion. Therefore, the presence of such a diverse collection of decompression-induced reaction rims in samples from each eruptive event with respect to thickness, texture, and mineralogy suggests that magma ascent probably occurred in one of two styles.

One ascent style that is consistent with observations from this study is that fresh, rapidly ascending magma mix with conduit-resident magma en route to the surface (e.g., Rutherford and Hill, 1993). As a result, amphiboles from conduit-resident magma with reaction rims that formed in response to decompression at different pressures and for different timescales are incorporated as fresh batches of magma move to the surface

through an established conduit (Fig. 2.17). Another ascent style that is consistent with this study is ascent that occurs initially at a constant rate, but stalls *en masse* in the conduit for a given amount of time. As a result, the upper portion of the magma column at low pressure will contain hornblendes with either very thin reaction rims (if stalled at 20-50 MPa), or no reaction rims at all if stalled at very low pressure (<10 MPa). Reaction rims will develop relative quickly in portions of the magma column at intermediate pressure (60-70 MPa), whereas hornblende crystals at higher pressure (80-90 MPa) will simply dissolve. Thus, subsequent effusion of the *en masse* magma column will result in a diverse collection of hornblende reaction rims.

Bearing in mind either ascent style, the ascent of Redoubt magma from depth through the conduit appears to have slowed over time, as indicated by the steady increase in hornblende and pargasite rim thickness in eruptive products from successive eruption events. This style of magma ascent is likely widespread, regardless of magma composition or tectonic setting, as indicated by the presence of amphibole decompression rim diversity in magmas erupted elsewhere, such as Mount St. Helens, Washington (Rutherford and Hill, 1993), Popocatepetl, Mexico (Athanasopoulos, 1997), Soufriere Hills, Montserrat (Devine et al., 1997; Rutherford and Devine, 2003), Tongariro Volcanic Centre, New Zealand (Nakagawa et al., 1998), Black Butte, California (McCanta and Rutherford, 1999), and the Crater Flat volcanic zone, Nevada (Nicholis and Rutherford, 2004).

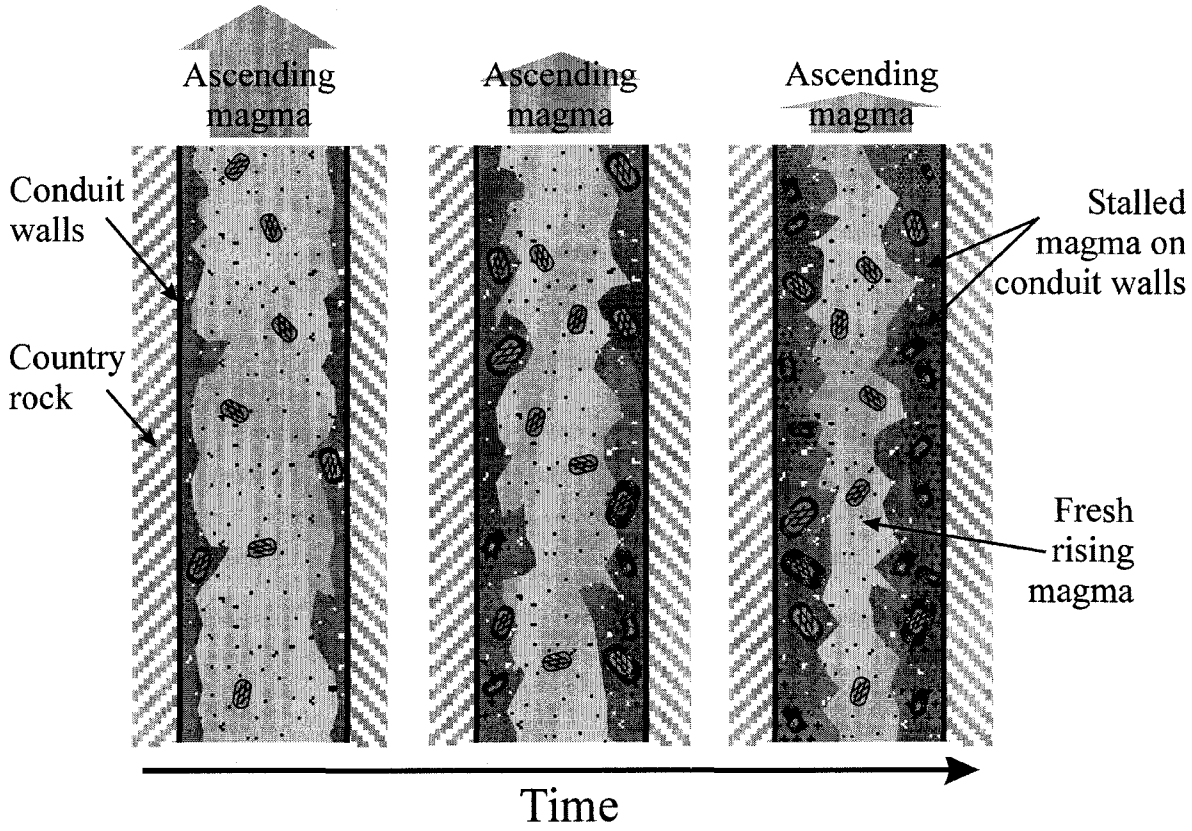

Figure 2.17
Schematic diagram for magma ascent during the 1989-90 eruptions of Redoubt. Fresh batches of magma rapidly ascend to the surface through an established conduit in all eruptive events. Some magma, probably near the flow-conduit boundary, stalls during ascent in response to cooling and increased viscosity. This conduit-resident magma is incorporated by subsequent batches of fresh rising magma. As a result, amphiboles from conduit-resident magma with reaction rims that formed in response to decompression at different pressures and for different timescales are brought to the surface with fresh batches of magma. Over time, the proportion of fresh magma decreases as the eruption wanes and eventually stops.

2.6 CONCLUSIONS

(1) Agreement between the compositions of plagioclase rims and coexisting matrix glass from natural dacite and andesite pumice samples and experimental phase and glass compositions at water saturated conditions suggests that the dacite last equilibrated at ~840°C, 150 MPa (±25 MPa) and the andesite last equilibrated at ~940°C, 170 MPa (±40 MPa).

(2) Decompression-induced reaction rims are composed of orthopyroxene and plagioclase, with minor titanomagnetite. Hornblende decompression reaction rim growth depends on the balance between the rate that reaction rim components are supplied from dissolving hornblende to the coexisting melt, and the rate that those components are transported through the melt away from the dissolving hornblende margin to other pre-existing mineral phases. This reaction is strongly influenced by the melt viscosity, which is controlled by the dissolved water content and crystallinity of the interstitial melt.

At relatively high pressures (<20 MPa below hornblende stability), the hornblende crystal faces dissolve while growth of new anhydrous phases occurs away from the hornblende -melt boundary on pre-existing crystal faces. Hornblende reaction rim growth in response to decompression is fastest 30- 40 MPa below the hornblende stability field (1.9- 6.9 x 10^{-9} cm/sec), and slowest 50- 90 MPa below the hornblende stability (0.18- 2.0 x 10^{-9} cm/sec), because the high viscosity and microlite-rich nature of the interstitial melt.

(3) Heating reaction rims exist around anhedral and pervasively embayed crystal edges, and are composed of clinopyroxene, calcic plagioclase, pargasite, and minor titanomagnetite. Heating rims grow 10- 100 times faster than decompression rims (0.8-2.1 x 10^{-7} cm/sec), where the rate and style of hornblende reaction rim growth in response to heating is mainly controlled by the rate at which necessary rim components are supplied from the hornblende to the coexisting melt through dissolution.

(4) Results from this study are generally consistent with the previous calibration of decompression-induced hornblende breakdown from magmas erupted during the 1980-86 eruption of Mount St. Helens, however the rate of reaction rim growth in Redoubt dacite occurs more slowly than Mount St. Helens dacite, probably because Redoubt dacite is lower temperature (~60°C) with a more silicic melt (~10 wt.% SiO_2).

(5) Two types of hornblende reaction rims occur together in nearly all magmas erupted from Redoubt during 1989-90. One type of reaction rim is interpreted to result from decompression, as suggested by their strong resemblance in texture and mineralogy to experimental rims that grew in response to decompression. Decompression rims are 3-40 μm thick, fine or medium grained, and composed of plagioclase, orthopyroxene, and titanomagnetite. These rims closely surround subangular to subrounded crystal margins. The second type is interpreted to form in response to thermal instability during an intrusion of hotter magma into the Redoubt magma storage chamber at depth prior to the eruption. This type is thicker (20- 120 μm), coarse-grained rims of clinopyroxene, calcic plagioclase, and minor pargasite and titanomagnetite that broadly enclose rounded and pervasively embayed grains.

(6) Magma ascent during the 1989-90 Redoubt eruption may be characterized in two styles based on the variety in texture, mineralogy, and thickness of reaction rim widths in products from the same eruptive events. One style may involve fresh ascending magma that mixes with stagnant conduit magma en route to the surface. Another style involves ascent that occurs initially at a constant rate, but stalls *en masse* in the conduit for a given amount of time. These styles of magma ascent are likely widespread, regardless of magma composition or tectonic setting. For either ascent styles, the residence time of ascending Redoubt magmas in the conduit increased with each successive eruptive event over the coarse of the eruption from <8 to 10 days in December 1989, to <8 to 14 days in January 1990, to <8 to 24 days in April and June 1990.

3.1 REFERENCES

Anderson, A.T. (1983). Oscillatory zoning of plagioclase: Nomarski interference contrast microscopy of etched polish sections. American Mineralogist 68, 125-129

Anderson, A.T., Jr., Swihart, G.H., Artioli, G., and Geiger, C.A. (1984). Segregation vesicles, gas filter-pressing, and igneous differentiation. Journal of Geology 92, 55-72

Anderson, D. J., Lindsley, D. H. (1988). Internally consistent solution models for Fe-Mg-Mn-Ti oxides: Fe-Ti oxides. American Mineralogist 73, 57-61

Athanasopoulos, P. (1997) The origin and ascent history of the 1996 dacitic dome, Volcan Popocatepetl, Mexico. University of Manitoba, Winnipeg, MB, Canada (Masters Thesis)

Bacon, C. R. (1986). Magmatic inclusions in silicic and intermediate volcanic rocks. Journal of Geophysical Research 91, 6091-6112

Bacon, C. R., Bruggman, P. E., Christiansen, R. L., Clynne, M. A., Donnelly-Nolan, J. M., and Hildreth, W. (1997). Primitive magmas at five Cascade volcanic fields; melts from hot, heterogeneous sub-arc mantle. The Canadian Mineralogist 35, 397-423

Bacon, C. R., Hirschmann, M. M. (1988). Mg/Mn partitioning as a test for equilibrium between coexisting Fe-Ti oxides. American Mineralogist 73, 57-61

Bacon, C. R., Metz, J. (1984). Magmatic inclusions in rhyolites, contaminated basalts, and compositional zonation beneath the Coso volcanic field, California. Contributions to Mineralogy and Petrology 85, 346-365

Barclay, J., Rutherford, M.J., Carroll, M. R., Murphy, M.D., Devine, J.D., Gardner, J., Sparks, R.S.J. (1998) Experimental phase equilibria constraints on pre-eruptive storage conditions of the Soufriere Hills magma. Geophysical Research Letters 25: 3437-3440

Beget, J.E., Nye, C.J. (1994) Postglacial eruption history of Redoubt Volcano, Alaska. Journal of Volcanology and Geothermal Research 62: 31-54

Bindeman, I.N., Bailey, J.C. (1999). Trace elements in anorthite megacrysts from the Kurile Arc: a window to across-arc geochemical variations in magma compositions. Earth and Planetary Science Letters 169, 209-226

Blundy, J. D., Sparks, R. S. J. (2002) Generation, ascent and crystallisation of calc-alkaline silicic magmas. Geochimica et Cosmochimica Acta 66: 83

Blundy, J.D., Wood, B.J. (1991). Crystal-chemical controls on the partitioning of Sr and Ba between plagioclase feldspar, silicate melts, and hydrothermal solutions. Geochimica et Cosmochimica 55, 193-209

Brantley, S.R. (1990) The eruption of Redoubt Volcano, Alaska, December 14, 1989-August 31, 1990. Casadevall, T.J., Chouet, B.A. (Eds.) U. S. Geological Survey Circular, Reston

Carey, S., Sigurdsson, H. (1987) Temporal variations in column height and magma discharge rate during the 79 A.D. eruption of Vesuvius. Geological Society of America Bulletin 99: 303-314

Cashman, K., Blundy, J. (2000) Degassing and crystallization of ascending andesite and dacite. Philosophical Transactions of the Royal Society, London 358: 1487-1513

Chen, C., Nakada, S., Shieh, Y., DePaolo, D.J. (1999) The Sr, Nd and O isotopic studies of the 1991-1995 eruption at Unzen, Japan. Journal of Volcanology and Geothermal Research 89, 243-253

Clynne, M.A. (1989). The disaggregation of quenched magmatic inclusions contributes to chemical diversity in silicic lavas of Lassen Peak, California. New Mexico Bureau of Mines and Mineral Resources 131, 54

Clynne, M. A. (1999). A complex magma mixing origin for rocks erupted in 1915, Lassen Peak, California. Journal of Petrology 40, 105-132

Clynne, M.A., and Borg, L.E. (1997). The composition of olivine and chromian spinel in primitive calc-alkaline and tholeiitic lavas from the southernmost Cascades Range, California: a reflection of relative fertility of the source. Canadian Mineralogist 35, 453-472

Coombs, M. C., Eichelberger, J. C., Rutherford, M. J. (2002). Experimental and textural constraints on mafic enclave formation in volcanic rocks. Journal of Volcanology and Geothermal Research 119, 125- 144

Criss, J. W. (1980). Fundamental parameters calculations on a laboratory microcomputer. Advanced X-ray Analysis 23, 93- 97

Davidson, J.P., Tepley, F.J. III (1997). Recharge in volcanic systems: evidence from isotopic profiles of phenocrysts. Science 275, 826-829

Davidson, J.P., Tepley, F.J. III, Knesel K.M. (1998). Isotopic fingerprinting may provide insights into evolution of magmatic systems. EOS Transactions, American Geophysical Union 79, 185-193

Davidson, J., Tepley, F., Palacz, Z., Meffan-Main, S. (2001). Magma recharge, contamination and residence times revealed by in situ laser ablation isotopic analysis of feldspar in volcanic rocks. Earth and Planetary Science Letters 184, 427-442

Deer, W.A., Howie, R.A., Zussman, J. (1992) An introduction to the rock-forming minerals (2^{nd} Edition). Addison Wesley Longman Limited, England

Devine, J.D., Gardner, J.E., Brack, H.P., Layne, G.D., Rutherford, M.J. (1995) Comparison of microanalytical methods for estimating H_2O contents of silicic volcanic glasses. American Mineralogist 80: 319-328

Devine, J.D., Rutherford, M.J., Gardner, J.E. (1997) Petrologic determination of ascent rates for the 1995-1997 Soufriere Hills Volcano andesitic magma. Geophysical Research Letters 25: 3673-3676

Didier, J. (1973).Granites and their enclaves; the bearing of enclaves on the origin of granites. Developments in Petrology 3

Dunbar, N.W., Cashman, K.V., Dupré, R. (1994). Crystallization processes of anorthoclase phenocrysts in the Mount Erebus magmatic system: Evidence from crystal composition, crystal size distributions, and volatile contents of melt inclusions. Antarctic Research Series 66, 129-146

Eichelberger, J. C. (1978). Andesitic volcanism and crustal evolution. Nature 275, 21-27

Eichelberger, J. C. (1980). Vesiculation of mafic magma during replenishment of silicic magma reservoirs. Nature 288, 446-450

Eichelberger, J. C., Chertkoff, D.G., Dreher, S. T., and Nye, C. T. (2000). Magmas in collision; rethinking chemical zonation in silicic magmas. Geology 28, 603-606

Eichelberger, J. C., Gooley, R.; Nitsan, U., and Rice, A. (1976). A mixing model for andesitic volcanism (abstract). Eos, Transactions, American Geophysical Union 57, 1024

Feeley, T. C., Dungan, M.A. (1996). Compositional and dynamic controls on mafic-silicic magma interactions at continental arc volcanoes; evidence from Cordon El Guadal, Tatara-San Pedro Complex, Chile. Journal of Petrology: 37: 1547-1577

Freundt, A., Tait, S.R. (1986). The entrainment of high-viscosity magma into low-viscosity magma in eruption conduits. Bulletin of Volcanology 48: 325-339

Gamble, J.A., Wood, C.P., Price, R.C., Smith, I.E.M., Stewart, R.B., Waight, T. (1999). A fifty year perspective of magmatic evolution on Ruapehu Volcano, New Zealand: Verification of open system behavior in an arc volcano. Earth and Planetary Science Letters 170, 301-314

Gardner, J.E., Rutherford, M., Carey, S., Sigurdsson, H. (1995) Experimental constraints on pre-eruptive water contents and changing magma storage prior to explosive eruptions of Mount St Helens Volcano. Bulletin of Volcanology 57: 1-17

Geschwind, C., Rutherford, M.J. (1992) Cummingtonite and the evolution of the Mount St. Helens (Washington) magma system; an experimental study. Geology 20: 1011-1014

Gill, J.B. (1981). *Orogenic andesites and plate tectonics*. Berlin: Springer

Grove, T.L., Baker, M.B., Kinzler, R.J. (1984). Coupled CaAl-NaSi diffusion in plagioclase feldspar: Experiments and applications to cooling rate speedometry. Geochimica et Cosmochimica 48, 2113-2121

Grove, T.L., Donnelly-Nolan, J.M., Housh, T.B. (1997) Magmatic processes that generated the rhyolite of Glass Mountain, Medicine Lake Volcano, N. California. Contributions to Mineralogy and Petrology 127: 205-223

Hammer, J.E., Rutherford, M.J. (2002). An experimental study of the kinetics of decompression-induced crystallization in silicic melt. Journal of Geophysical Research: 107

Hammer, J.E., Rutherford, M.J. (2002) Magma storage prior to the 1912 eruption at Novarupta, Alaska. Contributions to Mineralogy and Petrology 144: 144-162

Heiken, G., Eichelberger, J. C. (1980). Eruptions at Chaos Crags, Lassen Volcanic National Park, California. Journal of Volcanology and Geothermal Research 7, 443-481

Helz, R.T. (1973). Phase Relations of Basalts in their Melting Range at P_{H2O} = 5kb as a Function of Oxygen Fugacity; Part I, Mafic Phases. Journal of Petrology 14, 249-302

Helz, R. T. (1979). Alkali exchange between hornblende and melt: A temperature sensitive reaction. American Mineralogist 64, 953-965

Huppert, H.E., Sparks, R.S.J., Turner, J.S. (1982a). Effects of volatiles on mixing in calc-alkaline magma systems. Nature 297, 554-557

Huppert, H. E., Turner, J. S., Sparks, R. S. J. (1982b). Replenished magma chambers; effects of compositional zonation and input rates. Earth and Planetary Science Letters 57, 345-357

Hoshizumi, H., Uto, K., Watanabe, K. (1999). Geology and eruptive history of Unzen Volcano, Shimabara Peninsula, Kyushu, SW Japan. Journal of Volcanology and Geothermal Research 89, 81-94

Hoshizumi, H., Uto, K., Matsumoto, A., Xu, S., Oguri, K. (2002). Geology of Unzen volcano and core stratigraphy of the flank drilling (abstract). Unzen Workshop 2002: International Workshop on the Unzen Scientific Drilling Project, pp. 4- 8

Izbekov, P.E., Eichelberger, J.C., Patino, L.C., Vogel, B.V., Ivanov, B.V. (2002). Calcic cores of plagioclase phenocrysts in andesite from Karymsky volcano: Evidence for rapid introduction by basalt replenishment. Geology 30, 799-802

Jaeger, J.C. (1968). Cooling and solidification of igneous rocks. In: Hess, H.H., and Poldervaart, A. (ed.) *Basalts, volume 2*. New York, New York: John Wiley and Sons, Inc., pp. 503-536

Jaupart, C., Vergniolle, S. (1989). The generation and collapse of a foam layer at the top of a basaltic magma chamber. Journal of Fluid Mechanics 203, 347-380

Kouchi, A., Sunagawa, I. (1985). A model for mixing basaltic and dacitic magmas as deduced from experimental data. Contributions to Mineralogy and Petrology 89, 17-23

Koyaguchi, T., Blake, S. (1989) The dynamics of magma mixing in a rising magma batch. Bulletin of Volcanology 52: 127-137

Koyaguchi, T., Blake, S. (1991). Origin of mafic enclaves; constraints on the magma mixing model from fluid dynamic experiments. Enclaves and granite petrology, Developments in Petrology 13, 415-429

Le Bas, M. J., Le Maitre, R.W., Streckeisen, A., Zanettin, B.A., (1986). Chemical classification of volcanic rocks based on the total alkali-silica diagram. Journal of Petrology: 27: 745-750

Le Maitre, R.W., Bateman, P., Dudek, A., Keller, J., Lameyre Le Bas, M.J., Sabine, P.A., Schmid, R., Sorensen, H., Streckeisen, A., Woolley, A.R., and Zanettin, B. (1989). *A classification of Igneous Rocks and Glossery of Terms*. Oxford: Blakewell Press

Lofgren, G.E. (1980). Experimental studies on the dynamic crystallization of silicate melts. In: Hargraves, R. B. (Ed.) *Physics of Magmatic Processes*. Princeton, NJ: Princeton University Press, pp. 487-551

Lahr, J.C., Chouet, B.A., Stephens, C.D., Power, J.A., Page, R.A. (1994) Earthquake classification, location, and error analysis in a volcanic environment; implications for the magmatic system of the 1989-1990 eruptions at Redoubt Volcano, Alaska. Journal of Volcanology and Geothermal Research 62: 137-151

Luhr, J.F., and Carmichael I.S.E. (1985). Jorullo volcano, Michoacan, Mexico (1759-1774): the earliest stages of fractionation in calc-alkaline magmas. Contributions to Mineralogy and Petrology 90, 142-161

Martel, C., Pichavant, M., Bourdier, J. L., Traineau, H., Holtz, F., Scaillet, B. (1998) Magma storage conditions and control of eruption regime in silicic volcanoes; experimental evidence from Mt. Pelee. Earth and Planetary Science Letters 156: 89-99

Martin-del Pozzo, A.L., Cifuentes, G. (2003) Timing magma ascent at Popocatepetl Volcano, Mexico, 2000-2001. Journal of Volcanology and Geothermal Research 125: 107-120

McCanta, M.C., Rutherford, M.J. (1999) Black Butte, CA dacite dome; pre-eruption conditions, magma ascent, and links to Shasta. Eos, Transactions, American Geophysical Union 80: 1106

Miller, T.P. (1994) Dome growth and destruction during the 1989-1990 eruption of Redoubt Volcano. Journal of Volcanology and Geothermal Research 62: 197-212

Miller, T. P., Chertkoff, D. G., Eichelberger, J. C., Coombs, M. C. (1999). Mount Dutton Volcano, Alaska; Aleutian Arc analog to Unzen Volcano, Japan. Journal of Volcanology and Geothermal Research 89, 275-301

Miller, T.P., Chouet, B.A. (1994). The 1989-1990 eruptions of Redoubt Volcano; an introduction. Journal of Volcanology and Geothermal Research 62: 1-10

Miyashiro, A. (1974). Volcanic rock series in island arcs and active continental margins. American Journal of Science 274, 321-355

Moore, G., Vennemann, T., Carmichael, I.S.E. (1998). An empirical model for the solubility of H_2O in magmas to 3 kilobars. American Mineralogist 83: 36-42

Nakada, S., Bacon, C.R., Gartner, A.E. (1994). Origin of phenocrysts and compositional diversity in per-Mazama rhyodacite lavas, Crater Lake, Oregon. Journal of Petrology 35, 127-162

Nakada, S., Motomura, Y. (1999). Petrology of the 1991-1995 eruption at Unzen; effusion pulsation and groundmass crystallization. Journal of Volcanology and Geothermal Resources 89, 173-196

Nakada, S., Shimizu, H., Ohta, K. (1999). Overview of the 1990-1995 eruption at Unzen. Journal of Volcanology and Geothermal Research 89, 1-22

Nakagawa, M., Nairn, I.A., Kobayashi, T. (1998) The approximately 10 ka multiple vent pyroclastic eruption sequence at Tongariro Volcanic Centre, Taupo Volcanic Zone, New Zealand; Part 2, Petrological insights into magma storage and transport during regional extension. Journal of Volcanology and Geothermal Research 86: 45-65

Nakamura, M., Shimakita, S. (1998). Dissolution origin and syn-entrapment compositional change of melt inclusion in plagioclase. Earth and Planetary Science Letters 161, 119-133

NEDO (New Energy Development Organization) (1988). Western district of Unzen. Report on the Promotion and Development of Geothermal Energy 15, 1060 (in Japanese)

Nelson, S.T., Montana, A. (1992). Sieve-textured plagioclase in volcanic rocks produced by rapid decompression. American Mineralogist 77, 1242-1249

Nicholis, M.G., Rutherford, M.J. (2004) Experimental constraints on magma ascent rate for the Crater Flat volcanic zone hawaiite. Geology 32: 489-492

Nye, C.J., Swanson, S.E., Avery, V.F., Miller, T.P. (1994) Geochemistry of the 1989-1990 eruption of Redoubt Volcano; Part I, Whole-rock major- and trace-element chemistry. Journal of Volcanology and Geothermal Research 62: 429-452

Norman, M.D., Pearson, N.J., Sharma, A., and Griffin, W.L. (1996). Quantitative analysis of trace elements in geological materials by laser ablation ICP-MS: Instrumental operating conditions and calibration values of NIST glasses. Geostandards Newsletter 20, 776-798

Pallister, J.S., Hoblitt, R.P., Meeker, G.P., Knight, R.J., Siems, D.F. (1996). Magma mixing at Mount Pinatubo; petrographic and chemical evidence from the 1991 deposits. In: Newhall, C. G., and Punongbayan, R. S. (Ed.) *Fire and mud; eruptions and lahars of Mount Pinatubo, Philippines*. Seattle, WA: University of Washington Press, pp. 687-731

Pearce, T.H., Griffin, M.P., Kolisnik, A.M. (1987). Magmatic crystal stratigraphy and constraints on magma chamber dynamics: Laser interference results on individual phenocrysts. Journal of Geophysical Research 92, 13745-13752

Phillips, J. C., Woods, A. W. (2001). Bubble plumes generated during recharge of basaltic magma reservoirs. Earth and Planetary Science Letters 186, 297-309

Power, J.A., Lahr, J.C., Page, R.A., Chouet, B.A., Stephens, C.D., Harlow, D.H., Murray, T.L., Davies, J.N. (1994) Seismic evolution of the 1989-1990 eruption sequence of Redoubt Volcano, Alaska. Journal of Volcanology and Geothermal Research 62: 69-94

Pownceby, M.I., O'Neill, H. (1994) Thermodynamic data from redox reactions at high temperatures; III, Activity-composition relations in Ni-Pd alloys from EMF measurements at 850-1250 K, and calibration of the NiO+Ni-Pd assemblage as a redox sensor. Contributions to Mineralogy and Petrology 116: 327-339

Reed, B.L., Lanphere, M.A. (1973). Plutonic Rocks of Alaska-Aleutian Range Batholith. Arctic Geology 19, 421-428

Riehle, J.R. (1985) A reconnaissance of the major Holocene tephra deposits in the upper Cook Inlet region, Alaska. Journal of Volcanology and Geothermal Research 26: 37-74

Robinson, P., Spear, F. S., Schumacher, J. C., Laird, J., Klein, C., Evans, B. W., and Doolan, B. L. (1982). Amphiboles: Petrology and experimental phase relations. In: Veblen, D.R., and Ribbe, P.H. (Ed.) *Reviews in Mineralogy 9B*. Chelsea, MI: Mineralogical Society of America, pp. 3-42

Roeder, P. L., Emslie, R. F. (1970). Olivine-liquid equilibrium. Contributions to Mineralogy and Petrology 29, 275-289

Rutherford, M.J., Devine, J.D (1988) The May 18 1980 Eruption of Mount St. Helens; 3. Stability and chemistry of amphibole in the magma chamber. Journal of Geophysical Research 93: 11,949- 11,959

Rutherford, M.J., Devine, J.D. (2003) Magmatic conditions and magma ascent as indicated by hornblende phase equilibria and reactions in the 1995-2002 Soufriere Hills magma. Journal of Petrology 44: 1433-1454

Rutherford, M.J., Hill, P.M. (1993) Magma ascent rates from amphibole breakdown; an experimental study applied to the 1980-1986 Mount St. Helens eruptions. Journal of Geophysical Research 98: 19,667-19,685

Rutherford, M.J., Sigurdsson, H., Carey, S., Davis, A. (1985) The May 18, 1980, eruption of Mount St. Helens; 1, Melt composition and experimental phase equilibria. Journal of Geophysical Research 90: 2929-2947

Sack, R. O., Carmichael, I. S. E., Rivers, M., Ghiorso, M. S. (1980). Ferric-Ferrous equilibria in natural silicate liquids at 1 bar. Contributions to Mineralogy and Petrology 85, 116-132

Scandone, R., Malone, S.D. (1985) Magma supply, magma discharge and readjustment of the feeding system of Mount St. Helens during 1980. Journal of Volcanology and Geothermal Research 23: 239-262

Shaw, H.R. (1974) Diffusion of H_2O in granitic liquids; Part 1, Experimental data; Part 2, Mass transfer in magma chambers. Carnegie Institution of Washington Publication 634: 139-170

Sigurdsson, H., Cornell, W., Carey, S. (1990) Influence of magma withdrawal on compositional gradients during the AD 79 Vesuvius eruption. Nature 345: 519-521

Singer, B.S., Dungan, M.A., Layne, G.D. (1995). Textures and Sr, Ba, Mg, Fe, K, and Ti compositional profiles in volcanic plagioclase: Clues to the dynamics of calc-alkaline magma chambers. American Mineralogist 80, 776-798

Sisson, T.W. and Bacon, C.R. (1999). Gas-driven filter pressing in magmas. Geology 27, 613-616

Snyder, D., Tait, S. (1995). Magma mingling in Replenishment of magma chambers; comparison of fluid-mechanic experiments with field relations. Contributions to Mineralogy and Petrology 122, 230-240

Sparks, R.S.J., Marshall, L.A. (1986). Thermal and mechanical constraints on mixing between mafic and silicic magmas. Journal of Volcanology and Geothermal Research 29, 99-124

Spera, F.J. (1980) Aspects of magma transport. *Physics of magmatic processes.* Hargraves, R. B. (Ed.) Princeton University Press, Princeton, NJ p 265-324

Stimac, J.A., Pearce, T. H., Donnelly-Nolan, J. M., Hearn Jr., B. C. (1990). The origin and implications of undercooled andesitic inclusions in rhyolites, Clear Lake Volcanics, California. Journal of Geophysical Research 95, 17729- 17746

Stimac, J.A., Pearce, T. H. (1992). Textural evidence of mafic-felsic magma interaction in dacite lavas, Clear Lake, California. American Mineralogist 77, 795-809

Stormer, J.C. (1983). The effects of recalculation on estimates of temperature and oxygen fugacity from analyses of multicomponent iron-titanium oxides. American Mineralogist 68, 586-594

Swanson, S.E., Nye, C.J., Miller, T.P., Avery, V.F. (1994) Geochemistry of the 1989-1990 eruption of Redoubt Volcano; Part II, Evidence from mineral and glass chemistry. Journal of Volcanology and Geothermal Research 62: 453-468

Tepley, F.J. III, Davidson, J.P., Clynne, M.A. (1999). Magmatic interactions as recorded in plagioclase phenocrysts of Chaos Crags, Lassen Volcanic Center, California. Journal of Petrology 40, 787-806

Tepley, F.J. III, Davidson, J.P., Tilling, R.I., Arth, J.G. (2000). Magma mixing, recharge and eruption histories in plagioclase phenocrysts from El Chichón Volcano, Mexico. Journal of Petrology 41, 1397-1411

Till, A.B., Yount, M.E., Bevier, M.L. (1994) The geologic history of Redoubt Volcano, Alaska. Journal of Volcanology and Geothermal Research 62: 11-30

Tsuchiyama A. (1985). Dissolution kinetics of plagioclase in the melt of the system: diopside-albite-anorthite, and origin of dusty plagioclase in andesites. Contributions to Mineralogy and Petrology 89, 1-16

Tsuchiyama, A., Takahashi, E. (1983). Melting kinetics of a plagioclase feldspar. Contributions to Mineralogy Petrology 84, 345-354

Ulmer, P. (1989). The dependence of the Fe2+-Mg cation-partitioning between olivine and basaltic liquid on pressure, temperature and composition; an experimental study to 30 kbars. Contributions to Mineralogy and Petrology 101: 261-273

Uto, K., Nakada, S., Hoshizumi, H., Shimizu, H. (2002). Overview of the Unzen Scientific Drilling Project and the progress of its first phase [abstract: V10/01P/A01-001]. International Union of Geodesy and Geophysics 2003 Meeting, Sapporo, Japan

Vance, J.A. (1965). Zoning in igneous plagioclase: Patchy zoning. Journal of Geology 73, 636-651

Venezky, D.Y., Rutherford, M.J. (1999) Petrology and Fe-Ti oxide reequilibration of the 1991 Mount Unzen mixed magma. Journal of Volcanology and Geothermal Research 89: 213-230

Vernon, R. H. (1983). Restite, xenoliths and microgranitoid enclaves in granites. Journal and Proceedings of the Royal Society of New South Wales 116, 77-103

Vernon, R. H. (1984). Microgranitoid enclaves in granites; globules of hybrid magma quenched in a plutonic environment. Nature 309, 438-439

Wiebe, R. A. (1994). Silicic magma chambers as traps for basaltic magmas: The Cadillac Mountain Intrusive Complex, Mount Desert Island, Maine. The Journal of Geology 102, 423-437

Wiebe R. A., Collins, W. J. (1998). Depositional features and stratigraphic sections in granitic plutons: implications for the emplacement and crystallization of granitic magma, Journal of Structural Geology 20, 1273-1289

Wiebe, R. A., Blair, K. D., Hawkins, D. P., Sabine C. P. (2002). Mafic injections, in situ hybridization, and crystal accumulation in the Pyramid Peak Granite, California. Geological Society of America Bulletin 114, 909-920

Wolf, K.J., Eichelberger, J.C. (1997) Syn-eruptive mixing, degassing, and crystallization at Redoubt Volcano, eruption of December, 1989 to May 1990. Journal of Volcanology and Geothermal Research 75: 19-38

Zellmer, G.F., Blake, S., Vance, D., Hawkesworth, C., Turner, S. (1999). Plagioclase residence times at two island arc volcanoes (Kameni Islands, Satorini, and Soufriere, St. Vincent) determined by Sr diffusion systematics. Contributions to Mineralogy and Petrology 136, 345-357

3.2 APPENDICES

Appendix 1.1

Electron microprobe analyses of Unzen plagioclase (in wt.%). Plagioclase sample names are based on the sampling group (see **1.3 MATERIALS AND METHODS**), type of crystal (P, phenocryst; M, microphenocryst), and whether the grain exists in a host (H), enclave (E), or 1663 lava (1663) sample. For example, sample "103.8-103.85 Host Plag1" relates to a plagioclase crystal found in a host lava sample from an USDP drill depth of 103.8-103.85 m. Alternatively, sample "153.85-153.9 Enclave P-Plag1" relates to a plagioclase phenocryst found in an enclave from an USDP drill depth of 153.85-153.9 m. Or, sample "432.2-432.25 E1 M-Plag1" indicates a plagioclase microphenocryst found in an enclave from an USDP drill depth of 432.20-432.25 m. Finally; plagioclase crystals from 1991-1995 samples are indicated by a "U" prefix. *An, Anorthite mole %; **um, distance in microns from plagioclase core.

Appendix 1.1

Electron microprobe analyses of Unzen plagioclase (in wt.%).

Sample ID	SiO_2	Al_2O_3	FeO	CaO	Na_2O	K_2O	Total	An*	um**	Sr (ppm)	Ba (ppm)	Sr/ Ba
103.8-103.85 Host Plag-1	55.15	28.33	0.26	10.12	5.78	0.34	99.97	62.33	0			
	54.70	27.79	0.28	10.16	5.64	0.34	98.91	62.97	9			
	54.95	28.06	0.24	9.67	5.77	0.35	99.05	61.25	16			
	55.03	28.27	0.26	9.93	5.93	0.30	99.72	61.47	24			
	55.47	27.71	0.22	9.49	5.92	0.36	99.17	60.19	32			
	55.56	27.81	0.25	9.49	6.09	0.34	99.55	59.61	40			
	55.54	27.67	0.24	9.51	6.15	0.32	99.43	59.53	48			
	55.70	27.34	0.25	9.03	6.11	0.34	98.77	58.34	56			
	55.33	27.04	0.26	9.05	5.96	0.38	98.02	58.80	64			
	56.23	27.08	0.27	8.46	6.36	0.40	98.80	55.57	73			
	56.93	26.96	0.22	8.54	6.47	0.41	99.54	55.37	81			
	56.72	27.61	0.23	8.83	6.23	0.37	99.99	57.22	97			
	55.06	27.86	0.22	9.85	5.80	0.36	99.15	61.56	104			
	54.52	28.26	0.28	10.05	5.68	0.32	99.11	62.63	113			
	55.12	27.85	0.22	9.67	5.84	0.32	99.01	61.08	120			
	55.63	28.08	0.23	9.53	6.08	0.36	99.90	59.70	129			
	55.68	27.28	0.23	9.18	6.03	0.37	98.78	58.92	136			
	56.39	26.89	0.18	8.40	6.30	0.44	98.61	55.48	145			
	56.08	27.88	0.33	9.44	6.15	0.45	100.33	58.86	153			
	55.37	28.23	0.18	9.94	5.89	0.32	99.93	61.53	161			
	54.73	28.37	0.20	9.92	5.93	0.32	99.46	61.37	169			
	55.41	27.81	0.23	9.63	5.98	0.33	99.39	60.40	177			
	55.22	28.00	0.17	9.44	5.87	0.35	99.05	60.29	185			
	55.09	27.99	0.13	9.92	5.74	0.36	99.22	61.94	193			
	55.09	28.29	0.36	9.69	5.82	0.29	99.55	61.31	201			
	55.44	27.64	0.29	9.52	5.95	0.37	99.21	60.08	208			
	55.33	28.02	0.20	9.56	5.94	0.35	99.40	60.31	217			
	55.96	28.03	0.28	9.56	5.87	0.34	100.04	60.59	233			
	55.91	27.75	0.34	9.47	5.97	0.39	99.84	59.83	242			
	55.89	27.33	0.34	9.36	5.98	0.32	99.22	59.79	249			
	55.99	28.09	0.29	9.20	6.00	0.37	99.94	59.09	257			
	55.75	27.77	0.29	9.17	6.14	0.40	99.53	58.36	265			
	56.67	27.58	0.28	9.18	6.18	0.40	100.29	58.23	274			
	56.17	27.47	0.31	9.17	6.27	0.39	99.77	57.94	281			
	55.97	27.30	0.32	9.18	6.20	0.45	99.43	57.99	290			
	56.18	27.30	0.22	8.86	6.31	0.40	99.28	56.90	297			
	56.00	27.12	0.24	8.95	6.26	0.40	98.97	57.34	305			
	56.77	27.44	0.32	8.63	6.45	0.46	100.08	55.50	314			
	56.25	27.18	0.33	8.81	6.28	0.44	99.27	56.75	321			
	56.76	27.33	0.29	8.70	6.30	0.42	99.80	56.44	330			
	56.67	27.41	0.27	8.86	6.24	0.40	99.85	57.17	338			
	57.00	27.40	0.25	8.92	6.43	0.39	100.38	56.65	346			
	56.12	27.03	0.20	8.61	6.41	0.41	98.79	55.80	354			
	56.15	27.07	0.26	8.77	6.41	0.42	99.07	56.22	362			
	57.44	27.28	0.22	8.52	6.40	0.46	100.33	55.40	369			
	56.91	27.03	0.26	8.57	6.33	0.37	99.46	56.13	378			
	56.98	26.76	0.27	8.61	6.52	0.45	99.60	55.27	386			
	56.40	26.41	0.28	8.42	6.43	0.42	98.35	55.17	402			
	57.19	26.75	0.28	8.48	6.38	0.43	99.51	55.49	418			
	56.40	27.30	0.23	8.93	6.44	0.39	99.69	56.66	426			
	56.23	27.00	0.15	8.83	6.38	0.37	98.98	56.66	434			
	56.48	27.17	0.25	8.51	6.36	0.37	99.14	55.83	442			
	56.31	27.38	0.12	8.51	6.24	0.44	99.01	56.03	450			
	55.94	27.67	0.20	9.02	6.10	0.34	99.28	58.33	459			
	55.85	27.77	0.34	9.12	5.98	0.35	99.41	59.04	466			
	55.56	27.71	0.27	9.62	6.01	0.38	99.55	60.09	475			
	55.50	28.29	0.25	9.75	5.92	0.40	100.12	60.67	482			
	55.39	27.57	0.29	9.48	5.89	0.34	98.96	60.34	491			

Appendix 1.1 (cont.)

Electron microprobe analyses of Unzen plagioclase (in wt.%).

Sample ID	SiO_2	Al_2O_3	FeO	CaO	Na_2O	K_2O	Total	An*	um**	Sr (ppm)	Ba (ppm)	Sr/ Ba
	56.13	27.61	0.32	9.22	6.05	0.36	99.70	58.98	498			
	56.58	27.34	0.23	8.70	6.46	0.42	99.74	55.82	507			
	55.91	27.48	0.33	8.91	6.33	0.36	99.32	57.13	515			
	55.88	27.64	0.33	9.16	6.18	0.37	99.56	58.30	523			
	55.89	27.72	0.26	8.82	6.03	0.38	99.09	57.92	531			
	55.71	27.34	0.21	9.16	6.34	0.39	99.15	57.66	538			
	56.76	27.69	0.38	8.55	6.33	0.42	100.13	55.87	547			
	55.44	28.10	0.27	9.87	5.67	0.39	99.75	61.95	555			
	55.90	27.85	0.35	9.63	5.88	0.44	100.05	60.37	563			
	55.34	28.44	0.33	9.72	5.80	0.35	99.97	61.26	571			
	54.93	28.35	0.28	9.83	5.65	0.37	99.40	62.02	579			
	55.08	27.85	0.31	9.72	5.82	0.37	99.15	61.08	587			
	55.40	27.49	0.17	9.24	5.94	0.37	98.60	59.44	595			
	55.94	28.36	0.28	9.62	5.84	0.36	100.41	60.82	603			
	55.13	28.73	0.23	10.47	5.41	0.35	100.32	64.51	611			
	54.72	28.88	0.30	10.25	5.51	0.35	100.01	63.63	620			
	54.75	28.40	0.24	10.01	5.75	0.30	99.46	62.32	627			
	55.20	28.47	0.30	9.43	5.80	0.34	99.55	60.57	635			
	55.77	28.34	0.19	9.65	5.85	0.39	100.20	60.70	643			
	55.56	27.82	0.31	9.33	5.99	0.35	99.37	59.50	651			
	55.70	28.04	0.27	9.44	6.12	0.33	99.91	59.38	659			
	54.07	29.06	0.21	10.68	5.40	0.34	99.76	65.06	668			
	54.76	28.71	0.27	10.23	5.58	0.31	99.86	63.45	676			
	55.41	28.52	0.30	9.96	5.66	0.34	100.18	62.41	684			
	55.68	28.51	0.30	9.54	5.78	0.32	100.12	60.98	692			
	55.10	28.67	0.21	9.59	5.71	0.31	99.59	61.45	699			
	55.02	29.13	0.28	10.08	5.72	0.33	100.56	62.48	708			
	54.99	28.14	0.28	9.83	5.73	0.32	99.29	61.92	715			
	55.33	28.39	0.24	9.62	5.64	0.34	99.56	61.69	724			
	55.81	28.10	0.26	9.64	5.94	0.32	100.08	60.62	732			
	55.37	28.21	0.35	9.60	5.73	0.32	99.59	61.36	740			
	55.86	28.43	0.30	9.47	5.66	0.34	100.06	61.22	748			
	54.82	28.76	0.29	10.28	5.44	0.36	99.95	63.93	756			
	53.58	29.06	0.25	10.50	5.37	0.26	99.03	65.10	764			
	54.38	29.08	0.29	10.55	5.27	0.30	99.88	65.43	772			
	54.21	28.42	0.19	10.54	5.50	0.32	99.18	64.46	780			
	54.50	28.93	0.26	10.22	5.46	0.32	99.68	63.89	788			
	55.14	28.35	0.17	9.65	5.70	0.37	99.38	61.38	797			
	55.84	28.66	0.25	9.66	5.65	0.34	100.40	61.74	804			
	54.80	28.50	0.23	9.67	5.69	0.38	99.28	61.44	812			
	54.87	27.93	0.17	9.57	5.59	0.34	98.45	61.76	820			
	55.74	28.44	0.27	9.84	5.68	0.35	100.31	62.00	828			
	56.81	27.36	0.32	8.58	6.33	0.45	99.86	55.84	837			
	56.87	27.66	0.23	8.52	6.24	0.41	99.92	56.17	853			
	55.05	28.49	0.10	9.85	5.55	0.32	99.36	62.65	860			
	55.15	28.23	0.27	9.60	5.84	0.35	99.44	60.80	868			
	55.76	28.07	0.37	9.03	6.17	0.37	99.76	58.00	876			
	55.69	27.51	0.28	9.04	6.23	0.43	99.17	57.59	885			
	56.87	27.15	0.30	8.30	6.41	0.44	99.48	54.78	892			
	57.52	27.04	0.21	8.14	6.44	0.45	99.81	54.16	901			
	55.34	28.48	0.24	9.75	5.68	0.35	99.83	61.78	909			
	55.76	28.02	0.30	9.17	5.95	0.40	99.61	59.08	917			
	56.74	27.33	0.22	8.35	6.38	0.44	99.46	55.04	925			
	58.91	26.40	0.27	7.40	6.91	0.51	100.40	49.92	932			
	56.32	27.85	0.25	8.83	6.13	0.36	99.74	57.60	941			
	56.49	27.42	0.30	8.64	6.25	0.42	99.53	56.44	949			
	55.75	28.17	0.16	9.64	5.69	0.40	99.82	61.27	957			
	56.86	27.54	0.19	8.56	6.19	0.40	99.73	56.50	965			

Appendix 1.1 (cont.)

Electron microprobe analyses of Unzen plagioclase (in wt.%).

Sample ID	SiO_2	Al_2O_3	FeO	CaO	Na_2O	K_2O	Total	An*	um**	Sr (ppm)	Ba (ppm)	Sr/ Ba
	55.44	28.52	0.25	9.59	5.70	0.33	99.84	61.39	973			
	56.31	27.83	0.20	9.10	6.02	0.40	99.85	58.63	981			
	56.55	27.48	0.23	8.61	6.33	0.42	99.63	56.04	989			
	56.13	28.34	0.13	9.36	5.76	0.30	100.03	60.68	997			
	56.15	28.10	0.33	9.21	6.07	0.34	100.20	58.98	1005			
	55.94	28.06	0.33	9.38	5.99	0.39	100.10	59.52	1014			
	55.59	28.71	0.20	9.83	5.64	0.27	100.25	62.44	1029			
	55.38	28.73	0.20	9.63	5.80	0.36	100.11	61.01	1037			
	55.19	28.30	0.38	9.54	5.70	0.32	99.43	61.32	1045			
	55.73	28.50	0.24	9.79	5.76	0.34	100.37	61.60	1054			
	56.06	27.58	0.19	8.72	6.21	0.38	99.13	56.97	1062			
	56.67	27.22	0.31	8.45	6.19	0.36	99.19	56.37	1070			
	56.47	27.69	0.22	8.40	6.44	0.39	99.60	55.16	1078			
	56.89	26.99	0.20	8.07	6.59	0.48	99.22	53.29	1086			
	57.83	26.70	0.26	7.93	6.49	0.44	99.65	53.36	1094			
	56.99	27.18	0.23	7.92	6.49	0.53	99.34	53.00	1102			
	56.41	26.68	0.28	7.93	6.56	0.45	98.31	53.10	1109			
	56.73	27.21	0.21	8.37	6.35	0.46	99.33	55.15	1118			
	57.11	27.10	0.28	8.09	6.47	0.45	99.50	53.91	1127			
	56.82	26.92	0.15	8.39	6.41	0.47	99.15	54.95	1134			
	56.67	27.68	0.32	8.39	6.46	0.41	99.94	54.98	1142			
	56.42	27.58	0.31	8.81	6.14	0.44	99.70	57.26	1150			
	55.65	27.53	0.81	9.03	5.46	0.42	98.90	60.58	1158			
	54.79	28.34	0.22	9.60	5.66	0.33	98.95	61.58	1166			
	55.52	28.11	0.27	9.55	5.78	0.37	99.61	60.83	1174			
	54.84	28.43	0.32	9.61	5.63	0.30	99.13	61.86	1182			
	55.04	27.80	0.27	9.28	5.77	0.29	98.45	60.50	1198			
	55.77	28.21	0.29	9.01	6.00	0.41	99.69	58.43	1206			
103.8-103.85 Host Plag-2	55.69	27.81	0.11	8.62	6.23	0.43	98.90	56.40	0			
	56.64	27.13	0.27	8.35	6.42	0.39	99.19	55.04	8			
	57.21	27.18	0.23	8.25	6.42	0.43	99.72	54.61	17			
	56.97	26.96	0.19	8.32	6.56	0.48	99.47	54.15	24			
	56.96	27.22	0.26	8.38	6.52	0.47	99.81	54.54	32			
	57.60	26.93	0.24	8.08	6.49	0.55	99.89	53.43	41			
	58.34	26.58	0.30	7.83	6.72	0.48	100.24	52.09	49			
	57.50	26.71	0.20	8.05	6.59	0.49	99.53	53.24	56			
	54.85	28.54	0.20	9.76	5.74	0.33	99.41	61.68	65			
	58.18	26.44	0.32	8.86	5.44	0.86	100.10	58.44	81			
	54.49	28.85	0.16	9.92	5.52	0.32	99.26	62.92	89			
	54.17	28.32	0.25	9.77	5.71	0.33	98.56	61.80	105			
	55.58	28.34	0.30	9.34	5.76	0.32	99.63	60.58	114			
	55.34	28.29	0.24	9.68	5.69	0.32	99.56	61.71	121			
	55.96	27.86	0.30	8.85	6.08	0.44	99.50	57.58	138			
	53.98	28.87	0.29	10.47	5.10	0.36	99.07	65.71	146			
	55.76	27.93	0.31	8.98	6.10	0.38	99.47	58.07	154			
	54.11	29.64	0.29	10.38	5.11	0.31	99.85	65.67	162			
	55.37	27.21	0.39	9.47	5.06	0.62	98.12	62.54	187			
	55.97	27.83	0.27	8.95	6.05	0.39	99.46	58.17	194			
	54.85	28.28	0.24	9.89	5.73	0.30	99.30	62.11	202			
	54.12	29.03	0.23	10.32	5.45	0.28	99.43	64.31	211			
	51.17	30.51	0.41	12.14	4.37	0.15	98.75	72.84	219			
	56.44	27.38	0.28	8.78	6.37	0.46	99.72	56.22	227			
	56.56	27.39	0.23	8.64	6.44	0.37	99.63	55.93	243			
	55.70	28.39	0.25	9.70	5.90	0.32	100.27	60.94	251			
	55.79	27.79	0.29	9.35	6.01	0.38	99.60	59.42	260			
	55.40	28.62	0.22	9.61	5.81	0.40	100.06	60.76	267			
	56.18	27.73	0.23	8.85	6.20	0.35	99.55	57.46	275			

Appendix 1.1 (cont.)

Electron microprobe analyses of Unzen plagioclase (in wt.%).

Sample ID	SiO_2	Al_2O_3	FeO	CaO	Na_2O	K_2O	Total	An*	um**	Sr (ppm)	Ba (ppm)	Sr/ Ba
	56.95	27.49	0.27	8.36	6.41	0.42	99.91	55.04	284			
	56.85	27.28	0.25	8.82	6.35	0.40	99.96	56.65	292			
	53.97	28.76	0.28	10.28	5.43	0.27	98.99	64.32	299			
	57.76	26.69	0.35	8.83	5.21	0.71	99.55	59.86	308			
	51.54	30.37	0.31	13.02	3.74	0.35	99.33	76.11	316			
	49.12	31.80	0.27	13.73	3.45	0.18	98.55	79.11	332			
	49.86	31.84	0.36	13.51	3.25	0.20	99.02	79.68	340			
	51.94	29.73	0.35	13.24	3.32	0.65	99.24	76.90	357			
	52.92	30.91	0.46	13.16	2.89	0.54	100.88	79.30	364			
	48.40	32.27	0.40	14.25	3.13	0.17	98.62	81.19	373			
	55.29	28.20	0.33	9.22	5.83	0.38	99.26	59.75	381			
	58.70	25.85	0.52	8.34	5.27	1.02	99.69	57.00	389			
	54.79	28.58	0.42	10.40	4.99	0.49	99.67	65.51	430			
	55.59	27.25	0.27	9.33	6.22	0.40	99.06	58.52	438			
	55.99	27.44	0.29	8.88	6.06	0.38	99.04	57.95	446			
	56.13	27.73	0.09	9.16	6.19	0.43	99.72	58.08	454			
	54.72	27.76	0.21	9.79	5.81	0.32	98.62	61.49	462			
	49.21	31.98	0.31	13.62	3.44	0.14	98.71	79.17	470			
	52.02	29.93	0.41	11.75	4.57	0.32	98.99	70.64	478			
	49.95	32.30	0.41	14.03	3.30	0.22	100.22	79.90	486			
	48.95	32.73	0.36	14.32	3.13	0.12	99.61	81.49	495			
	50.27	31.85	0.37	12.98	3.61	0.19	99.26	77.37	502			
	51.36	30.56	0.24	12.77	3.93	0.24	99.10	75.36	510			
	55.94	27.58	0.31	8.81	6.41	0.45	99.49	56.26	519			
	49.72	32.15	0.32	13.22	3.30	0.17	98.89	79.19	527			
	47.93	33.89	0.35	15.38	2.55	0.11	100.22	85.25	583			
	50.46	30.90	0.33	13.30	3.26	0.34	98.58	78.73	592			
	50.73	31.51	0.44	13.65	3.79	0.17	100.30	77.49	600			
	47.04	32.92	0.61	15.81	1.93	0.29	98.60	87.65	607			
	55.12	28.23	0.31	9.65	5.73	0.36	99.40	61.31	616			
	46.48	34.26	0.43	16.29	2.02	0.12	99.60	88.40	624			
	52.86	29.56	0.33	11.39	4.79	0.32	99.25	69.04	632			
	52.93	29.76	0.32	11.12	4.97	0.27	99.37	67.98	640			
	53.43	29.12	0.31	10.77	5.21	0.28	99.12	66.22	648			
	46.94	33.39	0.30	15.87	1.88	0.27	98.66	88.05	657			
	45.68	34.34	0.48	16.76	1.61	0.06	98.92	90.95	665			
	49.97	31.75	0.56	13.22	3.80	0.20	99.50	76.75	673			
	51.92	30.54	0.53	11.78	4.34	0.25	99.36	71.94	681			
	49.86	31.13	0.58	13.26	3.68	0.23	98.74	77.21	689			
103.8-103.85 Enclave Plag-1	56.63	27.17	0.20	8.62	6.13	0.39	99.14	56.91	0			
	56.04	27.71	0.31	9.12	5.89	0.36	99.43	59.34	8			
	52.37	30.14	0.30	11.77	4.47	0.25	99.30	71.37	16			
	50.64	31.28	0.16	13.08	3.82	0.18	99.16	76.59	24			
	52.09	30.12	0.31	11.79	4.64	0.29	99.24	70.52	33			
	54.98	28.18	0.22	9.85	5.70	0.39	99.32	61.79	40			
	54.47	28.60	0.30	10.26	5.53	0.33	99.48	63.67	48			
	51.43	31.30	0.31	12.94	3.82	0.20	100.00	76.30	73			
	51.13	31.05	0.39	12.94	3.81	0.22	99.54	76.26	81			
	52.24	30.36	0.27	12.02	4.25	0.20	99.33	73.00	88			
	51.75	30.95	0.37	12.44	4.07	0.21	99.79	74.39	97			
	51.71	30.76	0.24	12.18	4.28	0.24	99.40	72.95	104			
	51.85	30.66	0.20	12.15	4.22	0.21	99.30	73.26	112			
	51.35	30.79	0.19	12.28	4.21	0.24	99.07	73.36	121			
	52.02	31.09	0.35	12.12	4.35	0.23	100.16	72.56	152			
	52.98	29.90	0.35	11.55	4.93	0.25	99.96	69.00	161			
	54.91	28.60	0.26	10.07	5.83	0.36	100.04	61.91	169			
	55.49	27.63	0.36	9.17	5.90	0.34	98.88	59.52	176			

Appendix 1.1 (cont.)
Electron microprobe analyses of Unzen plagioclase (in wt.%)

Sample ID	SiO_2	Al_2O_3	FeO	CaO	Na_2O	K_2O	Total	An*	um**	Sr (ppm)	Ba (ppm)	Sr/ Ba
	56.75	27.33	0.19	8.77	6.25	0.41	99.69	56.81	185			
103.8-103.85 Enclave Plag-2	55.51	28.10	0.23	9.70	5.76	0.35	99.64	61.35	0			
	51.02	31.29	0.32	12.62	3.82	0.22	99.30	75.75	8			
	51.45	31.34	0.35	12.24	3.80	0.20	99.39	75.36	16			
	56.15	27.87	0.23	9.02	5.87	0.34	99.49	59.22	25			
	55.63	28.11	0.32	9.52	5.86	0.37	99.81	60.47	41			
	56.06	28.21	0.19	9.35	5.98	0.31	100.09	59.82	50			
	55.43	28.45	0.26	9.57	5.78	0.40	99.91	60.75	57			
	55.67	28.22	0.15	9.43	5.87	0.38	99.72	60.15	66			
	55.59	27.71	0.31	9.44	6.01	0.43	99.48	59.46	74			
	50.56	31.53	0.23	12.63	3.93	0.20	99.08	75.36	83			
	50.89	31.50	0.29	12.70	3.88	0.20	99.47	75.68	91			
	50.55	30.94	0.26	12.69	3.90	0.16	98.50	75.76	99			
	51.33	31.40	0.28	12.40	3.95	0.18	99.54	75.01	108			
	50.98	31.12	0.37	12.65	3.98	0.14	99.23	75.43	116			
	51.31	31.19	0.24	12.64	4.06	0.16	99.61	74.95	124			
	51.12	31.22	0.28	12.54	4.11	0.20	99.47	74.42	132			
103.8-103.85 Enclave Plag-3	56.18	28.34	0.21	8.97	5.98	0.44	100.12	58.31	0			
	52.88	30.24	0.28	11.34	4.79	0.23	99.76	69.29	6			
	55.21	28.62	0.23	9.72	5.69	0.40	99.87	61.44	12			
	53.99	28.72	0.18	10.19	5.25	0.30	98.64	64.77	18			
	55.85	27.72	0.30	8.91	5.99	0.39	99.16	58.29	24			
	56.68	27.36	0.37	8.72	6.21	0.41	99.75	56.86	31			
	58.10	26.48	0.30	8.18	5.92	0.67	99.65	55.37	37			
	55.03	28.78	0.22	9.72	5.43	0.37	99.55	62.61	43			
	51.69	31.49	0.25	12.66	4.11	0.19	100.38	74.65	55			
	52.07	30.77	0.21	12.15	4.25	0.20	99.65	73.18	62			
	52.36	30.65	0.23	12.01	4.41	0.29	99.95	71.89	68			
	52.28	30.81	0.29	11.74	4.46	0.24	99.83	71.42	74			
	52.43	30.53	0.40	11.48	4.65	0.27	99.75	69.99	80			
	55.35	28.72	0.30	9.70	5.65	0.33	100.05	61.87	86			
	55.44	28.41	0.30	9.20	5.78	0.33	99.47	60.10	92			
103.8-103.85 Enclave Plag-4	55.20	28.23	0.21	9.67	5.87	0.35	99.53	60.85	8			
	56.65	27.44	0.26	8.52	6.26	0.45	99.59	55.91	16			
	55.88	28.35	0.31	9.74	5.89	0.38	100.55	60.87	25			
	51.59	30.14	0.26	12.10	4.43	0.28	98.81	71.95	33			
	51.94	30.79	0.34	12.67	4.22	0.22	100.19	74.01	41			
	51.53	31.36	0.37	11.99	3.99	0.19	99.43	74.15	49			
	51.50	30.99	0.34	12.22	4.29	0.23	99.57	73.00	57			
	51.92	30.81	0.23	11.68	4.21	0.23	99.09	72.46	65			
	51.50	30.81	0.37	12.20	4.31	0.24	99.43	72.82	73			
	51.32	30.65	0.20	12.36	4.18	0.25	98.96	73.62	82			
	51.42	30.73	0.26	12.00	4.32	0.22	98.95	72.55	90			
	51.89	30.65	0.22	12.14	4.29	0.25	99.44	72.78	98			
	51.28	30.49	0.26	12.23	4.24	0.19	98.69	73.42	105			
	51.24	30.77	0.16	12.08	4.24	0.26	98.75	72.88	113			
	51.78	31.09	0.21	12.41	4.27	0.21	99.96	73.49	121			
	52.10	30.77	0.28	12.17	4.14	0.24	99.70	73.55	130			
	51.66	30.63	0.26	12.30	4.26	0.24	99.35	73.21	138			
	52.72	30.77	0.26	11.97	4.38	0.18	100.27	72.41	146			
	51.78	30.72	0.33	12.39	4.18	0.20	99.58	73.92	154			
	52.03	30.88	0.28	12.01	4.32	0.27	99.80	72.33	162			
	55.01	28.78	0.32	10.11	5.46	0.33	100.00	63.59	170			
	54.73	28.03	0.22	10.02	5.71	0.27	98.98	62.63	179			
	54.95	28.30	0.18	9.22	5.98	0.32	98.94	59.45	187			

Appendix 1.1 (cont.)
Electron microprobe analyses of Unzen plagioclase (in wt.%)

Sample ID	SiO_2	Al_2O_3	FeO	CaO	Na_2O	K_2O	Total	An*	um**	Sr (ppm)	Ba (ppm)	Sr/ Ba
	56.07	27.86	0.32	8.90	5.97	0.41	99.53	58.23	195			
	55.81	28.08	0.24	9.69	5.88	0.35	100.05	60.86	203			
	49.67	32.56	0.26	13.87	3.07	0.18	99.61	81.03	211			
	52.31	30.65	0.34	11.76	4.10	0.23	99.39	73.09	219			
	51.54	30.64	0.27	12.36	4.20	0.19	99.19	73.78	228			
	51.72	30.92	0.29	11.85	4.25	0.26	99.29	72.46	236			
	51.43	30.58	0.28	12.28	4.34	0.17	99.09	73.13	244			
	51.38	30.70	0.29	12.56	4.25	0.24	99.42	73.65	252			
	52.02	30.67	0.27	11.60	4.31	0.23	99.10	71.86	268			
	52.19	30.35	0.29	12.38	4.39	0.21	99.81	72.90	276			
	51.65	30.49	0.30	11.95	4.38	0.20	98.96	72.33	285			
	51.44	30.39	0.33	12.12	4.33	0.18	98.79	72.86	292			
	52.22	30.86	0.17	12.39	4.32	0.20	100.16	73.27	300			
	51.65	30.64	0.28	12.17	4.23	0.19	99.16	73.38	308			
	51.33	30.77	0.21	12.53	4.19	0.23	99.25	73.93	316			
	50.92	31.30	0.31	12.99	3.89	0.19	99.59	76.13	325			
	51.04	30.98	0.16	12.79	3.96	0.21	99.14	75.39	333			
	52.40	30.80	0.33	12.09	4.53	0.23	100.39	71.73	341			
	51.86	30.58	0.29	11.84	4.46	0.22	99.25	71.66	349			
	54.89	28.10	0.26	9.78	5.79	0.36	99.19	61.40	357			
	56.72	27.28	0.29	8.25	6.23	0.39	99.15	55.51	365			
	56.32	27.58	0.23	8.58	6.35	0.41	99.47	55.94	374			
	55.98	27.08	0.29	9.10	6.19	0.40	99.03	58.01	382			
	56.99	27.08	0.29	8.00	6.50	0.46	99.32	53.47	390			
153.85-153.9 Host Plag-1	51.27	31.17	0.51	12.74	4.06	0.19	99.95	74.98	0			
	52.65	29.54	0.44	12.08	4.25	0.51	99.47	71.70	8			
	51.46	30.60	0.52	12.15	4.28	0.23	99.25	72.90	16			
	52.79	29.70	0.47	11.72	4.69	0.23	99.61	70.42	24			
	52.18	30.26	0.45	12.14	4.54	0.24	99.80	71.77	33			
	51.33	30.49	0.40	12.76	4.36	0.27	99.61	73.37	40			
	52.54	30.30	0.47	12.05	4.41	0.37	100.15	71.57	65			
	51.90	30.35	0.36	12.27	4.36	0.21	99.45	72.86	72			
	63.87	21.81	0.94	6.84	3.16	2.33	98.96	55.49	88			
	52.00	30.59	0.46	12.84	4.19	0.22	100.31	74.45	97			
	51.70	30.51	0.45	12.25	4.10	0.36	99.37	73.31	105			
	52.19	30.04	0.48	11.88	4.59	0.24	99.41	71.12	113			
	51.22	30.51	0.45	12.71	4.24	0.19	99.32	74.13	122			
	56.46	26.83	0.25	8.34	6.34	0.44	98.66	55.15	129			
	53.73	29.55	0.36	10.60	5.23	0.34	99.80	65.57	138			
	56.71	26.84	0.36	8.72	6.15	0.54	99.33	56.62	145			
	69.08	17.33	0.94	3.94	3.11	4.06	98.46	35.42	153			
	52.65	30.20	0.38	12.48	4.41	0.27	100.39	72.71	177			
	53.24	29.92	0.39	11.73	4.53	0.41	100.21	70.37	186			
	52.53	30.26	0.42	11.76	4.62	0.25	99.84	70.68	194			
	52.63	30.47	0.48	12.17	4.40	0.26	100.42	72.31	227			
	54.78	28.49	0.43	11.53	4.14	0.77	100.14	70.12	234			
	55.40	28.43	0.30	9.41	5.78	0.38	99.69	60.44	250			
	55.27	28.26	0.33	9.47	5.98	0.39	99.70	59.79	258			
	55.77	27.34	0.22	9.11	6.23	0.39	99.06	57.91	267			
	56.84	26.94	0.21	8.40	6.41	0.44	99.23	55.07	275			
	56.68	27.28	0.22	9.07	6.36	0.45	100.07	57.12	282			
	57.05	26.97	0.19	8.82	6.31	0.42	99.76	56.73	291			
	56.68	27.00	0.37	8.57	6.53	0.45	99.60	55.12	299			
	57.14	26.80	0.27	8.38	6.48	0.42	99.49	54.83	307			
	56.90	27.35	0.31	8.48	6.30	0.45	99.79	55.70	315			
	55.63	27.64	0.27	9.53	6.00	0.37	99.44	59.93	323			
	55.31	28.05	0.22	9.66	5.85	0.40	99.49	60.74	331			

Appendix 1.1 (cont.)
Electron microprobe analyses of Unzen plagioclase (in wt.%)

Sample ID	SiO_2	Al_2O_3	FeO	CaO	Na_2O	K_2O	Total	An*	um**	Sr (ppm)	Ba (ppm)	Sr/ Ba
	54.62	29.08	0.15	10.56	5.49	0.27	100.17	64.70	339			
	55.24	28.14	0.34	9.69	5.87	0.37	99.66	60.82	347			
	55.45	28.33	0.28	9.57	5.80	0.33	99.76	60.95	356			
	55.13	28.40	0.31	9.83	5.79	0.31	99.77	61.72	363			
	54.76	28.22	0.27	10.10	5.74	0.33	99.41	62.48	372			
	55.45	28.24	0.17	9.69	5.86	0.29	99.70	61.17	379			
	54.80	28.47	0.25	10.21	5.51	0.31	99.55	63.71	387			
	54.15	28.29	0.21	9.90	5.63	0.30	98.48	62.51	396			
	54.55	28.22	0.28	10.12	5.65	0.30	99.11	62.98	404			
	54.13	28.61	0.33	10.22	5.43	0.33	99.04	63.98	412			
	54.89	28.29	0.34	9.95	5.54	0.29	99.30	63.07	420			
	54.41	28.78	0.39	9.99	5.58	0.30	99.44	62.93	428			
	54.73	28.55	0.36	10.27	5.61	0.30	99.81	63.46	436			
	54.33	28.46	0.26	9.98	5.44	0.31	98.77	63.44	444			
	55.01	28.39	0.26	9.84	5.65	0.31	99.46	62.29	452			
	54.26	28.83	0.27	10.29	5.50	0.30	99.45	63.94	461			
	55.57	28.44	0.32	9.78	5.78	0.31	100.20	61.62	468			
	54.46	28.40	0.18	10.01	5.83	0.36	99.24	61.79	477			
	53.46	29.14	0.34	10.86	5.23	0.26	99.28	66.43	484			
	54.58	28.43	0.23	10.02	5.71	0.34	99.32	62.33	492			
	54.96	28.74	0.34	9.99	5.50	0.29	99.82	63.30	501			
	54.47	28.46	0.26	10.03	5.53	0.33	99.08	63.16	509			
	54.97	28.34	0.36	10.16	5.58	0.34	99.74	63.17	517			
	53.99	29.17	0.30	10.69	5.38	0.31	99.84	65.25	525			
	55.60	28.47	0.25	9.79	5.69	0.30	100.11	62.04	533			
	54.79	28.12	0.26	9.79	5.87	0.33	99.17	61.21	541			
	56.39	27.11	0.20	8.64	6.33	0.41	99.08	56.18	549			
	52.10	30.29	0.40	12.02	4.58	0.17	99.56	71.68	566			
	51.62	30.21	0.42	12.16	4.38	0.23	99.02	72.48	590			
	51.29	30.48	0.43	12.77	4.30	0.23	99.50	73.85	597			
	51.60	30.34	0.52	12.13	4.17	0.28	99.04	73.19	606			
	51.42	30.53	0.37	12.17	4.31	0.18	98.98	73.05	614			
	53.56	29.43	0.34	10.95	5.07	0.37	99.72	66.80	622			
	53.44	29.31	0.24	10.94	5.15	0.27	99.34	66.85	638			
	49.63	31.87	0.34	13.93	3.54	0.19	99.49	78.87	646			
	49.88	31.61	0.59	13.84	3.33	0.17	99.42	79.82	662			
	50.01	31.43	0.51	14.12	3.36	0.12	99.55	80.22	671			
	51.33	30.19	0.50	13.18	3.40	0.54	99.14	77.00	678			
	50.79	30.83	0.47	12.76	3.95	0.19	98.99	75.52	687			
	50.45	31.47	0.54	13.83	3.42	0.20	99.91	79.25	695			
	52.34	28.55	1.09	12.68	2.84	0.77	98.28	77.81	702			
	50.27	31.32	0.55	13.41	3.65	0.23	99.44	77.55	727			
	52.03	29.23	0.70	13.05	2.93	0.23	98.16	80.50	751			
	50.19	31.57	0.54	13.61	3.50	0.18	99.59	78.71	759			
	49.61	31.20	0.66	13.53	3.18	0.23	98.40	79.85	767			
	55.81	26.48	0.84	9.10	4.58	1.27	98.08	60.87	776			
	48.52	32.65	0.54	14.80	2.87	0.18	99.55	82.96	800			
	52.73	32.42	0.72	13.38	2.30	0.41	101.96	83.19	832			
	49.23	32.39	0.45	14.14	3.10	0.15	99.45	81.35	840			
	49.79	31.82	0.48	13.87	3.32	0.14	99.41	80.06	848			
	50.93	31.52	0.39	13.35	3.77	0.22	100.17	77.02	857			
	49.04	32.14	0.59	14.16	3.16	0.12	99.22	81.19	864			
	49.38	31.89	0.40	14.25	3.25	0.18	99.35	80.61	872			
	50.39	31.10	0.50	13.39	3.73	0.22	99.33	77.22	880			
	52.79	30.15	0.46	11.87	4.57	0.21	100.05	71.29	896			
	52.09	30.01	0.49	12.00	4.39	0.25	99.24	72.11	905			
	51.03	30.38	0.43	12.50	4.07	0.19	98.60	74.61	912			
	51.53	30.46	0.53	12.53	4.14	0.25	99.43	74.06	921			

Appendix 1.1 (cont.)
Electron microprobe analyses of Unzen plagioclase (in wt.%)

Sample ID	SiO_2	Al_2O_3	FeO	CaO	Na_2O	K_2O	Total	An*	um**	Sr (ppm)	Ba (ppm)	Sr/ Ba
	51.90	30.31	0.51	12.02	4.41	0.19	99.35	72.35	929			
	51.22	31.20	0.56	12.75	3.95	0.16	99.84	75.59	936			
	52.32	29.98	0.54	11.83	4.44	0.25	99.36	71.61	945			
	52.32	30.02	0.47	12.09	4.39	0.20	99.50	72.49	962			
	52.66	30.07	0.68	11.78	4.57	0.21	99.96	71.17	969			
153.85-153.9 Host Plag-2	56.48	27.45	0.23	8.73	6.18	0.37	99.45	57.16	0			
	56.37	28.13	0.29	8.79	6.08	0.35	100.00	57.76	8			
	56.24	27.72	0.21	8.57	6.16	0.37	99.28	56.75	16			
	55.86	27.65	0.31	8.62	6.12	0.36	98.93	57.08	25			
	56.51	27.75	0.20	9.00	6.10	0.33	99.89	58.31	33			
	55.87	27.94	0.29	9.14	6.09	0.45	99.77	58.29	40			
	56.61	27.67	0.27	8.85	6.07	0.40	99.86	57.78	48			
	56.44	27.97	0.36	8.98	5.94	0.30	100.00	59.01	57			
	56.54	27.93	0.18	8.92	6.05	0.39	100.01	58.08	65			
	56.06	27.66	0.24	8.93	6.12	0.36	99.38	57.94	73			
	55.99	27.70	0.28	8.86	6.11	0.35	99.30	57.80	81			
	56.01	27.68	0.38	8.82	6.09	0.34	99.32	57.81	89			
	56.09	27.49	0.32	8.30	6.28	0.35	98.82	55.60	98			
	56.75	27.57	0.28	9.15	6.13	0.45	100.32	58.17	106			
	56.14	27.99	0.20	8.78	6.21	0.40	99.73	57.03	113			
	57.15	27.28	0.30	8.49	6.39	0.42	100.03	55.49	122			
	57.78	27.01	0.33	7.95	6.57	0.44	100.09	53.11	138			
	57.50	27.11	0.25	8.16	6.65	0.48	100.17	53.36	146			
	57.58	26.84	0.32	8.01	6.72	0.42	99.90	52.84	154			
	57.65	26.50	0.23	7.65	6.71	0.45	99.19	51.69	162			
	57.97	26.96	0.29	7.80	6.72	0.47	100.21	52.02	171			
	55.93	28.13	0.18	9.40	6.05	0.32	100.00	59.60	179			
	54.87	28.08	0.33	9.31	5.91	0.28	98.79	60.06	186			
	55.57	27.63	0.22	9.03	6.16	0.38	99.00	57.98	195			
	55.87	27.88	0.28	9.21	6.05	0.36	99.65	58.99	203			
	56.56	28.03	0.23	8.91	6.05	0.36	100.15	58.17	211			
	56.00	28.11	0.15	9.31	5.94	0.38	99.89	59.59	219			
	55.33	28.21	0.24	9.15	6.01	0.37	99.31	58.93	227			
	56.18	27.91	0.20	8.66	6.30	0.40	99.64	56.38	236			
	56.29	27.62	0.26	8.62	6.26	0.38	99.43	56.49	244			
	55.01	28.24	0.33	9.11	5.73	0.30	98.72	60.15	252			
	55.42	28.67	0.20	9.89	5.78	0.30	100.26	61.94	260			
	54.49	28.87	0.18	9.94	5.45	0.31	99.23	63.33	268			
	55.00	28.32	0.16	9.70	5.72	0.32	99.21	61.62	285			
	55.54	28.11	0.24	9.12	5.87	0.39	99.27	59.30	292			
	56.32	28.25	0.28	9.14	5.96	0.38	100.33	59.03	300			
	55.61	28.84	0.25	9.49	5.87	0.33	100.39	60.47	309			
	55.00	28.61	0.36	9.61	5.58	0.38	99.53	61.76	317			
	55.06	28.62	0.24	9.21	5.78	0.36	99.27	60.00	325			
	55.76	28.19	0.22	9.29	5.79	0.36	99.61	60.16	332			
	55.15	28.51	0.29	9.46	5.66	0.35	99.41	61.15	341			
	56.07	28.62	0.25	9.28	6.01	0.40	100.63	59.15	350			
	55.55	27.30	0.13	9.14	6.04	0.50	98.66	58.30	357			
	55.96	28.11	0.22	9.51	5.99	0.34	100.12	60.01	365			
	56.03	27.89	0.22	8.97	5.98	0.34	99.43	58.64	373			
	54.85	29.18	0.24	9.97	5.46	0.32	100.02	63.28	382			
	52.55	29.75	0.23	11.16	4.99	0.24	98.92	68.09	390			
	54.92	28.71	0.29	10.21	5.53	0.35	100.02	63.46	398			
	56.05	27.96	0.23	9.06	6.12	0.37	99.80	58.24	414			
	55.83	27.77	0.21	9.03	6.21	0.39	99.45	57.75	423			
	56.67	27.13	0.24	8.47	6.51	0.44	99.46	54.92	431			
	56.71	27.41	0.30	8.30	6.44	0.38	99.54	54.89	438			

Appendix 1.1 (cont.)
Electron microprobe analyses of Unzen plagioclase (in wt.%)

Sample ID	SiO_2	Al_2O_3	FeO	CaO	Na_2O	K_2O	Total	An*	um**	Sr (ppm)	Ba (ppm)	Sr/ Ba
	57.44	26.95	0.24	8.00	6.72	0.43	99.78	52.81	446			
	54.85	28.54	0.33	9.87	5.65	0.41	99.65	61.96	455			
	52.46	29.90	0.53	11.46	4.58	0.22	99.15	70.50	463			
	52.60	29.86	0.32	11.40	4.74	0.25	99.18	69.53	471			
153.85-153.9 Enclave P-Plag-1	56.75	27.13	0.24	8.85	6.30	0.43	99.71	56.84	0			
	55.91	27.44	0.23	8.66	6.43	0.40	99.06	55.91	8			
	51.57	31.12	0.23	12.31	4.14	0.17	99.55	74.05	17			
	53.71	29.67	0.29	10.66	5.18	0.28	99.79	66.11	25			
	53.79	29.71	0.29	10.97	5.12	0.24	100.12	67.16	34			
	52.38	30.55	0.21	11.68	4.72	0.26	99.80	70.11	41			
	51.15	30.69	0.24	11.99	4.27	0.21	98.56	72.82	49			
	52.68	30.38	0.26	11.56	4.93	0.25	100.06	69.04	58			
	51.91	30.72	0.30	11.67	4.54	0.25	99.39	70.89	66			
	50.45	31.56	0.30	13.19	3.93	0.17	99.60	76.26	74			
	50.16	31.89	0.37	13.60	3.47	0.14	99.64	79.04	83			
	52.93	30.12	0.30	11.30	4.97	0.23	99.86	68.49	91			
	54.80	28.80	0.42	10.31	5.16	0.68	100.18	63.81	99			
	54.13	29.37	0.22	10.80	5.35	0.25	100.11	65.87	108			
	54.70	28.72	0.15	10.09	5.75	0.25	99.67	62.68	116			
	48.11	33.23	0.23	15.08	2.67	0.14	99.47	84.30	124			
	54.40	29.11	0.29	10.30	5.47	0.33	99.89	63.97	132			
	50.70	31.97	0.37	13.31	3.63	0.17	100.15	77.79	140			
	51.71	30.76	0.29	12.68	4.28	0.21	99.93	73.83	149			
	52.14	30.80	0.27	11.89	4.50	0.22	99.81	71.60	157			
153.85-153.9 Enclave P-Plag-2	52.12	29.19	0.61	11.44	4.55	0.30	98.23	70.20	0			
	54.25	29.55	0.22	10.51	5.32	0.29	100.15	65.20	8			
	52.03	29.86	0.21	11.89	4.68	0.24	98.92	70.70	17			
	52.41	30.02	0.15	11.82	4.48	0.18	99.06	71.71	25			
	53.49	28.52	0.29	10.84	4.53	0.58	98.24	67.99	33			
	52.67	30.07	0.32	11.59	4.69	0.24	99.57	70.14	42			
	50.84	31.33	0.23	13.19	4.00	0.21	99.80	75.83	50			
	54.80	28.91	0.15	10.44	5.49	0.26	100.05	64.49	59			
	54.13	29.85	0.25	11.08	4.98	0.24	100.52	68.00	67			
	54.14	29.37	0.17	10.99	5.22	0.27	100.17	66.69	75			
	54.94	28.72	0.10	10.34	5.51	0.36	99.96	63.78	84			
	53.99	29.09	0.32	10.50	5.28	0.31	99.49	65.25	92			
	55.37	28.49	0.20	9.82	5.75	0.33	99.97	61.76	99			
	55.59	28.09	0.27	9.67	6.01	0.34	99.97	60.35	108			
	54.53	28.80	0.25	9.92	5.74	0.34	99.57	61.99	116			
	54.91	28.72	0.24	10.34	5.47	0.28	99.95	64.28	124			
	54.35	29.12	0.21	10.86	5.29	0.33	100.15	65.90	133			
	51.87	31.22	0.28	12.81	3.92	0.18	100.27	75.76	141			
	52.21	30.09	0.38	12.18	4.34	0.20	99.40	72.85	150			
	51.05	31.21	0.21	13.09	3.98	0.18	99.73	75.88	158			
	51.83	30.94	0.26	12.78	4.31	0.24	100.35	73.73	166			
	51.20	31.23	0.35	13.11	3.93	0.18	100.00	76.16	175			
	51.51	31.06	0.31	12.71	4.26	0.21	100.05	73.99	183			
153.85-153.9 Enclave P-Plag-3	55.32	28.95	0.50	10.28	5.27	0.30	100.63	64.87	0			
	54.79	28.34	0.27	10.01	5.49	0.34	99.24	63.19	7			
	57.00	27.28	0.32	8.79	6.22	0.44	100.05	56.90	16			
	56.48	27.31	0.19	8.94	6.28	0.42	99.62	57.16	24			
	56.06	27.21	0.28	9.11	6.19	0.42	99.28	57.96	32			
	56.34	27.79	0.15	9.67	6.09	0.45	100.49	59.65	40			
	54.40	28.92	0.22	10.16	5.50	0.34	99.53	63.53	57			
	54.59	28.72	0.17	10.70	5.48	0.31	99.97	64.89	65			

Appendix 1.1 (cont.)
Electron microprobe analyses of Unzen plagioclase (in wt.%)

Sample ID	SiO_2	Al_2O_3	FeO	CaO	Na_2O	K_2O	Total	An*	um**	Sr (ppm)	Ba (ppm)	Sr/ Ba
	55.00	28.95	0.22	10.34	5.56	0.30	100.37	63.81	73			
	54.48	28.45	0.24	10.29	5.53	0.34	99.33	63.65	81			
	54.84	28.69	0.23	10.31	5.44	0.33	99.84	64.11	89			
	53.37	29.31	0.29	11.03	5.22	0.30	99.51	66.66	97			
	51.12	30.96	0.29	12.69	4.17	0.17	99.39	74.51	106			
	53.81	29.27	0.24	11.00	5.09	0.25	99.67	67.34	114			
	51.21	31.49	0.32	13.01	4.00	0.19	100.22	75.64	122			
	50.43	31.73	0.38	13.31	3.81	0.14	99.81	77.11	130			
	50.94	31.37	0.20	12.84	4.13	0.19	99.67	74.85	138			
	51.23	31.71	0.32	13.08	4.05	0.19	100.58	75.55	146			
	50.49	30.97	0.21	13.05	3.91	0.17	98.80	76.16	163			
	52.03	30.78	0.27	12.33	4.38	0.19	99.98	72.97	171			
	52.16	30.43	0.21	12.60	4.46	0.19	100.05	73.05	179			
	52.16	29.78	0.39	11.88	4.53	0.22	98.96	71.46	187			
198.9-198.95 Host Plag-1	57.07	27.49	0.27	8.50	6.36	0.37	100.06	55.81	0			
	56.03	27.21	0.33	9.33	6.17	0.35	99.42	58.86	8			
	57.04	27.87	0.24	8.72	6.44	0.38	100.68	56.10	16			
	57.02	27.01	0.23	8.63	6.32	0.38	99.59	56.30	25			
	57.31	27.19	0.20	8.18	6.74	0.41	100.03	53.35	32			
	57.50	27.10	0.29	8.42	6.50	0.40	100.21	54.98	40			
	57.21	27.65	0.20	8.79	6.40	0.39	100.64	56.42	48			
	57.39	27.18	0.17	8.36	6.71	0.49	100.30	53.72	57			
	57.98	27.10	0.23	7.68	6.66	0.41	100.05	52.05	64			
	57.40	26.67	0.21	8.01	6.61	0.40	99.29	53.34	73			
	57.61	26.85	0.29	8.18	6.73	0.44	100.10	53.31	81			
	57.24	27.94	0.27	8.81	6.24	0.36	100.86	57.16	89			
	54.60	29.19	0.18	10.55	5.32	0.31	100.15	65.20	96			
	54.97	28.69	0.36	9.89	5.60	0.36	99.87	62.36	105			
	55.43	28.00	0.20	9.27	5.80	0.34	99.04	60.17	113			
	56.91	28.00	0.22	9.02	6.05	0.34	100.54	58.53	121			
	55.79	28.44	0.20	9.30	5.86	0.36	99.93	59.93	129			
	56.97	27.43	0.23	8.43	6.38	0.46	99.91	55.19	137			
	57.91	26.99	0.23	8.21	6.62	0.41	100.36	53.88	145			
	58.00	26.70	0.20	7.45	6.72	0.44	99.52	50.99	161			
	59.08	26.38	0.22	7.01	7.05	0.52	100.27	48.10	169			
	59.34	25.97	0.27	6.87	7.28	0.61	100.34	46.54	177			
	59.17	26.11	0.20	6.88	7.23	0.50	100.08	47.09	186			
	58.93	25.88	0.22	7.08	7.12	0.57	99.80	47.96	193			
	59.08	26.12	0.22	6.87	7.03	0.53	99.85	47.60	202			
	59.40	26.55	0.29	7.09	6.97	0.57	100.87	48.47	209			
	58.46	26.58	0.30	7.27	7.11	0.57	100.29	48.60	217			
	56.29	27.23	0.29	8.68	6.33	0.42	99.25	56.26	225			
	56.34	27.91	0.27	8.65	6.28	0.40	99.84	56.44	234			
	56.86	27.89	0.20	8.61	6.37	0.37	100.30	56.10	246			
	56.79	27.39	0.20	8.21	6.42	0.46	99.46	54.41	254			
	58.88	25.93	0.19	7.01	7.03	0.62	99.66	47.82	262			
	55.10	28.74	0.12	10.06	5.55	0.30	99.87	63.24	270			
	54.97	29.15	0.33	10.62	5.51	0.29	100.86	64.65	278			
	55.59	28.59	0.21	9.97	5.69	0.26	100.33	62.60	286			
	55.49	28.70	0.25	9.88	5.63	0.41	100.35	62.05	294			
	54.71	28.88	0.24	10.30	5.56	0.30	99.99	63.77	302			
	55.06	28.46	0.28	10.22	5.55	0.36	99.93	63.36	310			
	55.11	28.93	0.30	10.36	5.46	0.37	100.54	64.00	318			
	54.61	28.62	0.26	10.43	5.46	0.41	99.80	63.97	334			
	54.87	29.05	0.27	9.90	5.56	0.31	99.96	62.78	342			
	55.63	28.64	0.27	9.93	5.70	0.37	100.53	62.04	350			
	55.40	28.32	0.29	9.85	5.82	0.29	99.97	61.75	358			

Appendix 1.1 (cont.)
Electron microprobe analyses of Unzen plagioclase (in wt.%)

Sample ID	SiO_2	Al_2O_3	FeO	CaO	Na_2O	K_2O	Total	An*	um**	Sr (ppm)	Ba (ppm)	Sr/ Ba
	54.95	28.13	0.22	10.12	5.65	0.36	99.45	62.71	366			
	53.22	29.88	0.28	11.16	5.10	0.27	99.93	67.51	374			
	50.98	31.47	0.27	13.55	3.76	0.20	100.22	77.40	382			
	55.20	28.95	0.15	9.98	5.63	0.31	100.23	62.70	390			
	55.70	28.93	0.29	9.85	5.78	0.26	100.81	61.96	399			
	54.32	29.31	0.20	10.68	5.29	0.29	100.08	65.68	405			
	54.80	28.71	0.27	10.22	5.54	0.36	99.90	63.40	413			
	53.94	29.77	0.31	11.36	5.00	0.26	100.63	68.37	421			
	55.37	28.62	0.13	10.13	5.69	0.35	100.30	62.65	429			
	55.11	28.97	0.14	9.95	5.53	0.34	100.03	62.92	437			
	55.30	28.97	0.32	10.28	5.41	0.34	100.64	64.14	446			
	55.04	28.98	0.25	10.05	5.40	0.35	100.08	63.63	454			
	54.30	28.99	0.26	10.71	5.21	0.36	99.83	65.81	470			
	53.59	29.73	0.24	10.70	5.19	0.29	99.73	66.15	478			
	54.65	28.79	0.25	10.25	5.68	0.31	99.92	63.15	486			
	55.54	28.20	0.26	10.08	5.69	0.42	100.18	62.27	494			
	54.73	29.11	0.28	10.39	5.44	0.37	100.33	64.15	502			
	55.07	28.85	0.22	10.11	5.67	0.34	100.25	62.73	510			
	55.29	28.56	0.34	10.17	5.83	0.37	100.55	62.13	518			
	53.92	29.60	0.44	10.96	5.10	0.32	100.33	66.91	526			
	54.49	29.04	0.38	10.57	5.32	0.35	100.14	65.12	534			
	54.60	29.11	0.19	10.59	5.40	0.34	100.24	64.83	542			
	55.35	28.86	0.26	9.92	5.60	0.36	100.35	62.51	550			
	54.91	29.04	0.24	10.17	5.59	0.38	100.32	63.04	558			
	54.53	29.15	0.25	10.15	5.52	0.34	99.93	63.39	566			
	54.70	28.38	0.37	10.25	5.66	0.50	99.87	62.44	574			
	54.11	29.29	0.30	10.37	5.16	0.63	99.87	64.14	582			
	49.71	32.37	0.38	13.73	3.33	0.37	99.90	78.75	606			
	53.40	29.61	0.30	11.08	5.09	0.41	99.88	66.82	614			
	47.02	34.12	0.41	16.30	2.03	0.07	99.94	88.61	622			
	48.01	34.15	0.33	15.79	2.55	0.11	100.96	85.54	630			
	52.60	30.27	0.18	11.76	5.00	0.27	100.08	69.07	638			
	50.09	31.92	0.39	13.59	3.65	0.13	99.78	78.22	646			
	47.50	34.39	0.31	16.22	2.20	0.06	100.67	87.77	654			
	46.11	34.91	0.17	17.04	1.62	0.05	99.89	91.05	662			
	49.41	32.26	0.30	14.36	3.18	0.14	99.65	81.24	670			
	50.61	31.89	0.22	13.18	3.76	0.19	99.84	76.95	678			
	54.74	29.14	0.23	10.80	5.33	0.26	100.51	65.86	687			
	52.29	30.56	0.25	12.29	4.45	0.22	100.07	72.44	695			
	52.81	29.31	0.38	11.21	4.88	0.24	98.83	68.61	703			
	58.35	26.60	0.28	7.66	6.77	0.48	100.14	51.39	711			
	58.24	26.47	0.21	7.64	7.01	0.51	100.07	50.40	719			
	56.68	27.85	0.14	8.88	6.22	0.39	100.14	57.34	725			
	55.95	27.85	0.27	9.22	6.26	0.33	99.89	58.30	734			
	55.12	28.13	0.16	9.57	5.85	0.28	99.12	60.95	742			
	55.20	27.64	0.39	9.12	5.74	0.34	98.43	59.99	750			
	56.98	27.49	0.07	8.90	6.20	0.38	100.02	57.51	758			
	56.93	27.61	0.27	8.98	6.40	0.42	100.60	56.85	766			
	56.66	27.77	0.24	9.00	6.16	0.34	100.17	58.05	774			
	56.78	27.39	0.16	9.06	6.39	0.40	100.18	57.19	782			
	56.68	27.71	0.21	8.84	6.07	0.44	99.95	57.61	790			
	58.52	26.68	0.34	7.72	6.77	0.54	100.58	51.35	798			
	56.49	27.67	0.25	9.15	6.15	0.37	100.07	58.41	806			
	56.35	28.06	0.31	9.45	6.08	0.36	100.61	59.48	814			
	56.39	27.74	0.29	9.17	6.05	0.43	100.07	58.61	822			
	54.74	27.70	0.15	9.10	5.96	0.48	98.13	58.56	846			
	56.56	27.54	0.36	9.10	5.89	0.57	100.02	58.48	854			
	55.20	29.31	0.34	10.01	5.55	0.55	100.97	62.14	862			

Appendix 1.1 (cont.)
Electron microprobe analyses of Unzen plagioclase (in wt.%)

Sample ID	SiO_2	Al_2O_3	FeO	CaO	Na_2O	K_2O	Total	An*	um**	Sr (ppm)	Ba (ppm)	Sr/ Ba
	54.55	28.59	0.42	10.44	5.37	0.48	99.84	64.11	870			
198.9-198.95 E1 P-Plag1	56.89	27.35	0.30	8.88	6.22	0.60	100.24	56.57	0			
	56.70	27.03	0.30	8.42	6.39	0.53	99.37	54.87	8			
	57.64	26.97	0.33	8.52	6.60	0.43	100.49	54.80	16			
	57.58	26.94	0.25	8.29	6.61	0.51	100.18	53.79	24			
	56.97	26.76	0.17	8.70	6.45	0.47	99.53	55.68	32			
	56.84	27.56	0.26	9.01	6.27	0.37	100.31	57.54	40			
	54.48	28.49	0.22	10.24	5.57	0.29	99.30	63.59	48			
	50.35	32.02	0.29	13.76	3.56	0.17	100.15	78.64	64			
	48.04	33.34	0.30	15.61	2.57	0.14	100.01	85.17	72			
	47.87	33.43	0.24	15.58	2.49	0.11	99.71	85.71	81			
	48.25	33.59	0.25	15.86	2.41	0.13	100.50	86.17	89			
	48.34	32.90	0.38	14.98	2.88	0.10	99.59	83.42	97			
	49.55	32.38	0.34	14.43	3.22	0.15	100.09	81.05	105			
	47.03	34.11	0.35	16.58	2.11	0.08	100.25	88.34	113			
	46.63	34.30	0.34	16.47	1.92	0.06	99.73	89.26	121			
	46.93	34.27	0.39	17.01	2.13	0.08	100.82	88.49	129			
	56.88	26.96	0.34	9.65	5.39	0.69	99.92	61.33	137			
	46.99	33.92	0.35	16.44	2.27	0.06	100.02	87.57	145			
	47.99	33.08	0.29	15.77	2.56	0.13	99.82	85.41	153			
	48.25	33.44	0.40	15.18	2.86	0.08	100.22	83.75	161			
	49.29	32.45	0.35	14.81	3.02	0.12	100.05	82.50	169			
	47.03	33.80	0.25	16.21	2.27	0.13	99.69	87.10	177			
	47.73	33.53	0.32	15.33	2.58	0.09	99.60	85.13	193			
	49.10	32.67	0.25	14.48	3.16	0.17	99.83	81.32	201			
	49.28	32.54	0.17	14.68	3.15	0.15	99.97	81.65	209			
	48.95	33.10	0.41	15.16	2.84	0.17	100.63	83.42	217			
	47.24	33.95	0.30	16.22	2.41	0.13	100.25	86.49	226			
	46.97	34.11	0.27	16.19	2.15	0.11	99.79	87.74	234			
	48.48	33.50	0.24	15.30	2.65	0.09	100.26	84.79	242			
	49.42	32.38	0.28	14.83	3.28	0.14	100.34	81.25	250			
	50.31	31.92	0.27	14.03	3.49	0.12	100.14	79.55	258			
	49.77	32.04	0.30	14.01	3.58	0.18	99.88	78.85	266			
	50.39	31.70	0.24	13.91	3.50	0.16	99.91	79.15	274			
	50.18	31.92	0.25	13.90	3.58	0.17	100.00	78.76	282			
	50.61	31.47	0.23	13.42	3.82	0.16	99.71	77.12	290			
	51.34	31.47	0.25	13.10	3.97	0.15	100.28	76.10	298			
	51.81	31.04	0.25	13.21	4.18	0.27	100.76	74.80	306			
	50.96	30.75	0.24	12.77	4.07	0.19	98.99	74.98	314			
	52.03	30.30	0.22	12.18	4.53	0.20	99.47	72.02	322			
	55.51	28.56	0.30	10.11	5.79	0.38	100.66	62.10	370			
	55.38	27.85	0.20	9.50	5.85	0.38	99.17	60.39	379			
	55.85	28.15	0.31	9.60	5.89	0.37	100.17	60.52	387			
	55.65	28.17	0.22	9.85	5.85	0.41	100.15	61.15	395			
	56.34	27.88	0.17	9.30	6.00	0.36	100.05	59.38	403			
	57.21	26.92	0.32	8.43	6.62	0.44	99.94	54.38	411			
	57.78	26.86	0.30	8.51	6.62	0.50	100.56	54.47	419			
	57.20	26.85	0.26	8.41	6.40	0.57	99.68	54.71	435			
198.9-198.95 E1 P-Plag2	55.93	27.78	0.23	9.66	5.84	0.46	99.91	60.52	0			
	56.45	27.46	0.28	9.01	6.28	0.41	99.89	57.40	8			
	54.93	28.25	0.26	9.68	5.98	0.39	99.49	60.34	17			
	55.20	28.51	0.32	10.01	5.73	0.35	100.13	62.20	24			
	50.19	32.10	0.26	14.29	3.58	0.14	100.56	79.36	32			
	50.26	31.90	0.25	14.07	3.58	0.19	100.23	78.90	41			
	50.58	31.62	0.24	14.13	3.56	0.15	100.29	79.19	49			
	50.57	31.83	0.29	13.86	3.51	0.14	100.20	79.16	57			

Appendix 1.1 (cont.)
Electron microprobe analyses of Unzen plagioclase (in wt.%)

Sample ID	SiO_2	Al_2O_3	FeO	CaO	Na_2O	K_2O	Total	An*	um**	Sr (ppm)	Ba (ppm)	Sr/ Ba
	49.99	31.82	0.27	13.96	3.52	0.16	99.73	79.11	66			
	49.73	31.90	0.37	14.57	3.45	0.13	100.14	80.27	81			
	50.37	31.76	0.36	13.94	3.55	0.13	100.12	79.09	90			
	49.49	31.91	0.24	14.06	3.56	0.14	99.40	79.17	98			
	49.81	31.51	0.43	13.67	3.55	0.17	99.13	78.61	106			
	50.24	31.18	0.21	13.67	3.70	0.20	99.19	77.81	114			
	50.08	31.78	0.25	13.55	3.92	0.19	99.77	76.74	130			
	50.06	31.40	0.35	13.29	3.69	0.16	98.95	77.54	139			
	51.47	31.83	0.23	14.05	3.74	0.17	101.48	78.24	147			
	51.42	31.53	0.33	13.41	3.72	0.22	100.63	77.28	156			
	51.81	31.19	0.27	12.86	3.62	0.31	100.06	76.61	164			
	51.49	31.22	0.34	13.33	4.03	0.23	100.63	75.80	179			
	51.27	31.00	0.31	13.24	4.07	0.19	100.09	75.64	187			
	51.96	30.87	0.32	12.98	4.23	0.22	100.58	74.45	196			
	51.55	30.92	0.26	12.98	4.26	0.18	100.15	74.49	204			
	55.35	28.39	0.21	10.05	5.70	0.38	100.07	62.32	213			
	55.72	27.69	0.25	9.67	5.94	0.41	99.68	60.37	220			
	57.46	26.61	0.35	8.27	6.51	0.59	99.80	53.78	229			
	57.18	26.61	0.20	8.68	6.41	0.63	99.71	55.22	237			
198.9-198.95 E1 P-Plag3	56.08	28.40	0.23	9.39	6.03	0.34	100.49	59.57	0			
	53.85	29.41	0.41	10.95	5.13	0.28	100.03	66.94	8			
	52.52	30.17	0.37	12.32	4.50	0.20	100.09	72.39	16			
	51.18	31.38	0.36	13.46	3.96	0.18	100.53	76.47	25			
	50.84	31.67	0.34	13.75	3.76	0.13	100.50	77.93	33			
	46.89	34.06	0.28	16.36	2.08	0.10	99.79	88.21	41			
	47.19	33.96	0.38	16.48	2.31	0.12	100.44	87.18	49			
	47.33	32.82	0.53	15.73	2.44	0.29	99.14	85.22	58			
	48.99	32.56	0.35	14.60	2.95	0.13	99.57	82.61	67			
	48.68	33.13	0.34	15.14	2.87	0.12	100.27	83.53	74			
	48.95	32.97	0.29	15.13	2.96	0.15	100.45	82.97	82			
	57.10	27.23	0.29	8.43	6.63	0.46	100.13	54.33	99			
	56.97	27.18	0.15	8.99	6.24	0.43	99.96	57.39	107			
	57.17	26.70	0.38	8.20	6.61	0.47	99.54	53.62	115			
	49.61	32.25	0.29	14.12	3.23	0.15	99.66	80.67	123			
	50.81	31.78	0.24	13.44	3.81	0.25	100.33	76.82	132			
	51.29	30.80	0.27	13.31	3.88	0.10	99.66	76.98	140			
	58.19	27.06	0.14	8.45	6.52	0.52	100.89	54.52	148			
	57.76	27.02	0.23	7.99	6.60	0.49	100.11	52.97	156			
	55.94	27.40	0.36	9.17	5.95	0.42	99.25	59.01	165			
	55.05	27.96	0.24	9.90	5.58	0.48	99.21	62.04	173			
	56.33	27.89	0.30	9.76	5.66	0.40	100.34	61.68	181			
199.1-199.15 Host Plag1	56.80	26.84	0.23	8.76	6.43	0.46	99.52	55.97	0			
	56.79	27.97	0.32	8.92	6.34	0.47	100.81	56.68	25			
	57.22	27.32	0.23	8.60	6.31	0.43	100.10	56.06	51			
	56.73	26.85	0.19	8.66	6.51	0.41	99.34	55.59	76			
	56.43	27.39	0.22	9.16	6.33	0.38	99.91	57.70	101			
	56.76	27.05	0.28	8.88	6.28	0.44	99.68	56.94	126			
	56.94	27.26	0.12	8.73	6.62	0.47	100.14	55.17	151			
	56.97	27.46	0.26	8.42	6.37	0.42	99.90	55.34	175			
	56.95	27.62	0.28	8.90	6.24	0.43	100.42	57.14	200			
	55.89	28.20	0.27	9.48	6.07	0.42	100.34	59.36	226			
	55.00	28.30	0.24	9.93	5.84	0.36	99.67	61.57	251			
	56.02	27.94	0.30	9.23	6.22	0.42	100.13	58.18	276			
	56.56	27.53	0.16	8.96	6.19	0.44	99.85	57.47	301			
	57.07	26.85	0.26	8.23	6.65	0.47	99.52	53.61	326			
	57.40	26.61	0.22	8.11	6.69	0.44	99.46	53.22	352			

Appendix 1.1 (cont.)
Electron microprobe analyses of Unzen plagioclase (in wt.%)

Sample ID	SiO_2	Al_2O_3	FeO	CaO	Na_2O	K_2O	Total	An*	um**	Sr (ppm)	Ba (ppm)	Sr/ Ba
	56.39	27.61	0.14	9.05	6.20	0.44	99.84	57.68	377			
	56.74	27.33	0.27	8.91	6.30	0.46	100.00	56.86	402			
	56.73	27.43	0.22	8.95	6.24	0.49	100.06	57.10	427			
	55.45	28.17	0.23	9.55	6.11	0.47	99.98	59.20	452			
	56.60	27.85	0.33	9.06	6.16	0.60	100.60	57.29	477			
	56.56	28.31	0.37	9.31	6.11	0.62	101.26	58.04	502			
	56.82	27.96	0.27	8.87	6.28	0.48	100.67	56.75	527			
	49.94	32.38	0.31	13.85	3.53	0.15	100.15	79.01	552			
	54.47	28.97	0.23	10.76	5.44	0.32	100.18	65.13	577			
	52.32	30.44	0.24	12.42	4.43	0.18	100.04	72.92	602			
	56.26	27.57	0.25	9.08	6.30	0.39	99.85	57.57	653			
	56.49	27.90	0.16	9.25	6.18	0.42	100.42	58.37	678			
	57.58	27.36	0.29	8.66	6.45	0.48	100.83	55.54	703			
	58.19	26.86	0.24	8.01	6.87	0.47	100.64	52.15	728			
	58.02	26.90	0.19	8.27	6.70	0.47	100.56	53.56	753			
	58.16	26.80	0.16	8.16	6.74	0.50	100.52	52.95	779			
	56.03	27.79	0.19	9.25	6.08	0.43	99.76	58.72	804			
	57.76	26.60	0.19	8.42	6.71	0.54	100.22	53.74	828			
	57.14	26.66	0.32	8.37	6.65	0.52	99.66	53.88	853			
	58.24	26.60	0.18	8.00	6.87	0.53	100.41	51.97	878			
	57.96	26.93	0.14	7.87	6.71	0.50	100.11	52.18	904			
	57.60	26.90	0.20	8.21	6.55	0.52	99.99	53.73	929			
	58.65	25.55	0.27	7.98	6.27	0.69	99.41	53.42	954			
	58.21	26.62	0.23	8.06	6.77	0.54	100.43	52.41	979			
	57.19	27.21	0.24	8.92	6.31	0.47	100.34	56.82	1004			
	62.95	22.53	0.51	3.86	8.02	1.88	99.75	28.03	1029			
	56.34	28.52	0.38	9.57	6.11	0.39	101.30	59.56	1080			
	56.07	28.47	0.18	9.77	5.93	0.37	100.79	60.78	1105			
	55.94	27.87	0.31	9.52	5.94	0.40	99.98	60.06	1129			
	57.52	26.97	0.14	8.46	6.65	0.46	100.21	54.35	1154			
	57.68	27.04	0.29	8.57	6.61	0.53	100.72	54.55	1180			
	56.43	28.07	0.24	9.47	6.13	0.39	100.74	59.20	1205			
	56.14	28.00	0.21	9.40	6.12	0.45	100.33	58.84	1230			
	57.13	27.13	0.14	8.51	6.63	0.50	100.05	54.39	1255			
	57.31	27.54	0.21	8.68	6.47	0.49	100.71	55.51	1280			
	56.92	27.43	0.19	8.84	6.44	0.41	100.23	56.34	1305			
	56.54	27.82	0.23	9.49	6.29	0.45	100.82	58.46	1331			
	56.77	27.48	0.14	8.69	6.25	0.42	99.75	56.57	1356			
	57.24	27.59	0.13	8.77	6.37	0.46	100.55	56.22	1381			
	57.10	27.10	0.24	8.87	6.51	0.49	100.30	55.91	1406			
	57.39	27.04	0.19	8.23	6.68	0.45	99.98	53.62	1431			
	56.28	27.84	0.20	9.07	6.28	0.45	100.13	57.41	1456			
	52.70	29.45	0.55	11.40	4.33	1.18	99.62	67.40	1481			
	54.91	29.32	0.21	10.33	5.49	0.38	100.63	63.74	1506			
	56.22	27.74	0.22	9.46	6.11	0.43	100.18	59.14	1531			
	57.71	27.12	0.10	8.43	6.56	0.52	100.45	54.34	1556			
	58.43	26.70	0.28	8.05	6.58	0.46	100.50	53.32	1581			
	52.85	30.90	0.25	12.64	4.41	0.21	101.26	73.22	1607			
	55.04	28.07	0.26	9.82	5.83	0.40	99.42	61.18	1632			
	56.11	28.00	0.14	9.35	6.12	0.39	100.12	58.95	1657			
	57.18	27.12	0.32	8.78	6.27	0.38	100.04	56.92	1682			
	55.57	28.03	0.18	9.57	6.01	0.39	99.74	59.92	1707			
	56.94	27.70	0.20	8.92	6.33	0.52	100.62	56.57	1758			
	56.13	27.69	0.16	9.22	6.13	0.40	99.73	58.58	1782			
	56.39	28.01	0.30	9.04	6.18	0.36	100.28	58.01	1807			
	56.97	27.25	0.32	8.73	6.48	0.42	100.18	55.86	1832			
	58.42	26.59	0.19	7.97	6.85	0.56	100.57	51.84	1857			
	57.92	26.72	0.27	7.98	6.90	0.48	100.27	51.96	1883			

Appendix 1.1 (cont.)
Electron microprobe analyses of Unzen plagioclase (in wt.%)

Sample ID	SiO_2	Al_2O_3	FeO	CaO	Na_2O	K_2O	Total	An*	um**	Sr (ppm)	Ba (ppm)	Sr/ Ba
	57.66	26.45	0.20	8.31	6.42	0.52	99.56	54.48	1908			
	56.18	26.99	0.23	8.76	6.35	0.45	98.97	56.29	1933			
	56.67	27.73	0.32	9.16	6.22	0.39	100.48	58.09	1958			
	57.19	27.35	0.19	8.81	6.55	0.45	100.55	55.73	1983			
	56.21	28.29	0.29	9.76	5.82	0.35	100.71	61.26	2009			
	55.97	28.26	0.29	9.70	5.84	0.40	100.45	60.83	2034			
	54.63	28.84	0.16	10.66	5.44	0.32	100.06	64.89	2059			
	55.50	27.98	0.34	9.74	6.03	0.38	99.97	60.34	2084			
	55.79	28.04	0.23	9.64	5.71	0.30	99.71	61.57	2108			
	54.64	28.85	0.42	10.19	5.55	0.31	99.96	63.49	2133			
	55.07	28.51	0.30	10.02	5.54	0.35	99.79	63.00	2159			
	55.07	28.52	0.34	10.01	5.82	0.37	100.14	61.80	2184			
	55.90	28.34	0.20	9.82	5.96	0.36	100.57	60.82	2209			
	56.07	28.71	0.13	9.94	5.73	0.33	100.91	62.16	2234			
	55.42	28.43	0.21	9.84	5.79	0.42	100.10	61.30	2259			
	56.45	27.73	0.22	9.27	6.04	0.37	100.08	59.13	2285			
	56.18	28.32	0.25	9.46	6.07	0.39	100.67	59.42	2310			
	54.98	28.30	0.19	9.85	5.87	0.42	99.62	61.02	2335			
	55.93	27.77	0.09	9.32	6.01	0.40	99.52	59.26	2360			
	55.82	27.71	0.28	9.33	5.94	0.39	99.48	59.57	2385			
	56.48	28.09	0.22	9.13	6.19	0.42	100.52	58.02	2410			
	57.01	27.43	0.22	8.89	6.44	0.38	100.37	56.56	2435			
	56.77	27.16	0.19	9.24	6.24	0.42	100.02	58.14	2460			
	56.54	27.54	0.29	9.26	6.12	0.46	100.21	58.47	2485			
	57.16	27.30	0.18	8.68	6.42	0.45	100.18	55.83	2510			
	57.59	27.42	0.30	8.61	6.59	0.39	100.90	55.21	2535			
	57.00	27.19	0.27	8.53	6.47	0.43	99.90	55.28	2561			
	55.80	28.03	0.22	9.67	5.86	0.37	99.95	60.82	2611			
	55.66	28.69	0.25	9.91	5.68	0.38	100.57	62.06	2636			
	57.23	26.92	0.23	8.37	6.50	0.42	99.67	54.74	2661			
	57.01	25.86	0.33	7.88	6.52	0.61	98.21	52.47	2712			
	55.92	28.40	0.21	9.54	5.93	0.42	100.41	60.07	2736			
	55.60	28.50	0.22	9.78	5.79	0.36	100.26	61.40	2761			
	57.96	26.72	0.31	7.99	6.70	0.46	100.14	52.74	2786			
	55.96	27.80	0.34	9.40	5.86	0.37	99.74	60.15	2811			
	57.96	26.68	0.29	8.09	6.62	0.49	100.13	53.24	2837			
	58.37	26.73	0.30	7.97	6.76	0.50	100.62	52.34	2862			
	55.65	27.79	0.23	9.57	5.88	0.40	99.51	60.40	2887			
	54.52	28.68	0.48	10.31	5.47	0.50	99.97	63.32	2912			
199.1-199.15 Host Plag2	57.87	26.86	0.20	8.57	6.77	0.50	100.77	54.10	0			
	57.03	27.03	0.14	8.64	6.51	0.44	99.78	55.42	16			
	57.09	27.24	0.35	8.75	6.50	0.46	100.38	55.71	30			
	56.72	27.10	0.30	8.52	6.31	0.42	99.36	55.88	45			
	57.05	26.81	0.21	8.64	6.45	0.58	99.76	55.12	60			
	57.31	27.08	0.24	8.47	6.46	0.63	100.19	54.43	75			
	57.20	26.81	0.23	8.37	6.44	0.48	99.52	54.76	91			
	57.30	27.04	0.29	8.41	6.54	0.48	100.06	54.50	105			
	57.17	26.91	0.31	8.33	6.73	0.42	99.87	53.81	121			
	57.78	27.04	0.28	8.30	6.53	0.51	100.45	54.09	135			
	57.44	26.93	0.30	8.68	6.65	0.50	100.51	54.83	151			
	57.13	27.46	0.19	8.96	6.49	0.36	100.59	56.67	165			
	56.33	27.22	0.32	8.73	6.43	0.45	99.48	55.93	181			
	56.61	27.36	0.28	8.74	6.39	0.45	99.84	56.07	196			
	57.32	27.33	0.27	8.84	6.40	0.42	100.58	56.43	211			
	57.28	26.77	0.25	8.41	6.60	0.51	99.83	54.18	226			
	57.25	26.65	0.12	8.37	6.72	0.51	99.63	53.66	241			
	56.92	26.79	0.20	8.16	6.77	0.49	99.32	52.92	256			

Appendix 1.1 (cont.)
Electron microprobe analyses of Unzen plagioclase (in wt.%)

Sample ID	SiO_2	Al_2O_3	FeO	CaO	Na_2O	K_2O	Total	An*	um**	Sr (ppm)	Ba (ppm)	Sr/ Ba
	57.46	26.73	0.17	8.18	6.56	0.51	99.60	53.65	272			
	58.37	26.27	0.22	7.72	7.18	0.48	100.24	50.20	286			
	57.82	26.74	0.35	8.03	6.89	0.53	100.37	51.97	302			
	57.96	26.67	0.23	7.89	6.74	0.47	99.96	52.26	316			
	56.51	27.37	0.29	8.80	6.47	0.47	99.91	55.92	331			
	56.67	27.27	0.23	9.07	6.44	0.43	100.12	56.90	347			
	56.97	27.15	0.24	8.86	6.64	0.41	100.26	55.67	362			
	56.73	27.09	0.24	9.08	6.38	0.48	100.01	56.93	377			
	56.44	27.32	0.21	8.54	6.57	0.46	99.54	54.86	391			
	57.75	26.40	0.28	7.93	6.72	0.50	99.58	52.36	407			
	57.65	26.42	0.19	7.87	6.80	0.49	99.41	51.94	422			
	58.12	26.56	0.25	7.92	6.89	0.48	100.23	51.78	437			
	57.07	26.85	0.21	8.31	6.63	0.42	99.49	54.11	452			
	56.76	27.38	0.23	8.76	6.32	0.50	99.94	56.23	467			
	57.13	27.25	0.21	8.70	6.42	0.46	100.17	55.86	482			
	57.43	26.57	0.25	8.13	6.78	0.46	99.62	52.87	498			
	58.31	27.05	0.31	7.97	6.93	0.51	101.07	51.74	512			
	57.27	27.73	0.22	8.87	6.36	0.39	100.85	56.75	528			
	58.13	27.08	0.27	8.48	6.58	0.50	101.03	54.52	542			
	57.70	26.17	0.23	7.87	6.82	0.57	99.36	51.54	558			
	56.80	27.00	0.28	8.83	6.55	0.45	99.92	55.78	573			
	57.13	26.79	0.25	8.63	6.60	0.47	99.87	54.96	588			
	57.37	27.02	0.20	8.55	6.57	0.47	100.17	54.86	603			
	57.90	27.06	0.23	8.25	6.84	0.48	100.77	52.99	618			
	57.33	27.12	0.20	8.48	6.60	0.50	100.23	54.43	633			
	57.71	26.52	0.17	8.09	6.77	0.45	99.70	52.86	649			
	57.51	26.83	0.29	8.13	6.83	0.49	100.09	52.60	663			
	56.91	27.84	0.18	8.96	6.48	0.40	100.76	56.56	679			
	56.24	27.49	0.19	9.23	6.16	0.39	99.70	58.47	693			
	56.98	27.66	0.13	9.29	6.10	0.34	100.50	59.08	709			
	56.57	27.51	0.16	9.61	6.19	0.40	100.45	59.34	723			
	55.93	28.24	0.22	9.38	6.10	0.42	100.28	59.02	739			
	56.28	28.36	0.27	9.53	6.06	0.37	100.87	59.73	754			
	58.07	26.67	0.21	7.99	6.95	0.53	100.42	51.64	784			
	57.72	26.49	0.23	8.04	6.80	0.49	99.77	52.46	798			
	58.23	26.44	0.21	7.82	6.80	0.54	100.05	51.57	814			
	58.22	26.16	0.27	7.41	7.04	0.51	99.60	49.52	829			
	58.01	26.28	0.18	7.40	7.09	0.51	99.47	49.35	844			
	58.37	26.70	0.26	8.16	6.70	0.45	100.64	53.32	859			
	57.10	26.62	0.21	7.78	6.71	0.51	98.93	51.89	874			
	57.79	26.55	0.29	8.10	6.74	0.50	99.97	52.78	889			
	57.61	26.91	0.31	8.16	6.70	0.46	100.16	53.25	905			
	56.66	27.40	0.15	9.16	6.19	0.36	99.93	58.30	919			
	56.55	27.53	0.26	9.03	6.41	0.45	100.22	56.85	935			
	57.00	27.11	0.22	8.51	6.37	0.42	99.64	55.59	949			
	58.52	25.99	0.13	7.70	6.89	0.54	99.77	50.90	965			
	57.81	26.72	0.30	7.91	6.63	0.50	99.86	52.59	980			
	57.09	27.42	0.26	8.67	6.55	0.47	100.46	55.27	995			
	56.89	27.04	0.23	8.52	6.45	0.41	99.55	55.37	1010			
	56.77	26.80	0.24	8.10	6.73	0.46	99.10	52.97	1040			
	57.85	27.03	0.14	8.23	6.54	0.50	100.28	53.90	1056			
	58.05	26.93	0.23	7.94	6.85	0.43	100.42	52.15	1070			
	58.31	26.73	0.21	7.62	6.94	0.47	100.27	50.74	1086			
	58.12	26.38	0.23	7.75	6.82	0.47	99.77	51.54	1100			
	58.00	26.28	0.14	8.03	6.86	0.55	99.87	52.00	1115			
	56.58	27.38	0.20	8.65	6.27	0.50	99.58	56.08	1131			
	56.62	27.92	0.29	9.03	6.14	0.48	100.48	57.69	1146			
	58.79	27.16	0.19	8.05	6.76	0.44	101.39	52.76	1161			

Appendix 1.1 (cont.)
Electron microprobe analyses of Unzen plagioclase (in wt.%)

Sample ID	SiO_2	Al_2O_3	FeO	CaO	Na_2O	K_2O	Total	An*	um**	Sr (ppm)	Ba (ppm)	Sr/ Ba
	56.27	27.73	0.24	9.17	6.20	0.42	100.03	58.08	1175			
	56.87	26.95	0.25	8.38	6.64	0.46	99.54	54.14	1191			
	57.98	27.09	0.27	8.56	6.57	0.43	100.90	55.00	1205			
	57.72	26.86	0.26	8.08	6.72	0.48	100.12	52.85	1221			
	57.14	27.31	0.25	8.49	6.49	0.43	100.11	55.08	1236			
	57.62	26.86	0.26	8.32	6.69	0.43	100.17	53.93	1251			
	56.36	27.64	0.29	9.09	6.17	0.40	99.95	58.03	1266			
	58.06	26.64	0.20	7.91	6.78	0.45	100.04	52.26	1281			
	57.92	26.57	0.24	7.88	6.77	0.45	99.82	52.20	1296			
	58.21	26.64	0.33	7.92	6.84	0.45	100.39	52.09	1312			
	57.92	26.37	0.25	7.70	6.85	0.46	99.57	51.32	1326			
	56.68	27.32	0.25	8.66	6.40	0.44	99.76	55.86	1342			
	56.85	27.40	0.27	8.44	6.64	0.48	100.08	54.26	1356			
	56.68	27.71	0.16	8.73	6.28	0.63	100.19	55.81	1372			
	56.61	27.83	0.30	9.23	6.02	0.57	100.57	58.35	1387			
	57.92	26.64	0.29	9.06	5.87	0.63	100.41	58.22	1402			
	54.29	29.05	0.17	10.50	5.23	0.31	99.55	65.47	1432			
	55.04	28.72	0.17	10.10	5.65	0.35	100.02	62.77	1447			
	55.10	28.77	0.27	9.83	5.77	0.35	100.08	61.61	1462			
	56.11	27.51	0.23	9.38	6.13	0.43	99.79	58.85	1477			
	55.89	28.21	0.25	9.33	5.95	0.39	100.02	59.53	1493			
	55.37	28.50	0.29	9.51	5.92	0.36	99.95	60.22	1507			
	56.64	27.64	0.18	9.26	6.12	0.34	100.19	58.89	1522			
	57.31	27.27	0.17	8.29	6.67	0.51	100.20	53.60	1538			
	56.31	28.36	0.24	9.44	5.98	0.41	100.73	59.66	1552			
	57.31	27.21	0.28	8.49	6.40	0.54	100.22	55.02	1568			
	57.42	26.64	0.25	7.89	6.42	0.81	99.43	52.19	1582			
	51.07	31.16	0.60	12.98	3.81	0.27	99.88	76.07	1598			
199.1-199.15 E1 P-Plag1	56.57	27.92	0.17	9.28	6.09	0.63	100.65	57.99	0			
	57.51	27.04	0.22	8.04	6.54	0.66	100.00	52.78	6			
	57.45	27.52	0.27	8.31	6.25	0.53	100.33	55.08	13			
	56.53	27.56	0.24	8.75	6.29	0.53	99.91	56.20	19			
	55.73	28.11	0.27	9.46	5.83	0.38	99.79	60.37	26			
	55.47	28.54	0.32	9.44	5.83	0.39	99.99	60.26	32			
	53.85	29.60	0.26	11.43	4.97	0.29	100.40	68.49	39			
	52.87	30.01	0.32	11.68	4.55	0.29	99.73	70.69	45			
	53.37	29.63	0.24	10.86	5.18	0.30	99.58	66.44	52			
	52.56	30.14	0.31	11.68	4.64	0.27	99.60	70.39	58			
	53.51	29.57	0.33	11.33	4.99	0.31	100.05	68.10	65			
	57.92	26.63	0.35	7.91	6.65	0.61	100.07	52.13	71			
	58.23	26.75	0.31	7.79	6.70	0.60	100.40	51.60	77			
	52.78	30.02	0.64	11.82	4.68	0.36	100.31	70.12	84			
	61.42	24.36	0.47	5.41	7.25	1.66	100.57	37.78	0			
	54.18	29.04	0.50	10.68	5.20	0.40	100.00	65.59	6			
199.1-199.15 E1 P-Plag2	56.69	27.61	0.30	8.58	6.21	0.44	99.84	56.34	12			
	55.31	28.84	0.23	9.82	5.69	0.35	100.24	61.91	18			
	56.03	28.65	0.30	9.75	5.88	0.33	100.95	61.09	24			
	55.56	27.98	0.25	9.60	5.90	0.37	99.66	60.49	30			
	54.98	28.90	0.18	9.90	5.70	0.37	100.03	61.99	36			
	54.61	29.76	0.22	10.70	5.16	0.26	100.70	66.38	42			
	53.54	29.89	0.25	11.13	4.92	0.30	100.04	68.08	48			
	52.61	30.36	0.30	11.79	4.48	0.23	99.77	71.46	55			
	53.85	29.37	0.13	11.14	5.06	0.25	99.81	67.69	60			
	57.21	27.16	0.19	7.94	6.64	0.50	99.65	52.62	67			
	57.71	26.81	0.19	8.28	6.60	0.38	99.97	54.28	72			
	56.99	27.30	0.31	8.16	6.39	0.45	99.61	54.37	79			
	55.41	28.88	0.21	9.87	5.45	0.31	100.13	63.11	84			

Appendix 1.1 (cont.)
Electron microprobe analyses of Unzen plagioclase (in wt.%)

Sample ID	SiO_2	Al_2O_3	FeO	CaO	Na_2O	K_2O	Total	An*	um**	Sr (ppm)	Ba (ppm)	Sr/ Ba
	54.06	29.34	0.19	10.53	5.21	0.29	99.63	65.68	91			
	54.43	29.23	0.29	10.70	5.37	0.33	100.35	65.25	96			
	53.85	29.52	0.31	11.25	5.06	0.42	100.42	67.22	0			
	52.93	29.76	0.31	11.48	4.76	0.26	99.50	69.58	6			
199.1-199.15 E1 P-Plag3	52.79	29.73	0.31	11.64	4.90	0.32	99.70	69.03	13			
	52.76	30.05	0.33	11.69	4.72	0.25	99.79	70.18	19			
	52.41	30.23	0.34	11.96	4.48	0.27	99.69	71.56	24			
	53.59	29.28	0.39	11.01	4.88	0.33	99.47	67.90	31			
	53.00	29.57	0.32	11.59	4.78	0.33	99.60	69.39	37			
	53.65	28.78	0.46	10.91	5.14	0.38	99.33	66.42	43			
	59.75	24.94	0.53	6.72	7.07	1.13	100.13	45.06	50			
	52.27	29.87	0.52	11.72	4.45	0.35	99.19	70.97	0			
	54.45	29.10	0.26	10.42	5.37	0.38	99.98	64.42	6			
199.1-199.15 E1 P-Plag4	55.09	28.70	0.23	10.42	5.51	0.34	100.29	64.04	12			
	57.34	26.46	0.16	8.18	6.62	0.45	99.22	53.63	18			
	57.65	27.09	0.30	8.15	6.50	0.38	100.06	54.22	24			
	55.34	28.58	0.32	9.53	5.90	0.36	100.04	60.36	31			
	54.82	28.69	0.21	10.10	5.60	0.30	99.73	63.12	36			
	52.07	30.28	0.20	11.84	4.59	0.22	99.21	71.12	43			
	52.98	30.43	0.13	11.56	4.64	0.27	100.01	70.17	49			
	53.06	30.11	0.33	11.70	4.65	0.26	100.12	70.43	55			
	55.83	28.41	0.22	9.55	5.84	0.30	100.15	60.89	61			
	56.73	27.70	0.25	8.91	6.24	0.41	100.23	57.28	67			
	54.42	29.01	0.18	10.71	5.31	0.31	99.93	65.59	73			
	54.97	28.37	0.26	10.15	5.68	0.28	99.71	62.99	80			
	57.25	27.50	0.18	8.74	6.43	0.41	100.50	56.11	86			
	55.74	28.36	0.23	9.70	5.67	0.35	100.07	61.70	92			
	54.59	29.04	0.35	10.41	5.47	0.37	100.24	64.06	98			
	53.08	29.61	0.30	11.37	5.02	0.28	99.66	68.20	105			
	52.76	30.27	0.33	11.80	4.51	0.23	99.89	71.35	110			
	52.19	30.34	0.28	12.17	4.54	0.23	99.75	71.85	116			
	47.76	34.18	0.36	15.93	2.22	0.10	100.54	87.32	123			
	47.02	33.92	0.30	15.48	2.34	0.08	99.13	86.49	128			
	47.66	33.64	0.23	15.86	2.34	0.07	99.79	86.82	134			
	47.34	34.25	0.34	16.25	2.29	0.08	100.54	87.29	141			
	47.37	33.89	0.30	15.73	2.40	0.11	99.80	86.23	147			
	47.76	33.80	0.43	15.63	2.42	0.10	100.13	86.14	153			
	47.90	33.51	0.29	15.10	2.48	0.12	99.38	85.34	159			
	48.18	33.18	0.35	15.57	2.52	0.15	99.95	85.32	165			
	50.37	31.61	0.29	13.27	3.68	0.19	99.42	77.39	172			
	53.21	30.00	0.33	11.45	4.87	0.28	100.14	68.98	177			
	52.95	30.42	0.44	11.58	4.89	0.33	100.62	68.95	183			
	50.33	31.33	0.37	13.34	4.00	0.22	99.61	75.95	189			
	51.43	31.95	0.30	13.05	3.89	0.20	100.82	76.15	197			
	52.41	30.56	0.33	12.05	4.60	0.24	100.18	71.36	202			
	52.56	30.83	0.23	11.83	4.60	0.28	100.32	70.80	208			
	51.98	31.09	0.36	12.33	4.28	0.26	100.31	73.05	215			
	50.97	31.05	0.42	12.67	4.00	0.21	99.32	75.05	221			
	52.64	29.98	0.29	11.77	4.72	0.26	99.65	70.29	226			
	53.69	29.97	0.31	10.65	4.98	0.26	99.86	67.02	233			
	53.57	29.39	0.36	11.07	5.10	0.26	99.76	67.37	239			
	53.13	29.82	0.36	10.90	4.97	0.32	99.50	67.32	245			
	53.74	30.10	0.28	10.84	5.12	0.24	100.32	66.91	251			
	53.53	29.39	0.46	10.85	5.09	0.25	99.57	67.04	257			
	53.05	29.90	0.30	11.50	4.90	0.24	99.90	69.10	264			
	53.16	30.10	0.33	11.60	4.73	0.29	100.21	69.78	269			
	52.08	29.83	0.35	11.88	4.59	0.25	98.99	71.04	275			

Appendix 1.1 (cont.)
Electron microprobe analyses of Unzen plagioclase (in wt.%)

Sample ID	SiO_2	Al_2O_3	FeO	CaO	Na_2O	K_2O	Total	An*	um**	Sr (ppm)	Ba (ppm)	Sr/ Ba
	54.50	29.36	0.30	10.30	5.31	0.33	100.10	64.63	282			
	55.52	28.47	0.33	9.17	5.82	0.39	99.70	59.62	288			
	56.43	27.59	0.31	9.52	5.84	0.50	100.18	60.04	293			
	53.64	29.19	0.49	11.02	5.14	0.41	99.89	66.52	300			
	54.06	29.16	0.66	10.70	4.86	0.39	99.84	67.08	307			
	53.34	28.67	0.71	10.77	4.78	0.42	98.69	67.45	313			
	54.14	28.82	0.67	10.49	5.10	0.57	99.79	64.88	318			
	56.37	27.29	0.24	8.91	6.20	0.54	99.54	56.94	8			
	54.86	28.55	0.33	9.78	5.80	0.43	99.75	61.07	17			
199.1-199.15 E1 P-Plag5	54.27	28.80	0.27	10.11	5.28	0.35	99.07	64.25	25			
	54.40	29.30	0.32	10.42	5.32	0.30	100.06	64.96	33			
	52.68	29.72	0.24	11.94	4.77	0.22	99.57	70.54	41			
	52.09	30.49	0.24	12.38	4.37	0.20	99.76	73.05	49			
	53.67	29.39	0.26	10.88	5.20	0.29	99.68	66.49	57			
	54.02	29.18	0.23	10.87	5.26	0.24	99.80	66.39	65			
	52.25	29.94	0.31	12.11	4.57	0.23	99.41	71.59	73			
	52.67	29.87	0.21	11.33	4.75	0.27	99.10	69.30	82			
	52.78	29.96	0.39	11.43	4.77	0.26	99.59	69.44	90			
	53.26	29.26	0.35	11.09	5.03	0.27	99.25	67.64	98			
	49.56	31.87	0.29	14.02	3.42	0.19	99.34	79.53	107			
	55.55	28.03	0.19	9.52	5.82	0.42	99.54	60.42	115			
	56.24	27.68	0.26	9.10	6.06	0.48	99.81	58.20	123			
	55.69	27.92	0.32	9.32	6.08	0.55	99.87	58.45	130			
	51.96	30.36	0.32	12.38	4.24	0.26	99.52	73.36	139			
	52.76	30.09	0.19	11.39	4.61	0.24	99.29	70.14	147			
	53.70	29.12	0.24	11.03	5.19	0.26	99.54	66.93	155			
	52.15	30.30	0.27	11.46	4.43	0.25	98.87	71.01	163			
	51.81	31.17	0.34	12.50	4.03	0.21	100.06	74.65	172			
	52.62	30.09	0.30	11.42	4.83	0.29	99.55	69.03	180			
	53.33	29.57	0.29	11.18	4.96	0.29	99.63	68.05	188			
	53.11	30.32	0.36	11.40	4.81	0.31	100.30	69.00	196			
	52.14	30.35	0.35	12.35	4.47	0.22	99.88	72.48	205			
	52.77	30.36	0.28	11.46	4.63	0.27	99.77	70.02	212			
	52.78	29.98	0.33	11.43	4.76	0.20	99.47	69.76	220			
	52.20	30.75	0.34	12.14	4.17	0.20	99.80	73.56	229			
	52.04	30.18	0.28	12.44	4.48	0.20	99.62	72.69	237			
	52.64	29.93	0.35	11.22	4.84	0.26	99.24	68.73	245			
	52.50	29.69	0.21	11.66	4.70	0.27	99.03	70.10	253			
	53.57	29.85	0.26	10.78	5.03	0.30	99.79	66.94	262			
	52.79	29.71	0.27	11.77	4.78	0.24	99.57	70.09	270			
	54.06	29.59	0.33	10.63	5.05	0.31	99.97	66.47	278			
	54.86	28.53	0.29	10.23	5.51	0.35	99.76	63.56	286			
	55.78	27.92	0.27	9.08	5.93	0.43	99.41	58.83	294			
	52.65	29.78	0.48	11.70	4.65	0.35	99.62	70.08	302			
199.1-199.15 E1 P-Plag6	56.74	27.55	0.27	8.60	6.22	0.65	100.03	55.61	0			
	54.21	29.23	0.34	10.68	5.11	0.34	99.91	66.22	13			
	54.41	29.28	0.28	10.30	5.11	0.30	99.68	65.57	19			
	54.72	29.06	0.30	10.37	5.40	0.31	100.17	64.48	25			
	51.19	30.98	0.25	12.38	4.19	0.25	99.24	73.58	31			
	52.42	30.47	0.30	11.64	4.54	0.23	99.61	70.89	38			
	53.13	30.09	0.37	11.33	4.81	0.29	100.02	68.93	44			
	54.93	29.28	0.31	10.18	5.22	0.40	100.31	64.43	50			
	56.67	27.84	0.34	8.41	6.10	0.60	99.96	55.65	57			
262.50-262.55 E1 P-Plag1	55.66	25.46	0.32	8.40	6.63	0.47	96.94	54.19	0	559.2	122.88	4.6
	56.11	26.55	0.40	8.87	6.23	0.37	98.51	57.35	20			

Appendix 1.1 (cont.)
Electron microprobe analyses of Unzen plagioclase (in wt.%)

Sample ID	SiO_2	Al_2O_3	FeO	CaO	Na_2O	K_2O	Total	An*	um**	Sr (ppm)	Ba (ppm)	Sr/ Ba
	56.72	26.60	0.21	8.83	6.12	0.38	98.86	57.62	40			
	56.69	26.79	0.18	8.87	6.13	0.46	99.11	57.38	61			
	56.81	26.28	0.22	8.44	6.40	0.49	98.65	55.03	81			
	56.64	25.82	0.24	8.25	6.34	0.52	97.81	54.59	101			
	58.04	25.89	0.33	7.84	6.41	0.47	98.97	53.29	122			
	56.98	25.78	0.23	8.21	6.36	0.45	98.01	54.68	143			
	57.34	25.64	0.19	7.92	6.67	0.42	98.17	52.77	163			
	57.51	25.30	0.32	7.82	6.53	0.66	98.14	52.10	183			
	57.18	25.94	0.35	8.02	6.87	0.50	98.86	52.12	203	566.3	113.26	5.0
	56.30	26.13	0.18	8.23	6.54	0.48	97.85	53.99	224			
	57.19	26.66	0.32	8.78	6.26	0.37	99.58	56.99	244			
	56.41	26.68	0.26	9.27	6.28	0.40	99.29	58.11	264			
	55.93	26.63	0.25	8.72	6.19	0.42	98.14	56.86	285			
	56.04	26.91	0.42	9.04	6.01	0.38	98.79	58.60	306			
	56.45	26.18	0.45	8.50	6.21	0.34	98.14	56.49	326			
	56.92	25.92	0.29	8.05	6.63	0.52	98.33	52.98	346			
	58.22	25.41	0.25	7.68	6.60	0.54	98.70	51.83	366			
	57.78	25.31	0.26	7.46	6.80	0.46	98.07	50.65	388			
	57.52	25.55	0.14	7.71	6.75	0.49	98.16	51.58	407	659.1	155.39	4.2
	57.20	26.22	0.32	8.39	6.74	0.43	99.30	53.91	427			
	57.07	26.15	0.34	8.14	6.59	0.43	98.71	53.68	447			
	58.57	24.95	0.36	7.19	6.94	0.64	98.65	48.66	469			
	57.76	25.56	0.36	7.93	6.83	0.47	98.91	52.09	489			
	57.38	26.17	0.32	8.09	6.55	0.45	98.96	53.63	509			
	57.32	26.28	0.32	8.13	6.54	0.42	99.00	53.88	550			
	56.07	26.82	0.29	8.99	6.03	0.40	98.60	58.30	570			
	55.42	27.16	0.26	9.55	5.69	0.28	98.36	61.53	590			
	56.47	26.53	0.20	8.59	6.17	0.40	98.35	56.67	610	568.2	119.76	4.7
	55.27	26.83	0.31	9.07	5.96	0.45	97.89	58.60	631			
	56.01	26.61	0.32	9.07	5.99	0.41	98.40	58.62	652			
	56.11	26.42	0.29	9.04	5.96	0.38	98.20	58.77	672			
	55.47	26.88	0.21	10.37	6.07	0.37	99.37	61.69	692	744.8	163.97	4.5
	51.50	29.77	0.14	12.22	4.17	0.22	98.01	73.59	713			
	54.18	27.45	0.35	10.37	5.28	0.27	97.91	65.09	733			
	54.81	27.65	0.39	9.96	5.59	0.29	98.69	62.89	753			
	56.28	26.34	0.29	8.87	6.08	0.38	98.24	57.88	773			
	55.61	26.70	0.48	9.29	6.02	0.37	98.46	59.25	794	650.1	170.25	3.8
	55.59	27.06	0.26	9.36	5.65	0.34	98.26	60.97	814			
	55.54	27.09	0.38	9.65	5.67	0.35	98.68	61.59	835			
	55.65	27.43	0.14	9.44	5.86	0.42	98.94	60.06	855			
	56.49	26.27	0.21	8.68	6.28	0.47	98.39	56.28	876			
	56.70	26.16	0.27	8.70	6.39	0.45	98.67	55.95	896	336.5	105.80	3.2
	54.69	27.53	0.43	10.05	5.25	0.27	98.23	64.52	916			
	37.44	22.63	1.08	7.97	1.77	0.27	71.17	79.65	936			
	48.58	29.81	0.67	13.33	3.51	0.23	96.13	78.10	957			
	51.75	28.86	0.44	12.15	3.69	0.40	97.30	74.81	977			
	52.83	26.58	0.98	11.22	2.97	0.71	95.29	75.30	997			
	55.45	26.77	1.05	11.53	2.94	0.79	98.52	75.56	1038			
	54.18	27.31	0.86	11.75	3.48	0.81	98.38	73.28	1059			
	56.37	27.01	0.35	9.35	5.71	0.40	99.20	60.47	1079			
262.50-262.55 E1 P-Plag2	55.40	26.92	0.30	9.75	5.82	0.41	98.60	61.03	0	566.0	121.00	4.7
	54.27	27.84	0.51	9.93	5.59	0.40	98.54	62.39	36			
	57.35	26.17	0.87	8.15	4.90	1.89	99.32	54.57	72			
	55.59	27.40	0.37	9.19	5.79	0.36	98.70	59.89	108			
	54.97	27.36	0.30	9.46	6.02	0.35	98.46	59.79	126			
	54.83	27.27	0.35	9.60	5.57	0.29	97.91	62.10	144			
	54.76	27.22	0.30	9.67	5.75	0.28	97.98	61.59	162			
	55.46	27.29	0.32	9.24	5.91	0.38	98.61	59.52	180			

Appendix 1.1 (cont.)
Electron microprobe analyses of Unzen plagioclase (in wt.%)

Sample ID	SiO_2	Al_2O_3	FeO	CaO	Na_2O	K_2O	Total	An*	um**	Sr (ppm)	Ba (ppm)	Sr/ Ba
	52.78	29.54	0.04	11.82	4.84	0.24	99.27	69.91	199			
	53.08	28.54	0.44	11.34	4.94	0.24	98.57	68.68	216	588.1	93.85	6.3
	55.20	27.59	0.10	9.78	5.76	0.36	98.80	61.49	233			
	54.87	28.02	0.23	10.12	5.41	0.34	98.99	63.80	252			
	56.26	27.71	0.32	9.25	5.38	0.50	99.41	61.14	270			
	51.67	29.35	0.35	11.86	4.35	0.23	97.81	72.14	289			
	52.96	29.61	0.32	12.01	4.36	0.27	99.52	72.14	306			
	53.97	28.12	0.29	10.11	5.27	0.31	98.06	64.47	324	722.4	122.47	5.9
	54.54	27.89	0.31	10.38	5.31	0.24	98.68	65.14	360			
	55.01	27.29	0.34	9.57	5.70	0.38	98.29	61.13	378			
	54.82	27.26	0.33	9.68	5.63	0.26	97.99	62.19	396			
	55.72	26.90	0.31	9.40	6.00	0.36	98.70	59.64	414			
	56.47	26.99	0.32	8.86	6.04	0.37	99.05	58.02	432			
	55.26	27.21	0.35	9.28	5.85	0.38	98.33	59.86	450			
	55.86	26.68	0.32	9.06	6.11	0.40	98.43	58.18	468			
	55.67	26.75	0.22	9.27	5.75	0.39	98.05	60.15	486			
	55.15	26.88	0.22	9.04	6.09	0.38	97.76	58.27	505			
	57.51	25.86	0.24	7.80	6.60	0.45	98.46	52.53	522			
	57.34	25.83	0.28	8.26	6.41	0.52	98.64	54.38	540			
	56.96	26.51	0.16	8.20	6.68	0.42	98.94	53.59	559			
	52.92	28.50	0.27	11.32	5.11	0.25	98.37	67.86	576			
	55.83	27.42	0.12	10.01	5.72	0.31	99.41	62.40	594			
	55.70	27.87	0.26	9.55	5.60	0.36	99.33	61.60	612			
	54.71	27.72	0.32	10.11	5.48	0.32	98.65	63.54	630			
	55.99	26.94	0.10	9.31	5.89	0.38	98.60	59.74	648			
	56.17	26.59	0.31	8.59	6.11	0.40	98.18	56.87	666			
	56.85	26.28	0.15	8.49	6.49	0.38	98.65	55.30	684			
	57.66	25.57	0.46	7.72	6.61	0.45	98.46	52.24	702			
	57.05	26.23	0.39	8.24	6.42	0.43	98.75	54.63	721			
	57.08	26.09	0.31	8.37	6.31	0.41	98.57	55.45	738	598.6	149.74	4.0
	56.55	26.07	0.16	8.40	6.22	0.40	97.80	55.92	757			
	54.68	27.71	0.23	9.95	5.51	0.32	98.40	63.06	775			
	55.76	27.25	0.11	9.07	5.74	0.32	98.25	59.94	792	553.5	106.24	5.2
	55.62	27.42	0.40	9.60	5.61	0.37	99.02	61.62	811			
	56.05	26.62	0.29	9.21	6.12	0.39	98.68	58.59	828			
	54.08	28.29	0.24	10.82	5.26	0.27	98.97	66.17	846			
	54.80	27.48	0.32	10.03	5.64	0.36	98.64	62.56	865			
	55.11	27.32	0.24	9.95	5.32	0.35	98.29	63.70	882			
	54.88	27.54	0.24	9.59	5.69	0.35	98.29	61.37	900			
	56.43	26.96	0.30	8.76	5.94	0.40	98.79	58.01	919			
	56.83	26.43	0.44	8.81	6.16	0.38	99.04	57.41	937			
	55.74	27.22	0.28	9.15	5.96	0.36	98.71	59.16	954			
	55.11	27.60	0.21	9.57	5.63	0.35	98.47	61.54	973			
	41.82	19.35	1.66	6.74	3.36	0.47	73.40	63.74	991			
	50.61	30.66	0.43	13.12	3.55	0.19	98.57	77.83	1008			
	50.31	30.46	0.46	13.31	3.62	0.11	98.27	78.12	1027	549.5	29.99	18.3
	51.38	29.53	0.37	12.35	4.29	0.18	98.10	73.42	1044			
	52.94	29.14	0.21	11.14	4.92	0.26	98.62	68.26	1063			
	54.66	27.74	0.49	9.98	5.26	0.26	98.39	64.39	1081			
	55.20	27.64	0.31	9.75	5.63	0.27	98.81	62.32	1098			
	55.72	27.25	0.26	9.31	5.64	0.37	98.55	60.76	1116			
	56.07	27.24	0.38	9.05	5.80	0.37	98.91	59.47	1135			
	54.63	27.71	0.39	9.61	5.69	0.33	98.35	61.48	1153			
	55.55	27.54	0.31	9.78	5.64	0.35	99.17	62.00	1170			
	54.99	27.66	0.33	10.05	5.46	0.31	98.81	63.51	1189			
	54.64	28.13	0.43	10.10	5.53	0.33	99.15	63.30	1207			
	54.73	28.29	0.24	10.13	5.36	0.35	99.09	63.95	1225	592.6	92.94	6.4
	54.99	27.15	0.42	9.67	5.69	0.34	98.26	61.60	1243			

Appendix 1.1 (cont.)
Electron microprobe analyses of Unzen plagioclase (in wt.%)

Sample ID	SiO_2	Al_2O_3	FeO	CaO	Na_2O	K_2O	Total	An*	um**	Sr (ppm)	Ba (ppm)	Sr/ Ba
	56.11	26.92	0.28	8.98	6.06	0.42	98.77	58.05	1261			
	53.34	29.61	0.78	13.13	3.21	0.44	100.50	78.27	1279			
	49.66	31.09	0.56	13.82	3.30	0.15	98.58	80.06	1297			
	49.78	31.24	0.61	14.33	2.89	0.17	99.02	82.40	1314			
	36.10	22.14	0.47	10.22	2.04	0.12	71.09	82.55	1333			
	52.43	31.70	0.63	13.59	2.80	0.22	101.38	81.80	1351			
	48.50	31.98	0.77	14.97	2.57	0.21	99.00	84.33	1369			
	57.06	24.16	0.84	8.71	3.47	1.25	95.49	64.83	1387			
	48.93	31.15	0.69	14.34	2.98	0.20	98.29	81.86	1405			
	47.76	32.06	0.50	15.31	2.53	0.13	98.28	85.21	1423			
	51.09	30.30	0.85	13.25	3.80	0.22	99.51	76.72	1441			
	50.68	29.67	0.52	12.56	3.87	0.14	97.44	75.79	1459			
	56.26	26.67	0.31	9.00	5.85	0.41	98.50	59.01	1477	416.3	45.91	9.1
262.50-262.55 E1 P-Plag3	57.62	25.51	0.30	8.08	6.61	0.43	98.54	53.43	0	572.8	140.95	4.1
	57.29	26.07	0.26	8.09	6.36	0.45	98.52	54.32	20			
	57.16	25.99	0.16	7.94	6.32	0.53	98.10	53.65	41			
	57.51	25.97	0.39	7.90	6.59	0.48	98.83	52.79	61			
	58.04	25.79	0.29	7.80	6.93	0.50	99.34	51.21	81			
	57.11	25.98	0.34	8.33	6.58	0.42	98.77	54.32	102	616.2	143.09	4.3
	54.44	27.76	0.24	10.26	5.23	0.32	98.25	64.90	122			
	55.03	27.22	0.27	9.61	5.91	0.41	98.44	60.34	142			
	57.07	25.83	0.14	8.05	6.55	0.46	98.10	53.43	163			
	57.10	26.03	0.20	8.14	6.49	0.45	98.41	53.97	183			
	57.53	26.13	0.29	7.99	6.68	0.46	99.08	52.82	205	581.9	826.18	0.7
	58.09	25.87	0.29	7.88	6.38	0.51	99.02	53.35	225			
	58.40	25.81	0.23	8.05	6.67	0.49	99.65	52.95	245			
	52.02	29.65	0.39	12.42	4.37	0.27	99.12	72.77	266			
	59.12	25.59	0.68	8.77	5.75	0.65	100.57	57.80	307	648.8	150.72	4.3
	55.27	27.80	0.32	9.97	5.71	0.37	99.45	62.11	327			
	56.30	26.87	0.38	9.12	5.80	0.36	98.82	59.66	347			
	53.25	28.70	0.29	11.02	4.88	0.24	98.38	68.26	368			
	52.35	29.51	0.18	11.92	4.60	0.23	98.79	71.14	388			
	55.52	27.19	0.22	9.73	5.63	0.29	98.58	62.19	408	639.3	160.01	4.0
	54.43	27.99	0.51	10.27	5.54	0.28	99.02	63.83	428			
	55.87	27.62	0.19	9.48	5.81	0.26	99.23	60.94	449			
	54.45	28.00	0.28	10.66	5.18	0.29	98.87	66.07	469			
	48.79	31.50	0.75	14.30	3.09	0.22	98.64	81.24	530	912.3	230.49	4.0
	48.50	28.32	2.71	12.60	2.63	0.16	94.92	81.82	551			
	57.79	26.15	0.74	10.72	3.66	1.04	100.10	69.53	571			
	50.71	30.34	0.59	13.58	3.13	0.36	98.71	79.59	592			
	48.62	31.86	0.71	15.50	2.33	0.23	99.24	85.84	613	930.4	230.49	4.0
	48.25	31.50	0.70	14.99	2.44	0.17	98.05	85.15	633			
	32.41	17.05	0.70	8.50	1.44	0.55	60.66	80.98	654			
	53.50	25.90	1.18	11.12	2.98	0.77	95.46	74.79	674			
	38.41	25.36	0.73	12.42	2.17	0.11	79.20	84.46	694	466.6	357.86	1.3
	51.68	29.21	0.68	12.29	4.18	0.23	98.26	73.61	715			
	52.03	28.72	0.79	11.69	4.58	0.25	98.06	70.74	796	527.3	312.88	1.7
390.00-390.05 Host Plag1	45.28	30.41	0.15	10.76	3.99	0.27	90.87	71.61	0			
	56.65	27.01	0.16	9.01	5.91	0.45	99.19	58.62	15			
	55.57	28.36	0.27	9.95	5.61	0.52	100.28	61.91	31			
	52.29	30.03	0.23	12.04	4.42	0.26	99.27	71.99	46			
	54.00	29.24	0.27	11.33	4.83	0.24	99.91	69.07	62			
	54.87	28.17	0.22	10.09	5.44	0.33	99.13	63.64	77			
	56.39	28.00	0.26	9.84	5.59	0.45	100.53	61.99	93			
	56.24	27.62	0.25	9.23	5.95	0.42	99.71	59.19	109			
	56.32	27.85	0.34	9.32	5.80	0.38	100.01	60.15	124			

Appendix 1.1 (cont.)
Electron microprobe analyses of Unzen plagioclase (in wt.%)

Sample ID	SiO_2	Al_2O_3	FeO	CaO	Na_2O	K_2O	Total	An*	um**	Sr (ppm)	Ba (ppm)	Sr/ Ba
	54.56	29.02	0.30	11.00	4.97	0.31	100.15	67.58	139			
	56.08	27.72	0.15	9.72	5.70	0.35	99.72	61.64	155			
	56.94	27.45	0.25	9.04	6.00	0.45	100.13	58.36	170			
	57.17	27.18	0.19	8.83	6.17	0.49	100.03	57.02	186			
	56.39	27.51	0.24	9.63	5.90	0.45	100.10	60.29	202			
	56.88	26.95	0.22	8.44	6.29	0.52	99.31	55.33	218			
	57.50	26.94	0.33	8.65	6.27	0.39	100.09	56.49	233			
	57.06	26.95	0.35	8.41	6.28	0.43	99.47	55.65	249			
	50.09	31.78	0.41	13.84	3.54	0.21	99.86	78.68	264			
	54.26	29.07	0.38	10.73	5.16	0.32	99.92	66.16	279			
	55.47	27.90	0.30	9.79	5.78	0.39	99.64	61.35	295			
	52.50	30.24	0.39	12.43	3.87	0.28	99.71	74.98	311			
	55.12	28.73	0.34	10.35	5.12	0.34	99.99	65.50	326			
	39.07	24.90	0.76	10.55	2.59	0.20	78.09	79.06	342			
	50.85	30.51	0.61	13.09	3.68	0.19	98.93	77.18	357			
	53.50	30.49	0.63	11.89	4.41	0.20	101.11	72.06	372			
390.00-390.05 Host Plag2	56.68	26.85	0.13	9.07	5.96	0.52	99.19	58.34	0	880.3	173.31	5.1
	56.88	27.21	0.32	8.81	6.21	0.41	99.84	57.09	18			
	56.13	27.31	0.22	9.26	5.91	0.37	99.19	59.58	37			
	56.25	27.08	0.20	9.24	5.96	0.40	99.14	59.21	55			
	56.37	27.35	0.20	9.12	6.04	0.44	99.52	58.47	73			
	57.37	27.26	0.29	8.93	6.09	0.39	100.32	57.96	92			
	57.01	27.07	0.23	8.69	6.12	0.43	99.55	57.04	110			
	56.73	26.78	0.26	8.95	5.85	0.45	99.01	58.70	129			
	57.41	26.37	0.25	8.34	6.37	0.51	99.26	54.78	147			
	58.02	26.10	0.21	8.36	6.32	0.58	99.58	54.81	166	790.1	161.79	4.9
	58.58	25.85	0.19	7.99	6.58	0.55	99.74	52.86	184			
	56.23	27.24	0.30	9.17	6.01	0.38	99.33	58.94	202			
	53.45	29.80	0.32	11.81	4.67	0.25	100.31	70.58	221			
	58.49	26.45	0.12	8.04	6.49	0.52	100.12	53.41	239			
	55.52	28.00	0.20	9.56	5.87	0.42	99.56	60.32	258			
	56.95	26.96	0.20	8.41	6.15	0.42	99.09	56.12	276			
	57.57	27.39	0.31	8.75	6.12	0.40	100.53	57.30	294	835.0	167.27	5.0
	57.92	26.35	0.17	8.31	6.37	0.48	99.60	54.80	313			
	55.78	28.41	0.24	9.97	5.63	0.31	100.35	62.65	331			
	57.09	26.99	0.24	8.33	6.08	0.49	99.22	55.89	350			
	56.65	26.79	0.14	8.42	6.36	0.51	98.88	55.09	368			
	55.87	28.17	0.27	9.93	5.70	0.34	100.27	62.18	387			
	56.86	27.16	0.19	9.03	6.09	0.38	99.71	58.28	405	859.3	165.85	5.2
	56.13	27.44	0.24	9.21	5.90	0.42	99.35	59.33	423			
	53.47	27.60	0.30	9.56	4.80	0.36	96.08	64.94	442			
390.00-390.05 Host Plag3	58.62	25.97	0.23	7.54	6.68	0.51	99.54	51.19	0			
	59.10	25.80	0.11	7.17	6.87	0.61	99.66	48.94	16			
	55.52	27.91	0.23	9.60	5.67	0.31	99.24	61.63	46			
	56.63	27.40	0.20	9.07	6.06	0.41	99.78	58.36	61			
	57.66	26.80	0.23	8.60	6.16	0.47	99.92	56.45	76			
	56.36	27.60	0.24	9.08	5.93	0.46	99.66	58.68	92			
	57.33	26.77	0.24	8.53	6.35	0.44	99.66	55.69	106			
	56.40	27.08	0.15	8.58	5.79	0.44	98.44	57.91	122			
	57.63	26.72	0.15	8.44	6.16	0.50	99.60	55.91	137			
	52.62	30.31	0.27	12.47	4.30	0.24	100.22	73.30	153			
	50.57	31.31	0.30	13.47	3.73	0.17	99.55	77.52	168			
	51.77	30.66	0.33	12.79	4.03	0.19	99.77	75.17	183			
	53.20	29.65	0.18	11.58	4.61	0.26	99.48	70.41	199			
	56.43	27.51	0.20	9.09	6.06	0.37	99.66	58.57	213			
	57.49	27.09	0.30	8.57	6.22	0.42	100.08	56.34	229			

Appendix 1.1 (cont.)
Electron microprobe analyses of Unzen plagioclase (in wt.%)

Sample ID	SiO_2	Al_2O_3	FeO	CaO	Na_2O	K_2O	Total	An*	um**	Sr (ppm)	Ba (ppm)	Sr/ Ba
	57.78	27.08	0.25	8.38	6.31	0.45	100.25	55.34	244			
	57.84	26.44	0.28	8.22	6.56	0.50	99.84	53.80	259			
	57.79	26.65	0.24	8.25	6.44	0.53	99.91	54.22	275			
	55.86	27.81	0.31	9.61	5.66	0.39	99.65	61.35	289			
	54.91	28.66	0.27	10.59	5.18	0.30	99.92	65.86	305			
390.00-390.05 Host Plag4	54.40	27.88	0.41	9.87	5.41	0.47	98.43	62.68	0	855.9	152.19	5.6
	53.16	29.42	0.27	12.15	4.62	0.24	99.85	71.40	82			
	56.61	27.32	0.26	8.28	6.22	0.47	99.17	55.30	124			
	57.80	26.46	0.19	8.51	6.25	0.63	99.84	55.32	165			
	54.61	29.12	0.29	10.71	5.18	0.28	100.18	66.24	206			
	56.30	27.74	0.21	9.37	5.93	0.36	99.91	59.86	248			
	54.45	24.58	0.52	7.94	5.03	0.49	93.00	58.99	288			
	58.23	26.04	0.28	7.74	6.67	0.48	99.44	51.95	330	885.7	176.28	5.0
	57.52	26.93	0.27	8.62	6.28	0.43	100.05	56.21	371			
	56.62	27.73	0.25	9.56	5.77	0.37	100.31	60.89	413			
	56.77	27.79	0.25	9.06	5.91	0.42	100.20	58.86	454			
	57.53	26.98	0.18	8.56	6.44	0.45	100.13	55.41	495			
	49.78	23.27	0.23	7.41	5.52	0.55	86.75	54.97	536			
	55.66	28.29	0.18	9.94	5.56	0.33	99.97	62.78	578			
	58.02	26.66	0.25	8.77	6.30	0.44	100.44	56.57	619			
	58.54	26.72	0.17	8.39	6.22	0.53	100.57	55.43	660	884.0	170.27	5.2
	57.94	26.19	0.14	8.20	6.53	0.50	99.50	53.84	702			
	56.59	27.46	0.15	9.03	5.98	0.43	99.64	58.46	742			
	57.23	27.19	0.33	9.23	5.96	0.41	100.35	59.18	784			
	58.12	26.34	0.25	8.31	6.52	0.50	100.04	54.23	825			
	57.63	27.08	0.29	8.87	6.16	0.46	100.48	57.28	866			
	57.12	27.08	0.19	8.58	6.15	0.48	99.61	56.44	908	741.0	148.23	5.0
	57.70	26.46	0.23	8.09	6.17	0.43	99.07	55.08	949			
	57.69	26.64	0.19	8.47	6.22	0.50	99.71	55.77	990			
	58.39	26.63	0.23	8.20	6.30	0.52	100.27	54.61	1031	815.5	186.53	4.4
	57.27	27.04	0.15	8.80	6.07	0.42	99.74	57.55	1073	858.2	176.27	4.9
	56.76	27.17	0.18	9.17	5.87	0.40	99.55	59.38	1114	829.4	163.71	5.1
390.00-390.05 Host Plag5	58.26	26.12	0.19	7.78	6.34	0.52	99.21	53.14	0			
	58.01	26.45	0.17	7.84	6.63	0.53	99.64	52.24	36			
	58.02	26.17	0.19	7.83	6.60	0.52	99.35	52.35	72			
	57.83	26.22	0.24	7.90	6.63	0.50	99.32	52.55	108			
	57.79	25.85	0.16	8.04	6.38	0.53	98.74	53.78	144			
	56.61	27.29	0.17	9.22	6.01	0.42	99.71	58.92	180			
	54.11	28.94	0.27	11.06	5.14	0.27	99.79	67.15	215			
	54.73	28.57	0.15	10.38	5.37	0.32	99.53	64.60	251			
	57.10	27.23	0.18	8.91	6.15	0.39	99.95	57.68	287			
	58.93	25.63	0.27	7.54	6.88	0.61	99.86	50.18	323			
	58.51	26.56	0.22	7.85	6.68	0.52	100.33	52.17	359			
	58.18	26.38	0.21	8.04	6.47	0.54	99.82	53.44	395			
	56.48	27.41	0.35	8.70	6.10	0.38	99.41	57.34	431			
	56.19	28.14	0.18	9.65	5.77	0.43	100.35	60.89	467			
	56.78	26.99	0.43	8.96	6.04	0.40	99.61	58.20	503			
	56.38	27.32	0.24	9.68	5.89	0.39	99.90	60.64	539			
	56.04	27.24	0.26	9.40	5.98	0.40	99.32	59.57	575			
	57.12	27.27	0.09	9.07	6.04	0.38	99.96	58.54	610			
	57.68	27.01	0.27	8.70	6.33	0.44	100.42	56.24	646			
	56.19	27.27	0.19	9.43	5.91	0.40	99.40	59.91	682			
	57.43	26.70	0.13	8.69	6.27	0.48	99.70	56.27	718			
	57.66	26.75	0.25	8.35	6.48	0.51	100.00	54.43	754			
	54.84	28.40	0.25	10.88	5.17	0.32	99.87	66.43	790			
	50.67	30.96	0.54	13.72	3.62	0.20	99.72	78.21	825			

Appendix 1.1 (cont.)
Electron microprobe analyses of Unzen plagioclase (in wt.%)

Sample ID	SiO_2	Al_2O_3	FeO	CaO	Na_2O	K_2O	Total	An*	um**	Sr (ppm)	Ba (ppm)	Sr/ Ba
390.00-390.05 Plag6	58.15	26.19	0.25	7.92	6.50	0.54	99.56	52.95	0	5.1	148.66	
	57.24	27.45	0.13	8.81	6.09	0.34	100.07	57.80	35	5.1	148.66	
	54.22	26.81	0.27	9.28	5.72	0.40	96.69	60.23	71			
	57.82	26.56	0.15	8.35	6.38	0.52	99.77	54.75	107	5.0	157.13	
	57.23	27.60	0.19	9.18	5.90	0.39	100.49	59.33	143			
	57.52	26.47	0.13	8.21	6.50	0.40	99.23	54.33	179			
	57.92	26.85	0.23	8.36	6.30	0.44	100.11	55.37	214	5.7	130.02	
	57.02	27.34	0.23	8.77	6.11	0.43	99.90	57.27	250			
	58.30	26.64	0.29	7.98	6.58	0.49	100.27	53.01	286			
	54.57	28.87	0.13	10.62	5.25	0.35	99.80	65.46	322			
	56.25	27.63	0.27	9.72	5.89	0.42	100.18	60.64	357			
	58.02	26.09	0.16	8.11	6.55	0.51	99.43	53.48	393	4.4	212.04	
	57.94	26.29	0.25	8.09	6.62	0.48	99.66	53.28	429			
	52.07	23.06	0.22	6.74	5.62	0.54	88.24	52.27	463			
	58.70	26.20	0.24	7.81	6.74	0.57	100.25	51.67	501	5.6	126.79	
	55.79	27.69	0.31	9.56	5.83	0.41	99.60	60.51	536			
	57.78	26.59	0.35	8.31	6.44	0.47	99.93	54.58	572	4.1	207.65	
	57.99	26.34	0.28	7.72	6.48	0.57	99.38	52.23	607			
	58.41	25.78	0.19	7.63	6.77	0.46	99.24	51.36	643			
	58.05	26.30	0.18	8.14	6.33	0.44	99.45	54.56	679			
	57.52	27.02	0.16	8.30	6.17	0.44	99.60	55.68	715			
	57.20	26.76	0.24	9.08	6.15	0.41	99.84	58.05	751			
	57.73	26.64	0.22	8.42	6.30	0.50	99.81	55.34	786			
	56.90	25.67	0.25	7.70	5.90	0.55	96.97	54.41	821	4.6	190.92	
	59.35	22.44	0.50	7.08	3.96	1.32	94.65	57.28	858			
	54.30	27.65	0.43	9.32	5.44	0.36	97.48	61.66	893	6.2	131.09	
	55.59	28.51	0.39	10.53	5.28	0.29	100.59	65.42	929			
390.00-390.05 Host Plag7	57.79	26.15	0.23	7.97	6.31	0.46	98.91	54.06	0	767.1	165.26	4.6
	57.54	26.84	0.23	8.58	6.31	0.47	99.97	55.86	15			
	57.70	26.66	0.31	8.65	6.30	0.47	100.10	56.06	31			
	57.99	26.44	0.24	8.40	6.48	0.42	99.98	54.91	46			
	57.51	26.80	0.19	8.40	6.21	0.47	99.58	55.70	61			
	56.30	27.61	0.28	9.12	5.85	0.36	99.53	59.51	76	842.9	181.10	4.7
	57.57	26.92	0.25	8.38	6.19	0.42	99.72	55.93	91			
	57.55	27.12	0.24	8.92	6.24	0.54	100.60	56.83	107			
	57.21	26.76	0.23	8.81	6.27	0.45	99.73	56.73	121			
	57.41	26.81	0.17	8.34	6.27	0.47	99.47	55.29	137			
	57.57	26.33	0.20	7.98	6.50	0.46	99.04	53.41	153			
	59.15	25.74	0.14	7.52	6.68	0.66	99.91	50.61	168	752.3	176.57	4.3
	55.98	28.03	0.18	9.93	5.70	0.38	100.20	62.03	183			
	56.32	27.69	0.16	9.13	5.82	0.42	99.56	59.39	198			
	57.74	27.03	0.06	8.12	6.26	0.49	99.69	54.62	213			
	56.58	27.90	0.29	9.53	5.91	0.33	100.55	60.39	228			
	54.33	28.90	0.12	10.96	5.05	0.32	99.67	67.15	244			
	56.17	27.62	0.23	9.61	6.09	0.35	100.06	59.91	259			
	56.53	27.94	0.26	9.48	5.84	0.40	100.44	60.31	274	832.0	183.44	4.5
	57.24	27.43	0.12	8.74	6.20	0.45	100.19	56.78	289			
	57.45	26.96	0.23	8.49	6.37	0.49	100.00	55.33	304			
	58.22	26.45	0.20	8.26	6.31	0.53	99.96	54.72	320			
	55.49	27.85	0.18	9.93	5.71	0.38	99.55	62.00	335			
	56.40	27.69	0.34	9.45	5.82	0.36	100.06	60.50	350			
	55.98	27.57	0.29	9.20	5.96	0.42	99.42	59.08	366			
	57.37	26.81	0.14	8.49	6.22	0.42	99.46	56.11	381	927.3	214.14	4.3
	55.62	28.39	0.23	9.97	5.58	0.36	100.15	62.66	396			
	55.22	26.70	0.25	8.66	5.85	0.43	97.11	58.00	411	839.4	163.88	5.1
	57.10	27.07	0.33	8.59	6.22	0.45	99.77	56.27	426			
	55.18	28.32	0.21	9.98	5.63	0.37	99.67	62.45	442			

Appendix 1.1 (cont.)
Electron microprobe analyses of Unzen plagioclase (in wt.%)

Sample ID	SiO_2	Al_2O_3	FeO	CaO	Na_2O	K_2O	Total	An*	um**	Sr (ppm)	Ba (ppm)	Sr/ Ba
	56.54	27.39	0.17	8.51	6.09	0.46	99.17	56.47	457			
	57.32	26.92	0.25	8.65	6.01	0.47	99.62	57.18	472			
390.00-390.05 Host Plag10	53.87	27.86	0.13	8.38	5.63	0.34	96.22	58.39	0	857.6	189.17	4.5
	57.79	26.98	0.24	8.55	6.15	0.40	100.11	56.60	20			
	57.46	27.21	0.27	8.31	6.25	0.41	99.91	55.49	40			
	57.43	27.24	0.17	8.55	6.23	0.46	100.08	56.13	60			
	57.40	27.17	0.07	8.71	6.13	0.43	99.90	57.07	80			
	57.16	27.01	0.23	8.51	6.13	0.41	99.44	56.55	101			
	57.73	26.47	0.20	8.26	6.41	0.51	99.58	54.41	121			
	57.72	26.47	0.27	7.79	6.60	0.47	99.32	52.39	141	740.2	131.85	5.6
	58.88	26.45	0.24	7.38	6.58	0.45	99.99	51.21	161			
	57.86	26.22	0.20	7.70	6.64	0.46	99.10	52.03	181			
	56.37	27.51	0.21	9.23	6.06	0.40	99.78	58.79	201			
	56.24	27.31	0.22	9.04	6.06	0.41	99.28	58.31	221			
	57.68	26.83	0.25	8.62	6.22	0.54	100.13	56.08	241	621.4	81.39	7.6
	56.32	27.68	0.25	9.18	5.90	0.39	99.72	59.34	261			
	56.06	27.67	0.11	9.32	5.73	0.35	99.24	60.54	282			
	56.07	27.74	0.22	9.59	5.48	0.40	99.48	62.01	303			
	56.93	27.18	0.37	8.98	6.11	0.38	99.95	58.03	323	944.0	215.85	4.4
	56.11	27.57	0.27	8.98	5.88	0.36	99.18	59.01	343			
	56.32	27.61	0.26	9.28	5.93	0.39	99.80	59.46	363			
	56.30	27.82	0.33	9.51	5.66	0.34	99.96	61.29	383			
	56.63	27.74	0.29	9.63	5.58	0.37	100.25	61.80	403	903.0	165.58	5.5
390.00-390.05 E1 M-Plag1	48.14	31.64	0.81	15.77	3.18	0.19	99.74	82.40	0			
	49.46	31.13	0.67	14.17	3.36	0.10	98.87	80.39	9	1662.6	144.57	11.5
	48.34	32.32	0.80	14.52	3.56	0.13	99.68	79.73	18			
	45.39	29.85	0.90	15.59	3.89	0.17	95.77	79.34	28	1160.5	121.35	9.6
	45.38	30.67	0.72	13.87	3.88	0.15	94.67	77.49	37			
	48.20	32.08	0.64	13.40	4.02	0.11	98.45	76.45	46			
	50.38	31.01	0.59	12.89	3.73	0.16	98.75	76.85	55	1420.3	360.51	3.9
	54.03	28.37	0.44	10.84	5.14	0.28	99.10	66.68	64			
	57.09	26.78	0.40	9.27	5.96	0.44	99.96	59.14	73			
390.00-390.05 E1 M-Plag2	48.88	31.50	0.74	15.79	3.39	0.54	100.84	80.06	0			
	49.82	31.56	0.69	14.58	2.82	0.82	100.29	80.02	14	1684.3	141.83	11.9
	48.20	32.46	0.75	14.21	3.17	0.05	98.83	81.51	27			
	48.80	29.80	0.71	15.55	3.77	0.16	98.80	79.81	41			
	45.99	30.52	0.82	13.13	3.75	0.15	94.37	77.07	54			
	47.09	32.16	0.86	13.21	4.71	0.13	98.17	73.15	68			
	50.99	31.46	0.77	12.51	3.62	0.62	99.96	74.70	81	1437.2	294.16	4.9
	45.54	29.59	0.42	10.35	5.12	0.81	91.82	63.59	95			
	49.15	29.47	0.41	9.30	5.62	0.36	94.29	60.87	109			
390.00-390.05 E1 M-Plag3	47.82	33.14	0.62	16.43	2.35	0.09	100.45	87.08	0			
	50.50	31.38	0.55	13.61	3.73	0.14	99.91	77.83	11			
	50.48	30.38	0.53	13.53	3.88	0.19	98.99	76.89	23	1463.5	149.69	9.8
	51.26	31.08	0.53	13.27	3.92	0.14	100.19	76.57	34			
	52.32	30.03	0.56	11.91	4.44	0.21	99.47	71.94	45			
	54.88	28.30	0.36	10.10	5.50	0.32	99.45	63.45	56			
	55.74	27.05	0.53	9.50	6.04	0.38	99.23	59.67	68	1466.0	306.03	4.8
	58.41	25.70	0.42	8.39	6.22	0.66	99.79	54.97	79			
	57.62	25.91	0.23	8.61	6.51	0.13	99.01	56.49	90			
	58.59	24.77	0.15	8.07	7.03	0.04	98.64	53.29	101			
432.20-432.25 Host Plag1	48.87	32.12	0.71	15.26	2.84	0.11	99.91	83.77	0			
	64.51	10.13	0.54	4.72	1.15	0.11	81.16	78.94	75			

Appendix 1.1 (cont.)
Electron microprobe analyses of Unzen plagioclase (in wt.%)

Sample ID	SiO_2	Al_2O_3	FeO	CaO	Na_2O	K_2O	Total	An*	um**	Sr (ppm)	Ba (ppm)	Sr/ Ba
	50.46	29.52	0.59	14.36	2.81	0.40	98.14	81.73	151			
	29.85	14.94	0.60	6.78	1.82	0.30	54.29	76.24	226			
	55.25	27.43	0.23	8.44	6.30	0.45	98.09	55.54	302			
	57.74	27.21	0.22	8.44	6.64	0.41	100.67	54.45	378			
	55.16	28.00	0.26	10.16	5.77	0.36	99.71	62.37	454			
	57.08	26.73	0.34	8.71	6.44	0.60	99.91	55.30	529			
	58.80	25.88	0.17	7.51	6.96	0.44	99.76	50.37	604			
	55.81	27.63	0.37	9.74	5.94	0.32	99.82	60.85	680			
	56.24	27.22	0.26	9.18	6.24	0.44	99.58	57.87	756			
	55.69	26.03	0.31	8.34	6.11	0.55	97.03	55.61	831			
	56.63	27.11	0.34	8.93	6.23	0.44	99.68	57.24	907			
	56.97	26.67	0.24	9.07	6.49	0.44	99.87	56.69	982			
	55.65	26.37	0.22	8.49	6.31	0.41	97.45	55.82	1057			
	54.61	28.57	0.36	10.72	5.34	0.32	99.92	65.45	1134			
	56.18	27.32	0.27	9.67	6.28	0.40	100.11	59.18	1209			
	54.66	28.58	0.24	10.59	5.42	0.29	99.77	64.98	1284			
	53.83	28.99	0.25	10.83	5.25	0.25	99.41	66.34	1360			
	56.80	26.81	0.18	9.15	6.24	0.34	99.51	58.18	1436			
	55.94	27.21	0.19	9.35	6.17	0.35	99.21	58.94	1511			
	56.28	27.19	0.26	9.23	6.13	0.35	99.43	58.75	1587			
	57.56	26.45	0.35	8.28	6.63	0.44	99.71	53.96	1662			
	56.65	26.50	0.27	8.97	6.44	0.41	99.24	56.71	1738			
	57.99	24.70	0.49	8.82	5.43	1.17	98.61	57.21	1813			
	45.29	27.46	0.70	12.81	2.36	0.44	89.07	82.08	1889			
	49.80	31.54	0.83	14.39	3.38	0.22	100.15	79.98	1964			
432.20-432.25 E1 M-Plag1	48.59	32.16	0.54	15.19	3.03	0.15	99.66	82.67	0			
	49.21	31.57	0.66	15.12	2.94	0.13	99.64	83.13	7			
	61.93	22.87	0.53	8.65	2.73	1.99	98.70	64.68	13			
	48.85	32.26	0.79	14.99	2.94	0.11	99.95	83.08	20			
	48.83	32.49	0.72	14.97	2.85	0.10	99.96	83.55	27			
	74.09	12.17	0.95	0.50	2.02	5.24	94.98	6.49	34			
432.20-432.25 E1 M-Plag2	74.35	11.24	1.13	0.58	1.36	5.31	93.97	8.06	0			
	52.43	29.84	0.61	12.44	4.25	0.28	99.85	73.31	9			
	49.56	31.65	0.46	14.42	3.21	0.13	99.43	81.20	17			
	49.74	31.63	0.62	14.77	3.23	0.17	100.16	81.26	25			
	49.97	31.98	0.74	14.85	3.11	0.10	100.75	82.24	33			
	49.97	31.26	0.60	14.27	3.39	0.16	99.65	80.08	42			
	46.05	28.94	0.68	13.35	3.21	0.12	92.35	80.05	50			
	49.25	31.73	0.53	14.99	3.13	0.13	99.76	82.12	58			
	49.68	31.73	0.63	14.46	3.27	0.11	99.88	81.04	67			
	49.33	31.67	0.63	14.26	3.23	0.17	99.28	80.73	74			
	49.44	31.05	0.76	13.49	3.21	0.21	98.17	79.76	83			
432.20-432.25 E1 M-Plag3	49.43	29.69	0.53	12.90	3.76	0.20	96.51	76.51	0			
	48.91	31.87	0.80	14.23	3.34	0.12	99.26	80.46	9			
	43.06	29.53	1.06	12.85	2.18	0.13	88.81	84.78	16			
	46.13	33.94	0.70	16.87	1.73	0.08	99.45	90.33	24			
	45.62	34.64	0.83	17.58	1.55	0.04	100.27	91.69	32			
	45.31	35.02	0.69	17.89	1.52	0.04	100.47	92.00	40			
	46.92	33.28	0.88	16.84	1.63	0.17	99.72	90.34	49			
	29.34	20.41	0.48	11.73	1.12	0.15	63.25	90.18	57			
	40.70	28.79	0.85	14.81	1.57	0.14	86.86	89.62	65			
	33.61	20.84	3.67	0.48	0.34	0.37	59.32	40.13	73			
	47.32	32.70	0.73	15.85	2.44	0.11	99.15	86.15	81			
	49.75	31.37	0.43	14.42	3.39	0.10	99.47	80.48	89			
	49.71	31.37	0.68	14.31	3.33	0.15	99.55	80.41	97			

Appendix 1.1 (cont.)
Electron microprobe analyses of Unzen plagioclase (in wt.%)

Sample ID	SiO_2	Al_2O_3	FeO	CaO	Na_2O	K_2O	Total	An*	um**	Sr (ppm)	Ba (ppm)	Sr/ Ba
	50.22	31.08	0.85	14.19	3.53	0.17	100.03	79.32	106			
	51.82	29.66	0.62	12.88	4.22	0.17	99.37	74.61	113			
	49.24	29.08	0.48	12.74	3.95	0.27	95.75	75.15	121			
432.20-432.25 E1 M-Plag4	54.59	29.16	0.72	11.13	4.92	0.39	100.92	67.67	0			
	48.75	32.26	0.78	14.77	3.00	0.12	99.69	82.55	9			
	49.46	32.05	0.67	14.76	3.30	0.10	100.33	81.25	18			
	49.19	32.43	0.79	15.06	3.00	0.11	100.58	82.92	27			
	48.12	32.94	0.86	15.45	2.51	0.06	99.93	85.77	37			
	46.87	33.51	0.80	16.63	2.17	0.09	100.07	88.02	45			
	49.54	32.05	0.50	15.02	3.05	0.09	100.25	82.72	55			
	50.05	31.29	0.62	13.70	3.61	0.17	99.42	78.41	63			
432.20-432.25 E1 M-Plag5	51.30	30.20	0.49	12.83	4.10	0.26	99.18	74.65	0			
	47.08	33.48	0.82	16.41	1.99	0.10	99.87	88.69	8			
	45.31	34.40	0.68	17.82	1.46	0.05	99.71	92.21	16			
	46.18	34.14	0.63	17.34	1.89	0.06	100.25	89.88	24			
	45.39	34.44	0.67	16.88	1.81	0.08	99.27	89.96	32			
	34.31	25.10	0.65	11.91	1.23	0.17	73.36	89.49	41			
	45.45	34.75	0.72	17.94	1.39	0.02	100.27	92.70	49			
	41.63	29.17	1.20	15.16	2.03	0.14	89.32	87.50	57			
	49.24	31.73	0.74	14.22	3.29	0.12	99.34	80.63	65			
	49.22	31.64	0.67	14.25	3.35	0.13	99.26	80.34	73			
	50.47	31.31	0.54	13.35	3.97	0.31	99.95	75.73	81			
432.20-432.25 E1 M-Plag6	49.95	30.69	0.82	12.05	3.59	0.28	97.38	75.69	0			
	51.37	30.59	0.49	12.85	3.89	0.17	99.37	75.97	7			
	50.73	30.60	0.45	13.43	3.69	0.16	99.05	77.74	14			
	50.42	30.62	0.63	13.18	3.67	0.18	98.70	77.39	21			
	51.41	30.58	0.63	12.82	4.01	0.30	99.75	74.84	28			
	55.33	26.21	0.82	6.20	5.92	0.76	95.25	48.15	35			
432.20-432.25 E1 M-Plag7	50.14	31.47	0.73	14.09	3.14	0.20	99.76	80.82	0			
	49.34	31.69	0.75	14.84	3.07	0.14	99.84	82.23	11			
	45.58	34.48	0.75	17.65	1.51	0.06	100.03	91.80	21			
	45.90	34.07	0.80	17.48	1.52	0.12	99.89	91.46	31			
	47.73	28.13	1.62	3.27	2.98	0.58	84.31	47.92	42			
	51.42	24.50	1.70	4.96	2.17	0.49	85.23	65.11	53			
	46.35	33.96	0.73	16.84	1.83	0.03	99.74	90.04	63			
	47.26	33.39	0.81	16.08	2.31	0.13	99.99	86.79	73			
	45.78	34.32	0.66	17.58	1.65	0.05	100.04	91.21	84			
	45.57	31.52	0.76	15.38	1.78	0.10	95.12	89.09	94			
	46.60	33.54	0.52	16.64	1.86	0.08	99.24	89.59	105			
	49.52	31.54	0.64	14.15	3.26	0.10	99.21	80.83	115			
	48.88	31.90	0.74	14.41	3.15	0.10	99.18	81.63	126			
	49.95	31.75	0.57	14.23	3.32	0.13	99.96	80.48	136			
	51.45	29.40	0.49	11.73	4.38	0.32	97.78	71.37	147			
432.20-432.25 E1 M-Plag8	53.10	28.86	0.39	11.48	4.63	0.45	98.91	69.32	0			
	29.26	20.24	0.58	10.16	1.19	0.13	61.56	88.50	10			
	46.89	32.94	0.61	16.59	2.23	0.12	99.37	87.62	21			
	46.39	33.72	0.82	16.93	1.78	0.03	99.66	90.33	31			
	20.94	14.64	0.69	6.04	0.73	0.17	43.22	86.98	42			
	46.14	34.10	0.86	17.50	1.80	0.06	100.45	90.41	52			
	48.04	32.08	0.61	15.57	2.51	0.10	98.91	85.66	63			
	49.00	32.10	0.67	15.09	2.93	0.13	99.92	83.13	73			
	50.60	31.17	0.54	13.47	3.84	0.29	99.92	76.52	83			

Appendix 1.1 (cont.)
Electron microprobe analyses of Unzen plagioclase (in wt.%)

Sample ID	SiO_2	Al_2O_3	FeO	CaO	Na_2O	K_2O	Total	An*	um**	Sr (ppm)	Ba (ppm)	Sr/ Ba
432.20-432.25 E1 M-Plag9	59.58	25.97	0.97	9.22	5.31	0.42	101.48	61.66	0			
	52.46	30.24	0.54	13.10	4.23	0.16	100.73	74.90	9			
	49.46	31.78	0.69	14.73	3.25	0.08	99.99	81.55	17			
	46.98	33.46	0.76	16.54	2.21	0.15	100.10	87.53	26			
	48.84	31.79	1.13	14.51	3.16	0.12	99.55	81.52	34			
	49.18	31.89	0.57	14.70	3.10	0.12	99.57	82.02	43			
	50.23	31.54	0.58	14.14	3.72	0.13	100.35	78.61	51			
435.20-435.25 Host Plag1	56.04	27.29	0.40	9.00	5.95	0.66	99.34	57.63	0	748.6	117.48	6.4
	54.96	28.65	0.29	10.48	5.09	0.48	99.96	65.28	12			
	54.29	28.65	0.30	10.49	5.04	0.36	99.13	66.02	24			
	54.78	28.56	0.27	10.73	5.20	0.43	99.97	65.59	36			
	54.71	25.83	0.28	8.77	5.30	0.56	95.45	59.97	48			
	57.80	26.20	0.19	8.07	6.38	0.67	99.30	53.38	60			
	53.43	28.94	0.31	11.17	4.83	0.39	99.07	68.13	72			
	52.13	29.61	0.28	12.04	4.34	0.25	98.64	72.40	84			
	52.08	30.98	0.37	13.33	3.91	0.20	100.87	76.44	96			
	53.57	29.93	0.44	12.15	4.38	0.23	100.70	72.48	108			
	52.64	29.63	0.43	11.53	4.51	0.23	98.97	70.85	120			
	52.95	28.97	0.16	11.88	4.27	0.32	98.55	72.13	132			
	52.75	29.32	0.28	11.70	4.12	0.25	98.41	72.79	144			
	55.20	28.08	0.29	10.07	5.43	0.42	99.49	63.26	157			
	49.62	29.03	0.38	12.27	3.78	0.27	95.35	75.18	181			
	58.44	25.50	0.37	9.34	4.09	0.89	98.63	65.22	193			
	56.13	28.19	0.46	10.00	5.61	0.45	100.84	62.23	205	1013.9	253.88	4.0
	53.12	29.50	0.36	11.61	4.78	0.35	99.72	69.37	217			
	53.58	29.27	0.36	11.38	4.50	0.37	99.46	70.03	229			
	56.34	26.73	0.56	9.08	5.51	0.56	98.78	59.91	241			
	54.77	28.54	0.41	10.54	5.08	0.30	99.64	66.21	253			
	54.79	28.82	0.31	10.84	5.07	0.29	100.12	66.92	265			
	54.67	28.49	0.27	10.63	5.14	0.30	99.49	66.16	278			
	54.37	28.54	0.18	10.83	5.14	0.34	99.40	66.41	290			
	54.46	28.28	0.14	10.58	5.33	0.31	99.10	65.22	302	900.9	165.15	5.5
	53.85	28.97	0.27	10.81	4.99	0.29	99.19	67.20	314			
	54.14	28.65	0.31	10.84	5.10	0.34	99.38	66.58	326			
	53.20	30.11	0.20	12.18	4.30	0.31	100.30	72.52	338			
	43.38	24.37	1.38	8.76	3.49	0.42	81.81	69.14	350			
	55.94	27.48	0.30	9.65	5.66	0.48	99.51	61.09	362			
	56.14	27.34	0.29	9.42	5.68	0.52	99.39	60.29	374			
	57.02	26.45	0.21	8.50	5.80	0.68	98.67	56.73	386			
	58.79	25.84	0.18	7.91	6.46	0.69	99.87	52.49	398	840.7	140.49	6.0
	57.88	25.60	0.24	7.73	6.33	0.71	98.49	52.35	410			
	54.30	24.97	0.79	7.35	5.56	0.59	93.57	54.47	422			
	58.26	26.31	0.13	8.33	6.39	0.63	100.05	54.27	434			
	55.58	27.87	0.32	10.03	5.67	0.34	99.80	62.55	446			
	56.04	27.47	0.34	9.34	5.76	0.44	99.39	60.10	458			
	54.94	28.28	0.10	10.28	5.22	0.32	99.14	64.94	471			
	50.66	26.66	0.24	9.78	5.12	0.35	92.81	64.13	483			
	52.24	29.91	0.28	12.37	4.30	0.25	99.36	73.10	495	681.4	107.51	6.3
	52.32	30.05	0.27	11.99	4.47	0.33	99.42	71.40	507			
	50.77	31.11	0.39	13.23	3.38	0.23	99.11	78.57	519			
	55.91	27.59	0.30	9.95	5.31	0.50	99.56	63.13	531			
	55.99	27.33	0.26	8.94	5.85	0.61	98.99	58.03	543			
	51.43	25.76	0.01	9.71	5.02	0.42	92.35	64.08	555			
	50.90	29.79	0.52	12.47	4.02	0.23	97.94	74.58	567			
	51.31	30.74	0.40	13.54	3.67	0.20	99.85	77.77	579			
	52.57	29.99	0.36	12.14	4.06	0.27	99.38	73.72	591	857.0	80.09	10.7
	55.49	27.81	0.17	10.08	5.34	0.55	99.44	63.11	615			

Appendix 1.1 (cont.)
Electron microprobe analyses of Unzen plagioclase (in wt.%)

Sample ID	SiO_2	Al_2O_3	FeO	CaO	Na_2O	K_2O	Total	An*	um**	Sr (ppm)	Ba (ppm)	Sr/ Ba
	55.08	28.16	0.23	10.13	5.24	0.38	99.21	64.32	627			
	55.03	27.88	0.28	10.26	5.51	0.36	99.30	63.61	639			
	56.34	27.27	0.18	9.01	5.79	0.41	99.00	59.23	651			
	56.62	27.14	0.43	9.07	6.05	0.43	99.73	58.32	663			
	56.60	27.09	0.16	8.78	5.85	0.45	98.94	58.21	675	927.2	138.34	6.7
	56.82	27.13	0.38	9.20	5.98	0.43	99.93	58.97	687			
	55.93	27.75	0.37	9.81	5.64	0.28	99.78	62.38	699			
	49.84	31.45	0.29	13.99	3.18	0.15	98.90	80.80	711			
	50.64	31.43	0.38	13.80	3.44	0.20	99.89	79.11	723	1107.4	213.03	5.2
	48.27	32.87	0.45	15.56	2.35	0.10	99.60	86.38	735			
	51.29	31.02	0.31	13.98	2.96	0.33	99.89	80.95	747			
	55.22	28.00	0.22	10.31	5.36	0.46	99.56	63.93	759			
	54.96	28.10	0.38	10.13	5.47	0.40	99.43	63.33	771			
	54.91	26.72	0.27	9.28	5.40	0.34	96.91	61.81	783			
	56.67	26.61	0.26	8.90	6.05	0.40	98.89	57.99	796			
	57.18	26.48	0.26	8.57	6.13	0.47	99.08	56.50	809			
	55.71	28.16	0.29	10.07	5.48	0.41	100.12	63.10	821			
	55.48	28.57	0.35	10.44	5.35	0.31	100.49	64.84	833			
	55.29	27.63	0.45	9.92	5.24	0.39	98.92	63.79	845			
	55.22	27.98	0.30	10.15	5.56	0.58	99.80	62.32	869			
	53.92	27.18	0.46	9.58	5.40	0.52	97.06	61.80	880			
	54.82	27.96	0.34	10.47	5.38	0.39	99.36	64.47	893			
	55.79	27.66	0.34	9.61	5.65	0.44	99.49	61.23	905			
	55.84	27.98	0.37	10.10	5.54	0.47	100.29	62.70	917			
435.20-435.25 Host Plag2	57.02	26.77	0.27	8.59	5.90	0.49	99.03	57.34	0	818.2	196.51	4.2
	55.81	28.17	0.18	10.18	5.71	0.34	100.39	62.74	17			
	56.28	27.44	0.19	9.43	5.91	0.36	99.61	60.06	36			
	56.82	27.48	0.23	9.35	5.95	0.42	100.25	59.49	55			
	56.10	27.27	0.25	9.13	5.70	0.39	98.84	59.99	73			
	57.24	26.44	0.16	8.41	6.38	0.49	99.11	55.08	91			
	58.12	26.53	0.21	7.70	6.40	0.54	99.49	52.63	109			
	56.74	27.07	0.01	8.89	6.27	0.36	99.34	57.27	128			
	56.47	27.46	0.22	8.99	6.07	0.39	99.59	58.18	146	831.4	204.14	4.1
	57.13	27.04	0.33	8.66	6.38	0.41	99.94	56.04	164			
	57.64	26.87	0.20	8.61	6.28	0.42	100.02	56.21	183			
	56.77	26.75	0.17	8.73	6.35	0.44	99.21	56.24	201			
	57.33	26.74	0.15	8.42	6.17	0.48	99.29	55.88	219			
	57.79	26.00	0.26	8.41	6.39	0.44	99.29	55.15	237			
	55.83	27.92	0.37	9.78	5.71	0.33	99.93	61.81	256			
	57.53	26.15	0.23	7.88	6.57	0.51	98.87	52.67	274			
	58.04	26.14	0.21	8.26	6.47	0.49	99.61	54.26	293	764.0	182.19	4.2
	57.00	26.96	0.15	9.11	5.85	0.41	99.48	59.27	311			
	55.15	27.04	0.26	9.58	5.49	0.40	97.91	61.97	329			
	55.10	28.27	0.24	10.22	5.46	0.33	99.62	63.85	347			
	55.78	27.66	0.21	9.90	5.59	0.35	99.49	62.51	366			
	55.53	26.94	0.45	9.14	6.21	0.35	98.62	58.22	384			
	56.41	27.24	0.14	9.17	5.85	0.39	99.20	59.51	402			
	56.74	26.73	0.24	9.07	6.05	0.43	99.26	58.29	420			
	57.55	26.29	0.12	8.09	6.14	0.48	98.67	55.00	439			
	58.98	25.21	0.24	8.02	6.07	0.70	99.21	54.25	457	726.8	157.00	4.6
	58.29	26.55	0.20	7.77	6.60	0.44	99.84	52.48	475			
	58.92	26.26	0.24	7.65	6.70	0.53	100.30	51.39	493			
	57.49	25.09	0.13	7.75	6.40	0.73	97.59	52.09	512			
	58.06	25.87	0.17	7.87	6.40	0.53	98.90	53.16	530			
	57.03	26.19	0.25	8.41	6.18	0.54	98.60	55.57	548			
	56.81	26.75	0.36	8.49	6.03	0.47	98.90	56.63	567			
	56.95	27.13	0.14	8.81	6.13	0.38	99.54	57.52	585			

Appendix 1.1 (cont.)
Electron microprobe analyses of Unzen plagioclase (in wt.%)

Sample ID	SiO_2	Al_2O_3	FeO	CaO	Na_2O	K_2O	Total	An*	um**	Sr (ppm)	Ba (ppm)	Sr/ Ba
	57.38	26.67	0.28	8.49	6.27	0.45	99.54	55.80	603	919.8	229.62	4.0
	58.16	26.50	0.34	8.43	6.57	0.48	100.47	54.47	621			
	57.35	26.93	0.12	8.36	6.18	0.45	99.38	55.80	640			
	57.69	26.07	0.12	8.29	6.32	0.51	98.99	54.82	658			
	55.77	27.66	0.23	9.88	5.55	0.43	99.52	62.29	676			
	57.91	26.76	0.28	8.27	6.38	0.45	100.05	54.77	694			
	56.84	25.58	0.36	7.61	6.42	0.49	97.28	52.42	713			
	57.78	26.45	0.26	7.95	6.34	0.40	99.18	54.14	731			
	58.92	26.15	0.17	7.77	6.49	0.54	100.03	52.50	749	837.6	203.59	4.1
	57.76	25.79	0.36	7.54	6.60	0.52	98.58	51.43	767			
	58.75	25.44	0.21	7.38	6.80	0.55	99.13	50.11	786			
	57.89	26.38	0.19	8.21	6.50	0.49	99.66	54.02	804			
	58.68	25.82	0.22	7.70	6.85	0.56	99.82	50.95	822			
	57.36	26.40	0.11	8.01	6.52	0.48	98.87	53.37	841			
	58.31	26.30	0.14	7.92	6.66	0.42	99.75	52.82	859			
	58.71	25.82	0.36	7.58	6.64	0.52	99.63	51.44	877			
	57.72	26.56	0.23	8.17	6.40	0.49	99.56	54.26	895			
	57.04	27.23	0.23	9.04	6.03	0.42	99.99	58.36	914			
	56.83	26.94	0.34	8.79	5.98	0.47	99.35	57.69	933			
	57.85	26.32	0.33	8.10	6.56	0.53	99.68	53.36	950			
	58.52	26.20	0.24	7.53	6.67	0.48	99.64	51.31	968			
	57.62	26.49	0.26	8.08	6.60	0.50	99.54	53.24	987			
	57.80	26.28	0.14	8.44	6.25	0.43	99.34	55.82	1005			
	57.95	26.20	0.31	7.99	6.63	0.52	99.59	52.77	1023			
	56.52	26.68	0.39	10.51	3.86	0.89	98.84	68.86	1041			
	55.37	29.05	0.30	11.68	4.15	0.53	101.08	71.36	1078			
	51.75	31.44	0.48	13.32	3.34	0.23	100.57	78.83	1096			
	51.23	30.74	0.56	13.30	3.68	0.26	99.76	77.13	1115			
	47.75	31.24	0.57	14.52	2.52	0.50	97.10	82.80	1169	914.8	36.42	25.1
	47.17	32.04	0.74	15.51	2.26	0.24	97.97	86.12	1188	943.9	43.86	21.5
	46.74	33.32	0.66	16.50	2.07	0.10	99.39	88.39	1206	1001.1	48.62	20.6
	49.38	31.95	0.77	14.94	2.64	0.12	99.80	84.45	1224	1057.4	54.98	19.2
	51.41	30.28	0.72	13.40	3.77	0.19	99.77	77.19	1242			
435.20-435.25 Host Plag3	58.00	26.36	0.27	8.04	6.39	0.45	99.51	54.01	0	839.8	192.41	4.4
	58.33	25.97	0.26	7.68	6.79	0.50	99.54	51.27	10			
	58.68	25.98	0.16	7.66	6.53	0.49	99.50	52.19	21			
	57.83	26.28	0.23	7.97	6.65	0.45	99.40	52.93	31			
	58.19	26.15	0.17	8.29	6.54	0.45	99.79	54.27	40			
	57.64	26.67	0.40	8.27	6.39	0.46	99.84	54.67	51			
	57.07	26.60	0.19	8.08	6.38	0.44	98.75	54.23	60			
	56.81	26.88	0.06	8.90	6.05	0.42	99.12	57.90	71			
	56.53	27.05	0.41	9.10	5.94	0.40	99.43	58.93	81			
	56.04	27.55	0.27	9.98	5.74	0.34	99.93	62.12	91			
	55.94	27.75	0.28	9.48	5.81	0.37	99.63	60.55	102	1009.2	255.18	4.0
	58.30	26.27	0.12	7.76	6.65	0.49	99.58	52.08	121			
	58.63	25.95	0.17	7.94	6.71	0.51	99.91	52.37	132			
	58.29	26.26	0.22	7.91	6.51	0.45	99.63	53.21	142			
	57.78	25.88	0.31	8.04	6.29	0.48	98.77	54.29	152			
	58.60	26.12	0.36	7.96	6.51	0.45	100.00	53.34	162			
	58.76	25.95	0.14	7.84	6.60	0.51	99.80	52.41	182	836.1	200.66	4.2
	57.95	26.17	0.24	7.86	6.66	0.57	99.45	52.11	192			
	58.65	25.96	0.27	7.74	6.71	0.50	99.83	51.75	202			
	54.44	23.50	0.34	8.13	6.00	0.69	93.10	54.85	213			
	58.61	25.90	0.22	8.06	6.60	0.52	99.91	53.06	223			
	58.29	26.56	0.32	8.13	6.68	0.46	100.44	53.25	233			
	58.54	25.99	0.27	7.75	6.71	0.45	99.71	51.97	243			
	56.96	27.07	0.39	8.84	6.09	0.40	99.74	57.67	253	882.6	221.94	4.0

Appendix 1.1 (cont.)
Electron microprobe analyses of Unzen plagioclase (in wt.%)

Sample ID	SiO_2	Al_2O_3	FeO	CaO	Na_2O	K_2O	Total	An*	um**	Sr (ppm)	Ba (ppm)	Sr/ Ba
	56.78	26.94	0.26	9.11	6.16	0.43	99.67	58.04	263			
	56.33	27.27	0.35	9.17	6.17	0.47	99.75	58.03	273			
	56.27	27.12	0.26	8.80	6.16	0.42	99.03	57.22	283			
	57.13	27.03	0.28	8.77	6.37	0.38	99.97	56.52	294			
	58.33	26.15	0.28	7.80	6.59	0.50	99.65	52.38	303			
	57.54	26.71	0.29	8.54	6.30	0.45	99.83	55.84	314			
	57.72	26.67	0.33	8.07	6.31	0.47	99.56	54.34	324			
	58.00	26.36	0.23	8.02	6.82	0.43	99.85	52.56	334			
	56.63	26.89	0.17	8.91	6.09	0.43	99.12	57.74	344			
	54.60	28.67	0.26	10.38	5.25	0.29	99.44	65.20	355	1028.0	254.64	4.0
	55.39	28.25	0.23	9.95	5.56	0.31	99.69	62.89	364			
	57.32	27.18	0.42	8.70	6.24	0.43	100.29	56.61	374			
	56.00	27.48	0.25	9.15	5.79	0.38	99.04	59.73	384			
	56.34	27.41	0.19	9.29	5.79	0.36	99.39	60.15	394			
	56.73	27.14	0.19	9.37	6.03	0.39	99.86	59.32	405			
	56.12	27.62	0.36	9.38	5.78	0.36	99.62	60.44	415			
	56.18	27.60	0.33	9.23	6.13	0.42	99.89	58.47	425			
	56.28	27.43	0.30	9.31	5.96	0.39	99.68	59.44	445			
	56.91	27.15	0.32	9.12	6.05	0.36	99.90	58.72	456			
	58.08	26.08	0.26	7.95	6.67	0.48	99.51	52.67	465			
	58.08	26.18	0.39	8.00	6.43	0.48	99.56	53.66	476			
	57.79	26.51	0.20	8.40	6.23	0.42	99.55	55.82	486			
	57.53	26.46	0.34	8.15	6.60	0.47	99.56	53.52	496	792.5	207.98	3.8
	58.70	25.82	0.30	7.81	6.33	0.51	99.46	53.33	506			
	58.05	26.42	0.23	8.33	6.67	0.44	100.14	53.97	516			
	57.91	26.38	0.18	8.31	6.47	0.47	99.72	54.51	526			
	57.12	26.95	0.09	8.66	6.29	0.43	99.55	56.31	537			
	56.02	27.22	0.20	9.53	5.86	0.38	99.21	60.43	547			
	55.37	27.81	0.22	9.76	5.44	0.38	98.97	62.64	556			
	56.69	26.84	0.44	9.26	5.74	0.42	99.39	60.09	567			
	57.15	26.61	0.35	8.85	6.05	0.47	99.48	57.57	577	780.9	164.98	4.7
	50.23	30.92	0.54	13.58	3.41	0.16	98.85	79.20	587			
435.20-435.25 Host Plag4	58.60	26.05	0.31	7.61	6.65	0.53	99.76	51.44	0	798.7	184.94	4.3
	59.91	25.80	0.18	7.26	6.90	0.58	100.62	49.26	18			
	59.00	25.79	0.41	7.59	6.54	0.57	99.88	51.63	36			
	58.24	26.19	0.22	7.75	6.66	0.47	99.52	52.07	54			
	58.52	26.00	0.21	7.51	6.49	0.53	99.25	51.69	72			
	57.85	26.19	0.22	8.27	6.37	0.47	99.38	54.72	90			
	57.79	25.89	0.13	7.96	6.50	0.52	98.78	53.15	108			
	58.26	26.11	0.28	7.69	6.51	0.50	99.35	52.30	126	796.1	201.54	4.0
	58.73	26.01	0.23	7.51	6.68	0.49	99.66	51.16	145			
	58.70	26.04	0.36	7.63	6.87	0.58	100.18	50.60	163			
	58.60	26.22	0.18	7.91	6.53	0.49	99.93	53.00	180			
	58.40	26.22	0.21	7.87	6.84	0.52	100.06	51.68	199			
	58.22	26.37	0.22	7.97	6.27	0.46	99.52	54.18	217			
	58.94	25.61	0.41	7.85	6.76	0.48	100.04	52.06	235	754.1	199.65	3.8
	58.27	26.37	0.28	7.99	6.60	0.55	100.06	52.77	252			
	54.60	28.67	0.25	10.39	5.09	0.34	99.33	65.70	272			
	56.38	27.64	0.15	9.74	5.63	0.31	99.85	62.11	290			
	57.82	26.23	0.15	8.35	6.59	0.49	99.62	54.09	308			
	57.73	26.25	0.31	8.11	6.32	0.43	99.14	54.57	325	877.5	239.74	3.7
	58.24	26.05	0.21	7.99	6.49	0.50	99.49	53.32	344			
	58.30	25.52	0.17	7.73	6.39	0.62	98.73	52.45	362			
	58.45	26.27	0.08	8.18	6.65	0.55	100.18	53.19	380			
	58.33	25.74	0.22	7.78	6.48	0.53	99.08	52.60	398			
	58.33	26.00	0.29	7.87	6.77	0.54	99.80	51.83	416			
	59.02	25.87	0.27	7.40	6.83	0.53	99.91	50.14	435			

Appendix 1.1 (cont.)
Electron microprobe analyses of Unzen plagioclase (in wt.%)

Sample ID	SiO_2	Al_2O_3	FeO	CaO	Na_2O	K_2O	Total	An*	um**	Sr (ppm)	Ba (ppm)	Sr/ Ba
	55.54	27.67	0.20	9.47	5.66	0.37	98.92	61.10	453			
	58.51	26.33	0.22	8.07	6.19	0.50	99.82	54.64	470			
	59.26	25.44	0.21	7.41	6.88	0.51	99.71	50.05	488			
	56.21	27.46	0.22	9.34	5.63	0.36	99.23	60.89	507			
	56.67	27.07	0.25	8.89	5.93	0.49	99.30	58.04	525	820.5	193.87	4.2
	56.97	27.29	0.11	8.81	5.93	0.33	99.44	58.46	542			
	56.09	27.94	0.36	9.46	6.00	0.38	100.24	59.72	560			
	56.86	27.52	0.17	9.29	5.99	0.35	100.17	59.47	579			
	57.65	26.77	0.34	8.25	6.36	0.45	99.82	54.78	597			
	57.78	26.79	0.21	8.30	6.20	0.46	99.74	55.46	615			
	57.61	26.13	0.17	8.13	6.45	0.45	98.95	54.08	633			
	58.18	26.26	0.19	8.31	6.31	0.43	99.68	55.24	652			
	56.47	27.65	0.18	9.48	5.68	0.43	99.90	60.77	670			
	55.54	27.80	0.27	9.94	5.55	0.29	99.39	63.00	687			
	56.89	26.65	0.12	8.75	5.98	0.43	98.82	57.72	705			
	58.34	26.15	0.20	7.99	6.46	0.42	99.57	53.74	724	888.6	206.38	4.3
	58.41	26.56	0.27	7.94	6.53	0.43	100.14	53.30	742			
	57.93	26.08	0.22	8.20	6.56	0.47	99.46	53.84	760			
	57.96	26.47	0.28	8.05	6.56	0.50	99.81	53.27	778			
	58.19	26.20	0.19	7.97	6.52	0.48	99.55	53.23	796			
	59.26	26.10	0.16	7.74	6.78	0.53	100.57	51.40	815	669.5	142.26	4.7
	58.78	26.00	0.26	7.74	6.57	0.50	99.85	52.26	832			
	57.91	26.51	0.15	8.03	6.51	0.44	99.56	53.60	850			
	57.02	26.88	0.32	8.61	6.03	0.49	99.34	56.93	868			
	57.84	26.64	0.37	8.34	6.27	0.48	99.92	55.29	887			
	55.61	27.90	0.37	10.10	5.56	0.34	99.88	63.12	905			
	56.01	27.96	0.31	9.45	5.69	0.39	99.82	60.82	923	1342.8	285.72	4.7
	57.79	26.69	0.21	8.21	6.44	0.41	99.75	54.52	941			
	57.51	27.21	0.08	8.69	6.02	0.52	100.03	57.08	960			
	54.22	26.37	0.37	9.14	5.63	0.77	96.50	58.78	977			
	52.54	29.55	0.45	12.09	3.72	0.71	99.06	73.17	995			
	51.19	30.80	0.94	14.01	2.71	0.47	100.13	81.49	1013			
	48.44	32.26	0.61	15.25	2.71	0.15	99.42	84.21	1032			
	50.57	30.84	0.43	13.68	3.55	0.19	99.26	78.54	1049			
435.20-435.25 Host Plag5	56.90	27.12	0.21	8.85	6.18	0.42	99.68	57.28	0	646.4	96.84	6.7
	55.40	27.92	0.28	9.58	5.49	0.31	98.98	62.29	12			
	56.16	27.54	0.17	9.50	5.78	0.35	99.50	60.77	25			
	55.92	27.31	0.24	9.17	6.01	0.34	98.98	59.07	37			
	56.75	27.13	0.22	9.00	6.22	0.40	99.72	57.63	48			
	56.77	27.25	0.19	8.80	6.21	0.38	99.60	57.20	60	655.2	108.69	6.0
	57.44	26.83	0.19	8.38	6.28	0.41	99.53	55.60	72			
	57.87	26.56	0.25	8.32	6.69	0.54	100.22	53.49	85			
	57.75	26.69	0.30	8.28	6.45	0.44	99.92	54.56	97			
	57.80	26.76	0.23	8.45	6.68	0.54	100.46	53.93	109			
	57.51	26.91	0.22	8.88	6.28	0.40	100.21	57.06	121			
	57.50	26.72	0.17	8.72	6.21	0.42	99.73	56.78	133			
	57.35	26.48	0.22	8.18	6.60	0.45	99.27	53.70	145	800.7	174.10	4.6
	57.38	26.49	0.29	8.36	6.29	0.46	99.27	55.31	157			
	57.36	27.09	0.16	8.63	6.21	0.49	99.95	56.28	169			
	56.75	27.15	0.15	9.12	5.86	0.42	99.44	59.26	181			
	56.72	27.31	0.28	8.95	6.23	0.42	99.91	57.33	193			
	56.50	26.95	0.07	9.16	6.05	0.40	99.13	58.68	205			
	57.04	26.66	0.23	8.30	6.30	0.43	98.96	55.22	218			
	56.60	26.93	0.15	8.40	6.28	0.45	98.81	55.54	229			
	57.66	26.86	0.31	8.44	6.44	0.43	100.15	55.12	241			
	57.58	26.57	0.17	8.67	6.29	0.46	99.74	56.20	253			
	58.14	26.69	0.17	8.72	6.28	0.47	100.47	56.37	266			

Appendix 1.1 (cont.)
Electron microprobe analyses of Unzen plagioclase (in wt.%)

Sample ID	SiO_2	Al_2O_3	FeO	CaO	Na_2O	K_2O	Total	An*	um**	Sr (ppm)	Ba (ppm)	Sr/ Ba
	57.57	26.71	0.38	8.28	6.57	0.40	99.91	54.26	278			
	58.02	26.22	0.16	8.13	6.48	0.45	99.46	54.00	290			
	57.12	25.43	0.23	10.14	5.94	0.44	99.30	61.38	302	745.4	161.38	4.6
	52.89	2.99	0.06	1.13	0.95	0.46	58.49	44.44	314			
	57.12	26.23	0.15	8.18	6.20	0.47	98.35	55.05	326			
	58.71	26.29	0.31	7.82	6.83	0.49	100.44	51.63	338			
	58.31	26.17	0.22	7.97	6.28	0.48	99.43	54.10	350			
	57.11	26.70	0.39	9.03	5.97	0.42	99.61	58.58	362			
	57.39	26.92	0.27	8.53	6.21	0.42	99.74	56.25	375			
	55.62	27.81	0.34	9.72	5.68	0.35	99.51	61.73	387			
	55.69	28.28	0.30	9.82	5.61	0.39	100.09	62.06	398			
	57.45	26.51	0.19	8.34	6.16	0.52	99.17	55.51	410			
	55.54	26.15	0.33	8.44	5.94	0.39	96.79	57.15	422			
	52.54	25.71	0.65	6.87	5.06	0.42	91.26	55.60	447	662.4	153.38	4.3
	56.69	27.62	0.13	9.41	5.68	0.58	100.12	60.07	459			
	52.65	30.33	0.55	12.73	4.01	0.36	100.64	74.44	471			
	55.74	27.70	0.35	9.64	5.67	0.48	99.57	61.06	494			
	56.11	27.55	0.29	9.24	5.97	0.32	99.47	59.51	507			
	57.36	27.59	0.74	11.47	3.00	1.30	101.47	72.75	531	1093.2	244.85	4.5
	53.67	29.26	0.39	13.11	2.81	0.76	99.99	78.63	543			
	59.30	23.55	0.55	8.91	2.79	1.60	96.70	66.99	556			
	54.39	21.73	0.65	9.02	2.30	1.59	89.68	69.86	568	1197.4	305.99	3.9
	51.96	27.93	0.39	12.01	2.35	0.88	95.52	78.80	579			
	47.07	32.12	0.87	15.30	2.12	0.23	97.72	86.66	591	892.4	37.94	23.5
	49.20	31.73	0.68	14.66	2.72	0.12	99.11	83.79	604	874.9	27.80	31.5
	49.20	31.73	0.68	14.66	2.72	0.12	99.11	83.79	604	921.9	37.13	24.8
	52.50	29.93	0.63	12.01	4.29	0.33	99.68	72.24	616			
437.15-437.20 Host Plag1	57.74	26.44	0.22	8.25	6.42	0.51	99.58	54.35	0	886.7	213.92	4.1
	56.73	26.73	0.21	8.90	6.04	0.43	99.04	57.89	25			
	57.23	26.87	0.23	8.86	6.20	0.43	99.82	57.20	50			
	58.93	25.86	0.05	7.45	6.78	0.50	99.57	50.57	100			
	58.84	26.05	0.26	7.92	6.76	0.52	100.35	52.09	125			
	59.05	25.79	0.14	7.57	6.72	0.54	99.82	51.04	151			
	35.72	17.75	0.33	5.61	4.27	0.43	64.10	54.38	175	559.5	156.60	3.6
	55.82	27.76	0.18	9.84	5.84	0.41	99.84	61.15	201			
	56.46	27.43	0.26	9.15	6.11	0.45	99.87	58.23	226			
	56.37	27.40	0.25	9.40	5.99	0.39	99.81	59.53	251			
	57.40	27.24	0.32	8.91	6.13	0.47	100.46	57.44	276			
	57.25	26.94	0.21	8.86	6.07	0.41	99.75	57.76	301			
	56.62	27.55	0.33	9.10	6.37	0.45	100.41	57.16	326			
	49.93	25.85	0.12	8.37	5.51	0.33	90.10	58.90	352			
	55.25	27.85	0.19	9.72	5.59	0.37	98.96	61.98	376			
	51.56	27.18	0.25	9.74	5.21	0.30	94.24	63.87	402			
	55.48	28.05	0.18	9.80	5.70	0.42	99.62	61.58	426			
	57.15	27.01	0.21	8.93	6.13	0.46	99.88	57.55	452			
	57.78	26.58	0.22	8.36	6.40	0.49	99.83	54.82	477	857.5	194.55	4.4
	57.00	27.18	0.25	9.18	6.14	0.53	100.27	57.92	502			
	57.28	27.30	0.26	8.84	6.16	0.40	100.23	57.40	527			
	56.44	26.97	0.17	8.80	6.10	0.43	98.92	57.40	553			
	56.72	26.86	0.26	8.97	6.24	0.42	99.49	57.37	577			
	56.86	27.08	0.23	8.99	5.93	0.40	99.50	58.67	602			
	56.22	27.33	0.27	9.47	5.98	0.38	99.64	59.82	627			
	56.26	27.21	0.21	9.13	5.98	0.45	99.25	58.68	652			
	56.79	27.43	0.18	9.26	5.91	0.45	100.01	59.31	678			
	56.88	27.24	0.22	8.99	6.13	0.45	99.90	57.75	702			
	58.39	26.33	0.07	7.83	6.61	0.50	99.72	52.41	728			
	57.96	27.25	0.29	8.81	6.22	0.45	100.98	56.92	752			

Appendix 1.1 (cont.)
Electron microprobe analyses of Unzen plagioclase (in wt.%)

Sample ID	SiO_2	Al_2O_3	FeO	CaO	Na_2O	K_2O	Total	An*	um**	Sr (ppm)	Ba (ppm)	Sr/ Ba
	56.35	27.91	0.13	9.64	5.74	0.41	100.17	61.06	778			
	56.20	27.85	0.18	9.84	5.78	0.39	100.24	61.47	803			
	56.84	26.86	0.27	9.03	6.12	0.48	99.59	57.80	828			
	56.69	26.74	0.21	8.81	6.10	0.50	99.05	57.17	853			
	52.25	27.36	0.41	10.53	4.91	0.40	95.86	66.47	879			
	57.78	26.60	0.14	8.18	6.37	0.45	99.50	54.56	903	776.4	181.62	4.3
	56.78	27.25	0.27	8.84	5.98	0.41	99.53	58.03	929			
	56.25	27.77	0.36	9.37	5.81	0.34	99.91	60.38	979			
	46.18	25.06	0.18	7.23	5.32	0.31	84.28	56.16	1004			
	46.72	25.07	0.17	7.86	4.92	0.24	84.97	60.34	1029			
	50.67	24.45	0.13	8.54	5.39	0.30	89.49	59.98	1054			
	50.21	25.87	0.35	8.32	5.54	0.33	90.62	58.64	1078			
	44.02	23.38	0.05	6.16	5.40	0.36	79.36	51.66	1104			
	56.20	27.33	0.26	9.13	5.94	0.43	99.29	58.90	1129	894.5	137.54	6.5
	52.28	25.97	0.04	6.23	6.13	0.52	91.17	48.35	1154			
	51.74	24.55	0.07	7.84	5.80	0.31	90.32	56.19	1179			
	56.18	26.53	0.30	8.35	6.06	0.41	97.83	56.35	1205			
	49.94	24.89	0.17	7.49	5.72	0.28	88.49	55.52	1229			
	58.06	26.40	0.26	8.29	6.48	0.49	99.97	54.33	1255			
	57.37	26.79	0.28	8.51	6.36	0.46	99.78	55.48	1279			
437.15-437.20 Host Plag2	56.91	26.55	0.14	8.46	6.27	0.48	98.81	55.61	0			
	57.74	26.38	0.25	8.53	6.53	0.50	99.94	54.82	20			
	57.74	26.54	0.21	8.36	6.48	0.54	99.87	54.38	41			
	57.89	26.51	0.27	8.15	6.66	0.49	99.98	53.27	61			
	59.03	26.03	0.26	7.52	6.97	0.57	100.38	49.94	82			
	58.48	26.08	0.18	8.22	6.51	0.51	99.98	53.91	102			
	47.23	22.77	0.37	7.56	4.97	0.41	83.31	58.40	122			
	57.59	26.66	0.25	8.36	6.48	0.51	99.85	54.48	142			
	57.73	26.36	0.15	8.26	6.53	0.45	99.48	54.24	163			
	58.10	25.98	0.13	8.10	6.62	0.51	99.44	53.16	183			
	51.99	25.66	0.21	8.94	5.57	0.39	92.76	59.97	204			
	56.12	27.49	0.25	9.29	6.11	0.45	99.72	58.59	224			
	56.82	27.29	0.21	8.97	6.07	0.47	99.83	57.83	245			
	58.60	25.84	0.24	7.91	6.69	0.58	99.85	52.09	264			
	58.92	25.89	0.22	7.76	6.79	0.57	100.15	51.32	285			
	55.15	27.98	0.37	10.08	5.55	0.50	99.62	62.52	305			
	55.05	28.55	0.40	10.42	5.30	0.37	100.09	64.79	325			
	57.56	26.38	0.24	8.11	6.49	0.56	99.35	53.49	346			
	57.99	26.20	0.19	8.15	6.63	0.52	99.68	53.28	366			
	54.50	28.41	0.22	10.29	5.52	0.32	99.27	63.81	387			
	56.11	27.47	0.32	9.54	5.83	0.36	99.64	60.65	406			
	57.93	26.33	0.05	8.29	6.51	0.49	99.60	54.20	428			
	58.93	25.83	0.26	7.58	6.82	0.56	99.98	50.66	447			
	53.08	29.96	0.24	11.96	4.57	0.27	100.08	71.21	468			
	56.18	27.98	0.29	9.58	5.55	0.37	99.96	61.82	488			
	56.89	26.49	0.07	8.63	6.40	0.42	98.90	55.84	509			
	57.50	26.90	0.15	8.47	6.47	0.49	99.97	54.91	529			
	55.68	27.82	0.37	9.57	5.74	0.35	99.53	61.12	550			
	57.45	26.29	0.27	8.07	6.29	0.55	98.92	54.12	570			
	58.00	26.35	0.26	8.15	6.60	0.58	99.94	53.15	590			
	56.51	27.25	0.13	9.06	6.04	0.45	99.44	58.27	611			
	58.45	26.11	0.24	8.08	6.56	0.54	99.99	53.21	631			
	57.65	26.45	0.16	8.10	6.48	0.56	99.40	53.49	651			
	57.94	26.73	0.27	8.15	6.45	0.53	100.06	53.90	671			
	58.59	26.36	0.31	7.84	6.78	0.62	100.50	51.46	692			
	57.58	26.03	0.22	8.08	6.53	0.52	98.95	53.43	712			
	59.62	25.44	0.16	7.03	6.86	0.61	99.73	48.47	733			

Appendix 1.1 (cont.)
Electron microprobe analyses of Unzen plagioclase (in wt.%)

Sample ID	SiO_2	Al_2O_3	FeO	CaO	Na_2O	K_2O	Total	An*	um**	Sr (ppm)	Ba (ppm)	Sr/ Ba
	59.46	25.80	0.21	7.61	6.89	0.60	100.56	50.42	753			
	59.66	25.43	0.17	7.04	6.93	0.61	99.85	48.29	774			
	57.76	26.63	0.22	8.15	6.38	0.52	99.66	54.14	793			
	56.67	27.55	0.22	9.31	5.85	0.46	100.06	59.59	814			
	54.96	24.40	0.36	7.40	5.06	0.96	93.15	55.15	834			
	56.19	27.33	0.21	9.39	5.99	0.40	99.52	59.50	855			
437.15-437.20 Host Plag3	57.90	26.61	0.21	8.39	6.47	0.50	100.09	54.63	0	888.6	212.33	4.2
	58.26	26.40	0.18	8.26	6.31	0.46	99.87	54.98	21			
	58.46	26.84	0.32	8.51	6.35	0.44	100.93	55.59	40			
	57.69	27.72	0.26	9.38	5.86	0.40	101.31	60.00	61			
	56.82	27.47	0.21	8.81	6.05	0.48	99.83	57.46	81			
	58.64	25.87	0.18	7.63	6.55	0.61	99.48	51.59	102			
	58.91	25.91	0.19	7.34	6.78	0.58	99.72	49.92	122			
	57.73	26.64	0.19	8.43	6.28	0.49	99.76	55.44	141			
	57.44	26.97	0.20	8.51	6.45	0.44	100.01	55.26	162			
	58.02	26.40	0.25	8.30	6.30	0.50	99.75	55.00	182			
	56.88	27.06	0.20	8.71	6.06	0.46	99.37	57.19	203			
	55.51	25.42	0.16	8.56	7.38	0.50	97.54	52.07	223			
	56.25	26.74	0.36	8.53	5.94	0.52	98.34	56.88	243			
	56.76	27.34	0.22	9.31	5.93	0.42	99.99	59.43	263			
	57.36	26.88	0.16	8.67	6.23	0.47	99.76	56.39	283			
	57.85	26.98	0.17	8.42	6.33	0.50	100.26	55.20	303			
	55.34	28.73	0.18	10.69	5.30	0.37	100.60	65.35	324			
	56.57	27.45	0.27	9.51	5.73	0.41	99.93	60.78	344			
	57.86	26.84	0.24	8.55	6.47	0.53	100.48	54.97	365			
	57.65	26.46	0.29	8.52	6.30	0.41	99.64	55.94	384			
	57.22	26.77	0.15	8.72	6.00	0.42	99.27	57.57	405	850.8	229.62	3.7
	58.56	25.99	0.26	7.85	6.68	0.62	99.96	51.79	426			
	58.35	26.60	0.27	8.38	6.40	0.48	100.47	54.94	445			
	58.09	26.61	0.17	8.15	6.51	0.56	100.07	53.53	465			
	58.27	26.14	0.25	7.94	6.64	0.58	99.82	52.36	485			
	57.32	27.01	0.28	8.74	6.29	0.46	100.10	56.42	506			
	57.63	26.83	0.30	8.48	6.46	0.49	100.20	54.97	526			
	58.17	26.61	0.25	7.95	6.62	0.53	100.14	52.64	546			
	58.51	26.02	0.15	7.82	6.85	0.57	99.93	51.31	567			
	57.67	26.82	0.28	8.50	6.24	0.48	100.00	55.86	587			
	57.75	26.68	0.22	8.69	6.27	0.48	100.10	56.25	607			
	57.50	26.48	0.21	8.39	6.49	0.53	99.60	54.45	627			
	57.57	26.61	0.27	8.08	6.54	0.48	99.55	53.54	647	801.8	190.49	4.2
	58.00	26.18	0.20	8.44	6.45	0.46	99.74	54.98	668			
	58.87	25.97	0.18	7.68	6.66	0.57	99.93	51.50	688			
	58.07	27.21	0.27	8.76	6.00	0.46	100.77	57.55	708			
	57.84	26.42	0.27	8.55	6.34	0.42	99.84	55.86	728			
	58.17	26.28	0.21	7.98	6.49	0.52	99.65	53.24	749			
	58.87	25.89	0.25	7.94	6.72	0.55	100.22	52.17	769			
	58.88	26.08	0.19	7.71	6.81	0.57	100.25	51.09	789			
	58.49	26.05	0.33	7.94	6.63	0.61	100.05	52.30	809			
	58.97	25.75	0.37	7.69	6.63	0.53	99.93	51.78	829			
	57.90	26.40	0.11	8.19	6.58	0.50	99.69	53.62	850			
	56.25	27.53	0.23	9.42	5.77	0.37	99.58	60.52	870			
	58.79	26.64	0.08	8.33	6.59	0.43	100.87	54.28	890			
	58.13	26.44	0.26	8.14	6.53	0.48	99.98	53.71	911	767.4	179.27	4.3
	58.18	26.42	0.13	8.51	6.29	0.51	100.06	55.57	931			
	58.91	26.22	0.29	7.85	6.57	0.55	100.39	52.47	951			
	58.07	26.78	0.26	8.46	6.31	0.49	100.38	55.42	971			
	57.85	27.11	0.24	8.66	6.28	0.40	100.55	56.44	991			
	54.02	25.05	0.17	7.87	5.63	0.50	93.24	56.19	1012			

Appendix 1.1 (cont.)
Electron microprobe analyses of Unzen plagioclase (in wt.%)

Sample ID	SiO_2	Al_2O_3	FeO	CaO	Na_2O	K_2O	Total	An*	um**	Sr (ppm)	Ba (ppm)	Sr/ Ba
	57.76	26.26	0.38	8.82	5.74	0.69	99.65	57.81	1032	871.3	207.59	4.2
	58.11	26.12	1.52	10.31	3.48	1.02	100.56	69.64	1052			
437.15-437.20 Host Plag4	57.15	27.23	0.17	9.01	5.93	0.44	99.92	58.58	0	817.8	189.35	4.3
	57.73	27.20	0.21	8.45	6.33	0.44	100.36	55.49	20			
	57.73	26.53	0.21	8.26	6.50	0.49	99.71	54.18	40			
	59.10	25.94	0.25	7.63	6.72	0.55	100.20	51.21	60			
	57.23	24.77	0.44	7.65	6.33	0.83	97.26	51.65	80			
	57.57	27.26	0.04	8.66	6.27	0.44	100.23	56.35	100			
	58.72	25.99	0.16	7.97	6.56	0.46	99.85	53.16	120			
	55.21	24.45	0.23	7.62	6.15	0.66	94.33	52.77	140			
	58.84	25.96	0.23	7.95	6.54	0.53	100.05	52.93	160			
	58.07	26.66	0.13	8.43	6.32	0.48	100.09	55.35	180			
	57.41	27.24	0.21	8.93	6.14	0.39	100.32	57.80	201			
	57.93	26.83	0.24	8.34	6.53	0.49	100.36	54.33	220			
	57.68	26.75	0.18	8.56	6.56	0.46	100.19	54.96	241	800.6	203.89	3.9
	58.10	26.64	0.34	8.32	6.63	0.49	100.53	53.87	261			
	57.10	26.61	0.17	8.82	6.19	0.46	99.35	57.04	280			
	57.27	27.08	0.35	8.63	6.46	0.44	100.22	55.54	300			
	57.56	27.22	0.25	8.63	6.20	0.57	100.43	56.05	321			
	58.39	26.80	0.17	8.23	6.39	0.47	100.44	54.55	341			
	56.72	26.95	0.23	8.50	6.33	0.44	99.18	55.65	360			
	57.37	26.57	0.24	8.13	6.51	0.48	99.31	53.75	381			
	59.00	26.24	0.10	7.84	6.54	0.61	100.33	52.29	401			
	55.92	25.15	0.28	7.58	6.45	0.61	96.01	51.77	420			
	58.42	25.96	0.21	8.06	6.55	0.53	99.73	53.25	440			
	58.77	26.10	0.19	8.10	6.65	0.49	100.29	53.16	461			
	57.96	26.44	0.11	8.12	6.53	0.45	99.61	53.80	481			
	58.44	26.28	0.30	8.11	6.59	0.55	100.28	53.16	501			
	58.53	26.18	0.10	7.51	6.78	0.58	99.67	50.52	521	782.2	218.19	3.6
	58.20	26.40	0.22	7.87	6.55	0.50	99.74	52.72	541			
	57.77	27.08	0.34	8.64	6.32	0.52	100.66	55.82	561			
	57.12	26.54	0.17	8.42	6.46	0.43	99.13	54.98	581			
	58.37	26.85	0.22	8.28	6.44	0.45	100.61	54.59	601			
	58.62	25.92	0.26	7.87	6.77	0.52	99.96	51.90	621			
	59.77	24.93	0.28	6.66	7.31	0.63	99.58	45.60	641			
	58.87	25.87	0.22	7.43	6.72	0.57	99.68	50.49	661			
	58.79	26.12	0.22	7.80	6.66	0.57	100.15	51.89	681			
	57.78	26.26	0.21	8.22	6.61	0.56	99.64	53.39	701			
	56.36	27.70	0.20	9.29	6.00	0.38	99.93	59.30	722			
	57.93	26.85	0.13	8.60	6.42	0.44	100.37	55.65	741			
	58.36	26.56	0.30	8.11	6.67	0.51	100.52	53.02	761			
	58.25	26.34	0.26	8.19	6.55	0.50	100.09	53.74	781			
	58.78	26.00	0.26	7.61	6.73	0.55	99.94	51.10	801	825.7	208.76	4.0
	59.18	26.11	0.22	7.77	6.49	0.53	100.31	52.54	821			
	57.38	27.10	0.30	8.87	6.28	0.44	100.37	56.89	841			
	57.34	27.43	0.27	8.96	6.21	0.45	100.67	57.37	862			
	58.24	27.07	0.25	8.42	6.17	0.50	100.66	55.79	882			
	54.91	25.24	0.16	7.92	6.14	0.43	94.80	54.69	901			
	58.76	26.55	0.16	8.05	6.50	0.52	100.53	53.41	921			
	58.61	26.15	0.34	7.53	6.54	0.59	99.76	51.38	942			
	55.80	27.56	0.08	9.66	5.75	0.38	99.24	61.16	961			
	55.82	28.13	0.09	9.83	5.79	0.41	100.08	61.34	981			
	56.86	27.25	0.33	9.25	6.10	0.44	100.24	58.59	1002			
	56.44	27.81	0.21	9.53	5.76	0.37	100.12	60.87	1022			
	56.56	27.61	0.12	9.50	5.86	0.39	100.05	60.31	1041			
	58.93	26.46	0.27	8.15	6.67	0.55	101.02	53.05	1062	718.1	184.22	3.9
	55.69	28.08	0.27	9.83	5.72	0.40	99.99	61.62	1101			

Appendix 1.1 (cont.)
Electron microprobe analyses of Unzen plagioclase (in wt.%)

Sample ID	SiO_2	Al_2O_3	FeO	CaO	Na_2O	K_2O	Total	An*	um**	Sr (ppm)	Ba (ppm)	Sr/ Ba
	56.82	27.23	0.31	8.72	6.22	0.41	99.70	56.83	1122			
	56.42	27.54	0.28	9.20	5.91	0.47	99.81	59.05	1142			
	57.13	27.00	0.16	8.74	6.19	0.46	99.69	56.79	1162			
	55.89	27.78	0.18	9.68	5.77	0.45	99.75	60.89	1182			
	57.74	26.71	0.14	8.49	6.55	0.49	100.12	54.70	1202			
	56.16	27.13	0.28	9.56	6.01	0.41	99.54	59.84	1222			
	57.23	27.10	0.16	8.73	6.17	0.41	99.80	57.05	1242			
	53.09	25.31	0.78	7.92	5.31	0.45	92.86	57.89	1262			
	56.68	27.59	0.24	9.17	6.10	0.43	100.22	58.41	1282	953.1	240.32	4.0
	55.27	28.48	0.10	10.40	5.36	0.35	99.96	64.57	1302	900.6	177.43	5.1
546.40-546.45 E1 M-Plag1	48.02	32.51	0.57	15.48	2.39	0.11	99.08	86.10	0			
	46.87	30.08	1.25	13.89	2.67	0.21	94.97	82.85	8			
	49.02	32.65	0.53	15.24	2.84	0.09	100.37	83.90	18			
	49.05	32.42	0.45	15.01	2.68	0.12	99.73	84.26	26			
	49.27	31.93	0.57	14.72	3.00	0.15	99.63	82.38	35			
	50.31	31.99	0.44	14.50	3.39	0.14	100.77	80.43	44			
	57.11	26.53	1.03	10.36	3.38	0.86	99.27	70.96	53			
	53.18	29.67	0.58	11.66	4.81	0.44	100.33	68.98	62			
	62.40	22.90	0.97	7.87	3.54	1.54	99.22	60.77	70			
546.40-546.45 E1 M-Plag2	47.90	32.81	0.70	15.69	2.40	0.12	99.61	86.15	0			
	48.05	32.83	0.54	15.38	2.50	0.08	99.37	85.64	6			
	48.81	32.89	0.55	15.49	2.69	0.12	100.55	84.63	13			
	48.55	32.72	0.55	15.08	2.78	0.12	99.80	83.87	19			
	49.70	32.28	0.59	14.86	3.08	0.12	100.64	82.28	25			
	49.97	32.10	0.54	14.72	2.94	0.13	100.40	82.73	31			
	49.43	32.16	0.52	14.49	3.10	0.23	99.92	81.30	38			
	52.54	30.21	0.45	12.46	4.27	0.32	100.25	73.07	44			
	61.80	20.42	0.57	5.24	6.32	1.05	95.40	41.56	50			
546.40-546.45 E1 M-Plag3	48.22	31.47	0.83	14.82	2.67	0.21	98.21	83.73	0			
	48.34	32.45	0.79	15.28	2.67	0.15	99.68	84.42	8			
	48.41	31.97	0.62	15.05	2.80	0.09	98.93	83.88	17			
	49.58	32.34	0.70	15.36	2.68	0.09	100.75	84.75	25			
	48.53	32.19	0.60	14.96	2.76	0.17	99.21	83.60	33			
	49.10	31.86	0.73	15.54	2.85	0.20	100.27	83.59	40			
	49.37	32.29	0.50	15.06	2.81	0.12	100.14	83.73	50			
	48.85	32.39	0.57	14.85	2.83	0.13	99.62	83.38	57			
	48.38	32.18	0.45	15.07	2.80	0.14	99.01	83.69	65			
	49.71	31.57	0.63	14.57	3.31	0.13	99.93	80.86	73			
	49.90	31.01	0.44	13.71	3.45	0.27	98.78	78.65	82			
	56.23	27.05	0.58	9.10	5.91	0.55	99.43	58.48	90			
546.40-546.45 E M-Plag4	48.57	32.49	0.52	15.36	2.70	0.13	99.77	84.46	0			
	48.64	32.26	0.68	14.90	3.00	0.13	99.61	82.62	8			
	49.40	32.14	0.82	14.83	2.87	0.10	100.15	83.34	16			
	49.34	32.24	0.66	14.98	2.97	0.13	100.33	82.82	25			
	49.40	32.37	0.80	14.82	3.03	0.15	100.57	82.32	33			
	48.87	32.61	0.57	14.95	2.72	0.15	99.87	83.86	42			
	54.47	28.77	0.55	11.14	4.81	0.45	100.20	67.93	50			
546.40-546.45 E2 M-Plag1	49.16	32.38	0.53	15.19	2.89	0.13	100.27	83.43	0			
	49.19	32.44	0.64	14.92	2.86	0.13	100.19	83.29	9			
	49.56	32.33	0.44	15.18	2.93	0.16	100.61	83.08	17			
	49.39	32.37	0.72	14.93	2.82	0.14	100.37	83.47	26			
	49.74	32.30	0.69	14.64	3.15	0.11	100.62	81.81	35			
	48.97	32.37	0.38	15.17	2.81	0.09	99.78	83.97	43			

Appendix 1.1 (cont.)
Electron microprobe analyses of Unzen plagioclase (in wt.%)

Sample ID	SiO_2	Al_2O_3	FeO	CaO	Na_2O	K_2O	Total	An*	um**	Sr (ppm)	Ba (ppm)	Sr/ Ba
	53.73	29.28	0.57	11.28	5.01	0.53	100.40	67.07	52			
	61.95	23.61	0.49	5.28	7.66	1.26	100.26	37.17	61			
546.40-546.45 E2 M-Plag2	48.22	31.86	0.56	15.34	2.83	0.12	98.94	83.83	0			
	48.19	32.48	0.46	15.22	2.76	0.10	99.22	84.16	8			
	48.37	32.28	0.67	15.05	2.77	0.14	99.29	83.78	16			
	48.99	32.14	0.66	15.51	2.78	0.09	100.17	84.39	25			
	48.81	32.50	0.54	15.36	2.79	0.16	100.16	83.89	33			
	44.96	28.24	0.93	12.99	2.41	0.19	89.73	83.29	41			
	44.70	30.26	0.54	13.05	2.67	0.13	91.35	82.31	50			
	42.66	29.51	0.52	12.34	3.08	0.09	88.20	79.55	58			
	48.22	30.80	0.49	13.47	3.07	0.13	96.18	80.82	66			
	49.51	31.53	0.57	14.22	3.17	0.19	99.20	80.89	75			
	49.70	32.18	0.61	14.88	3.12	0.15	100.65	81.96	82			
	50.80	30.98	0.55	13.15	3.88	0.20	99.57	76.31	90			
	51.46	30.05	0.71	12.60	4.09	0.29	99.21	74.19	100			
	54.84	28.36	0.67	10.74	5.37	0.54	100.51	64.52	108			
546.40-546.45 E2 M-Plag3	48.88	32.45	0.65	15.13	2.73	0.13	99.97	84.11	0			
	48.49	31.66	1.14	14.54	2.70	0.15	98.69	83.58	5			
	48.85	32.75	0.74	15.27	2.72	0.16	100.49	84.11	11			
	49.07	32.46	0.62	15.35	2.78	0.11	100.40	84.16	17			
	49.38	32.27	0.58	15.14	3.03	0.14	100.55	82.69	22			
	49.60	32.15	0.77	14.85	2.86	0.10	100.34	83.39	28			
	49.46	31.96	0.58	14.61	3.13	0.20	99.93	81.43	33			
	50.96	31.35	0.55	13.76	3.73	0.20	100.56	77.75	39			
	56.69	26.79	0.50	8.65	6.14	0.75	99.51	55.66	44			
	93.68	2.30	0.00	0.29	0.72	0.18	97.17	24.35	50			
546.40-546.45 E2 M-Plag4	49.10	31.61	0.49	14.73	3.02	0.16	99.12	82.22	0			
	48.45	32.08	0.66	14.88	2.83	0.10	98.99	83.53	5			
	49.57	32.36	0.63	14.98	2.84	0.14	100.53	83.38	11			
	49.04	31.82	0.58	14.90	3.00	0.11	99.46	82.69	16			
	49.00	32.18	0.62	14.87	2.92	0.13	99.73	82.96	22			
	48.89	31.82	0.73	15.14	2.93	0.12	99.63	83.24	27			
	49.16	32.40	0.70	14.93	2.96	0.10	100.25	82.97	32			
	48.63	31.65	0.57	14.82	2.92	0.13	98.73	82.94	37			
	48.68	32.03	0.59	14.81	3.00	0.12	99.23	82.59	43			
	32.32	5.82	30.53	5.78	0.40	0.15	74.99	91.37	48			
546.45-546.50 Host Plag1	57.87	26.50	0.18	7.97	6.73	0.45	99.70	52.62	0			
	58.73	26.28	0.26	7.91	6.62	0.52	100.32	52.57	21			
	58.60	26.40	0.32	7.81	6.75	0.60	100.49	51.49	40			
	58.75	26.46	0.31	7.73	6.52	0.61	100.38	52.02	60			
	58.15	26.57	0.38	8.33	6.51	0.51	100.46	54.27	80			
	59.35	26.01	0.33	7.32	6.79	0.59	100.40	49.81	100			
	58.76	25.80	0.09	7.42	6.69	0.57	99.34	50.55	121			
	58.45	26.76	0.25	8.24	6.47	0.53	100.70	54.08	140			
	58.27	26.66	0.24	7.91	6.40	0.49	99.96	53.45	161			
	58.33	26.76	0.26	8.05	6.45	0.46	100.30	53.83	180			
	58.10	26.31	0.09	7.99	6.49	0.54	99.53	53.20	200			
	57.88	26.69	0.22	8.32	6.31	0.52	99.93	54.91	221			
	59.07	25.89	0.11	7.52	6.81	0.62	100.02	50.31	240			
	58.34	26.20	0.34	7.74	6.70	0.56	99.87	51.61	261			
	58.63	26.36	0.18	7.98	6.65	0.51	100.30	52.69	280			
	59.04	26.55	0.24	7.86	6.87	0.53	101.09	51.50	300			
	57.30	27.35	0.31	8.68	6.11	0.50	100.24	56.74	321			
	57.95	26.54	0.28	8.55	6.26	0.48	100.07	55.93	341			

Appendix 1.1 (cont.)
Electron microprobe analyses of Unzen plagioclase (in wt.%)

Sample ID	SiO_2	Al_2O_3	FeO	CaO	Na_2O	K_2O	Total	An*	um**	Sr (ppm)	Ba (ppm)	Sr/ Ba
	56.67	27.41	0.28	9.49	5.96	0.44	100.26	59.71	361			
	57.79	26.68	0.23	8.56	6.33	0.43	100.01	55.86	380			
	58.39	26.34	0.20	7.84	6.72	0.54	100.02	51.93	401			
	58.25	26.33	0.20	7.90	6.86	0.54	100.08	51.64	422			
	59.05	26.25	0.26	7.38	6.73	0.55	100.22	50.35	441			
	58.35	26.21	0.24	8.19	6.49	0.43	99.91	54.19	461			
	57.44	26.39	0.19	8.45	6.44	0.46	99.37	55.03	481			
	57.95	26.96	0.28	8.47	6.61	0.52	100.79	54.31	501			
	57.45	27.30	0.18	8.68	6.25	0.42	100.28	56.55	520			
	57.10	27.91	0.12	9.17	5.90	0.40	100.61	59.25	541			
	56.52	27.78	0.12	9.36	5.91	0.36	100.06	59.89	562			
	57.54	27.48	0.35	8.73	6.09	0.44	100.62	57.22	581			
	59.06	26.37	0.28	7.59	6.75	0.50	100.54	51.17	602			
	58.96	26.23	0.22	7.66	6.61	0.62	100.30	51.44	621			
	58.79	26.25	0.22	7.81	6.85	0.52	100.44	51.45	641			
	58.27	26.70	0.18	8.11	6.49	0.46	100.20	53.85	661			
	57.85	26.51	0.21	8.03	6.65	0.41	99.66	53.23	681			
	58.81	26.48	0.16	7.97	6.57	0.47	100.46	53.11	702			
	58.88	26.32	0.27	7.66	6.54	0.59	100.27	51.78	721			
	57.55	27.04	0.22	8.97	6.14	0.42	100.35	57.76	742			
	56.78	27.45	0.18	9.16	6.05	0.39	100.00	58.73	762			
	58.47	26.61	0.26	7.88	6.69	0.58	100.49	52.02	781			
	59.21	26.27	0.23	7.63	6.78	0.51	100.64	51.11	802			
	59.17	25.68	0.25	7.55	6.94	0.60	100.19	50.04	821			
	59.38	26.14	0.35	7.87	6.70	0.67	101.11	51.61	842			
	58.49	26.09	0.23	8.04	6.58	0.53	99.96	53.05	862			
	60.01	26.06	0.12	7.31	7.17	0.58	101.25	48.52	882			
	58.61	26.71	0.28	7.70	6.62	0.50	100.41	51.99	902			
	56.57	27.50	0.29	9.31	6.07	0.42	100.16	58.94	922			
	58.22	26.75	0.31	8.43	6.57	0.48	100.75	54.45	942			
	57.31	27.28	0.18	8.85	6.34	0.37	100.33	56.84	963			
	58.18	27.18	0.26	8.55	6.48	0.46	101.10	55.23	982			
	58.35	26.53	0.12	7.85	6.56	0.55	99.96	52.51	1003			
	58.51	26.24	0.22	7.77	6.82	0.54	100.09	51.33	1022			
	57.04	27.53	0.31	9.03	6.12	0.45	100.49	57.90	1042			
	56.73	27.84	0.36	9.39	6.08	0.38	100.79	59.26	1063			
	58.40	26.98	0.15	8.20	6.57	0.53	100.83	53.61	1082			
	58.13	26.67	0.23	8.24	6.26	0.46	100.00	55.06	1103			
	58.16	26.21	0.12	8.21	6.84	0.50	100.05	52.81	1122			
	59.66	25.77	0.00	7.59	6.60	0.58	100.20	51.39	1143			
	59.01	25.79	0.26	7.28	6.86	0.59	99.79	49.42	1163			
	59.32	25.91	0.15	7.60	7.04	0.57	100.60	49.93	1182			
	59.34	26.01	0.17	7.34	6.95	0.58	100.39	49.38	1203			
	58.92	25.76	0.23	7.30	6.90	0.62	99.74	49.25	1222			
	59.94	25.84	0.23	7.26	6.90	0.54	100.70	49.39	1243			
	58.07	26.63	0.22	8.23	6.40	0.51	100.06	54.37	1263			
	59.56	25.95	0.23	7.20	6.69	0.66	100.29	49.49	1283			
	58.57	25.89	0.22	7.55	6.85	0.54	99.61	50.53	1302			
	58.88	26.32	0.27	7.87	6.68	0.57	100.58	52.07	1323			
	59.26	25.30	0.23	7.23	7.00	0.58	99.59	48.85	1343			
	58.31	26.28	0.35	7.70	6.56	0.58	99.78	51.89	1364			
	58.70	26.21	0.21	7.94	6.60	0.56	100.21	52.58	1383			
	58.97	25.81	0.08	7.68	6.67	0.54	99.76	51.55	1404			
	58.36	26.68	0.27	8.46	6.50	0.45	100.73	54.88	1423			
	57.81	26.93	0.26	8.46	6.44	0.49	100.38	54.99	1443			
	57.52	27.14	0.13	8.79	6.22	0.40	100.21	57.01	1463			
	57.70	26.34	0.13	8.11	6.27	0.47	99.03	54.61	1483			
	57.82	26.80	0.21	8.21	6.56	0.54	100.15	53.63	1504			

Appendix 1.1 (cont.)
Electron microprobe analyses of Unzen plagioclase (in wt.%)

Sample ID	SiO_2	Al_2O_3	FeO	CaO	Na_2O	K_2O	Total	An*	um**	Sr (ppm)	Ba (ppm)	Sr/ Ba
	56.82	27.53	0.22	9.05	6.18	0.46	100.26	57.67	1523			
	57.43	26.78	0.25	8.38	6.37	0.45	99.66	55.14	1544			
	59.04	25.85	0.22	7.73	6.80	0.61	100.26	51.03	1563			
	55.93	28.11	0.21	9.88	5.56	0.35	100.04	62.57	1583			
	56.51	27.75	0.27	9.35	5.81	0.41	100.10	60.05	1604			
	57.63	27.20	0.23	8.85	6.23	0.54	100.68	56.67	1623			
	57.74	26.73	0.26	8.38	6.41	0.55	100.06	54.66	1644			
	57.79	26.73	0.32	8.40	6.48	0.48	100.20	54.70	1663			
	57.96	26.64	0.31	8.63	6.34	0.47	100.36	55.86	1684			
	58.25	26.62	0.29	8.05	6.54	0.51	100.27	53.31	1704			
	58.70	26.12	0.15	7.67	6.69	0.57	99.88	51.40	1724			
	58.15	26.09	0.17	8.04	6.48	0.50	99.43	53.51	1744			
	58.31	26.09	0.20	7.92	6.69	0.51	99.73	52.38	1763			
	58.57	25.66	0.16	7.80	6.74	0.50	99.44	51.84	1784			
546.45-546.50 Host Plag2	57.71	26.16	0.30	7.67	6.59	0.45	98.88	52.13	0			
	58.35	26.31	0.33	8.28	6.69	0.46	100.41	53.68	15			
	58.65	26.23	0.22	8.05	6.54	0.56	100.25	53.15	30			
	58.17	26.64	0.33	8.13	6.26	0.47	100.00	54.73	45			
	58.64	26.73	0.26	8.36	6.27	0.41	100.67	55.57	61			
	58.21	27.00	0.26	8.40	6.53	0.54	100.95	54.30	76			
	57.14	26.91	0.15	8.90	6.28	0.42	99.81	57.04	91			
	57.25	27.72	0.23	9.07	6.19	0.39	100.84	57.97	107			
	57.18	27.16	0.30	8.87	6.26	0.39	100.15	57.17	123			
	57.36	26.68	0.25	8.64	6.12	0.49	99.56	56.67	137			
	58.37	26.41	0.15	8.16	6.55	0.50	100.14	53.67	152			
	58.25	26.38	0.23	7.90	6.65	0.55	99.96	52.33	167			
	58.75	26.40	0.26	8.05	6.64	0.54	100.64	52.84	183			
	57.75	26.76	0.29	8.17	6.49	0.50	99.95	53.89	198			
	58.49	26.28	0.12	8.24	6.54	0.43	100.10	54.15	212			
	58.29	26.56	0.23	8.12	6.58	0.56	100.34	53.26	228			
	58.97	25.96	0.22	7.77	6.65	0.50	100.07	52.08	243			
	59.01	25.34	0.25	7.42	7.04	0.66	99.72	49.10	259			
	59.84	25.46	0.25	7.20	6.90	0.59	100.26	48.99	274			
	59.37	25.51	0.11	7.10	6.90	0.61	99.60	48.58	289			
	58.25	26.66	0.22	8.00	6.41	0.51	100.05	53.60	304			
	58.85	26.37	0.21	7.85	6.56	0.52	100.36	52.58	319			
	58.01	27.03	0.24	8.50	6.37	0.47	100.62	55.42	335			
	55.84	27.62	0.28	9.70	5.55	0.41	99.40	61.94	350			
	58.19	26.21	0.22	8.20	6.66	0.55	100.03	53.21	365			
	58.64	26.53	0.24	8.05	6.56	0.52	100.53	53.22	381			
	58.40	26.22	0.27	7.93	6.75	0.52	100.09	52.18	395			
	59.00	26.35	0.30	7.82	6.52	0.48	100.47	52.80	411			
	58.75	26.22	0.17	8.22	6.73	0.53	100.62	53.08	426			
	58.38	26.17	0.11	8.12	6.43	0.51	99.72	53.95	441			
	58.20	26.64	0.23	8.11	6.37	0.52	100.08	54.02	457			
	58.57	26.51	0.31	7.94	6.38	0.50	100.22	53.56	471			
	153.84	7.37	0.85	23.36	13.35	0.01	198.78	63.62	487			
	54.33	25.07	0.22	7.58	6.33	0.40	93.94	52.97	503			
	56.64	26.62	0.20	8.07	6.49	0.46	98.48	53.75	517			
	57.98	26.30	0.07	8.28	6.68	0.48	99.79	53.65	533			
	57.62	25.95	0.26	7.62	6.70	0.52	98.66	51.36	548			
	58.06	26.71	0.29	7.75	6.56	0.54	99.91	52.20	563			
	57.30	25.37	0.18	7.40	5.98	0.50	96.72	53.36	579			
	56.05	26.93	0.28	8.54	6.17	0.38	98.35	56.56	593			
	57.81	25.54	0.26	7.30	6.70	0.59	98.20	50.03	609			
	58.09	25.79	0.16	7.86	6.55	0.50	98.95	52.73	624			
	57.60	25.13	0.04	7.65	6.59	0.64	97.66	51.42	639			

Appendix 1.1 (cont.)
Electron microprobe analyses of Unzen plagioclase (in wt.%)

Sample ID	SiO_2	Al_2O_3	FeO	CaO	Na_2O	K_2O	Total	An*	um**	Sr (ppm)	Ba (ppm)	Sr/ Ba
	58.26	26.04	0.19	7.98	6.44	0.61	99.53	53.11	655			
	57.12	26.44	0.12	8.70	6.32	0.42	99.12	56.33	669			
	58.34	26.24	0.19	7.74	6.82	0.47	99.80	51.50	684			
	58.43	25.26	0.00	7.43	6.78	0.47	98.37	50.60	700			
	57.73	26.75	0.28	8.27	6.42	0.38	99.83	54.89	715			
	56.33	26.45	0.23	8.55	6.33	0.40	98.30	55.95	731			
	57.66	25.49	0.16	7.96	6.49	0.55	98.31	53.08	745			
	58.07	26.27	0.07	8.01	6.03	0.38	98.83	55.58	760			
	55.74	27.46	0.26	9.73	5.74	0.33	99.27	61.57	776			
	56.38	27.44	0.31	9.21	6.01	0.36	99.70	59.10	791			
	57.90	26.36	0.16	7.45	6.65	0.48	98.99	51.13	807			
	57.51	26.44	0.31	7.90	6.54	0.53	99.22	52.77	821			
	55.69	27.77	0.20	9.29	5.92	0.41	99.28	59.46	836			
	54.58	28.02	0.17	10.18	5.33	0.31	98.60	64.37	852			
	54.83	27.37	0.16	9.90	5.51	0.40	98.18	62.63	867			
	55.82	27.25	0.16	9.49	5.56	0.30	98.58	61.84	883			
	56.21	27.29	0.22	9.29	5.75	0.40	99.16	60.15	898			
	56.51	26.78	0.32	8.60	6.02	0.42	98.65	57.17	912			
	56.19	27.27	0.20	9.55	6.21	0.27	99.69	59.57	928			
	54.65	27.59	0.15	9.52	5.80	0.34	98.03	60.82	943			
	56.16	27.18	0.29	9.40	5.73	0.32	99.08	60.84	958			
	56.58	26.91	0.32	8.64	6.50	0.42	99.37	55.53	974			
	57.13	26.34	0.00	7.60	6.55	0.52	98.15	51.83	989			
	57.50	26.27	0.20	8.12	6.31	0.45	98.85	54.59	1005			
	58.56	26.77	0.19	7.69	6.35	0.40	99.96	53.25	1019			
	57.21	26.24	0.31	8.06	6.40	0.39	98.62	54.27	1034			
	52.89	24.53	0.29	8.79	5.66	0.39	92.56	59.23	1050			
	57.71	25.70	0.13	8.20	6.06	0.44	98.26	55.78	1065			
	56.91	25.91	0.32	8.58	6.49	0.45	98.66	55.29	1081			
	50.08	22.79	0.42	7.21	5.19	0.55	86.25	55.69	1095			
546.45-546.50 Host Plag3	54.94	27.45	0.20	9.62	5.78	0.29	98.29	61.29	0			
	56.17	26.30	0.45	8.71	6.23	0.49	98.36	56.44	25			
	54.81	27.98	0.18	9.85	5.42	0.40	98.63	62.87	51			
	56.78	26.85	0.23	8.23	6.19	0.43	98.72	55.39	76			
	55.04	27.01	0.15	9.53	5.67	0.35	97.74	61.29	101			
	55.06	27.32	0.36	9.77	5.43	0.45	98.40	62.41	126			
	56.65	26.91	0.45	9.02	6.26	0.45	99.74	57.35	152			
	56.83	26.53	0.26	8.48	6.31	0.60	99.01	55.09	202			
	55.36	25.54	0.70	7.97	5.79	0.61	95.97	55.43	229			
	56.09	26.96	0.26	8.98	6.12	0.31	98.71	58.29	254			
	58.06	25.93	0.19	7.83	6.36	0.45	98.82	53.50	279			
	55.19	25.29	0.45	8.74	6.19	0.53	96.38	56.57	305			
	57.46	26.37	0.32	8.68	5.98	0.49	99.29	57.27	330			
	57.28	26.25	0.31	8.68	6.30	0.45	99.26	56.25	355			
	56.48	26.79	0.31	9.46	5.85	0.40	99.28	60.22	380			
	56.93	25.91	0.41	8.79	6.41	0.42	98.87	56.26	406			
	54.12	28.26	0.35	10.32	5.69	0.34	99.08	63.11	432			
	55.79	26.72	0.18	8.99	5.96	0.36	98.00	58.74	456			
	43.71	20.10	0.67	10.19	4.56	1.40	80.62	63.13	482			
	43.08	23.92	0.66	10.19	6.09	1.53	85.47	57.20	507			
	57.25	26.13	0.16	8.00	6.41	0.59	98.54	53.32	532			
	56.97	26.92	0.28	8.42	6.09	0.52	99.20	56.01	559			
	57.02	26.78	0.25	8.67	6.13	0.61	99.45	56.27	584			
	54.54	27.39	0.07	9.75	5.25	0.43	97.43	63.20	609			
	56.86	26.98	0.47	8.79	6.34	0.45	99.89	56.38	634			
	54.00	29.29	0.25	10.67	5.02	0.31	99.54	66.70	659			
	53.51	28.22	0.19	10.57	5.19	0.37	98.05	65.52	685			

Appendix 1.1 (cont.)
Electron microprobe analyses of Unzen plagioclase (in wt.%)

Sample ID	SiO_2	Al_2O_3	FeO	CaO	Na_2O	K_2O	Total	An*	um**	Sr (ppm)	Ba (ppm)	Sr/ Ba
	56.02	26.90	0.47	8.83	6.01	0.30	98.53	58.33	710			
	55.91	27.17	0.13	9.29	5.70	0.42	98.62	60.30	736			
	55.61	26.40	0.39	7.88	6.70	0.44	97.42	52.48	761			
	56.46	27.02	1.14	8.60	6.17	0.37	99.76	56.79	786			
	57.08	26.27	0.04	8.60	6.54	0.46	98.98	55.13	812			
	57.29	26.69	0.23	8.68	6.17	0.45	99.51	56.71	837			
	56.19	26.62	0.38	8.57	6.31	0.39	98.46	56.12	862			
	54.87	27.74	0.51	10.17	5.19	0.29	98.78	64.98	887			
	54.71	27.16	0.53	9.80	5.23	0.38	97.81	63.58	914			
	55.76	26.88	0.29	8.28	6.36	0.42	98.00	54.97	939			
	55.90	26.73	0.32	8.89	6.01	0.49	98.33	57.76	964			
	51.35	30.12	0.42	12.79	4.38	0.22	99.28	73.53	989			
	51.76	30.20	0.23	12.43	4.35	0.21	99.18	73.13	1014			
	55.66	28.14	0.00	10.26	5.24	0.38	99.68	64.62	1040			
	57.43	25.79	0.18	8.76	6.38	0.59	99.14	55.67	1066			
	50.84	24.00	0.80	7.34	5.47	0.51	88.96	55.14	1091			
	49.97	21.60	0.12	6.57	6.02	0.45	84.73	50.35	1116			
	57.49	24.92	0.31	7.57	6.86	0.50	97.65	50.72	1141			
	58.64	24.56	0.19	7.13	7.00	0.72	98.24	47.99	1167			
	57.40	26.23	0.38	7.93	6.47	0.59	99.00	52.88	1192			
	57.31	25.87	0.37	7.32	6.98	0.55	98.40	49.29	1217			
	57.96	26.03	0.26	8.07	6.66	0.66	99.65	52.43	1243			
	57.74	25.29	0.13	7.21	6.92	0.46	97.75	49.40	1267			
	58.51	25.94	0.19	7.31	6.81	0.64	99.39	49.54	1294			
	55.73	27.55	0.41	8.69	5.63	0.47	98.48	58.72	1320			
	55.69	25.55	0.23	7.95	6.27	0.54	96.24	53.83	1370			
	57.74	26.26	0.03	8.74	6.24	0.38	99.40	56.87	1395			
546.45-546.50 Host Plag4	58.32	25.17	0.32	7.34	6.49	0.56	98.21	51.00	0			
	55.92	27.14	0.25	9.50	5.99	0.39	99.18	59.81	21			
	57.06	26.37	0.29	8.43	6.44	0.46	99.04	54.97	41			
	58.84	25.90	0.09	8.04	6.41	0.56	99.84	53.57	61			
	56.85	26.51	0.00	7.97	6.39	0.63	98.35	53.15	82			
	54.64	24.51	0.80	7.22	6.07	0.57	93.82	52.08	102			
	56.72	25.94	0.34	8.41	6.22	0.44	98.06	55.83	122			
	58.25	25.89	0.18	7.52	6.86	0.55	99.25	50.37	142			
	57.98	25.49	0.20	7.71	6.53	0.53	98.44	52.22	162			
	57.74	26.14	0.29	8.18	6.50	0.50	99.35	53.86	183			
	58.38	25.12	0.23	7.16	6.81	0.48	98.19	49.54	204			
	58.31	25.04	0.19	7.26	6.59	0.55	97.94	50.41	224			
	57.87	25.37	0.28	7.55	6.55	0.54	98.15	51.56	245			
	57.78	25.31	0.38	7.81	6.13	0.64	98.06	53.56	265			
	57.44	26.02	0.20	8.13	6.39	0.66	98.86	53.54	286			
	58.08	26.92	0.10	8.17	5.93	0.51	99.71	55.95	306			
	57.77	26.17	0.13	8.10	6.55	0.58	99.29	53.19	326			
	55.38	27.97	0.31	10.30	5.59	0.33	99.88	63.50	346			
	56.71	27.45	0.00	8.96	5.99	0.40	99.51	58.37	365			
	57.40	26.48	0.32	7.77	6.74	0.56	99.27	51.55	387			
	56.77	26.23	0.09	8.51	6.39	0.47	98.44	55.38	408			
	56.18	26.18	0.09	8.60	6.03	0.51	97.58	56.81	448			
	57.64	25.54	0.10	7.81	6.70	0.52	98.30	51.99	469			
	58.30	24.63	0.38	7.65	6.65	0.52	98.14	51.61	489			
	56.59	27.23	0.44	9.12	6.18	0.53	100.10	57.61	510			
	55.65	27.85	0.23	9.90	5.63	0.38	99.64	62.23	530			
	58.13	26.41	0.40	8.07	6.94	0.56	100.50	51.83	551			
	56.99	27.00	0.29	8.91	5.97	0.37	99.53	58.43	570			
	57.08	26.95	0.06	8.74	6.36	0.45	99.64	56.20	591			
	56.84	26.88	0.25	9.02	6.00	0.46	99.45	58.29	611			

Appendix 1.1 (cont.)
Electron microprobe analyses of Unzen plagioclase (in wt.%)

Sample ID	SiO_2	Al_2O_3	FeO	CaO	Na_2O	K_2O	Total	An*	um**	Sr (ppm)	Ba (ppm)	Sr/ Ba
	55.06	27.43	0.18	9.04	6.07	0.41	98.18	58.24	632			
	57.29	26.25	0.01	8.13	6.72	0.52	98.92	52.91	652			
602.80-602.85 Host Plag1	54.89	27.49	0.37	9.65	5.85	0.53	98.79	60.19	0			
	56.98	26.79	0.21	8.95	6.26	0.58	99.76	56.67	72			
	57.43	26.36	0.34	8.38	6.73	0.45	99.68	53.89	144			
	45.42	19.39	1.85	6.20	3.62	0.36	76.84	60.87	216			
	56.20	26.68	0.30	9.07	6.28	0.43	98.96	57.50	287			
	57.09	26.50	0.27	8.40	6.72	0.51	99.49	53.75	359			
	56.11	27.58	0.35	9.26	6.09	0.32	99.71	59.09	431			
	55.98	27.53	0.30	9.05	6.28	0.38	99.51	57.61	503			
	55.81	27.62	0.25	9.21	6.01	0.39	99.28	59.04	575			
	56.72	26.66	0.09	8.85	6.32	0.43	99.08	56.73	647			
	57.78	25.95	0.20	7.80	6.81	0.59	99.12	51.31	719			
	57.63	25.98	0.23	8.11	6.80	0.59	99.33	52.33	790			
	57.19	26.76	0.37	8.86	6.54	0.50	100.22	55.74	862			
	56.41	27.00	0.24	8.90	6.16	0.52	99.24	57.08	934			
	55.99	27.30	0.33	9.29	6.12	0.39	99.41	58.79	1006			
	57.61	26.63	0.25	8.18	6.56	0.52	99.76	53.60	1078			
	57.59	26.36	0.21	8.36	6.54	0.56	99.63	54.07	1150			
	57.67	26.23	0.22	8.24	6.44	0.65	99.45	53.72	1222			
	60.11	27.99	0.32	8.96	5.88	0.58	103.84	58.08	1293			
	57.32	25.67	0.40	7.97	6.64	0.64	98.65	52.26	1365			
	56.45	26.93	0.27	8.46	6.53	0.66	99.29	54.04	1438			
	53.96	28.56	0.34	10.90	5.27	0.46	99.51	65.53	1510			
602.80-602.85 E M-Plag1	50.77	28.40	0.95	11.43	4.19	0.37	96.11	71.48	0			
	43.33	20.63	3.71	9.42	2.77	1.39	81.24	69.38	9			
	53.83	27.79	0.79	10.71	5.20	0.40	98.72	65.66	17			
	53.87	28.02	0.63	11.19	5.09	0.36	99.16	67.23	25			
	53.51	28.20	0.71	11.21	5.13	0.40	99.16	66.97	33			
	52.65	28.77	0.89	11.35	4.76	0.34	98.77	69.00	42			
	52.20	27.42	0.89	10.73	4.97	0.38	96.59	66.74	50			
	50.52	27.06	1.48	11.09	4.31	0.40	94.86	70.20	58			
602.80-602.85 E M-Plag2	54.97	28.50	0.35	10.53	5.66	0.48	100.48	63.18	0			
	51.80	29.85	0.69	11.87	4.44	0.33	98.98	71.30	9			
	51.61	30.45	0.66	13.01	3.96	0.38	100.07	74.96	17			
	54.23	29.04	0.53	10.98	5.07	0.55	100.40	66.14	26			
	53.14	29.07	0.69	11.14	5.05	0.56	99.65	66.51	34			
	42.60	22.67	0.71	8.73	3.88	0.41	79.00	67.01	43			
	49.48	22.55	2.55	13.06	3.36	0.35	91.36	77.84	51			
602.80-602.85 E P-Plag3	56.87	26.25	0.20	8.55	6.28	0.58	98.73	55.48	0			
	57.16	26.64	0.21	8.53	6.63	0.53	99.70	54.35	41			
	52.89	29.65	0.24	11.83	4.97	0.28	99.86	69.27	83			
	57.07	27.11	0.18	8.87	6.24	0.45	99.93	57.00	124			
	53.46	28.78	0.28	11.16	5.24	0.34	99.25	66.66	165			
	55.28	28.10	0.32	10.39	5.60	0.34	100.03	63.62	206			
	56.43	27.09	0.26	8.95	6.42	0.41	99.56	56.71	248			
	57.39	26.15	0.34	8.15	6.67	0.47	99.16	53.30	289			
	56.50	26.24	0.24	8.59	6.28	0.39	98.24	56.30	330			
	55.98	27.13	0.24	9.29	6.12	0.38	99.13	58.85	371			
	56.82	26.60	0.23	8.70	6.45	0.38	99.18	56.02	413			
	56.94	27.34	0.18	9.09	6.32	0.37	100.26	57.60	454			
	55.96	27.31	0.20	9.28	5.99	0.37	99.10	59.36	495			
	55.59	26.88	0.67	9.17	5.60	0.36	98.26	60.61	536			
	57.28	25.81	0.28	7.77	6.92	0.56	98.62	50.94	578			

Appendix 1.1 (cont.)
Electron microprobe analyses of Unzen plagioclase (in wt.%)

Sample ID	SiO_2	Al_2O_3	FeO	CaO	Na_2O	K_2O	Total	An*	um**	Sr (ppm)	Ba (ppm)	Sr/ Ba
	58.19	25.96	0.30	8.12	6.72	0.51	99.79	52.91	620			
	56.39	27.27	0.24	8.87	6.38	0.41	99.56	56.63	661			
	55.70	27.75	0.15	9.66	5.86	0.33	99.45	60.98	702			
	56.29	27.01	0.34	9.18	6.27	0.43	99.52	57.83	744			
	55.27	27.87	0.22	9.93	5.98	0.37	99.64	60.99	785			
	55.83	27.65	0.19	9.55	5.94	0.39	99.55	60.14	826			
	54.63	28.75	0.16	11.39	5.20	0.30	100.43	67.40	867			
	57.01	26.81	0.26	8.11	6.64	0.50	99.34	53.16	909			
	56.40	26.79	0.25	8.69	6.40	0.55	99.09	55.58	950			
	55.53	27.44	0.38	9.53	5.96	0.48	99.31	59.67	991			
602.80-602.85 E M-Plag4	53.06	28.12	0.67	11.41	5.14	0.39	98.78	67.35	0			
	52.65	29.16	0.65	11.84	4.59	0.28	99.17	70.84	9			
	50.86	30.44	0.68	13.38	4.04	0.27	99.66	75.64	17			
	50.73	31.01	0.71	13.69	3.89	0.28	100.33	76.63	26			
	50.53	30.38	0.63	13.41	3.82	0.31	99.09	76.45	34			
	50.95	30.56	0.64	13.27	3.91	0.28	99.61	76.02	44			
	51.20	30.46	0.59	12.95	4.18	0.30	99.69	74.28	53			
	52.82	28.41	0.51	11.14	5.22	0.32	98.41	66.79	61			
	78.66	11.64	0.15	0.68	2.28	5.47	98.87	8.03	70			
	58.59	25.50	0.44	7.82	6.81	0.53	99.69	51.59	78			
602.80-602.85 E M-Plag5	58.75	24.67	0.53	7.28	6.90	0.58	98.71	49.31	0			
	53.25	29.12	0.45	10.97	5.20	0.38	99.38	66.28	7			
	53.11	29.01	0.76	11.71	4.89	0.36	99.83	69.07	17			
	52.74	28.82	0.88	11.34	5.04	0.36	99.18	67.72	24			
	47.19	25.98	1.32	10.61	3.87	0.31	89.26	71.75	32			
	52.02	30.06	0.91	12.53	4.39	0.33	100.24	72.64	41			
	52.85	29.24	0.71	11.53	4.77	0.36	99.46	69.23	49			
	50.44	27.50	1.86	10.81	4.58	0.42	95.61	68.39	58			
	51.78	29.75	0.85	12.43	4.50	0.32	99.61	72.08	66			
	52.28	29.09	0.63	11.71	4.74	0.37	98.83	69.60	73			
	54.20	28.60	0.54	11.00	5.20	0.41	99.94	66.20	82			
	53.33	27.62	0.52	11.46	5.34	0.49	98.77	66.25	90			
602.80-602.85 E M-Plag6	55.83	22.60	1.39	6.52	5.06	3.04	94.44	44.60	0			
	53.35	29.32	0.68	11.60	4.76	0.34	100.05	69.46	9			
	53.59	29.35	0.63	11.58	4.80	0.39	100.35	69.05	16			
	53.06	29.38	0.57	11.75	4.91	0.35	100.02	69.08	26			
	54.16	28.77	0.47	11.03	5.17	0.40	100.00	66.44	35			
	56.21	27.32	0.50	9.26	5.96	0.57	99.82	58.66	44			
	51.68	30.16	0.50	12.60	4.35	0.43	99.74	72.48	52			
	54.15	28.01	0.82	10.35	5.50	0.40	99.23	63.70	61			
602.80-602.85 E M-Plag7	52.83	29.36	0.51	11.57	4.78	0.32	99.38	69.37	0	136.7	1251.50	9.2
	53.14	29.54	0.62	11.85	4.85	0.37	100.36	69.43	8			
	53.14	29.09	0.65	11.59	4.80	0.39	99.66	69.10	16			
	53.25	29.02	0.44	11.15	5.06	0.41	99.32	67.10	25			
	44.59	21.12	2.08	8.33	2.78	1.29	80.18	67.18	34			
	54.37	28.03	0.43	10.64	5.29	0.46	99.21	64.91	42			
	57.20	26.35	0.40	8.42	6.27	0.74	99.38	54.56	51			
	53.14	29.22	0.69	11.29	4.95	0.45	99.74	67.62	59			
	56.82	26.83	0.48	8.66	6.46	0.44	99.70	55.65	67			
602.80-602.85 E M-Plag8	54.48	28.29	0.92	10.57	5.06	0.63	99.95	65.01	0	85.1	1052.50	12.4
	52.77	29.36	0.68	11.75	4.67	0.38	99.60	69.97	6			
	52.65	29.88	0.61	12.08	4.75	0.36	100.32	70.28	12			
	52.58	29.57	0.65	11.94	4.51	0.38	99.64	70.96	18			
	52.99	29.57	0.72	11.81	4.63	0.37	100.10	70.26	25			

Appendix 1.1 (cont.)
Electron microprobe analyses of Unzen plagioclase (in wt.%)

Sample ID	SiO_2	Al_2O_3	FeO	CaO	Na_2O	K_2O	Total	An*	um**	Sr (ppm)	Ba (ppm)	Sr/ Ba
	53.15	30.04	0.56	11.81	4.61	0.35	100.52	70.40	31			
	64.18	22.64	0.52	6.18	4.67	2.55	100.74	46.13	37			
	73.21	14.76	0.36	2.99	4.53	1.73	97.58	32.35	43			
602.80-602.85 E M-Plag9	57.20	26.39	0.48	8.50	6.11	0.67	99.35	55.64	0	122.5	1243.85	10.2
	55.07	27.63	0.54	9.80	5.79	0.43	99.26	61.18	7			
	55.30	27.55	0.56	9.83	5.70	0.39	99.33	61.76	13			
	60.31	20.27	1.21	2.99	4.33	5.78	94.89	22.83	20			
	53.29	28.94	0.52	11.53	4.66	0.35	99.29	69.68	26			
	51.67	30.13	0.48	12.44	4.39	0.28	99.39	72.70	33			
	51.41	30.10	0.58	12.78	4.28	0.32	99.48	73.55	39			
	50.72	28.44	1.05	12.23	4.06	0.32	96.83	73.62	46			
602.80-602.85 E M-Plag10	52.94	27.86	1.16	11.02	4.88	0.36	98.21	67.81	0			
	56.99	26.94	0.40	8.46	6.13	0.66	99.59	55.46	10			
	55.27	28.22	0.44	10.16	5.55	0.43	100.07	62.92	20			
	53.41	29.17	0.48	11.20	5.08	0.38	99.72	67.21	30			
	53.47	29.11	0.53	11.51	4.99	0.42	100.03	68.05	41			
	53.29	29.28	0.37	11.60	4.79	0.47	99.80	68.81	51			
	53.53	29.21	0.44	11.73	4.72	0.35	99.99	69.84	61			
	53.82	28.75	0.54	11.40	5.05	0.45	100.01	67.47	71			
	53.20	28.60	0.34	11.02	5.05	0.45	98.66	66.72	81			
	53.62	28.87	0.30	10.87	5.26	0.52	99.44	65.32	90			
	54.71	28.60	0.32	10.52	5.35	0.54	100.04	64.10	102			
	54.71	28.79	0.28	10.20	5.46	0.48	99.93	63.20	112			
	55.97	27.51	0.32	9.25	5.86	0.56	99.46	59.02	122			
	57.60	26.49	0.26	8.21	6.51	0.78	99.85	52.95	132			
	51.97	30.14	0.40	12.85	4.20	0.31	99.86	74.04	142			
	54.73	25.81	0.94	9.13	4.42	2.64	97.67	56.38	152			
	57.15	26.41	0.67	8.37	6.47	0.59	99.66	54.27	162			
602.80-602.85 E M-Plag11	57.01	26.82	0.49	8.64	6.28	0.56	99.80	55.80	0			
	58.08	26.14	0.29	7.90	6.45	0.72	99.58	52.41	7			
	55.60	27.69	0.25	9.96	5.90	0.47	99.86	61.01	14			
	50.19	27.23	0.38	10.98	4.37	0.38	93.54	69.80	21			
	52.72	29.56	0.36	11.73	4.76	0.34	99.48	69.67	28			
602.80-602.85 E M-Plag12	54.54	28.55	0.68	10.76	5.37	0.34	100.25	65.33	0			
	52.01	29.81	0.42	12.25	4.50	0.34	99.34	71.69	9			
	55.60	27.56	0.43	9.99	5.61	0.53	99.72	61.92	18			
	55.17	28.06	0.36	10.35	5.37	0.50	99.81	63.80	27			
	53.87	29.08	0.51	11.05	5.23	0.43	100.17	66.11	35			
	53.28	29.34	0.46	11.48	4.97	0.45	99.99	67.96	44			
	52.95	29.03	0.39	11.39	4.98	0.37	99.11	68.01	53			
	53.47	28.94	0.51	11.67	4.86	0.41	99.86	68.89	61			
	53.06	29.73	0.31	11.51	4.79	0.33	99.73	69.24	71			
	55.00	27.68	0.56	9.95	5.57	0.46	99.22	62.27	79			
602.80-602.85 Host Plag2	56.32	27.85	0.27	9.30	5.76	0.41	99.90	60.13	0	915.7	189.41	4.8
	56.15	27.66	0.21	9.56	5.96	0.39	99.93	60.09	18			
	56.09	27.71	0.21	9.12	5.65	0.41	99.18	60.09	36			
	57.17	27.18	0.33	8.99	5.94	0.39	99.99	58.69	55			
	58.20	27.01	0.23	8.51	6.00	0.45	100.39	56.89	72			
	58.19	26.63	0.33	8.07	6.31	0.47	99.99	54.36	90			
	57.45	26.68	0.05	8.42	6.29	0.40	99.29	55.73	108			
	58.24	26.72	0.17	8.56	6.38	0.42	100.49	55.70	126			
	57.05	26.27	0.18	8.51	6.37	0.43	98.80	55.61	144			
	56.93	27.06	0.16	8.83	6.19	0.43	99.60	57.17	163			

Appendix 1.1 (cont.)
Electron microprobe analyses of Unzen plagioclase (in wt.%)

Sample ID	SiO_2	Al_2O_3	FeO	CaO	Na_2O	K_2O	Total	An*	um**	Sr (ppm)	Ba (ppm)	Sr/ Ba
	57.45	26.99	0.24	8.59	6.30	0.41	99.99	56.12	181			
	57.14	27.41	0.16	8.64	6.13	0.43	99.90	56.85	199	877.5	164.30	5.3
	56.58	27.01	0.25	8.61	6.10	0.36	98.91	57.15	216			
	57.00	26.99	0.24	8.57	5.96	0.40	99.16	57.42	234			
	56.40	27.20	0.25	8.94	6.09	0.40	99.29	57.92	252			
	56.96	26.92	0.30	8.51	6.29	0.38	99.36	56.06	271			
	57.80	26.74	0.24	8.30	6.28	0.48	99.84	55.12	288			
	58.00	26.33	0.20	7.88	6.22	0.53	99.16	53.86	306			
	57.35	26.79	0.19	8.59	6.15	0.45	99.51	56.56	324			
	57.52	27.09	0.17	8.49	6.03	0.43	99.72	56.79	342			
	56.83	27.04	0.20	8.76	6.25	0.43	99.51	56.75	361			
	56.94	26.96	0.21	8.75	6.03	0.42	99.31	57.55	379			
	58.07	26.29	0.23	7.91	6.42	0.50	99.41	53.35	397	833.8	160.97	5.2
	58.01	26.35	0.28	8.07	6.44	0.48	99.63	53.81	415			
	56.38	27.85	0.29	9.43	5.68	0.37	99.99	60.96	432			
	56.45	27.53	0.19	9.42	5.60	0.34	99.54	61.31	450			
	57.20	27.39	0.14	9.05	5.85	0.37	100.00	59.31	469			
	57.16	25.98	0.31	7.89	6.54	0.57	98.45	52.59	541			
	58.64	26.79	0.29	8.38	6.33	0.51	100.93	55.08	560	1012.6	239.33	4.2
	58.18	26.43	0.25	7.83	6.63	0.51	99.85	52.30	577			
	58.40	25.64	0.30	7.40	6.60	0.50	98.85	51.04	595			
	58.22	25.92	0.35	7.34	6.65	0.48	98.95	50.74	613			
	58.42	26.33	0.20	7.52	6.32	0.49	99.28	52.44	631			
	58.21	26.10	0.34	7.72	6.53	0.54	99.44	52.18	649			
	56.68	26.72	0.26	8.89	5.94	0.42	98.91	58.29	668			
	58.91	26.32	0.26	7.60	6.53	0.56	100.19	51.75	686	788.9	166.24	4.7
	58.91	25.95	0.19	7.90	6.61	0.49	100.05	52.66	704			
	58.08	26.85	0.29	8.55	6.24	0.41	100.42	56.27	721			
	57.37	27.05	0.24	8.78	6.26	0.39	100.09	56.89	739			
	56.93	27.41	0.26	8.62	5.91	0.43	99.56	57.62	757			
	57.73	26.23	0.17	8.00	6.58	0.45	99.15	53.21	776			
	59.34	25.40	0.24	7.17	6.77	0.56	99.47	49.41	794	1047.6	256.36	4.1
	58.68	25.90	0.30	7.33	6.98	0.55	99.74	49.33	812			
	58.49	25.89	0.18	7.88	6.30	0.59	99.33	53.34	830			
	59.15	25.42	0.17	7.25	6.86	0.56	99.41	49.40	847			
	58.35	26.10	0.15	7.79	6.51	0.57	99.47	52.39	866			
	58.91	25.93	0.20	7.28	6.62	0.52	99.46	50.51	884			
	57.73	26.58	0.28	8.32	6.51	0.43	99.85	54.52	902			
	58.05	26.41	0.21	8.00	6.61	0.48	99.76	53.01	920			
	58.47	25.71	0.27	7.79	6.80	0.52	99.57	51.56	937			
	58.96	25.93	0.18	7.38	6.63	0.55	99.63	50.67	955	983.4	208.80	4.7
	58.03	26.34	0.31	7.92	6.53	0.50	99.63	52.95	974			
	57.75	26.50	0.27	8.40	6.17	0.46	99.56	55.86	992			
	59.03	25.99	0.18	7.59	6.74	0.54	100.07	51.03	1010	947.5	200.36	4.7
	58.63	25.59	0.19	7.60	6.53	0.64	99.18	51.45	1028	958.7	200.59	4.8
	58.68	25.88	0.23	7.75	6.36	0.59	99.50	52.71	1046			
	59.12	25.42	0.17	7.03	6.87	0.74	99.34	48.02	1064			
	56.85	26.98	0.32	8.74	5.95	0.49	99.32	57.57	1082			
	58.78	25.69	0.27	7.56	6.61	0.69	99.60	50.86	1100			
	52.84	30.13	0.86	12.03	4.19	0.26	100.31	73.01	1118			
602.80-602.85 Host Plag3	57.22	26.84	0.60	8.54	5.40	0.23	98.83	60.27	0	1297.7	143.60	9.0
	55.78	27.48	0.23	9.56	5.31	0.53	98.89	62.09	15			
	57.34	27.14	0.09	9.04	5.77	0.51	99.88	59.03	30			
	54.67	28.18	0.31	9.91	5.10	0.40	98.57	64.31	45			
	56.20	26.82	0.21	9.11	5.65	0.49	98.47	59.76	61			
	55.73	27.50	0.22	9.96	5.57	0.46	99.44	62.29	75			
	57.20	26.46	0.29	8.35	6.06	0.60	98.95	55.64	91			

Appendix 1.1 (cont.)
Electron microprobe analyses of Unzen plagioclase (in wt.%)

Sample ID	SiO_2	Al_2O_3	FeO	CaO	Na_2O	K_2O	Total	An*	um**	Sr (ppm)	Ba (ppm)	Sr/ Ba
	56.89	26.45	0.21	8.59	5.80	0.48	98.42	57.75	106			
	56.90	26.77	0.16	9.06	6.12	0.49	99.50	57.82	122			
	57.80	26.21	0.21	7.86	6.35	0.69	99.12	52.76	137			
	57.34	26.62	0.28	8.63	5.89	0.55	99.30	57.27	152			
	57.24	26.68	0.30	8.23	6.17	0.71	99.33	54.46	167			
	57.05	26.08	0.27	8.07	6.05	0.58	98.09	54.91	183	1019.6	119.70	8.5
	57.49	26.67	0.21	8.53	6.01	0.56	99.48	56.48	197			
	56.99	27.29	0.30	8.70	6.04	0.58	99.90	56.82	213			
	57.17	26.77	0.30	8.33	6.14	0.54	99.25	55.53	228			
	56.88	26.22	0.22	8.48	6.38	0.57	98.74	54.98	243			
	57.14	26.92	0.25	8.56	6.05	0.59	99.49	56.34	258			
	57.24	26.71	0.21	8.52	6.15	0.56	99.38	55.95	274			
	57.36	26.86	0.14	8.43	6.29	0.48	99.55	55.46	288			
	57.29	26.69	0.36	8.32	6.21	0.59	99.46	55.02	319			
	57.17	26.91	0.22	8.47	6.20	0.57	99.53	55.56	334			
	58.97	26.24	0.29	7.58	6.41	0.67	100.15	51.70	349			
	57.96	26.62	0.19	8.17	6.32	0.63	99.89	54.04	365			
	59.38	25.68	0.18	7.10	6.70	0.65	99.69	49.12	380			
	58.24	26.24	0.04	7.33	6.52	0.67	99.04	50.52	396			
	57.96	26.52	0.11	8.24	6.34	0.58	99.76	54.36	411			
	55.14	28.24	0.48	10.13	4.72	0.26	98.97	67.04	426	1157.3	141.96	8.2
	57.23	26.52	0.18	8.46	6.11	0.54	99.04	55.97	441			
	57.90	26.66	0.28	8.43	6.09	0.58	99.93	55.84	456			
	57.37	26.57	0.20	8.43	6.10	0.54	99.22	55.90	487			
	57.52	26.63	0.19	8.34	6.16	0.56	99.41	55.38	501			
	57.55	26.85	0.25	8.40	6.06	0.52	99.63	56.08	517			
	56.80	26.87	0.09	8.70	6.03	0.57	99.06	56.86	532			
	56.26	27.17	0.28	9.07	5.85	0.51	99.13	58.77	547			
	55.88	27.46	0.28	9.57	5.69	0.50	99.37	60.72	562			
	56.23	27.34	0.25	8.79	5.86	0.48	98.95	58.08	578			
	57.01	27.34	0.20	9.14	5.90	0.51	100.10	58.79	593			
	56.31	27.03	0.29	8.79	5.78	0.56	98.75	58.11	608			
	51.29	31.74	0.21	13.47	3.69	0.22	100.62	77.47	623	1201.8	62.93	19.1
	47.81	32.52	0.29	15.38	2.66	0.14	98.80	84.60	639	1259.3	65.33	19.3
	49.02	32.56	0.30	14.66	2.93	0.19	99.66	82.44	654	1242.9	58.62	21.2
	49.02	32.04	0.52	14.49	3.10	0.18	99.34	81.56	670			
	59.78	24.98	0.11	7.09	6.84	0.90	99.69	47.80	700			
	59.94	25.13	0.32	6.79	6.88	0.94	100.00	46.45	715			
	57.85	26.15	0.28	7.89	6.12	0.67	98.95	53.74	730			
	56.67	26.64	0.22	8.60	5.79	0.66	98.59	57.13	745			
	57.48	26.34	0.19	8.25	6.18	0.79	99.23	54.21	760			
	58.08	26.05	0.26	7.90	6.50	0.72	99.52	52.25	775			
	58.47	26.05	0.29	7.79	6.22	0.82	99.62	52.55	791			
	57.37	26.12	0.31	7.78	6.08	0.77	98.41	53.18	806			
	56.49	27.08	0.16	9.40	5.60	0.58	99.30	60.32	821	1311.8	159.39	8.2
	63.05	22.68	0.37	5.60	6.84	0.86	99.40	42.09	836			
	54.53	28.24	0.87	10.59	4.94	0.30	99.47	66.93	852	1028.3	149.50	6.9
	58.93	25.21	0.88	7.74	5.28	0.48	98.52	57.33	867	1021.3	127.37	8.0
U1A Host Plag1	57.40	26.46	0.38	7.84	6.47	0.42	98.97	53.22	0			
	57.63	26.09	0.20	7.86	6.37	0.42	98.57	53.64	12			
	57.59	26.65	0.29	8.33	6.39	0.46	99.71	54.88	24			
	57.70	26.18	0.23	7.86	6.37	0.47	98.81	53.50	36			
	58.64	25.90	0.19	7.37	6.61	0.49	99.20	50.93	48			
	58.11	25.87	0.17	7.47	6.70	0.50	98.83	50.92	60			
	57.76	26.12	0.21	8.00	6.72	0.46	99.27	52.69	72			
	58.51	26.37	0.25	7.94	6.47	0.52	100.05	53.19	84			
	57.68	26.34	0.18	7.99	6.44	0.53	99.16	53.41	97			

Appendix 1.1 (cont.)
Electron microprobe analyses of Unzen plagioclase (in wt.%)

Sample ID	SiO_2	Al_2O_3	FeO	CaO	Na_2O	K_2O	Total	An*	um**	Sr (ppm)	Ba (ppm)	Sr/ Ba
	58.16	26.08	0.22	7.65	6.58	0.46	99.15	52.08	109			
	57.80	26.07	0.27	7.61	6.55	0.48	98.78	51.98	120			
	57.21	26.14	0.12	7.89	6.52	0.43	98.32	53.15	132			
	57.79	26.46	0.34	8.17	6.48	0.36	99.60	54.42	144			
	56.98	26.75	0.28	8.15	6.38	0.40	98.94	54.58	156			
	57.43	26.31	0.31	8.50	6.39	0.36	99.28	55.77	169			
	57.67	26.58	0.25	8.31	6.27	0.41	99.49	55.40	181			
	56.96	26.51	0.21	7.93	6.12	0.44	98.17	54.70	192			
	57.20	26.76	0.20	8.19	6.40	0.37	99.11	54.77	204			
	57.18	26.37	0.12	8.04	6.31	0.38	98.41	54.59	216			
	57.63	26.53	0.21	7.70	6.30	0.42	98.80	53.37	229			
	56.69	26.48	0.30	8.49	6.28	0.44	98.67	55.83	241			
	57.32	26.22	0.41	8.36	6.28	0.43	99.02	55.46	253			
	57.30	26.45	0.31	8.32	6.00	0.43	98.80	56.40	265			
	57.59	26.20	0.25	7.66	6.52	0.44	98.67	52.41	276			
	55.64	25.76	0.07	7.76	6.30	0.47	95.99	53.44	288			
	48.37	24.67	0.43	9.11	5.56	0.36	88.50	60.62	301			
	54.64	28.58	0.19	10.04	5.45	0.27	99.16	63.72	313			
	53.10	29.39	0.31	11.35	4.76	0.23	99.13	69.48	325			
	55.59	28.00	0.32	9.41	5.44	0.36	99.11	61.82	337			
	56.41	26.95	0.15	8.82	6.08	0.36	98.77	57.79	348			
	57.10	26.48	0.25	8.14	6.49	0.46	98.91	53.93	361			
	56.66	26.43	0.23	8.30	6.08	0.38	98.08	56.26	373			
	56.58	27.12	0.11	8.58	6.05	0.35	98.79	57.27	385			
	53.89	27.20	0.15	9.58	5.42	0.30	96.54	62.60	397			
	55.96	27.02	0.30	8.70	5.93	0.38	98.29	57.95	409			
	55.96	26.88	0.27	8.35	5.75	0.39	97.60	57.59	421			
	52.57	29.63	0.42	11.93	4.62	0.24	99.41	71.06	433			
	47.19	25.63	0.30	9.63	4.52	0.53	87.80	65.58	457			
	51.54	30.56	0.37	12.81	3.90	0.16	99.34	75.91	469			
	53.39	29.30	0.22	10.96	4.98	0.23	99.07	67.78	482			
	56.44	27.01	0.33	8.75	6.47	0.44	99.44	55.90	505			
	50.87	31.12	0.46	13.26	3.70	0.22	99.64	77.19	541			
	49.59	31.71	0.32	13.87	3.30	0.18	98.97	79.95	554			
	49.20	31.08	0.56	14.19	3.12	0.17	98.32	81.20	577			
	57.79	26.06	0.26	7.59	6.52	0.49	98.69	51.98	601			
	54.03	29.08	0.20	10.91	4.76	0.32	99.30	68.24	614			
	53.20	29.20	0.33	11.01	5.19	0.27	99.18	66.88	626			
	49.53	31.53	0.48	13.72	3.17	0.14	98.57	80.59	638			
	49.68	31.33	0.38	13.93	3.42	0.16	98.90	79.55	649			
	48.37	32.37	0.43	14.55	2.66	0.08	98.46	84.14	661			
	50.45	31.10	0.53	13.36	3.42	0.09	98.96	79.18	674			
	50.12	31.57	0.60	13.85	3.26	0.12	99.51	80.41	686			
	51.16	30.24	0.64	12.52	4.01	0.12	98.69	75.21	698			
	50.20	30.81	0.40	13.36	3.47	0.14	98.37	78.75	710			
	54.97	28.10	0.51	10.22	5.44	0.33	99.57	63.93	722			
	56.07	6.77	7.79	11.89	1.06	1.79	85.37	80.65	902			
U1A Host Plag2	56.77	26.33	0.18	8.39	6.34	0.38	98.40	55.54	0			
	56.97	26.15	0.13	8.16	6.12	0.33	97.86	55.83	15			
	55.70	26.15	0.11	8.10	5.88	0.52	96.46	55.87	30			
	56.50	26.80	0.27	8.46	6.28	0.40	98.70	55.89	45			
	56.25	27.00	0.39	8.73	6.02	0.40	98.79	57.61	60			
	56.11	26.78	0.17	8.76	6.09	0.38	98.28	57.51	76			
	55.94	27.28	0.20	9.00	5.86	0.39	98.67	59.02	91			
	56.20	27.05	0.19	8.49	5.91	0.36	98.20	57.53	105			
	56.65	26.96	0.22	8.56	6.25	0.41	99.06	56.24	121			
	56.78	26.72	0.23	8.37	6.40	0.36	98.85	55.33	136			

Appendix 1.1 (cont.)
Electron microprobe analyses of Unzen plagioclase (in wt.%)

Sample ID	SiO_2	Al_2O_3	FeO	CaO	Na_2O	K_2O	Total	An*	um**	Sr (ppm)	Ba (ppm)	Sr/ Ba
	56.29	26.44	0.25	8.42	6.08	0.40	97.88	56.51	150			
	56.86	26.55	0.31	8.35	6.20	0.46	98.72	55.63	166			
	56.50	26.89	0.23	8.47	6.10	0.36	98.55	56.74	181			
	56.61	26.38	0.21	8.47	6.48	0.43	98.57	55.07	197			
	57.15	26.31	0.04	8.18	6.45	0.41	98.53	54.37	211			
	57.33	26.32	0.19	7.92	6.47	0.44	98.68	53.42	226			
	56.44	27.40	0.21	8.71	6.02	0.34	99.11	57.79	242			
	55.30	27.46	0.17	9.35	5.54	0.33	98.14	61.45	257			
	57.31	26.52	0.30	8.42	6.15	0.39	99.09	56.31	271			
	56.23	26.04	0.23	8.14	6.16	0.37	97.17	55.49	287			
	57.75	26.46	0.00	8.20	6.52	0.48	99.41	53.98	302			
	56.46	26.63	0.44	8.56	5.96	0.33	98.37	57.66	316			
	55.99	27.02	0.18	9.01	5.83	0.33	98.35	59.40	332			
	56.02	27.29	0.25	8.68	6.09	0.37	98.70	57.32	347			
	56.38	26.41	0.14	8.62	6.12	0.36	98.03	57.09	362			
	56.60	26.95	0.24	8.83	6.06	0.37	99.05	57.89	377			
	56.56	26.98	0.30	8.64	6.11	0.36	98.95	57.15	392			
	56.49	27.12	0.39	8.71	6.27	0.44	99.42	56.50	407			
	56.29	27.31	0.25	8.57	6.36	0.34	99.12	56.12	423			
	57.06	26.75	0.21	8.22	6.29	0.44	98.96	54.97	437			
	57.43	26.85	0.22	8.60	6.27	0.47	99.83	56.05	452			
	56.26	27.31	0.14	9.05	5.87	0.38	99.02	59.15	468			
	55.07	28.01	0.34	10.02	5.37	0.34	99.14	63.68	483			
	56.12	27.12	0.19	9.03	5.99	0.38	98.83	58.66	497			
	57.57	26.49	0.18	8.09	6.32	0.39	99.05	54.66	513			
	57.49	26.65	0.04	8.31	6.44	0.45	99.38	54.70	528			
	57.30	26.72	0.23	8.41	6.43	0.36	99.45	55.31	544			
	57.82	26.03	0.24	7.87	6.38	0.47	98.80	53.49	558			
	57.46	26.41	0.14	7.95	6.44	0.46	98.86	53.56	573			
	57.20	26.36	0.15	7.97	6.28	0.41	98.37	54.35	589			
	56.55	26.41	0.20	8.25	6.43	0.49	98.34	54.39	604			
	56.53	26.50	0.44	8.34	6.31	0.34	98.46	55.61	618			
	56.44	26.66	0.14	8.78	6.30	0.49	98.81	56.38	634			
	57.75	26.38	0.26	8.30	6.34	0.39	99.42	55.20	649			
	56.65	26.53	0.32	8.57	6.07	0.38	98.52	57.08	663			
	57.56	26.53	0.36	8.15	6.29	0.37	99.26	55.02	679			
	57.96	26.15	0.21	7.93	6.69	0.40	99.35	52.78	694			
	57.99	25.82	0.32	7.23	6.84	0.48	98.68	49.68	709			
	56.73	26.65	0.30	8.55	6.44	0.45	99.11	55.42	725			
	56.92	26.99	0.15	8.40	6.31	0.36	99.12	55.76	739			
	57.32	26.31	0.22	8.33	6.43	0.46	99.07	54.71	754			
	56.58	26.74	0.20	8.42	6.39	0.40	98.73	55.33	770			
	57.39	25.85	0.24	7.83	6.46	0.44	98.21	53.16	784			
	57.66	26.51	0.23	8.35	6.36	0.46	99.56	55.03	799			
	58.65	25.07	0.28	6.57	6.79	0.62	97.98	46.98	815			
	57.29	26.24	0.28	8.08	6.69	0.42	98.98	53.22	830			
	57.57	26.79	0.42	8.06	6.50	0.45	99.79	53.72	844			
	56.80	26.09	0.21	8.10	6.65	0.48	98.32	53.21	860			
	58.41	26.07	0.18	7.55	6.58	0.49	99.28	51.61	875			
	57.05	26.70	0.40	8.29	6.40	0.39	99.21	54.99	891			
	58.06	26.02	0.25	8.02	6.71	0.54	99.60	52.52	905			
	40.51	15.87	0.23	5.07	3.64	0.36	65.70	55.87	920			
	57.85	26.20	0.23	8.03	6.52	0.48	99.31	53.42	936			
	57.78	26.24	0.25	8.19	6.57	0.45	99.47	53.85	950			
	60.08	24.56	0.18	6.05	7.34	0.65	98.85	43.08	965			
	59.15	21.91	0.85	6.97	5.00	0.91	94.79	54.15	996			

Appendix 1.1 (cont.)
Electron microprobe analyses of Unzen plagioclase (in wt.%)

Sample ID	SiO_2	Al_2O_3	FeO	CaO	Na_2O	K_2O	Total	An*	um**	Sr (ppm)	Ba (ppm)	Sr/ Ba
U1A Host Plag3	54.89	28.20	0.20	10.11	5.26	0.29	98.96	64.55	0			
	55.34	28.13	0.23	10.11	5.51	0.28	99.60	63.60	15			
	53.65	28.63	0.39	10.43	5.18	0.18	98.47	66.04	31			
	54.23	28.82	0.13	10.42	5.25	0.31	99.15	65.21	45			
	55.25	28.30	0.11	10.18	5.40	0.30	99.54	64.13	60			
	54.24	28.35	0.18	10.43	4.97	0.31	98.47	66.42	75			
	53.16	28.95	0.26	10.96	4.71	0.25	98.28	68.83	90			
	53.43	29.35	0.25	10.97	4.64	0.25	98.89	69.16	105			
	54.46	28.51	0.33	10.31	5.15	0.22	98.99	65.73	120			
	55.08	28.12	0.08	9.81	5.70	0.36	99.14	61.84	135			
	56.04	27.84	0.42	9.44	5.60	0.29	99.61	61.58	151			
	55.71	27.53	0.10	9.44	5.58	0.40	98.75	61.22	165			
	55.04	27.59	0.20	9.39	5.51	0.29	98.02	61.82	181			
	56.01	27.19	0.30	9.28	6.07	0.32	99.17	59.21	196			
	55.86	27.82	0.27	9.33	5.62	0.33	99.23	61.07	211			
	54.07	28.63	0.30	10.63	5.10	0.24	98.96	66.58	226			
	54.91	27.88	0.28	9.92	5.67	0.27	98.94	62.54	241			
	54.61	27.72	0.14	10.05	5.36	0.32	98.19	63.87	256			
	54.33	28.46	0.21	10.39	5.23	0.33	98.94	65.13	271			
	55.25	27.90	0.31	10.03	5.55	0.30	99.33	63.14	286			
	55.09	27.56	0.32	9.30	5.63	0.38	98.29	60.73	301			
	55.25	27.73	0.24	9.42	5.84	0.33	98.81	60.44	316			
	55.43	27.87	0.27	9.84	5.66	0.33	99.39	62.18	332			
	54.48	27.80	0.18	9.74	5.23	0.31	97.73	63.78	347			
	55.58	27.80	0.37	9.94	5.80	0.27	99.76	62.09	362			
	52.73	29.47	0.28	11.57	4.64	0.17	98.85	70.64	377			
	52.58	29.71	0.24	11.54	4.47	0.21	98.75	71.15	392			
	55.23	27.52	0.29	9.27	5.73	0.30	98.34	60.57	407			
	56.19	27.28	0.18	8.83	6.29	0.33	99.10	57.18	422			
	57.01	26.81	0.32	8.50	6.46	0.39	99.48	55.41	436			
	56.57	26.99	0.20	8.76	6.28	0.38	99.18	56.78	452			
	50.83	30.85	0.25	13.16	3.96	0.15	99.20	76.20	467			
	51.61	30.26	0.12	12.87	3.96	0.18	99.01	75.65	483			
	50.51	31.19	0.25	13.42	3.75	0.14	99.26	77.51	497			
	51.02	30.71	0.37	13.60	3.71	0.20	99.62	77.65	512			
	55.02	28.04	0.15	10.21	5.64	0.30	99.36	63.22	558			
	55.19	27.44	0.10	9.72	5.87	0.33	98.64	61.06	572			
	55.30	27.78	0.22	9.72	5.80	0.31	99.13	61.41	587			
	55.38	28.18	0.20	9.85	5.80	0.34	99.74	61.62	603			
	55.13	28.20	0.42	10.13	5.54	0.29	99.71	63.44	618			
	44.36	20.93	0.27	7.54	3.98	0.27	77.34	63.98	633			
	56.21	26.69	0.09	8.89	5.95	0.35	98.18	58.53	648			
	56.60	27.05	0.25	8.87	6.09	0.37	99.22	57.88	663			
	54.97	27.94	0.19	9.58	5.73	0.33	98.73	61.25	679			
	55.35	27.50	0.17	9.27	5.67	0.37	98.34	60.52	694			
	55.89	26.80	0.22	8.71	5.96	0.32	97.91	58.08	708			
	55.26	28.01	0.22	9.54	5.55	0.35	98.92	61.83	723			
	54.34	28.03	0.16	10.27	5.23	0.30	98.32	65.01	738			
	55.86	27.82	0.21	9.80	5.54	0.34	99.57	62.52	754			
	55.41	28.02	0.22	9.90	5.71	0.33	99.59	62.08	768			
	57.20	26.54	0.21	8.45	6.25	0.43	99.08	55.87	784			
	55.87	27.90	0.35	9.68	5.68	0.34	99.82	61.63	799			
	56.72	26.51	0.02	8.20	6.27	0.45	98.17	54.98	814			
	57.66	26.85	0.14	8.61	6.29	0.41	99.96	56.21	829			
	56.87	27.01	0.34	8.87	6.29	0.45	99.82	56.82	844			
	55.82	27.06	0.29	9.39	5.66	0.34	98.55	61.03	859			
	57.17	26.52	0.32	8.65	6.12	0.42	99.20	56.92	874			
	57.99	26.53	0.33	8.10	6.37	0.43	99.75	54.37	889			

Appendix 1.1 (cont.)
Electron microprobe analyses of Unzen plagioclase (in wt.%)

Sample ID	SiO_2	Al_2O_3	FeO	CaO	Na_2O	K_2O	Total	An*	um**	Sr (ppm)	Ba (ppm)	Sr/ Ba
	57.77	26.23	0.32	8.18	6.40	0.43	99.33	54.48	904			
	57.63	26.44	0.29	8.00	6.56	0.44	99.36	53.34	919			
	56.85	26.44	0.31	8.72	6.16	0.41	98.88	57.03	950			
	56.80	26.68	0.21	8.69	6.35	0.42	99.16	56.21	964			
	57.12	26.45	0.20	8.41	6.24	0.42	98.83	55.81	980			
U1A Host Plag4	55.82	27.46	0.17	9.40	5.79	0.37	99.01	60.41	0			
	55.11	27.52	0.07	9.21	5.98	0.41	98.30	59.05	18			
	56.36	27.74	0.23	9.07	6.16	0.32	99.88	58.32	35			
	56.67	27.18	0.17	9.28	6.16	0.33	99.78	58.85	54			
	56.70	26.73	0.18	8.85	6.20	0.39	99.04	57.32	71			
	56.39	27.21	0.10	9.10	6.10	0.37	99.27	58.45	91			
	56.99	26.90	0.18	8.78	6.06	0.42	99.33	57.55	108			
	56.47	26.60	0.18	8.68	6.14	0.41	98.49	56.96	127			
	57.29	27.02	0.22	8.76	6.21	0.42	99.93	56.93	145			
	56.85	26.46	0.24	8.70	6.19	0.45	98.89	56.69	163			
	56.96	26.97	0.23	8.66	6.31	0.38	99.51	56.40	180			
	56.81	26.91	0.29	8.96	6.22	0.42	99.60	57.44	199			
	57.04	27.10	0.20	8.66	6.18	0.46	99.63	56.62	217			
	56.08	27.07	0.31	9.27	5.85	0.30	98.88	60.08	236			
	56.18	27.50	0.27	9.14	5.97	0.31	99.36	59.28	253			
	55.91	27.40	0.25	8.87	6.13	0.37	98.93	57.72	271			
	56.74	26.91	0.16	8.53	6.42	0.39	99.14	55.61	290			
	56.61	27.14	0.26	8.86	6.41	0.36	99.64	56.70	308			
	56.46	27.38	0.19	9.28	5.82	0.35	99.48	60.08	325			
	55.74	27.25	0.20	9.29	5.66	0.35	98.49	60.71	344			
	56.40	27.35	0.23	9.17	5.98	0.34	99.46	59.19	362			
	56.46	27.46	0.34	9.28	5.94	0.33	99.80	59.72	380			
	55.84	27.68	0.23	9.33	6.00	0.33	99.41	59.58	398			
	56.83	27.03	0.28	9.16	6.17	0.40	99.87	58.21	416			
	56.91	27.01	0.16	8.51	6.41	0.38	99.38	55.63	435			
	56.87	27.06	0.18	8.93	6.33	0.40	99.78	57.03	452			
	56.85	26.99	0.31	8.84	6.11	0.36	99.46	57.76	470			
	56.30	27.43	0.09	9.16	6.13	0.32	99.43	58.66	489			
	56.97	26.74	0.17	8.60	6.30	0.40	99.18	56.22	507			
	55.63	27.38	0.21	9.27	5.86	0.37	98.73	59.79	524			
	55.70	27.06	0.35	9.09	5.92	0.40	98.52	58.98	543			
	56.72	27.09	0.32	8.89	6.05	0.32	99.39	58.24	561			
	56.57	26.62	0.32	8.64	6.09	0.37	98.61	57.21	580			
	58.29	26.74	0.37	8.12	6.67	0.48	100.67	53.18	597			
	54.91	28.41	0.25	10.31	5.49	0.30	99.68	64.01	615			
	55.49	27.76	0.27	9.22	5.83	0.32	98.89	59.99	634			
	56.88	26.73	0.14	8.90	6.08	0.40	99.13	57.86	652			
	55.93	27.57	0.16	9.24	5.66	0.34	98.89	60.67	669			
	57.25	26.70	0.16	8.69	6.07	0.41	99.28	57.31	688			
	57.11	26.58	0.28	8.43	6.48	0.44	99.31	54.91	706			
	57.55	26.55	0.23	8.17	6.73	0.43	99.66	53.32	724			
	57.54	26.64	0.01	8.22	6.52	0.42	99.35	54.21	742			
	44.83	21.22	0.33	6.87	4.90	0.35	78.51	56.68	760			
	57.46	25.97	0.21	7.85	6.64	0.47	98.60	52.49	778			
	57.40	26.44	0.21	8.04	6.50	0.45	99.03	53.66	796			
	58.00	26.29	0.27	7.88	6.64	0.39	99.46	52.88	814			
	57.57	26.23	0.18	7.90	6.58	0.45	98.92	52.88	832			
	57.58	26.76	0.24	7.97	6.65	0.51	99.71	52.69	851			
	53.68	29.33	0.13	11.38	5.00	0.24	99.76	68.49	868			
	51.09	30.77	0.26	13.44	3.97	0.13	99.67	76.62	887			
	52.14	30.04	0.28	12.44	4.23	0.21	99.34	73.70	905			
	52.63	29.55	0.39	11.73	4.68	0.21	99.18	70.59	923			

Appendix 1.1 (cont.)
Electron microprobe analyses of Unzen plagioclase (in wt.%)

Sample ID	SiO_2	Al_2O_3	FeO	CaO	Na_2O	K_2O	Total	An*	um**	Sr (ppm)	Ba (ppm)	Sr/ Ba
	53.07	29.22	0.30	11.16	4.66	0.22	98.64	69.58	941			
	55.92	27.80	0.19	9.33	5.75	0.30	99.28	60.67	959			
	57.23	26.76	0.23	8.81	6.32	0.34	99.68	56.94	977			
	57.14	26.44	0.21	8.08	6.75	0.48	99.10	52.80	996			
	57.58	26.51	0.10	8.04	6.46	0.45	99.14	53.77	1013			
	58.13	26.28	0.12	8.11	6.57	0.42	99.63	53.73	1031			
	57.21	26.56	0.26	8.16	6.45	0.47	99.11	54.11	1050			
	57.53	26.86	0.35	8.32	6.28	0.42	99.76	55.41	1068			
	56.17	27.12	0.13	9.04	5.96	0.38	98.79	58.77	1086			
	66.73	19.16	0.93	5.90	3.24	2.02	97.98	52.90	1104			
	51.89	28.63	0.65	13.05	3.41	0.34	97.97	77.71	1122			
	58.38	24.04	0.67	9.45	3.29	1.05	96.87	68.56	1141			
	50.20	30.96	0.65	14.11	2.86	0.32	99.11	81.60	1158			
	60.21	25.73	0.81	10.30	3.42	1.08	101.54	69.64	1176			
	63.90	22.77	0.86	8.68	2.59	1.74	100.55	66.71	1195			
	56.10	27.87	0.93	12.54	2.70	0.79	100.93	78.25	1212			
	55.61	25.85	0.86	11.02	2.48	1.09	96.91	75.51	1249			
U1A Host Plag5	55.74	27.73	0.25	9.35	5.76	0.28	99.11	60.72	0			
	54.55	28.49	0.31	10.45	5.02	0.27	99.09	66.39	25			
	55.10	27.83	0.15	9.71	5.39	0.30	98.47	63.06	51			
	55.46	27.85	0.31	9.49	5.75	0.35	99.21	60.88	76			
	55.03	27.73	0.06	9.92	5.30	0.30	98.32	63.93	101			
	54.75	28.16	0.27	10.01	5.40	0.33	98.90	63.60	126			
	54.42	27.80	0.21	9.78	5.50	0.33	98.04	62.66	152			
	55.71	27.65	0.06	9.60	5.92	0.35	99.29	60.51	177			
	55.16	27.58	0.21	9.43	5.91	0.35	98.63	60.10	202			
	54.56	28.32	0.27	10.59	5.30	0.27	99.31	65.56	228			
	54.72	27.84	0.06	10.03	5.39	0.28	98.31	63.91	252			
	49.10	23.89	0.11	8.15	4.43	0.35	86.02	63.02	278			
	56.07	27.29	0.20	8.95	6.05	0.34	98.90	58.32	303			
	55.56	27.77	0.25	9.62	5.62	0.37	99.19	61.65	328			
	55.69	27.39	0.18	9.30	5.80	0.35	98.70	60.21	354			
	55.94	27.87	0.25	9.67	5.70	0.34	99.77	61.54	379			
	56.33	27.74	0.53	9.35	5.76	0.35	100.08	60.46	405			
	55.33	27.98	0.32	9.60	5.55	0.34	99.13	61.96	429			
	55.48	27.48	0.13	9.35	5.85	0.36	98.65	60.11	455			
	57.21	26.36	0.15	8.40	6.24	0.32	98.69	56.15	480			
	57.39	26.58	0.28	8.35	6.47	0.45	99.52	54.69	505			
	57.13	26.66	0.25	8.57	6.34	0.40	99.34	55.98	531			
	57.19	26.27	0.19	7.95	6.34	0.49	98.44	53.80	556			
	54.78	27.89	0.13	9.98	5.20	0.28	98.26	64.57	581			
	54.52	28.40	0.16	10.45	5.04	0.27	98.84	66.28	606			
	55.48	28.12	0.18	9.75	5.60	0.37	99.49	62.03	631			
	55.24	27.96	0.21	9.81	5.35	0.22	98.78	63.80	657			
	56.46	27.06	0.34	8.88	6.21	0.39	99.34	57.39	682			
	56.64	26.96	0.19	8.62	6.22	0.42	99.05	56.50	708			
	57.64	26.61	0.20	8.20	6.20	0.40	99.24	55.42	732			
	56.10	26.95	0.26	8.87	6.04	0.37	98.59	58.03	758			
	56.46	27.33	0.20	9.07	6.00	0.28	99.35	59.08	783			
	56.25	26.95	0.22	8.95	5.87	0.47	98.71	58.50	809			
	56.92	26.87	0.30	8.50	6.30	0.41	99.30	55.86	834			
	56.64	26.57	0.21	8.13	6.20	0.43	98.19	55.07	859			
	55.59	27.81	0.19	9.82	5.75	0.34	99.50	61.71	885			
	55.74	27.03	0.22	9.26	5.78	0.30	98.33	60.34	909			
	55.77	27.93	0.17	9.31	5.71	0.34	99.24	60.57	934			
	55.80	28.07	0.33	9.98	5.50	0.29	99.96	63.32	960			
	56.57	26.86	0.27	8.68	6.21	0.38	98.97	56.84	985			

Appendix 1.1 (cont.)
Electron microprobe analyses of Unzen plagioclase (in wt.%)

Sample ID	SiO_2	Al_2O_3	FeO	CaO	Na_2O	K_2O	Total	An*	um**	Sr (ppm)	Ba (ppm)	Sr/ Ba
	56.59	27.10	0.37	9.02	5.83	0.37	99.27	59.25	1011			
	56.72	26.37	0.38	8.12	6.39	0.44	98.42	54.31	1036			
	57.18	26.54	0.30	8.24	6.42	0.39	99.08	54.76	1061			
	57.19	26.88	0.25	8.18	6.29	0.37	99.16	55.10	1086			
	57.12	26.87	0.11	8.34	6.14	0.40	98.98	56.06	1112			
	55.60	27.92	0.25	9.81	5.62	0.34	99.55	62.19	1137			
	54.70	27.82	0.28	9.71	5.63	0.34	98.48	61.92	1162			
	55.81	27.29	0.24	9.16	5.90	0.41	98.80	59.24	1188			
	56.34	26.88	0.35	8.61	6.28	0.42	98.88	56.24	1213			
	56.59	27.37	0.23	9.13	5.97	0.35	99.64	59.10	1238			
	56.45	26.96	0.19	8.81	6.21	0.43	99.03	57.02	1263			
	57.13	26.75	0.23	8.31	6.08	0.39	98.88	56.24	1288			
	55.59	27.29	0.19	9.49	5.74	0.40	98.69	60.70	1314			
	56.78	26.66	0.15	8.23	6.31	0.43	98.55	54.99	1339			
	56.17	26.82	0.19	8.60	6.23	0.33	98.34	56.71	1365			
	55.60	27.63	0.22	9.83	5.70	0.31	99.29	62.08	1389			
	53.67	28.85	0.16	10.95	4.74	0.23	98.60	68.77	1415			
	55.82	26.96	0.18	8.85	6.11	0.38	98.28	57.72	1440			
	56.53	26.89	0.13	8.50	6.23	0.39	98.67	56.25	1466			
	57.62	26.70	0.13	8.45	6.40	0.45	99.75	55.21	1491			
	54.69	27.64	0.10	9.61	5.43	0.32	97.79	62.58	1516			
	55.58	26.86	0.20	8.88	6.10	0.40	98.02	57.74	1541			
	56.12	27.48	0.22	9.07	5.92	0.36	99.17	59.11	1566			
	57.03	26.55	0.24	8.46	6.23	0.40	98.90	56.09	1591			
	56.87	27.00	0.02	8.82	6.09	0.37	99.17	57.74	1617			
	57.07	26.70	0.17	8.28	6.05	0.40	98.67	56.23	1642			
	57.72	26.44	0.16	7.97	6.55	0.39	99.22	53.47	1668			
	56.40	27.16	0.28	9.01	6.19	0.31	99.35	58.09	1693			
	56.80	26.82	0.21	8.51	6.13	0.42	98.89	56.52	1718			
	57.84	26.33	0.32	8.02	6.46	0.47	99.43	53.64	1743			
	58.50	25.96	0.33	7.52	6.49	0.43	99.23	52.05	1769			
	58.05	26.14	0.20	7.87	6.80	0.48	99.53	51.93	1794			
	57.86	26.60	0.19	7.97	6.44	0.41	99.47	53.76	1819			
	57.72	26.39	0.25	8.48	6.13	0.37	99.33	56.61	1845			
	57.12	26.79	0.09	8.24	6.07	0.43	98.73	55.88	1869			
	54.81	27.96	0.39	10.02	5.46	0.25	98.89	63.71	1894			
	51.94	29.48	0.67	12.24	4.37	0.21	98.90	72.79	1945			
U1A Host Plag6	55.25	28.01	0.50	9.94	5.59	0.31	99.60	62.73	0			
	53.85	28.52	0.17	10.79	5.07	0.23	98.62	67.09	11			
	53.74	28.68	0.22	10.94	4.97	0.30	98.84	67.49	24			
	54.77	28.79	0.23	10.43	5.22	0.26	99.70	65.57	36			
	54.46	28.44	0.21	10.47	5.29	0.32	99.20	65.06	48			
	54.49	28.95	0.15	10.68	5.39	0.21	99.86	65.61	60			
	53.98	28.67	0.42	10.55	5.36	0.21	99.18	65.44	72			
	55.04	28.64	0.10	10.60	5.35	0.24	99.97	65.46	84			
	53.07	29.02	0.16	11.32	4.99	0.22	98.77	68.49	96			
	56.42	27.43	0.26	9.27	5.94	0.33	99.65	59.67	108			
	56.11	27.93	0.37	9.19	5.93	0.33	99.85	59.50	120			
	55.51	27.50	0.18	9.32	5.81	0.34	98.66	60.25	133			
	56.33	27.13	0.28	9.16	6.03	0.39	99.32	58.81	145			
	56.65	27.48	0.29	9.23	6.02	0.34	100.01	59.21	157			
	56.51	26.79	0.35	8.85	5.78	0.36	98.63	59.04	169			
	57.90	27.18	0.13	8.60	6.02	0.40	100.22	57.25	181			
	56.01	27.26	0.18	9.21	6.25	0.26	99.18	58.57	193			
	52.27	25.62	0.20	8.92	5.14	0.32	92.47	62.03	205			
	56.14	27.63	0.28	9.25	6.00	0.32	99.61	59.43	217			
	57.39	26.75	0.23	8.67	6.34	0.41	99.80	56.22	229			

Appendix 1.1 (cont.)
Electron microprobe analyses of Unzen plagioclase (in wt.%)

Sample ID	SiO_2	Al_2O_3	FeO	CaO	Na_2O	K_2O	Total	An*	um**	Sr (ppm)	Ba (ppm)	Sr/ Ba
	56.05	27.06	0.31	9.07	6.04	0.37	98.90	58.60	241			
	55.49	27.81	0.25	10.09	5.62	0.35	99.62	62.82	252			
	56.17	27.14	0.20	9.07	5.89	0.39	98.85	59.09	265			
	55.70	27.57	0.30	9.30	6.26	0.34	99.47	58.46	277			
	57.05	26.60	0.30	8.44	6.48	0.45	99.32	54.90	289			
	56.69	27.06	0.19	8.85	6.17	0.38	99.35	57.43	301			
	56.18	27.67	0.21	9.61	5.74	0.38	99.79	61.09	313			
	57.53	26.68	0.16	8.35	6.27	0.40	99.38	55.58	325			
	57.79	26.27	0.26	8.14	6.71	0.52	99.69	52.98	337			
	56.79	26.71	0.36	8.43	6.37	0.45	99.10	55.27	349			
	58.05	26.23	0.29	7.82	6.65	0.50	99.54	52.24	361			
	57.42	26.88	0.17	8.33	6.35	0.48	99.63	54.96	373			
	56.75	26.99	0.31	8.71	6.31	0.34	99.42	56.69	385			
	56.93	26.35	0.14	8.31	6.56	0.38	98.67	54.49	398			
	58.30	25.63	0.15	7.84	6.78	0.46	99.16	52.02	410			
	56.94	27.21	0.23	8.60	6.28	0.42	99.69	56.18	422			
	58.39	26.28	0.32	7.92	6.52	0.44	99.86	53.23	434			
	57.29	26.86	0.26	8.58	6.39	0.39	99.77	55.84	446			
	56.67	26.70	0.22	8.38	6.32	0.38	98.66	55.58	458			
	57.51	26.42	0.21	8.20	6.31	0.45	99.10	54.82	470			
	57.62	26.30	0.17	8.16	6.68	0.47	99.39	53.30	482			
	58.06	26.37	0.22	8.21	6.60	0.49	99.95	53.62	494			
	56.58	26.85	0.27	8.63	6.26	0.42	99.00	56.38	506			
	57.64	26.02	0.17	8.22	6.63	0.50	99.17	53.52	518			
	58.02	26.20	0.15	8.16	6.33	0.42	99.28	54.71	530			
	56.84	26.74	0.21	8.50	6.39	0.37	99.04	55.72	542			
	52.79	29.57	0.25	11.68	4.52	0.23	99.05	71.10	555			
	53.85	28.23	0.36	10.86	5.14	0.27	98.71	66.76	566			
	56.03	27.66	0.24	9.49	5.95	0.40	99.77	59.91	578			
	56.54	27.26	0.41	9.09	6.36	0.39	100.04	57.40	590			
	57.23	26.62	0.29	8.74	6.15	0.43	99.45	57.07	602			
	56.43	26.92	0.35	9.14	6.03	0.35	99.21	58.88	614			
	57.17	26.78	0.12	8.76	5.76	0.45	99.04	58.51	626			
	57.36	26.79	0.18	8.80	5.82	0.47	99.42	58.32	638			
	55.98	26.29	0.72	10.99	3.51	0.80	98.30	71.81	650			
	50.27	31.11	0.52	13.96	3.22	0.18	99.27	80.40	663			
	50.88	30.26	0.73	13.78	3.03	0.34	99.03	80.34	675			
	57.50	23.55	0.88	9.67	2.51	0.98	95.10	73.45	687			
	59.79	23.00	0.72	9.08	2.60	1.12	96.32	70.93	699			
	50.70	33.15	0.65	14.76	2.67	0.17	102.11	83.87	711			
	48.67	32.22	0.37	14.92	2.82	0.10	99.10	83.61	735			
	54.66	28.56	0.69	12.61	2.86	0.65	100.03	78.22	747			
	49.26	31.33	0.57	14.02	3.32	0.14	98.64	80.23	759			
	51.02	30.27	0.60	13.67	3.74	0.17	99.48	77.76	771			
U2A E P-Plag1	54.82	27.61	0.22	9.91	5.65	0.31	98.52	62.44	0	863.6	169.18	5.1
	55.82	27.09	0.13	9.01	6.04	0.31	98.41	58.64	19			
	54.65	27.73	0.16	10.08	5.54	0.27	98.44	63.42	37			
	54.96	27.18	0.18	9.65	5.86	0.32	98.14	60.97	55			
	54.72	27.22	0.10	9.86	5.82	0.32	98.04	61.64	74			
	54.89	27.79	0.30	10.13	5.79	0.28	99.17	62.55	92			
	54.39	28.33	0.22	10.68	5.30	0.24	99.16	65.85	111			
	53.21	28.25	0.27	10.90	5.14	0.28	98.04	66.82	130			
	52.86	28.83	0.40	10.88	4.97	0.29	98.23	67.41	148			
	54.39	28.13	0.24	10.20	5.28	0.29	98.54	64.70	166			
	55.98	26.92	0.20	9.34	5.93	0.35	98.71	59.80	185			
	56.26	26.70	0.29	9.15	6.13	0.38	98.90	58.43	204			
	56.78	26.04	0.30	8.48	5.95	0.58	98.13	56.50	222	926.2	173.75	5.3

Appendix 1.1 (cont.)
Electron microprobe analyses of Unzen plagioclase (in wt.%)

Sample ID	SiO_2	Al_2O_3	FeO	CaO	Na_2O	K_2O	Total	An*	um**	Sr (ppm)	Ba (ppm)	Sr/ Ba
	55.92	26.74	0.23	8.52	6.27	0.34	98.02	56.31	241			
	56.45	26.41	0.24	8.69	6.06	0.43	98.29	57.23	259			
	55.81	26.91	0.27	9.23	5.95	0.38	98.55	59.32	277			
	55.06	27.56	0.18	9.66	5.68	0.39	98.53	61.42	296			
	55.63	27.33	0.18	9.41	5.92	0.43	98.90	59.70	315			
	56.57	26.28	0.22	8.12	6.46	0.41	98.08	54.16	334			
	55.58	27.07	0.22	9.03	6.01	0.33	98.24	58.73	352			
	57.75	25.51	0.10	7.71	6.70	0.49	98.26	51.78	370			
	58.02	25.98	0.25	7.89	6.53	0.49	99.17	52.92	389			
	55.76	27.01	0.16	9.13	5.93	0.42	98.40	59.01	407	939.8	151.76	6.2
	57.56	25.92	0.25	8.09	6.70	0.50	99.01	52.92	426			
	61.62	18.78	1.30	5.70	2.90	2.71	93.00	50.36	445			
	55.15	27.09	0.90	10.92	4.05	0.48	98.59	70.68	463			
	50.35	30.70	0.60	13.36	3.70	0.22	98.92	77.35	481			
	55.47	26.70	0.53	10.26	4.13	0.75	97.83	67.78	500			
	52.74	29.08	0.57	12.24	4.08	0.29	99.00	73.70	519			
	48.88	31.37	0.48	14.40	3.05	0.17	98.36	81.71	537			
	51.83	30.21	0.45	13.53	3.58	0.24	99.83	77.99	556			
	48.23	31.26	0.59	14.46	2.96	0.11	97.60	82.51	574	870.3	43.83	19.9
	50.25	30.72	0.64	13.88	3.26	0.13	98.88	80.37	592	983.2	62.39	15.8
	53.97	28.60	0.41	10.85	5.06	0.26	99.15	67.11	611	789.5	62.71	12.6
U2A E P-Plag2	56.29	26.79	0.32	8.82	6.28	0.32	98.83	57.19	0	934.4	147.65	6.3
	56.75	26.15	0.39	8.59	6.45	0.41	98.75	55.59	19			
	57.10	25.96	0.14	8.64	6.48	0.41	98.73	55.67	36			
	54.78	24.87	0.31	8.07	6.34	0.42	94.80	54.42	55			
	57.18	26.15	0.22	8.04	6.46	0.45	98.50	53.77	73			
	56.45	26.35	0.31	8.71	6.12	0.43	98.37	57.07	91			
	55.69	26.55	0.11	9.04	6.08	0.31	97.78	58.59	109			
	55.88	26.80	0.13	9.17	5.84	0.41	98.22	59.48	128			
	55.23	27.11	0.26	9.63	5.83	0.38	98.45	60.78	144			
	55.57	26.63	0.18	8.95	5.97	0.30	97.60	58.82	163			
	55.56	27.20	0.29	9.10	5.89	0.38	98.42	59.20	182			
	55.33	27.12	0.24	9.37	5.96	0.37	98.38	59.70	200			
	55.78	26.53	0.21	9.23	5.92	0.36	98.03	59.51	218			
	55.59	26.79	0.13	9.39	5.97	0.34	98.21	59.77	236			
	56.01	26.69	0.22	9.37	5.95	0.32	98.55	59.93	255			
	55.79	26.50	0.24	8.95	6.13	0.38	97.99	57.89	273	896.8	166.88	5.4
	56.19	26.85	0.14	8.63	6.15	0.37	98.33	57.01	291			
	56.69	26.79	0.13	9.08	6.18	0.40	99.27	57.98	309			
	56.31	26.48	0.21	8.98	6.16	0.43	98.57	57.69	328			
	56.22	26.73	0.29	9.22	6.19	0.42	99.07	58.25	345			
	55.80	27.01	0.16	9.37	6.03	0.37	98.75	59.42	364			
	56.18	26.79	0.28	9.20	5.99	0.45	98.89	58.83	382			
	55.54	26.63	0.12	9.08	6.03	0.33	97.72	58.83	400			
	55.83	26.69	0.00	9.01	5.96	0.36	97.85	58.77	419			
	55.60	27.06	0.22	9.35	5.99	0.36	98.58	59.54	436			
	57.26	26.81	0.18	9.26	6.11	0.37	100.00	58.83	455			
	56.26	26.78	0.14	9.25	6.27	0.45	99.15	57.94	473			
	55.75	26.72	0.19	9.31	6.05	0.38	98.40	59.14	491			
	56.07	26.54	0.42	9.01	6.09	0.39	98.52	58.15	509			
	56.34	26.48	0.24	8.89	6.11	0.37	98.44	57.80	527			
	56.93	26.37	0.11	8.54	6.15	0.41	98.50	56.59	546	870.8	178.87	4.9
	56.69	26.58	0.13	8.49	6.48	0.46	98.84	55.00	564			
	57.19	26.11	0.14	8.17	6.65	0.40	98.66	53.68	582			
	58.16	26.07	0.39	8.27	6.38	0.44	99.71	54.79	600			
	57.17	26.22	0.28	8.48	6.53	0.43	99.12	54.91	619			
	56.78	26.34	0.21	8.34	6.45	0.45	98.56	54.71	637			

Appendix 1.1 (cont.)
Electron microprobe analyses of Unzen plagioclase (in wt.%)

Sample ID	SiO_2	Al_2O_3	FeO	CaO	Na_2O	K_2O	Total	An*	um**	Sr (ppm)	Ba (ppm)	Sr/ Ba
	56.97	26.61	0.30	8.45	6.40	0.38	99.11	55.47	655			
	56.70	26.27	0.14	8.84	6.37	0.37	98.69	56.73	673			
	56.59	26.31	0.24	8.51	6.45	0.41	98.51	55.39	691			
	57.10	26.05	0.17	8.29	6.43	0.42	98.47	54.78	709			
	57.00	25.84	0.27	8.05	6.53	0.44	98.13	53.61	728			
	57.43	26.13	0.16	8.22	6.53	0.48	98.97	53.96	746			
	56.43	26.20	0.20	8.46	6.46	0.40	98.15	55.22	764			
	58.29	25.67	0.11	7.79	6.76	0.49	99.11	51.81	783			
	58.05	25.66	0.21	7.58	6.88	0.50	98.88	50.64	800	886.8	150.06	5.9
	57.86	25.38	0.31	7.39	6.93	0.52	98.38	49.77	819			
	58.84	25.07	0.21	7.28	6.88	0.53	98.81	49.57	836			
	59.52	24.27	0.21	7.00	6.65	0.73	98.38	48.70	855			
	58.26	25.06	0.15	7.13	7.00	0.60	98.20	48.41	873			
	57.26	26.15	0.35	8.07	6.72	0.41	98.97	53.09	891			
	56.48	26.52	0.24	8.64	6.39	0.32	98.58	56.30	909			
	56.91	26.02	0.29	8.35	6.45	0.43	98.45	54.78	928			
	56.86	26.04	0.25	8.42	6.20	0.43	98.20	55.95	946	975.8	115.77	8.4
	56.76	26.66	0.13	8.60	6.10	0.40	98.66	56.92	964			
	56.67	26.45	0.13	8.47	6.45	0.43	98.59	55.18	983			
	56.88	25.83	0.13	8.12	6.63	0.47	98.06	53.36	1000			
	53.95	28.20	0.18	10.70	5.17	0.29	98.49	66.22	1019			
	54.60	27.87	0.26	10.10	5.38	0.30	98.52	63.99	1036			
	55.92	27.02	0.18	9.31	6.12	0.37	98.93	58.90	1055	824.4	147.30	5.6
	57.17	25.84	0.21	8.19	6.55	0.41	98.38	54.05	1073			
	56.99	26.48	0.04	8.35	6.32	0.40	98.58	55.37	1091			
	56.05	26.13	0.13	8.59	6.08	0.43	97.41	56.92	1110			
	56.41	26.08	0.17	8.61	6.44	0.40	98.11	55.73	1128			
	55.47	26.55	0.28	8.75	5.95	0.36	97.35	58.11	1146			
	56.54	26.08	0.22	8.48	6.41	0.41	98.14	55.45	1164			
	57.28	26.03	0.28	8.16	6.57	0.46	98.77	53.72	1182			
	57.62	26.20	0.31	7.81	6.57	0.41	98.92	52.82	1200			
	56.25	26.74	0.19	8.78	6.20	0.41	98.57	57.09	1219			
	51.23	29.79	0.16	12.54	4.12	0.19	98.03	74.41	1236			
	56.52	26.44	0.31	8.67	6.12	0.42	98.47	57.00	1255			
	57.22	26.16	0.27	8.08	6.59	0.42	98.74	53.52	1274			
	55.13	27.36	0.28	9.42	5.94	0.36	98.50	59.91	1292			
	56.78	26.37	0.24	8.40	6.62	0.42	98.82	54.41	1310			
	57.24	25.96	0.12	8.24	6.61	0.48	98.65	53.72	1328			
	56.34	26.43	0.16	8.77	6.30	0.40	98.40	56.67	1346			
	57.71	25.93	0.22	7.62	6.68	0.44	98.60	51.70	1364			
	57.06	26.13	0.13	8.50	6.28	0.43	98.52	55.91	1382			
	57.80	25.63	0.12	7.83	6.62	0.50	98.49	52.36	1400			
	56.33	26.06	0.16	8.46	6.32	0.46	97.79	55.51	1419			
	60.70	24.12	0.49	7.19	6.02	1.28	99.80	49.63	1438			
	53.23	28.44	0.58	12.47	3.22	0.60	98.54	76.52	1490			
	56.77	26.42	0.92	11.28	2.91	1.29	99.59	72.87	1510			
	48.76	32.17	0.50	15.00	2.80	0.21	99.45	83.27	1528	914.1	77.38	11.8
	50.52	28.33	0.43	12.05	4.00	0.17	95.49	74.33	1546	885.6	87.58	10.1
U2A E P-Plag3	52.53	29.27	0.37	11.65	4.53	0.27	98.61	70.82	0	1050.5	170.44	6.2
	56.75	27.24	0.28	8.98	5.77	0.51	99.53	58.83	18			
	55.93	27.08	0.14	8.61	6.10	0.35	98.21	57.18	36			
	55.15	28.09	0.10	9.95	5.67	0.32	99.28	62.44	55			
	53.39	28.57	0.28	11.01	4.98	0.23	98.45	67.91	72			
	54.62	27.57	0.18	9.66	5.21	0.28	97.53	63.75	92			
	54.30	26.89	0.26	9.22	5.55	0.35	96.57	60.98	110			
	55.36	28.02	0.26	9.79	5.64	0.30	99.36	62.22	128			
	54.66	27.95	0.26	9.99	5.70	0.30	98.86	62.47	146	929.8	136.05	6.8

Appendix 1.1 (cont.)
Electron microprobe analyses of Unzen plagioclase (in wt.%)

Sample ID	SiO_2	Al_2O_3	FeO	CaO	Na_2O	K_2O	Total	An*	um**	Sr (ppm)	Ba (ppm)	Sr/ Ba
	54.28	28.34	0.23	10.37	5.23	0.34	98.79	65.06	164			
	54.04	28.24	0.24	10.59	5.24	0.33	98.69	65.53	183			
	55.22	27.57	0.29	9.71	5.79	0.32	98.88	61.37	200			
	55.38	26.95	0.30	9.18	5.78	0.40	97.99	59.74	219			
	54.79	28.13	0.11	10.41	5.75	0.34	99.53	63.10	238			
	50.92	25.37	0.33	9.05	5.49	0.35	91.50	60.81	256			
	54.37	28.11	0.33	10.31	5.52	0.35	99.01	63.69	274			
	53.66	28.02	0.15	10.45	5.19	0.30	97.76	65.57	292	934.2	189.33	4.9
	49.94	23.41	0.89	8.01	5.30	0.39	87.93	58.44	311			
	56.24	26.74	0.22	8.73	6.33	0.37	98.63	56.58	328			
	55.83	27.11	0.11	9.42	5.90	0.35	98.72	60.15	347			
	54.95	26.76	0.22	9.50	5.85	0.30	97.59	60.67	365			
	55.65	27.17	0.19	9.62	5.68	0.33	98.64	61.51	384	909.1	144.44	6.3
	55.10	27.04	0.10	9.10	5.95	0.29	97.58	59.30	402			
	54.42	26.22	0.18	8.94	5.96	0.35	96.05	58.63	420			
	54.85	27.79	0.33	9.92	5.69	0.32	98.90	62.29	438			
	56.60	26.46	0.31	8.67	6.31	0.45	98.80	56.18	456			
	53.35	28.14	0.41	10.66	5.01	0.42	97.99	66.28	475			
	51.58	29.94	0.34	12.84	3.83	0.25	98.77	75.90	493			
	51.35	30.30	0.31	13.05	3.72	0.29	99.02	76.52	511			
	44.74	23.87	0.38	9.43	3.27	0.55	82.24	71.19	530			
	50.45	29.49	0.56	13.23	3.50	0.22	97.44	78.07	548			
	48.49	30.87	0.65	13.88	3.13	0.16	97.19	80.85	566			
	48.26	32.01	0.41	15.23	2.50	0.06	98.48	85.61	584	828.9	52.27	15.9
	51.33	29.53	0.43	12.42	4.04	0.21	97.95	74.53	657	873.7	61.13	14.3
	50.08	30.19	0.56	13.06	3.70	0.15	97.73	77.23	676			
	49.57	30.56	0.51	13.81	3.48	0.15	98.08	79.19	694			
	49.65	29.69	0.46	13.16	3.58	0.14	96.68	77.96	712			
	52.98	28.35	0.57	10.62	4.78	0.24	97.54	67.90	730			
U4A E P-Plag1	57.27	26.71	0.25	8.63	6.44	0.38	99.68	55.84	0			
	56.50	26.63	0.19	8.61	6.35	0.42	98.69	55.99	15			
	57.40	26.71	0.27	8.57	6.28	0.32	99.55	56.49	31			
	57.36	26.78	0.19	8.36	6.26	0.42	99.36	55.59	45			
	57.37	26.49	0.18	8.77	6.12	0.40	99.33	57.35	60			
	57.17	26.71	0.43	8.53	6.19	0.41	99.45	56.37	76			
	57.26	26.65	0.31	8.33	6.23	0.38	99.15	55.76	91			
	56.41	26.68	0.12	8.49	6.10	0.40	98.19	56.62	106			
	56.60	26.63	0.12	8.54	6.34	0.41	98.64	55.86	121			
	57.34	26.57	0.22	8.60	6.33	0.43	99.49	56.00	136			
	56.83	26.66	0.33	8.58	6.30	0.43	99.13	56.03	151			
	56.58	26.46	0.36	8.45	6.30	0.39	98.54	55.82	167			
	56.71	26.33	0.26	8.56	6.16	0.36	98.37	56.80	182			
	56.10	27.29	0.28	9.61	5.49	0.34	99.12	62.22	197			
	56.88	26.45	0.66	10.63	3.60	0.66	98.88	71.41	211			
	50.13	31.18	0.57	13.57	3.16	0.18	98.79	80.26	227			
	50.45	31.08	0.59	13.65	3.38	0.15	99.31	79.48	242			
	57.57	26.69	0.53	10.55	3.46	1.02	99.82	70.23	257			
	53.65	29.62	0.63	12.95	3.42	0.30	100.57	77.71	273			
	49.48	31.53	0.53	14.32	3.07	0.18	99.12	81.48	287			
	54.76	25.83	0.72	10.39	2.84	1.14	95.69	72.31	318			
	58.79	24.82	0.87	9.80	3.20	1.06	98.54	69.67	348			
	56.59	25.21	1.05	10.23	3.24	0.99	97.30	70.73	363			
	49.26	32.05	0.67	15.06	2.40	0.16	99.60	85.43	378			
	60.23	23.11	0.93	8.97	2.56	1.42	97.23	69.27	409			
	57.94	23.97	0.66	9.58	3.16	1.01	96.33	69.65	424			
	67.34	20.18	1.40	6.26	3.08	2.01	100.27	55.13	454			
	57.69	28.58	0.61	11.85	3.65	0.72	103.11	73.06	469			

Appendix 1.1 (cont.)
Electron microprobe analyses of Unzen plagioclase (in wt.%)

Sample ID	SiO_2	Al_2O_3	FeO	CaO	Na_2O	K_2O	Total	An*	um**	Sr (ppm)	Ba (ppm)	Sr/ Ba
	60.05	25.14	1.05	10.31	3.04	1.21	100.80	70.81	484			
	57.29	25.30	1.15	10.07	2.84	1.09	97.73	71.94	500			
	43.33	24.85	1.02	11.00	1.56	0.79	82.55	82.44	514			
	48.03	32.69	0.41	15.32	2.52	0.11	99.07	85.36	529			
	50.28	30.12	0.69	14.05	2.69	0.40	98.23	81.97	590			
	47.88	32.19	0.59	15.33	2.48	0.11	98.58	85.53	605			
	49.52	31.31	0.52	14.38	2.78	0.20	98.72	82.84	620			
	48.14	32.41	0.62	15.16	2.23	0.15	98.72	86.42	635			
	59.46	27.04	0.97	10.94	3.41	0.91	102.73	71.65	666			
	56.66	26.02	1.09	10.79	3.34	0.80	98.70	72.25	680			
	48.75	31.77	0.52	14.60	2.85	0.13	98.61	83.05	696			
	47.29	33.28	0.62	16.37	1.93	0.08	99.57	89.04	711			
	61.84	23.14	0.50	8.95	2.46	1.32	98.21	70.33	742			
	46.99	33.48	0.55	16.12	2.08	0.08	99.32	88.15	771			
	47.91	32.08	0.75	15.31	1.98	0.15	98.18	87.80	787			
	56.65	28.10	0.53	12.35	2.49	0.86	100.98	78.67	802			
	55.15	28.21	0.59	12.21	3.29	0.69	100.15	75.43	832			
	49.41	31.02	0.50	14.72	2.30	0.35	98.29	84.78	847			
	50.77	23.42	2.92	11.77	2.30	0.47	91.64	80.97	908			
	47.00	33.31	0.58	16.16	1.93	0.06	99.04	89.02	923			
	58.93	25.39	0.73	10.17	3.41	1.00	99.63	69.76	938			
	51.91	31.79	0.74	14.69	2.84	0.31	102.27	82.36	953			
	47.17	32.93	0.57	15.80	2.30	0.09	98.85	86.84	968			
	57.56	26.61	0.95	11.65	2.88	0.81	100.45	75.98	998			
	47.17	32.94	0.69	16.24	1.93	0.13	99.11	88.75	1029			
	49.41	32.48	0.45	15.67	2.33	0.12	100.47	86.44	1059			
	46.80	33.55	0.60	16.01	1.90	0.10	98.96	88.88	1104			
U4A E P-Plag2	55.40	27.51	0.66	10.69	3.24	0.76	98.27	72.75	0			
	67.29	18.63	1.21	5.14	3.70	2.11	98.08	46.95	21			
	69.98	18.17	1.28	5.17	3.19	2.17	99.95	49.12	30			
	69.78	18.43	1.06	5.55	2.66	2.30	99.78	52.78	40			
	48.14	24.35	1.31	11.32	2.82	0.75	88.70	76.01	51			
	49.91	31.00	0.73	14.19	2.99	0.26	99.08	81.37	71			
	54.94	26.21	0.95	10.70	3.11	0.85	96.76	73.01	91			
	59.31	26.40	0.90	10.93	3.32	0.99	101.85	71.70	102			
	48.85	31.79	0.51	15.25	2.20	0.25	98.86	86.15	121			
	51.85	30.79	0.64	13.72	3.24	0.30	100.54	79.51	132			
	47.03	31.18	0.41	14.87	2.60	0.10	96.19	84.61	152			
	47.90	32.62	0.52	15.26	2.51	0.08	98.90	85.50	162			
	48.53	32.15	0.48	15.08	2.69	0.12	99.05	84.30	173			
	47.72	32.61	0.60	15.70	2.29	0.12	99.04	86.69	183			
	49.89	31.62	0.55	15.31	2.37	0.26	100.01	85.33	193			
	61.84	23.28	0.52	9.01	2.80	1.44	98.90	67.98	223			
	48.83	32.09	0.35	15.01	2.90	0.11	99.28	83.27	234			
	48.36	32.37	0.57	14.77	2.40	0.14	98.61	85.34	243			
	51.43	28.81	0.58	13.08	2.21	0.59	96.70	82.41	264			
	47.39	32.34	0.50	15.61	2.26	0.17	98.26	86.56	284			
	48.96	32.76	0.50	15.61	2.28	0.14	100.24	86.61	294			
	47.10	33.51	0.40	16.12	1.88	0.09	99.11	89.10	315			
	46.76	32.70	0.68	16.03	2.14	0.12	98.44	87.63	334			
	50.16	30.71	0.63	14.48	2.23	0.39	98.60	84.70	345			
	47.17	32.93	0.36	15.81	2.11	0.08	98.46	87.84	355			
	51.85	29.55	0.80	13.30	3.33	0.35	99.19	78.32	365			
	56.55	24.69	1.02	10.03	3.08	0.85	96.22	71.85	375			
	59.15	24.37	0.82	9.83	2.86	1.35	98.39	70.00	396			
	47.89	31.05	0.55	14.91	2.88	0.14	97.42	83.17	406			
	47.96	33.20	0.49	15.70	2.07	0.09	99.52	87.89	416			

Appendix 1.1 (cont.)
Electron microprobe analyses of Unzen plagioclase (in wt.%)

Sample ID	SiO_2	Al_2O_3	FeO	CaO	Na_2O	K_2O	Total	An*	um**	Sr (ppm)	Ba (ppm)	Sr/ Ba
	47.05	33.38	0.50	15.85	2.03	0.09	98.90	88.24	426			
	55.77	26.17	0.73	10.55	2.27	1.09	96.58	75.82	437			
	46.86	33.67	0.72	15.74	1.93	0.05	98.96	88.83	447			
	59.82	22.00	1.11	8.11	2.56	1.38	94.98	67.34	456			
	46.87	32.99	0.60	15.72	2.28	0.10	98.57	86.87	466			
	50.78	30.67	0.71	13.27	3.77	0.11	99.31	77.38	477			
	50.95	30.96	0.45	13.15	3.64	0.12	99.27	77.76	487			
	54.07	28.55	0.17	10.77	5.05	0.20	98.80	67.21	496			
	54.57	24.87	0.77	9.17	5.47	0.33	95.18	61.25	548			
	40.67	12.47	15.13	10.77	2.18	0.51	81.71	80.06	558			
U4A E P-Plag3	56.42	27.30	0.28	9.21	6.03	0.35	99.58	59.05	0			
	56.22	27.19	0.33	9.08	6.02	0.32	99.17	58.87	15			
	56.35	27.23	0.36	8.94	6.11	0.37	99.35	57.97	30			
	54.88	26.46	0.31	8.74	5.69	0.40	96.48	58.94	45			
	55.84	27.31	0.34	9.24	5.77	0.38	98.88	60.05	60			
	55.97	27.51	0.17	9.31	5.77	0.33	99.07	60.43	75			
	55.92	27.41	0.41	9.44	6.00	0.37	99.54	59.69	90			
	56.46	27.16	0.26	8.82	6.15	0.36	99.20	57.51	105			
	56.87	26.92	0.30	8.67	6.22	0.38	99.35	56.78	120			
	57.18	26.57	0.34	8.09	6.21	0.44	98.83	54.88	135			
	57.41	26.42	0.26	8.19	6.65	0.40	99.32	53.77	150			
	55.07	25.72	0.35	8.03	5.48	0.44	95.10	57.53	165			
	49.55	23.94	0.27	7.95	4.89	0.36	86.96	60.24	180			
	56.00	27.08	0.26	8.86	5.96	0.37	98.52	58.31	195			
	56.92	27.01	0.21	8.97	6.21	0.39	99.71	57.61	210			
	68.22	23.07	0.56	6.84	4.32	1.39	104.41	54.47	225			
	55.40	28.08	0.41	9.62	5.63	0.28	99.42	61.93	255			
	53.60	29.40	0.43	10.98	4.77	0.35	99.53	68.21	271			
	50.13	31.05	0.61	14.09	3.03	0.22	99.13	81.27	301			
	49.73	32.00	0.59	14.63	2.59	0.09	99.64	84.49	315			
	63.64	22.73	0.78	8.33	2.78	1.70	99.96	65.04	331			
	49.43	31.78	0.44	14.37	2.76	0.19	98.98	82.97	345			
	54.90	28.73	0.48	12.10	2.99	0.52	99.73	77.51	375			
	47.12	32.09	0.61	15.31	2.38	0.11	97.61	86.02	390			
	60.40	25.62	0.78	10.60	2.22	1.32	100.94	74.96	435			
	50.57	31.16	0.37	14.37	2.72	0.27	99.46	82.78	450			
	50.30	31.39	0.48	14.28	2.66	0.28	99.39	82.94	495			
	50.12	30.95	0.46	14.13	2.98	0.22	98.86	81.54	510			
	48.15	32.55	0.40	15.45	2.36	0.09	99.00	86.30	540			
	49.02	31.97	0.56	14.83	2.58	0.17	99.14	84.34	556			
	50.80	30.65	0.62	14.20	2.41	0.45	99.15	83.22	570			
	47.79	32.89	0.65	15.74	2.38	0.07	99.52	86.56	616			
	47.03	34.04	0.61	16.58	1.91	0.06	100.24	89.35	855			
	55.42	30.48	0.64	13.85	2.48	0.59	103.47	81.84	871			
	46.79	33.29	0.64	16.76	1.94	0.07	99.49	89.29	885			
	50.31	30.60	0.58	14.49	2.39	0.43	98.80	83.70	915			
	54.43	27.33	0.67	11.64	2.69	0.66	97.42	77.67	931			
	46.11	33.76	0.77	16.73	1.83	0.06	99.27	89.81	945			
	59.08	23.02	0.68	7.90	4.46	1.02	96.15	59.09	975			
	47.88	32.46	0.51	15.18	2.12	0.14	98.29	87.08	1005			
	45.87	32.83	0.66	16.22	1.94	0.08	97.60	88.91	1036			
	46.02	33.77	0.39	17.11	1.67	0.05	99.00	90.91	1065			
	46.58	33.19	0.42	16.32	1.93	0.07	98.51	89.06	1081			
	51.34	30.21	0.58	12.70	3.98	0.15	98.95	75.49	1095			
	51.73	30.28	0.40	12.81	4.05	0.13	99.41	75.37	1111			

Appendix 1.1 (cont.)
Electron microprobe analyses of Unzen plagioclase (in wt.%)

Sample ID	SiO_2	Al_2O_3	FeO	CaO	Na_2O	K_2O	Total	An*	um**	Sr (ppm)	Ba (ppm)	Sr/ Ba
UZN1663A Plag1	54.47	29.37	0.27	11.07	5.00	0.27	100.44	67.75	0			
	52.47	31.29	0.18	13.10	4.19	0.21	101.44	74.84	10	752.4	131.31	5.7
	52.46	31.29	0.24	13.15	4.10	0.14	101.38	75.61	20	757.0	125.00	6.1
	55.61	28.22	0.13	10.21	5.52	0.28	99.97	63.77	30			
	56.09	28.46	0.22	9.90	5.79	0.30	100.76	61.92	41			
	56.95	28.52	0.11	9.72	5.70	0.33	101.33	61.70	50			
	57.17	27.83	0.26	9.35	6.14	0.32	101.08	59.12	60			
	56.10	27.76	0.26	9.06	5.84	0.34	99.35	59.44	71			
	57.33	27.86	0.24	9.09	6.08	0.34	100.94	58.59	80			
	56.81	27.64	0.31	9.18	6.07	0.38	100.39	58.74	91			
	57.60	27.59	0.25	9.31	6.08	0.37	101.20	59.07	101			
	57.16	27.40	0.17	9.27	5.91	0.37	100.29	59.59	111	524.8	84.03	6.2
	57.46	27.70	0.08	9.01	6.23	0.36	100.85	57.74	121			
	58.16	27.31	0.20	8.70	6.29	0.42	101.07	56.45	131			
	56.16	28.13	0.22	10.29	5.57	0.34	100.71	63.52	141			
	54.58	29.07	0.25	10.96	5.25	0.26	100.37	66.59	151			
	54.74	28.91	0.25	10.81	5.28	0.29	100.29	66.01	161			
	56.13	28.04	0.15	9.84	5.83	0.30	100.30	61.59	172			
	56.84	27.70	0.20	9.38	6.22	0.34	100.67	58.84	181			
	56.10	28.54	0.17	9.87	5.62	0.30	100.60	62.50	192			
	56.27	28.27	0.18	9.62	5.79	0.30	100.44	61.24	202			
	56.43	28.08	0.20	9.68	5.99	0.34	100.74	60.45	211			
	56.78	27.49	0.14	8.97	6.08	0.37	99.83	58.17	232			
	56.66	28.24	0.23	9.79	5.83	0.28	101.04	61.57	242			
	56.01	28.06	0.27	9.55	5.65	0.29	99.82	61.64	252			
	56.47	27.96	0.11	9.49	5.88	0.33	100.23	60.47	262			
	57.11	27.85	0.19	9.39	5.86	0.35	100.74	60.19	272			
	55.62	28.41	0.31	10.41	5.49	0.28	100.51	64.33	282			
	55.92	28.48	0.24	10.38	5.53	0.29	100.84	64.05	292			
	54.55	27.93	0.24	9.81	5.55	0.37	98.45	62.36	302			
	55.59	28.50	0.26	10.00	5.61	0.27	100.23	62.95	312			
	57.10	28.26	0.35	9.55	5.81	0.34	101.42	60.82	323			
	56.26	28.03	0.30	9.92	5.75	0.33	100.59	62.02	332			
	57.55	27.37	0.17	9.24	6.19	0.35	100.86	58.55	343			
	57.32	28.30	0.20	9.72	6.01	0.34	101.89	60.49	353	626.4	127.35	4.9
	57.26	27.59	0.25	9.03	6.03	0.34	100.51	58.63	362			
	56.60	27.45	0.11	9.40	5.69	0.27	99.52	61.20	373			
	56.91	26.65	0.21	8.59	6.07	0.39	98.82	57.08	383			
	57.05	28.13	0.21	9.59	5.90	0.30	101.17	60.73	393			
	56.25	28.05	0.18	9.64	5.71	0.34	100.17	61.41	403			
	56.67	28.14	0.27	9.44	5.81	0.39	100.72	60.37	413			
	57.65	27.23	0.27	8.93	6.25	0.39	100.71	57.37	423			
	55.56	28.72	0.26	10.13	5.53	0.32	100.53	63.40	433			
	57.24	27.31	0.16	9.29	5.71	0.31	100.02	60.69	444			
	56.86	28.06	0.19	9.29	6.03	0.37	100.79	59.23	453			
	56.60	28.21	0.19	9.76	5.71	0.30	100.76	61.87	464			
	58.00	27.25	0.12	8.80	6.37	0.35	100.89	56.70	474			
	56.12	27.82	0.16	10.14	5.67	0.28	100.19	63.02	484			
	55.78	28.58	0.27	10.29	5.63	0.27	100.81	63.57	494			
	56.89	27.95	0.17	9.58	6.00	0.37	100.96	60.06	504			
	57.58	27.56	0.16	9.13	6.20	0.38	101.00	58.12	524			
	58.14	26.91	0.19	8.65	6.47	0.43	100.79	55.62	534			
	57.46	27.09	0.34	8.73	6.36	0.41	100.40	56.33	545			
	57.38	27.04	0.13	9.04	6.04	0.33	99.98	58.65	554			
	56.09	28.25	0.14	10.00	5.65	0.29	100.42	62.75	564			
	57.05	28.06	0.26	9.28	6.05	0.32	101.03	59.29	575			
	57.64	27.52	0.14	8.79	6.15	0.40	100.64	57.29	584			
	57.68	26.77	0.20	8.45	6.66	0.42	100.20	54.41	595			

Appendix 1.1 (cont.)
Electron microprobe analyses of Unzen plagioclase (in wt.%)

Sample ID	SiO_2	Al_2O_3	FeO	CaO	Na_2O	K_2O	Total	An*	um**	Sr (ppm)	Ba (ppm)	Sr/ Ba
	58.03	26.66	0.13	8.69	6.44	0.39	100.34	56.00	605			
	58.26	27.05	0.27	8.60	6.64	0.42	101.24	54.92	614			
	58.02	27.35	0.24	8.80	6.45	0.31	101.17	56.51	625			
	58.89	26.97	0.18	8.40	6.36	0.40	101.20	55.41	635			
	57.60	27.18	0.13	8.85	6.15	0.37	100.28	57.59	645			
	55.25	28.61	0.33	10.15	5.44	0.31	100.09	63.84	655			
	55.51	29.32	0.26	10.52	5.28	0.26	101.15	65.48	665			
	56.31	28.16	0.30	9.87	5.65	0.40	100.70	62.00	675			
	56.87	27.45	0.16	9.29	5.98	0.28	100.03	59.75	685			
	58.18	27.26	0.23	8.76	6.33	0.43	101.18	56.45	696	506.0	97.17	5.2
	58.95	26.57	0.09	8.20	6.49	0.40	100.70	54.36	705			
	58.83	26.82	0.16	8.31	6.48	0.40	101.00	54.71	715			
	58.70	26.92	0.26	8.55	6.46	0.36	101.25	55.63	726			
	57.72	27.25	0.30	8.58	6.09	0.38	100.31	57.01	735			
	59.14	26.94	0.18	8.18	6.52	0.47	101.43	53.93	746			
	57.97	27.02	0.09	8.43	6.37	0.44	100.32	55.29	756			
	58.64	27.11	0.16	8.77	6.46	0.37	101.51	56.23	776	600.2	135.19	4.4
	58.88	26.28	0.14	7.95	6.60	0.44	100.29	53.01	786			
	60.20	26.00	0.23	7.25	6.90	0.46	101.04	49.62	797			
	57.52	27.45	0.38	8.89	6.13	0.46	100.84	57.45	806			
	54.66	29.59	0.30	11.55	4.88	0.30	101.29	69.02	816			
	55.10	29.03	0.36	10.71	5.02	0.40	100.63	66.42	836			
	56.26	28.81	0.94	11.43	3.97	0.74	102.13	70.82	847			
	49.80	32.59	0.53	14.91	2.83	0.17	100.84	83.26	857			
	56.90	26.33	1.65	9.95	3.03	1.52	99.39	68.58	867			
	48.83	33.21	0.47	15.65	2.50	0.15	100.82	85.50	877			
	49.48	32.46	0.55	15.26	2.88	0.08	100.71	83.75	887	487.5	31.88	15.3
	49.26	32.53	0.54	15.12	2.76	0.13	100.34	83.93	897	482.1	28.46	16.9
	48.97	32.92	0.49	15.50	2.55	0.12	100.54	85.34	907	528.9	37.57	14.1
	50.08	32.64	0.68	15.13	2.81	0.11	101.46	83.81	917	508.7	39.13	13.0
	50.21	31.91	0.67	14.39	3.14	0.14	100.45	81.46	927			
	50.46	30.46	0.91	13.09	3.64	0.23	98.77	77.21	937			
UZN1663A Plag2	57.81	26.88	0.06	8.39	6.38	0.40	99.91	55.32	0			
	57.76	26.49	0.21	8.68	6.49	0.34	99.96	55.97	12			
	58.31	26.89	0.15	8.68	6.20	0.44	100.67	56.68	25			
	57.93	27.44	0.18	9.18	6.22	0.41	101.37	58.04	36			
	57.71	27.24	0.14	8.79	6.09	0.36	100.33	57.69	48			
	58.04	27.17	0.26	8.48	6.41	0.41	100.78	55.42	60			
	56.69	27.49	0.23	9.26	5.94	0.30	99.92	59.74	73			
	54.73	28.95	0.19	10.95	5.38	0.24	100.45	66.06	84			
	57.93	27.05	0.17	8.85	6.26	0.37	100.63	57.19	96			
	56.70	27.38	0.19	9.39	6.07	0.31	100.05	59.53	108			
	55.17	29.01	0.25	10.51	5.19	0.31	100.43	65.68	121			
	55.90	28.08	0.21	9.96	5.60	0.28	100.05	62.86	133			
	55.40	28.72	0.37	10.38	5.35	0.31	100.52	64.73	144	508.3	42.92	11.8
	51.54	31.42	0.26	13.96	3.91	0.20	101.29	77.27	156	510.7	59.07	8.6
	52.23	30.82	0.27	12.49	4.38	0.17	100.36	73.28	169			
	55.44	28.68	0.16	10.52	5.64	0.26	100.71	64.05	181			
	56.56	27.97	0.30	10.10	5.79	0.30	101.02	62.39	193			
	56.69	28.23	0.13	10.03	5.68	0.35	101.11	62.44	204			
	55.82	28.46	0.22	10.27	5.62	0.30	100.68	63.42	217			
	55.40	28.89	0.20	10.51	5.42	0.25	100.66	64.95	229			
	56.47	28.10	0.27	9.69	5.85	0.29	100.67	61.20	241			
	56.52	28.03	0.20	9.53	5.88	0.37	100.53	60.39	252			
	56.95	28.13	0.16	9.78	5.84	0.35	101.22	61.23	265			
	56.31	27.92	0.24	9.80	5.69	0.28	100.24	62.12	277			
	56.39	28.11	0.24	10.15	5.92	0.29	101.10	62.01	289			

Appendix 1.1 (cont.)
Electron microprobe analyses of Unzen plagioclase (in wt.%)

Sample ID	SiO_2	Al_2O_3	FeO	CaO	Na_2O	K_2O	Total	An*	um**	Sr (ppm)	Ba (ppm)	Sr/ Ba
	56.89	28.12	0.27	9.46	6.02	0.33	101.09	59.84	301			
	56.68	28.04	0.12	9.75	5.91	0.33	100.81	60.99	313			
	56.47	28.17	0.19	9.59	5.96	0.29	100.67	60.57	325			
	56.74	27.51	0.26	9.42	5.93	0.36	100.21	59.99	337			
	57.10	27.78	0.11	9.23	5.94	0.27	100.43	59.76	350			
	55.52	27.77	0.24	9.63	5.62	0.34	99.11	61.79	362			
	56.72	27.66	0.20	9.38	6.09	0.37	100.41	59.21	373			
	57.83	27.21	0.26	8.66	6.12	0.40	100.47	57.04	385			
	57.86	26.95	0.05	8.97	6.35	0.39	100.58	57.08	397			
	57.89	26.99	0.21	8.44	6.52	0.44	100.48	54.84	410			
	56.64	27.70	0.17	9.83	6.07	0.28	100.69	60.75	433			
	57.57	27.05	0.14	8.78	6.56	0.32	100.42	56.07	446			
	58.10	26.77	0.15	8.47	6.61	0.40	100.50	54.71	458			
	58.49	27.02	0.18	8.62	6.35	0.37	101.04	56.20	470			
	57.98	27.09	0.04	8.77	6.52	0.39	100.79	55.93	481			
	58.43	26.57	0.14	8.30	6.46	0.39	100.30	54.79	494			
	57.90	26.62	0.16	8.41	6.57	0.39	100.06	54.71	506			
	58.26	26.81	0.19	8.52	6.50	0.45	100.74	55.05	518			
	58.43	26.68	0.27	8.53	6.58	0.35	100.84	55.20	529			
	58.12	26.81	0.25	8.32	6.54	0.37	100.42	54.62	542			
	57.46	27.07	0.18	8.59	6.47	0.46	100.22	55.34	554			
	58.58	27.11	0.27	8.38	6.54	0.39	101.27	54.76	566			
	58.08	27.10	0.24	8.47	6.52	0.44	100.85	54.91	578			
	57.82	27.25	0.08	9.01	6.25	0.40	100.81	57.49	590			
	57.11	26.91	0.78	8.64	4.02	0.34	97.81	66.46	602			
	57.36	28.05	0.20	9.30	6.13	0.34	101.38	58.97	614			
	56.44	27.66	0.30	9.72	6.08	0.37	100.56	60.14	626			
	56.70	28.08	0.34	9.74	5.96	0.32	101.15	60.81	639			
	56.77	28.22	0.23	9.80	5.58	0.31	100.91	62.47	650			
	55.97	28.27	0.33	10.41	5.96	0.31	101.25	62.40	662			
	56.70	27.75	0.24	9.59	5.97	0.28	100.53	60.53	675			
	57.53	27.13	0.18	8.94	6.39	0.36	100.53	56.99	687			
	57.88	26.86	0.27	8.53	6.51	0.46	100.53	55.02	698			
	57.22	27.51	0.25	8.87	6.28	0.34	100.47	57.25	722			
	57.44	26.93	0.19	8.76	6.38	0.43	100.12	56.29	735	559.8	123.18	4.5
	58.23	27.02	0.21	8.67	6.19	0.38	100.70	56.92	747			
	58.69	26.76	0.21	8.83	6.57	0.36	101.42	56.03	758			
	57.50	26.89	0.15	8.57	6.12	0.37	99.59	56.91	771			
	57.62	27.14	0.08	8.90	6.33	0.38	100.45	57.05	783			
	57.55	27.19	0.18	8.95	6.13	0.40	100.40	57.85	795			
	57.75	27.31	0.18	9.32	6.36	0.37	101.29	58.05	807			
	56.89	27.25	0.14	8.79	6.14	0.36	99.58	57.49	819			
	57.33	27.72	0.09	9.24	6.25	0.37	100.99	58.29	831			
	56.76	27.89	0.16	9.72	6.06	0.29	100.88	60.45	843			
	57.40	27.96	0.28	9.75	6.03	0.33	101.76	60.52	855			
	56.91	27.92	0.17	9.45	6.00	0.31	100.74	59.98	867			
	56.39	28.14	0.17	9.63	6.03	0.30	100.67	60.32	879			
	57.43	27.92	0.16	9.61	5.99	0.33	101.44	60.32	891			
	56.67	28.23	0.27	9.64	5.96	0.27	101.04	60.73	903	520.3	121.73	4.3
	57.10	27.59	0.14	9.16	5.99	0.36	100.34	59.05	927			
	55.11	28.01	0.21	9.89	5.72	0.31	99.25	62.12	939			
	56.82	28.09	0.33	10.20	5.73	0.34	101.51	62.68	952			
	55.28	28.32	0.39	9.98	5.32	0.41	99.70	63.53	964			
	55.82	28.80	0.18	10.67	5.42	0.25	101.15	65.29	976			
	55.07	29.22	0.33	10.95	5.40	0.29	101.26	65.81	987			
	55.18	28.90	0.21	10.70	5.52	0.30	100.81	64.73	999			
	56.14	28.24	0.28	10.08	5.91	0.34	100.99	61.71	1012			
	56.87	27.82	0.21	9.88	5.97	0.37	101.12	60.91	1024			

Appendix 1.1 (cont.)
Electron microprobe analyses of Unzen plagioclase (in wt.%)

Sample ID	SiO_2	Al_2O_3	FeO	CaO	Na_2O	K_2O	Total	An*	um**	Sr (ppm)	Ba (ppm)	Sr/ Ba
	57.00	27.72	0.23	9.58	6.10	0.32	100.94	59.92	1035			
	57.27	27.40	0.22	9.49	6.14	0.34	100.86	59.43	1048			
	57.51	28.03	0.08	9.64	5.90	0.32	101.48	60.80	1060			
	56.71	28.69	0.24	10.24	5.63	0.32	101.83	63.28	1072			
	57.43	27.60	0.17	9.36	6.22	0.37	101.14	58.69	1084			
	56.73	28.28	0.16	9.99	5.84	0.32	101.32	61.88	1096			
	52.23	27.45	0.16	12.83	5.08	0.27	98.01	70.59	1108			
	56.13	28.23	0.14	9.94	5.57	0.36	100.37	62.65	1120			
	57.12	27.33	0.15	9.09	6.16	0.34	100.19	58.31	1132			
	57.07	27.40	0.16	9.18	6.12	0.42	100.36	58.38	1144			
	56.93	27.30	0.31	9.03	6.28	0.32	100.18	57.77	1156			
	55.57	28.53	0.17	10.82	5.46	0.24	100.81	65.48	1168			
	56.67	27.34	0.25	9.06	6.00	0.35	99.66	58.80	1180			
	57.58	27.19	0.23	8.97	6.05	0.42	100.43	58.13	1193			
	57.68	27.12	0.12	8.75	6.44	0.39	100.51	56.13	1204			
	58.32	26.92	0.21	8.51	6.46	0.40	100.81	55.36	1216			
	57.95	26.95	0.03	8.55	6.50	0.43	100.41	55.22	1229			
	58.18	26.98	0.21	8.69	6.37	0.42	100.85	56.13	1241			
	57.75	26.76	0.21	8.43	6.46	0.43	100.04	55.02	1253			
	56.54	27.69	0.17	9.55	5.85	0.30	100.10	60.83	1264			
	56.18	28.18	0.28	9.74	5.86	0.34	100.58	61.09	1276			
	56.48	27.59	0.15	9.55	6.10	0.32	100.19	59.82	1289			
	57.06	27.42	0.24	9.12	5.99	0.36	100.19	58.95	1301			
	54.49	27.31	0.24	10.60	5.53	0.34	98.51	64.34	1312			
	57.46	27.79	0.30	9.26	6.20	0.38	101.39	58.49	1325			
	54.46	29.48	0.20	11.15	5.06	0.21	100.56	67.88	1337			
	55.36	29.18	0.16	10.92	5.35	0.27	101.25	66.01	1349			
	56.23	28.05	0.13	10.21	5.70	0.32	100.64	62.91	1361	647.1	133.62	4.8
	57.55	27.21	0.14	9.02	6.19	0.39	100.49	57.84	1373			
	56.72	28.18	0.20	9.78	5.60	0.33	100.81	62.24	1385			
	55.98	28.68	0.11	10.57	5.50	0.26	101.10	64.76	1397			
	56.75	27.51	0.31	9.75	6.13	0.35	100.79	60.09	1409			
	57.56	27.82	0.26	9.20	6.02	0.32	101.19	59.19	1422			
	58.28	27.34	0.18	9.08	6.30	0.38	101.56	57.62	1433			
	58.60	26.48	0.19	8.14	6.67	0.37	100.45	53.62	1445			
	56.28	28.10	0.30	9.95	5.78	0.31	100.71	62.03	1457			
	57.67	27.39	0.34	9.00	6.22	0.36	100.99	57.76	1470			
	57.49	27.38	0.22	8.82	6.33	0.33	100.56	56.97	1481			
	57.29	27.11	0.10	9.02	6.32	0.35	100.20	57.48	1493			
	58.33	26.22	0.18	8.38	6.47	0.40	99.97	54.95	1506			
	58.77	26.02	0.16	7.95	6.70	0.41	100.01	52.80	1518			
	58.17	26.27	0.23	8.31	6.45	0.41	99.85	54.78	1530			
	57.41	27.73	0.25	8.88	6.18	0.39	100.85	57.43	1541			
	57.67	27.13	0.22	8.95	6.16	0.39	100.52	57.73	1554			
	58.04	26.77	0.22	8.70	6.46	0.42	100.61	55.84	1566			
	57.43	27.43	0.22	8.72	6.06	0.33	100.19	57.71	1578			
	57.83	27.01	0.22	8.48	6.34	0.43	100.30	55.61	1590			
	55.96	28.16	0.24	10.03	5.78	0.31	100.48	62.21	1601			
	57.95	27.14	0.09	8.79	6.44	0.42	100.83	56.16	1614	574.2	139.08	4.1
	59.17	26.66	0.18	8.02	6.78	0.46	101.27	52.57	1626			
	57.35	27.44	0.17	9.28	6.28	0.35	100.88	58.33	1638			
	57.21	27.55	0.11	9.50	6.16	0.30	100.83	59.52	1650			
	58.41	27.46	0.25	8.45	6.37	0.41	101.34	55.50	1662			
	57.82	27.06	0.11	8.66	6.29	0.36	100.30	56.56	1674			
	58.28	27.30	0.20	8.89	6.30	0.37	101.34	57.13	1686			
	57.71	27.36	0.09	8.85	6.12	0.35	100.49	57.78	1699			
	57.60	26.81	0.19	8.45	6.47	0.45	99.97	54.98	1710			
	57.35	27.23	0.25	9.39	6.21	0.42	100.84	58.59	1734	635.7	147.61	4.3

Appendix 1.1 (cont.)
Electron microprobe analyses of Unzen plagioclase (in wt.%)

Sample ID	SiO_2	Al_2O_3	FeO	CaO	Na_2O	K_2O	Total	An*	um**	Sr (ppm)	Ba (ppm)	Sr/ Ba
	58.21	27.18	0.19	9.03	6.47	0.41	101.48	56.76	1747			
	58.08	27.15	0.30	9.06	6.12	0.32	101.03	58.43	1758			
	58.98	26.77	0.21	7.91	6.85	0.43	101.15	52.03	1770			
	57.80	27.04	0.29	8.55	6.40	0.32	100.39	55.99	1782			
	57.89	27.07	0.26	8.46	6.55	0.40	100.63	54.90	1795			
	57.98	26.83	0.14	8.90	6.06	0.40	100.30	57.97	1807			
	57.66	27.48	0.20	8.82	6.19	0.43	100.78	57.13	1818			
	58.23	26.74	0.15	8.64	6.39	0.41	100.56	55.96	1831			
	57.32	27.16	0.30	9.05	6.09	0.37	100.28	58.34	1843			
	58.56	26.55	0.12	8.47	6.40	0.52	100.61	55.07	1855			
	50.17	31.81	0.59	14.81	3.12	0.20	100.71	81.69	1903			
	53.69	30.36	0.83	13.80	3.20	0.58	102.46	78.52	1926	451.7	27.53	16.4
	51.03	30.69	0.66	13.97	3.08	0.43	99.86	79.88	1939	471.4	106.49	4.4
	51.26	31.08	0.64	14.28	3.34	0.27	100.86	79.83	1951	466.9	84.53	5.5
UZN1663A Plag3	57.37	27.58	0.17	9.15	5.99	0.37	100.63	58.99	0			
	58.22	27.60	0.25	8.87	6.33	0.40	101.66	56.90	10			
	56.08	27.53	0.44	8.68	6.11	0.41	99.24	57.10	20			
	55.84	26.78	0.35	8.73	5.99	0.50	98.19	57.36	30			
	57.29	26.97	0.23	8.50	6.41	0.46	99.87	55.28	40			
	58.00	27.36	0.15	8.89	6.34	0.42	101.17	56.77	50			
	58.09	26.95	0.07	8.78	6.49	0.45	100.83	55.86	60			
	57.57	27.27	0.22	8.78	6.25	0.42	100.51	56.84	70			
	57.87	26.77	0.10	8.59	6.35	0.45	100.13	55.85	80			
	58.53	26.44	0.12	8.05	6.65	0.40	100.18	53.31	90			
	55.81	28.24	0.24	10.02	5.69	0.35	100.34	62.38	100			
	57.96	26.89	0.23	8.71	6.56	0.45	100.79	55.39	110			
	59.37	26.06	0.15	7.39	6.90	0.53	100.40	49.89	121			
	59.17	26.16	0.31	7.62	6.94	0.45	100.65	50.74	132			
	57.85	26.89	0.25	8.24	6.41	0.42	100.07	54.68	142			
	57.13	27.14	0.20	8.88	6.06	0.39	99.81	57.93	152			
	57.97	27.26	0.17	8.90	6.45	0.37	101.13	56.61	162			
	57.61	26.99	0.27	8.78	6.37	0.42	100.45	56.40	172			
	58.28	27.14	0.24	8.70	6.75	0.40	101.50	54.87	182			
	58.87	26.82	0.33	8.24	6.55	0.40	101.20	54.25	192			
	58.16	26.74	0.28	8.30	6.54	0.39	100.41	54.54	202	413.9	86.61	4.8
	58.77	26.28	0.05	7.95	6.58	0.43	100.06	53.12	212			
	58.83	26.63	0.33	8.02	6.92	0.37	101.09	52.41	222			
	55.97	28.42	0.11	10.27	5.52	0.33	100.62	63.73	232			
	57.05	27.12	0.31	8.86	6.20	0.35	99.89	57.49	242			
	57.67	27.18	0.23	8.65	6.28	0.46	100.46	56.20	252			
	57.13	27.38	0.13	9.18	6.35	0.38	100.54	57.70	262			
	56.68	27.84	0.19	9.28	6.34	0.36	100.69	58.06	272			
	57.59	27.45	0.21	9.19	6.15	0.38	100.97	58.49	282			
	55.94	27.22	0.30	9.12	6.30	0.47	99.34	57.40	292			
	57.78	27.00	0.23	8.46	6.39	0.38	100.23	55.57	302	561.2	108.85	5.2
	58.96	26.39	0.25	7.99	6.77	0.39	100.75	52.72	312			
	57.47	27.08	0.28	8.90	6.41	0.40	100.55	56.63	322			
	58.05	27.19	0.23	8.85	6.40	0.43	101.14	56.48	332			
	58.31	27.11	0.24	8.51	6.53	0.34	101.04	55.35	343			
	59.15	26.76	0.10	8.24	6.85	0.45	101.56	53.04	353	576.9	116.72	4.9
	58.28	26.77	0.17	8.36	6.60	0.42	100.60	54.35	364			
	54.76	29.17	0.17	11.09	5.29	0.28	100.77	66.54	374			
	59.17	27.03	0.15	8.34	6.71	0.41	101.81	53.92	384			
	58.34	26.81	0.25	8.28	6.53	0.45	100.65	54.27	394			
	59.30	26.10	0.15	7.99	6.73	0.52	100.78	52.42	404			
	58.21	26.96	0.12	8.75	6.24	0.46	100.73	56.63	414	540.9	57.66	9.4
	51.88	30.40	0.67	13.20	3.82	0.28	100.25	76.33	454	542.8	96.95	5.6

Appendix 1.1 (cont.)
Electron microprobe analyses of Unzen plagioclase (in wt.%)

Sample ID	SiO_2	Al_2O_3	FeO	CaO	Na_2O	K_2O	Total	An*	um**	Sr (ppm)	Ba (ppm)	Sr/ Ba
	51.88	30.40	0.67	13.20	3.82	0.28	100.25	76.33	454	461.4	53.99	8.5
UZN1663A Plag4	58.42	26.37	0.26	8.37	6.55	0.43	100.39	54.53	0			
	58.61	27.20	0.07	8.35	6.57	0.39	101.19	54.53	10			
	58.34	26.91	0.23	8.09	6.64	0.47	100.69	53.22	20			
	58.01	27.53	0.31	8.79	6.30	0.34	101.28	56.96	30			
	57.22	27.41	0.17	9.09	6.31	0.36	100.56	57.69	40			
	57.66	27.16	0.22	8.52	6.34	0.39	100.29	55.86	51			
	57.84	27.44	0.25	8.56	6.40	0.39	100.88	55.76	61			
	58.53	27.02	0.17	8.63	6.52	0.47	101.34	55.25	71			
	58.21	26.66	0.13	8.20	6.88	0.57	100.65	52.40	81			
	58.86	26.30	0.18	7.89	6.70	0.40	100.33	52.61	91			
	59.78	26.40	0.18	7.52	6.79	0.50	101.17	50.74	101			
	58.12	26.11	0.10	8.30	6.66	0.43	99.72	53.91	111			
	56.65	27.96	0.28	9.24	6.08	0.37	100.57	58.86	121			
	57.53	27.41	0.15	9.05	6.23	0.32	100.69	58.02	131			
	58.35	27.17	0.34	8.60	6.64	0.43	101.53	54.85	141			
	58.88	26.20	0.24	8.11	6.67	0.44	100.53	53.31	151			
	58.61	26.40	0.16	7.94	6.83	0.44	100.38	52.20	161			
	57.86	27.34	0.07	9.06	6.32	0.33	100.98	57.67	171			
	57.50	27.36	0.23	9.32	6.08	0.33	100.83	59.26	181			
	57.97	27.09	0.18	8.71	6.47	0.40	100.81	55.92	191			
	59.08	26.18	0.28	7.89	6.79	0.45	100.66	52.13	201			
	58.92	26.04	0.22	8.01	6.70	0.50	100.38	52.65	211			
	58.01	26.61	0.18	8.05	6.51	0.42	99.77	53.75	222	467.4	118.55	3.9
	58.09	27.37	0.21	8.77	6.51	0.40	101.35	55.93	232			
	57.67	26.75	0.16	8.56	6.42	0.39	99.96	55.65	242			
	58.41	26.95	0.18	8.76	6.47	0.37	101.14	56.12	252			
	59.06	26.71	0.35	7.97	6.75	0.40	101.23	52.70	262			
	59.04	26.47	0.27	7.93	6.67	0.47	100.84	52.65	272			
	58.79	26.34	0.19	7.93	6.96	0.48	100.68	51.59	282			
	58.96	25.97	0.15	7.95	6.98	0.45	100.45	51.72	292			
	58.30	26.65	0.25	8.35	6.48	0.44	100.46	54.67	303			
	59.24	26.64	0.27	8.02	6.74	0.50	101.42	52.56	313	529.1	136.93	3.9
	59.04	26.61	0.17	7.80	6.81	0.40	100.83	51.96	323			
	58.79	26.40	0.04	8.06	6.57	0.41	100.27	53.57	333			
	58.11	27.10	0.14	8.49	6.60	0.43	100.87	54.70	343			
	57.82	27.26	0.28	9.03	6.30	0.35	101.04	57.61	353			
	56.96	27.40	0.21	9.13	6.21	0.39	100.30	58.04	363			
	58.04	27.53	0.21	8.93	6.23	0.34	101.28	57.59	373			
	57.81	26.47	0.15	8.27	6.65	0.38	99.73	54.06	383			
	58.18	26.91	0.12	8.24	6.40	0.43	100.28	54.68	394			
	58.37	26.21	0.36	8.25	6.71	0.42	100.31	53.65	404			
	58.03	26.97	0.22	8.45	6.27	0.33	100.27	56.14	414	515.4	113.32	4.5
	58.11	26.93	0.21	9.08	6.28	0.39	101.00	57.67	424			
	58.40	26.76	0.13	8.21	6.38	0.36	100.25	54.89	434			
	58.43	26.54	0.16	8.36	6.25	0.39	100.13	55.73	444			
	58.53	26.57	0.23	8.52	6.47	0.47	100.80	55.09	454			
	57.97	26.43	0.16	8.22	6.53	0.40	99.70	54.29	464			
	58.91	26.48	0.18	7.93	6.58	0.43	100.52	53.06	475			
	58.77	27.03	0.17	8.27	6.57	0.47	101.28	54.03	485			
	57.69	26.84	0.13	8.66	6.32	0.41	100.05	56.26	495			
	58.89	26.39	0.15	7.80	6.81	0.52	100.56	51.56	505			
	58.69	26.26	0.16	8.11	6.68	0.42	100.31	53.33	515	520.0	153.59	3.4
	58.22	26.83	0.25	8.41	6.48	0.39	100.58	55.03	545			
	58.73	26.72	0.16	8.02	6.63	0.48	100.74	53.02	555			
	58.30	26.88	0.11	8.23	6.29	0.50	100.32	54.79	565			
	56.26	28.13	0.41	10.51	5.06	0.55	100.91	65.21	575			

Appendix 1.1 (cont.)
Electron microprobe analyses of Unzen plagioclase (in wt.%)

Sample ID	SiO_2	Al_2O_3	FeO	CaO	Na_2O	K_2O	Total	An*	um**	Sr (ppm)	Ba (ppm)	Sr/ Ba
	55.93	25.42	0.66	9.45	5.65	0.98	98.09	58.77	585			
	53.03	29.34	0.47	12.15	4.73	0.39	100.10	70.36	595			
	50.87	30.11	0.75	13.23	3.62	0.36	98.95	76.88	615			
	57.20	24.82	2.51	10.31	3.44	1.48	99.76	67.70	635			
	48.95	32.52	0.65	15.50	2.80	0.09	100.52	84.28	646	513.4	64.09	8.0
	50.02	32.34	0.69	15.05	3.14	0.09	101.32	82.36	656	528.5	61.14	8.6
	49.87	31.54	0.46	14.65	3.18	0.13	99.83	81.57	666	486.3	62.38	7.8
	51.70	31.05	0.68	13.59	3.65	0.20	100.87	77.94	676	469.9	46.34	10.1
	51.79	30.41	0.62	13.31	3.73	0.18	100.04	77.26	686			
UZN1663A Plag5	56.13	28.54	0.22	10.26	5.42	0.29	100.85	64.25	0			
	55.90	28.80	0.24	10.37	5.54	0.23	101.08	64.27	10			
	55.73	28.36	0.21	10.28	5.63	0.27	100.48	63.53	21	738.9	156.10	4.7
	55.19	28.51	0.17	10.21	5.51	0.32	99.91	63.63	30			
	55.85	28.63	0.14	10.24	5.53	0.32	100.72	63.61	40			
	55.79	28.29	0.21	10.03	5.43	0.29	100.03	63.71	50			
	56.08	28.99	0.19	10.03	5.55	0.24	101.08	63.41	60			
	54.84	28.67	0.19	10.54	5.38	0.25	99.88	65.19	70			
	55.61	28.60	0.26	10.63	5.41	0.27	100.78	65.19	80			
	56.24	27.89	0.25	9.44	5.90	0.35	100.06	60.17	90			
	57.19	27.79	0.20	9.61	5.99	0.38	101.16	60.15	101			
	55.68	28.15	0.26	9.89	5.55	0.51	100.03	62.03	110			
	56.76	27.98	0.19	9.14	5.95	0.43	100.45	58.89	120			
	55.87	28.61	0.22	10.24	5.68	0.31	100.92	63.09	130			
	56.39	28.57	0.23	9.79	5.79	0.28	101.05	61.72	151			
	56.52	28.11	0.22	9.64	5.79	0.32	100.60	61.22	161			
	56.79	27.71	0.25	9.59	6.08	0.33	100.74	59.94	170			
	57.33	27.60	0.18	8.99	6.12	0.37	100.59	58.03	181			
	57.34	27.33	0.12	8.97	6.18	0.35	100.29	57.84	190			
	57.92	27.28	0.23	8.32	6.42	0.35	100.53	55.12	200			
	58.51	27.18	0.15	8.68	6.45	0.39	101.35	55.93	211			
	57.85	27.20	0.21	8.62	6.45	0.38	100.72	55.80	221			
	58.26	27.45	0.11	8.72	6.14	0.40	101.07	57.15	231	560.9	116.92	4.8
	56.28	28.11	0.15	9.55	5.87	0.35	100.32	60.57	241			
	53.17	30.23	0.16	12.25	4.47	0.18	100.45	72.51	251			
	50.70	21.66	4.31	11.24	3.81	1.17	92.89	69.33	261			
	52.31	30.97	0.34	13.02	4.17	0.24	101.05	74.70	271			
	52.96	30.61	0.34	12.29	4.33	0.21	100.74	73.01	280			
	53.03	30.49	0.24	12.32	4.52	0.23	100.83	72.16	291			
	52.58	30.01	0.33	11.73	4.55	0.13	99.33	71.47	301			
	56.34	28.55	0.17	10.23	5.57	0.30	101.16	63.52	311			
	56.80	28.20	0.21	9.77	5.82	0.32	101.11	61.42	321			
	55.23	27.46	0.44	9.34	5.90	0.30	98.67	60.07	331			
	57.76	27.44	0.21	9.04	6.19	0.43	101.07	57.75	341			
	57.77	27.41	0.12	8.89	6.43	0.31	100.93	56.85	351			
	57.45	27.26	0.25	8.86	6.18	0.35	100.34	57.59	361			
	57.31	27.65	0.15	9.25	6.06	0.29	100.71	59.28	372			
	57.61	27.66	0.16	9.26	6.06	0.36	101.11	59.04	381			
	57.46	27.44	0.20	8.64	6.33	0.34	100.41	56.44	391			
	56.13	28.28	0.20	9.77	5.76	0.34	100.48	61.57	401			
	58.08	27.08	0.29	8.62	6.45	0.44	100.95	55.59	411			
	56.71	27.95	0.16	9.17	5.98	0.43	100.40	58.86	421			
	56.85	27.96	0.11	9.24	5.83	0.32	100.32	60.04	431			
	57.01	27.60	0.12	8.75	6.36	0.34	100.19	56.64	442			
	55.76	28.76	0.32	10.10	5.57	0.28	100.80	63.29	452			
	57.44	27.40	0.10	9.04	6.36	0.39	100.73	57.25	461			
	57.34	27.71	0.23	9.47	5.84	0.37	100.97	60.40	471			
	55.10	29.43	0.22	10.89	5.15	0.23	101.02	66.92	482			

Appendix 1.1 (cont.)
Electron microprobe analyses of Unzen plagioclase (in wt.%)

Sample ID	SiO_2	Al_2O_3	FeO	CaO	Na_2O	K_2O	Total	An*	um**	Sr (ppm)	Ba (ppm)	Sr/ Ba
	55.69	28.24	0.19	10.20	5.51	0.31	100.14	63.65	492			
	57.17	28.08	0.23	10.09	5.95	0.34	101.85	61.59	501			
	56.27	27.83	0.12	9.82	5.83	0.34	100.22	61.40	511			
	55.60	28.62	0.28	10.52	5.40	0.44	100.86	64.29	522			
	56.82	28.72	0.23	9.79	5.71	0.42	101.68	61.53	532			
	58.32	27.04	0.15	8.24	6.27	0.46	100.48	55.03	541			
	57.69	27.53	0.20	9.19	6.34	0.42	101.36	57.60	552			
	56.23	28.50	0.29	10.29	5.56	0.30	101.17	63.70	562			
	52.30	31.23	0.24	12.59	4.00	0.20	100.55	74.96	572			
	57.98	27.13	0.12	9.03	6.31	0.43	101.00	57.26	582			
	51.21	32.06	0.16	14.42	3.51	0.19	101.55	79.59	592			
	50.53	31.87	0.22	14.71	3.37	0.15	100.85	80.68	602			
	56.34	28.18	0.22	9.97	5.73	0.41	100.85	61.89	612			
	55.59	28.28	0.35	10.25	5.42	0.47	100.36	63.49	621			
	56.16	28.42	0.10	9.93	5.75	0.38	100.75	61.83	662			
	55.93	28.55	0.16	10.20	5.78	0.38	101.00	62.36	672			
	56.46	27.84	0.12	9.59	6.00	0.43	100.44	59.90	682			
	56.29	28.17	0.11	9.75	5.88	0.50	100.71	60.43	702			
	54.11	29.42	0.25	11.28	4.90	0.31	100.27	68.41	713			
	56.83	27.05	0.39	8.69	6.15	0.96	100.07	55.00	732			
	57.51	27.54	0.20	9.25	6.24	0.43	101.17	58.11	742			
	53.57	30.47	0.23	12.43	4.61	0.21	101.52	72.04	752			
	58.30	26.86	0.27	8.49	6.50	0.38	100.80	55.22	762			
	57.23	27.76	0.26	9.37	6.01	0.27	100.89	59.89	772			
	55.61	28.42	0.27	10.02	5.60	0.28	100.20	63.01	783			
	56.89	27.38	0.40	9.24	6.08	0.32	100.31	59.08	793			
	51.27	31.04	0.25	13.77	3.71	0.13	100.17	78.22	803			
	49.36	32.87	0.21	15.70	2.73	0.09	100.96	84.78	812			
	56.76	28.16	0.21	9.99	6.11	0.35	101.58	60.74	823			
	55.72	28.72	0.16	10.17	5.84	0.31	100.92	62.33	832			
	55.57	29.30	0.15	10.94	5.53	0.27	101.77	65.33	842			
	56.34	28.41	0.14	9.88	5.64	0.26	100.68	62.59	852			
	57.10	27.86	0.29	9.60	5.76	0.61	101.22	60.10	863			
	55.49	28.26	0.42	10.03	5.09	1.02	100.32	62.13	883			
	55.48	29.31	0.37	10.96	5.13	0.35	101.59	66.69	892			
	57.06	27.86	0.12	9.59	5.83	0.32	100.77	60.94	913			
	57.76	27.26	0.27	8.93	6.57	0.39	101.19	56.22	923			
	58.40	26.48	0.13	8.07	6.52	0.47	100.07	53.56	934			
	58.28	27.00	0.31	8.56	6.40	0.46	101.01	55.51	943			
	58.18	26.75	0.13	8.70	6.49	0.37	100.62	55.92	953			
	56.91	27.20	0.20	9.27	6.21	0.38	100.17	58.47	963	592.0	125.96	4.7
	58.53	27.11	0.31	8.83	6.44	0.38	101.61	56.44	973			
	58.13	27.09	0.17	9.02	6.35	0.42	101.18	57.11	983			
	57.96	27.36	0.24	9.00	6.34	0.42	101.33	57.12	1003			
	57.69	27.05	0.16	8.81	6.38	0.37	100.46	56.62	1014			
	58.38	26.65	0.21	8.72	6.31	0.47	100.73	56.29	1023			
	51.96	30.87	0.71	13.82	3.76	0.34	101.46	77.14	1053	482.7	54.28	8.9
	51.96	30.87	0.71	13.82	3.76	0.34	101.46	77.14	1053	478.0	49.72	9.6
	52.11	29.78	1.55	13.43	3.49	0.33	100.68	77.87	1063	474.1	47.04	10.1
	51.49	29.97	1.15	13.48	3.33	0.26	99.68	79.00	1073	420.3	72.48	5.8
	58.76	24.82	1.34	9.44	3.90	1.52	99.77	63.49	1094			
	50.19	31.86	0.69	15.28	3.01	0.18	101.21	82.76	1103	502.6	88.23	5.7
UZN1663A Plag6	56.76	27.59	0.22	9.59	6.11	0.35	100.61	59.77	0			
	56.62	28.19	0.21	9.78	6.03	0.35	101.20	60.51	10			
	56.41	27.86	0.21	9.87	5.87	0.28	100.51	61.58	20			
	56.46	27.95	0.18	9.82	5.85	0.35	100.61	61.29	30			
	56.79	28.12	0.31	9.96	5.76	0.32	101.26	62.07	40			

Appendix 1.1 (cont.)
Electron microprobe analyses of Unzen plagioclase (in wt.%)

Sample ID	SiO_2	Al_2O_3	FeO	CaO	Na_2O	K_2O	Total	An*	um**	Sr (ppm)	Ba (ppm)	Sr/ Ba
	56.37	28.43	0.29	10.08	5.96	0.30	101.43	61.69	50			
	57.04	27.58	0.15	9.98	5.81	0.33	100.88	61.93	60			
	56.62	27.27	0.28	9.75	5.81	0.35	100.09	61.27	71			
	57.10	27.66	0.17	9.84	5.89	0.35	101.00	61.19	81			
	56.91	27.40	0.14	9.13	6.25	0.36	100.20	58.00	91			
	56.96	27.62	0.14	9.26	6.03	0.34	100.36	59.24	101	591.4	106.17	5.6
	57.21	27.80	0.21	9.26	6.32	0.39	101.19	57.99	111			
	56.93	27.47	0.23	9.51	6.23	0.37	100.73	59.04	121			
	57.52	27.45	0.12	9.41	6.07	0.38	100.96	59.33	131			
	57.36	27.70	0.17	9.45	5.83	0.39	100.90	60.29	141			
	57.76	27.11	0.31	9.03	6.19	0.39	100.79	57.86	151			
	58.03	27.33	0.25	9.07	6.23	0.36	101.28	57.92	161			
	56.47	27.57	0.17	9.77	5.90	0.40	100.28	60.76	171			
	56.60	27.87	0.21	9.72	5.83	0.38	100.61	61.06	181			
	57.56	27.22	0.28	8.61	6.47	0.40	100.54	55.63	191			
	58.37	26.80	0.21	8.62	6.38	0.42	100.79	55.91	202			
	58.06	27.36	0.24	8.80	6.30	0.43	101.19	56.66	212			
	56.12	28.32	0.21	10.30	5.84	0.33	101.12	62.54	222			
	56.53	27.54	0.60	9.32	5.78	0.35	100.12	60.34	232			
	56.62	27.93	0.08	9.95	5.73	0.33	100.64	62.16	242			
	56.28	28.17	0.23	10.34	5.87	0.34	101.22	62.47	253			
	56.47	28.18	0.21	10.27	5.59	0.26	100.98	63.72	273			
	57.38	27.16	0.10	8.88	6.53	0.39	100.45	56.20	283			
	57.48	27.42	0.21	8.98	6.22	0.38	100.70	57.62	293			
	57.42	27.27	0.20	9.37	6.39	0.40	101.05	57.97	303			
	56.51	27.91	0.16	10.11	5.83	0.31	100.82	62.24	313			
	57.74	27.08	0.22	8.95	6.31	0.39	100.70	57.21	323			
	59.43	25.62	0.13	7.45	7.00	0.44	100.06	50.05	334			
	58.82	27.04	0.20	8.62	6.46	0.38	101.52	55.76	344			
	57.10	26.94	0.07	9.21	6.15	0.39	99.86	58.47	354	638.6	137.45	4.6
	58.42	26.53	0.21	8.61	6.30	0.41	100.47	56.19	364			
	58.42	26.81	0.17	9.03	6.55	0.39	101.38	56.53	374			
	57.86	27.25	0.23	9.24	6.36	0.40	101.34	57.79	384			
	58.22	27.21	0.23	8.84	6.43	0.40	101.32	56.41	394			
	58.20	26.95	0.13	8.19	6.46	0.37	100.31	54.54	404	543.4	116.00	4.7
	58.05	26.80	0.26	8.87	6.62	0.44	101.04	55.68	414			
	58.16	27.01	0.16	9.03	6.52	0.40	101.28	56.64	424			
	58.37	27.10	0.21	9.18	6.37	0.36	101.60	57.67	434			
	58.19	27.01	0.25	8.62	6.37	0.40	100.85	56.02	444			
	57.40	27.02	0.13	8.94	6.22	0.42	100.13	57.39	454	580.9	123.40	4.7
	57.35	27.44	0.21	9.26	6.18	0.36	100.81	58.58	465			
	57.73	26.67	0.18	8.90	6.47	0.55	100.51	55.90	475			
	57.43	25.82	0.69	9.18	5.91	0.84	99.88	57.62	485			
	52.83	28.59	1.28	11.78	3.64	0.39	98.51	74.51	495	523.3	48.54	10.8
	49.78	31.95	0.71	15.50	2.98	0.14	101.06	83.24	505	548.0	65.20	8.4
	50.73	31.29	0.73	14.94	3.27	0.14	101.09	81.44	515	542.3	64.22	8.4
UZN1663A Plag7	57.27	27.14	0.18	9.29	6.45	0.43	100.77	57.46	0			
	57.58	27.13	0.15	9.02	6.34	0.33	100.55	57.51	10			
	57.57	27.24	0.04	9.04	6.34	0.36	100.59	57.45	20			
	56.31	28.30	0.23	10.20	5.79	0.34	101.17	62.46	30	717.4	134.73	5.3
	55.11	28.34	0.23	10.35	5.66	0.25	99.94	63.63	41			
	55.02	28.84	0.22	11.04	5.26	0.30	100.67	66.55	51	771.0	156.88	4.9
	57.14	27.98	0.10	9.51	6.02	0.32	101.07	59.99	60			
	57.23	27.64	0.29	9.48	6.22	0.33	101.19	59.11	70			
	56.96	27.76	0.30	9.57	6.20	0.39	101.18	59.24	80	625.5	108.32	5.8
	57.50	27.58	0.32	9.30	6.20	0.37	101.27	58.60	90			
	57.36	27.60	0.23	9.49	6.13	0.38	101.19	59.30	101			

Appendix 1.1 (cont.)
Electron microprobe analyses of Unzen plagioclase (in wt.%)

Sample ID	SiO_2	Al_2O_3	FeO	CaO	Na_2O	K_2O	Total	An*	um**	Sr (ppm)	Ba (ppm)	Sr/ Ba
	57.02	28.51	0.28	10.12	5.67	0.25	101.86	63.10	111			
	56.08	28.49	0.47	10.19	5.81	0.34	101.39	62.32	131			
	56.17	28.36	0.28	10.36	5.89	0.30	101.36	62.59	141			
	55.64	28.55	0.15	10.59	5.44	0.28	100.64	64.93	151			
	56.24	28.43	0.21	10.03	5.86	0.31	101.09	61.90	161			
	56.99	27.64	0.25	9.27	6.37	0.36	100.88	57.95	171			
	54.56	29.60	0.20	11.62	4.93	0.32	101.22	68.86	181			
	55.98	28.30	0.18	10.61	5.43	0.31	100.81	64.87	221			
	55.88	28.75	0.20	10.61	5.24	0.31	100.99	65.67	232			
	56.28	28.42	0.22	10.44	5.57	0.32	101.25	63.92	242			
	57.38	25.53	0.23	7.90	6.49	0.43	97.96	53.33	252			
	58.00	26.49	0.21	8.27	6.83	0.40	100.20	53.38	262			
	57.12	27.10	0.26	9.41	5.82	0.45	100.16	60.01	272			
	54.98	29.36	0.23	11.29	4.99	0.24	101.08	68.36	281			
	54.58	29.08	0.29	11.11	5.12	0.18	100.36	67.69	291			
	56.50	27.78	0.22	9.89	5.97	0.30	100.66	61.20	302			
	55.48	26.10	0.35	9.01	5.91	0.39	97.24	58.85	312			
	57.83	27.35	0.24	9.41	6.16	0.33	101.32	59.17	322			
	57.29	27.65	0.18	9.70	5.96	0.35	101.13	60.58	342			
	57.10	27.62	0.17	9.59	6.15	0.35	100.98	59.63	352			
	58.19	27.71	0.37	9.23	6.23	0.39	102.12	58.23	363			
	55.08	29.67	0.31	11.77	4.99	0.23	102.05	69.29	373			
	57.94	27.34	0.25	9.31	6.25	0.41	101.50	58.28	383			
	56.35	27.38	0.20	9.76	5.91	0.35	99.95	60.95	392			
	57.21	27.64	0.20	9.81	5.78	0.39	101.03	61.40	402			
	57.83	26.85	0.23	8.95	6.59	0.34	100.79	56.37	412			
	56.00	28.17	0.31	10.31	5.91	0.32	101.02	62.31	423			
	56.52	27.84	0.27	9.75	5.73	0.28	100.39	61.87	433			
	56.84	27.82	0.20	9.38	5.81	0.35	100.41	60.37	443			
	57.22	27.64	0.22	9.46	6.01	0.36	100.91	59.76	453	619.8	137.55	4.5
	58.40	26.81	0.19	8.74	6.34	0.42	100.90	56.38	463			
	56.36	28.33	0.45	9.96	5.76	0.47	101.32	61.54	473			
	57.66	24.92	1.99	9.75	4.20	1.58	100.09	62.79	483			
	53.57	29.12	0.71	12.26	4.28	0.58	100.52	71.62	493			
	50.71	31.35	0.59	14.29	3.44	0.28	100.66	79.32	503			
	52.80	30.58	0.58	13.41	3.74	0.55	101.66	75.77	513			
	50.55	31.05	0.42	14.69	3.34	0.22	100.27	80.48	523			
	52.07	31.85	0.43	14.17	3.46	0.24	102.21	79.30	543			
	51.62	30.87	0.34	13.63	4.01	0.24	100.72	76.20	553			
	52.85	29.90	0.73	13.49	3.43	0.77	101.17	76.23	584			
	49.81	32.05	0.31	15.47	2.81	0.26	100.70	83.47	594			
	53.73	29.71	0.72	13.05	3.28	0.77	101.25	76.32	644			
	56.25	28.98	0.94	12.20	3.54	1.15	103.06	72.24	654			
	51.29	30.96	0.63	14.54	3.18	0.51	101.12	79.76	664			
	50.77	31.58	0.70	15.15	2.87	0.42	101.48	82.16	674			
	52.66	30.90	0.74	13.30	3.86	0.30	101.76	76.15	694			
	50.46	32.02	0.50	15.08	3.03	0.23	101.32	82.21	705			
	48.56	33.00	0.65	16.51	2.45	0.17	101.34	86.30	734			
	51.01	31.95	0.55	15.01	3.19	0.31	102.02	81.08	765			
	48.54	33.34	0.60	16.28	2.17	0.27	101.20	86.94	785			
	48.14	33.53	0.69	16.92	2.15	0.09	101.52	88.34	795			
	48.72	33.24	0.64	16.66	2.61	0.08	101.95	86.09	805			
	47.03	32.48	0.39	16.06	2.27	0.09	98.32	87.18	815			
	48.31	33.62	0.48	16.82	2.19	0.07	101.49	88.16	825	507.5	25.32	20.0
	47.43	34.39	0.50	17.54	1.76	0.06	101.68	90.64	835	561.6	32.35	17.4
	48.68	33.05	0.40	16.50	2.53	0.06	101.22	86.43	845	504.0	24.44	20.6
	48.88	32.80	0.63	15.95	2.76	0.09	101.11	84.83	855			
	49.42	32.51	0.58	15.58	2.81	0.09	101.00	84.28	865			

Appendix 1.1 (cont.)
Electron microprobe analyses of Unzen plagioclase (in wt.%)

Sample ID	SiO_2	Al_2O_3	FeO	CaO	Na_2O	K_2O	Total	An*	um**	Sr (ppm)	Ba (ppm)	Sr/ Ba
	49.87	32.26	0.82	15.76	2.83	0.08	101.63	84.42	875			
UZN1663B Plag1	50.76	31.95	0.21	14.12	3.70	0.14	100.88	78.62	0			
	55.39	28.91	0.28	10.98	5.34	0.28	101.17	66.16	10			
	56.08	28.25	0.12	10.49	5.72	0.32	100.98	63.45	20			
	51.98	31.09	0.26	13.52	4.02	0.17	101.04	76.33	30	569.1	87.60	6.5
	51.75	31.20	0.22	13.79	3.81	0.17	100.94	77.60	41			
	51.58	30.79	0.09	13.66	3.98	0.19	100.30	76.59	51	593.5	83.55	7.1
	51.90	30.56	0.30	13.46	4.38	0.16	100.77	74.79	61			
	53.09	30.38	0.29	12.86	4.44	0.18	101.24	73.57	71			
	54.18	29.60	0.30	11.82	5.01	0.24	101.16	69.24	81			
	55.57	28.42	0.23	10.44	5.51	0.31	100.49	64.21	91			
	56.23	28.06	0.21	10.20	5.75	0.36	100.81	62.55	101			
	57.25	27.45	0.18	9.35	6.26	0.41	100.89	58.39	112			
	58.85	26.71	0.13	8.53	6.30	0.47	101.00	55.77	122	449.1	74.07	6.1
	58.69	27.05	0.13	8.26	6.82	0.44	101.39	53.21	132			
	56.15	28.09	0.18	10.11	5.80	0.33	100.65	62.25	142			
	56.56	28.03	0.23	10.24	5.78	0.31	101.16	62.72	152			
	57.95	26.76	0.22	8.87	6.53	0.44	100.76	56.00	162	537.2	134.70	4.0
	58.29	27.20	0.21	8.70	6.47	0.38	101.24	55.95	172			
	56.69	28.18	0.27	10.14	5.82	0.32	101.42	62.28	182			
	57.95	26.98	0.27	8.85	6.24	0.39	100.69	57.17	192			
	57.93	27.07	0.17	8.93	6.62	0.46	101.18	55.78	202			
	57.22	27.50	0.05	9.38	6.26	0.39	100.79	58.52	212			
	58.18	26.65	0.24	8.86	6.59	0.39	100.91	55.93	222	69.8	189.89	0.4
	57.58	27.10	0.16	8.99	6.14	0.34	100.30	58.11	232			
	57.20	27.24	0.18	9.54	6.19	0.40	100.74	59.18	242			
	57.95	27.12	0.00	9.31	6.28	0.42	101.07	58.13	253			
	60.02	25.88	0.11	8.01	6.81	0.46	101.29	52.43	263			
	57.19	27.30	0.25	9.31	6.33	0.43	100.80	57.92	273			
	55.73	27.94	0.25	9.71	5.62	0.41	99.66	61.69	283			
	58.13	26.88	0.08	8.83	6.37	0.41	100.69	56.56	293			
	54.98	28.55	0.80	11.86	4.31	0.56	101.05	70.88	303			
	50.33	31.80	0.58	14.71	3.39	0.19	101.00	80.44	354	520.7	65.74	7.9
	50.33	31.80	0.58	14.71	3.39	0.19	101.00	80.44	354	440.6	217.64	2.0
	50.57	31.46	0.58	14.93	3.27	0.17	100.97	81.27	364	508.0	70.91	7.2
UZN1663B Plag2	60.22	25.06	0.12	6.92	7.51	0.62	100.45	46.01	0			
	60.86	24.84	0.22	6.95	7.13	0.73	100.73	46.96	10	508.3	133.65	3.8
	59.02	26.05	0.21	7.70	7.05	0.50	100.53	50.47	20			
	57.29	26.58	0.21	8.76	6.82	0.43	100.08	54.71	30			
	58.06	26.27	0.25	8.77	6.63	0.45	100.42	55.36	40			
	58.31	27.00	0.29	8.86	6.40	0.45	101.31	56.39	51			
	58.29	26.69	0.22	8.57	6.52	0.44	100.75	55.18	61			
	58.38	26.95	0.10	8.20	6.54	0.44	100.60	54.03	71			
	58.33	26.70	0.22	8.88	6.27	0.57	100.97	56.49	81			
	57.40	27.79	0.29	9.84	6.06	0.39	101.77	60.41	91			
	58.54	27.09	0.14	8.50	6.39	0.44	101.11	55.44	101			
	56.57	27.40	0.30	9.65	5.94	0.42	100.28	60.29	121			
	57.75	27.09	0.20	9.11	6.26	0.35	100.76	57.93	131			
	58.07	26.51	0.30	8.92	6.72	0.38	100.90	55.67	141			
	57.91	26.42	0.31	8.47	6.60	0.53	100.23	54.30	152			
	58.49	26.45	0.15	8.54	6.67	0.46	100.75	54.50	162	641.2	195.52	3.3
	58.00	26.85	0.20	8.95	6.26	0.47	100.74	57.08	171			
	56.92	27.45	0.17	9.52	6.08	0.35	100.49	59.67	182			
	57.69	27.37	0.33	9.26	6.25	0.43	101.32	58.09	192			
	57.59	27.42	0.27	9.21	6.39	0.40	101.29	57.55	201			
	57.21	27.55	0.22	9.70	6.12	0.38	101.18	59.84	212			

Appendix 1.1 (cont.)
Electron microprobe analyses of Unzen plagioclase (in wt.%)

Sample ID	SiO_2	Al_2O_3	FeO	CaO	Na_2O	K_2O	Total	An*	um**	Sr (ppm)	Ba (ppm)	Sr/ Ba
	57.94	27.15	0.32	9.25	6.35	0.37	101.36	57.94	222			
	57.69	27.32	0.20	9.32	6.17	0.37	101.06	58.78	231			
	58.45	26.86	0.19	8.89	6.39	0.43	101.21	56.60	242			
	58.10	27.25	0.19	8.68	6.59	0.40	101.22	55.38	252			
	58.96	26.58	0.20	8.21	6.63	0.46	101.04	53.67	262			
	58.56	26.78	0.13	8.64	6.63	0.39	101.14	55.15	273			
	57.78	27.28	0.32	9.40	6.23	0.49	101.50	58.28	282			
	51.25	29.11	0.55	12.71	4.76	0.33	98.70	71.43	312			
	52.08	29.82	0.69	12.84	4.35	0.25	100.03	73.63	322			
	54.87	28.84	0.39	11.28	5.21	0.49	101.07	66.43	333			
	57.94	27.83	0.37	9.90	5.33	0.69	102.05	62.22	342	655.0	159.48	4.1
	54.75	28.08	0.78	11.97	3.96	1.02	100.56	70.62	373			
	48.91	32.54	0.46	15.73	2.74	0.13	100.50	84.60	403			
	48.91	32.64	0.45	15.95	2.73	0.13	100.82	84.78	423	556.3	59.99	9.3
	48.84	32.75	0.51	16.29	2.57	0.08	101.04	86.02	433	509.7	47.56	10.7
	49.80	32.92	0.46	15.79	2.83	0.09	101.89	84.42	443			
	49.54	32.56	0.43	15.79	2.78	0.11	101.21	84.53	454			
	49.57	32.12	0.39	15.61	2.91	0.09	100.70	83.87	464	555.4	45.52	12.2
	50.41	32.33	0.52	15.35	2.98	0.14	101.73	83.11	474			
	49.78	32.10	0.67	15.28	2.98	0.11	100.92	83.17	484			
	49.55	31.75	0.59	15.64	2.90	0.11	100.54	83.82	494			
	51.29	31.57	0.66	14.14	3.58	0.19	101.44	78.97	504			
UZN1663B Plag3	57.98	27.26	0.28	8.97	6.32	0.43	101.23	57.07	0			
	57.54	27.18	0.28	9.30	6.39	0.43	101.12	57.71	10			
	57.70	27.10	0.05	9.24	6.33	0.39	100.81	57.92	21			
	57.34	27.13	0.19	9.01	6.23	0.33	100.22	57.89	30			
	57.08	27.63	0.18	9.34	5.96	0.34	100.53	59.75	40			
	56.42	28.16	0.18	9.94	5.87	0.34	100.91	61.55	50			
	57.32	27.82	0.22	9.51	6.07	0.39	101.33	59.57	60			
	57.04	28.05	0.14	9.96	6.07	0.32	101.59	60.91	71			
	56.18	27.74	0.22	9.82	5.87	0.28	100.11	61.45	80			
	57.91	26.98	0.23	8.90	6.42	0.41	100.85	56.56	90			
	57.95	27.15	0.31	8.87	6.34	0.36	100.97	56.98	100			
	57.10	27.74	0.19	9.81	6.18	0.37	101.40	59.94	111			
	57.71	27.63	0.16	9.18	6.25	0.35	101.29	58.15	121			
	57.76	27.73	0.08	9.55	6.09	0.34	101.55	59.78	130			
	57.69	27.25	0.23	9.19	6.29	0.37	101.02	57.97	150			
	55.08	28.88	0.20	10.67	5.37	0.29	100.49	65.36	161			
	57.53	27.70	0.28	9.65	6.42	0.29	101.87	58.95	171			
	58.05	26.70	0.10	8.54	6.44	0.46	100.29	55.30	180	560.6	121.37	4.6
	57.33	27.37	0.17	9.44	5.95	0.38	100.64	59.88	190			
	57.84	27.60	0.20	9.47	6.31	0.38	101.80	58.58	201			
	57.63	27.33	0.07	9.23	6.27	0.43	100.95	57.93	211			
	56.93	27.62	0.25	9.85	5.98	0.40	101.02	60.71	221			
	57.80	26.96	0.24	8.93	6.40	0.46	100.79	56.58	230			
	57.81	26.93	0.19	8.80	6.56	0.42	100.71	55.77	240			
	58.95	26.61	0.18	8.00	6.78	0.52	101.05	52.31	251			
	58.67	26.62	0.12	8.67	6.43	0.40	100.92	55.92	261			
	57.47	27.17	0.14	8.92	6.13	0.41	100.23	57.69	271			
	57.92	26.82	0.26	8.97	6.32	0.42	100.71	57.12	280			
	56.83	26.89	0.20	8.57	6.42	0.43	99.34	55.57	291			
	58.54	27.09	0.28	8.58	6.40	0.42	101.30	55.75	301			
	58.19	26.61	0.17	8.72	6.33	0.41	100.43	56.38	311	555.8	138.15	4.0
	58.65	26.45	0.07	8.43	6.49	0.44	100.54	54.90	320			
	58.32	26.68	0.26	8.64	6.46	0.38	100.73	55.81	330			
	58.17	26.16	0.10	7.85	6.71	0.44	99.42	52.34	341			
	59.06	25.80	0.17	7.75	6.86	0.51	100.15	51.26	351			

Appendix 1.1 (cont.)
Electron microprobe analyses of Unzen plagioclase (in wt.%)

Sample ID	SiO_2	Al_2O_3	FeO	CaO	Na_2O	K_2O	Total	An*	um**	Sr (ppm)	Ba (ppm)	Sr/ Ba
	57.63	27.06	0.21	8.97	6.39	0.45	100.72	56.72	361			
	58.81	26.75	0.12	8.12	6.71	0.51	101.01	52.96	370			
	59.44	26.56	0.05	8.17	6.76	0.44	101.43	53.16	380			
	58.30	26.77	0.12	8.38	6.35	0.45	100.37	55.21	391			
	58.71	26.53	0.29	8.24	6.72	0.50	101.01	53.26	401			
	59.85	25.98	0.23	7.48	6.94	0.46	100.93	50.27	411			
	59.87	26.22	0.10	7.64	6.88	0.52	101.23	50.81	420	852.0	324.81	2.6
	59.12	26.06	0.12	7.39	7.02	0.56	100.26	49.36	431			
	58.31	27.29	0.25	8.83	6.28	0.36	101.30	57.10	441			
	57.94	27.14	0.23	9.34	6.15	0.35	101.15	58.95	451			
	58.50	27.37	0.35	9.02	5.98	0.39	101.63	58.59	461			
	58.51	27.21	0.22	8.91	6.37	0.40	101.62	56.83	470			
	50.97	32.48	0.62	15.29	3.08	0.14	102.58	82.61	481	817.6	177.20	4.6
	50.97	32.48	0.62	15.29	3.08	0.14	102.58	82.61	481	869.1	188.94	4.6
	50.97	32.48	0.62	15.29	3.08	0.14	102.58	82.61	481	973.6	228.83	4.3
UZN1663B Plag4a	51.58	31.41	0.37	14.09	3.75	0.19	101.39	78.15	0	691.4	91.26	7.6
	51.81	31.45	0.37	13.94	3.75	0.21	101.52	77.85	10			
	51.26	31.53	0.19	14.16	3.68	0.17	100.99	78.62	20			
	52.12	31.11	0.24	13.39	3.84	0.12	100.83	77.15	30			
	52.06	31.26	0.38	13.30	4.02	0.19	101.20	75.96	40			
	52.39	30.86	0.23	12.95	4.14	0.19	100.77	74.91	51			
	52.58	31.17	0.22	13.37	4.13	0.20	101.67	75.53	61			
	52.48	30.80	0.24	13.20	4.01	0.17	100.90	75.94	71			
	52.10	31.01	0.21	13.49	3.77	0.24	100.81	77.09	81			
	52.48	30.75	0.30	13.11	4.14	0.25	101.03	74.94	91			
	52.45	30.77	0.18	13.11	4.16	0.20	100.87	75.01	101	767.7	117.12	6.6
	52.29	31.49	0.36	13.59	3.87	0.18	101.77	77.05	111			
	53.04	30.33	0.26	12.81	4.26	0.26	100.96	73.90	122			
	54.29	29.89	0.22	11.75	5.10	0.25	101.50	68.69	132			
	52.88	30.79	0.33	13.26	4.31	0.19	101.76	74.66	141			
	53.79	29.78	0.26	12.01	4.58	0.21	100.63	71.47	152			
	53.21	30.27	0.14	12.27	4.59	0.17	100.64	72.07	162			
	55.67	28.59	0.21	10.59	5.52	0.26	100.84	64.70	172			
	53.25	30.13	0.32	12.42	4.59	0.21	100.91	72.13	182			
	53.27	30.21	0.21	12.08	4.65	0.22	100.64	71.26	192			
	55.43	29.34	0.17	11.19	5.34	0.25	101.72	66.67	202	749.1	136.73	5.5
	56.05	28.36	0.21	10.43	5.60	0.33	100.99	63.74	212			
	56.35	28.76	0.18	10.64	5.46	0.28	101.67	64.96	222			
	56.69	27.78	0.16	9.52	5.90	0.32	100.36	60.49	242			
	56.35	28.00	0.38	9.98	5.85	0.36	100.92	61.64	253			
	57.21	27.46	0.19	9.47	6.12	0.34	100.79	59.45	263			
	56.78	27.43	0.19	9.35	6.43	0.44	100.63	57.67	273			
	56.60	27.52	0.21	9.57	6.12	0.32	100.33	59.77	284			
	53.79	30.48	0.37	12.21	4.45	0.18	101.47	72.50	293			
	54.57	29.48	0.15	11.50	5.05	0.26	101.01	68.41	303	772.6	133.57	5.8
	56.37	28.72	0.25	10.22	5.74	0.33	101.65	62.72	314			
	57.38	27.53	0.33	9.45	6.22	0.28	101.19	59.21	324			
	57.31	27.75	0.25	9.89	6.10	0.34	101.65	60.53	333			
	56.14	27.94	0.17	10.20	5.74	0.31	100.51	62.74	343			
	55.64	28.49	0.16	10.49	5.56	0.29	100.62	64.22	354			
	56.53	27.64	0.24	9.95	5.94	0.30	100.61	61.46	364			
	57.81	26.91	0.03	9.00	6.23	0.37	100.35	57.69	373			
	57.77	27.11	0.15	8.82	6.20	0.34	100.41	57.40	384			
	57.92	26.75	0.22	8.48	6.62	0.40	100.38	54.71	394			
	56.59	27.74	0.17	9.98	5.93	0.37	100.77	61.32	404			
	56.38	28.40	0.22	9.91	5.92	0.33	101.16	61.33	415			
	55.29	28.53	0.18	10.79	5.49	0.30	100.58	65.07	425			

Appendix 1.1 (cont.)
Electron microprobe analyses of Unzen plagioclase (in wt.%)

Sample ID	SiO_2	Al_2O_3	FeO	CaO	Na_2O	K_2O	Total	An*	um**	Sr (ppm)	Ba (ppm)	Sr/ Ba
	55.33	28.98	0.10	11.11	5.15	0.26	100.93	67.27	435			
	55.95	28.36	0.15	10.66	5.58	0.27	100.96	64.58	445			
	56.27	28.24	0.27	10.18	5.82	0.28	101.06	62.55	455			
	56.45	27.94	0.24	10.00	5.90	0.31	100.84	61.70	465			
	56.27	28.15	0.11	9.73	5.82	0.32	100.38	61.34	476			
	57.58	27.41	0.15	9.41	6.11	0.38	101.04	59.18	486	694.9	148.21	4.7
	57.15	27.60	0.15	9.34	6.24	0.32	100.80	58.76	495			
	58.21	27.02	0.14	8.99	6.50	0.37	101.23	56.67	505			
	57.97	26.98	0.15	8.77	6.59	0.41	100.87	55.61	516			
	58.68	27.12	0.21	8.89	6.66	0.42	101.98	55.65	525			
	58.17	26.67	0.27	8.69	6.34	0.47	100.61	56.07	535			
	58.85	25.96	0.17	8.31	6.99	0.48	100.77	52.63	546			
	58.80	26.20	0.32	8.36	6.60	0.51	100.79	54.04	556			
	57.80	27.07	0.15	8.98	6.46	0.35	100.81	56.87	566			
	57.54	27.84	0.15	9.15	6.12	0.41	101.22	58.39	576			
	58.29	26.76	0.21	8.85	6.42	0.42	100.94	56.41	586			
	58.31	26.99	0.22	8.60	6.57	0.46	101.14	55.01	596			
	58.33	26.90	0.24	8.60	6.54	0.37	100.98	55.46	607			
	57.43	27.20	0.19	9.13	6.47	0.41	100.83	57.04	617			
	57.63	26.88	0.10	9.01	6.36	0.42	100.40	57.06	627			
	58.30	26.64	0.27	8.47	6.68	0.47	100.83	54.21	637			
	58.73	26.52	0.19	8.35	6.68	0.43	100.91	54.01	647			
	58.18	27.19	0.26	9.05	6.38	0.35	101.41	57.39	657			
	58.15	27.23	0.23	8.62	6.60	0.40	101.24	55.18	667	634.5	143.88	4.4
	58.72	26.90	0.18	8.85	6.26	0.38	101.29	57.16	678			
	57.92	27.47	0.31	8.82	6.35	0.38	101.24	56.73	687			
	57.59	26.95	0.23	8.96	6.40	0.37	100.50	56.94	697			
	57.63	26.83	0.32	8.66	6.34	0.43	100.21	56.13	708			
	58.48	26.94	0.20	8.44	6.64	0.42	101.12	54.44	718			
	57.91	27.26	0.28	8.95	6.35	0.41	101.16	56.98	727			
	58.43	26.99	0.22	9.14	6.16	0.40	101.34	58.23	738	660.8	139.57	4.7
	58.15	26.64	0.23	8.90	6.54	0.41	100.85	56.15	748			
	57.19	27.56	0.28	9.38	6.23	0.34	100.97	58.82	758			
	59.18	26.30	0.16	8.12	6.55	0.50	100.80	53.52	768			
	58.03	26.08	0.14	8.47	6.30	0.61	99.63	55.07	779			
	58.02	25.58	0.45	8.79	5.98	0.80	99.61	56.48	789			
	52.77	30.20	0.89	13.92	3.43	0.46	101.67	78.16	809	601.1	76.34	7.9
	49.74	31.75	0.61	15.22	3.04	0.14	100.50	82.69	819	565.3	52.97	10.7
	51.31	29.02	0.75	15.56	3.24	0.30	100.18	81.46	819	569.8	49.60	19.5
UZN1663B Plag4c	51.72	31.80	0.12	14.37	3.76	0.16	101.93	78.57	0	728.0	93.05	7.8
	51.71	30.94	0.19	13.91	4.22	0.17	101.14	76.02	10	763.8	110.24	6.9
	55.89	28.08	0.20	10.78	5.57	0.35	100.87	64.56	20			
	56.88	27.79	0.23	9.90	6.00	0.31	101.10	61.08	30			
	56.81	27.72	0.15	9.30	6.03	0.39	100.41	59.17	40			
	58.35	26.59	0.16	8.75	6.28	0.38	100.51	56.78	51			
	59.37	28.08	0.22	9.13	6.06	0.52	103.39	58.11	61			
	57.61	27.52	0.32	10.00	5.89	0.41	101.76	61.31	71			
	57.90	27.16	0.18	9.01	6.11	0.48	100.84	57.74	90			
	57.10	27.04	0.18	9.39	6.25	0.28	100.24	58.99	110	670.8	129.63	5.2
	56.99	27.22	0.32	9.14	6.16	0.38	100.20	58.31	121			
	58.22	26.65	0.21	8.35	6.51	0.47	100.40	54.47	131			
	58.71	26.75	0.12	8.60	6.47	0.38	101.03	55.67	141			
	58.43	26.52	0.19	8.35	6.50	0.38	100.37	54.83	151			
	58.10	27.00	0.11	8.96	6.50	0.40	101.06	56.52	161			
	58.07	26.84	0.12	8.49	6.55	0.43	100.50	54.86	171			
	58.11	26.89	0.16	8.76	6.33	0.39	100.65	56.60	181			
	58.34	26.49	0.18	8.42	6.29	0.47	100.18	55.49	191			

Appendix 1.1 (cont.)
Electron microprobe analyses of Unzen plagioclase (in wt.%)

Sample ID	SiO_2	Al_2O_3	FeO	CaO	Na_2O	K_2O	Total	An*	um**	Sr (ppm)	Ba (ppm)	Sr/ Ba
	56.91	28.14	0.24	9.69	5.99	0.35	101.33	60.43	201	597.0	109.13	5.5
	56.12	28.56	0.22	10.65	5.57	0.27	101.39	64.59	212			
	55.78	28.86	0.13	10.50	5.54	0.26	101.06	64.40	222			
	56.83	28.13	0.11	9.60	6.04	0.35	101.07	60.02	232			
	56.95	27.88	0.18	9.88	5.97	0.37	101.24	60.90	241			
	56.86	27.89	0.23	9.63	6.16	0.34	101.09	59.73	251			
	55.08	28.74	0.25	11.12	5.14	0.28	100.62	67.23	261			
	56.00	28.20	0.14	10.17	5.74	0.33	100.58	62.60	271			
	56.63	28.25	0.21	10.23	5.78	0.33	101.44	62.60	281			
	54.96	29.12	0.35	11.10	5.02	0.25	100.80	67.80	292			
	57.52	27.66	0.29	9.45	6.01	0.40	101.34	59.58	302	622.2	139.31	4.6
	56.13	27.87	0.31	9.81	5.66	0.13	99.91	62.89	312	635.0	136.04	4.7
	56.11	28.23	0.15	10.22	5.60	0.26	100.58	63.55	322			
	56.48	28.40	0.14	10.47	5.98	0.29	101.76	62.56	332			
	57.55	27.49	0.15	9.43	6.32	0.33	101.27	58.65	342			
	57.55	27.46	0.25	9.29	6.05	0.37	100.97	59.12	352			
	57.91	27.16	0.08	8.81	6.25	0.42	100.64	56.93	362			
	58.31	27.20	0.24	8.85	6.33	0.44	101.37	56.64	372			
	57.95	27.22	0.15	9.02	6.27	0.38	101.01	57.54	383			
	57.79	26.97	0.27	8.98	6.40	0.42	100.84	56.84	393			
	58.78	26.74	0.18	8.48	6.45	0.41	101.05	55.30	402	582.1	149.77	3.9
	57.57	27.37	0.16	8.76	6.29	0.37	100.51	56.80	412	598.0	162.68	3.7
	58.67	26.59	0.37	8.41	6.67	0.41	101.13	54.29	422			
	58.57	27.07	0.46	8.71	6.19	0.41	101.40	56.91	432			
	57.01	26.53	0.24	9.02	6.03	0.53	99.37	57.88	442			
	52.07	30.81	0.69	13.69	3.70	0.26	101.21	77.58	452	555.6	194.34	2.9
	52.07	30.81	0.69	13.69	3.70	0.26	101.21	77.58	452	536.9	60.58	8.9
	53.94	29.13	0.88	12.15	4.09	0.50	100.69	72.57	463	507.9	186.85	2.7
	52.61	29.57	0.77	12.74	4.09	0.27	100.04	74.51	473	552.4	74.99	7.4
UZN1663B Plag5	52.70	30.73	0.18	12.76	4.24	0.17	100.77	74.32	0	878.4	225.07	3.9
	55.07	29.09	0.19	10.97	5.02	0.25	100.60	67.51	10			
	56.91	27.86	0.37	9.85	5.89	0.33	101.21	61.30	20			
	56.05	28.05	0.18	9.88	5.78	0.31	100.25	61.85	30			
	56.77	28.06	0.27	9.56	5.96	0.30	100.91	60.43	40			
	56.75	27.80	0.15	9.43	5.99	0.33	100.45	59.88	50			
	57.65	27.00	0.17	8.99	6.39	0.45	100.64	56.79	60			
	57.06	27.45	0.17	9.41	5.99	0.33	100.40	59.86	70			
	55.58	28.16	0.25	10.40	5.64	0.33	100.35	63.53	80			
	56.26	28.25	0.21	10.04	5.58	0.30	100.65	63.05	91			
	57.82	27.08	0.16	9.22	6.20	0.34	100.82	58.51	101			
	57.96	26.59	0.24	8.37	6.33	0.43	99.91	55.30	111			
	58.02	26.91	0.24	8.35	6.33	0.41	100.26	55.31	121			
	58.24	26.27	0.24	8.04	6.66	0.45	99.91	53.07	131			
	58.17	26.46	0.20	8.77	6.42	0.43	100.45	56.14	141	589.9	140.96	4.2
	57.41	27.00	0.15	8.94	6.30	0.41	100.20	57.13	151			
	56.26	28.34	0.15	9.87	5.61	0.30	100.53	62.54	161			
	56.49	27.81	0.17	9.87	6.00	0.30	100.65	61.04	171			
	56.88	26.96	0.18	9.49	6.13	0.39	100.04	59.26	181			
	56.89	27.80	0.20	10.09	5.72	0.37	101.08	62.35	191			
	55.85	28.25	0.16	10.34	5.48	0.32	100.40	64.04	201			
	56.86	28.03	0.24	9.33	6.00	0.34	100.80	59.55	211			
	55.89	28.76	0.13	10.33	5.79	0.34	101.24	62.78	221			
	55.22	29.00	0.26	10.71	5.31	0.29	100.79	65.68	231			
	54.52	27.86	0.19	9.72	5.49	0.34	98.12	62.55	241	572.0	131.97	4.3
	56.60	27.88	0.19	9.71	5.77	0.33	100.48	61.39	252			
	56.80	27.95	0.24	9.95	5.87	0.36	101.17	61.52	262			
	56.07	27.78	0.22	9.87	5.76	0.27	99.98	62.06	272			

Appendix 1.1 (cont.)
Electron microprobe analyses of Unzen plagioclase (in wt.%)

Sample ID	SiO_2	Al_2O_3	FeO	CaO	Na_2O	K_2O	Total	An*	um**	Sr (ppm)	Ba (ppm)	Sr/ Ba
	56.95	27.76	0.16	9.47	5.95	0.30	100.60	60.22	282			
	56.60	27.82	0.25	9.68	6.04	0.32	100.71	60.34	292			
	56.15	28.80	0.18	10.37	5.88	0.30	101.69	62.62	312			
	56.48	27.70	0.21	10.06	5.78	0.28	100.51	62.38	322			
	56.40	28.17	0.25	10.13	5.83	0.33	101.11	62.20	332			
	56.67	28.20	0.22	10.05	5.68	0.31	101.13	62.67	342	657.9	128.69	5.1
	56.62	27.27	0.13	9.14	6.21	0.43	99.81	57.93	352			
	57.00	27.87	0.17	9.94	6.08	0.43	101.49	60.44	362			
	52.84	30.14	0.41	13.12	4.21	0.29	101.01	74.45	372			
	54.52	29.46	0.24	11.11	4.97	0.31	100.61	67.79	382			
	54.87	28.67	0.26	11.08	5.19	0.33	100.40	66.73	392			
	55.61	28.82	0.19	10.80	5.28	0.38	101.07	65.65	402			
	57.50	27.73	0.17	9.46	5.96	0.45	101.27	59.62	412			
	52.32	30.47	0.64	13.10	3.97	0.30	100.79	75.41	443	760.6	165.46	4.6
	56.37	27.83	1.03	10.19	5.21	0.53	101.16	63.98	453			
	55.26	30.57	0.50	12.08	4.28	0.41	103.10	72.04	473			
	54.15	28.99	1.00	12.94	3.76	0.51	101.36	75.17	503			
	38.04	20.83	0.69	8.13	3.15	0.31	71.14	70.14	523			
	48.60	29.16	0.63	12.99	3.41	0.31	95.11	77.73	553			
	49.96	29.16	0.92	13.33	3.43	0.35	97.15	77.93	594			
	49.28	30.25	0.91	13.67	2.90	0.24	97.25	81.31	604			
	49.72	31.96	0.65	15.50	3.07	0.13	101.04	82.89	654	567.3	73.33	7.7
	50.61	31.22	0.62	14.27	3.29	0.16	100.17	80.56	664	570.3	56.54	10.1
	51.15	31.11	0.67	14.14	3.54	0.17	100.78	79.22	674	541.4	47.01	11.5
UZN1663B Plag6	57.13	27.33	0.31	9.30	6.25	0.35	100.68	58.46	0			
	57.67	27.41	0.24	9.24	6.17	0.50	101.22	58.09	10			
	57.81	27.44	0.18	9.14	6.11	0.42	101.10	58.32	20			
	57.66	27.01	0.28	9.15	6.41	0.39	100.89	57.38	31			
	57.28	27.46	0.11	9.67	5.94	0.36	100.83	60.54	41			
	55.90	28.28	0.22	10.31	5.36	0.29	100.35	64.61	51			
	55.78	28.39	0.22	10.36	5.49	0.29	100.53	64.19	61	667.6	127.18	5.2
	55.79	28.54	0.23	10.41	5.64	0.30	100.90	63.67	71			
	55.14	28.66	0.22	10.83	5.17	0.25	100.28	66.63	81			
	55.56	28.63	0.27	10.77	5.28	0.28	100.79	65.96	91			
	53.91	30.02	0.25	12.08	4.70	0.20	101.16	71.14	101			
	54.54	29.26	0.12	11.85	4.97	0.29	101.03	69.22	111			
	53.63	29.97	0.21	12.02	4.84	0.22	100.88	70.40	121			
	54.04	30.01	0.23	12.13	5.06	0.22	101.68	69.68	131			
	54.10	29.57	0.28	11.68	4.79	0.23	100.64	69.97	141			
	54.80	29.27	0.24	11.19	5.08	0.27	100.84	67.68	151			
	54.50	28.90	0.31	11.13	5.26	0.24	100.34	66.95	162			
	55.22	28.56	0.16	10.69	5.32	0.23	100.18	65.84	172			
	55.99	28.09	0.16	10.04	5.66	0.29	100.24	62.79	182			
	56.89	27.99	0.18	9.72	6.03	0.32	101.13	60.51	191			
	56.74	27.92	0.19	9.61	5.91	0.33	100.70	60.65	202			
	56.97	27.27	0.12	9.34	6.12	0.33	100.14	59.16	212			
	57.40	27.53	0.18	9.07	6.22	0.34	100.74	58.04	222			
	57.60	27.49	0.26	9.04	6.24	0.33	100.96	57.93	232			
	57.20	27.26	0.20	8.99	6.08	0.33	100.06	58.36	242			
	57.45	27.38	0.23	8.99	6.14	0.35	100.54	58.04	252			
	57.95	27.77	0.19	9.15	6.33	0.43	101.81	57.54	262			
	57.22	27.61	0.27	9.54	6.02	0.42	101.08	59.70	272			
	56.95	27.53	0.26	9.37	6.17	0.38	100.66	58.85	282			
	58.02	27.41	0.19	9.31	6.27	0.38	101.57	58.36	293			
	57.75	27.38	0.17	8.76	6.29	0.37	100.73	56.80	303	575.5	112.53	5.1
	56.86	28.06	0.20	9.82	5.84	0.29	101.07	61.58	313			
	56.84	27.72	0.14	9.56	6.03	0.35	100.64	59.99	322			

Appendix 1.1 (cont.)
Electron microprobe analyses of Unzen plagioclase (in wt.%)

Sample ID	SiO_2	Al_2O_3	FeO	CaO	Na_2O	K_2O	Total	An*	um**	Sr (ppm)	Ba (ppm)	Sr/ Ba
	56.71	27.78	0.19	9.78	5.80	0.34	100.60	61.43	333			
	57.34	27.73	0.29	9.60	6.02	0.34	101.32	60.14	343			
	57.63	27.71	0.22	8.92	6.35	0.30	101.14	57.27	353			
	57.68	27.13	0.14	8.80	6.09	0.37	100.21	57.67	363			
	57.73	27.70	0.20	9.46	6.12	0.36	101.57	59.38	373			
	57.30	27.94	0.34	9.62	5.95	0.31	101.47	60.56	383			
	57.57	27.45	0.16	9.20	6.37	0.35	101.09	57.79	393			
	57.92	27.49	0.11	9.15	6.12	0.34	101.13	58.61	403			
	57.71	27.56	0.29	9.11	6.19	0.41	101.26	58.00	413			
	57.95	27.40	0.15	8.77	6.33	0.43	101.03	56.48	424			
	57.46	27.71	0.22	9.35	6.23	0.31	101.28	58.82	434			
	55.82	28.79	0.32	10.53	5.60	0.29	101.35	64.12	443			
	56.10	28.58	0.15	10.29	5.51	0.24	100.86	64.18	453			
	57.86	27.11	0.22	8.84	6.47	0.36	100.86	56.40	474			
	58.16	26.88	0.25	8.97	6.72	0.35	101.33	55.93	484			
	58.11	26.64	0.31	8.85	6.46	0.45	100.83	56.15	494			
	58.37	27.01	0.18	8.57	6.78	0.38	101.28	54.48	504			
	57.19	26.95	0.18	8.75	6.16	0.35	99.59	57.35	514			
	57.96	27.06	0.27	9.13	6.22	0.33	100.97	58.22	524			
	57.97	27.05	0.17	8.64	6.59	0.35	100.78	55.43	534			
	58.31	26.68	0.18	8.55	6.37	0.42	100.51	55.75	544			
	57.92	26.81	0.09	8.44	6.30	0.37	99.93	55.86	555			
	58.88	26.45	0.13	8.63	6.47	0.39	100.95	55.71	565			
	58.35	26.86	0.18	8.54	6.56	0.44	100.92	54.94	574			
	59.00	26.14	0.19	8.10	6.51	0.44	100.38	53.85	584			
	59.11	26.34	0.21	8.11	6.87	0.47	101.10	52.46	594			
	59.71	26.55	0.27	7.80	6.94	0.51	101.77	51.16	605			
	58.20	26.42	0.22	8.50	6.59	0.41	100.35	54.82	615			
	57.61	26.88	0.21	9.10	6.39	0.42	100.61	57.17	625			
	58.50	27.11	0.19	8.83	6.44	0.46	101.53	56.14	635			
	58.43	26.86	0.27	8.52	6.46	0.43	100.97	55.29	646			
	59.35	26.76	0.21	8.58	6.82	0.44	102.16	54.15	656			
	58.92	26.19	0.13	7.81	7.05	0.48	100.58	50.88	666			
	58.58	26.80	0.24	8.39	6.47	0.41	100.88	54.97	676			
	58.16	26.24	0.20	8.20	7.06	0.47	100.33	52.13	686			
	58.75	26.68	0.27	8.36	6.74	0.41	101.21	53.91	695			
	58.80	26.50	0.22	7.67	6.46	0.44	100.09	52.68	705	509.7	121.40	4.2
	58.94	26.38	0.18	8.62	6.67	0.40	101.18	54.92	715			
	58.56	26.77	0.19	8.21	6.53	0.48	100.74	53.97	725			
	57.93	27.33	0.22	8.73	6.28	0.39	100.87	56.67	736			
	58.57	26.72	0.18	8.73	6.57	0.43	101.20	55.49	746			
	58.77	26.73	0.19	8.39	6.64	0.37	101.11	54.46	756			
	59.19	26.73	0.30	8.14	6.52	0.40	101.29	54.07	766			
	58.47	26.54	0.24	8.58	6.65	0.41	100.88	54.84	777			
	58.62	26.35	0.15	8.15	6.10	0.47	99.85	55.39	787			
	59.20	26.06	0.15	8.00	6.86	0.46	100.71	52.22	797			
	59.36	26.20	0.14	7.64	6.87	0.40	100.60	51.23	807			
	60.00	25.63	0.18	7.29	7.46	0.53	101.10	47.69	817			
	60.00	25.82	0.20	7.28	7.11	0.55	100.96	48.72	827			
	59.96	25.99	0.14	7.65	7.05	0.51	101.30	50.29	837			
	59.22	26.90	0.24	8.26	6.94	0.49	102.06	52.65	847			
	59.03	26.63	0.09	8.36	6.66	0.47	101.25	53.95	857			
	59.05	26.10	0.14	8.08	6.69	0.46	100.51	53.08	867			
	59.53	26.41	0.16	7.71	6.89	0.48	101.17	51.15	877			
	59.25	26.43	0.25	7.85	6.79	0.43	101.00	52.06	887			
	59.62	25.98	0.32	8.04	6.82	0.45	101.22	52.53	897	544.0	136.38	4.0
	58.90	26.26	0.30	8.14	6.60	0.50	100.70	53.41	907			
	59.31	26.30	0.22	8.20	6.83	0.55	101.41	52.65	918			

Appendix 1.1 (cont.)
Electron microprobe analyses of Unzen plagioclase (in wt.%)

Sample ID	SiO_2	Al_2O_3	FeO	CaO	Na_2O	K_2O	Total	An*	um**	Sr (ppm)	Ba (ppm)	Sr/ Ba
	59.14	26.40	0.25	7.90	6.68	0.67	101.04	51.84	928			
	54.55	29.46	0.49	12.22	4.26	0.56	101.55	71.72	938			
	56.77	25.53	1.36	9.95	3.92	1.57	99.11	64.44	958			
	56.23	28.28	0.90	11.48	3.73	0.92	101.54	71.15	988			
	50.11	28.69	0.69	12.64	4.60	0.30	97.02	72.07	998			
	51.75	30.41	0.75	13.65	3.28	0.49	100.33	78.39	1008			
	48.98	32.24	0.45	15.85	2.75	0.12	100.39	84.66	1018	542.1	34.37	15.8
	48.98	32.24	0.45	15.85	2.75	0.12	100.39	84.66	1018	549.9	46.35	11.9
	48.98	32.24	0.45	15.85	2.75	0.12	100.39	84.66	1018	528.0	31.75	16.6
	48.98	32.24	0.45	15.85	2.75	0.12	100.39	84.66	1018	529.7	30.50	17.4
UZN1663B Plag7	46.91	34.26	0.78	17.31	1.79	0.06	101.11	90.33	0			
	50.29	30.98	0.78	15.36	2.23	0.59	100.23	84.49	11			
	46.67	34.42	0.70	17.66	1.78	0.08	101.31	90.45	21			
	47.40	34.16	0.56	17.24	1.87	0.04	101.26	90.04	31			
	47.21	33.92	0.66	16.56	1.97	0.13	100.45	88.75	41			
	48.95	33.01	0.56	15.90	2.44	0.15	101.01	85.99	52			
	48.36	33.70	0.72	17.05	2.08	0.07	101.98	88.79	82			
	48.39	33.20	0.83	16.44	2.18	0.11	101.16	87.79	93			
	51.38	31.76	0.96	14.94	2.96	0.17	102.17	82.68	104			
	48.15	33.66	0.63	16.65	2.26	0.10	101.45	87.58	114			
	49.56	32.73	0.60	15.76	2.41	0.19	101.23	85.87	124			
	47.21	34.31	0.62	17.28	1.63	0.07	101.12	91.04	145			
	47.52	34.40	0.51	17.49	1.94	0.08	101.95	89.61	186			
	48.97	33.21	0.50	15.80	2.59	0.04	101.12	85.71	197			
	49.16	32.60	0.49	15.19	2.76	0.12	100.32	84.04	207			
	50.18	31.91	0.38	15.22	2.87	0.10	100.66	83.68	217	508.5	39.25	13.0
	50.00	32.26	0.62	15.13	3.11	0.12	101.25	82.42	227			
	50.73	32.12	0.50	14.52	3.21	0.14	101.21	81.26	238			
	49.85	31.80	0.51	14.56	3.30	0.15	100.17	80.81	248			
	51.47	30.98	0.58	13.79	3.49	0.17	100.49	79.01	258			
	51.69	31.18	0.52	14.16	3.53	0.17	101.25	79.30	268	490.9	47.56	10.3
	51.69	31.18	0.52	14.16	3.53	0.17	101.25	79.30	268	501.2	44.62	11.2
	51.69	31.18	0.52	14.16	3.53	0.17	101.25	79.30	268	480.2	49.01	9.8
	52.82	29.75	0.72	12.86	4.23	0.24	100.62	74.22	279			

Appendix 1.2
Electron microprobe analyses of Unzen glasses (in wt.%)

Sample ID	SiO_2	TiO_2	Al_2O_3	Fe_2O_3	MgO
199.1-199.15H					
	73.81	0.30	12.83	0.89	0.05
	74.09	0.36	11.96	2.11	0.50
	72.68	0.49	11.26	2.49	1.03
	74.11	0.24	11.68	1.43	0.19
	73.67	0.35	11.93	1.73	0.45
153.85-153.9E	73.96	0.26	12.25	1.39	0.16
	73.90	0.02	12.41	1.50	0.18
	74.18	0.18	12.37	1.30	0.24
	72.09	0.06	12.16	1.17	0.12
	73.73	0.16	12.47	1.42	0.13
	73.76	0.16	12.80	1.27	0.16
	73.56	0.38	12.32	1.11	0.13
	74.41	0.12	12.01	1.41	0.18
	73.59	0.18	12.15	1.32	0.17
	73.50	0.06	11.98	1.45	0.23
	73.67	0.16	12.29	1.33	0.17
153.85-153.9H	74.56	0.14	12.51	0.72	0.02
	75.92	0.26	11.12	1.12	0.21
	76.39	0.42	10.38	0.80	0.17
	75.64	0.16	11.43	1.19	0.16
	73.51	0.28	14.17	1.00	0.14
	76.10	0.14	11.07	1.09	0.30
	74.88	0.42	11.67	1.15	0.06
	74.14	0.36	12.00	1.21	0.13
	74.54	0.36	11.71	1.15	0.25
	75.07	0.28	11.78	1.05	0.16
435.2-435.25H	74.53	0.32	13.36	0.79	0.16
	74.01	0.40	12.90	0.88	0.09

CaO	Na_2O	K_2O	Cl	Total	Sr	Ba	Sr/Ba
0.77	2.48	5.75	0.05	96.93			
0.69	2.32	5.76	0.03	97.83			
0.69	1.98	5.69	0.02	96.34			
0.57	2.45	5.70	0.01	96.37			
0.68	2.31	5.72	0.03	96.86			
0.81	2.66	5.12	0.09	96.70	72.0	702.52	0.10
0.83	2.70	5.05	0.11	96.69	86.4	677.63	0.13
0.79	2.82	5.17	0.13	97.19	93.8	692.12	0.14
0.76	2.77	5.11	0.13	94.36			
0.76	2.75	5.42	0.09	96.93			
0.87	2.82	5.16	0.08	97.07			
0.82	2.84	5.20	0.12	96.48			
0.68	2.94	4.97	0.10	96.80			
0.85	2.65	5.30	0.05	96.26			
0.96	2.95	5.21	0.11	96.43			
0.81	2.79	5.17	0.10	96.49			
1.17	3.06	4.54	0.04	96.75			
0.88	2.51	4.19	0.06	96.27			
0.25	2.36	5.12	0.07	95.96			
0.71	2.66	5.59	0.05	97.59			
1.65	3.39	4.12	0.03	98.29			
0.49	2.21	5.12	0.01	96.53			
0.49	2.81	5.52	0.03	97.02			
0.55	2.57	5.82	0.08	96.85			
0.80	2.01	5.17	0.02	96.00			
0.78	2.62	5.02	0.04	96.81			
1.64	3.22	4.32	0.04	98.38			
1.31	2.76	5.11	0.03	97.49			

Appendix 1.2 (cont.)
Electron microprobe analyses of Unzen glasses (in wt.%)

Sample ID	SiO_2	TiO_2	Al_2O_3	Fe_2O_3	MgO
	74.20	0.46	12.74	1.19	0.18
	74.86	0.10	12.46	0.91	0.09
	74.87	0.32	11.90	0.96	0.06
	73.68	0.32	13.30	0.95	0.09
	74.64	0.10	12.16	0.87	0.03
	74.00	0.00	12.84	1.17	0.20
	74.35	0.25	12.71	0.96	0.11
435.2-435.25E	71.26	0.26	13.48	1.31	0.12
	71.83	0.34	13.88	0.99	0.09
	71.49	0.36	13.64	0.93	0.07
	71.68	0.30	13.86	1.01	0.05
	70.84	0.22	13.99	1.13	0.06
	71.04	0.51	13.39	1.24	0.09
	72.00	0.42	12.88	1.05	0.06
	71.45	0.34	13.59	1.09	0.08
390.00-390.05E	74.26	0.32	11.31	1.15	0.17
	74.84	0.20	11.13	1.09	0.13
	74.50	0.12	11.47	1.07	0.13
	74.72	0.30	11.74	1.08	0.16
	74.98	0.20	11.44	0.94	0.08
	74.74	0.20	11.50	1.00	0.09
	74.39	0.20	11.49	1.30	0.08
	74.56	0.34	11.71	1.05	0.11
	74.72	0.02	11.29	1.23	0.09
	74.85	0.22	11.61	1.04	0.14
	74.66	0.21	11.47	1.09	0.12
390.00-390.05H	75.38	0.30	11.01	1.19	0.39
	74.38	0.24	12.11	0.93	0.12

CaO	Na_2O	K_2O	Cl	Total	Sr	Ba	Sr/Ba
1.34	3.03	5.24	0.07	98.44			
1.04	2.59	5.46	0.08	97.58			
0.77	2.31	5.78	0.08	97.04			
1.50	3.10	4.75	0.09	97.78			
0.90	2.48	5.41	0.11	96.68			
1.46	3.09	4.61	0.06	97.42			
1.24	2.82	5.09	0.07	97.60			
0.34	2.57	7.22	0.06	96.62			
0.75	3.46	6.28	0.04	97.64			
0.35	2.62	7.28	0.06	96.78			
0.55	2.68	7.29	0.04	97.47			
0.54	2.79	6.93	0.04	96.53			
0.38	2.62	7.02	0.07	96.35			
0.67	2.77	6.35	0.03	96.23			
0.51	2.79	6.91	0.05	96.80			
1.00	2.85	4.55	0.14	95.76	86.3	1075.87	0.08
0.66	2.60	4.92	0.11	95.67	45.1	307.90	0.15
0.74	2.97	4.93	0.06	95.97	50.1	322.75	0.16
0.65	2.45	5.00	0.12	96.20	55.0	320.19	0.17
0.71	2.41	5.16	0.09	96.01			
0.58	2.86	5.14	0.07	96.18			
0.69	2.82	5.23	0.10	96.29			
0.74	3.06	4.74	0.11	96.40			
0.71	2.62	5.00	0.10	95.77			
0.72	2.79	5.12	0.10	96.59			
0.72	2.74	4.98	0.10	96.08			
0.74	3.12	4.30	0.04	96.46	60.9	589.67	0.10
0.94	3.07	4.56	0.03	96.37	113.2	630.93	0.18

Appendix 1.2 (cont.)
Electron microprobe analyses of Unzen glasses (in wt.%)

Sample ID	SiO_2	TiO_2	Al_2O_3	Fe_2O_3	MgO
	73.84	0.00	12.70	0.80	0.06
	75.12	0.38	10.94	1.09	0.24
	75.28	0.18	11.59	1.06	0.22
	74.76	0.00	12.17	0.85	0.13
	75.22	0.26	11.32	0.87	0.17
	75.33	0.46	11.60	0.87	0.17
	74.91	0.23	11.68	0.96	0.19
546.45-546.5E	73.48	0.12	11.95	0.96	0.16
	73.47	0.10	12.17	0.72	0.09
	73.51	0.28	12.13	0.76	0.11
	73.47	0.28	11.88	0.71	0.07
	73.06	0.04	12.08	0.90	0.11
	73.68	0.14	12.29	0.81	0.13
	73.34	0.14	11.99	0.63	0.03
	74.12	0.32	12.12	0.66	0.07
	74.43	0.20	11.73	0.53	0.08
	74.23	0.00	11.95	0.48	0.07
	73.68	0.16	12.03	0.71	0.09
546.45-546.5H	74.82	0.14	12.54	0.62	0.11
	75.65	0.24	12.09	0.86	0.29
	73.62	0.28	13.75	0.87	0.04
	75.37	0.32	11.56	1.30	0.25
	74.51	0.20	12.36	0.77	0.21
	75.14	0.02	12.69	0.55	0.08
	76.54	0.18	11.55	0.58	0.12
	73.84	0.10	13.00	1.14	0.31
	72.51	0.06	14.78	0.70	0.06
	75.07	0.04	12.49	1.24	0.38
	74.71	0.16	12.68	0.86	0.18

CaO	Na_2O	K_2O	Cl	Total	Sr	Ba	Sr/Ba
1.21	3.39	4.55	0.04	96.60			
0.51	2.65	4.76	0.07	95.75			
0.68	2.80	4.86	0.06	96.73			
0.87	2.87	4.81	0.05	96.51			
0.58	2.67	4.96	0.04	96.09			
0.68	2.79	4.67	0.06	96.63			
0.78	2.92	4.68	0.05	96.39			
0.55	2.25	6.31	0.01	95.78	26.3	182.57	0.14
0.55	2.34	6.64	0.02	96.09	48.8	322.77	0.15
0.62	2.64	6.29	0.05	96.37	48.5	316.06	0.15
0.46	2.36	5.84	0.07	95.14	51.7	323.09	0.16
0.55	2.47	6.46	0.02	95.69	64.4	284.03	0.23
0.56	2.46	5.89	0.00	95.97	48.4	312.95	0.15
0.50	2.54	6.07	0.02	95.25	51.7	336.80	0.15
0.52	2.45	6.52	0.03	96.82			
0.41	2.22	6.20	0.02	95.82			
0.38	2.42	6.44	0.03	95.99			
0.51	2.41	6.27	0.03	95.89			
0.81	2.94	5.63	0.02	97.62	50.8	252.35	0.20
0.97	3.01	4.70	0.04	97.83	62.8	424.95	0.15
1.19	3.29	5.15	0.03	98.22	51.5	283.73	0.18
0.48	2.55	5.97	0.06	97.86			
0.70	2.89	5.61	0.01	97.26			
0.77	3.05	5.33	0.02	97.65			
0.49	2.35	5.66	0.04	97.50			
1.04	3.11	5.47	0.06	98.07			
1.58	3.57	5.05	0.04	98.34			
0.96	2.86	5.09	0.04	98.16			
0.90	2.96	5.37	0.04	97.85			

Appendix 1.2 (cont.)
Electron microprobe analyses of Unzen glasses (in wt.%)

Sample ID	SiO_2	TiO_2	Al_2O_3	Fe_2O_3	MgO
U-5E	73.65	0.18	14.24	1.86	0.25
	73.43	0.50	14.17	2.20	0.21
	74.74	0.56	13.58	1.79	0.25
	73.04	0.48	14.66	1.76	0.19
	73.25	0.46	15.02	1.50	0.17
	72.28	0.62	13.96	2.84	0.43
	72.53	0.60	15.10	2.02	0.33
	73.68	0.57	13.53	2.74	0.40
	73.99	0.72	14.35	1.53	0.20
	73.40	0.52	14.29	2.03	0.27
U-5 Host	76.62	0.14	12.76	1.28	0.14
	76.96	0.32	12.67	1.75	0.25
	76.26	0.42	13.18	1.51	0.18
	76.28	0.26	12.91	1.49	0.26
	76.85	0.44	12.49	1.08	0.09
	75.44	0.64	13.97	1.23	0.04
	75.55	0.26	13.24	1.44	0.29
	77.37	0.50	11.76	1.11	0.08
	77.38	0.44	12.30	1.35	0.08
	76.52	0.38	12.81	1.36	0.16
602.8-602.85H	73.43	0.20	14.43	1.52	0.14
	76.81	0.28	12.91	0.69	0.06
	78.74	0.36	11.56	0.53	0.00
	78.08	0.56	11.64	0.66	0.03
	77.00	0.06	12.49	0.61	0.03
	77.96	0.20	11.76	0.59	0.15
	75.97	0.34	12.23	0.86	0.12
	74.60	0.04	13.43	0.74	0.03
	77.15	0.16	11.72	0.45	0.07
	76.64	0.24	12.46	0.74	0.07

CaO	Na_2O	K_2O	Cl	Total	Sr	Ba	Sr/Ba
1.79	4.06	3.67	0.11	99.81			
2.29	3.63	2.87	0.16	99.46			
2.20	3.64	3.03	0.03	99.82			
2.35	3.97	3.29	0.10	99.82			
2.71	4.20	3.00	0.06	100.37			
2.35	3.73	2.96	0.11	99.28			
2.96	3.89	2.45	0.12	99.99			
2.11	4.51	2.78	0.16	100.49			
2.38	3.72	3.09	0.08	100.05			
2.35	3.93	3.01	0.10	99.90			
1.05	3.13	4.47	0.05	99.62			
0.83	3.12	4.31	0.06	100.25			
1.22	3.22	4.12	0.07	100.18			
1.43	3.48	4.37	0.05	100.52			
0.89	3.02	4.40	0.03	99.28			
1.67	3.78	3.92	0.05	100.73			
1.47	3.34	4.13	0.04	99.75			
0.69	3.25	4.78	0.06	99.58			
0.80	3.55	4.73	0.06	100.68			
1.12	3.32	4.36	0.05	100.07			
1.79	3.52	4.80	0.01	99.84	134.5	595.70	0.23
1.29	3.67	4.08	0.02	99.81	235.9	436.29	0.54
0.66	3.39	4.85	0.04	100.12	140.6	556.20	0.25
0.67	2.74	4.81	0.00	99.18			
0.78	3.27	4.94	0.01	99.20			
0.78	2.67	5.00	0.00	99.10			
0.62	2.04	6.45	0.02	98.64			
1.78	3.35	3.99	0.00	97.97			
0.84	2.68	5.37	0.03	98.46			
1.02	3.04	4.92	0.02	99.15			

Appendix 1.2 (cont.)
Electron microprobe analyses of Unzen glasses (in wt.%)

Sample ID	SiO_2	TiO_2	Al_2O_3	Fe_2O_3	MgO	CaO	Na_2O	K_2O	Cl	Total	Sr	Ba	Sr/Ba
602.8-602.85E	78.24	0.22	12.86	0.40	0.00	1.64	4.34	2.38	0.02	100.09			
	76.47	0.14	13.35	0.37	0.00	0.26	2.85	7.35	0.00	100.79			
	77.06	0.08	12.02	0.44	0.10	0.26	2.34	7.32	0.02	99.64			
	73.88	0.24	15.26	0.43	0.02	1.13	3.67	6.24	0.02	100.87			
	73.31	0.24	13.87	0.95	0.39	1.44	2.98	5.20	0.03	98.41			
	78.28	0.20	11.70	0.60	0.05	0.34	2.13	6.91	0.00	100.21			
	75.97	0.46	13.01	0.51	0.02	0.38	2.22	7.56	0.00	100.13			
	77.69	0.30	10.93	1.11	0.52	0.43	1.88	6.03	0.01	98.90			
	76.36	0.23	12.87	0.60	0.14	0.74	2.80	6.12	0.01	99.88			
U-1AE	72.94	0.60	14.06	1.67	0.12	0.94	3.30	5.73	0.05	99.40			
	73.06	0.24	14.52	1.80	0.13	0.97	3.07	5.45	0.12	99.36			
	71.46	0.42	14.32	1.90	0.12	1.03	3.73	5.44	0.09	98.51			
	71.71	0.46	14.55	2.12	0.14	1.66	4.21	4.33	0.07	99.25			
	71.93	0.22	14.48	2.53	0.12	1.07	4.08	5.43	0.13	99.98			
	73.09	0.52	13.79	1.87	0.13	0.98	3.74	5.35	0.06	99.53			
	73.54	0.04	13.85	1.75	0.16	1.01	4.05	5.28	0.08	99.77			
	72.98	0.44	14.03	1.68	0.14	1.03	4.08	5.44	0.06	99.87			
	72.90	0.26	14.59	1.85	0.14	1.10	3.42	5.33	0.10	99.68			
	72.62	0.35	14.24	1.91	0.13	1.09	3.74	5.31	0.09	99.48			
U-1AH	76.21	0.56	12.06	1.63	0.14	1.03	3.09	4.69	0.04	99.44	125.9	521.37	0.24
	75.31	0.36	13.18	1.19	0.10	1.54	3.27	4.19	0.03	99.15	97.1	509.43	0.19
	75.40	0.44	12.43	1.81	0.60	1.27	3.22	4.38	0.02	99.56	231.6	542.99	0.43
	75.52	0.60	12.79	1.47	0.33	1.38	3.77	4.38	0.03	100.27	119.9	523.81	0.23
	75.61	0.49	12.61	1.52	0.29	1.31	3.34	4.41	0.03	99.61	146.3	490.25	0.30
U-2AE	74.33	0.28	12.63	1.01	0.08	0.63	2.58	6.02	0.03	97.59			
	73.92	0.46	13.43	1.40	0.08	0.52	3.33	6.25	0.05	99.42			
	74.14	0.70	12.97	1.38	0.12	0.46	2.87	6.38	0.05	99.07			
	74.83	0.66	12.99	1.43	0.10	0.50	2.92	6.72	0.05	100.20			
	73.70	0.74	13.20	1.45	0.07	0.50	3.25	6.70	0.06	99.66			

Appendix 1.2 (cont.)
Electron microprobe analyses of Unzen glasses (in wt.%)

Sample ID	SiO_2	TiO_2	Al_2O_3	Fe_2O_3	MgO
	72.97	0.40	13.48	1.69	0.11
	74.79	0.60	13.19	1.27	0.04
	74.09	0.55	13.13	1.38	0.08
262.5-262.55E	71.57	0.69	13.51	1.82	0.17
	70.97	0.73	13.25	2.00	0.20
	71.15	0.46	13.37	2.17	0.19
	70.28	0.54	14.31	1.75	0.10
	71.22	0.50	13.25	1.78	0.20
	71.38	0.81	13.94	1.53	0.08
	71.21	0.48	13.04	1.88	0.19
	71.12	0.58	13.56	1.85	0.11
	71.30	0.50	13.69	1.86	0.19
	71.13	0.59	13.55	1.85	0.16
U-4A Enclave	72.73	0.14	13.91	2.35	0.74
	73.41	0.46	13.60	1.88	0.15
	73.42	0.38	13.93	1.75	0.16
	73.49	0.40	13.31	1.63	0.17
	73.36	0.38	14.06	1.79	0.16
	72.78	0.24	14.17	1.81	0.16
	74.64	0.26	12.68	1.71	0.17
	74.61	0.34	12.83	1.81	0.22
	73.55	0.32	13.56	1.84	0.24

CaO	Na_2O	K_2O	Cl	Total	Sr	Ba	Sr/Ba
0.47	3.11	6.45	0.07	98.75			
0.63	3.27	6.09	0.06	99.93			
0.53	3.05	6.37	0.05	99.23			
1.01	3.25	5.15	0.08	97.25			
1.12	3.37	5.04	0.08	96.76			
1.03	3.47	4.81	0.07	96.72			
1.44	3.44	4.81	0.04	96.70			
0.98	3.12	4.88	0.05	95.97			
1.42	3.28	4.61	0.05	97.11			
0.88	3.07	5.09	0.06	95.88			
1.07	3.67	5.35	0.09	97.38			
1.10	3.41	4.96	0.07	97.07			
1.12	3.34	4.97	0.06	96.76			
1.29	3.59	4.66	0.10	99.53			
1.19	3.92	4.39	0.06	99.05			
1.27	3.42	4.39	0.05	98.76			
1.16	3.56	4.31	0.04	98.04			
1.30	3.93	4.37	0.12	99.46			
1.40	3.67	4.15	0.07	98.44			
1.12	3.24	3.97	0.04	97.82			
1.08	3.09	4.24	0.10	98.29			
1.23	3.55	4.31	0.07	98.67			

Appendix 1.3
Electron microprobe analyses of Unzen Fe-Ti oxides (in wt.%)

Sample ID	Loc.	SiO_2	TiO_2	Al_2O_3	FeO	MgO	MnO	Cr_2O_3	Total
199.10-199.15 H									
Ilmenite-1	core	0.04	39.31	0.05	54.21	1.77	0.66	0.02	96.07
		0.00	44.10	0.06	50.83	1.50	0.75	0.07	97.32
		0.00	47.02	0.05	46.20	1.30	0.60	0.05	95.22
		0.03	45.59	0.06	48.71	1.65	0.71	0.01	96.75
		0.09	45.57	0.06	48.46	1.60	0.77	0.06	96.61
	rim	0.00	43.19	0.06	51.93	2.24	0.83	0.01	98.26
Magnetite-1	rim	0.08	9.53	1.21	86.53	1.25	0.56	0.03	99.19
		0.18	8.30	0.95	89.62	0.57	0.23	0.16	100.00
		0.05	8.24	1.07	89.53	0.84	0.57	0.23	100.53
		0.02	7.76	1.25	89.11	0.88	0.55	0.16	99.74
		0.12	6.47	1.16	88.90	0.83	0.23	0.19	97.90
		0.07	5.91	1.18	89.18	0.96	0.67	0.11	98.08
	core	0.06	5.90	0.81	89.36	1.19	0.51	0.12	97.96
Ilmenite-2	core	0.39	39.65	0.11	51.47	1.25	0.43	0.12	93.41
		0.14	39.95	0.14	53.78	4.16	0.76	0.04	98.96
		0.09	36.76	0.12	55.79	1.14	0.40	0.13	94.44
		0.03	43.03	0.08	53.15	1.26	0.32	0.05	97.92
	rim	0.16	39.85	0.11	53.55	1.95	0.48	0.09	96.18
Magnetite-2	rim	0.05	8.30	0.89	89.30	0.48	0.31	0.16	99.49
		0.06	8.90	0.91	89.40	0.51	0.32	0.19	100.29
		0.04	7.90	0.99	89.76	0.62	0.51	0.11	99.93
		0.05	8.60	0.98	88.76	0.88	0.48	0.23	99.98
		0.05	8.47	1.01	88.90	0.81	0.29	0.21	99.73
		0.06	8.10	1.03	88.98	0.91	0.38	0.22	99.68
	core	0.05	8.10	1.01	89.70	0.85	0.46	0.19	100.36
199.10-199.15 E (Equigranular)									
Ilmenite-1	core	0.07	36.15	0.18	57.42	2.24	0.55	0.00	96.62
		0.13	37.11	0.09	58.57	1.39	0.61	0.00	97.91
		0.02	43.02	0.07	52.79	1.76	0.95	0.06	98.66
		0.09	49.72	0.07	48.53	1.28	0.48	0.10	100.28
		0.09	42.62	0.08	54.73	1.61	0.85	0.06	100.04
	rim	0.08	43.21	0.10	52.94	2.21	0.83	0.04	99.42
Magnetite-2	rim	0.07	7.58	0.68	88.57	1.29	0.53	0.12	98.84
		0.11	8.78	0.92	87.42	1.05	0.41	0.10	98.79
		0.02	9.77	1.03	88.23	0.88	0.32	0.14	100.38
		0.12	10.86	0.85	83.23	0.90	0.46	0.06	96.47
		0.08	9.22	1.11	87.79	1.24	0.56	0.09	100.09
		0.09	10.67	0.76	87.33	0.72	0.33	0.06	99.97
	core	0.08	7.70	0.61	88.51	1.23	0.44	0.04	98.62
262.50-262.55 E (Porphyritic)									
Ilmenite-1	core	0.00	43.28	0.20	51.65	2.61	0.44	0.09	98.27
		0.01	43.36	0.22	51.08	2.48	0.51	0.09	97.76
		0.04	43.51	0.23	51.31	2.53	0.46	0.13	98.21
		0.05	43.94	0.20	51.72	2.63	0.58	0.01	99.12
	rim	0.10	44.92	0.11	51.18	3.02	0.54	0.01	99.87
Magnetite-1	rim	0.71	10.66	2.32	81.03	1.34	0.48	0.15	96.71
		0.13	11.26	2.41	80.85	1.34	0.32	0.17	96.48
		0.15	10.98	2.78	79.37	1.44	0.48	0.04	95.24
		0.08	11.07	2.38	81.24	1.26	0.31	0.14	96.47
	core	0.14	11.16	2.11	83.50	1.25	0.46	0.14	98.75
Ilmenite-2	core	0.07	41.73	0.24	53.78	2.53	0.53	0.02	98.90
		0.05	42.79	0.20	53.95	2.63	0.51	0.06	100.19
		0.05	43.16	0.22	53.10	2.85	0.55	0.06	100.00

Appendix 1.3 (cont)
Electron microprobe analyses of Unzen Fe-Ti oxides (in wt.%)

Sample ID	Loc.	SiO_2	TiO_2	Al_2O_3	FeO	MgO	MnO	Cr_2O_3	Total
	rim	0.04	44.26	0.22	51.08	2.74	0.51	0.08	98.93
Magnetite-2	rim	0.13	8.04	1.21	88.16	0.94	0.28	0.19	98.94
		0.07	9.68	1.25	87.82	0.96	0.32	0.26	100.34
		0.03	9.01	1.16	88.64	0.96	0.30	0.15	100.25
		0.04	8.22	1.24	87.59	0.93	0.16	0.14	98.32
		0.00	8.44	1.22	88.66	0.93	0.26	0.14	99.65
		0.12	9.37	1.30	87.77	0.96	0.28	0.11	99.90
		0.03	9.27	1.27	88.81	1.00	0.29	0.21	100.88
		0.03	10.54	1.41	85.98	1.10	0.38	0.18	99.61
		0.10	10.44	1.06	85.84	0.93	0.32	0.11	98.80
		0.03	10.33	1.06	87.71	0.89	0.29	0.12	100.43
		0.06	9.03	1.22	87.00	0.96	0.29	0.16	98.71
	core	0.06	10.18	1.37	86.79	1.08	0.32	0.18	100.00
Ilmenite-3	core	0.00	41.24	0.20	55.87	0.11	0.49	0.09	98.00
		0.01	41.36	0.22	55.08	2.48	0.51	0.09	99.76
		0.04	41.51	0.23	55.31	2.53	0.46	0.13	100.21
		0.05	40.94	0.20	55.72	2.63	0.58	0.01	100.12
		0.10	40.92	0.11	55.18	3.02	0.54	0.01	99.87
		0.07	41.73	0.24	53.78	2.53	0.53	0.02	98.90
		0.05	40.79	0.20	54.95	2.63	0.51	0.06	99.19
	rim	0.05	40.16	0.12	54.61	1.65	0.51	0.06	97.17
Magnetite-3	rim	1.00	7.36	0.82	86.40	0.92	0.37	0.19	97.06
		1.44	11.40	1.58	84.27	0.94	0.33	0.13	100.08
		0.15	12.90	1.39	83.21	0.90	0.44	0.04	99.03
		0.70	12.81	1.41	83.80	1.12	0.33	0.07	100.23
		0.82	12.72	1.47	83.87	1.01	0.37	0.08	100.33
	core	0.94	11.86	0.68	84.35	1.01	0.62	0.04	99.51
390.00-390.15 H									
Ilmenite-1	core	0.00	39.90	0.11	56.95	1.94	0.67	0.03	99.60
		0.00	39.79	0.12	56.07	1.70	0.76	0.00	98.45
		0.00	40.42	0.08	54.87	1.79	0.53	0.09	97.78
		0.01	38.61	0.09	54.90	1.68	0.65	0.07	96.02
		0.00	39.41	0.10	54.18	1.74	0.63	0.03	96.10
		0.02	38.90	0.10	56.25	1.83	0.82	0.00	97.92
	rim	0.00	41.66	0.11	56.36	1.74	0.69	0.14	100.71
Magnetite-1	rim	0.17	9.39	0.71	87.12	1.23	0.56	0.02	99.20
		0.10	8.40	0.69	87.90	1.19	0.47	0.05	98.80
		0.10	8.28	0.65	88.95	1.30	0.57	0.00	99.86
		0.06	8.42	0.67	88.47	1.19	0.57	0.00	99.37
		0.05	8.38	0.67	88.31	1.21	0.49	0.01	99.13
	core	0.10	8.37	0.68	89.35	1.23	0.53	0.01	100.27
Ilmenite-2	core	0.00	38.24	0.07	55.48	1.75	0.64	0.01	96.18
		0.04	40.78	0.09	54.64	1.86	0.61	0.00	98.02
	rim	0.03	44.48	0.09	51.16	2.09	0.64	0.00	98.48
Magnetite-2	rim	0.09	9.30	0.77	86.70	1.27	0.58	0.01	98.72
		0.87	6.70	1.62	86.44	0.76	0.31	0.00	96.70
		0.66	8.54	0.86	87.74	1.15	0.61	0.03	99.59
		0.14	8.70	0.75	88.74	0.93	0.51	0.00	99.76
	core	0.05	5.81	0.82	85.13	1.20	0.57	0.11	93.70
Ilmenite-3	core	0.00	39.33	0.09	54.26	1.74	0.41	0.00	95.84
		0.06	39.79	0.12	53.67	1.75	0.52	0.05	95.96
		0.01	39.31	0.10	54.21	1.78	0.65	0.03	96.11
	rim	0.02	40.90	0.10	56.40	1.86	0.68	0.04	100.00
Magnetite-3	rim	1.25	6.98	0.90	88.12	0.97	0.56	0.00	98.80

Appendix 1.3 (cont)
Electron microprobe analyses of Unzen Fe-Ti oxides (in wt.%)

Sample ID	Loc.	SiO_2	TiO_2	Al_2O_3	FeO	MgO	MnO	Cr_2O_3	Total
		0.01	7.18	0.85	88.46	0.84	0.70	0.04	98.08
		0.06	9.00	0.96	87.70	0.88	0.62	0.00	99.21
	core	0.04	9.07	0.93	87.65	0.95	0.55	0.00	99.20
390.00-390.15 E (Equigranular)									
Ilmenite-1	core	1.46	38.63	0.06	55.62	1.52	0.58	0.09	97.97
		0.03	39.61	0.13	55.18	1.62	0.77	0.05	97.40
		0.01	40.22	0.11	53.51	1.55	0.85	0.05	96.29
		0.02	39.82	0.11	54.13	1.56	0.76	0.07	96.45
		0.08	39.56	0.12	54.02	1.52	0.77	0.00	96.06
		0.55	39.67	0.17	52.57	1.59	0.76	0.00	95.32
	rim	0.36	38.24	0.14	55.53	1.78	0.55	0.03	96.62
Magnetite-1	rim	0.15	6.10	0.77	88.91	1.20	0.48	0.00	97.59
		0.10	9.01	0.64	87.22	1.28	0.58	0.00	98.83
		1.48	7.66	0.97	88.23	1.19	0.51	0.02	100.05
	core	0.57	6.29	0.85	89.79	1.20	0.52	0.01	99.23
Ilmenite-2	core	0.00	38.64	0.13	55.64	1.50	0.64	0.07	96.63
		0.00	37.96	0.08	55.54	1.69	0.54	0.02	95.84
		0.03	38.99	0.13	54.85	1.72	0.79	0.03	96.55
		0.06	38.05	0.11	55.59	1.82	0.56	0.00	96.19
		0.01	38.22	0.10	56.04	1.78	0.61	0.00	96.77
		0.03	38.10	0.09	55.50	1.81	0.60	0.01	96.14
		0.00	38.29	0.09	55.54	1.95	0.35	0.00	96.23
		0.01	37.66	0.10	55.65	1.91	0.44	0.05	95.83
		0.02	38.24	0.11	55.54	1.77	0.57	0.02	96.27
	rim	0.06	38.97	0.72	55.45	1.15	0.71	0.17	97.23
Magnetite-2	rim	0.08	6.75	0.84	88.60	1.17	0.41	0.09	97.93
		0.01	6.08	0.85	89.00	1.18	0.57	0.13	97.82
		0.18	9.87	0.82	85.45	1.14	0.57	0.11	98.13
		0.00	9.66	0.84	85.72	1.23	0.53	0.08	98.06
		0.07	6.02	0.88	86.56	1.09	0.50	0.22	95.35
		0.07	9.89	0.85	86.96	1.12	0.39	0.13	99.40
		0.07	5.60	0.85	86.15	1.19	0.40	0.13	94.39
		0.03	5.98	0.92	89.50	1.17	0.43	0.11	98.14
		0.03	5.72	0.82	89.96	1.07	0.86	0.23	98.70
		0.09	5.75	0.90	89.62	1.16	0.43	0.09	98.03
		0.05	5.87	0.84	88.07	1.26	0.33	0.06	96.47
		0.04	5.76	0.81	88.75	1.11	0.58	0.10	97.14
		0.03	5.83	0.84	88.44	1.23	0.43	0.06	96.86
		0.02	5.26	0.78	89.07	1.15	0.52	0.11	96.90
		0.06	5.76	0.82	89.98	1.18	0.60	0.06	98.46
		0.06	5.95	0.88	89.94	1.21	0.58	0.12	98.73
	core	0.06	5.86	0.85	89.92	1.17	0.51	0.11	98.47
435.20-435.25 H									
Ilmenite-1	core	0.00	41.98	0.10	54.07	1.39	0.82	0.03	98.39
		0.02	41.33	0.52	54.61	0.97	0.32	0.05	97.82
		0.05	41.34	0.42	54.44	1.59	0.65	0.06	98.56
		0.10	33.50	0.45	63.07	1.57	0.39	0.05	99.12
	rim	0.17	30.33	0.43	68.05	1.17	0.35	0.08	100.58
Magnetite-2	rim	0.36	12.71	1.12	82.94	1.19	0.54	0.14	99.00
		0.13	10.66	1.06	84.13	1.26	0.59	0.15	97.99
		0.12	6.12	0.59	88.90	1.31	0.52	0.08	97.64
	core	0.13	8.82	0.65	88.29	1.44	0.58	0.09	100.00

Appendix 1.3 (cont)
Electron microprobe analyses of Unzen Fe-Ti oxides (in wt.%)

Sample ID	Loc.	SiO_2	TiO_2	Al_2O_3	FeO	MgO	MnO	Cr_2O_3	Total
435.20-235.25 E (Porphyritic)									
Ilmenite-1	core	0.05	31.39	0.10	66.76	0.47	0.18	0.00	98.95
		0.02	36.28	0.20	59.64	0.94	0.47	0.06	97.60
		0.01	38.12	0.29	59.80	0.96	0.61	0.06	99.85
		0.02	38.20	0.24	58.22	0.95	0.54	0.06	98.23
	rim	0.02	39.34	0.26	57.70	1.03	0.59	0.07	99.00
Magnetite	rim	0.05	7.72	0.74	89.44	1.00	0.60	0.03	99.57
		0.08	8.05	1.03	87.08	0.93	0.41	0.11	97.69
		0.13	12.02	0.98	85.78	0.89	0.40	0.10	100.31
		0.11	11.80	1.10	85.17	0.90	0.53	0.11	99.71
		0.09	12.78	1.17	83.15	0.92	0.49	0.14	98.74
	core	0.09	13.87	1.00	81.72	0.93	0.48	0.10	98.20
546.40-546.45 E (Porphyritic)									
Ilmenite-1	core	0.14	37.91	0.59	59.09	1.17	0.63	0.13	99.65
		0.21	39.72	0.73	57.69	1.16	0.74	0.00	100.25
	rim	0.81	41.13	8.42	48.98	0.03	0.00	0.00	99.37
Magnetite-1	rim	0.07	6.56	0.65	88.14	1.04	0.53	0.02	97.02
		0.11	10.40	1.04	87.59	1.28	0.43	0.04	100.88
		0.13	9.37	0.52	88.37	0.83	0.58	0.05	99.84
		0.07	11.09	0.57	85.45	0.78	0.36	0.03	98.35
		0.16	12.11	0.67	85.04	0.99	0.18	0.00	99.14
	core	0.11	13.90	0.69	83.52	0.98	0.42	0.03	99.65
Ilmenite-2	core	0.09	36.84	1.16	60.77	0.01	0.05	0.01	98.93
		0.09	39.46	0.63	55.84	1.97	0.68	0.08	98.76
	rim	0.71	40.95	0.51	56.47	0.87	0.42	0.04	99.98
	rim	0.08	7.46	1.07	89.60	0.92	0.61	0.01	99.75
Magnetite-2		0.23	6.36	1.12	89.71	0.85	0.61	0.05	98.94
		0.62	8.18	1.24	88.18	1.04	0.28	0.06	99.59
		0.12	8.25	1.02	85.90	1.05	0.62	0.04	97.00
		0.13	11.48	1.04	84.22	1.20	0.58	0.03	98.67
	core	0.26	12.06	1.11	83.10	0.97	0.53	0.04	98.07
602.80-602.85 H									
Ilmenite-1	core	0.00	41.18	0.01	50.84	2.23	0.53	0.03	94.83
		0.00	42.69	0.03	50.18	2.23	0.66	0.12	95.92
		0.29	43.02	0.06	52.88	2.30	0.67	0.01	99.23
		0.01	43.10	0.05	51.09	2.11	0.60	0.12	97.08
		0.00	44.23	0.04	51.75	2.27	0.43	0.02	98.74
		0.05	44.57	0.06	52.23	2.20	0.44	0.00	99.55
		0.00	39.34	0.05	56.65	2.33	0.46	0.02	98.85
	rim	0.05	41.24	0.05	52.08	2.11	0.71	0.01	96.26
Magnetite-1	rim	0.14	7.63	0.84	88.74	1.17	0.41	0.03	98.96
		0.17	8.77	0.53	87.41	1.11	0.29	0.15	98.43
		0.09	6.86	0.52	87.95	1.16	0.33	0.05	96.95
		0.05	5.97	0.52	88.75	1.03	0.51	0.01	96.85
		3.48	5.13	0.92	89.13	1.23	0.45	0.03	100.37
	core	0.79	6.71	0.66	89.44	1.20	0.40	0.05	99.25
Ilmenite-2	core	0.02	44.13	0.04	50.68	2.16	0.89	0.02	97.93
		0.07	44.51	0.06	50.18	2.01	0.56	0.00	97.39
		0.00	44.33	0.06	51.43	2.07	0.72	0.06	98.67
		0.00	44.32	0.06	52.42	2.09	0.55	0.00	99.44
		0.02	44.92	0.03	51.86	2.21	0.61	0.10	99.75
		0.00	44.69	0.06	51.01	2.18	0.64	0.00	98.56
		0.01	44.97	0.07	50.65	2.12	0.62	0.04	98.48
		0.01	44.93	0.05	51.81	2.26	0.60	0.00	99.66

Appendix 1.3 (cont)
Electron microprobe analyses of Unzen Fe-Ti oxides (in wt.%)

Sample ID	Loc.	SiO_2	TiO_2	Al_2O_3	FeO	MgO	MnO	Cr_2O_3	Total
		0.05	44.87	0.06	50.91	2.05	0.71	0.08	98.73
		0.00	45.16	0.05	50.56	2.09	0.62	0.00	98.48
		0.04	45.06	0.06	52.85	2.27	0.64	0.09	100.99
		0.00	40.59	0.05	54.34	2.08	0.70	0.01	97.76
		0.08	41.04	0.03	54.38	2.03	0.66	0.05	98.27
		0.55	39.74	0.09	56.15	2.09	0.76	0.13	99.49
	rim	0.06	39.02	0.05	58.02	2.12	0.66	0.04	99.97
Magnetite-2	rim	0.32	11.21	0.76	83.41	1.13	0.35	0.03	97.20
		0.10	10.42	0.75	83.81	0.99	0.41	0.01	96.49
		0.28	9.60	0.77	88.51	1.13	0.22	0.01	100.52
		1.66	6.17	0.84	88.66	1.06	0.49	0.00	98.88
		0.16	7.21	0.60	88.02	1.25	0.51	0.09	97.83
		0.10	7.35	0.68	88.05	1.13	0.33	0.00	97.64
		0.47	7.43	0.58	88.91	1.20	0.44	0.03	99.07
		0.10	8.05	0.61	88.42	1.25	0.47	0.05	98.95
	core	0.40	7.05	0.70	89.97	1.14	0.40	0.03	99.70
602.80-602.85 E (Equigranular)									
Ilmenite-1	core	0.08	42.23	0.05	54.30	2.42	0.52	0.06	99.65
		0.10	43.39	0.56	54.39	0.97	0.42	0.05	99.88
		0.06	42.32	0.03	51.54	2.48	0.72	0.00	97.16
		0.00	42.82	0.05	52.41	2.55	0.47	0.05	98.35
		0.21	44.24	0.06	51.55	2.51	0.47	0.00	99.04
	rim	0.09	41.20	0.15	51.44	2.19	0.52	0.03	95.62
Magnetite-1	rim	0.20	5.97	0.63	89.86	1.06	0.54	0.09	98.35
		0.31	6.52	0.64	89.12	1.13	0.21	0.01	97.93
		0.99	6.45	0.65	88.66	1.17	0.34	0.00	98.25
		0.17	6.40	0.58	89.66	1.12	0.40	0.03	98.37
		0.23	6.53	0.63	89.78	1.11	0.52	0.09	98.88
		0.04	8.14	0.66	87.29	1.16	0.43	0.01	97.72
	core	0.33	9.33	0.63	87.39	1.13	0.41	0.04	99.25
U2A E (Porphyritic)									
Ilmenite-1	core	0.05	44.23	0.14	49.63	1.83	0.43	0.07	96.39
		0.07	45.70	0.14	50.36	1.53	0.39	0.02	98.21
		0.01	46.13	0.11	50.56	1.63	0.39	0.12	98.95
		0.03	46.79	0.15	50.72	1.66	0.49	0.06	99.89
		0.04	46.12	0.14	50.61	1.57	0.67	0.00	99.15
		0.00	46.05	0.14	50.11	1.57	0.50	0.00	98.37
		0.00	47.72	0.14	50.77	1.60	0.39	0.00	100.61
		0.08	47.16	0.15	47.69	1.68	0.65	0.00	97.42
		0.05	46.70	0.16	49.31	1.48	0.52	0.00	98.22
		0.05	45.68	0.13	49.60	1.69	0.58	0.10	97.83
	rim	0.04	48.93	0.14	47.70	1.60	0.50	0.04	98.95
Magnetite-1	rim	0.09	9.18	0.99	84.63	1.00	0.53	0.11	96.53
		0.13	11.24	0.85	85.37	1.00	0.35	0.22	99.17
		0.07	8.65	0.83	86.91	0.89	0.32	0.22	97.89
		0.09	9.44	0.77	87.21	1.07	0.37	0.24	99.20
		0.06	17.16	0.76	80.94	1.08	0.40	0.16	100.57
		0.03	19.14	0.79	78.77	0.97	0.48	0.15	100.32
		0.14	10.52	0.81	85.52	0.96	0.45	0.18	98.59
		0.08	16.09	0.86	82.31	0.85	0.42	0.19	100.79
		0.07	19.61	0.91	77.74	0.82	0.49	0.23	99.86
		0.08	18.78	0.88	77.80	0.83	0.48	0.27	99.11
	core	0.08	19.74	0.84	74.42	1.69	0.63	0.31	97.70
Ilmenite-2	core	0.10	44.13	0.09	50.74	2.12	0.75	0.00	97.92
		0.02	44.79	0.14	51.72	1.89	0.51	0.00	99.06

Appendix 1.3 (cont)
Electron microprobe analyses of Unzen Fe-Ti oxides (in wt.%)

Sample ID	Loc.	SiO_2	TiO_2	Al_2O_3	FeO	MgO	MnO	Cr_2O_3	Total
		0.04	43.90	0.15	51.08	1.73	0.59	0.00	97.50
		0.05	45.36	0.11	49.94	1.71	0.58	0.03	97.79
		0.06	43.65	0.14	51.08	1.87	0.49	0.07	97.36
		0.51	39.22	0.17	55.82	1.64	0.53	0.00	97.88
		0.09	39.52	0.12	55.31	1.72	0.75	0.07	97.58
	rim	0.12	39.08	0.13	56.24	1.81	0.60	0.02	98.01
Magnetite-2	rim	0.20	9.40	1.16	84.65	0.97	0.41	0.25	97.03
		0.09	9.28	1.02	86.76	0.91	0.39	0.19	98.64
		0.15	16.14	0.97	81.50	0.93	0.42	0.14	100.25
		0.38	16.04	0.92	76.72	0.72	0.42	0.15	95.34
		4.91	15.72	1.11	76.99	1.56	0.42	0.17	100.88
		0.07	16.63	1.05	80.23	0.88	0.53	0.23	99.63
	core	0.97	16.20	1.04	79.81	1.00	0.43	0.19	99.63
Ilmenite-3	core	0.13	46.66	1.01	50.39	1.14	0.41	0.15	99.89
	rim	0.08	41.05	0.94	53.67	0.96	0.43	0.19	97.31
Magnetite-3	rim	0.15	9.99	1.02	85.92	1.10	0.43	0.15	98.76
		0.04	9.91	0.86	86.04	1.02	0.46	0.17	98.52
		0.32	16.77	0.89	80.44	1.02	0.40	0.14	99.98
		0.04	16.90	1.02	80.60	1.08	0.52	0.22	100.37
		0.05	17.17	1.07	80.76	0.97	0.35	0.14	100.50
		0.12	17.18	1.01	79.55	0.98	0.54	0.19	99.57
		0.12	17.22	1.05	80.32	0.87	0.46	0.24	100.28
		0.09	17.72	1.03	79.60	0.83	0.41	0.21	99.88
	core	0.11	17.06	0.99	80.93	1.00	0.44	0.18	100.71

Appendix 1.4
Electron microprobe analyses of Unzen amphiboles (in wt.%)

Sample ID	Loc.	SiO_2	TiO_2	Al_2O_3
103.80 H				
P-HBL-1	core	47.30	1.10	9.80
P-HBL-1	rim	47.20	2.30	7.70
P-HBL-2	core	46.40	1.35	9.60
P-HBL-2	rim	46.88	1.44	9.18
P-HBL-3	core	46.31	1.38	9.62
P-HBL-3	rim	47.26	1.00	9.79
P-HBL-4	core	46.52	1.12	9.39
P-HBL-4	rim	46.97	1.22	8.93
P-HBL-5	core	44.77	1.49	9.69
P-HBL-5	rim	46.58	1.23	9.08
103.80 E (Equigranular)				
M-HBL-1	core	46.90	1.50	8.90
M-HBL-1	rim	47.40	1.90	8.20
M-HBL-2	core	48.41	0.77	10.08
M-HBL-2	rim	49.81	1.07	8.65
M-HBL-3	core	47.65	1.16	8.88
M-HBL-3	rim	47.68	1.12	8.03
M-HBL-4	core	45.17	1.50	9.12
M-HBL-4	rim	46.40	1.35	7.60
262.80-H				
P-HBL-1	core	46.19	1.39	9.64
P-HBL-1	rim	46.98	1.41	9.46

FeO	Fe_2O_3	MgO	MnO	CaO	Na_2O	K_2O	F	Cl	Total
10.89	4.25	14.72	0.41	9.48	1.20	0.43	0.10	0.20	99.88
13.15	1.81	13.97	0.40	11.41	1.32	0.71	0.00	0.10	100.07
11.14	2.81	14.20	0.53	9.65	1.33	0.75	0.19	0.07	98.02
9.96	2.77	14.56	0.45	9.32	1.19	0.48	0.07	0.06	96.35
10.96	2.67	14.09	0.38	9.60	1.33	0.55	0.00	0.09	96.99
9.89	2.83	14.84	0.43	9.43	1.20	0.38	0.09	0.09	97.24
0.38	11.09	2.52	14.11	9.87	1.25	0.49	0.10	0.09	96.94
8.64	4.31	15.90	0.56	8.42	1.10	0.41	0.30	0.08	96.83
11.27	2.21	14.08	0.37	9.66	1.50	0.57	0.00	0.12	95.73
10.83	2.73	14.01	0.53	9.37	1.25	0.43	0.05	0.08	96.17
11.01	3.13	14.71	0.40	10.52	1.32	0.54	0.10	0.23	99.26
11.14	3.49	14.65	0.33	9.88	1.21	0.63	0.21	0.21	99.25
10.69	1.18	14.66	0.29	9.89	2.23	0.67	1.19	0.05	100.11
10.33	2.76	14.08	0.58	9.02	1.09	0.34	0.14	0.05	97.93
10.75	2.71	14.53	0.59	11.78	1.17	0.45	0.19	0.06	99.94
10.15	3.00	14.37	0.45	10.02	1.30	0.47	0.23	0.07	96.89
11.78	2.40	12.81	0.57	9.70	1.46	0.58	0.26	0.08	95.41
11.14	2.81	14.20	0.53	9.65	1.33	0.75	0.19	0.07	96.02
11.18	2.61	14.18	0.51	9.42	1.19	0.68	0.09	0.20	97.28
10.01	2.81	14.51	0.49	9.31	1.25	0.49	0.04	0.01	96.77

Appendix 1.4 (cont)
Electron microprobe analyses of Unzen amphiboles (in wt.%)

Sample ID	Loc.	SiO_2	TiO_2	Al_2O_3
P-HBL-2	core	46.38	1.41	9.54
P-HBL-2	rim	46.98	1.15	9.89
262.80-E (Porphyritic)				
M-HBL-1	core	45.72	2.51	11.99
M-HBL-1	rim	45.50	2.53	11.16
M-HBL-2	core	44.77	2.50	12.08
M-HBL-2	rim	44.91	1.96	10.12
M-HBL-3	core	43.97	2.02	11.11
M-HBL-3	rim	43.16	2.28	10.21
M-HBL-4	core	41.00	2.20	14.20
M-HBL-4	rim	46.80	1.40	8.10
M-HBL-5	core	45.21	2.45	12.47
M-HBL-5	rim	44.73	2.59	12.65
578.75-H				
P-HBL-1	core	48.20	1.40	9.04
P-HBL-1	rim	48.20	1.22	9.63
578.75-E (Equigranular)				
M-HBL-1	core	48.43	0.82	10.04
M-HBL-1	rim	49.82	1.14	9.25
M-HBL-2	core	46.38	1.68	8.16
M-HBL-2	rim	48.62	1.46	7.09
M-HBL-3	core	43.80	1.94	11.61
M-HBL-3	rim	48.20	1.23	9.46

FeO	Fe_2O_3	MgO	MnO	CaO	Na_2O	K_2O	F	Cl	Total
10.46	2.68	14.81	0.30	9.45	1.11	0.59	0.20	0.10	97.03
10.15	2.84	14.35	0.31	9.18	1.29	0.31	0.10	0.18	96.73
7.32	3.01	15.22	0.09	9.38	2.11	0.45	0.36	0.01	98.15
7.42	3.37	15.20	0.23	8.80	1.98	0.43	0.78	0.02	97.41
8.86	2.46	14.06	0.17	9.50	2.21	0.46	0.00	0.02	97.09
8.69	2.89	15.14	0.28	9.44	1.97	0.43	0.36	0.03	96.22
7.66	1.87	15.73	0.07	10.89	2.08	0.39	0.14	0.01	95.95
10.33	3.05	14.07	0.31	9.64	1.82	0.39	0.42	0.03	95.71
10.73	3.97	14.20	0.43	10.48	2.21	0.44	0.30	0.10	100.26
11.68	2.85	14.33	0.51	10.17	1.34	0.64	0.61	0.14	98.57
8.90	2.63	13.88	0.16	9.46	2.08	0.44	0.63	0.03	98.35
9.80	2.55	13.29	0.07	9.77	1.85	0.47	0.00	0.03	97.80
11.11	2.53	14.83	0.64	9.97	2.21	0.54	0.00	0.13	100.60
10.44	3.95	14.91	0.54	9.16	1.44	0.41	0.11	0.14	100.15
10.78	1.21	14.32	0.21	9.78	2.21	0.74	0.20	0.04	98.78
10.43	3.76	12.82	0.46	8.98	2.56	0.26	0.01	0.02	99.51
9.79	2.85	14.86	0.46	11.85	1.19	0.39	0.04	0.10	97.75
10.19	3.16	12.44	0.45	9.86	2.01	0.58	0.00	0.20	96.06
10.20	3.98	15.39	0.24	9.97	2.23	0.51	0.00	0.11	99.98
10.85	3.81	14.51	0.44	9.46	1.83	0.62	0.32	0.14	100.87

Appendix 1.4 (cont)
Electron microprobe analyses of Unzen amphiboles (in wt.%)

Sample ID	Loc.	SiO_2	TiO_2	Al_2O_3
U3-H				
P-HBL-1	core	47.89	1.05	9.14
P-HBL-1	rim	45.73	1.27	9.87
P-HBL-2	core	47.93	0.93	9.48
P-HBL-2	rim	47.10	1.39	9.52
U3-E (Porphyritic)				
M-HBL-1	core	45.72	2.51	11.99
M-HBL-1	rim	45.50	2.53	11.16
M-HBL-2	core	45.21	2.45	12.47
M-HBL-2	rim	44.73	2.59	12.65
M-HBL-3	core	44.77	2.50	12.08
M-HBL-3	rim	44.91	1.96	10.12
M-HBL-4	core	43.97	2.02	11.11
M-HBL-4	rim	43.16	2.28	10.21
M-HBL-5	core	45.53	1.74	13.16
M-HBL-5	rim	44.94	2.21	11.72

FeO	Fe_2O_3	MgO	MnO	CaO	Na_2O	K_2O	F	Cl	Total
10.81	2.46	14.72	0.50	9.30	1.25	0.44	0.14	0.07	97.78
10.92	1.98	14.39	0.40	9.66	1.44	0.53	0.14	0.05	96.38
10.19	2.24	14.12	0.52	9.22	1.36	0.36	0.23	0.04	96.61
9.49	2.47	14.48	0.20	9.33	1.89	0.35	0.35	0.04	96.62
7.32	3.01	15.22	0.09	9.38	2.11	0.45	0.36	0.01	98.15
7.42	3.37	15.20	0.23	8.80	1.98	0.43	0.78	0.02	97.41
8.90	2.63	13.88	0.16	9.46	2.08	0.44	0.63	0.03	98.35
9.80	2.55	13.29	0.07	9.77	1.85	0.47	0.00	0.03	97.80
8.86	2.46	14.06	0.17	9.50	2.21	0.46	0.00	0.02	97.09
8.69	2.89	15.14	0.28	9.44	1.97	0.43	0.36	0.03	96.22
7.66	1.87	15.73	0.07	10.89	2.08	0.39	0.14	0.01	95.95
10.33	3.05	14.07	0.31	9.64	1.82	0.39	0.42	0.03	95.71
9.02	0.87	14.13	0.29	10.10	1.36	0.26	0.22	0.07	96.75
10.11	2.47	13.17	0.28	9.67	2.06	0.53	0.00	0.01	97.16

Appendix 2. 1
Electron microprobe analyses of Redoubt amphiboles (in wt.%)

Sample	Event	microns	SiO_2	TiO_2	Al_2O_3
92MHR6-1 HBL01	Dec 15 1989	0.00	45.57	1.81	8.49
		16.28	44.64	2.44	8.07
		49.67	45.73	2.11	8.45
		66.79	45.38	2.40	8.50
		83.07	46.13	2.14	9.34
92MHR6-1 HBL02	Dec 15 1989	0.00	46.35	0.76	8.35
		15.62	46.55	0.92	8.59
		47.52	46.32	1.21	8.34
		63.92	45.82	1.56	9.04
		79.54	46.76	1.44	8.54
		95.82	47.14	1.36	8.48
		111.44	45.96	0.96	8.48
92MHR9-1 PG01	Dec 15 1989	0.00	40.94	1.64	14.59
		16.82	41.67	1.87	12.93
		33.64	40.98	1.74	13.76
		50.46	41.85	1.93	12.70
92MHR6-1 HBL03	Dec 15 1989	0.00	45.18	1.29	9.68
		25.00	45.07	1.32	10.54
		60.00	45.59	1.72	9.35
92MHR20-1 HBL01	Jan 2 1990	0.00	45.33	1.62	8.94
		16.76	46.97	1.85	7.49
		32.57	44.71	1.97	9.41
		49.34	44.44	1.97	9.23
		66.10	45.29	1.46	9.31
		82.86	47.78	1.40	7.31
		98.67	48.34	1.38	6.72
92MHR20-1 HBL02	Jan 2 1990	0.00	44.34	1.44	11.07
		33.54	43.35	1.13	11.29
		60.84	43.56	1.25	11.23
		86.02	43.94	1.38	11.19
		127.99	44.54	1.32	10.06

FeO	MnO	MgO	CaO	Na_2O	K_2O	F	Cl	Total
12.56	0.40	14.54	10.79	1.87	0.72	0.46	0.42	97.62
12.62	0.40	14.10	10.66	1.80	0.32	0.20	0.14	95.37
12.99	0.49	14.66	11.06	1.77	0.47	0.00	0.09	97.82
12.21	0.70	14.68	11.10	1.79	0.43	0.00	0.10	97.29
11.64	0.33	14.90	11.35	2.13	0.36	0.39	0.09	98.81
13.64	0.52	13.73	11.46	1.45	0.29	0.00	0.11	96.65
13.38	0.40	14.25	11.81	1.61	0.31	0.00	0.13	97.96
13.32	0.54	14.27	11.40	1.46	0.31	0.00	0.14	97.31
13.72	0.43	13.95	10.49	1.28	0.33	0.13	0.09	96.83
13.36	0.54	14.44	10.51	1.42	0.27	0.71	0.12	98.10
12.95	0.39	14.02	10.58	1.60	0.35	0.00	0.12	96.99
13.31	0.55	13.93	10.56	1.42	0.29	0.07	0.10	95.61
11.68	0.11	14.08	11.64	2.21	0.64	0.00	0.01	97.54
13.95	0.38	12.93	11.47	2.36	0.46	0.32	0.03	98.38
12.82	0.24	13.51	11.55	2.28	0.55	0.16	0.02	97.62
13.22	0.27	13.45	11.16	2.22	0.43	0.45	0.00	97.69
13.09	0.39	14.16	10.60	1.89	0.38	0.00	0.05	96.70
11.86	0.33	14.15	10.69	2.05	0.34	0.26	0.00	96.62
12.61	0.41	14.69	9.83	1.72	0.28	0.20	0.05	96.46
13.21	0.65	14.33	11.09	1.75	0.35	0.00	0.05	97.32
11.76	0.40	15.12	10.85	1.42	0.33	0.00	0.07	96.25
13.48	0.60	13.96	11.14	1.79	0.38	0.00	0.09	97.53
12.87	0.48	14.00	10.93	1.79	0.39	0.26	0.07	96.43
12.57	0.55	13.96	11.19	1.79	0.38	0.00	0.09	96.58
11.89	0.64	15.80	11.00	1.38	0.23	0.20	0.07	97.70
11.65	0.42	15.97	10.96	1.48	0.29	0.39	0.07	97.68
13.39	0.42	13.83	10.19	1.85	0.33	0.00	0.06	96.90
13.94	0.38	13.41	10.62	1.91	0.31	0.19	0.01	96.53
13.82	0.40	13.86	10.74	2.09	0.26	0.51	0.02	97.75
13.07	0.31	13.65	10.66	1.77	0.37	0.13	0.02	96.47
12.49	0.26	14.72	10.80	1.98	0.29	0.00	0.05	96.51

Appendix 2. 1 (cont.)
Electron microprobe analyses of Redoubt amphiboles (in wt.%)

Sample	Event	microns	SiO_2	TiO_2	Al_2O_3
		138.99	45.80	1.40	9.22
92MHR20-1 HBL03	Jan 2 1990	0.00	46.65	1.91	7.41
		16.28	46.71	1.61	7.57
		31.41	46.51	2.20	7.80
		47.69	46.84	2.01	7.76
		63.81	46.47	1.60	7.80
		79.11	46.52	1.62	7.61
		95.24	45.95	1.28	8.94
92MHR20-1 PG01	Jan 2 1990	0.00	41.85	1.93	12.70
		12.96	40.38	1.76	14.15
		25.92	41.51	2.10	13.23
		38.88	40.72	2.21	13.42
		51.84	41.58	2.47	13.26
92MHR12-1 HBL01	Feb 15 1989	15.30	48.29	1.77	6.70
		30.82	47.93	1.32	6.61
		62.40	46.30	1.40	6.35
		77.92	48.12	1.61	6.58
		93.22	48.33	1.65	6.55
		109.50	48.33	1.47	6.55
		125.02	47.44	1.53	6.35
		140.32	48.17	1.54	6.44
92MHR12-2 HBL02	Feb 15 1989	0.00	47.32	1.95	7.72
		11.00	45.62	2.40	8.71
		22.00	46.29	2.06	7.85
		34.00	46.70	1.98	7.74
		45.00	47.00	2.16	7.61
		56.00	47.36	1.50	7.35
92MHR12-2 HBL03	Feb 15 1989	0.00	53.33	0.12	0.80
		17.46	52.76	0.24	0.77
		36.25	53.49	0.10	0.83
		53.72	32.67	0.14	0.49

FeO	MnO	MgO	CaO	Na_2O	K_2O	F	Cl	Total
12.65	0.36	14.70	10.21	1.82	0.30	0.19	0.06	96.71
12.87	0.44	14.93	11.52	1.68	0.26	0.26	0.03	97.98
12.15	0.44	15.02	11.05	1.65	0.30	0.00	0.07	96.56
12.56	0.52	14.92	10.90	1.68	0.34	0.26	0.11	97.80
12.63	0.63	14.73	11.01	1.66	0.38	0.00	0.10	97.75
12.66	0.33	15.01	11.28	1.61	0.33	0.00	0.07	97.18
12.35	0.40	14.95	10.97	1.68	0.30	0.59	0.11	97.10
11.73	0.42	14.96	10.25	1.76	0.28	0.13	0.06	95.77
13.22	0.27	13.45	11.16	2.22	0.43	0.16	0.00	97.39
11.69	0.08	13.68	11.95	2.18	0.68	0.10	0.20	96.85
11.87	0.21	14.66	11.04	2.51	0.37	0.20	0.01	97.70
11.30	0.15	14.38	11.95	2.42	0.41	0.00	0.03	96.99
11.15	0.23	14.10	11.24	2.51	0.45	0.33	0.03	97.35
11.69	0.43	15.46	11.34	1.59	0.26	0.20	0.11	97.84
10.69	0.39	15.88	11.29	1.47	0.29	0.00	0.08	95.95
10.93	0.36	15.11	11.16	1.42	0.26	0.33	0.11	93.73
11.70	0.35	15.87	11.14	1.38	0.32	0.00	0.06	97.13
11.59	0.52	15.88	10.83	1.53	0.22	0.00	0.12	97.21
11.10	0.35	15.60	11.21	1.42	0.31	0.00	0.11	96.44
11.25	0.43	15.80	10.82	1.49	0.29	0.00	0.11	95.51
11.95	0.41	15.60	10.99	1.29	0.27	0.07	0.11	96.84
12.11	0.45	15.22	11.10	1.69	0.40	0.13	0.07	98.17
12.56	0.56	14.49	11.39	1.90	0.35	0.33	0.10	98.41
11.85	0.53	15.38	11.53	1.76	0.37	0.00	0.07	97.69
11.65	0.48	14.92	11.35	1.66	0.38	0.00	0.07	96.92
11.71	0.29	15.38	11.13	1.68	0.28	0.00	0.06	97.31
11.68	0.53	15.15	10.39	1.68	0.38	0.00	0.07	96.08
18.86	1.08	23.67	1.04	0.04	0.01	0.00	0.03	98.98
19.69	1.15	23.57	1.04	0.02	0.00	0.59	0.01	99.85
20.25	0.97	23.55	0.95	0.01	0.00	0.18	0.01	100.34
11.96	0.70	14.80	19.34	0.03	0.00	0.48	0.66	81.27

Appendix 2. 1 (cont.)
Electron microprobe analyses of Redoubt amphiboles (in wt.%)

Sample	Event	microns	SiO_2	TiO_2	Al_2O_3
		72.51	51.36	0.10	0.86
		89.97	51.42	0.06	0.85
92MHR12-2 HBL04	Feb 15 1989	0.00	46.59	1.89	8.05
		11.00	46.77	2.04	8.21
		22.00	47.42	1.65	7.31
		33.00	47.99	1.36	7.28
		44.00	48.03	1.53	7.29
92MHR22-1 HBL01	April 15 1990	0.00	42.04	2.06	12.54
		35.23	42.69	1.52	13.79
		70.67	72.46	0.63	11.12
92MHR22-1 HBL02	April 15 1990	46.12	43.49	1.09	11.55
		62.61	43.97	1.36	9.71
		77.91	45.28	1.50	9.46
		93.20	44.82	1.60	9.32
		108.73	44.30	1.25	9.70
		124.03	41.16	2.08	12.84
		139.32	34.71	1.28	20.44
		155.82	41.14	1.96	12.84
		171.11	41.13	1.62	13.13
		186.64	41.19	1.79	13.30
		201.93	40.83	1.59	12.73
92MHR22-1 HBL03	April 15 1990	0.00	42.20	2.20	12.31
		43.32	41.31	1.85	13.04
		64.91	41.58	1.93	12.33
		110.22	40.67	1.81	13.26
		167.08	40.86	1.91	12.68
RDT-1 HBL02		0.00	45.58	2.03	9.12
		16.12	45.22	1.54	9.02
		31.94	45.15	1.58	9.28
		48.06	44.04	1.44	11.10
		64.70	44.73	1.27	10.51

FeO	MnO	MgO	CaO	Na_2O	K_2O	F	Cl	Total
19.16	0.67	22.73	1.02	0.00	0.00	0.24	0.01	96.14
18.47	1.10	23.68	1.04	0.00	0.01	0.00	0.04	96.67
12.01	0.35	15.02	11.22	1.73	0.33	0.00	0.11	97.31
12.43	0.40	14.97	11.37	1.84	0.33	0.13	0.14	98.63
11.57	0.30	15.27	11.30	1.52	0.39	0.00	0.09	96.82
11.48	0.47	15.25	11.21	1.52	0.42	0.33	0.12	97.41
11.84	0.30	15.54	11.14	1.56	0.29	0.39	0.09	98.00
12.36	0.27	14.35	11.34	2.23	0.37	0.13	0.00	97.68
12.57	0.26	12.63	9.57	2.18	0.37	0.00	0.03	95.61
2.38	0.10	1.64	1.06	1.19	3.10	0.00	0.15	93.83
11.78	0.31	13.82	9.91	1.92	0.32	0.19	0.07	94.45
11.87	0.52	14.24	10.80	1.78	0.30	0.20	0.08	94.82
11.73	0.31	14.49	10.59	1.76	0.45	0.00	0.08	95.66
11.74	0.49	14.50	9.98	1.67	0.42	0.00	0.08	94.63
11.87	0.36	14.63	10.05	1.83	0.38	0.07	0.10	94.55
11.63	0.16	13.75	10.55	2.23	0.41	0.00	0.04	94.84
10.01	0.18	11.64	9.74	1.77	0.31	0.07	0.10	90.23
11.27	0.15	14.08	10.61	2.24	0.43	0.33	0.00	95.05
11.79	0.25	13.85	10.44	2.41	0.32	0.26	0.03	95.23
11.84	0.18	13.50	10.42	2.41	0.50	0.00	0.02	95.16
11.10	0.14	13.86	11.42	2.23	0.41	0.00	0.00	94.31
11.51	0.17	14.36	11.12	2.39	0.39	0.00	0.02	96.68
11.50	0.14	13.87	11.69	2.39	0.40	0.00	0.03	96.22
12.14	0.25	13.94	11.75	2.34	0.32	0.00	0.03	96.60
10.88	0.21	13.87	11.04	2.34	0.39	0.00	0.02	94.49
11.55	0.19	13.96	10.57	2.62	0.36	0.07	0.03	94.81
12.74	0.34	14.19	10.84	1.90	0.37	0.00	0.10	97.22
13.04	0.33	14.40	10.27	1.95	0.42	0.32	0.11	96.63
13.48	0.37	14.57	11.43	1.85	0.35	0.20	0.13	98.39
12.17	0.33	14.05	10.74	1.82	0.41	0.13	0.04	96.29
13.35	0.22	14.25	11.03	1.93	0.35	0.06	0.03	97.73

Appendix 2. 1 (cont.)
Electron microprobe analyses of Redoubt amphiboles (in wt.%)

Sample	Event	microns	SiO_2	TiO_2	Al_2O_3
		80.83	44.83	1.25	10.25
		96.64	44.71	1.32	10.00
		112.76	48.55	1.32	6.88
RDT-2 HBL01		0.00	46.07	2.10	8.38
		14.76	46.60	1.95	8.60
		30.42	46.34	1.62	8.45
		45.18	46.60	1.79	8.48
		60.83	46.19	1.73	8.55
		75.60	49.43	1.05	5.92
RDT-4 HBL01		0.00	45.67	2.05	8.99
		16.49	45.26	2.78	8.77
RDT-4 HBL02		0.00	45.81	1.95	8.78
		22.81	45.77	1.27	9.68
RDT-4 HBL03		0.00	45.68	2.06	8.62
RDT-4 HBL04		0.00	45.92	2.08	8.61
RDT-4 HBL05		0.00	45.71	2.11	8.28
RDT-4 HBL06		0.00	45.39	2.16	8.56
RDT-4 HBL07		0.00	44.67	2.05	8.99
RDT-4 HBL08		0.00	45.26	1.78	8.77
RDT-4 HBL09		0.00	44.81	1.95	8.78
RDT-4 HBL10		0.00	44.77	2.27	9.68
RDT-4 HBL11		0.00	45.82	1.50	8.23
RDT-4 HBL12		0.00	45.95	2.37	8.12
RDT-A-1 PG01		0.00	41.74	1.75	14.06
		13.04	41.32	1.86	14.19
RDT-A-1 PG02		0.00	41.39	2.39	13.37
		9.12	41.07	2.49	13.22
		18.24	42.00	1.94	13.46
RDT-A-1 PG03		0.00	41.67	1.87	12.93

FeO	MnO	MgO	CaO	Na_2O	K_2O	F	Cl	Total
13.18	0.47	14.15	10.36	1.90	0.38	0.00	0.07	96.83
12.66	0.41	13.97	10.59	1.83	0.34	0.00	0.06	95.87
12.09	0.64	16.01	10.92	1.51	0.38	0.00	0.03	98.33
12.53	0.36	14.97	11.14	1.68	0.39	0.13	0.07	97.82
12.81	0.48	14.87	10.67	1.72	0.32	0.20	0.10	98.30
12.58	0.57	14.89	9.91	1.63	0.38	0.00	0.09	96.46
12.73	0.43	14.94	10.78	1.67	0.38	0.46	0.04	98.30
12.67	0.63	15.05	10.33	1.67	0.31	0.00	0.06	97.17
12.00	0.78	17.05	8.69	1.41	0.19	0.39	0.03	96.93
12.75	0.29	14.28	11.10	1.98	0.40	0.65	0.11	98.27
12.91	0.36	14.00	11.29	1.90	0.44	0.20	0.10	97.99
12.38	0.28	14.26	10.80	1.86	0.44	0.46	0.13	97.15
12.42	0.55	14.10	10.86	1.99	0.30	0.00	0.02	96.95
12.69	0.41	14.32	11.06	1.68	0.86	0.24	0.01	97.63
12.79	0.50	14.09	11.46	1.85	0.82	0.21	0.12	98.45
12.91	0.62	13.68	11.21	1.71	0.43	0.19	0.04	96.89
13.06	0.89	13.98	11.16	1.64	0.39	0.08	0.10	97.41
12.75	0.29	14.28	11.10	1.98	0.40	0.65	0.11	97.27
12.91	0.36	14.00	11.29	1.90	0.44	0.20	0.10	96.99
12.38	0.28	14.26	10.80	1.86	0.44	0.46	0.13	96.15
12.42	0.55	14.10	10.86	1.99	0.30	0.00	0.02	96.95
13.48	0.37	14.13	10.82	1.89	0.45	0.39	0.14	97.23
14.16	0.61	14.25	9.89	1.79	0.40	0.00	0.16	97.70
11.97	0.23	12.37	12.07	2.55	0.44	0.00	0.07	97.26
11.27	0.14	12.35	12.08	2.60	0.44	0.20	0.02	96.46
11.34	0.26	14.39	11.61	2.56	0.44	0.52	0.06	98.33
11.19	0.11	14.42	11.76	2.50	0.39	0.00	0.06	97.22
11.58	0.19	14.72	11.86	2.56	0.43	0.00	0.00	98.72
13.95	0.38	12.93	11.47	2.36	0.46	0.32	0.03	98.38

Appendix 2. 1 (cont.)
Electron microprobe analyses of Redoubt amphiboles (in wt.%)

Sample	Event	microns	SiO_2	TiO_2	Al_2O_3
RDT-A-1 PG04		0.00	41.85	1.93	12.70
RDT-A-1 PG05		0.00	41.67	1.97	12.37
RDT-A-1 PG06		0.00	41.76	2.13	12.38
RDT-A-1 PG07		0.00	41.32	1.86	13.19
RDT-A-1 PG08		0.00	41.39	2.39	13.37
RDT-A-1 PG09		0.00	41.07	2.49	13.22
RDT-A-2 PG01		0.00	40.51	2.10	16.23
		9.44	40.72	2.21	16.42
		18.88	40.58	2.47	16.26
RDT-A-2 PG02		0.00	39.39	2.64	15.96
RDT-A-2 PG03		0.00	39.98	2.71	14.58
RDT-A-2 PG04		0.00	40.16	2.49	14.96
RDT-A-2 PG05		0.00	40.18	2.37	14.67
RDT-A-2 PG06		0.00	39.99	2.66	15.86
RDT-7 HBL01		0.00	41.74	1.75	13.06
		13.04	41.32	1.86	13.19
		26.08	41.39	2.39	13.37
		39.12	41.07	2.49	13.22
		50.78	42.00	1.94	13.46
		63.82	41.51	2.10	13.23
		79.44	40.72	2.21	13.42
		90.21	41.58	2.47	13.26
RDT-7 HBL02		0.00	47.82	2.00	6.47
		13.93	47.89	1.59	6.41
		28.79	45.30	1.63	6.08
		42.72	47.86	1.44	6.43
RDT-8 HBL01		0.00	45.48	1.15	10.04
		18.11	44.47	1.21	10.95
		36.22	44.55	1.52	10.32
		54.47	44.39	1.31	10.21
		72.58	49.28	1.59	6.12

FeO	MnO	MgO	CaO	Na_2O	K_2O	F	Cl	Total
13.22	0.27	13.45	11.16	2.22	0.43	0.45	0.00	97.69
13.28	0.33	12.67	10.34	2.34	0.43	0.00	0.02	95.42
13.14	0.31	13.05	10.27	2.36	0.38	0.77	0.02	96.56
11.27	0.14	14.35	12.08	2.60	0.44	0.20	0.02	97.46
11.34	0.26	14.39	11.61	2.56	0.44	0.52	0.06	98.33
11.19	0.11	14.42	11.76	2.50	0.39	0.00	0.06	97.22
11.87	0.21	14.66	10.04	2.51	0.37	0.20	0.01	98.70
11.30	0.15	14.38	10.95	2.42	0.41	0.00	0.03	98.99
11.15	0.23	14.10	10.24	2.51	0.45	0.33	0.03	98.35
10.69	0.21	15.86	10.11	3.58	0.62	0.00	0.06	99.12
11.06	0.28	15.86	10.08	3.64	0.68	0.10	0.01	98.98
11.14	0.34	15.67	9.06	3.82	0.74	0.00	0.14	98.52
10.79	0.21	15.10	10.46	3.11	0.74	0.00	0.00	97.63
10.68	0.28	14.83	10.18	3.16	0.19	0.15	0.00	97.98
10.97	0.23	14.37	12.07	2.55	0.44	0.00	0.07	97.26
11.27	0.14	14.35	12.08	2.60	0.44	0.20	0.02	97.46
11.34	0.26	14.39	11.61	2.56	0.44	0.52	0.06	98.33
11.19	0.11	14.42	11.76	2.50	0.39	0.00	0.06	97.22
11.58	0.19	14.72	11.86	2.56	0.43	0.00	0.00	98.72
11.87	0.21	14.66	11.04	2.51	0.37	0.20	0.01	97.70
11.30	0.15	14.38	11.95	2.42	0.41	0.00	0.03	96.99
11.15	0.23	14.10	11.24	2.51	0.45	0.33	0.03	97.35
11.88	0.34	16.20	9.92	1.44	0.27	0.00	0.05	96.38
11.45	0.27	15.92	10.53	1.44	0.28	0.20	0.12	96.11
11.58	0.45	15.68	10.56	1.36	0.31	0.00	0.05	93.00
11.50	0.52	16.52	11.09	1.50	0.27	0.00	0.08	97.23
13.66	0.45	14.66	10.20	1.64	0.26	0.32	0.05	97.91
13.69	0.57	14.09	10.79	1.91	0.31	0.06	0.06	98.11
12.41	0.25	14.53	11.22	1.81	0.36	0.00	0.06	97.03
12.97	0.35	14.80	10.77	1.66	0.25	0.06	0.05	96.83
10.50	0.49	16.62	10.46	1.32	0.21	0.33	0.09	97.01

Appendix 2. 1 (cont.)
Electron microprobe analyses of Redoubt amphiboles (in wt.%)

Sample	Event	microns	SiO_2	TiO_2	Al_2O_3
RDT-58 HBL01		0.00	46.55	2.28	7.56
		15.23	47.16	2.06	7.61
		30.00	46.85	1.92	7.33
		45.23	45.88	1.87	7.04
		60.88	48.00	1.42	6.41
		75.20	48.42	1.46	6.26
		90.85	46.50	1.32	7.16
		106.08	47.18	1.44	7.53
		120.85	46.89	1.65	7.55
		136.08	47.26	1.71	7.34
RDT-58 HBL02		0.00	44.86	2.37	9.15
		15.00	44.13	2.08	9.16
		24.00	44.08	2.04	8.98
		41.46	44.74	2.27	9.31
RDT-58 HBL04		0.00	46.38	1.69	7.88
		16.49	46.62	1.96	7.50
		31.79	46.99	1.84	7.50
		48.28	47.70	1.72	6.74
RDT-58 HBL05		0.00	45.63	1.34	9.84
		11.00	45.78	1.38	9.67
		19.00	45.04	1.57	9.86
		31.00	44.85	1.30	9.75
		47.00	44.97	1.79	9.64
(rx rim)		90.84	53.83	0.26	0.40
RDT-58 HBL06		0.00	45.71	0.91	9.51
		14.56	45.50	1.55	9.29
		24.05	45.30	1.67	9.34
		35.75	46.22	1.65	8.40
(rx rim)		87.95	53.61	0.24	0.60
(rx rim)		107.80	53.27	0.04	0.32
RDT-58 HBL07		0.00	45.63	1.90	8.28
		37.12	45.60	2.43	8.44

FeO	MnO	MgO	CaO	Na_2O	K_2O	F	Cl	Total
12.55	0.44	14.66	10.57	1.51	0.39	0.39	0.12	97.03
11.73	0.48	15.09	11.04	1.64	0.38	0.00	0.09	97.28
12.52	0.41	14.91	11.17	1.58	0.34	0.00	0.10	97.13
12.54	0.53	16.19	10.93	1.54	0.36	0.59	0.10	97.56
11.87	0.34	15.72	10.45	1.31	0.32	0.85	0.07	96.75
12.11	0.65	16.13	11.43	1.36	0.29	0.79	0.08	98.98
12.51	0.53	15.17	11.64	1.46	0.32	0.33	0.09	97.02
12.75	0.64	15.28	11.42	1.65	0.36	0.46	0.06	98.77
12.14	0.42	14.96	11.17	1.63	0.26	0.33	0.08	97.09
12.41	0.47	15.18	11.02	1.64	0.37	0.00	0.05	97.46
12.53	0.34	14.45	11.10	2.05	0.38	0.00	0.08	97.33
12.44	0.35	14.63	10.91	2.00	0.39	0.07	0.12	96.29
12.22	0.27	14.28	10.61	2.02	0.36	0.00	0.12	94.98
12.67	0.28	14.32	11.42	1.98	0.43	0.07	0.08	97.57
12.36	0.21	14.83	11.13	1.67	0.34	0.33	0.05	96.88
12.12	0.49	15.13	10.62	1.64	0.34	0.00	0.10	96.53
12.00	0.50	15.18	10.79	1.46	0.37	0.07	0.08	96.77
11.46	0.40	15.41	10.82	1.62	0.33	0.33	0.12	96.64
12.43	0.38	14.85	10.59	1.77	0.33	0.07	0.04	97.24
13.06	0.32	14.88	10.91	1.71	0.32	0.00	0.03	98.05
11.95	0.47	14.74	11.30	1.78	0.32	0.46	0.10	97.59
12.22	0.48	14.71	11.23	1.80	0.37	0.20	0.07	96.97
12.61	0.56	14.48	10.54	1.95	0.38	0.20	0.07	97.18
19.37	1.35	23.79	1.09	0.02	0.02	0.24	0.01	100.39
12.01	0.42	14.78	10.88	1.73	0.25	0.33	0.05	96.56
12.37	0.49	14.90	11.12	1.92	0.23	0.00	0.07	97.46
11.79	0.50	14.56	11.11	1.84	0.24	0.00	0.07	96.43
12.53	0.56	15.39	11.15	1.71	0.34	0.72	0.05	98.72
18.00	1.06	25.00	1.29	0.01	0.01	0.00	0.02	99.85
18.70	1.63	23.78	2.12	0.04	0.00	0.00	0.03	99.93
12.90	0.43	14.48	11.03	1.89	0.44	0.00	0.07	97.05
12.96	0.48	14.83	11.50	1.90	0.40	0.39	0.06	98.98

Appendix 2. 1 (cont.)
Electron microprobe analyses of Redoubt amphiboles (in wt.%)

Sample	Event	microns	SiO_2	TiO_2	Al_2O_3
		95.30	46.03	2.10	8.42
		138.26	46.69	1.83	8.53
		369.21	45.47	1.77	8.53
(rx rim)		389.31	59.87	1.40	9.96
RDT-73 HBL01		0.00	49.37	0.28	0.48
		19.92	49.91	0.22	0.26
		88.58	48.92	0.22	0.25
RDT-73 HBL02		0.00	46.94	1.44	7.54
		16.00	46.32	1.91	7.67
		34.00	46.67	1.85	7.70
		51.00	47.09	1.47	7.34
RDT-73 HBL03		0.00	45.53	1.56	8.22
		26.93	45.16	1.70	8.29
		65.21	45.37	1.79	8.18
		91.46	45.35	1.54	8.14
RDT-74 HBL01		0.00	47.06	1.22	7.02
		16.28	47.53	1.86	6.61
		47.34	48.34	1.71	6.89
RDT-74 HBL02		0.00	49.24	1.58	9.59
		26.40	46.04	2.43	8.62
		57.71	47.79	1.77	6.89
		77.71	48.22	1.57	8.21
RDT-74 HBL05		0.00	45.22	2.01	8.80
		16.28	45.18	1.91	8.81
		31.90	45.07	1.81	8.85
		48.18	45.30	2.05	8.78
		64.46	45.16	1.95	8.71
		80.74	45.27	2.01	8.92
		96.36	44.85	1.94	8.69
		112.64	45.30	1.76	8.79

FeO	MnO	MgO	CaO	Na_2O	K_2O	F	Cl	Total
12.94	0.26	14.81	11.14	1.85	0.40	0.00	0.19	98.16
13.08	0.24	12.99	9.65	1.89	0.50	0.00	0.11	95.52
12.76	0.31	14.76	11.44	1.88	0.36	0.07	0.11	97.45
7.21	0.19	7.78	6.54	1.23	1.23	0.00	0.14	95.53
27.54	1.53	14.50	2.07	0.02	0.00	0.23	0.02	96.04
26.07	1.27	14.67	3.19	0.00	0.00	0.00	0.02	95.61
25.86	1.19	13.94	2.64	0.00	0.00	0.12	0.00	93.12
11.19	0.57	14.67	10.34	1.56	0.31	0.00	0.07	94.65
11.25	0.30	15.15	9.01	1.62	0.35	0.00	0.12	93.71
11.46	0.38	15.03	11.04	1.76	0.22	0.13	0.06	96.30
10.70	0.32	15.31	10.77	1.69	0.34	0.72	0.07	95.82
12.64	0.40	14.23	9.94	1.75	0.37	0.00	0.10	94.73
13.62	0.35	14.15	9.93	1.65	0.41	0.39	0.14	95.78
12.78	0.22	14.36	10.14	1.62	0.41	0.00	0.15	95.02
12.66	0.38	14.19	10.24	1.65	0.35	0.00	0.20	94.70
10.23	0.38	13.12	8.25	1.56	0.64	0.46	0.11	90.03
13.58	0.58	14.68	9.19	1.63	0.34	0.00	0.08	96.08
12.31	0.45	15.38	9.87	1.68	0.42	0.00	0.11	97.15
11.73	0.35	11.50	10.10	2.30	0.44	0.00	0.07	96.90
11.89	0.33	14.35	10.92	1.92	0.40	0.07	0.14	97.11
11.64	0.41	15.59	11.56	1.62	0.31	0.07	0.08	97.71
11.64	0.34	13.88	10.79	1.58	0.36	0.13	0.09	96.80
13.32	0.46	14.64	11.47	1.85	0.37	0.00	0.10	98.24
13.87	0.37	14.41	10.88	1.71	0.40	0.26	0.13	97.93
13.58	0.24	14.50	11.13	1.83	0.39	0.00	0.10	97.51
13.37	0.26	14.42	10.92	1.74	0.38	0.33	0.18	97.73
13.49	0.52	14.40	11.41	1.86	0.33	0.20	0.10	98.13
14.05	0.34	14.51	11.25	1.72	0.40	0.00	0.08	98.55
14.39	0.50	14.33	10.63	1.87	0.31	0.45	0.14	98.10
13.17	0.42	14.46	10.67	1.82	0.36	0.13	0.09	96.97

Appendix 2.2

Experiment sample preparation. "Sample #", indicates sample identification number as listed in Tables 2.5 and 2.6; "C", experimental capsule types of $Ag_{70}Pd_{30}$ (AP) or Ag (A); "F", furnace types of Rene or TZM; "Capsule (g)", empty capsule weight in grams; "w/ H2O (g)", capsule weight plus added distilled water in grams; "[H_2O_T (g)]", total distilled water added in grams; "Total (g)", total weight of the capsule, water, and sample after ~1 hour on 150 °C hot plate in grams; "[$Sample_T$ (g)]", total weight of sample in grams; "H_2O (wt.%)", weight percent added distilled water; "Ni, NiO (g)", weight of added Ni foil and NiO powder for TZM experiments in grams; "T (°C)", temperature of experiment run in °C; "P (MPa)", pressure of experiment run in MPa; "In (d,h)", Date and hour of start of experiment; "Drop (d,h)", Date and hour of decompression; "P_D (MPa)", Pressure to which experiment was decompressed in MPa; "T_H °C", Temperature to which experiment was heated in °C; "Quench (d,h)", Date and hour of end of when experiment was quenched; "Time $_{D,H}$ (d)", Total number of days outside of hornblende stability; "Time $_T$ (d)", Total number of days of experiment.

Appendix 2. 2
Experiment sample preparation

Exp #:	C	F	Capsule	w/ H2O	H_2O_T	Total	$Sample_T$	H_2O	Ni, NiO	T (°C)	P (MPa)	In (d, h)	Drop (d,h)	P_D (MPa)	T_H (°C)	Quench (d,h)	$Time_{D,H}$ (d)	$Time_T$ (d)
RDT-1	AP	R	0.9126	0.9227	0.0101	1.0860	0.1633	6.18		840	150	2/16/2002, 0930	2/20, 0915	120				
													2/21, 1030	90				
													2/22, 0930	60				
													2/23, 0915	30		2/23, 1715	3.5	7.5
RDT-2	AP	R	0.9842	1.0024	0.0182	1.3125	0.3101	5.87		840	150	2/16/2002, 0930	2/20, 0915	140				
													2/21, 0900	130				
													2/22, 0930	120				
													2/23, 0900	110				
													2/24, 0900	100				
													2/25, 0900	90				
													2/26, 0900	80				
													2/27, 0915	70				
													2/28, 0900	60				
													3/1, 0900	50				
													3/2, 0930	40				
													3/3, 0900	30		3/4, 0930	11.0	15.0
RDT-3	AP	R	0.9648	0.9712	0.0064	1.0984	0.1272	5.03		840	125	2/16/2002, 0930				2/21, 0900		4.9
RDT-4	AP	R	0.9137	0.9191	0.0054	0.9987	0.0796	6.78		840	150	2/16/2002, 0930				2/21, 0930		5.0
RDT-5	AP	R	1.6139	1.6222	0.0083	1.7636	0.1414	5.87		840	150	3/5/2002, 1245	3/9, 0915	130				
													3/9, 2100	110				
													3/10, 0900	90				
													3/10, 2130	70				
													3/11, 0915	50				
													3/11, 2110	30				
													3/12, 0900	10		3/12, 2215	3.5	7.5
RDT-6	AP	R	1.5004	1.5091	0.0087	1.6890	0.1799	4.84		840	150	3/5/2002, 1245	3/9, 0915	135				
													3/9, 2100	120				
													3/10, 0900	105				
													3/10, 2130	90				
													3/11, 0915	80		3/11, 2110	2.5	6.5
RDT-7	AP	R	0.8923	0.9042	0.0119	1.1383	0.2341	5.08		840	150	5/14/2002, 1230	8/19, 2100	140				
													8/20, 0910	130				
													8/20, 2050	120				
													8/21, 0925	110				
													8/21, 2230	100				
													8/22, 0900	90				
													8/22, 2110	80				
													8/23, 2135	60				
													8/24, 0905	50				
													8/24, 2045	40				
													8/25, 0910	30				
													8/25, 2100	20				
													8/26, 1030	10		8/26, 2100	7.0	10.5

Appendix 2. 2 (cont.)
Experiment sample preparation

Exp #:	C	F	Capsule	w/ H2O	H_2O_T	Total	$Sample_T$	H_2O	Ni, NiO	T (°C)	P (MPa)	In (d, h)	Drop (d,h)	P_D (MPa)	T_H (°C)	Quench (d,h)	$Time_{D,H}$ (d)	$Time_T$ (d)
RDT-8	AP	R	0.7357	0.7458	0.0101	0.9308	0.1850	5.46		840	150	8/14/2002, 1230	8/19, 2100	140				
													8/20, 0900	130				
													8/20, 2050	120				
													8/21, 0925	110				
													8/21, 2230	100				
													8/22, 0900	90				
													8/22, 2100	80				
													8/23, 0915	70		8/23, 2135	3.5	8.8
RDT-9	AP	R	0.7261	0.7358	0.0097	0.9392	0.2034	4.77		840	150	8/26/2002, 1405	8/30, 0905	100	900	9/1, 0850	1.9	5.5
RDT-10	AP	R	0.6987	0.7139	0.0152	0.9259	0.2120	7.17		840	150	8/26/2002, 1405	8/30, 0905	150	880	9/4, 1410	4.5	9.0
RDT-11	AP	R	0.7182	0.7319	0.0137	0.9402	0.2083	6.58		840	150	8/26/2002, 1405	8/30, 0905	100	880	9/4, 1410	4.5	9.0
RDT-12	AP	R	0.8352	0.8591	0.0239	1.1752	0.3161	7.56		840	150	8/26/2002, 1425	8/30, 0905	10		9/17, 1350	16.5	21.0
RDT-13	AP	R	0.8451	0.8875	0.0424	1.3984	0.5109	8.30		840	150	8/26/2002, 1425	8/30, 0905	10		9/21, 1510	21.5	27.0
RDT-14	AP	R	0.9483	0.9598	0.0115	1.2355	0.2757	4.17		875	125	9/15/2002, 0900				9/20, 1105		5.1
RDT-15	AP	R	1.0269	1.0417	0.0148	1.3540	0.3123	4.74		900	100	9/15/2002, 0900				9/20, 1115		5.1
RDT-16	AP	R	0.9681	0.9716	0.0035	1.0312	0.0596	5.84		900	150	9/15/2002, 0900				9/20, 1120		5.1
RDT-17	AP	R	0.9560	0.9571	0.0011	1.0384	0.0813	1.35		775	30	9/15/2002, 0900				9/20, 1130		5.1
RDT-14b	AP	R	0.6511	0.6658	0.0147	0.8776	0.2118	6.94		840	150	10/20/2002, 1515	10/25, 1245	100				
													10/27, 0800	87.5				
													10/27, 2100	75				
													10/28, 0900	62.5				
													10/28, 2100	50		10/28, 2000	3.5	8.3
RDT-16b	AP	R	0.6812	0.7010	0.0198	0.9942	0.2932	6.76		840	150	10/20/2002, 1600	10/25, 1245	100				
													10/27, 0800	87.5				
													10/27, 2100	75				
													10/28, 0900	62.5				
													10/28, 2100	50				
													10/29, 0900	40		10/29, 2000	4.5	9.3
RDT-17b	AP	R	0.6599	0.6810	0.0211	0.9913	0.3103	6.81		840	150	10/20/2002, 1600	10/25, 1245	100		10/29, 0900	3.8	8.5
RDT-18	AP	R	0.6141	0.6189	0.0048	0.6981	0.0792	6.06		840	150	10/30/2002, 1200	11/3, 1615	110		11/7, 2035	4.3	8.5
RDT-19	AP	R	0.6459	0.6512	0.0053	0.7827	0.1315	4.03		840	150	10/30/2002, 1145	11/3, 1615	85		11/11, 1805	8.1	12.4
RDT-20	AP	R	0.6278	0.6363	0.0085	0.7741	0.1378	6.17		840	150	10/30/2002, 1145	11/3, 1615	85		11/7, 2035	4.3	8.4
RDT-21	AP	R	0.6568	0.6665	0.0097	0.8136	0.1471	6.59		840	150	11/8/2002, 1100	11/15, 1255	90		11/23, 1505	8.2	14.3
RDT-22	AP	R	0.5289	0.5341	0.0052	0.6351	0.1010	5.15		840	150	11/8/2002, 1100	11/15, 1255	90				
													11/17, 1125	80				
													11/18, 1720	75				
													11/19, 1655	70				
													11/20, 1405	65				
													11/21, 1620	60				
													11/23, 1505	50				
													11/24, 1100	45				
													11/25, 1410	40		11/26, 1540	10.1	17.4
RDT-23	AP	R	0.6297	0.6398	0.0101	0.8051	0.1653	6.11		840	150	11/14/2002, 1420	11/19, 1650	100				

Appendix 2. 2 (cont.)
Experiment sample preparation

Exp #:	C	F	Capsule	w/ H2O	H_2O_T	Total	$Sample_T$	H_2O	Ni, NiO	T (°C)	P (MPa)	In (d, h)	Drop (d,h)	P_D (MPa)	T_H (°C)	Quench (d,h)	$Time_{D,H}$ (d)	$Time_T$ (d)
													11/20, 1255	95				
													11/21, 1620	90				
													11/22, 1305	85		11/23, 1505	3.8	9.1
RDT-27	AP	R	1.5422	1.5521	0.0099	1.7529	0.2008	4.93		840	150	12/8/2002, 1420	12/12, 1945	20		12/19, 1705	6.8	11.3
RDT-30	AP	R	1.5025	1.5114	0.0089	1.6831	0.1717	5.18		900	150	1/20/2003, 1405				1/23, 1630		3.2
RDT-31	AP	R	1.6079	1.6167	0.0088	1.8339	0.2172	4.05		900	200	1/20/2003, 1410				1/23, 1620		3.2
RDT-32	AP	R	1.4496	1.4563	0.0067	1.6004	0.1441	4.65		940	50	1/20/2003, 1605				1/23/1815		3.2
RDT-35	AP	R	1.5025	1.5114	0.0089	1.6831	0.1717	5.18		840	150	11/13/2003, 1530	11/25, 1650	60		12/8, 0940	7.5	18.5
RDT-37	AP	T	1.1821	1.1882	0.0061	1.2942	0.1060	5.75	0.127, 0.192	940	150	11/23/2003, 0900				11/23, 1110	0.1	0.1
RDT-38	AP	T	1.0326	1.0371	0.0045	1.1151	0.0780	5.77	0.287, 0.327	940	150	11/23/2003, 1420				11/23, 1835	0.2	0.2
RDT-39	AP	T	1.0796	1.0823	0.0027	1.1347	0.0524	5.15	0.816, 0.878	940	150	11/24/2003, 0945				11/24, 1550	0.4	0.4
RDT-40	AP	T	1.1509	1.1575	0.0066	1.2976	0.1401	4.71	0.221, 0.435	940	150	11/25/2003, 0840				11/25, 1635	0.5	0.5
RDT-41	AP	R	1.0481	1.0606	0.0125	1.3233	0.2627	4.76		840	150	1/20/2004, 1100	1/23, 2130	145				
													1/25, 1300	140				
													1/25, 1715	135				
													1/26, 1440	130				
													1/27, 1720	125				
													1/28, 1915	120				
													1/29, 1330	115				
													1/30, 1730	110				
													1/31, 1615	105				
													2/1, 1935	100				
													2/2, 1525	95				
													2/3, 1720	90				
													2/4, 2030	85				
													2/5, 1410	80				
													2/6, 1605	75				
													2/7, 1520	70				
													2/8, 1220	65				
													2/9, 1445	60				
													2/10, 1620	55				
													2/11, 1405	50				
													2/12, 1205	45				
													2/13, 1320	40				
													2/14, 1620	35				
													2/15, 1510	30				
													2/16, 1100	25				
													2/17, 0920	20		2/18, 0715	24.5	27.0
RDT-42	AP	R	1.1742	1.1913	0.0171	1.4612	0.2699	6.34		840	150	1/20/2004, 1100	1/23, 2130	145				
													1/25, 1300	140				
													1/25, 1715	135				
													1/26, 1440	130				
													1/27, 1720	125				

Appendix 2. 2 (cont.)
Experiment sample preparation

Exp #:	C	F	Capsule	w/ H2O	H_2O_T	Total	$Sample_T$	H_2O	Ni, NiO	T (°C)	P (MPa)	In (d, h)	Drop (d,h)	P_D (MPa)	T_H (°C)	Quench (d,h)	$Time_{D,H}$ (d)	$Time_T$ (d)
													1/28, 1915	120				
													1/29, 1330	115				
													1/30, 1730	110				
													1/31, 1615	105				
													2/1, 1935	100				
													2/2, 1525	95				
													2/3, 1720	90				
													2/4, 2030	85				
													2/5, 1410	80				
													2/6, 1605	75				
													2/7, 1520	70				
													2/8, 1220	65				
													2/9, 1445	60				
													2/10, 1620	55				
													2/11, 1405	50				
													2/12, 1205	45				
													2/13, 1320	40		2/14, 1620	20.5	23.0
RDT-43	AP	R	1.1368	1.1547	0.0179	1.5168	0.3621	4.94		840	150	1/20/2004, 1100	1/23, 2130	145				
													1/25, 1300	140				
													1/25, 1715	135				
													1/26, 1440	130				
													1/27, 1720	125				
													1/28, 1915	120				
													1/29, 1330	115				
													1/30, 1730	110				
													1/31, 1615	105				
													2/1, 1935	100				
													2/2, 1525	95				
													2/3, 1720	90				
													2/4, 2030	85				
													2/5, 1410	80				
													2/6, 1605	75				
													2/7, 1520	70				
													2/8, 1220	65				
													2/9, 1445	60		2/10, 1620	16.5	19.0
RDT-44	AP	R	1.1878	1.2049	0.0171	1.5349	0.3300	5.18		840	150	1/20/2004, 1100	1/23, 2130	145				
													1/25, 1300	140				
													1/25, 1715	135				
													1/26, 1440	130				
													1/27, 1720	125				
													1/28, 1915	120				
													1/29, 1330	115				
													1/30, 1730	110				

Appendix 2. 2 (cont.)
Experiment sample preparation

Exp #:	C	F	Capsule	w/ H2O	H_2O_T	Total	$Sample_T$	H_2O	Ni, NiO	T (°C)	P (MPa)	In (d, h)	Drop (d,h)	P_D (MPa)	T_H (°C)	Quench (d,h)	$Time_{D,H}$ (d)	$Time_T$ (d)
													1/31, 1615	105				
													2/1, 1935	100				
													2/2, 1525	95				
													2/3, 1720	90				
													2/4, 2030	85				
													2/5, 1410	80		2/6, 1605	12.5	15.0
RDT-46	A	R	0.2030	0.2063	0.0033	0.2526	0.0463	7.13		840	150	7/12/2004, 1315	7/16, 0850	110		7/18, 1510	3	6.1
RDT-47	A	R	0.2310	0.2340	0.0030	0.2902	0.0562	5.34		840	150	7/12/2004, 1310	7/16, 0850	90		7/18, 1510	3	6.1
RDT-48	A	R	0.2445	0.2484	0.0039	0.3284	0.0800	4.88		840	150	7/12/2004, 1310	7/16, 0850	75		7/18, 1510	3	6.1
RDT-49	A	R	0.2273	0.2309	0.0036	0.2936	0.0627	5.74		840	150	7/24/2004, 1430	7/27, 0745	60		7/29, 0845	2.1	4.5
RDT-50	AP	R	0.6771	0.6927	0.0156	0.9448	0.2521	6.19		840	150	7/24/2004, 1430	7/27, 0745	100		7/29, 0835	2.1	4.5
RDT-51	AP	R	0.6681	0.6830	0.0149	0.9347	0.2517	5.92		840	150	7/24/2004, 1430	7/27, 0745	80		7/29, 0840	2.1	4.5
RDT-52	AP	R	0.6945	0.7042	0.0097	0.9087	0.2045	4.74		840	150	8/12/2004, 1245	8/15, 1115	50		8/17, 1055	1.9	4.9
RDT-53	AP	R	0.6457	0.6541	0.0084	0.8090	0.1549	5.42		840	150	8/12/2004, 1245	8/15, 1115	40		8/17, 1100	1.9	4.9
RDT-54	A	R	0.1993	0.2033	0.0040	0.2731	0.0698	5.73		840	150	8/18/2004, 1530	8/21, 1300	45		8/24, 0950	2.8	5.5
RDT-55	AP	R	0.6672	0.6753	0.0081	0.8530	0.1777	4.56		840	150	8/12/2004, 1245	8/15, 1115	20		8/17, 1110	2.0	4.9
RDT-58	A	R	0.1980	0.1998	0.0018	0.2330	0.0332	5.42		840	150	8/18/2004, 1530	8/21, 1530	65		8/24, 0945	2.8	5.5
RDT-59	AG	R	1.0010	1.0282	0.0272	1.3771	0.3489	7.80		840	150	8/18/2004, 1530	8/21, 1530	70		8/24, 1300	2.8	5.5
RDT-60	A	R	0.1963	0.1990	0.0027	0.2522	0.0532	5.09		840	150	8/24/2004, 1640	8/30, 1020	145				
													8/31, 1320	140				
													9/1, 1125	135				
													9/2, 1400	130				
													9/3, 1100	125				
													9/4, 1050	120				
													9/5, 1140	115				
													9/6, 1045	110				
													9/7, 1030	100				
													9/8, 1050	95				
													9/9, 0930	90				
													9/10, 0945	85				
													9/11, 1040	80				
													9/12, 0945	78		9/12, 2130	13.5	19.6
RDT-63	A	R	0.1867	0.1901	0.0034	0.2434	0.0533	6.38		840	150	8/26/2004, 1220	8/29, 1610	145				
													8/30, 1020	140				
													8/31, 1320	135				
													9/1. 1125	130				
													9/2, 1400	125				
													9/3, 1100	120				
													9/4, 1050	115				
													9/5, 1140	110				
													9/6, 1045	105				
													9/7, 1030	100				
													9/8, 1050	95				

Appendix 2. 2 (cont.)
Experiment sample preparation

Exp #:	C	F	Capsule	w/ H2O	H_2O_T	Total	$Sample_T$	H_2O	Ni, NiO	T (°C)	P (MPa)	In (d, h)	Drop (d,h)	P_D (MPa)	T_H (°C)	Quench (d,h)	$Time_{D,H}$ (d)	$Time_T$ (d)
													9/9, 0930	90				
													9/10, 0945	85				
													9/11, 1040	80				
													9/12, 0945	75				
													9/13, 0925	70				
													9/14, 0940	65				
													9/15, 0950	60				
													9/16, 0945	55				
													9/17, 0930	50				
													9/18, 1145	40		9/22, 1215	24.0	27.0
RDT-64	A	R	0.1841	0.1865	0.0024	0.2338	0.0473	5.07		840	150	10/1/2004, 1120	10/4, 1200	65				
													10/5, 1105	55				
													10/6, 1115	45				
													10/7, 1600	35				
													10/8, 1330	25				
													10/9, 1535	15				
													10/10, 1345	5		10/11, 1320	7.2	10.2
RDT-65	AG	R	0.2431	0.2487	0.0056	0.3252	0.0765	7.32		840	150	10/5/2004, 1220	10/8, 1330	20		10/12, 1000	3.8	6.9
RDT-68	AG	R	1.3969	1.4115	0.0146	1.6012	0.1897	7.70		840	150	10/12/2004, 0845	10/16, 1025	20		10/22, 1025	6.0	10.1
RDT-69	AG	R	1.3727	1.3910	0.0183	1.7211	0.3301	5.54		840	150	10/12/2004, 1020	10/16, 1020	10		10/22, 1025	6.0	10.0
RDT-70	AG	R	1.0573	1.0705	0.0132	1.2752	0.2047	6.45		840	150	10/26/2004, 1500	10/31, 1815	30		11/10, 1505	9.9	15.0
RDT-73	A	R	0.2353	0.2375	0.0022	0.2766	0.0391	5.63		840	150	12/18/2004, 1310	12/21, 1740	20		1/7, 0930	17.0	20.0
RDT-74	A	R	0.2438	0.2451	0.0013	0.2760	0.0309	4.21		840	150	12/18/2004, 1310	12/21, 1740	30		1/7, 0930	17.0	20.0
RDT-76	A	R	0.2486	0.2498	0.0012	0.2791	0.0293	4.10		840	150	1/12/2005, 1345	1/17, 1335	5		2/12, 1335	26.0	31.0
RDT-A-1	AP	T	0.6290	0.6403	0.0113	0.8162	0.1759	6.42	0.017, 0.016	940	150	9/2/2004, 0955				9/2, 2350		0.6
RDT-A-2	AP	T	0.1870	0.1928	0.0058	0.2586	0.0658	8.81	0.025, 0.023	940	210	9/3/2004, 0915				9/3, 2300		0.6
RDT-A-3	AP	T	0.4393	0.4471	0.0078	0.5567	0.1096	7.12	0.023, 0.042	940	100	9/7/2004, 1045				9/9, 0920		1.9
RDT-A-4	AP	T	0.1482	0.1517	0.0035	0.1901	0.0384	9.11	0.0253, 0.036	1000	200	9/8/2004, 0955				9/9, 0905		0.9
RDT-A-5	AP	T	0.1941	0.1988	0.0047	0.2581	0.0593	7.93	0.036, 0.031	1000	210	9/14/2004, 0950				9/15, 1000		1.0
RDT-A-6	AP	T	0.1953	0.2124	0.0171	0.4587	0.2463	6.94	0.033, 0.0265	1050	200	9/15/2004, 1020				9/15, 2230		0.5
RDT-A-7	AP	T	0.2738	0.2789	0.0051	0.3469	0.0680	7.50	0.026, 0.043	1000	150	9/17/2004, 1000				9/18, 1015		1.0
RDT-A-8	AP	T	0.3350	0.3440	0.0090	0.7640	0.4200	2.14	0.029, 0.044	1050	50	9/20/2004, 0955				9/22, 1000		2.0
RDT-A-9	AP	T	0.3078	0.3120	0.0042	0.3870	0.0750	5.60	0.028, 0.019	1050	150	9/28/2004, 1000				9/29, 0945		0.9
RDT-A-10	AP	T	0.2692	0.2737	0.0045	0.3398	0.0661	6.81	0.036, 0.021	1000	100	9/29/2004, 1015				10/1, 0945		1.9
RDT-A-11	AP	R	0.2391	0.2437	0.0046	0.3328	0.0891	5.16		880	100	10/1/2004, 1120				10/4/0825		2.8
RDT-A-12	AP	R	0.3128	0.3137	0.0009	0.3491	0.0354	2.54		900	75	10/1/2004, 1120				10/4/0835		2.8